

# UNCLASSIFIED

AD NUMBER
AD476882
NEW LIMITATION CHANGE
TO Approved for public release, distribution unlimited
FROM Distribution authorized to U.S. Gov't. agencies only; Administrative/Operational Use; JUL 1965. Other requests shall be referred to Air Force Materials Lab., Attn: Plastics and Composites Branch [MANC], Nonmetallic Materials Div., Wright-Patterson AFB, OH 45433.
AUTHORITY
AFML ltr dtd 7 Dec 1972

THIS PAGE IS UNCLASSIFIED

AFML-TR-65-245  
PART I

ABLATIVE PLASTIC CHARACTERIZATION IN  
SIMULATED MOTOR EXHAUST

C. S. Mayo  
S. L. Ostrow  
R. E. Marcus

Aeronutronic Division of Philco Corporation

TECHNICAL REPORT AFML-TR-65-245, Part I

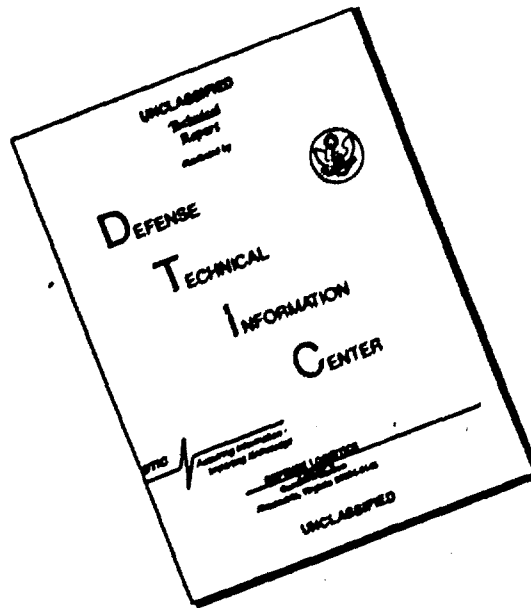
July 1965

Each transmittal of this document outside the agencies of the U.S. Government must have prior approval of the Plastics and Composites Branch, MANC, Nonmetallic Materials Division, Air Force Materials Laboratory, Wright-Patterson AFB, Ohio 45433.

Air Force Materials Laboratory  
Research and Technology Division  
Air Force Systems Command  
Wright-Patterson Air Force Base, Ohio



# DISCLAIMER NOTICE



**THIS DOCUMENT IS BEST  
QUALITY AVAILABLE. THE COPY  
FURNISHED TO DTIC CONTAINED  
A SIGNIFICANT NUMBER OF  
PAGES WHICH DO NOT  
REPRODUCE LEGIBLY.**

## NOTICES

When Government drawings, specifications, or other data are used for any purpose other than in connection with a definitely related Government procurement operation, the United States Government thereby incurs no responsibility nor any obligation whatsoever; and the fact that the Government may have formulated, furnished, or in any way supplied the said drawings, specifications, or other data, is not to be regarded by implication or otherwise as in any manner licensing the holder or any other person or corporation, or conveying any rights or permission to manufacture, use, or sell any patented invention that may in any way be related thereto.

Copies of this report should not be returned to the Research and Technology Division unless return is required by security considerations, contractual obligations, or notice on a specific document.

**PHILCO CORPORATION**

A SUBSIDIARY OF *Ford Motor Company*

January 19, 1966

AERONUTRONIC DIVISION

FORD ROAD NEWPORT BEACH, CALIFORNIA

REFCA-66-1057

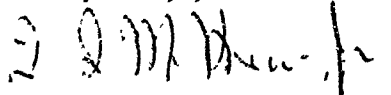
To: Distributees

Subject: First Yearly Summary Technical Report, prepared for  
Submittal under Air Force Contract AF33(615)-1632

The subject Aeronutronic Division technical report was distributed in November, 1965. Subsequently, certain changes in the report have been accomplished. Enclosed for substitution in your copy(s) of the report are revised pages 4, 23, and Figures 206. These pages reflect all of the changes made to date.

For your information, the data sheet numbers appearing in Table 7, Pages 43 through 46, were furnished from the Hughes Aircraft Company reports listed in the Foreword.

Very truly yours,



T. I. McKnew, Jr., Supervisor  
Contract Administration  
Applied Research Laboratories

Enclosures

**ABLATIVE PLASTIC CHARACTERIZATION IN  
SIMULATED MOTOR EXHAUST**

C. S. Mayo  
S. L. Ostrow  
R. E. Marcus

Each transmittal of this document outside the agencies of the U.S. Government must have prior approval of the Plastics and Composites Branch, MANC, Nonmetallic Materials Division, Air Force Materials Laboratory, Wright-Patterson AFB, Ohio 45433.

## FOREWORD

This report was prepared by Aeronutronic, a division of the Philco Corporation, Newport Beach, California under USAF Contract No. AF 33(615)-1632. This contract was initiated under Project No. 7340, "Nonmetallic and Composite Materials", Task No. 734001, "Thermally Protective Plastic and Composites". The work was administered under the direction of the Nonmetallic Materials Division, AF Materials Laboratory, Research and Technology Division, with Mr. Paul F. Pirrung as project engineer. The Aeronutronic Publication number is U-3356.

All research nozzles were furnished by the Nonmetallic Materials Division, Air Force Materials Laboratory, Research and Technology Division. Most of the rocket nozzle inserts were fabricated by the Hughes Aircraft Company under Air Force Contract. Further information on the fabrication of these nozzle inserts is in ML-TDR-64-222 and AFML-TR-65-94, dated June 1964 and April 1965 respectively. Both reports are titled, "New Ablative Plastics and Composites, Their Formulation and Processing" and both were authored by L. B. Keller, B. G. Kimmel and G. Schwartz.

This report covers work from 15 June 1964 to 30 June 1965.

Manuscript released by authors, 1 July 1965, for publication as an AFML Technical Report.

This technical report has been reviewed and is approved.

*H. S. Schwartz*  
H. S. SCHWARTZ, Chief  
Plastics and Composites Branch  
Nonmetallic Materials Division  
Air Force Materials Laboratory

### ABSTRACT

New chemical compositions and physical constructions of ablative materials were exposed in a small scale, high temperature Aeronutronic solid propellant rocket motor simulator and a liquid propellant (nitrogen tetroxide - 50 percent hydrazine and 50 percent unsymmetrical dimethylhydrazine) combustion gas environment to determine the potential usefulness of these materials for hyperenvironmental conditions associated with current and future solid and liquid propellant motors.

Material erosion and thermal insulation characteristics of the research nozzles were evaluated by comparisons of chamber pressure versus time data, erosion and resin degradation rates, and visual photographic data.

Research nozzle specimens were exposed in two (2) groups to the exhaust environment of a simulated solid propellant having a flame temperature of 5800°F and being highly aluminized. Test Series 1 contained thirty (30) nozzle specimens and Test Series 2 contained twenty-four (24) specimens. Test results and preliminary specimen evaluation indicated that the Aeronutronic solid propellant simulator exhaust environment provided the specified exhaust environment with the required repeatable test screening characteristics to enable valid material evaluations.

A total of seventy (70) nozzles were exposed to the exhaust environment of the liquid rocket motor (NTO/50-50). In the initial phase the motor injector was modified to provide optimum erosion geometry characteristics prior to research nozzle testing. Test results indicated that the specified nominal test conditions were met and enabled valid material evaluation.

Several new ablative plastic composites were found to have ablative performance characteristics superior to the state-of-the-art carbon-phenolic and silica-phenolic composites.

## CONTENTS

	PAGE
INTRODUCTION . . . . .	1
SOLID PROPELLANT COMBUSTION GAS SIMULATION TESTS . . . . .	2
General Discussion . . . . .	2
The Aeronutronic Solid Propellant Combustion Gas Simulator . . . . .	3
Test Conditions . . . . .	8
Check Run Performance . . . . .	8
Test Evaluation Techniques . . . . .	9
Nozzle Specimen Tests and Materials Evaluation Summary . . . . .	11
Identical Materials Performance - Test Series 1 and 2 . . . . .	16
Test Operation Conditions . . . . .	18
LIQUID PROPELLANT COMBUSTION GAS TEST . . . . .	19
General Discussion . . . . .	19
Liquid Propellant Rocket Motor, Propellant Fuel Systems, Controls and Instrumentation . . . . .	20
Test Conditions . . . . .	21
Check Run Performance . . . . .	22
Test Evaluation Techniques . . . . .	23
NOZZLE SPECIMEN TESTS AND MATERIALS EVALUATION SUMMARY . . . . .	24
Coatings on Prepyrolyzed Substrates . . . . .	24
Reinforcements . . . . .	25
Filled Composites . . . . .	26
Pyrolytic Coatings on Reinforcements . . . . .	26
Resin Systems . . . . .	27
TEST OPERATION CONDITIONS . . . . .	28

## ILLUSTRATIONS

FIGURE		PAGE
1	Aerothermochemical Laboratory Test Cells 6 and 7 . . . . .	63
2	ATC Test Cell 6 Control Room . . . . .	64
3	ATC Test Cell 6 Simulator Firing . . . . .	65
4	Solid Propellant Simulator Rocket Motor Injector - Wright Field Nozzle Test (Copper) . . . . .	66
5	Solid Propellant Simulator Rocket Motor Hardware . . . . .	67
6	Typical Test Nozzle Specimen Schematic . . . . .	68
7	Solid Propellant Simulation Rocket Motor Test Cell Schematic . . . . .	69
8	Chamber Pressure Versus Time - MANC-1 Nozzle . . . . .	70
9	Chamber Pressure Versus Time - MANC-2 Nozzle . . . . .	71
10	Chamber Pressure Versus Time - MANC-3 Nozzle . . . . .	72
11	Chamber Pressure Versus Time - MANC-4 Nozzle . . . . .	73
12	Chamber Pressure Versus Time - ASD 394 Nozzle . . . . .	74
13	Chamber Pressure Versus Time - ASD 397 Nozzle . . . . .	75
14	Chamber Pressure Versus Time - ASD 398 Nozzle . . . . .	76
15	Chamber Pressure Versus Time - ASD 400 Nozzle . . . . .	77



# ILLUSTRATIONS (Continued)

FIGURE		PAGE
16	Chamber Pressure Versus Time - ASD 414 Nozzle . . . . .	78
17	Chamber Pressure Versus Time - ASD 416 Nozzle . . . . .	79
18	Chamber Pressure Versus Time - ASD 418 Nozzle . . . . .	80
19	Chamber Pressure Versus Time - ASD 419 Nozzle . . . . .	81
20	Chamber Pressure Versus Time - ASD 421 Nozzle . . . . .	82
21	Chamber Pressure Versus Time - ASD 428 Nozzle . . . . .	83
22	Chamber Pressure Versus Time - ASD 430 Nozzle . . . . .	84
23	Chamber Pressure Versus Time - ASD 431 Nozzle . . . . .	85
24	Chamber Pressure Versus Time - ASD 432 Nozzle . . . . .	86
25	Chamber Pressure Versus Time - ASD 433 Nozzle . . . . .	87
26	Chamber Pressure Versus Time - ASD 434 Nozzle . . . . .	88
27	Chamber Pressure Versus Time - ASD 435 Nozzle . . . . .	89
28	Chamber Pressure Versus Time - ASD 437 Nozzle . . . . .	90
29	Chamber Pressure Versus Time - ASD 439 Nozzle . . . . .	91
30	Chamber Pressure Versus Time - ASD 440 Nozzle . . . . .	92
31	Chamber Pressure Versus Time - ASD 441 Nozzle . . . . .	93
32	Chamber Pressure Versus Time - ASD 442 Nozzle . . . . .	94
33	Chamber Pressure Versus Time - ASD 443 Nozzle . . . . .	95
34	Chamber Pressure Versus Time - ASD 444 Nozzle . . . . .	96
35	Chamber Pressure Versus Time - ASD 446 Nozzle . . . . .	97
36	Chamber Pressure Versus Time - ASD 448 Nozzle . . . . .	98

# ILLUSTRATIONS (Continued)

FIGURE		PAGE
37	Chamber Pressure Versus Time - ASD 452 Nozzle . . . . .	99
38	Chamber Pressure Versus Time - ASD 556 Nozzle . . . . .	100
39	Chamber Pressure Versus Time - ASD 358 Nozzle . . . . .	101
40	Chamber Pressure Versus Time - ASD 360 Nozzle . . . . .	102
41	Chamber Pressure Versus Time - ASD 366 Nozzle . . . . .	103
42	Chamber Pressure Versus Time - ASD 368 Nozzle . . . . .	104
43	Chamber Pressure Versus Time - ASD 417 Nozzle . . . . .	105
44	Chamber Pressure Versus Time - ASD 422 Nozzle . . . . .	106
45	Chamber Pressure Versus Time - ASD 423 Nozzle . . . . .	107
46	Chamber Pressure Versus Time - ASD 429 Nozzle . . . . .	108
47	Chamber Pressure Versus Time - ASD 449 Nozzle . . . . .	109
48	Chamber Pressure Versus Time - ASD 455 Nozzle . . . . .	110
49	Chamber Pressure Versus Time - ASD 456 Nozzle . . . . .	111
50	Chamber Pressure Versus Time - ASD 457 Nozzle . . . . .	112
51	Chamber Pressure Versus Time - ASD 459 Nozzle . . . . .	113
52	Chamber Pressure Versus Time - ASD 460 Nozzle . . . . .	114
53	Chamber Pressure Versus Time - ASD 463 Nozzle . . . . .	115
54	Chamber Pressure Versus Time - ASD 467 Nozzle . . . . .	116
55	Chamber Pressure Versus Time - ASD 468 Nozzle . . . . .	117
56	Chamber Pressure Versus Time - ASD 471 Nozzle . . . . .	118
57	Chamber Pressure Versus Time - ASD 480 Nozzle . . . . .	119
58	Chamber Pressure Versus Time - ASD 482 Nozzle . . . . .	120

# ILLUSTRATIONS (Continued)

FIGURE		PAGE
59	Chamber Pressure Versus Time - ASD 483 Nozzle . . . . .	121
60	Chamber Pressure Versus Time - ASD 489 Nozzle . . . . .	122
61	Chamber Pressure Versus Time - ASD 490 Nozzle . . . . .	123
62A	Erosion Rate Versus Nozzle Number Ablative Nozzle Characterization - Test Series 1 . . . . .	124
62A-1	Erosion Rate Versus Nozzle Number Ablative Nozzle Characteristics - Test Series 1 . . . . .	125
62B	Erosion Rate Versus Nozzle Number Ablative Nozzle Characterization - Test Series 2 . . . . .	126
63	Profile and Axial Nozzle Photographs . . . . .	127
64	Profile and Axial Nozzle Photographs . . . . .	128
65	Profile and Axial Nozzle Photographs . . . . .	129
66	Profile and Axial Nozzle Photographs . . . . .	130
67	Profile and Axial Nozzle Photographs . . . . .	131
68	Profile and Axial Nozzle Photographs . . . . .	132
69	Profile and Axial Nozzle Photographs . . . . .	133
70	Profile and Axial Nozzle Photographs . . . . .	134
71	Profile and Axial Nozzle Photographs . . . . .	135
72	Profile and Axial Nozzle Photographs . . . . .	136
73	Profile and Axial Nozzle Photographs . . . . .	137
74	Profile and Axial Nozzle Photographs . . . . .	138
75	Profile and Axial Nozzle Photographs . . . . .	139
76	Profile and Axial Nozzle Photographs . . . . .	140

# ILLUSTRATIONS (Continued)

FIGURE		PAGE
77	Profile and Axial Nozzle Photographs . . . . .	141
78	Profile and Axial Nozzle Photographs . . . . .	142
79	Profile and Axial Nozzle Photographs . . . . .	143
80	Profile and Axial Nozzle Photographs . . . . .	144
81	Profile and Axial Nozzle Photographs . . . . .	145
82	Profile and Axial Nozzle Photographs . . . . .	146
83	Profile and Axial Nozzle Photographs . . . . .	147
84	Profile and Axial Nozzle Photographs . . . . .	148
85	Profile and Axial Nozzle Photographs . . . . .	149
86	Profile and Axial Nozzle Photographs . . . . .	150
87	Profile and Axial Nozzle Photographs . . . . .	151
88	Profile and Axial Nozzle Photographs . . . . .	152
89	Profile and Axial Nozzle Photographs . . . . .	153
90	Test-to-Test Propellant Flowrate Variation From Nominal Condition . . . . .	154
91	Test-to-Test Propellant Flowrate Variation From Nominal Condition . . . . .	155
92	Aeronutronic El Toro Test Site . . . . .	156
93	Control Complex at El Toro . . . . .	157
94	Aeronutronic Remote Test Site - Test Cell B - NTO/50-50 Ablative Nozzle Test Firing . . . . .	158
95	$N_2O_4$ - Aerozine Injector - Wright Field Nozzle Test (Copper) . . . . .	159

# ILLUSTRATIONS (Continued)

FIGURE		PAGE
96	N <sub>2</sub> O <sub>4</sub> - Aerozine Injector - Wright Field Nozzle Test (Stainless) . . . . .	160
97	El Toro Cell B Schematic - Wright Field Ablative Nozzle Test Series . . . . .	161
98	Theoretical C* Versus Mixture Ratio N <sub>2</sub> O <sub>4</sub> /50% N <sub>2</sub> H <sub>4</sub> -50% UDMH Propellant at 300 Psia Chamber Pressure . . . . .	162
99	Chamber Pressure Versus Time - ASD 352 Nozzle . . . . .	163
100	Chamber Pressure Versus Time - ASD 377 Nozzle . . . . .	164
101	Chamber Pressure Versus Time - ASD 380 Nozzle . . . . .	165
102	Chamber Pressure Versus Time - ASD 381 Nozzle . . . . .	166
103	Chamber Pressure Versus Time - ASD 382 Nozzle . . . . .	167
104	Chamber Pressure Versus Time - ASD 390 Nozzle . . . . .	168
105	Chamber Pressure Versus Time - ASD 391 Nozzle . . . . .	169
106	Chamber Pressure Versus Time - ASD 392 Nozzle . . . . .	170
107	Chamber Pressure Versus Time - ASD 395 Nozzle . . . . .	171
108	Chamber Pressure Versus Time - ASD 396 Nozzle . . . . .	172
109	Chamber Pressure Versus Time - ASD 408 Nozzle . . . . .	173
110	Chamber Pressure Versus Time - ASD 409 Nozzle . . . . .	174
111	Chamber Pressure Versus Time - ASD 412 Nozzle . . . . .	175
112	Chamber Pressure Versus Time - ASD 415 Nozzle . . . . .	176
113	Chamber Pressure Versus Time - ASD 420 Nozzle . . . . .	177
114	Chamber Pressure Versus Time - ASD 424 Nozzle . . . . .	178

# ILLUSTRATIONS (Continued)

FIGURE		PAGE
115	Chamber Pressure Versus Time - ASD 425 Nozzle . . . . .	179
116	Chamber Pressure Versus Time - ASD 426 Nozzle . . . . .	180
117	Chamber Pressure Versus Time - ASD 427 Nozzle . . . . .	181
118	Chamber Pressure Versus Time - ASD 436 Nozzle . . . . .	182
119	Chamber Pressure Versus Time - ASD 438 Nozzle . . . . .	183
120	Chamber Pressure Versus Time - ASD 445 Nozzle . . . . .	184
121	Chamber Pressure Versus Time - ASD 447 Nozzle . . . . .	185
122	Chamber Pressure Versus Time - ASD 450 Nozzle . . . . .	186
123	Chamber Pressure Versus Time - ASD 453 Nozzle . . . . .	187
124	Chamber Pressure Versus Time - ASD 461 Nozzle . . . . .	188
125	Chamber Pressure Versus Time - ASD 462 Nozzle . . . . .	189
126	Chamber Pressure Versus Time - ASD 465 Nozzle . . . . .	190
127	Chamber Pressure Versus Time - ASD 466 Nozzle . . . . .	191
128	Chamber Pressure Versus Time - ASD 472 Nozzle . . . . .	192
129	Chamber Pressure Versus Time - ASD 473 Nozzle . . . . .	193
130	Chamber Pressure Versus Time - ASD 475 Nozzle . . . . .	194
131	Chamber Pressure Versus Time - ASD 476 Nozzle . . . . .	195
132	Chamber Pressure Versus Time - ASD 477 Nozzle . . . . .	196
133	Chamber Pressure Versus Time - ASD 478 Nozzle . . . . .	197
134	Chamber Pressure Versus Time - ASD 479 Nozzle . . . . .	198
135	Chamber Pressure Versus Time - ASD 481 Nozzle . . . . .	199

# ILLUSTRATIONS (Continued)

FIGURE		PAGE
136	Chamber Pressure Versus Time - ASD 484 Nozzle . . . . .	200
137	Chamber Pressure Versus Time - ASD 485 Nozzle . . . . .	201
138	Chamber Pressure Versus Time - ASD 486 Nozzle . . . . .	202
139	Chamber Pressure Versus Time - ASD 487 Nozzle . . . . .	203
140	Chamber Pressure Versus Time - ASD 488 Nozzle . . . . .	204
141	Chamber Pressure Versus Time - ASD 492 Nozzle . . . . .	205
142	Chamber Pressure Versus Time - ASD 493 Nozzle . . . . .	206
143	Chamber Pressure Versus Time - ASD 494 Nozzle . . . . .	207
144	Chamber Pressure Versus Time - ASD 495 Nozzle . . . . .	208
145	Chamber Pressure Versus Time - ASD 496 Nozzle . . . . .	209
146	Chamber Pressure Versus Time - ASD 497 Nozzle . . . . .	210
147	Chamber Pressure Versus Time - ASD 498 Nozzle . . . . .	211
148	Chamber Pressure Versus Time - ASD 499 Nozzle . . . . .	212
149	Chamber Pressure Versus Time - ASD 500 Nozzle . . . . .	213
150	Chamber Pressure Versus Time - ASD 501 Nozzle . . . . .	214
151	Chamber Pressure Versus Time - ASD 502 Nozzle . . . . .	215
152	Chamber Pressure Versus Time - ASD 503 Nozzle . . . . .	216
153	Chamber Pressure Versus Time - ASD 504 Nozzle . . . . .	217
154	Chamber Pressure Versus Time - ASD 505 Nozzle . . . . .	218
155	Chamber Pressure Versus Time - ASD 507 Nozzle . . . . .	219
156	Chamber Pressure Versus Time - ASD 509 Nozzle . . . . .	220

# ILLUSTRATIONS (Continued)

FIGURE		PAGE
157	Chamber Pressure Versus Time - ASD 514 Nozzle . . . . .	221
158	Chamber Pressure Versus Time - ASD 515 Nozzle . . . . .	222
159	Chamber Pressure Versus Time - ASD 516 Nozzle . . . . .	223
160	Chamber Pressure Versus Time - ASD 517 Nozzle . . . . .	224
161	Chamber Pressure Versus Time - ASD 518 Nozzle . . . . .	225
162	Chamber Pressure Versus Time - ASD 519 Nozzle . . . . .	226
163	Chamber Pressure Versus Time - ASD 520 Nozzle . . . . .	227
164	Chamber Pressure Versus Time - ASD 522 Nozzle . . . . .	228
165	Chamber Pressure Versus Time - ASD 524 Nozzle . . . . .	229
166	Chamber Pressure Versus Time - ASD 526 Nozzle . . . . .	230
167	Chamber Pressure Versus Time - ASD 527 Nozzle . . . . .	231
168	Chamber Pressure Versus Time - ASD 528 Nozzle . . . . .	232
169	Profile and Axial Nozzle Photographs . . . . .	233
170	Profile and Axial Nozzle Photographs . . . . .	234
171	Profile and Axial Nozzle Photographs . . . . .	235
172	Profile and Axial Nozzle Photographs . . . . .	236
173	Profile and Axial Nozzle Photographs . . . . .	237
174	Profile and Axial Nozzle Photographs . . . . .	238
175	Profile and Axial Nozzle Photographs . . . . .	239
176	Profile and Axial Nozzle Photographs . . . . .	240
177	Profile and Axial Nozzle Photographs . . . . .	241



# ILLUSTRATIONS (Continued)

FIGURE		PAGE
178	Profile and Axial Nozzle Photographs . . . . .	242
179	Profile and Axial Nozzle Photographs . . . . .	243
180	Profile and Axial Nozzle Photographs . . . . .	244
181	Profile and Axial Nozzle Photographs . . . . .	245
182	Profile and Axial Nozzle Photographs . . . . .	246
183	Profile and Axial Nozzle Photographs . . . . .	247
184	Profile and Axial Nozzle Photographs . . . . .	248
185	Profile and Axial Nozzle Photographs . . . . .	249
186	Profile and Axial Nozzle Photographs . . . . .	250
187	Profile and Axial Nozzle Photographs . . . . .	251
188	Profile and Axial Nozzle Photographs . . . . .	252
189	Profile and Axial Nozzle Photographs . . . . .	253
190	Profile and Axial Nozzle Photographs . . . . .	254
191	Profile and Axial Nozzle Photographs . . . . .	255
192	Profile and Axial Nozzle Photographs . . . . .	256
193	Profile and Axial Nozzle Photographs . . . . .	257
194	Profile and Axial Nozzle Photographs . . . . .	258
195	Profile and Axial Nozzle Photographs . . . . .	259
196	Profile and Axial Nozzle Photographs . . . . .	260
197	Profile and Axial Nozzle Photographs . . . . .	261
198	Profile and Axial Nozzle Photographs . . . . .	262

# ILLUSTRATIONS (Continued)

FIGURE		PAGE
199	Profile and Axial Nozzle Photographs . . . . .	263
200	Profile and Axial Nozzle Photographs . . . . .	264
201	Profile and Axial Nozzle Photographs . . . . .	265
202	Profile and Axial Nozzle Photographs . . . . .	266
203	Profile and Axial Nozzle Photographs . . . . .	267
204A	Test-to-Test Propellant Mixture Ratio and Total Propellant Flowrate Variation . . . . .	268
204B	Test-to-Test Propellant Mixture Ratio and Total Propellant Flowrate Variation . . . . .	269
204C	Test-to-Test Propellant Mixture Ratio and Total Propellant Flowrate Variation . . . . .	270
205A	Test-to-Test Propellant Flowrate Variation From Nominal Condition . . . . .	271
205B	Test-to-Test Propellant Flowrate Variation From Nominal Condition . . . . .	272
205C	Test-to-Test Propellant Flowrate Variation From Nominal Condition Nozzle Number . . . . .	273
206A	Erosion Rate Versus Nozzle Number Ablative Nozzle Characterization - Test Series III . . . . .	274
206B	Erosion Rate Versus Nozzle Number Ablative Nozzle Characterization - Test Series III . . . . .	275
206C	Erosion Rate Versus Nozzle Number Ablative Nozzle Characterization - Test Series III . . . . .	276

## TABLES

TABLE		PAGE
1A	Description of Test Specimens Ablative Nozzle Characterization Test Series 1 . . . . .	30
1B	Description of Test Specimens Ablative Nozzle Characterization Test Series 2 . . . . .	32
1C	Details of Post-Cure Cycles as Enumerated in Table of Test Specimens Description . . . . .	33
2	Solid Propellant Simulator Check Run Performance . . . . .	34
3A	Calculated and Measured Values Used in Erosion Property Analysis . . . . .	35
3B	Calculated and Measured Values Used in Erosion Property Analysis . . . . .	36
4A	Post Test Nozzle Erosion Evaluation MANC-Ablative Nozzle Characterization Test Series 1 . . . . .	37
4B	Post Test Nozzle Erosion Evaluation Ablative Nozzle Characterization Test Series 2 . . . . .	38
5A	Post Test Nozzle Visual Evaluation MANC-Ablative Nozzle Characterization Test Series 1 . . . . .	39
5B	Post Test Nozzle Visual Evaluation Ablative Nozzle Characterization Test Series 2 . . . . .	40
6A	Solid Propellant Simulator Performance Data During MANC-Ablative Nozzle Characterization Test Series 1 . . . . .	41

# TABLES (Continued)

TABLE		PAGE
6B	Solid Propellant Simulator Performance Data Ablative Nozzle Characterization Test Series 2 . . . . .	42
7	Liquid Propellant Test Series Test Specimen Description Ablative Nozzle Characterization . . . . .	43
8	Liquid Propellant Motor Check Run Performance Ablative Nozzle Characterization . . . . .	47
9	Calculated and Measured Values Used in Erosion Property Analysis Liquid Propellant Test Series . . . . .	48
10	Liquid Propellant Motor Performance Data Ablative Nozzle Characterization . . . . .	51
11	Post Test Nozzle Erosion Evaluation Ablative Nozzle Characterization . . . . .	55
12	Post Test Nozzle Visual Evaluation Ablative Nozzle Characterization . . . . .	59

## INTRODUCTION

A variety of high performance thermally protective materials are being generated on a continuing basis as a result of numerous research programs in this area. Many of these materials, because of their unique properties and characteristics, are intended for use in future solid propellant and liquid motor exhaust environments. Many of the new ablative composites or their components are sensitive to temperature, erosion, and chemical attack by certain rocket exhaust gases.

The object of this program is to determine the material erosion and thermal insulation characteristics of new ablative plastic and composite materials intended for use in current and future rocket nozzle environments. Research materials are exposed in an exhaust environment which will allow comparisons of behaviour among different ablative materials and provide reliable information on rocket motor performance characteristics in the throat of a rocket nozzle. Test device capability includes simulation of the chemical composition of current and future solid and liquid propellant exhausts.

The work done during this twelve month period of the program consisted of testing fifty-four (54) research nozzles in a solid propellant exhaust environment which had a flame temperature of 5800°F and which was highly aluminized; and testing seventy (70) additional research nozzles in a liquid propellant motor exhaust environment. The liquid propellants were nitrogen tetroxide (NTO) and a mixture by volume of 50 percent hydrazine and 50 percent unsymmetrical dimethylhydrazine (50-50) at an oxidizer to fuel mixture ratio of 1.6 to 1.0. Nozzle specimens and test data were evaluated and presented in tabulated, graphical, and photographic forms to allow comparisons of behaviour by the Air Force Materials Laboratory. A summary materials evaluation is included based on these data.

## SOLID PROPELLANT COMBUSTION GAS SIMULATION TESTS

### GENERAL DISCUSSION

The solid propellant combustion gas simulation tests were conducted in two groupings. Test Series 1 comprised thirty ablative nozzle test specimens and Test Series 2 comprised twenty-four ablative nozzle test specimens. Tables 1A and 1B present description of the nozzle test specimens tested.

The solid propellant simulators located at the Aeronutronic Aerothermochemical (ATC) laboratory at the Newport Beach location were utilized for these tests. Figure 1 is an overall view of a portion of the ATC complex showing some of these test cells. Figure 2 is an overall view of the test cell control room. Figure 3 shows the rocket motor firing in a test cell.

Check run data calculations resulted in the solid propellant simulator average combustion efficiency for Test Series 1 being 97.1 percent and for Test Series 2 being 96.2 percent. This was sufficient indication that simulation was being achieved.

An initial evaluation of conical versus tubular throat nozzle specimens was conducted as part of Test Series 1 to determine if resultant test data would indicate an optimum configuration. Although the tubular throat had an advantage in evaluating nozzle char depth, the conical throat was retained as the permanent configuration due to its previous standardization and acceptability of data for evaluation.

Also, one nozzle in Test Series 2 was fitted with a graphite entrance section rather than the standard phenolic configuration to evaluate the effect of nozzle section undercutting. Post test evaluation indicated side effects due to heat absorption characteristics that resulted in no advantage of the graphite entrance section to that of the standard configuration.

The summary nozzle specimen materials evaluations consisted of a preliminary review to indicate trends some of which were exhibited.

## The Aeronutronic Solid Propellant Combustion Gas Simulator

### Simulation Procedure

The rocket engine exhaust gas generator used for this program is a sophisticated device for identically reproducing the combustion products composition and temperature of a solid propellant by use of a propellant system employing only liquids, gases, or slurries. This Aeronutronic developed device has been perfected over the past six years, so that it is now operating on a routine basis as a highly successful research tool.

A given solid propellant can be exactly duplicated by any of a large number of combinations of liquid, gaseous, and/or slurry systems. The duplications are achieved with respect to both chamber temperature and chamber combustion products.

The composition and thermodynamic properties of the equilibrium products of a combustion process are uniquely determined by the atomic composition, the temperature, and the pressure. Pressure, as an independent variable, is usually specified in advance. The adiabatic flame temperature is determined by the heats of formation of the reacting propellant ingredients and their products.

Thus, in order to simulate a solid propellant with a liquid or gaseous system, the important parameters are atomic composition and enthalpy change. For example, if the solid propellant to be simulated contains six atomic species, it is possible to select six chemicals which contain the desired elements. Then, by a simple mass-balance process, the composition can be precisely determined. If an additional chemical is added, the heat balance equation can also be satisfied, such that not only the atomic composition, but also the temperature of the combustion products is reproduced. In the completely general case,  $n + 1$  ingredients are needed, where  $n$  is the number of elements in the solid propellant. In practice, however, fluid propellants can usually be found which combine several of the requisite elements, and then fewer than  $n + 1$  ingredients are required.

Finally, as a control on the simulation procedure, every proposed simulator composition is checked on the Aeronutronic computer before firing to assure that the flame temperature and gas composition are identical to the solid propellant being simulated.

The exhaust gas composition for the highly aluminized 5800°F solid propellant used in this program is shown on the following page.

# ALUMINIZED SOLID PROPELLANT SIMULATION

<u>Species</u>	<u>Molecular Weight</u>	<u>Moles/100 Grams</u>	<u>Weight %</u>
Al Cl (g)	62.44	0.0113	0.71
Al Cl <sub>2</sub> (g)	97.89	0.0209	2.04
CO (g)	28.01	0.7857	22.01
CO <sub>2</sub> (g)	44.01	0.0787	3.46
Cl (g)	35.46	0.0588	2.08
H Cl (g)	36.47	0.5081	18.53
HO (g)	17.00	0.0551	0.94
H <sub>2</sub> (g)	2.02	0.8845	1.78
H <sub>2</sub> O (g)	18.02	0.6992	12.60
N <sub>2</sub> (g)	28.02	0.3101	8.68
Al <sub>2</sub> O <sub>3</sub> (c)	101.96	0.2613	26.64
Other (minor species)			<u>0.53</u> 100.00%

---

Note: Simulation is at 500 psia chamber pressure and 3425°K chamber temperature



## The Aeronutronic Solid Propellant Combustion Gas Simulator

### Simulation Procedure

The rocket engine exhaust gas generator used for this program is a sophisticated device for identically reproducing the combustion products composition and temperature of a solid propellant by use of a propellant system employing only liquids, gases, or slurries. This Aeronutronic developed device has been perfected over the past six years, so that it is now operating on a routine basis as a highly successful research tool.

A given solid propellant can be exactly duplicated by any of a large number of combinations of liquid, gaseous, and/or slurry systems. The duplications are achieved with respect to both chamber temperature and chamber combustion products.

The composition and thermodynamic properties of the equilibrium products of a combustion process are uniquely determined by the atomic composition, the temperature, and the pressure. Pressure, as an independent variable, is usually specified in advance. The adiabatic flame temperature is determined by the heats of formation of the reacting propellant ingredients and their products.

Thus, in order to simulate a solid propellant with a liquid or gaseous system, the important parameters are atomic composition and enthalpy change. For example, if the solid propellant to be simulated contains six atomic species, it is possible to select six chemicals which contain the desired elements. Then, by a simple mass-balance process, the composition can be precisely determined. If an additional chemical is added, the heat balance equation can also be satisfied, such that not only the atomic composition, but also the temperature of the combustion products is reproduced. In the completely general case,  $n + 1$  ingredients are needed, where  $n$  is the number of elements in the solid propellant. In practice, however, fluid propellants can usually be found which combine several of the requisite elements, and then fewer than  $n + 1$  ingredients are required.

Finally, as a control on the simulation procedure, every proposed simulator composition is checked on the Aeronutronic computer before firing to assure that the flame temperature and gas composition are identical to the solid propellant being simulated.

The exhaust gas composition for the highly aluminized 5800°F solid propellant used in this program is shown on the following page.

<u>Constituent</u>	<u>Percent by Weight</u>
H <sub>2</sub> O	18.73
H <sub>2</sub>	1.22
CO	17.24
CO <sub>2</sub>	10.32
N <sub>2</sub>	9.33
H Cl	24.12
Cl	0.09
PO	0.04
Al <sub>2</sub> O <sub>2</sub> (S)	18.89
Other (minor species)	<u>0.02</u>
	100.00 percent

Solid Propellant Simulator, Propellant Feed Systems, Controls  
and Instrumentation

Aeronutronic has designed the solid propellant simulator especially for material testing. In achieving this goal, the simulator system has been designed to provide a constant flow of propellants independent of variations in chamber pressure. The simulator rocket motor hardware consists of a combustion chamber, a propellant feed injector, a nozzle holder, and the ablative nozzle test specimen. During the past five years the design of a representative solid propellant simulator has evolved into its present configuration.

The combustion chamber is a water cooled copper lined combustion chamber with an inside diameter of 3 inches at the injector end and 2.56 inches at the nozzle specimen end, with an overall length of 22-5/8 inches.

The propellant feed injector is made of copper. The injectants for the specified simulation were gaseous oxygen, gaseous nitrogen, gaseous hydrogen, and an aluminized slurry. Criteria pertinent to heat transfer, pressure drop, and impingement patterns were carefully employed in the design of the injector. The chamber and nozzle holder were designed to accept the test nozzle specimens which were furnished to Aeronutronic for this test evaluation program. These test specimens consist of an assembly comprising of a nozzle housing insert mold of refrasil phenolic into which the test ablative nozzle materials are inserted. Figure 4 presents a schematic of the injector. Figure 5 is a photo of the injector, chamber, and nozzle holder assembly. Figure 6 is a schematic of a typical test nozzle specimen.

The propellant feed systems are designed to provide constant flow independent of chamber pressure. The flow of each gas and the slurry propellant is independent of chamber pressure and each of the other propellants. Each of the gaseous oxygen, hydrogen, and nitrogen propellants feed systems includes a block valve, regulator, sonic nozzle, firing valve, bleed valve, pressure transducers, and thermocouples. The gases flow rate is controlled and measured by setting and recording the pressure upstream of the sonic nozzle. The setting of the flows are made under the exact flow conditions as during the run thus assuring reproducibility of the desired propellant flow rates. The slurry propellant is prepared in a mixer under carefully controlled conditions and then transferred into a run tank containing a floating piston. The slurry is expelled from the run tank during a test run by displacing the slurry with RP-1 fluid. Metering of the slurry is provided by controlling the volumetric amount of RP-1 which is used to displace the slurry. The metering of the RP-1 is provided by the setting of the RP-1 tank pressure and the use of a cavitating venturi. The flow rate through the cavitating venturi is determined by the area of the venturi, the upstream pressure, and the vapor pressure of the RP-1 fluid.

The system employed during these tests provides a differential ( $\Delta P$ ) pressure in the order of 1200 psi, thus the small variations in tank pressure results in minute changes in slurry flow rate. Figure 7 presents a test schematic of Aeronutronic's solid propellant simulator system.

In order to achieve the desired starting transients which are representative of a solid propellant motor, extreme care has to be observed in the timing of the firing valves. The timing of the control valves are controlled through a sequenced timer. During this test sequence, two shutdown criteria were used--one was time, the other pressure, whichever occurred first. The pressure shutdown was accomplished by the use of an automatic pressure control electronic circuit. The actual shutdown occurred approximately 1 second after the initiation of the shutdown circuit, thus allowing the shutdown to be accomplished with the sequence timer.

The instrumentation used during this sequence of tests is as follows: Dynisco "direct current" transducers were employed for all pressure measurements. The combined linearity and hysteresis of these transducers were held to better than 0.25 percent. Individual 10 volt excitation is provided to each transducer using Systems Research range and balance units. All temperatures were recorded using thermocouples conditioned for recording, utilizing a Pace thermocouple control unit. Gaseous flows were determined by measuring sonic nozzle upstream pressure and by the configuration of the sonic nozzle. The flow rate is then calculated by the appropriate flow equation and a series of correction graphs which compensates for temperature, upstream pressure, and gas medium. These formulas and corrections were developed through a computer program especially designed for determining propellant flow using high pressure sonic nozzles in the appropriate size range. The verification of this method of measuring flow has been documented using turbine type flow meters which were calibrated at the University of Colorado. RP-1 flow is measured using a Waugh turbine type flow meter. All data recorded during this test series were on a CEC oscillograph. The overall system accuracy achieved during this test series is better than  $\pm 1.5$  percent.

#### Propellant System Characterization

The solid propellant which was simulated is characterized by its combustion temperature, characteristic velocity, and its exhaust species. The theoretical values were then calculated based upon the ingredients which make up the propellant and the chamber pressure at which the system is to operate (i.e., 500 psia).

When the selected chemical ingredients are introduced into the combustion chamber and are allowed to react, the system is treated as a conventional rocket motor, which it is, wherein the combustion performance can be evaluated in accordance with accepted techniques. Utilizing the relationships among pressure, mass flow rates, and geometry to determine characteristic velocity ( $C^*$ ); if the experimental value approaches the theoretical  $C^*$ , then this is sufficient indication that simulation has been achieved.

Prior to testing any ablative nozzle specimens, short check runs were conducted on basically noneroding (graphite) nozzles. This permitted accurate definition of the throat area for simulation efficiency evaluation. Measurements made during each check firing are chamber pressure, propellant flow rates, and initial and final throat areas. From these measurements the experimental characteristic velocity is determined and combustion efficiency calculated.

Chamber pressure is obtained in a straightforward manner, employing a pressure transducer to sense pressure at a tap in the combustion chamber. The output from this transducer is converted to an oscillogram. Two transducers are utilized to provide redundancy for this parameter.

Flow rates are measured by methods best suited to each propellant. Gas flows are determined by measuring temperature and pressure upstream of sonic nozzles with known effective flow areas.

By virtue of the displacement technique employed to transfer the aluminized slurry (which contains solids in suspension), slurry flow rates are determined by measuring the volumetric flow rate of the displacement fluid.

Reproducibility of experimental or test conditions to ensure a common comparative base is largely dependent on the measurement of propellant flow meter outputs, pressures, and system temperatures.

Current technology for measurement of slurry flow rates in the Aeronutronic solid propellant simulator is based on measuring the flow rate of the transfer medium which displaces a known volume within a zero-leakage cylinder. A turbine type flow-meter is utilized to measure this flow rate. Overall accuracy of the measurement is dependent primarily on dynamic fluid correction, basic flow meter calibration, and instrumentation system accuracies.

Preset flow rates, monitored by means of pulse counting techniques (electronic counter), provides a system accuracy of better than  $\pm 0.5$  percent, while flow measurement conducted during the run via analog recording provides an overall accuracy of  $\pm 1.5$  percent.

Gaseous flow rates are measured by utilizing critical flow venturis designed according to classic principles and flow calibration techniques. Here again the accuracy is primarily dependent on following good design and fabrication techniques and verification of discharge characteristics. Measurement of flow-associated pressures and temperatures by pressure transducers and thermocouples provide the remaining basis for computation of the flow rates. Overall accuracy of this flow measurement and recorded data is  $\pm 1.5$  percent.

Measurement of all pressure parameters is made utilizing high-frequency bonded strain-gage pressure transducers, associated conditioning equipment, and galvanometer oscillographic recorders. Transfer function of each transducer channel is periodically verified with pressure standards and derived electrical equivalents. System accuracy is better than 1.5 percent.

### Test Conditions

All simulator testing was conducted utilizing a solid propellant simulation specified by the Nonmetallic Materials Division, Air Force Materials Laboratory, Research and Technology Division. The specified propellant had an equilibrium characteristic velocity ( $C^*$ ) of 5212 ft/sec and a flame temperature of 5800°F.

The weight flows "desired" for each propellant system were as follows:

$\text{GO}_2$	= 0.215 pps	Slurry Composition (% of Total Propellant)	
$\text{GN}_2$	= 0.051 pps		
$\text{GH}_2$	= 0.014 pps	Al	10.68%
Slurry	= <u>0.313</u> pps	$\text{Al}_2\text{O}_3$	8.04
Total	= 0.593 pps	Trichlorethane	27.67
		RP-1	5.28
		Gelling Agent	1.00

Test firing standard parameters for all nozzle specimen runs were as follows:

Initial Chamber Pressure: 500 psia (as determined by checkrun graphite nozzles)

Run Duration: 60 seconds or chamber pressure reduction to 150 psia, whichever occurred first.

### Check Run Performance

Check runs were completed prior to the actual specimen nozzle firings in each group. Check runs were performed for the following reasons:

- (1) To demonstrate proper simulation.
- (2) To optimize start transients of the various propellants.
- (3) To optimize simulator propellant flows, rocket motor performance, and demonstrate repeatability.
- (4) To experimentally verify a constant  $C^*$  value for the simulator, to enable calculations for the equivalent erosion rate based on chamber pressure.

The solid propellant simulator check run performance is presented in Table 2. All check runs were conducted utilizing graphite nozzles with a 0.500 inch nominal throat. Nine (9) performance check runs were made for the first test series. Because the solid propellant simulation performance had been optimized in the first test series only three (3) check runs were required for conducting the second test series.

During the check run series, a realistic value of characteristic velocity ( $C^*$ ) was obtained which was subsequently used for area calculations. The solid propellant simulator combustion efficiency was calculated at the end of each run. For these calculations the nozzle throat diameter was measured after each run. Due to the short test durations (about nine seconds), the graphite check nozzle throat usually had eroded very slightly and was easily measured.

The average combustion efficient for the check runs was 97.1 percent for the first set and 96.2 percent for the second set.

#### Test Evaluation Techniques

##### Chamber Pressure versus Time Curves

For each motor firing, a chamber pressure versus time graph has been prepared.

These graphs have been plotted so that a minimum of six points were used to define the curve and that no point is more than 4 seconds from an adjacent point. The graphs also note the pertinent research nozzle material.

Figures 8 through 37 present these data from Test Series 1; Figures 38 through 61 cover Test Series 2.

##### Erosion and Resin Degradation Rate Evaluation

Erosion rates were based on calculated nozzle specimen throat areas for the fired nozzles at rocket motor combustion chamber pressures of 350, 300, 250, 200, and 150 (or final) psia. The following standard formula was used:

$$A_t = \frac{W C^*}{g P_c}$$

where

$A_t$  = throat area (inch<sup>2</sup>)

$W$  = total weight flow (pounds per second)

$C^*$  = (equilibrium  $C^*$ ) x (average combustion efficiency) feet/second

$g$  = constant (32.2 feet/second<sup>2</sup>)

$P_c$  = chamber pressure (pounds per square inch absolute)

Resin degradation rates were calculated by adding the erosion rate at the end of the test run to the similar char depth rate. The char depth was measured on the post test sectioned nozzle at the resultant throat location.

The erosion rates per nozzle were plotted graphically to evaluate individual nozzles and nozzle groupings by materials. The resin degradation rates are tabulated for similar evaluations.

The above data are presented as follows:

- (1) Tables 3A and 3B present the tabulated, calculated, and measured values used in erosion property analysis.
- (2) Tables 4A and 4B present the tabulated char depths and resin degradation rates.
- (3) Figures 62A and 62B present the erosion rate versus nozzle number at the five specified combustion chamber pressures.

#### Nozzle Post Test Sectioning and Photographic Methods

Each of the ablative nozzles were sectioned and polished. All of the nozzles were sectioned with relation to the "12 O'clock" position of the simulator and so marked. The photographed section of each nozzle has been returned to the Nonmetallics Material Division.

Two different types of post test photographs were taken of each nozzle: an axial photograph of the complete nozzle and a profile photograph of a bisected nozzle.

A cross section throat area axial photograph was taken of the complete nozzle. The throat image was projected on a negative utilizing a point light source on the ceiling in the high bay photographic laboratory. A new nozzle was used to cast the original throat shape on a then reproduced negative. The negative was then aligned in a plexiglass fixture which also held the outside diameter of the phenolic nozzle holder, thus aligning the centers. A nozzle number and an injector orientation mark was also photographed through the plexiglass.

Profile photographs of the sectioned nozzles were taken utilizing a grid overlay, which consisted of a five lines per inch grid around the perimeter of the overlay and an original nozzle outline to emphasize and indicate erosion. The photographs emphasize the background highlights of the nozzles as well as the sanded nozzle plane for a more complete visual description of the post-fired nozzle section. For visual clarity only a perimeter grid was used. Both the grid and the outline were drawn with



white ink on a clear mylar sheet. The grid was aligned to the bisected nozzle utilizing the exit end of the insert and the 2.56 inch phenolic holder diameter. White chalk was placed on the nozzle contour for clarification.

Figures 63 through 77 present the photographic data for Test Series 1; Figures 78 through 89 cover Test Series 2.

Tables 5A and 5B present a brief tabulated post test nozzle visual evaluation.

#### NOZZLE SPECIMEN TESTS AND MATERIALS EVALUATION SUMMARY

##### Test Series 1

##### Tubular Throat Specimens Tests

Four tubular throat nozzles were tested to determine if the unique chamber pressure versus time trace resulting from this configuration would have more potential for material analysis than the previous conical throat configuration.

Theoretically, assuming no radial erosion, the tubular throat would erode longitudinally resulting in a constant chamber pressure until the original throat diameter disappeared, at which time the chamber pressure would drop. In ablative materials the radial erosion is a function of the material; and, therefore, this does not happen. In these tests a higher chamber pressure and a more evenly rounded trace peak was obtained from the tubular throat. Figures No. 8 and No. 9 (MANC 1 and 2) can be compared with Figure No. 14 (ASD 398). Figures No. 10 and No. 11 (MANC 3 and 4) can be compared with Figure No. 15 (ASD 400). For some reason, peak pressure and run duration on MANC 1 did not agree with this analysis.

Another erosion characteristic which was noted, and can be seen from the cross-sectioned photographs (Figures 63 and 64) is that a "true" nozzle char depth was obtained from the tubular throat nozzles. The post-run nozzle throat on the conical specimens usually has moved downstream and into the prerun conical section so that a combination throat and skirt char depth is obtained which could be difficult to evaluate. Because of this significant erosion characteristic it is believed that the tubular throat would have more potential than a conical configuration for evaluating ablative coatings. However, the conical throat nozzle can still be utilized as an acceptable configuration as long as it is standardized. Should it prove desirable to utilize the tubular throat, a correlation of a few test firings of similar materials in the two configurations should allow the use of previous conical throat nozzle data.

### Conical Throat Specimen Tests

Twenty-six conical throat specimens were tested as part of these series. The pressure versus time traces are presented as Figures No. 12 through 37. Table 3A presents the calculated and measured values used in the erosion property analysis. The calculated erosion rates at chamber pressures of 350, 300, 250, 200, and 150 psia are also presented in Table 3A. Table 5A includes post-test visual evaluations of each nozzle. Figures 63 through 77 are photographs of the post-test nozzle condition showing bisected nozzle profile axial views.

A preliminary review of the post-test nozzle visual data as presented in Table 5A and in the photographs of Figures 63 through 77 indicates that in all tests exceeding 35 seconds duration, "undercutting" of the nozzle insert was present. This condition may not be desirable because hot gas recirculation effects could affect material evaluation.

### Materials Evaluation

Some preliminary materials characteristics can be deduced from data obtained during this test series. With additional analysis, additional meaningful information could be obtained such as: chemical considerations of exhaust products, analysis of ablation products, X-ray and metallographic analyses of the chars to determine continuity of reinforcement and char, reaction of reinforcement with chars, and interaction of reinforcement-char product with combustion species.

The thirty runs considered here allow some deductions, if specimen fabrication is assumed optimum and constant for any material.

A comparison of specimens MANC 1 and 2, MANC 3 and 4, 398 and 400 indicates that the erosion rates are reproducible in this environment.

The substitution of carbon cloth for graphite cloth in nozzle specimens 3, 4, 400, 421, 428, 435, 437, 444 and 446 indicates a consistently higher erosion rate for the carbon cloth and that the influence of pyrolytic fabric coatings is only minor.

If one compares the rates of resin degradation (the erosion rate plus the rate at which the char layer advances relative to the hot wall) the carbon, high silica and graphite fabric reinforcements appear to be equivalent using the 91-ID resin system, 11.5 to 13 mils/sec, (Table 4A presents this tabulation). This can be an important consideration in material utilization because in general it will determine the insulation requirements for this combustion environment. This observation is somewhat unique and is probably due to a combination of nozzle heat transfer and exhaust chemistry which would control the rate at which char and carbonaceous reinforcements would be oxidized. This might be substantiated if these observations were coupled with temperature measurements in the test structure of selected nozzles and thermochemical analyses of the ablating wall.

Pregraphitized inserts were fabricated with WCA graphite cloth and R120 phenolic resin. The total composite was heat treated at graphitizing temperatures. The composites were then either impregnated with a resin or a coating was deposited onto the throat surface of the nozzle insert. A 5 mil pyrolytic graphite coated (No. 439) insert exhibited a 5 to 6 second period of no erosion during motor firings, while a 15 mil pyrolytic graphite coated (No. 440) insert exhibited a 12 second period of no erosion. Some of the lowest erosion rates of Test Series 1 were exhibited by the inserts which were impregnated with R120 phenolic resin (No. 441), X8-furane resin (No. 442), and LTV-X22 polyimide resin (No. 443).

With carbon cloth as the control reinforcement it appears the following resin matrix composites had erosion rates within the values exhibited by the phenolic (No. MANC-3, No. MANC-4, No. 400 and No. 421) composites: 2,2-Bis p-hydroxyphenyl) propane-formaldehyde (No. 394); 2,7 dihydroxy-naphthalene phenol formaldehyde (No. 431 and 432); m-hydroxybenzoic acid phenol formaldehyde (No. 433). The following had higher erosion rates than the standard phenolic (No. MANC-3, No. MANC-4, No. 400 and No. 421) composites: M-hydroxybenzoic acid phenol formaldehyde (No. 430); polyphenylene (No. 434); and I-8, polyimide (No. 452).

The performance of some of the experimental resins with standard CCA or C-100-48 reinforcements can be observed from some of the tests. The propane-formaldehyde resin was run with both carbon and high silica reinforcements. The resin degradation rate of the carbon cloth specimen (No. 394) was lower than the phenolic bonded analog (No. 4). The high silica-propane-formaldehyde exhibited lower resin degradation than the high silica-phenolic (No. 1, 2, and 418).

It is also interesting to note that the combined erosion and char rates of these experimental resin materials are the lowest in this series (refer to Table 4A).

Figure 62A is a graphical presentation of the erosion rates tabulated in Table 3A.

## Test Series 2

### Nozzle Specimen Tests

Twenty-four conical throat nozzle specimens were tested in this series. The pressure versus time curves of the tests are presented in Figures 38 through 61. The nozzle erosion property analysis at various chamber pressure increments of each nozzle test are presented in Table 3B. Figure 62B is a graphical presentation of these erosion rates. Table 5B covers the post-test visual analysis of each nozzle specimen. Table 4B tabulates the specimen char depth and resin degradation. Photographs of the post-test nozzle showing the bisected profile section and the axial throat view are presented in Figures 78 through 89.

In contrast to the Test Series No. 1, where eight (8) test specimens did not sufficiently erode to cause the test termination within 60 seconds, only three (3) specimens in this series maintained a chamber pressure above 150 psia at the end of 60 seconds test duration. The median test duration was 49 seconds.

In general, all specimens, except 366 and 368, exhibited a material erosion rate of 3 to 5 mils/seconds. Most specimens exhibited a total resin degradation rate between 11 and 16 mils/second.

#### Materials Evaluation

There were not as many single variable material changes within the nozzle specimens of this test series as there were in Test Series No. 1, which does not allow for many direct comparisons of specific material erosion or char rates. However, some observations can be made on some of the individual test specimens.

#### Prechar-Nonprechar Materials

A comparison of the char rates and erosion rates of specimens No. 356 and No. 358 shows that the precharred reimpregnated material erodes less and has a lesser degree of heat penetration than the noncharred material. A possible cause of this comparatively high erosion during the test of specimen No. 358 may be the observed spalling or "chunking" of the virgin resin matrix material. This gross removal of char is due to the fact that pyrolysis products are generated at the resin decomposition zone rapidly and must transpire through the char. If the permeability of the char is low, a pressure gradient develops across the char layer; the pressure gradient can be high enough so that mechanical failure of the char (chunking) results. Chunking has been observed during tests of carbon cloth reinforced phenolic ablators at relatively high heat fluxes. The graphite reinforcement in specimens No. 356 and No. 358 has a higher thermal conductivity than a carbon reinforcement and therefore the tendency to experience chunking would be expected to be greater for the nonprecharred specimen No. 358.

Specimens No. 368 and No. 366 are assumed to be analogous materials with silica reinforcement substituted for the graphite cloth of specimens No. 356 and No. 358. This substitution results in a reinforcement thermal conductivity which is significantly less than that of the graphite. Consequently the tendency toward chunking would be reduced significantly. The observed smooth, even erosion would seem to bear out this reinforcement comparison.

#### Pyrolytic Graphite Coated G-1550 Graphite Cloth

The graphite fiber reinforced materials with 91LD resin matrix exhibited comparable erosion rates regardless of whether or not the fiber reinforcement was coated with pyrolytic graphite. The charring rate of the uncoated fiber specimen (No. 429) was slightly less than those with coated fibers (Nos. 417, 459, and 460), although the difference in char rate was small. If significant, the difference in charring rate was most probably due to an increase in the effective conductivity of the fibers by means of the oriented graphite coating.

#### Pyrolytic Graphite Coated Specimens

The effect of a coating of pyrolytic graphite on the interior surface of a precharred specimen would be entirely different than the effect of pyrolytic graphite coating on the fibers of the reinforcing agent. The orientation of the deposit on the interior surface would be expected to serve as an insulator which would decrease heat penetration to the bulk of the specimen until the layer was either eroded or ablated off. At that time the erosion rate, as well as heat penetration, would approach that of the uncoated specimen. The effectiveness of the low thermal conductivity of the coating is obvious from Table 4B (Specimens No. 480 versus No. 482 and No. 483). However, throughout all portions of the run, the erosion rate is higher for the uncoated specimen than the coated specimens. The exit cone coating on nozzle No. 482, although cracked, was still adherent at the termination of the test. It is of interest to note that the pyrolytic graphite coated specimens (No. 439 and 440) of test series number one exhibited periods of no erosion. However, inserts No. 482 and No. 483 do not exhibit similar plateau regions. This difference of performance may be due to differences in the coating process. Inserts No. 439 and No. 440 were coated by a vapor deposition process utilizing the decomposition products of a hydrocarbon gas. Inserts No. 482 and 483 were coated by a vapor deposition process utilizing the sublimation products of bulk graphite. All insert substrates were pregraphitized similar to inserts No. 439 and No. 440.

#### Resin Comparison

With carbon cloth as the control reinforcement, it appears that the following resin matrix composites had equivalent or higher erosion rates than those of the 91 LD (No. 422) phenolic composite: I-8, polyimide, (No. 449); polyphenylene (No. 471 and No. 413). The following had lower erosion rates: p-phenyl-phenol-phenol-formaldehyde, (No. 455, No. 490, and No. 456) with respective erosion rates of 5%, 14%, and 16% below phenolic); Den 438, epoxy novolac (No. 489, erosion rate 12% below phenolic); 2-7 dihydroxynaphthalene phenol formaldehyde (No. 457 and 463 with respective erosion rates of 6% and 12% below phenolic); and polyphenylene (No. 468, erosion rate 5% below phenolic).

### Carbon and Graphite Fabric

It is interesting to note that most ablative specimens containing carbon cloth reinforcement in nonprecharred matrices exhibit delamination and fabric distortion. The graphite reinforced ablatives on the other hand appear to be stable with little evidence of delamination or fabric reorientation.

### Erosion Rate

In general, the erosion rates of the graphite cloth materials is lower than those of the carbon cloth materials. The two silica cloth specimens exhibited a relatively high erosion rate, but, because of the shallow char layer formed during these tests, the resin degradation rates are comparable to the other materials tested.

### Graphite Entrance Section

For the first test of this series, nozzle No. 423 was fitted with a graphite entrance section to diminish the nozzle section undercutting effects experienced on previous testing. Post-test inspection revealed that the nozzle section was not undercut but that the nozzle experienced an appreciably higher erosion rate than the No. 422 specimen which is of the same material but was not fitted with the graphite entrance section. Apparently, the graphite entrance section did not absorb as much heat as the regularly used phenolic material, causing more heat absorption and therefore more erosion by the nozzle section. Also, no pyrolysis or ablation products are injected into the bonding layer upstream of the nozzle throat when the graphite entrance section is used. This would tend to increase the chemical reactivity of the bonding layer at the throat section.

### IDENTICAL MATERIALS PERFORMANCE - TEST SERIES 1 AND 2

A superficial comparison of the identical nozzle materials that were used in both Test Series 1 and Test Series 2 has been made by examining the calculated erosion rates and resin degradation rates. Comparisons were made between the following nozzles:

ASD 416 - Test Series 1 and ASD 417 - Test Series 2; identically made of graphite cloth G1550 coated with 1.0 - 1.2 microns of pyrolytic graphite and CTL91-LD phenolic.

ASD 428 - Test Series 1 and ASD 429 - Test Series 2; identically made of graphite cloth G1550 and CTL91-LD phenolic.

ASD 448 - Test Series 1 and ASD 449 - Test Series 2; identically made of carbon cloth CCA-1 and polyimide I-8.

On the basis of this evaluation it would appear that there are differences between identical material performance in both test series. These differences do not seem attributable to the rocket motor simulator exhaust environment.

#### TEST OPERATION CONDITIONS

During the check runs prior to each ablative nozzle testing group, simulator operational performance was optimized and documented. As part of the documentation during the ablative nozzle tests, the simulator flow rates were tabulated. Tables 6A and 6B present these results.

Two test operation conditions were changed from the previous test series to ensure more consistent data production in this test series.

By use of an automatic cutoff relay, a consistent test pressure cutoff of almost exactly 150 psia chamber pressure was obtained. This factor allowed a more standardized evaluation of the nozzle material degradation and char formation rates.

This second series of nozzle evaluation tests was run in a test cell which has an operational digital voltage unit. With the use of this unit the pretest propellant pressures upstream of the gas systems sonic nozzles and the slurry system cavitating venturi can be very accurately adjusted and set. The small test-to-test variation of the propellant flow rates attests to the accuracy of this pretest set condition. This is shown graphically in Figures 90 and 91. The total flowrate variation range is within only  $\pm 1$  percent for both the total propellant flowrate and the slurry propellant flowrate. For the smaller value gaseous flowrates the variation is slightly higher, but the oxygen and nitrogen flowrate variation is within  $\pm 1$  percent from the nominal value in 88 percent (21 tests) of the tests while the hydrogen flowrate variation is between +2 percent and -1.2 percent of nominal with 71 percent (17 tests) falling within the  $\pm 1$  percent range. The inability to correct for the exact gaseous propellant run temperature is partially responsible for the gaseous flowrate variations.

## LIQUID PROPELLANT COMBUSTION GAS TESTS

### GENERAL DISCUSSION

The liquid propellant combustion gas nozzle specimen tests were conducted in one grouping of seventy nozzles. Table 7 presents a test specimen description. The liquid propellants were nitrogen tetroxide (NTO) and a 50 percent hydrazine and 50 percent unsymmetrical dimethyl hydrazine (50-50) mixture by volume at an oxidizer to fuel mixture ratio of 1.6 to 1.

The liquid propellant testing was conducted at the Aeronutronic Remote Test Site located about 15 miles from the main plant. Figure 92 is an overall view of the test cell - control room arrangement. Figure 93 is a view of the control room instrumentation area. Figure 94 shows the liquid propellant motor in Test Cell B during a test firing.

An extensive series of check runs were made to fully evaluate and optimize the rocket motor hardware. These initial runs were required as the erosion pattern exhibited on the graphite check nozzle after a sixty second run was such as to negate nozzle specimen testing even though combustion efficiency was very good (95.8 percent). This geometric deficiency was traced back to the copper 4 doublet configuration injector. Once the oxidizer-fuel impingement patterns were optimized, specimen nozzle testing was initiated. Thirteen nozzles were tested with this injector, following which the injector had to be discarded due to severe face erosion. Based on the experience with this copper injector the next injector was a water cooled stainless steel configuration incorporating 8 doublets to reduce geometric sensitivity. Check runs with this injector indicated very good nozzle erosion patterns and combustion efficiency was almost identical to that obtained with the copper unit (95.7 percent). No wear patterns have been observed on the injector face so that "life" characteristics should be good.



### Liquid Propellant Rocket Motor, Propellant Feed Systems, Controls and Instrumentation

Aeronutronic also designed the liquid propellant rocket motor ( $N_2O_4$  - 50/50) especially for material testing. In achieving this goal extreme care was utilized to get even nozzle erosion characteristics from the rocket engine. The liquid rocket motor hardware consists of a combustion chamber, a propellant feed injector, ablative-nozzle holder, and the test specimen.

The final combustion chamber used during this test sequence was the same as that utilized for the solid propellant simulator tests. Initially, check runs were run with a chamber which is 2.5 inches in diameter and 8 inches long. The length of this chamber was insufficient to allow for complete combustion before the gases entered in the test section.

Two propellant feed injectors have been used. The first injector was made of copper having four doublet stainless steel inserts at the injection face part. Although the efficiency of this injector was very good, many check runs were required to optimize the impingement geometry so that nozzle erosion would not be influenced by the injector characteristics. Thirty-eight check runs were required in this optimization evaluation. Fourteen nozzle specimens were evaluated with this copper injector prior to its failure due to excessive erosion at the injector face in the area of the stainless steel inserts. Figure 95 presents a schematic of the copper injector. Based on the results of the copper injector, the new injector configuration was designed. This is the stainless steel, water cooled unit shown in Figure 96. This injector has eight doublets which decreases its geometric sensitivity. Its combustion efficiency is almost exactly that of the initial copper injector so that it has been utilized with no qualification as to evaluation or comparison of data.

The propellant fuel systems are of a constant flow design. The flow of each liquid propellant is "set" by utilizing a specially designed cavitating venturi having a pressure drop of approximately 700 psi. This large drop results in the flow rates being very constant and repeatable.

Each of the two propellant systems includes a nitrogen pressurized propellant tank, block valve, cavitating venturi, firing valve, purge systems, pressure transducers, and thermocouples. Two purge systems are utilized: Gaseous nitrogen and water. The nitrogen purge is automatic at the start and finish of each run. The water purge is a post-test operation conducted to efficiently purge and clean the system. Figure 97 presents a test schematic of the Aeronutronic liquid propellant  $NTO/50-50$  system.

The instrumentation system employed during the liquid propellant tests is basically the same as that employed during simulator tests with the exception that the data are recorded using an analog to digital recorder in addition to the oscillograph recording. The analog to digital recorder is a

paper tape, three digit system which an accuracy of better than 0.2 percent. This system is manufactured by Applied Development Corporation. By use of the digital recorder, the overall system accuracy will be better than  $\pm 1/2$  percent.

The data was obtained by recording thirty channels of test pressure information per second in a sequential manner. Each channel being recorded in sequence every two-thirds ( $2/3$ ) of a second. Ten chamber pressure channels per each two-thirds ( $2/3$ ) second scan were employed to enable data analysts to more easily "pick out" desired data points and to insure that these points were consistent with the pressure values within a range as short as one-tenth ( $1/10$ ) second from the selected data point.

#### Test Conditions

All NTO/50-50 testing was conducted at an oxidizer to fuel mixture ratio of 1.6 to 1.0 as specified by the Nonmetallic Materials Division, Air Force Materials Laboratory, Research and Technology Division.

At the desired initial chamber pressure of 300 psia at the specified mixture ratio, the theoretical equilibrium characteristic velocity ( $C^*$ ) was 5627 feet/second; and the flame temperature was approximately 5300°F (reference Figure 98, Theoretical  $C^*$  Versus Mixture Ratio).

The weight flows "desired" for each propellant system were as follows:

NTO = 0.2164 pps

50-50 = 0.1352 pps

Total = 0.3516 pps

The firing standard parameters for all nozzle specimen runs were as follows:

Initial Chamber Pressure: 300 psia (as determined by check run graphite nozzles).

Run Duration: 120 seconds or chamber pressure reduction to 100 psia, whichever occurred first.

### Check Run Performance

Check runs were completed prior to the actual specimen nozzle firings and after any significant rocket motor or system modification. In addition, a check run was made after a run of approximately 15 nozzles to insure consistent data. Check runs were performed for the following reasons:

- (1) To demonstrate proper mixture ratio, chamber pressure, and uniform combustion.
- (2) To demonstrate reliable and repeatable hardware performance.
- (3) To optimize starting and stopping transients.

The liquid propellant check runs are presented in Table 8. All check runs were conducted utilizing graphite nozzles with 0.500 inch nominal throats.

The first large grouping of check runs was necessary because of the geometric sensitivity of the 4 doublet injector design on the nozzle erosion pattern. Impingement patterns were changed incrementally in order to optimize the pattern. Nine additional check runs were made to optimize the starting transient conditions and document performance with the copper injector. Average combustion efficiency was 95.8 percent.

Four check runs were made on the stainless steel 8 doublet injector. After one specimen nozzle had been tested, a water leak developed at the weld joints adjacent to the 50-50 doublets. A minor redesign was required. Following this modification, check run five was made. Combustion efficiency was 95.7 percent.

Table 8 presents the check run performance data. The invalid tests (check runs 24, 26, 39, and 44) were due to hot gas leakage past the check nozzle-nozzle holder assembly which resulted in erroneous data.

### Test Evaluation Techniques

Test evaluation for the specimen nozzles subjected to the liquid propellant environment were the same as for those exposed to the solid propellant simulator exhaust (refer to page 10). Erosion rates were based on calculated nozzle specimen throat areas for the fired nozzles at rocket motor combustion chamber pressures of 250, 200, 150, and 100 (or final) psia.

Data are presented as follows:

Chamber pressure versus time curves as shown on Figures 99 through 168.

Table 9 presents the tabulated, calculated, and measured values used in erosion property analysis.

Figure 206 presents the erosion rate versus nozzle member at the four specified combustion chamber pressures.

Figures 169 through 203 present the photographic data.

Table 10 presents liquid propellant motor performance data.

Table 11 presents the post test nozzle erosion evaluation consisting of char depth and resin degradation rates.

Table 12 is the post test nozzle visual evaluation.

Figure 204 is the test-to-test propellant mixture ratio and total propellant flowrate variation.

Figure 205 is the test-to-test propellant flowrate variation from nominal conditions.

#### NOZZLE SPECIMEN TESTS AND MATERIALS EVALUATION SUMMARY

The large number of nozzles tested here allow some comparison of the various materials and their performance. These are, however, limited since test duplication was not possible in many cases. Additional limitations on the conclusions which may be drawn are that the specimens were of small size, and the complete history and fabrication data processing of the materials were not completely known.

Due to the large number of specimens it is convenient to divide them and consider them separately in various groupings. By this means the effect of material variations can be assessed. There are some specimens which appear in more than one group, generally as the control element or the standard element in that group, such as a Refrasil phenolic reinforcement in a 91-LD resin which has been used throughout the rocket industry and with which a good deal of experience has been obtained. This material can be used as a baseline comparison not only for other resin systems but also for the influence of other reinforcements.

#### Coatings on Prepyrolized Substrates

The protection afforded by hard or oxidation resistant coatings is relatively easy to assess by means of chamber pressure time curves; in that, once a flaw is formed in the continuous coating, local and rapid nozzle degradation ensues. The change in slope can be utilized to define the point at which coating failure began. There is a problem in the utilization of coatings, however, since the anticipated performance of the structure must be based on the time duration when the coating remains continuous and completely protected. This imposes rather severe process, quality control and inspection requirements on the coating systems. This first group consists of the three nozzles, specimens numbered 380, 381, and 382. Specimens 380 and 381 exhibited similar performance; however, specimens 381 and 382 were intended to be identical. Of the three specimens it appears that the carbide based (mixed zirconium and silicon carbides) coating over the throat of Specimen 380 is superior to the zirconium diboride coating. However, the coating of 381 does not appear to provide as good performance in terms of erosion resistance as the majority of the normal Refrasil phenolic materials.

Some nozzle insert specimens of the group are No. 475, 476, 481, 484, 485, 486, 487, 488, 509, 514 and 515. For all of these specimens the erosion rate was quite low with the exception of the molybdenum-silicon coating.

As can be seen in the photograph of specimen No. 484 (consisting of a tantalum-sodium fluoride coating over the throat) there was a small spot oxidized or eroded through the coating and into the specimen. Post test examination of this spot revealed that the area around the coating discontinuity was undercut, implying the oxidation of underlying material and the subsequent mechanical failure of the unsupported coating. Further examination after sectioning revealed that the oxidized pocket was free of foreign material. This would imply that the coating failure occurred almost simultaneously with the end of the run or perhaps even slightly after the end of the run since the high flow rates over the surface of these nozzles normally result in coating material upstream being transported down and into cracks or other surface discontinuities.

The time versus chamber pressure curves for these coated specimens indicate that the body failed rapidly after pressure had decayed to about 250 psi; this is equivalent to a nominal 0.018 inch recession which is assumed to be approximately the initial coating thickness. The curves also indicate that value of such self protective coatings in providing low recession rates, limited, however, by the failure or potential failure within any local area.

#### Reinforcements

A total of six Refrasil phenolic specimens were run. All exhibited very low erosion. Five of the six exhibited erosion rates within 0.25 mil/sec indicating the high degree of reproducibility of both the material and the experiment. This low erosion rate has been experienced before in nitrogen tetroxide hydrazine rocket motor nozzles. A substitution of Irish Refrasil for the normal Refrasil does not drastically change the performance. The erosion rate data for the Irish Refrasil-phenolic specimen is within the scatter for that of the Refrasil-phenolic (0.25 to 1.75 mils/sec).

The substitution of carbon for some of the Refrasil (specimen No. 420) which consists of alternate plies of CCA carbon fabric and Refrasil fabric, appears to be slightly inferior to the performance of carbon and silica within the same woven fabric (specimen No. 524). This difference in performance is believed to be due to the close proximity of the silica sources (fibers) which coat and protect the underlying char from chemical attack by the  $N_2O_4$ - $N_2H_4$  exhaust products. These exhaust products have been shown in the past by both thermo-chemical analysis and experimental rocket nozzles to oxidize carbons or graphites quite rapidly.

The substitution of rayon into a silica fabric (specimen No. 527) results in a performance similar to silica phenolic. However, when all of the silica is replaced by rayon (specimen No. 516) the material seems to suffer from a lack of strength of the pyrolyzing reinforcement. As a result the surface recedes quite rapidly.

The use of zirconium fiber as reinforcement in a virgin resin system (specimen No. 377) results in an unusually high surface recession rate. This performance has been observed in solid propellant rocket motor firings at Aeronutronic. An extensive analysis of the nozzles from those solid propellant firings have been made. The high surface recession rate has been attributed to structural discontinuities within the char and at the char pyrolyzing zone interface. This is due to reactions within the char layer in which zirconia is converted to zirconium carbide with a large disruptive change in volume.

The performance of the oxidation resistant carbon reinforcements show considerable difference in two samples. The data for the specially prepared carbon reinforcements (specimens No. 503, 504, and 522) extend over the range of those observed for standard carbon and graphite reinforcements (specimens 505 and 507). They, therefore, do not appear to afford an advantage over the normal commercially available material in this environment.

#### Filled Composites

In addition to the filler materials incorporated in some specimens, other variables were changed and conclusions are difficult to draw from the series of specimens composed of samples 352, 425, 427, and 507.

Specimen No. 352 exhibited significantly higher erosion than the Refrasil phenolic. Whether this high erosion is due to the molybdenum-diboride filler or the propane formaldehyde resin system cannot be ascertained directly. Specimens 425, 426, and 427, indicate the influence of the various foreign materials. Most of the fillers perform as well as comparable materials without 91-LD. The erosion rates for specimen 427 is slightly superior to specimen 507, the carbon cloth phenolic control; however, in no case was the erosion rate as low as that obtained with silica as the fabric reinforcement.

#### Reimpregnated Prepyrolyzed Composites

This group consists of specimens 477, 478, and 479. The insert reimpregnated with phenolic (No. 477) resins had the lowest erosion rate of the three with the polyimide (No. 479) being second lowest.

### Pyrolytic Coatings on Reinforcements

The influence of pyrolytic graphite thickness on graphite reinforcement (specimens No. 461, 462, 494, and 495) is only minor. The heavier deposits may result in a slightly higher effective conductivity and strength; and hence, a lower surface temperature and lower initial erosion rate although the difference in material performance is small. The agreement from test to test for identical specimens is, however, obvious. The higher initial rate of erosion of pyrolytic graphite on carbon cloths compared to graphite cloth specimens No. 436, 461, and 462) is believed to be due to the lower effective thermal conductivity.

There does not appear to be an influence of doping pyrolytic graphite reinforcement coatings (Zr, Hf, Ti or B used in specimens No. 438, 445, 447, 461, 462, 494, 495, 496, 497, 501 and 502). All appear very similar with the exception of specimen 496. The cause of the anomaly between 496 and 497 is unknown at this time. The reduction of erosion rate (in this propellant system) achieved by the use of pyrolytic graphite deposits on graphite cloth reinforcements is immediately evident from a comparison of specimen 505 with any of the above nozzles.

### Resin Systems

The resin systems can be compared by means of a large group of specimens which evaluate resin performance with both Refrasil and carbon cloth as controlled variables. Considering 91-LD resin as the standard, a comparison can be made of specimens 396, 424, 498, 499, or 500 (all 91-LD). When used with carbon CCA (specimens 409 and 507), the resin degradation rate of PBI was lower than that of 91-LD phenolic resin. It is interesting to note that PBI and 91-LD as matrices for CCA exhibit identical erosion resistance in a fluorine oxidized system where mass loss is by thermal degradation and not oxidation; while in the oxygen oxidizing environment of the  $N_2O_4/50-50$  propellant system the PBI appears to be superior. When used with a higher conductivity reinforcement (G-1550) the PBI appears to be equivalent or slightly inferior to 91-LD (specimens 505 and 408). When used with Refrasil the PBI appears to be slight superior.

The polyimide resin appears to be inferior to 91-LD (specimens 450, 453, 507, and the 91-LD Refrasil series) as a matrix resin for carbon or Refrasil reinforcements. The 2,7 dihydroxynaphthalene phenol formaldehyde appears to be equivalent to 91-LD resin when reinforced with "Refrasil" as is shown by comparing the specimens 465 and 466 with 91-LD analogues.



### TEST OPERATION CONDITIONS

The test-to-test propellant mixture ratio and total propellant flowrate variation is presented in Figures 204A, 204B and 204C. The associated test-to-test propellant flowrate variation from nominal conditions is shown in Figures 205A, 205B, and 205C.

Through the first portion of the test series (Nozzles 352 through 424 and 505 and 507) the propellant flowrate variation from the nominal desired condition was rather excessive, considering the relative insensitivity of the propellant cavitating venturis to upstream pressure variations caused by the pressure regulation system characteristics. For these eighteen (18) tests the NTO flowrate variation was between +1% and -2% of the nominal and the 50/50 fuel flowrate was between +4% and -1% of the nominal value. After this series of tests was analyzed corrective steps were successfully introduced into the test procedure to minimize the inherent system pressure variations. In particular, the 50/50 fuel flowrate scatter was finally reduced (in the last 29 tests) to between 0 and -1% of the nominal value. Throughout the entire test series 77% (54 tests) of the tests ran with the NTO propellant within 1% of the nominal value. 88% (62 tests) of the tests ran with the total propellant flowrate within 1% of the nominal value. The control of the flowrate variation is best seen in the propellant mixture ratio variation figures (Figure 127). Throughout the first eighteen (18) tests the mixture ratio varied considerably from 1.500 to 1.625, but all of the last thirty-seven (37) tests ran between a 1.575 and 1.625 propellant mixture ratio as compared to the desired value of 1.600.

During the liquid motor test series a few tests were prematurely terminated for a variety of reasons as follows:

Four (4) tests were terminated due to facility malfunctions. The tests were then continued to specified completion to enable evaluation of data neglecting the effect of re-ignition. These tests are as follows:

Nozzle 478 - The water coolant booster pump was inadvertently not turned on for the first portion of this test. At approximately 25 seconds through the test,

the chamber and injector water exit temperature monitor recorder indicated a high value and the test was terminated. The booster pump, allowing for the flow of considerably more coolant water, was then turned on and the test was resumed.

Nozzle 479 - A leak past a chamber plug was noticed on the closed circuit TV monitor at the start of the test. The test was terminated and then resumed when the plug was replaced.

Nozzle 514 - Apparently the nozzle throat was partially plugged during the test. For a period of approximately 5 seconds the chamber pressure increased from 260 psia to 320 psia and the test was cut off. Coincidentally there was a leak in the propellant fuel system which was repaired and the remainder of the test was then completed.

Nozzle 520 - A leak in the propellant oxidizer system at 41 seconds through the test was noted on the TV monitor and the test was terminated. Upon repair of the leak the test was resumed and completed.

Eleven (11) tests were terminated prior to specified decrease in chamber pressure to 100 psia due to a test procedural error. The automatic chamber pressure cutoff relay was employed to cutoff the test whenever the nozzle ablation caused the rocket motor chamber pressure to reduce to 100 psia. After initial calibration this device functioned with a high degree of consistency in terminating tests at the 100 psia pressure. However, for a short span of time, but affecting a total of thirteen tests (nozzle numbers 438, 496, 497, 501, 502, 503, 504, 516, 517, 518, 522), the calibration of the device was inadvertently allowed to lapse, resulting in a premature test cutoff relay signal at approximately 115 psia chamber pressure.

Two (2) nozzle tests were terminated early due to nozzle material characteristics.

Nozzle 526 - Material flow into the nozzle throat caused an increasingly higher chamber pressure. The test was terminated at 26 seconds through the test at a pressure of 502 psia.

Nozzle 527 - After 25 seconds through the test, material flow into the nozzle throat caused an increasingly higher chamber pressure. At a pressure of 333 psia the nozzle section flew out of the nozzle holder.

TABLE 1A  
DESCRIPTION OF TEST SPECIMENS RELATIVE NOZZLE CHARACTERIZATION  
TEST SERIES 1

Data No.	Nozzle Number	Reinforcing Agent	Resin Chemical Type	Holding Conditions				Post Cure Cycle*	Barcol Hardness	Density g/cc
				Resin Content (percent)	Pressure/ Load (psi)	Temperature (°F)	Time (min)			
40	MANC 1	Refrasil cloth C100-48	CTL 91-1D phenolic	39.0	10,000	300	120	II	75	1.56
41	MANC 2	Refrasil cloth C100-48	CTL 91-1D phenolic	40.0	10,000	300	120	II	74	1.58
42	MANC 3	Carbon cloth CCA-1	CTL 91-1D phenolic	40.9	N.A.	N.A.	N.A.	N.A.	N.A.	N.A.
43	MANC 4	Carbon cloth CCA-1	CTL 91-1D phenolic	40.6						
44	MANC 5	Carbon cloth CCA-1	2, 2-Bis (p-hydroxyphenyl) propane- formaldehyde	40.6	11 Ton load	300	120	I	N.A.	N.A.
45	MANC 6	Refrasil cloth C100-48	CTL 91-1D phenolic	31.5	10,000	280	120	I	55	1.50
46	MANC 7	Refrasil cloth C100-48	CTL 91-1D phenolic	39.9	10,000	290	120	I	68	1.61
47	MANC 8	Carbon cloth CCA-1	CTL 91-1D phenolic	42.5	10,000	290	120	I	87	1.41
48	MANC 9	Carbon cloth CCA-1	CTL 91-1D phenolic	38.1	10,000	300	150	I	70	1.63
49	MANC 10	Graphite cloth C1550 coated with 1.0 to 1.2 microns of pyrolytic graphite	CTL 91-1D phenolic	40.5	10,000	290	120	I	40	1.37
50	MANC 11	Refrasil cloth C100-48	2, 2-Bis (p-hydroxyphenyl) propane- phenol-formaldehyde (B2153-20)	33.8	11 Ton load	300	120	I	N.A.	N.A.
51	MANC 12	Alternate Refrasil cloth C100-28 and carbon cloth CCA-1	CTL 91-1D phenolic	39.6	10,000	300	120	II	75	1.54
52	MANC 13	Carbon cloth CCA-1	CTL 91-1D phenolic	41.5	10,000	300	120	II	70	1.37
53	MANC 14	Graphite cloth C1550	CTL 91-1D phenolic	41.5	10,000	300	120	II	35	1.33
54	MANC 15	Carbon cloth CCA-1	N-hydroxybenzoic acid-phenol-formaldehyde (B6102-10A)	40.5	11 Ton load	300	120	I	N.A.	N.A.
55	MANC 16	Carbon cloth CCA-1	2, 7 dihydroxynaphthalene-phenol- formaldehyde (B6102-61)	41.6	11 Ton load	300	120	I	N.A.	N.A.
56	MANC 17	Carbon cloth CCA-1	2, 7 Naphthenediol-phenol-formaldehyde (B2153-25)	40.6	11 Ton load	300	120	I	N.A.	N.A.
57	MANC 18	Carbon cloth CCA-1	N-hydroxybenzoic acid-phenol-formaldehyde- copolymer (B6102-46-1)	39.1	11 Ton load	300	120	I	N.A.	N.A.

\* See Introduction for meaning of Data Sheet numbers.

† The carbon or graphite cloth of these nozzle inserts were coated with the indicated material (pyrolytic graphite, pyrolytic graphite-metal alloy or metal carbide) by vapor deposition before being fabricated into laminates.

TABLE 1A (Continued)

Data Sheet	Nozzle Number	Reinforcing Agent	Resin Chemical Type	Resin Content (percent)	Molding Conditions			Post Cure Cycle*	Barcol Hardness	Density g/cc
					Pressure/Load (psi)	Temperature (°F)	Time (min)			
APRL	434	Carbon cloth CCA-1	COP Polyphenylene cured with poly (xylylene) glycol (C1414-55-2)	33.2	11 Ton load	330	120	I	N.A.	N.A.
256	435 <sup>3</sup>	Carbon cloth CCA-1 coated with 1.0 to 1.4 microns of pyrolytic graphite-zirconium	CTL 91-ID phenolic	41.5	10,000	300	120	II	N.A.	1.36
257	437 <sup>3</sup>	Graphite cloth G1550 coated with 1.0 to 1.4 microns of pyrolytic graphite-zirconium	CTL 91-ID phenolic	41.1	10,000	300	120	II	N.A.	1.38
APRL	439 <sup>4,2</sup>	Graphite cloth WCA coated with 0.005 inch of pyrolytic graphite	R120 phenolic	42.1	N.A.	N.A.	N.A.	N.A.	N.A.	N.A.
APRL	440 <sup>4,2</sup>	Graphite cloth WCA coated with 0.015 inch of pyrolytic graphite	R120 phenolic	42.1	N.A.	N.A.	N.A.	N.A.	N.A.	N.A.
APRL	441 <sup>2</sup>	Graphite cloth WCA impregnated with R120 phenolic resin	R120 phenolic	42.1	N.A.	N.A.	N.A.	N.A.	N.A.	1.317
APRL	442 <sup>2</sup>	Graphite cloth WCA impregnated with X-8 furane resin	R120 phenolic	42.1	N.A.	N.A.	N.A.	N.A.	N.A.	1.198
APRL	443 <sup>2</sup>	Graphite cloth WCA impregnated with LTV-222 polyimide resin	R120 phenolic	42.1	N.A.	N.A.	N.A.	N.A.	N.A.	1.219
264	444 <sup>3</sup>	Graphite cloth G1550 coated with 1.0 to 1.5 microns of pyrolytic-graphite-hafnium	CTL 91-ID phenolic	40.7	10,000	300	120	II	30	1.42
265	446 <sup>3</sup>	Graphite cloth G1550 coated with 1.0 to 1.5 microns of pyrolytic graphite-titanium	CTL 91-ID phenolic	41.6	10,000	300	120	II	30	1.41
274	448	Carbon cloth CCA-1	Polyimide I-8	40.6	10,000	710	120	II	N.A.	1.38
275	452	Refrasil cloth C100-48	Polyimide I-8		4,000	710	120	II	N.A.	1.55

\*See attached Table 1-C (table of post-cure cycles).

\*\*See Introduction for meaning of Data Sheet numbers.

1 These nozzle throats were coated with the listed slurry or coating.

2 All of these nozzle inserts were machined from the same laminate. The laminate was fabricated from 42 wt % R/20 phenolic resin and 58 wt % WCA graphite cloth. Before machining the laminate was carbonized and graphitized. After machining the inserts were treated as shown.

3 The carbon or graphite cloth of these nozzle inserts were coated with the indicated material (pyrolytic graphite, pyrolytic graphite-metal alloy or metal carbide) by vapor deposition before being fabricated into laminates.

TABLE 1B  
TEST SERIES 2  
DESCRIPTION OF TEST SPECIMENS  
ABRATIVE NOZZLE CHARACTERIZATION

DATA SHEET NUMBER	REINFORCING AGENT	RESIN CHEMICAL TYPE	RESIN CONTENT (percent)	MOULDING CONDITIONS			POST CURE CYCLE *	BARCOL HARDNESS	DENSITY gm/cc
				PRESSURE (psi)	TEMPERATURE (°F)	TIME (Min.)			
APPL 356	Precharred graphite cloth	Modified epoxy novolac	N.A.	N.A.	N.A.	N.A.	N.A.	N.A.	1.32
APPL 358	Non precharred graphite cloth	Modified epoxy novolac	35	N.A.	N.A.	N.A.	N.A.	N.A.	1.36
APPL 360	Precharred carbon cloth	Modified epoxy novolac	N.A.	N.A.	N.A.	N.A.	N.A.	N.A.	1.34
APPL 366	Non precharred silica cloth	Modified epoxy novolac	32	N.A.	N.A.	N.A.	N.A.	N.A.	1.39
APPL 368	Precharred silica cloth	Modified epoxy novolac	N.A.	N.A.	N.A.	N.A.	N.A.	N.A.	1.39
217 417 <sup>3</sup>	Graphite cloth G1550 1.0 to 1.2 micron pyrolytic graphite coating	CTL91-LD phenolic	39.9	10,000	290	120	II	40	1.36
229 422	Carbon cloth CCA-1	CTL91-LD phenolic	41.3	10,000	300	120	II	70	1.40
229 423	Carbon cloth CCA-1	CTL91-LD phenolic	42.3	10,000	300	120	II	70	1.42
244 429	Graphite cloth G-1550	CTL91-LD phenolic	40.7	10,000	300	120	II	40	1.33
274 449	Carbon cloth CCA-1	Polyimide I-8	40.6	10,000	710	120	II	N.A.	1.38
APPL 455	Carbon cloth CCA-1	P-phenylphenol phenol formaldehyde (B2353-35)	41.2	300	300	120	II	N.A.	N.A.
APPL 456	Carbon cloth CCA-1	P-phenylphenol phenol formaldehyde (B2353-35)	41.2	300	300	120	II	N.A.	N.A.
APPL 457	Carbon cloth CCA-1	2,7 dihydroxynaphthalene phenol formaldehyde (B2353-36)	41.2	300	300	120	II	N.A.	N.A.
289 459 <sup>3</sup>	Graphite cloth G-1550 2.5 micron pyrolytic graphite coating	CTL91-LD phenolic	38.1	10,000	300	120	II	N.A.	1.47
289 460 <sup>3</sup>	Graphite cloth G-1550 2.5 micron pyrolytic graphite coating	CTL 91-LD phenolic	39.9	10,000	300	120	II	N.A.	1.45
303 463	Carbon cloth CCA-1	2,7 dihydroxynaphthalene phenol formaldehyde (B2353-41)	38.8	100	300	120	II	75	1.44
311 467	Carbon cloth CCA-1	Polyphenylene (M1000-1500) (B2353-42)	39.8	300	425	130	III	N.A.	1.28
311 468	Carbon cloth CCA-1	Polyphenylene (M1000-1500) (B2353-42)	39.9	300	425	180	III	N.A.	1.28
APPL 471	Carbon cloth CCA-1	Polyphenylene (B2353-40A) (cured with xylolene glycol)	39.9	1) TON LOAD	360	120	IV	N.A.	N.A.
APPL 480 <sup>2</sup>	WCA graphite cloth	R120 phenolic	42.1	N.A.	N.A.	N.A.	N.A.	N.A.	1.138
APPL 482 <sup>1,2</sup>	WCA graphite cloth .026 inch pyrolytic graphite coating	R120 phenolic	42.1	N.A.	N.A.	N.A.	N.A.	N.A.	1.138
APPL 483 <sup>1,2</sup>	WCA graphite cloth .034 inch pyrolytic graphite coating	R120 phenolic	42.1	N.A.	N.A.	N.A.	N.A.	N.A.	1.138
309 489	Carbon cloth CCA-1	DEN-438	40.2	300	300	960	II	70	1.34
320 490	Carbon cloth CCA-1	P-phenylphenol phenol formaldehyde	40.4	300	300	120	II	62	1.42

\*See attached Table 1C (table of post-cure cycles)

\*\* See Introduction for meaning of Data Sheet numbers.

<sup>1</sup>These nozzle throats were coated with the listed slurry or coating.

<sup>2</sup>All of these nozzle inserts were machined from the same laminate. The laminate was fabricated from 42 wt % R/20 phenolic resin and 58 wt % WCA graphite cloth. Before machining the laminate was carbonized and graphitized. After machining the inserts were treated as shown.

<sup>3</sup>The carbon or graphite cloth of these nozzle inserts were coated with the indicated material (pyrolytic graphite, pyrolytic graphite-metal alloy or metal carbide) by vapor deposition before being fabricated into laminates.

TABLE 1C

DETAILS OF POST-CURE CYCLES  
AS ENUMERATED IN TABLE OF TEST SPECIMENS DESCRIPTION

- I. 18 hours at 275°F, 48 hours from 275°F to 400°F, 4 hours at 400°F, cooled to below 200°F. (2.6°/hr temperature rise)
- II. 18 hours at 275°F, 72 hours from 275°F to 400°F, 4 hours at 400°F, 7 hours cooling to below 200°F. (1.7°/hr temperature rise)
- III. 18 hours at 275°F, 72 hours from 275°F to 450°F, 6 hours at 450°F, cooled to below 200°F. (2.4°/hr temperature rise)
- IV. 18 hours at 275°F, 48 hours from 275°F to 400°F, 6 hours from 400°F to 450°F. Cool to 200°F (2.7°/hr temperature rise to 400°F, 8.3°/hr temperature rise from 400° to 450°)
- V. 24 hours each at temperatures of 600°, 650°, 700° and 750°, 8 hours at 800°, and 3 hours at 700° in an atmosphere of nitrogen\*.  
\*Material placed in 600°F mold. Temperature increased to 700°F over period of 10 minutes.
- VI. 24 hours at 600°F, 24 hours at 650°F, 24 hours at 700°F, 6 hours at 750°F, 6 hours at 800°F, 6 hours at 850°F. Cool to room temperature. Nozzle was postcured in helium atmosphere.
- VII. 24 hours at 600°F, 24 hours at 650°F, 48 hours at 700°F, 6 hours at 750°F, 12 hours at 800°F, 12 hours at 850°F under Helium. Cool to room temperature under Helium before removing.
- VIII. 18 hours at 275°F, 114 hours from 275°F to 600°F, 6 hours cooling to below 200°F. Postcured under helium atmosphere (2.9°/hr temperature rise)
- IX. 3 hours each at temperatures of 150°, 200°, 250°, 300°, 350°, and 6 hours at 400°F.

TABLE 2  
SOLID PROPELLANT SIMULATOR CHECK RUN PERFORMANCE

Test Series	Simulator Checkout Number	Test Duration (sec)	Total Flow Rate (lb/sec)	Maximum Chamber Pressure (psia)	Final Chamber Pressure (psia)	Initial Throat Diameter (in.)	Final Throat Diameter (in.)	Calculated G <sub>f</sub> (lb/sec)	Efficiency (Percent)	Oxygen Flow Rate (lb/sec)	Hydrogen Flow Rate (lb/sec)	Nitrogen Flow Rate (lb/sec)	Slurry Flow Rate (lb/sec)	Remarks
1	1	9.0	0.6095	515.0	468.0	0.5020	0.509	5050	96.8	0.2169	0.0140	0.0495	0.330	Initial Checkout
1	2	60.0	0.5975	520.0	339.0	0.5020	N.A.			0.2130	0.0140	0.0515	0.3190	Full Duration Checkout
1	3	50.0	0.5940	504.6	312.0	0.5015	N.A.			0.2140	0.0140	0.0510	0.3190	Full Duration Checkout
1	4	9.0	0.587	508.3	474.1	0.5015	0.504	5130	98.3	0.2070	0.0140	0.0520	0.3140	Optimize start transients and verify motor performance. Note - slurry tankage piston jammed after test
														Slurry Tank Checkout
1	5	9.0	0.598	494.6	456.6	0.4980	0.507	5060	97.0	0.2120	0.0137	0.0516	0.3170	Optimize Starting Transients
1	6	9.0	0.5915	510.0	467.0	0.5020	0.504	5080	97.5	0.2160	0.0138	0.0507	0.3110	Optimize Starting Transients
1	7	9.0	0.6009	495.0	467.0	0.5070	0.504	5000	96.0	0.2150	0.0139	0.0510	0.3210	Optimize Starting Transients
1	8	9.0	0.5980	522.0	478.0	0.5030	0.503	5160	98.5	0.2160	0.0139	0.0510	0.3170	Optimize Starting Transients
1	9	10.0	0.6067	505.0	470.0	0.5010	0.502	4920	94.3	0.2140	0.0138	0.0519	0.3270	Optimize Starting Transients
2	1	10.8	0.5971	541.8	477.0	0.5060	0.503	5106	98.0	0.2208	0.0139	0.0510	0.3124	Optimize Starting Transients
2	2	13.4	0.5966	496.9	433.0	0.5030	0.519	4940	94.8	0.2206	0.0141	0.0515	0.3114	Performance Checkout
2	3	12.7	0.6001	507.1	468.0	0.5020	0.502	4965	95.3	0.2184	0.0142	0.0515	0.3160	Performance Checkout

TABLE 3A  
CALCULATED AND MEASURED VALUES USED IN EROSION PROPERTY ANALYSIS

NOZZLE NUMBER	TIME (sec)	MAXIMUM CHAMBER PRESSURE (psia)	ORIGINAL THROAT DIAMETER (inch)	MINIMUM CHAMBER PRESSURE (psia)	TOTAL FLOW RATE (lb/ sec)	TIME 350 psia (sec)	CALC. THROAT AREA 350 psia (in <sup>2</sup> )	CALC. THROAT RADIUS 350 psia (in)	CALC. EROSION RATE 350 psia (mils/sec)	TIME 300 psia (sec)	CALC. THROAT AREA 300 psia (in <sup>2</sup> )	CALC. THROAT RADIUS 300 psia (inch)	CALC. EROSION RATE 300 psia (mils/sec)	TIME 250 psia (sec)	CALC. THROAT AREA 250 psia (in <sup>2</sup> )	CALC. THROAT RADIUS 250 psia (inch)	CALC. EROSION RATE 250 psia (mils/sec)	TIME 200 psia (sec)
MANC 1	26.9	429	.5000	148	.6008	5.9	.2697	.2930	7.29	8.	.3147	.3165	7.15	12.9	.3776	.3667	7.50	18.2
MANC 2	28.4	441	.5005	140	.6069	7.2	.2725	.2945	6.15	10.0	.3179	.3181	6.79	13.7	.3815	.3485	7.18	19.0
MANC 3	59.3	462	.5000	150	.6010	13.6	.2698	.2931	3.17	19.2	.3148	.3166	3.47	28.7	.3778	.3468	3.37	41.1
MANC 4	59.2	446	.5010	150	.5946	13.5	.2669	.2915	3.04	18.9	.3115	.3149	3.41	25.7	.3736	.3469	3.67	36.3
394	59.2	442	.5015	145	.6017	10.6	.2702	.2932	4.01	15.6	.3152	.3167	4.23	22.4	.3782	.3469	4.39	35.6
397	25.7	419	.5015	143	.6046	5.0	.2715	.2939	8.64	7.9	.3167	.3175	8.46	11.3	.3800	.3478	8.59	15.9
398	29.6	434	.5000	139	.6056	6.1	.2719	.2942	7.25	9.0	.3172	.3177	7.52	12.4	.3807	.3481	7.91	18.1
400	55.5	442	.5015	144	.5996	9.1	.2692	.2927	4.62	13.7	.3141	.3162	4.78	20.0	.3769	.3464	4.79	30.4
414	27.9	419	.5010	134	.6066	5.9	.2724	.2944	7.44	8.6	.3177	.3180	8.04	11.6	.3813	.3484	8.44	16.5
416	59.1	495	.5015	163	.5870	14.8	.2636	.2896	2.63	21.0	.3075	.3128	2.96	29.6	.3690	.3427	3.11	42.8
418	29.2	432	.5010	126	.6007	4.5	.2697	.2930	9.44	6.9	.3146	.3165	9.57	9.8	.3776	.3467	9.82	15.8
419	39.6	445	.5030	135	.5973	8.7	.2682	.2922	4.68	12.3	.3129	.3156	5.21	17.7	.3755	.3457	5.32	24.6
421	59.3	429	.5000	150	.5994	9.0	.2691	.2927	4.74	14.2	.3140	.3161	4.65	22.7	.3768	.3463	4.24	37.5
428	58.3	488	.5010	182	.6050	18.1	.2716	.2940	2.40	25.6	.3169	.3176	2.62	35.1	.3803	.3479	2.77	50.5
430	47.4	440	.5010	140	.6021	10.3	.2703	.2933	4.16	14.8	.3154	.3168	4.46	20.8	.3785	.3471	4.64	28.8
431	59.2	434	.5005	150	.6044	11.4	.2714	.2939	3.83	16.5	.3166	.3174	4.07	24.1	.3799	.3478	4.05	38.3
432	59.0	454	.5005	149	.6001	9.2	.2694	.2928	4.63	15.6	.3143	.3163	4.24	23.4	.3772	.3465	4.12	38.0
433	57.3	446	.5000	141	.6002	10.6	.2695	.2929	4.05	15.1	.3144	.3163	4.39	21.6	.3773	.3465	4.47	33.7
434	28.2	415	.5010	140	.5877	6.7	.2639	.2898	5.87	9.1	.3078	.3130	6.04	11.4	.3694	.3429	8.11	16.8
435	59.4	476	.5015	150	.5815	13.9	.2611	.2833	4.74	20.7	.3114	.3114	3.25	25.1	.3655	.3411	3.60	36.0
437	59.4	491	.5010	174	.5779	15.4	.2595	.2874	2.40	22.6	.3027	.3104	2.65	33.0	.3633	.3420	2.71	48.0
439	59.2	511	.5025	151	.5944	17.8	.2669	.2915	2.26	23.7	.3114	.3148	2.68	32.6	.3736	.3448	2.87	44.1
440	54.3	511	.5020	151	.5811	25.7	.2609	.2852	1.45	28.7	.3044	.3113	2.10	35.1	.3653	.3410	2.56	43.0
441	59.3	510	.5010	183	.5886	15.8	.2643	.2900	2.50	24.3	.3083	.3133	2.70	35.0	.3700	.3432	2.65	52.5
442	59.1	498	.5020	179	.5795	18.2	.2602	.2878	2.02	28.4	.3035	.3108	2.11	38.0	.3645	.3405	2.36	57.8
443	59.3	481	.5040	169	.5949	14.6	.2671	.2916	2.71	20.7	.3116	.3149	3.03	29.3	.3739	.3450	2.17	45.3
444	59.3	482	.5000	167	.5986	14.7	.2688	.2924	2.88	21.4	.3135	.3159	3.08	20.2	.3763	.3461	3.18	44.0
445	59.3	467	.5020	171	.5953	15.3	.2673	.2917	2.56	21.6	.3118	.3151	2.97	30.6	.3742	.3451	3.09	45.4
448	30.5	435	.5015	156	.6063	8.6	.2722	.2944	5.08	12.3	.3176	.3179	5.46	16.2	.3911	.3483	8.17	21.8
452	18.4	410	.5015	150	.5996	4.9	.2692	.2927	8.57	7.5	.3141	.3162	8.73	10.0	.3769	.3494	9.17	13.1

\*150 psia or chamber pressure at termination of test



ABLATIVE NOZZLE CHARACTERIZATION  
PHILCO-AERONAUTRONIC DIVISION  
EXPERIMENTAL EQUIPMENT DEPARTMENT

CALC. THROAT RADIUS 250 psia (inch)	CALC. EROSION RATE 250 psia (mils/sec)	TIME 200 psia (sec)	CALC. THROAT AREA 200 psia (in <sup>2</sup> )	CALC. THROAT RADIUS 200 psia (inch)	CALC. EROSION RATE 200 psia (mils/sec)	TIME 150 psia (sec)	CALC. THROAT AREA 150 psia (in <sup>2</sup> )	CALC. THROAT RADIUS 150 psia (inch)	CALC. EROSION RATE 150 psia (mils/sec)	NOZZLE NUMBER	MATERIAL RESIN/REINFORCEMENT
.3467	7.50	18.2	.6721	.3876	7.36	26.2	.6294	.4476	7.54	MANC-1	91-LD 39.0% C100-48
.3485	7.18	19.0	.6769	.3896	7.34	27.6	.6363	.4501	7.24	MANC-2	91-LD 43.0% C100-48
.3468	3.57	41.1	.6722	.3877	3.35	59.3	.6296	.4477	3.33	MANC-3	91-LD 40.9% CCA-1
.3449	3.67	36.3	.6672	.3856	3.72	59.2	.6229	.4453	3.29	MANC-4	91-LD 40.9% CCA-1
.3489	4.29	35.6	.6728	.3879	3.85	56.0	.6303	.4479	3.52	394	Propene-Formaldehyde 40.6/CCA-1
.3478	8.59	15.9	.6750	.3889	8.69	24.4	.6338	.4492	8.14	397	CTL-91LD-31.3% C100-48 1/2" Sq.
.3481	7.93	18.1	.6708	.3892	7.69	27.7	.6350	.4495	7.21	398	91-LD 40% C100-48
.3464	4.79	30.4	.6711	.3873	4.49	52.0	.6281	.4472	3.78	400	91-LD 40% CCA-1
.3484	8.44	16.5	.6766	.3895	8.42	24.0	.6360	.4489	8.31	414	CTL 91-LD/1534-48 59.1%
.3427	3.11	42.8	.6612	.3832	3.10	59.1	.6659	.4244	2.94	416	CTL 91-LD/G1550-Coated with 1.0 Microns Pyrolytic Graphite
.3487	9.82	15.8	.6720	.3876	8.68	25.7	.6293	.4476	7.67	418	B2353-23/33.8% C100-48 59.5%
.3457	5.32	24.6	.6693	.3865	5.49	35.1	.6257	.4463	5.55	419	91-LD/Alternate C100-28 and CCA-1 40.4%
.3463	6.24	37.5	.6710	.3872	3.66	59.3	.6279	.4471	3.32	421	91-LD/CCA-1 58.5%
.3479	2.77	50.5	.6734	.3890	2.74	58.3	.5228	.4079	2.70	428	91-LD/G-1550 58.5%
.3471	4.64	28.6	.6731	.3881	4.78	43.5	.6308	.4481	4.54	430	B6102-10A/CCA-1 59.5%
.3478	4.05	38.3	.6749	.3888	3.62	59.2	.6357	.4491	3.34	431	B6102-41/CCA-1 58.6%
.3465	4.12	38.0	.6715	.3877	3.62	58.7	.6287	.4473	3.36	432	B2353-23/CCA-1 59.4%
.3465	4.47	33.7	.6716	.3878	4.09	52.9	.6263	.4474	3.73	433	B6102-46-1/CCA-1 60.9%
.3429	8.11	16.8	.6618	.3834	7.91	25.4	.6157	.4427	7.57	434	C1414-55-2/CCA-1 66.8%
.3411	3.60	36.0	.6569	.3814	3.63	59.4	.6092	.4403	3.19	435	91-LD/CCA-1 58.5% Coated 1.0 Microns Pyrolytic Graphite-Zirconium
.3400	2.71	48.0	.6541	.3892	2.70	59.4	.5219	.4076	2.64	437	91-LD/G1550 59.9% Coated 1.0 Microns Pyrolytic Graphite-Zirconium
.3448	2.87	44.1	.6670	.3856	3.05	59.2	.6227	.4452	3.28	439	R120/WCA-0.003" Pyrolytic Graphite Coating 57.9%
.3410	2.56	43.0	.6566	.3812	3.18	54.3	.6048	.4388	3.46	440	R120/WCA-0.015" Pyrolytic Graphite Coating 57.9%
.3432	2.65	52.5	.6625	.3837	2.54	59.3	.5060	.4011	2.54	441	R120/WCA-0.015" Pyrolytic Graphite Coating 57.9%
.3405	2.36	52.8	.6553	.3807	2.46	59.1	.5088	.4024	2.56	442	R120/WCA-0.015" Pyrolytic Graphite Coating 57.9%
.3450	3.17	45.3	.6674	.3857	3.05	59.3	.5532	.4196	2.83	443	R120/WCA-0.015" Pyrolytic Graphite Coating 57.9%
.3461	3.18	44.0	.6703	.3869	3.11	59.3	.5633	.4229	2.92	444	R120/WCA-0.015" Pyrolytic Graphite Coating 57.9%
.3451	3.08	45.6	.6677	.3859	3.06	59.3	.5471	.4173	2.80	446	91-LD/G1550-Pyrolytic Graphite Hafnium 59.3%
.3483	6.02	21.8	.6764	.3894	6.36	30.5	.6113	.4421	6.24	448	91-LD/G1550-Pyrolytic Graphite Titanium 58.4%
.3464	9.57	13.1	.6711	.3873	10.43	18.4	.6281	.4472	10.68	452	I-8/CCA-1 59.4%
											I-8/C100-48 60.0%

2

TABLE 35  
CALCULATED AND MEASURED VALUES USED IN EROSION PROPERTY ANALYSIS

NOZZLE NUMBER	TIME (sec)	MAXIMUM CHAMBER PRESSURE (psia)	ORIGINAL THROAT DIAMETER (inches)	MINIMUM CHAMBER PRESSURE (psia)	TOTAL FLOW RATE (lb/sec)	TIME (sec)	CALC. 150 THROAT AREA (in <sup>2</sup> )	CALC. 150 THROAT RADIUS (inches)	CALC. 150 THROAT EROSION RATE (mil/sec)	TIME (sec)	CALC. 150 THROAT AREA (in <sup>2</sup> )	CALC. 150 THROAT RADIUS (inches)	CALC. 150 THROAT EROSION RATE (mil/sec)	TIME (sec)	CALC. 150 THROAT AREA (in <sup>2</sup> )	CALC. 150 THROAT RADIUS (inches)	CALC. 150 THROAT EROSION RATE (mil/sec)	TIME (sec)	CALC. 150 THROAT AREA (in <sup>2</sup> )	CALC. 150 THROAT RADIUS (inches)	CALC. 150 THROAT EROSION RATE (mil/sec)
356	32.8	511	.502	153	.5935	11.7	.2639	.2898	3.26	20.3	.3079	.3131	3.87	28.7	.3499	.3430	3.20	37.0	.4619	.3834	
358	34.1	501	.501	148	.5907	10.4	.2627	.2892	3.77	16.5	.3065	.3123	4.26	18.3	.3478	.3421	3.00	26.7	.4197	.3875	
360	39.7	509	.502	154	.5851	11.0	.2615	.2886	3.10	18.8	.3057	.3117	3.23	27.7	.3463	.3414	2.28	42.1	.6378	.3818	
366	22.6	502	.501	145	.5902	3.8	.2624	.2890	10.33	0.0	.3062	.3122	10.28	8.9	.3455	.3420	10.28	13.7	.6593	.3824	
368	23.5	456	.503	140	.5916	4.2	.2631	.2895	8.41	7.3	.3069	.3123	8.32	10.2	.3473	.3426	8.91	13.7	.6404	.3828	
417	33.0	499	.501	150	.5954	16.8	.2648	.2904	2.27	21.4	.3049	.3136	2.67	30.4	.3707	.3435	3.09	38.0	.6434	.3841	
417	46.3	482	.502	150	.5947	11.2	.2645	.2901	3.49	16.8	.3066	.3136	3.71	23.5	.3703	.3435	3.62	30.6	.6478	.3878	
423	33.6	480	.503	159	.5991	9.0	.2646	.2912	3.57	12.2	.3108	.3165	3.78	15.9	.3730	.3466	4.18	23.2	.6442	.3832	
429	34.5	495	.502	150	.5941	15.3	.2642	.2900	2.95	20.4	.3042	.3132	3.04	27.0	.3499	.3431	3.64	35.8	.6679	.3824	
449	42.1	639	.502	150	.5965	8.8	.2653	.2906	4.20	14.3	.3095	.3197	8.33	23.8	.4214	.3486	6.94	29.8	.6947	.3866	
453	49.2	508	.501	150	.5969	7.1	.2651	.2907	3.64	11.3	.3097	.3160	3.61	16.6	.4114	.3479	3.82	47.8	.8067	.3843	
456	55.6	456	.501	150	.5953	10.3	.2647	.2903	2.86	17.3	.3089	.3156	3.64	23.1	.3706	.3478	4.82	36.7	.6837	.3860	
457	49.4	473	.501	150	.5925	7.9	.2639	.2898	4.97	13.4	.3079	.3131	4.97	21.0	.3493	.3439	4.67	31.9	.6419	.3836	
459	59.2	499	.501	155	.5904	15.8	.2626	.2891	2.44	22.1	.3044	.3123	2.79	20.9	.3477	.3421	2.96	46.2	.4391	.3834	
460	49.1	499	.501	150	.5976	11.2	.2638	.2908	2.85	18.7	.3101	.3162	3.90	24.4	.4721	.3441	3.81	52.4	.6853	.3868	
462	57.3	432	.501	161	.5937	8.2	.2640	.2899	4.80	25.0	.3098	.3181	4.81	25.7	.4494	.3480	4.80	52.0	.6823	.3875	
467	46.3	504	.501	150	.5934	6.2	.2639	.2898	6.33	13.0	.3079	.3130	4.80	20.1	.3495	.3429	4.59	27.9	.6418	.3844	
468	48.9	518	.502	150	.5936	7.9	.2639	.2899	4.92	12.2	.3079	.3131	3.09	23.9	.3494	.3473	4.80	41.8	.6423	.3835	
471	42.2	493	.501	150	.5921	9.0	.2633	.2895	3.97	14.4	.3073	.3127	4.78	28.0	.3494	.3479	4.60	27.4	.6408	.3830	
480	37.4	448	.505	150	.5935	9.0	.2639	.2898	4.14	12.4	.3079	.3131	4.80	17.0	.3493	.3439	4.32	23.4	.6419	.3834	
482	59.8	528	.484	139	.5939	15.5	.2641	.2900	2.03	21.8	.3081	.3132	3.22	24.2	.3498	.3431	3.42	48.0	.6422	.3836	
483	54.1	511	.499	150	.5927	12.0	.2636	.2897	3.25	17.3	.3073	.3129	3.44	21.9	.3490	.3477	3.94	35.8	.6413	.3837	
489	52.6	502	.500	150	.5923	9.9	.2640	.2899	4.03	14.1	.3079	.3131	4.47	20.6	.3494	.3430	4.51	31.0	.6431	.3836	
490	53.9	509	.500	150	.5919	7.4	.2632	.2895	3.33	13.0	.3071	.3127	4.82	20.9	.3485	.3425	4.42	34.6	.6407	.3829	

\* 150 PSIA or chamber pressure at termination of test.

ABLATIVE NOZZLE CHARACTERIZATION  
PHILCO-AERONAUTIC DIVISION  
EXPERIMENTAL EQUIPMENT IN ORIENT

TEST NO.	CALC. EROSION RATE 150 psi (in./sec)	TIME 200 psi (sec)	CALC. THROAT RADIUS 200 psi (in.)	CALC. EROSION RATE 200 psi (in./sec)	TIME 150 psi (sec)	CALC. THROAT RADIUS 150 psi (in.)	CALC. EROSION RATE 150 psi (in./sec)	NOZZLE NUMBER	MATERIAL RESIN/REINFORCEMENT
10	3.20	27.0	.4015	3.35	32.0	.4032	3.52	356	Epoxy novolac/francharred-graphite cloth
11	5.00	24.7	.4597	3.24	32.5	.4629	3.74	358	Epoxy novolac, 35%francharred-graphite cloth
14	3.24	42.3	.4574	3.10	39.7	.4570	3.03	360	Epoxy novolac/francharred-graphite cloth
15	10.73	13.7	.4593	9.43	21.0	.4124	9.40	366	Epoxy novolac, 35%francharred-graphite cloth
16	0.91	15.2	.4624	8.50	22.9	.4139	8.32	368	Epoxy novolac/francharred-graphite cloth
17	3.05	15.4	.4634	3.67	30.0	.4170	3.64	412	W-10 10.0%W-1000 covered with 1.0 to 1.2 microns pyrolytic-graphite
18	2.92	20.6	.4629	3.20	40.3	.4141	4.12	412	W-10 10.0%W-1000 covered with 1.0 to 1.2 microns pyrolytic-graphite
19	0.15	23.3	.4642	3.71	73.6	.4663	0.10	412	W-10 10.0%W-1000 covered with 1.0 to 1.2 microns pyrolytic-graphite
20	3.61	27.0	.4621	3.51	38.5	.4144	3.28	412	W-10 10.0%W-1000 covered with 1.0 to 1.2 microns pyrolytic-graphite
21	4.44	27.0	.4642	4.46	42.3	.4130	4.73	412	W-10 10.0%W-1000 covered with 1.0 to 1.2 microns pyrolytic-graphite
22	3.25	27.0	.4642	3.26	49.2	.4134	3.93	412	W-10 10.0%W-1000 covered with 1.0 to 1.2 microns pyrolytic-graphite
23	4.22	34.7	.4643	3.84	50.6	.4134	4.40	412	W-10 10.0%W-1000 covered with 1.0 to 1.2 microns pyrolytic-graphite
24	4.40	31.8	.4610	4.27	48.4	.4138	4.62	412	W-10 10.0%W-1000 covered with 1.0 to 1.2 microns pyrolytic-graphite
25	3.95	44.2	.4592	3.83	59.3	.4205	3.19	412	W-10 10.0%W-1000 covered with 1.0 to 1.2 microns pyrolytic-graphite
26	3.87	22.3	.4634	4.10	49.3	.4201	3.97	412	W-10 10.0%W-1000 covered with 1.0 to 1.2 microns pyrolytic-graphite
27	0.87	32.0	.4632	4.1	72.1	.4188	1.86	412	W-10 10.0%W-1000 covered with 1.0 to 1.2 microns pyrolytic-graphite
28	4.79	19.8	.4618	4.56	40.3	.4137	4.13	412	W-10 10.0%W-1000 covered with 1.0 to 1.2 microns pyrolytic-graphite
29	4.00	23.5	.4620	3.97	40.3	.4138	3.93	412	W-10 10.0%W-1000 covered with 1.0 to 1.2 microns pyrolytic-graphite
30	0.64	17.4	.4602	3.80	42.2	.4144	4.34	412	W-10 10.0%W-1000 covered with 1.0 to 1.2 microns pyrolytic-graphite
31	1.37	21.3	.4610	3.83	37.4	.4139	3.20	412	W-10 10.0%W-1000 covered with 1.0 to 1.2 microns pyrolytic-graphite
32	3.47	24.8	.4632	3.84	59.8	.4144	3.13	412	W-10 10.0%W-1000 covered with 1.0 to 1.2 microns pyrolytic-graphite
33	3.95	27.0	.4632	3.82	56.1	.4130	3.27	412	W-10 10.0%W-1000 covered with 1.0 to 1.2 microns pyrolytic-graphite
34	4.51	31.8	.4621	4.30	54.8	.4141	3.87	412	W-10 10.0%W-1000 covered with 1.0 to 1.2 microns pyrolytic-graphite
35	4.42	34.8	.4607	3.91	57.9	.4142	3.77	412	W-10 10.0%W-1000 covered with 1.0 to 1.2 microns pyrolytic-graphite

2

TABLE 4A

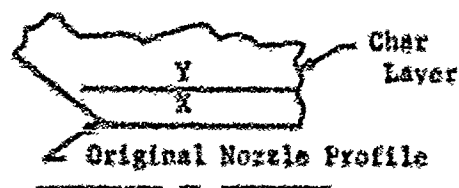
POST TEST NOZZLE EROSION EVALUATION  
MANC-ABLATIVE NOZZLE CHARACTERIZATION  
Test Series 1

NOZZLE NUMBER	CHAR <sup>(1)</sup> DEPTH (in.)	RESIN <sup>(2)</sup> DEGRADATION RATE (mils/sec)
No. 1	0.15	12.8
No. 2	0.15	12.8
No. 3	0.50	11.8
No. 4	0.55	12.6
394	0.40	9.4
397	0.15	13.9
398	0.20	13.9
400	0.45	11.2
414	0.20	15.3
416	0.65	17.0
418	0.70	10.6
419	0.35	14.4
421	0.50	11.7
428	0.55	12.2
430	0.50 to 0.40	11.3 to 13.0
431	0.50	11.9
432	0.45	11.0
433	0.40	10.6
434	0.40 to 0.40	11.5 to 21.1
435	0.55	12.4
437	0.60	12.6
439	0.60	11.5
440	0.60 to 0.75	8.1 to 14.6
441	0.60	12.7
442	0.60 to 0.75	12.8 to 15.3
443	0.65	13.8
444	0.55 to 0.70	12.0
445	0.55	12.0
448	0.30 to 0.50	15.9 to 22.5
452	0.10	15.8

## NOTES:

(1) Char depth measured at resultant throat with 6 inch scale.

(2) Resin degradation rate (d) calculated by adding calc erosion rate and char depth rate.



$$d = \frac{X}{t} + \frac{Y}{t}$$

where:

x = erosion  
y = char depth  
t = run time

TABLE 4B

POST TEST NOZZLE EROSION EVALUATION  
 ABLATIVE NOZZLE CHARACTERIZATION  
 Test Series 2

NOZZLE NUMBER	CHAR <sup>(1)</sup> DEPTH (in.)	RESIN <sup>(2)</sup> DEGRADATION RATE (mils/sec)	
356	0.51	13.2	NOTES:
358	0.33 to 0.44	15.4 to 18.6	
360	0.40 to 0.50	9.7 to 11.4	(1) Char depth measured at resultant throat with 6 inch scale.
366	0.14	15.0	(2) Resin degradation rate (d) calculated by adding calc erosion rate and char depth rate.
368	0.13	13.9	
417	0.37 to 0.68	11.3 to 17.5	
422	0.34 to 0.48	11.5 to 14.5	
423	0.36	16.1	
429	0.41 to 0.63	10.3 to 14.0	
449	0.40	14.1	
455	0.48	13.7	
456	0.47	11.9	
457	0.42	12.4	
459	0.54 to 0.74	12.2 to 15.6	
460	0.45 to 0.67	13.1 to 17.6	
463	0.45	11.4	
467	0.38 to 0.54	12.3 to 15.7	
468	0.47	13.6	
471	0.30 to 0.42	11.7 to 14.5	
480	0.54 to 0.62	19.5 to 21.7	
482	0.64	13.8	
483	0.57 to 0.66	14.1 to 15.8	
489	0.39	11.1	
490	0.41	11.2	



$$d = \frac{x}{t} + \frac{y}{t}$$

where:

x = erosion  
 y = char depth  
 t = run time

TABLE 5A

POST TEST NOZZLE VISUAL EVALUATION  
MANG-ABLATIVE NOZZLE CHARACTERIZATION  
Test Series 1

<u>Nozzle</u>	<u>Evaluation</u>
M No. 1	Bore smooth, even erosion
M No. 2	Bore smooth, even erosion
M No. 3	Bore rough, uneven erosion, insert undercut
M No. 4	Bore rough, uneven erosion, insert undercut
394	Bore rough, even erosion, insert undercut
397	Bore smooth, even erosion, glass flow
398	Bore smooth, even erosion, glass flow
400	Bore rough, spalling, uneven erosion, insert undercut
414	Bore smooth, even erosion
416	Bore rough but even, slight spalling, insert undercut
418	Bore smooth, even erosion
419	Bore rough, but erosion even, lamination standout, insert undercut slightly
421	Bore rough, cylindrical cracks, insert undercut
428	Bore rough, cylindrical cracks, insert undercut
430	Bore rough, cylindrical cracks, insert undercut
431	Bore rough, cylindrical cracks, insert undercut
432	Bore rough, cylindrical cracks, insert undercut
433	Bore rough, cylindrical cracks, insert undercut
434	Bore rough, cylindrical cracks
435	Bore smooth, even erosion, insert undercut
437	Bore smooth, cylindrical cracks, insert undercut
439	Spalling, one cylindrical crack, graphite coating left on exit cone. insert undercut
440	Extreme spalling, undercut, large difference between comparator and calculated area
441	Bore smooth, even erosion, insert undercut
442	Bore smooth, uneven erosion, some spalling, insert undercut
443	Bore smooth, even erosion, insert undercut
444	Spalling, cylindrical cracks, insert undercut, uneven erosion
446	Bore smooth, uneven erosion, cylindrical cracks, insert undercut
448	Cylindrical cracks, rough bore, uneven erosion
452	Some spalling, exit portion of nozzle gone

TABLE 5B

POST TEST NOZZLE VISUAL EVALUATION  
 ABLATIVE NOZZLE CHARACTERIZATION  
 Test Series 2

<u>Nozzle</u>	<u>Evaluation</u>
356	Bore smooth, one cylindrical crack, insert undercut
358	Bore smooth, uneven erosion, spalling, cylindrical cracks
360	Bore rough, even erosion, laminations, insert undercut
366	Bore smooth, even erosion
368	Bore smooth, even erosion
417	Bore rough, uneven erosion, cylindrical cracks, insert partially undercut
422	Bore rough, uneven erosion, laminations, insert undercut
423	Bore rough, uneven erosion, laminations, graphite entrance section used
429	Bore smooth, uneven erosion, cylindrical cracks, insert undercut
449	Bore rough, even erosion, laminations, insert undercut
455	Spalling, even erosion, cylindrical cracks and laminations, insert undercut
456	Bore rough, even erosion, laminations, insert undercut
457	Bore smooth, even erosion, cylindrical cracks and laminations, insert undercut
459	Bore smooth, uneven erosion, slight spalling, insert undercut
460	Bore smooth, uneven erosion, insert undercut
463	Bore rough, even erosion, laminations, insert undercut
467	Bore rough, uneven erosion, cylindrical cracks, insert undercut
468	Bore rough, even erosion, cylindrical cracks, insert undercut
471	Bore rough, uneven erosion, cylindrical cracks, insert undercut
480	Bore smooth, uneven erosion, insert undercut
482	Bore smooth, even erosion, slight cylindrical cracks, graphite coating remaining on exit cone, insert undercut
483	Bore smooth, even erosion, insert undercut
489	Bore rough, uneven erosion, cylindrical cracks, insert undercut
490	Bore rough, even erosion, laminations, insert undercut

TABLE 6A

SOLID PROPELLANT SIMULATOR PERFORMANCE DATA  
DURING MANC-ABLATIVE NOZZLE CHARACTERIZATION

## Test Series 1

Nozzle No.	Total Flow Rate (lb/sec)	Oxygen Flow Rate (lb/sec)	Hydrogen Flow Rate (lb/sec)	Nitrogen Flow Rate (lb/sec)	Slurry Flow Rate (lb/sec)
M No. 1	0.6008	0.2174	0.0140	0.0514	0.3180
M No. 2	0.6069	0.2164	0.0141	0.0500	0.3210
M No. 3	0.6010	0.2176	0.0141	0.0513	0.3180
M No. 4	0.5946	0.2152	0.0141	0.0512	0.3141
394	0.6017	0.2206	0.0143	0.0515	0.3153
397	0.6046	0.2219	0.0141	0.0527	0.3159
398	0.6056	0.2208	0.0143	0.0525	0.3180
400	0.5996	0.2173	0.0140	0.0512	0.3171
414	0.6066	0.2206	0.0142	0.0517	0.3201
416	0.5870	0.2181	0.0140	0.0514	0.3035
418	0.6007	0.2178	0.0141	0.0517	0.3171
419	0.5973	0.2144	0.0136	0.0506	0.3186
421	0.5994	0.2217	0.0140	0.0511	0.3126
428	0.6050	0.2200	0.0140	0.0530	0.3180
430	0.6021	0.2198	0.0139	0.0528	0.3156
431	0.6044	0.2172	0.0140	0.0516	0.3216
432	0.6001	0.2204	0.0141	0.0514	0.3141
433	0.6002	0.2189	0.0145	0.0497	0.3171
434	0.5877	0.2058	0.0143	0.0505	0.3171
435	0.5815	0.2116	0.0139	0.0499	0.3025
437	0.5779	0.2106	0.0140	0.0499	0.3070
439	0.5944	0.2178	0.0137	0.0504	0.3124
440	0.5811	0.2117	0.0138	0.0507	0.3048
441	0.5886	0.2130	0.0138	0.0501	0.3116
442	0.5795	0.2040	0.0138	0.0509	0.3108
443	0.5949	0.2163	0.0138	0.5010	0.3146
444	0.5986	0.2126	0.0139	0.0507	0.3213
446	0.5953	0.2166	0.0139	0.0504	0.3124
448	0.6063	0.2168	0.0138	0.0506	0.3251
452	0.5996	0.2169	0.0139	0.0513	0.3175



TABLE 6B  
SOLID PROPELLANT SIMULATOR PERFORMANCE DATA  
ABLATIVE NOZZLE CHARACTERIZATION  
Test Series 2

Nozzle No.	Total Flow Rate (lb/sec)	Oxygen Flow Rate (lb/sec)	Hydrogen Flow Rate (lb/sec)	Nitrogen Flow Rate (lb/sec)	Slurry Flow Rate (lb/sec)
356	0.5935	0.2172	0.01403	0.0510	0.3113
358	0.5907	0.2152	0.01409	0.0511	0.3103
360	0.5883	0.2126	0.01402	0.0501	0.3116
366	0.5902	0.2130	0.01407	0.0509	0.3122
368	0.5916	0.2138	0.01396	0.0510	0.3128
417	0.5954	0.2162	0.01414	0.0512	0.3139
422	0.5947	0.2157	0.01388	0.0512	0.3139
423	0.5991	0.2200	0.01425	0.0515	0.3133
429	0.5941	0.2149	0.01421	0.0513	0.3137
449	0.5965	0.2178	0.01403	0.0516	0.3131
455	0.5969	0.2169	0.01398	0.0515	0.3146
456	0.5953	0.2153	0.01413	0.0513	0.3146
457	0.5938	0.2171	0.01405	0.0512	0.3112
459	0.5906	0.2138	0.01402	0.0507	0.3121
460	0.5976	0.2162	0.01415	0.0510	0.3163
463	0.5937	0.2151	0.01394	0.0507	0.3140
467	0.5934	0.2155	0.01385	0.0511	0.3142
468	0.5936	0.2167	0.01388	0.0514	0.3114
471	0.5921	0.2152	0.01398	0.0511	0.3118
480	0.5935	0.2137	0.01389	0.0506	0.3154
482	0.5939	0.2171	0.01425	0.0513	0.3113
483	0.3927	0.2171	0.01422	0.0511	0.3103
489	0.5937	0.2153	0.01407	0.0506	0.3138
490	0.5919	0.2141	0.01384	0.0505	0.3135

TABLE I  
LIQUID PENETRANT TEST STAINS TEST SPECIES DESCRIPTION ABILITY TO  
CHARACTERIZATION

Data** Sheet	Nozzle Number	Reinforcing Agent	Resin Chemical Type	Resin Content (percent)	Molding Conditions		Post-Cure* Cycle	Barcol Hardness	Density (g/cc)
					Pressure (psi)	Time (minutes)			
APHL	332	Refrasil cloth C100-48 with molybdenum diboride filler	2,2-Bis (p-hydroxyphenyl) propane formaldehyde	40	12 Ton load	1000	1	NA	NA
APHL	377	Zirconia fiber	Phenolic	74.5	1500 psi	3500	NA	NA	2.83
APHL	3802	Graphite cloth WCA graphitized and coated with ZrC and SiC (throat)	R 120 phenolic	NA	NA	NA	NA	NA	NA
APHL	3812	Graphite cloth WCA graphitized and coated with ZrB <sub>2</sub> (throat)	R 120 phenolic	NA	NA	NA	NA	NA	NA
APHL	3822	Graphite cloth WCA graphitized and coated with ZrB <sub>2</sub> (throat)	R 120 phenolic	NA	NA	NA	NA	NA	NA
APHL	390	Carbon cloth with hafnia filler (RZ-1)	Phenolic	NA	NA	NA	NA	NA	NA
APHL	391	Carbon cloth with zirconia filler (Zr-1)	Phenolic	NA	NA	NA	NA	NA	NA
APHL	392	Carbon cloth with zirconia filler (Zr-2)	Phenolic	NA	NA	NA	NA	NA	NA
173	395	Refrasil cloth C100-48 (1 1/2" squares)	Polybenzotriazole (Bakelite)	NA	NA	NA	NA	NA	NA
162	396	Refrasil cloth C100-48 (1 1/2" squares)	CTE191-120 phenolic	NA	NA	NA	NA	NA	1.59
APHL	408	Graphite cloth G-1350	Polybenzotriazole (Bakelite)	NA	NA	NA	NA	NA	1.56
APHL	409	Carbon cloth CCA-1	Polybenzotriazole (Bakelite)	NA	NA	NA	NA	NA	NA
APHL	412	Refrasil cloth C100-48	Polybenzotriazole (Bakelite)	NA	NA	NA	NA	NA	NA
200	415	Refrasil (1250) 1554-48	CTE 191-120 phenolic	NA	NA	NA	NA	NA	1.66
232b	420	Alternate Refrasil cloth C100-26 and carbon cloth CCA-1	CTE 191-120 phenolic	NA	NA	NA	NA	NA	1.52
231	424	Refrasil cloth C100-48	CTE 191-120 phenolic	NA	NA	NA	NA	NA	1.53
241	425	Carbon cloth CCA-1 with zirconia diboride filler	CTE 191-120 phenolic	NA	NA	NA	NA	NA	1.36
242	426	Carbon cloth CCA-1 with molybdenum diboride filler	CTE 191-120 phenolic	NA	NA	NA	NA	NA	1.50
243	427	Carbon cloth CCA-1 with hafnia carbide (HfC) filler	CTE 191-120 phenolic	NA	NA	NA	NA	NA	1.36
254	428	Carbon cloth CCA-1 coated with 10 to 15 mils of polyimide	CTE 191-120 phenolic	NA	NA	NA	NA	NA	1.36
257	438	Graphite cloth G-1350 coated with 10 to 15 mils of polyimide	CTE 191-120 phenolic	NA	NA	NA	NA	NA	1.36
264	445	Graphite cloth G-1350 coated with 10 to 15 mils of polyimide	CTE 191-120 phenolic	NA	NA	NA	NA	NA	1.36

1. The first step is to identify the problem or question that needs to be answered. This involves understanding the context and the specific information required.

[illegible][illegible]

TABLE 7 (Continued)

Data** Sheet Number	Nozzle Number	Reinforcing Agent	Resin Chemical Type	Resin Content (percent)	Holding Conditions		Post-Cure* Cycle	Barcol Hardness	Density (g/cc)
					Pressure (psi) Load	Temperature (°F)	Time (minutes)		
265	447 <sup>3</sup>	Graphite cloth G-1550 coated with graphite-titanium	CTL 91-1D phenolic	41.4	10,000 psi	300°	120	30	1.41
274	450	Carbon cloth CCA-1	Polyimide I-8	40.6	10,000 psi	710°	120	NA	1.38
275	453	Refrasil cloth C100-48	Polyimide I-8	NA	2 Ton load	710°	120	NA	1.55
289	461 <sup>3</sup>	Graphite cloth G-1550 coated with 2.5 microns of pyrolytic graphite	CTL 91-1D phenolic	39.7	10,000 psi	300°	120	NA	1.46
289	462 <sup>3</sup>	Graphite cloth G-1550 coated with 3.5 microns of pyrolytic graphite	CTL 91-1D phenolic	38.2	10,000 psi	300°	120	NA	1.47
304	465	Refrasil cloth C100-48	2,7 dihydroxyphenylthale- ne phenol formaldehyde (R2353-41)	38.4	300 psi	300°	120	70	1.68
304	466	Refrasil cloth C100-48	2,7 dihydroxyphenylthale- ne phenol formaldehyde (R2353-41)	38.0	300 psi	300°	120	70	1.72
APHL	472	Refrasil cloth C100-48	Polyphenylene (prepolymer MW 1000 to 1500) cured with xylylene glycol (R2353-48AB)	39.8	11 Ton load	360°	120	NA	NA
313	473	Refrasil cloth C100-48	Polyphenylene (R2353-42) (Prepolymer MW 1000 to 1500)	40.9	300 psi	425°	180	30	1.43
APHL	475 <sup>1,2</sup>	Graphite cloth WCA coated with 0.010 inch of pyrolytic graphite	R 120 phenolic	42.1	NA	NA	NA	NA	NA
APHL	476 <sup>1,2</sup>	Graphite cloth WCA coated with 0.015 inch of pyrolytic graphite	R 120 phenolic	42.1	NA	NA	NA	NA	NA
APHL	477 <sup>2</sup>	Graphite cloth WCA impregnated with R 120 phenolic (total graphitized-- impregnated with phenolic resin)	R 120 phenolic	42.1	NA	NA	NA	NA	NA
APHL	478 <sup>2</sup>	Graphite cloth WCA impregnated with Jetkote X-8 furfuryl resin (total graphitized)	R 120 phenolic	42.1	NA	NA	NA	NA	NA
APHL	479 <sup>2</sup>	Graphite cloth WCA impregnated with LTV-222 polyimide resin (total graphitized)	R 120 phenolic	42.1	NA	NA	NA	NA	NA
APHL	481 <sup>2</sup>	Graphite cloth WCA (total graphitized)	R 120 phenolic	42.1	NA	NA	NA	NA	NA
APHL	484 <sup>1,2</sup>	Graphite cloth WCA (total graphi- tized) coated with a 98 percent Ta and 2 percent NaF Slurry	R 120 phenolic	42.1	NA	NA	NA	NA	NA
APHL	485 <sup>1,2</sup>	Graphite cloth WCA (total graphi- tized) coated with a 90 percent Ta and 10 percent Si Slurry	R 120 phenolic	42.1	NA	NA	NA	NA	NA

\*See Table 1C for details of post-cure cycle.

\*\*See Introduction for meaning of Data Sheet numbers.

<sup>1</sup>These nozzle throats were coated with the listed slurry or coating.<sup>2</sup>All of these nozzle inserts were machined from the same laminate. The laminate was fabricated from 42 wt % R/20 phenolic resin and 58 wt % WCA graphite cloth. Before machining the laminate was carbonized and graphitized. After machining the inserts were treated as shown.<sup>3</sup>The carbon or graphite cloth of these nozzle inserts was coated with the indicated material (pyrolytic graphite, pyrolytic graphite-metal alloy or metal carbide) by vapor deposition before being fabricated into laminates.

TABLE 7 (continued)

Data <sup>1</sup> Sheet Number	Nozzle Number	Reinforcing Agent	Resin Chemical Type	Resin Content (%)	Curing Conditions			Post-Cure <sup>2</sup> Cycles	Barcol Hardness	Density (gm/cc)
					Pressure (psi)	Temperature (°F)	Time (minutes)			
APYL	486 <sup>1,2</sup>	Graphite cloth WCA (total graphi- cized) coated with an 88% ZrB <sub>2</sub> 10% Si and 2% NaF Slurry	R 120 phenolic	42.1	NA	NA	NA	NA	NA	NA
APYL	487 <sup>1,2</sup>	Graphite cloth WCA (total graphi- cized) coated with a 90% W and 10% Si Slurry	R 120 phenolic	42.1	NA	NA	NA	NA	NA	NA
APYL	488 <sup>1,2</sup>	Graphite cloth WCA (total graphi- cized) coated with a 96% Si and 2% NaF Slurry	R 120 phenolic	42.1	NA	NA	NA	NA	NA	NA
326	492	Refrasil cloth C100-48	P-phenylphenol phenol formaldehyde (82553-40)	40.1	300 psi	300°	120	II	85	1.63
326	493	Refrasil cloth C100-48	P-phenylphenol phenol formaldehyde (82553-40)	40.1	300 psi	300°	120	II	63	1.62
308	494 <sup>3</sup>	Graphite cloth G-1550 coated with 1 micron of pyrolytic graphite	CTL 91-LD phenolic	37.5	300 psi	300°	120	II	30	1.42
308	495 <sup>3</sup>	Graphite cloth G-1550 coated with 1 micron of pyrolytic graphite	CTL 91-LD phenolic	37.4	300 psi	300°	120	II	32	1.42
314	496 <sup>3</sup>	Graphite cloth G-1550 coated with 1 micron of pyrolytic graphite-boron	CTL 91-LD phenolic	39.0	300 psi	300°	120	II	45	1.45
314	497 <sup>3</sup>	Graphite cloth G-1550 coated with 1 micron of pyrolytic graphite-boron	CTL 91-LD phenolic	39.1	300 psi	300°	120	II	47	1.45
319	498	Refrasil cloth C100-48	CTL 91-LD phenolic	38.4	300 psi	300°	120	II	77	1.61
APYL	499	Refrasil cloth C100-48	CTL 91-LD phenolic	39.1	300 psi	300°	120	II	NA	NA
APYL	500	Refrasil cloth C100-48	CTL 91-LD phenolic	38.5	300 psi	300°	120	II	NA	NA
320	501 <sup>3</sup>	Graphite cloth G-1550 coated with 2.5 microns of pyrolytic graphite- boron	CTL 91-LD phenolic	39.1	300 psi	300°	120	II	53	1.42
320	502 <sup>3</sup>	Graphite cloth G-1550 coated with 2.5 microns of pyrolytic graphite- boron	CTL 91-LD phenolic	38.6	300 psi	300°	120	II	54	1.42
321	503	Carbon cloth SS1620 (oxidation- resistant)	CTL 91-LD phenolic	39.7	300 psi	300°	120	II	70	1.41

<sup>1</sup> See Table 1C for details of post-cure cycle.<sup>2</sup> See Introduction for meaning of Data Sheet numbers.<sup>3</sup> These nozzle throats were coated with the listed slurry or coating.<sup>4</sup> All of these nozzle inserts were machined from the same laminate. The laminate was fabricated from 42 wt % R/50 phenolic resin and 58 wt % WCA graphite cloth. Before machining the laminate was carbonized and graphitized. After machining the inserts were treated as shown.<sup>5</sup> The carbon or graphite cloth of these nozzle inserts was coated with the indicated material (pyrolytic graphite, pyrolytic graphite-metal alloy or metal carbide) by vapor deposition before being fabricated into laminates.

TABLE 7 (continued)

Data** Sheet Number	Nozzle Number	Reinforcing Agent	Resin Chemical Type	Resin Content (%)	Holding Conditions			Post-Cure* Cycle	Barcol Hardness	Density (gm/cc)
					Pressure (psi) Load	Temperature (°F)	Time (minutes)			
321	504	Carbon cloth SS 1670 (oxidation-resistant)	CTL 91-LD phenolic	40.9	300 psi	300°	120	II	70	1.42
323	505	Graphite cloth G-1550	CTL 91-LD phenolic	42.6	300 psi	300°	120	II	50	1.33
329	507	Carbon cloth CCA-1	CTL 91-LD phenolic	43.6	300 psi	300°	120	II	73	1.42
APDL	509 <sup>1,2</sup>	Graphite cloth WCA (total graphitized) with an Hf-Si inside surface coating.	R 120 phenolic	42.1	NA	NA	NA	NA	NA	NA
APDL	514 <sup>1,2</sup>	Graphite cloth WCA (total graphitized) coated with .0285 inch of pyrolytic graphite	R 120 phenolic	42.1	NA	NA	NA	NA	NA	NA
APDL	515 <sup>1,2</sup>	Graphite cloth WCA (total graphitized) coated with .030 inch of pyrolytic graphite	R 120 phenolic	42.1	NA	NA	NA	NA	NA	NA
337	516	Rayon Fabric	CTL 91-LD phenolic	41.3	10,000	300°	120	II	68	1.34
364	517	Refrasil cloth C100-48	Polybenzimidazole (AF 151)	40.5	10,000	700	180	VII	65	1.64
356	518	Glass cloth style 181, A1100 finish	Polybenzimidazole (AF 151)	43.6	3,000	700	180	VI	45	1.42
365	519	Refrasil cloth C100-48	Polyphenylene (Abchor 413) prepolymer MW 1000 to 1500, 82353-51	40.3	3,000	400	120	VIII	38	1.45
365	520	Refrasil cloth C100-48	Polyphenylene (Abchor 413) prepolymer MW 1000 to 1500, 82353-51	40.3	3,000	400	120	VIII	37	1.46
359	522	Carbon cloth CCA-1 Low alkalinity (SS 1641)	CTL 91-LD phenolic	42.6	10,000	300	120	II	70	1.41
364	524	Carbon silica fabric	CTL 91-LD phenolic	41.9	10,000	300	120	II	78	1.53
366	526	Refrasil cloth C100-48	DEN 438 epoxy nonolac	38.9	10,000	300	960	II	70	1.60
APDL	527	Rayon silica fabric	CTL 91-LD phenolic	40	10,000	300	120	NA	NA	NA
APDL	528	Refrasil cloth C100-48	Chrome-P	38.7	NA	NA	NA	IX	NA	NA

\* See Table 1C for details of post-cure cycle.

\*\* See Introduction for meaning of Data Sheet numbers.

1 These nozzle throats were coated with the listed slurry or coating.

2 All of these nozzle inserts were machined from the same laminate. The laminate was fabricated from 42 wt % R/20 phenolic resin and 58 wt % WCA graphite cloth. Before machining the laminate was carbonized and graphitized. After machining the inserts were treated as shown.

TABLE 2  
LIQUID PROPELLANT MOTOR CHECK RUN PERFORMANCE  
ABLATIVE NOZZLE CHARACTERIZATION

Simulator Checkout Number	Test Duration (sec)	Total Flow Rate (lb/sec)	Initial Stabilized Chamber Pressure (psia)	Initial Throat Diameter (in.)	Calculated C <sub>d</sub> (ft/sec)	Efficiency (percent)	NTU Flow Rate (lb/sec)	50/50 Flow Rate (lb/sec)	Mixture Ratio (o/p)	Remarks
1-22	Variable	~0.36	~300	~0.500	--	--	~0.22	~0.14	~1.60	Various check runs for optimization of liquid motor system.
23	56	0.3555	303.2	0.501	5408	96.1	0.2193	0.1362	1.610	Performance check run.
24	56	0.3558	301.1	0.5015	5377	95.6	0.2199	0.1359	1.618	Performance check run.
25-26	--	--	--	--	--	--	--	--	--	Invalid tests.
27	62	0.3555	302.3	0.502	5414	96.1	0.2180	0.1377	1.582	Performance check run.
28	8	0.3535	298.9	0.501	5361	95.1	0.2172	0.1353	1.594	Performance check run.
29-34	10	~0.36	~300	~0.500	--	--	~0.22	~0.14	~1.60	Optimization of start transient.
35-36	8	~0.36	~300	~0.500	--	--	~0.22	~0.14	~1.60	Optimization of start transient with stainless steel injector.
37	58	0.3525	294.0	0.505	5374	95.4	0.2144	0.1381	1.552	Performance check run.
38	8	0.3517	297.0	0.500	5356	94.8	0.2166	0.1371	1.585	Performance check run.
39	--	--	--	--	--	--	--	--	--	Invalid test.
40	8	0.3546	302.0	0.5007	5394	95.8	0.2167	0.1368	1.571	Performance check run.
41	60	0.3538	302.3	0.5018	5437	96.6	0.2159	0.1379	1.566	Performance check run.
42-43	30	~0.36	~300	~0.500	--	--	~0.22	~0.14	~1.60	Optimization of start transient.
44	8	--	--	--	--	--	--	--	--	Invalid test.
45	8	0.3491	278.3	0.516	5363	95.3	0.2134	0.1337	1.611	Performance Checkrun
46	8	0.3467	292.1	0.503	5385	95.7	0.2121	0.1346	1.576	Performance Checkrun

TABLE 9  
CALCULATED AND MEASURED VALUES USED IN EROSION PROPERTY ANALYSIS  
LIQUID PROPELLANT TEST SERIES

NOZZLE NUMBER	TIME (sec)	MEASURED CHAMBER PRESSURE (psia)	ORIGINAL THROAT DIAMETER (inch)	MEASURED CHAMBER PRESSURE (psia)	TOTAL FLOW RATE (lb/sec)	TIME 250 psia (sec)	CALC. THROAT AREA 250 psia (in. <sup>2</sup> )	CALC. THROAT RADIUS 250 psia (inch)	CALC. EROSION RATE 250 psia (mils/sec)	TIME 200 psia (sec)	CALC. THROAT AREA 200 psia (in. <sup>2</sup> )	CALC. THROAT RADIUS 200 psia (inch)	CALC. EROSION RATE 200 psia (mils/sec)	TIME 150 psia (sec)	CALC. THROAT AREA 150 psia (in. <sup>2</sup> )
352	68.0	344	.502	98	.3497	12.5	.2363	.2731	1.64	18.2	.2927	.3052	2.82	29.8	.2903
377	55.5	312	.496	88	.3536	5.3	.2369	.2744	5.02	7.3	.2960	.3070	8.08	16.1	.2946
380	78.3	301	.505	100	.3487	26.6	.2336	.2727	.82	27.8	.2919	.3049	1.88	29.1	.2891
381	55.7	300	.5025	100	.3498	11.3	.2342	.2730	1.95	17.6	.2928	.3033	3.11	24.9	.2904
382	73.4	319	.506	109	.3517	2.1	.2356	.2739	6.74	6.5	.2944	.3063	8.20	12.5	.2925
390	42.6	326	.4975	110	.3538	7.8	.2370	.2757	3.33	14.5	.2962	.3070	3.94	24.7	.2948
391	81.7	322	.5003	100	.3508	8.7	.2349	.2735	2.48	16.3	.2936	.3057	3.40	23.0	.2915
392	16.2	391	.498	100	.3521	4.3	.2359	.2740	3.81	6.6	.2949	.3063	8.68	9.7	.2922
393	123.3	328	.501	131	.3477	21.3	.2379	.2733	1.02	29.5	.2910	.3045	1.27	74.3	.2880
396	111.8	328	.501	159	.3515	12.9	.2354	.2737	1.81	33.3	.2942	.3060	1.67	111.8	.2904
408	47.0	344	.5013	104	.3542	7.6	.2378	.2748	3.17	13.2	.2965	.3072	4.28	25.9	.2953
409	39.9	377	.5025	93	.3507	16.1	.2348	.2735	1.39	21.0	.2926	.3057	2.60	26.4	.2914
412	107.5	323	.503	161	.3536	31.9	.2370	.2747	.71	40.3	.2963	.3071	.92	107.5	.2940
415	119.6	316	.500	164	.3530	50.2	.2364	.2743	.68	79.5	.2955	.3067	.71	119.6	.2907
420	115.5	316	.501	141	.3521	31.1	.2358	.2740	.76	55.5	.2947	.3063	1.00	96.2	.2929
424	60.9	345	.5015	153	.3541	18.5	.2372	.2748	1.30	44.5	.2944	.3072	1.27	60.9	.2978
425	38.3	337	.502	102	.3531	5.5	.2367	.2745	4.27	12.1	.2959	.3069	4.62	20.3	.2945
426	17.6	320	.5005	101	.3543	4.4	.2375	.2750	5.64	6.3	.2969	.3074	9.06	10.0	.2956
427	39.1	321	.505	100	.3495	8.3	.2343	.2731	2.48	14.1	.2928	.3033	3.74	22.6	.2905
436	57.4	334	.5005	100	.3504	14.1	.2346	.2733	1.64	22.6	.2932	.3055	2.45	35.4	.2909
438	56.4	319	.500	114	.3489	13.4	.2339	.2729	1.71	24.2	.2922	.3050	2.27	39.5	.2898
445	61.3	331	.501	100	.3505	13.7	.2347	.2733	1.46	23.0	.2934	.3055	2.39	34.0	.2912

\*100 psia or chamber pressure at termination of test

RELATIVE NOZZLE CHARACTERIZATION  
PHILCO-ASTRONAUTICS DIVISION  
EXPERIMENTAL EQUIPMENT DEPARTMENT

UNITES

CALC. EROSION RATE 200 psia (mils/sec)	TIME 150 psia (sec)	CALC. THROAT AREA 150 psia (in. <sup>2</sup> )	CALC. THROAT RADIUS 150 psia (inch)	CALC. EROSION RATE 150 psia (mils/sec)	TIME 100 psia (sec)	CALC. THROAT AREA 100 psia (in. <sup>2</sup> )	CALC. THROAT RADIUS 100 psia (inch)	CALC. EROSION RATE 100 psia (mils/sec)	NOZZLE NUMBER	MATERIAL RESIN/REINFORCEMENT
2.82	29.8	.3903	.3524	3.41	45.7	.5834	.4317	2.75	352	2,2-Bis (p-hydroxyphenyl) propane formaldehyde 401/C100-48
8.08	16.1	.3546	.3344	6.62	40.8	.5850	.4330	6.55	377	Phenolic 26.52/silica fiber
1.28	39.1	.3691	.3321	7.55	76.9	.5838	.4311	2.31	380	R 120 phenolic/WCA coated with ZrO <sub>2</sub> and SiC (throat)
3.11	24.9	.3904	.3525	4.07	54.7	.5834	.4318	5.30	381	R 120 phenolic/WCA coated with ZrO <sub>2</sub> (throat)
6.20	12.5	.3925	.3535	8.04	25.4	.5806	.4148	6.91	382	R 120 phenolic/WCA coated with ZrO <sub>2</sub> (throat)
3.84	24.7	.3948	.3545	4.29	42.6	.5890	.4142	5.88	390	Phenolic/carbon cloth with hafnia filler (H-1)
3.40	33.0	.3915	.3532	3.12	81.7	.5878	.4324	2.23	391	Phenolic/carbon cloth with silica filler (Zr-1)
8.48	9.7	.3929	.3538	10.40	16.2	.5900	.4334	11.36	392	Phenolic/carbon cloth with silica filler (Zr-2)
1.37	74.3	.3680	.3316	1.34	125.3	.4447	.3762	1.02	395	Insulite 27.42/C100-48
1.67	111.8	.3704	.3434	.83					396	CTL 91-LD phenolic 33.72/C100-48
4.22	26.9	.3953	.3548	3.87	47.0	.5707	.4262	3.73	404	Insulite/G-1550
2.40	26.4	.3916	.3531	3.86	38.2	.5813	.4201	4.48	405	Insulite/OCA-1
.92	107.5	.3690	.3422	.84					412	Insulite/C 100-48
.71	119.8	.3607	.3388	.74					415	CTL 91-LD/49.92/1550-48
1.00	96.2	.3929	.3538	1.07	115.5	.4182	.3643	.99	420	CTL 91-LD 39.51/alternate C100-28 and OCA-1
1.27	60.9	.3878	.3513	1.65					424	CTL 91-LD phenolic 40.62/C100-48
4.62	20.3	.3945	.3543	5.09	38.3	.5801	.4297	4.67	425	CTL 91-LD 39.92/OCA-1 with titanium diboride filler
9.04	10.0	.3958	.3550	10.48	17.6	.5878	.4224	10.35	426	CTL 91-LD 41.61/ OCA-1with molybdenum diboride filler
3.74	22.6	.3905	.3525	4.42	39.3	.5857	.4318	4.59	427	CTL 91-LD 41.22/OCA-1 with boron carbide (B <sub>4</sub> C) filler
2.45	35.4	.3909	.3527	2.90	57.6	.5864	.4320	3.17	436	CTL 91-LD 40.07/OCA-1 coated with 1.0 to 1.4 microns of pyrolytic graphite
2.27	39.6	.3898	.3522	2.58	56.4	.5129	.4041	2.73	438	CTL 91-LD 41.92/G-1550 coated with 1.0 to 1.4 microns of pyrolytic graphite-sirconium
2.39	38.0	.3912	.3528	2.69	61.3	.5846	.4321	2.96	445	CTL 91-LD 40.42/G-1550 coated with 1.0 to 1.5 microns of pyrolytic graphite-hafnia



TABLE 9

\*100 psi or chamber pressure at termination of test.

TIME 150 psi (sec)	CALC. THROAT AREA 150 psi (in <sup>2</sup> )	CALC. THROAT RADIUS 150 psi (inch)	CALC. EROSION RATE 150 psi (mil/sec)	TIME 150 psi (sec)	CALC. THROAT AREA 150 psi (in <sup>2</sup> )	CALC. THROAT RADIUS 150 psi (inch)	CALC. EROSION RATE 150 psi (mil/sec)	NOZZLE NUMBER	MATERIAL RESIN/REINFORCEMENT
45.3	.3841	.3314	2.44	46.5	.3872	.6505	2.70	447	CTL 91-LD 41.4% G-1550 coated with 1.0 to 1.5 microns of pyrolytic graphite-titanium
19.3	.3913	.3333	3.21	31.0	.5884	.6328	5.84	450	I-8 40.6% DCL-1
36.0	.3913	.3329	1.82	104.3	.3766	.6283	1.67	453	X-8/ C100-48
36.8	.3914	.3329	1.76	72.3	.3871	.6223	2.48	461	CTL 91-LD 39.7% G-1550 coated with 2.5 microns of pyrolytic graphite
36.3	.3904	.3323	1.80	67.8	.5836	.6317	2.62	462	CTL 91-LD 38.7% G-1550 coated with 2.5 microns of pyrolytic graphite
104.5	.3904	.3323	.96					445	(R2333-41)/ C100-48 61.6%
109.4	.3903	.3324	1.01	115.0	.6316	.3643	.96	444	(R2333-41)/ C100-48 92.0%
43.2	.3902	.3324	1.92	17.1	.5822	.6317	1.65	472	(R2333-48A2)/ C100-48 60.7%
118.3	.3893	.3429	.1					473	(R2333-42)/ C100-48 59.1%
36.5	.3914	.3329	1.93	60.2	.5971	.6322	2.49	475	R 120 42.1% MCA coated with 0.010 inch of pyrolytic graphite
30.5	.3909	.3327	3.22	48.3	.5864	.6320	3.46	476	R 120 42.1% MCA coated with 0.015 inch of pyrolytic graphite
43.3	.3932	.3339	2.36	69.6	.5898	.6335	2.62	477	R 120 42.1% MCA impregnated with R 120 phenolic
37.0	.3978	.3313	2.21	54.3	.5709	.6263	3.13	478	R 120 42.1% MCA impregnated with Jethote X-8 furfuryl
38.9	.3913	.3331	2.40	61.5	.5877	.6324	2.94	479	R 120 42.1% MCA impregnated with LTV-X22 polyimide
32.9	.3905	.3326	2.50	54.1	.5836	.6318	3.17	481	R 120 42.1% MCA (total graphitized)
								484	R 120 42.1% MCA coated with 98% Ta and 2% NaF Slurry
95.0	.3892	.3322	1.67	116.5	.5648	.6314	1.55	483	R 120 42.1% MCA coated with a 90% Ta and 10% Si Slurry
93.5	.3870	.3310	1.08	109.6	.5803	.6299	1.64	486	R 120 42.1% MCA coated with an 88% ZrO <sub>2</sub> , 10% Si and 2% NaF Slurry
19.2	.3899	.3322	9.44	28.8	.5648	.6314	6.21	467	R 120 42.1% MCA coated with a 90% Mo and 10% Si Slurry
101.1	.3886	.3317	1.00	119.1	.5628	.6307	1.51	488	R 120 42.1% MCA coated with a 98% Si and 2% NaF Slurry
118.2	.3736	.3448	.80					492	(R2333-40)/ C100-48 59.9%
118.7	.3927	.3336	.86					493	(R2333-40)/ C100-48 59.9%
64.0	.3837	.3304	1.55	85.4	.3728	.6270	2.06	494	CTL 91-LD 37.5% G-1550 coated with 1 micron of pyrolytic graphite
49.1	.3919	.3332	2.08	79.0	.5878	.6324	2.50	495	CTL 91-LD 37.4% G-1550 coated with 1 micron of pyrolytic graphite

TABLE 4  
CALCULATED AND MEASURED VALUES USED IN EROSION TESTS  
LIQUID PROPellant TEST SERIES  
PAGE 3

MOUSE NUMBER	TIME (sec)	MAXIMUM CHAMBER PRESSURE (psia)	ORIGINAL THROAT DIAMETER (inch)	MINIMUM CHAMBER PRESSURE (psia)	TOTAL FLOW RATE (lb/sec)	TIME 750 psia (sec)	CALC. THROAT AREA 750 psia (in <sup>2</sup> )	CALC. THROAT RADIUS 750 psia (inch)	CALC. EROSION RATE 750 psia (mil/sec)	TIME 200 psia (sec)	CALC. THROAT AREA 200 psia (in <sup>2</sup> )	CALC. THROAT RADIUS 200 psia (inch)	CALC. EROSION RATE 200 psia (mil/sec)	TIME 150 psia (sec)	CALC. THROAT AREA 150 psia (in <sup>2</sup> )
495	52.0	378	.5015	110	.3575	15.1	.2344	.2743	1.34	76.0	.2955	.3067	2.25	39.4	.3546
497	30.6	377	.501	114	.3498	7.5	.2345	.2737	3.03	13.6	.2931	.3035	4.04	21.6	.3390
498	119.2	374	.5015	155	.3497	34.5	.2341	.2730	.65	73.0	.2945	.3037	.75	119.2	.3377
499	119.0	309	.5005	196	.3491	47.2	.2340	.2729	.67	109.0	.2925	.3021	.50		
500	119.1	307	.501	760	.3514	119.1	.2345	.2744	.70						
501	54.2	335	.501	116	.3537	14.3	.2347	.2745	1.48	24.6	.2959	.3069	2.27	34.6	.3546
502	61.8	375	.501	116	.3471	16.2	.2327	.2722	1.34	28.4	.2908	.3042	1.89	44.4	.3478
503	51.4	379	.5005	115	.3514	7.7	.2355	.2739	3.08	13.4	.2944	.3063	4.19	21.8	.3376
504	47.2	378	.5027	113	.3501	19.4	.2347	.2733	1.13	29.8	.2953	.3056	1.82	40.3	.3311
505	40.8	349	.505	108	.3579	8.7	.2344	.2743	2.50	15.5	.2957	.3068	3.50	32.8	.3543
507	53.2	315	.503	101	.3545	6.8	.2375	.2750	3.45	12.6	.2970	.3074	4.63	21.6	.3540
509	119.3	336	.498	135	.3481	56.5	.2333	.2725	.62	90.5	.2917	.3047	.62	108.5	.3489
514	114.4	304	.5025	171	.3511	69.5	.2353	.2737	.57	89.4	.2947	.3060	.61	102.7	.3322
515	118.4	329	.499	126	.3489	47.5	.2339	.2729	.49	62.8	.2933	.3050	.88	83.0	.3498
516	10.1	334	.5003	117	.3509	2.6	.2353	.2736	9.00	4.1	.2940	.3059	13.59	6.8	.3320
517	89.1	335	.498	114	.3506	16.0	.2351	.2736	1.54	26.5	.2939	.3059	2.14	53.3	.3319
518	17.6	336	.4975	117	.3506	4.8	.2350	.2735	5.17	7.9	.2938	.3058	7.23	12.6	.3317
519	119.0	319	.499	140	.3490	22.7	.2339	.2729	1.03	52.9	.2924	.3051	1.05	103.7	.3499
520	113.7	330	.500	189	.3487	34.2	.2334	.2726	.62	96.7	.2918	.3048	.57	113.7	.3087
522	37.1	311	.501	119	.3518	8.2	.2358	.2740	2.87	15.5	.2948	.3064	3.61	26.4	.3330
524	118.4	310	.5003	154	.3507	34.6	.2351	.2736	.66	65.1	.2939	.3059	.81	118.4	.3416
526	29.0	502	.501	307	.3510										
527	41.3	333	.503	213	.3570	14.3	.2358	.2740	1.57	24.6	.2969	.3069	1.85		
528	119.4	337	.5025	149	.3504	56.7	.2350	.2735	.39	91.7	.2938	.3058	.60	117.6	.3317

0100 psia or chamber pressure at termination of test.

CALC. EROSION RATE 200 psia (mil/sec)	TIME 150 psia (sec)	CALC. THROAT AREA 150 psia (in <sup>2</sup> )	CALC. THROAT RADIUS 150 psia (inch)	CALC. EROSION RATE 150 psia (mil/sec)	TIME 100 psia (sec)	CALC. THROAT AREA 100 psia * (in <sup>2</sup> )	CALC. THROAT RADIUS 100 psia * (inch)	CALC. EROSION RATE 100 psia * (mil/sec)	NOZZLE NUMBER	MATERIAL RESIN/REINFORCEMENT
2.25	39.6	.3940	.3541	2.62	32.0	.5373	.4135	3.13	496	CTL 91-LD 39.07/ C-1550 coated vit 1 micron of pyrolytic graphite-boron
4.04	21.6	.3908	.3527	4.73	30.6	.5142	.4044	5.04	497	CTL 91-LD 39.12/ G-1550 coated vit 1 micron of pyrolytic graphite-boron
.75	119.2	.3775	.3444	.80					498	CTL 91-LD 38.47/ C100-48
.50									499	CTL 91-LD 39.12/ C100-48
									500	CTL 91-LD 38.52/ C100-48
2.29	39.8	.3946	.3544	2.69	36.2	.5103	.4030	2.81	501	CTL 91-LD 39.12/ G-1550 coated with 2.5 microns of pyrolytic graphite-boron
1.89	44.4	.3878	.3513	2.27	61.8	.5014	.3993	2.41	502	CTL 91-LD 38.67/ G-1550 coated with 2.5 microns of pyrolytic graphite-boron
4.19	21.8	.3926	.3535	4.74	31.4	.5170	.4027	4.89	503	CTL 91-LD 39.73/ S1620 (oxidation-resistant)
1.82	40.3	.3911	.3528	2.32	47.2	.5192	.4083	2.29	504	CTL 91-LD 40.91/ S5 1620 (oxidation-resistant)
3.30	32.8	.3943	.3542	3.10	60.8	.5476	.4175	2.71	505	CTL 91-LD 42.62/ G-1550
4.43	21.6	.3960	.3550	4.79	33.2	.5481	.4327	3.41	507	CTL 91-LD 43.62/ CCA-1
.42	108.5	.3889	.3518	.95	119.3	.4321	.3708	1.02	509	R 120 42.12/ WCA with an Hf-Si inside surface coating
.61	102.7	.3922	.3533	.99	114.4	.4862	.3934	1.24	514	R120 42.12/ WCA coated with .0283 inch of pyrolytic graphite
.88	83.0	.3898	.3522	1.24	118.4	.4715	.3874	1.16	515	R120 42.12/ WCA coated with .030 inch of pyrolytic graphite
13.39	6.8	.3920	.3532	15.13	10.1	.5026	.4000	14.83	516	CTL 91-LD 41.31/ Rayon fabric
8.14	33.3	.3919	.3532	1.95	89.1	.5156	.4051	1.75	517	AP 151 40.52/ C100-48
7.23	12.6	.3917	.3531	8.29	17.6	.5021	.3998	8.39	518	AP 151 43.62/ Glass cloth style 181, A1100 finish
1.05	103.7	.3899	.3522	.99	119.0	.4172	.3747	.97	519	(R2353-51)/ C100-48 39.72
.37	113.7	.3887	.3515	.56					520	(R2353-51)/ C100-48 39.72
3.61	26.4	.3930	.3534	3.91	37.1	.4954	.3971	3.95	522	CTL 91-LD 42.62/ CCA-1
.81	118.4	.3816	.3435	.83					524	CTL 91-LD 41.92/ Carbon silica fabric
									526	DIN 438 38.72/ C100-48
									527	CTL 91-LD 402/ Rayon silica fabric
1.85									528	Chrome-F 38.72/C100-48
.60	117.6	.3917	.3531	.87						

Experimental Equipment Department  
Philco-Aeronutronic Division

TABLE 10

LIQUID PROPELLANT MOTOR PERFORMANCE DATA  
ABLATIVE NOZZLE CHARACTERIZATION

NOZZLE NO.	TOTAL FLOW RATE (lb/sec)	NTD FLOW RATE (lb/sec)	50/50 FLOW RATE (lb/sec)	PROPELLANT MIXTURE RATIO
352	.3497	.2143	.1354	1.582
377	.3536	.2184	.1352	1.615
380	.3487	.2135	.1352	1.579
381	.3498	.2156	.1342	1.600
382	.3517	.2152	.1365	1.576
390	.3538	.2132	.1406	1.516
391	.3508	.2134	.1374	1.553
392	.3521	.2131	.1390	1.533
395	.3477	.2129	.1348	1.579
396	.3515	.2161	.1354	1.596
408	.3542	.2143	.1399	1.532
409	.3507	.2130	.1377	1.546
412	.3536	.2129	.1407	1.513
415	.3530	.2127	.1403	1.516
420	.3521	.2128	.1393	1.527
424	.3541	.2176	.1365	1.594
425	.3531	.2172	.1359	1.598
426	.3543	.2169	.1374	1.578

TABLE 10 (Continued)

NOZZLE NO.	TOTAL FLOW RATE (lb/sec)	NTG FLOW RATE (lb/sec)	50/50 FLOW RATE (lb/sec)	PROPELLANT MIXTURE RATIO
427	.3495	.2166	.1329	1.629
436	.3504	.2173	.1331	1.632
438	.3489	.2138	.1351	1.582
445	.3505	.2175	.1330	1.635
447	.3478	.2147	.1331	1.613
450	.3516	.2183	.1333	1.637
453	.3506	.2177	.1329	1.638
461	.3507	.2174	.1333	1.631
462	.3498	.2161	.1337	1.616
465	.3498	.2169	.1329	1.632
466	.3497	.2168	.1329	1.631
472	.3495	.2159	.1336	1.616
473	.3482	.2147	.1335	1.608
475	.3509	.2178	.1331	1.636
476	.3503	.2167	.1336	1.622
477	.3522	.2178	.1344	1.620
478	.3475	.2137	.1338	1.597
479	.3510	.2167	.1343	1.613
481	.3499	.2163	.1336	1.619
484	.3485	.2142	.1343	1.594
485	.3490	.2156	.1334	1.616
486	.3464	.2127	.1337	1.590
487	.3490	.2145	.1345	1.594

TABLE 10 (Continued)

NOZZLE NO.	TOTAL FLOW RATE  (lb/sec)	HTO FLOW RATE  (lb/sec)	50/50 FLOW RATE  (lb/sec)	PROPELLANT MIXTURE RATIO
488	.3478	.2134	.1344	1.587
492	.3478	.2137	.1341	1.593
493	.3515	.2167	.1348	1.607
494	.3452	.2115	.1337	1.582
495	.3508	.2165	.1343	1.612
496	.3527	.2180	.1347	1.618
497	.3498	.2153	.1345	1.600
498	.3492	.2147	.1345	1.596
499	.3491	.2148	.1343	1.599
500	.3514	.2166	.1348	1.606
501	.3532	.2185	.1347	1.622
502	.3471	.2125	.1346	1.578
503	.3514	.2167	.1347	1.608
504	.3501	.2153	.1348	1.597
505	.3529	.2165	.1364	1.587
507	.3545	.2178	.1367	1.593
509	.3481	.2135	.1346	1.586
514	.3511	.2164	.1347	1.606
515	.3489	.2147	.1342	1.599
516	.3509	.2168	.1341	1.616
517	.3508	.2159	.1349	1.600
518	.3506	.2158	.1348	1.600
519	.3490	.2148	.1342	1.600
520	.3482	.2144	.1338	1.602
522	.3518	.2170	.1348	1.609

TABLE 10 (Continued)

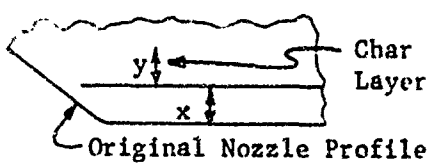
NOZZLE NO.	TOTAL FLOW RATE  (lb/sec)	NTC FLOW RATE  (ob/sec)	50/50 FLOW RATE  (lb/sec)	PROPELLANT MIXTURE RATIO
524	.3507	.2168	.1339	1.619
526	.3510	.2161	.1349	1.601
527	.3520	.2171	.1349	1.609
528	.3506	.2160	.1346	1.604



TABLE 11

POST TEST NOZZLE EROSION EVALUATION  
ABLATIVE NOZZLE CHARACTERIZATION

## Liquid Propellant Test Series

NOZZLE NUMBER	CHAR <sup>(1)</sup> DEPTH (in.)	RESIN (2) DEGRADATION RATE (mils/sec)	
352	0.35 to 0.43	7.9 to 9.1	NOTES:
377	0.18	7.8	
380	0.43	7.8	(1) Char depth measured at resultant throat with 6 inch scale.
381	0.33 to 0.49	9.2 to 12.1	
382	0.30 to 0.47	19.7 to 27.0	(2) Resin degradation rate (d) calculated by adding calc. erosion rate and char depth rate.
390	0.14	7.2	
391	0.37	6.7	
392	0.08	16.3	
395	0.25 to 0.35	3.0 to 3.9	
396	0.42	4.6	
408	0.45	13.3	
409	0.20	9.7	
410	0.27	3.3	
415	0.33 to 0.40	3.5 to 4.1	
420	0.38	4.3	
424	0.28	6.3	
425	0.26	11.5	
426	0.15	18.9	
427	0.25 to 0.35	11.0 to 13.6	
436	0.32	8.8	

$$d = \frac{x}{t} + \frac{y}{t}$$

where:

x - erosion  
y - char depth  
t - run time

TABLE 11 (continued)  
 POST TEST NOZZLE EROSION EVALUATION  
 ABLATIVE NOZZLE CHARACTERIZATION  
 Liquid Propellant Test Series

NOZZLE NUMBER	CHAR. (1) DEPTH (in.)	RESIN (2) DEGRADATION RATE (mils/sec)
438	0.40	9.8
445	0.35	8.7
447	0.32	7.5
450	0.20	12.3
453	0.32	4.7
461	0.29 to 0.39	6.5 to 7.9
462	0.15	4.8
465	0.35 to 0.45	4.0 to 4.8
466	0.37 to 0.45	4.1 to 4.8
472	0.10 to 0.50	2.6 to 6.2
473	0.41	4.2
475	0.20 to 0.30	5.6 to 7.1
476	0.39	11.7
477	0.37	7.9
478	0.35	9.3
479	0.37	9.0
481	0.37	10.0
484	0.53	4.6
485	0.24 to 0.50	3.6 to 5.8
486	0.30 to 0.43	4.3 to 5.5

TABLE 11 (Continued)

POST TEST NOZZLE EROSION EVALUATION  
ABLATIVE NOZZLE CHARACTERIZATION

## Liquid Propellant Test Series

NOZZLE NUMBER	CHAR <sup>(1)</sup> DEPTH (in.)	RESIN (2) DEGRADATION RATE (mils/sec)
487	0.18	12.5
488	0.42	5.0
492	0.40	4.2
493	0.40	4.2
494	0.35	6.2
495	0.34	6.6
496	0.34 to 0.43	9.7 to 11.4
497	0.17	10.5
498	0.42	4.3
499	0.52	4.9
500	0.40 to 0.60	3.6 to 5.2
501	0.40	10.2
502	0.35 to 0.48	8.1 to 10.2
503	0.20	11.3
504	0.36	10.9
505	0.38	9.0
507	0.30 to 0.40	9.1 to 10.5
509	0.40 to 0.50	4.4 to 5.2
514	0.40	4.7
515	0.20	2.9
516	0.38	52.4

TABLE 11 (Continued)  
 POST TEST NOZZLE EROSION EVALUATION  
 ABLATIVE NOZZLE CHARACTERIZATION  
 Liquid Propellant Test Series

NOZZLE NUMBER	CHAR <sup>(1)</sup> DEPTH (in.)	RESIN (2) DEGRADATION RATE (mils/sec)
517	0.32	5.3
518	0.04	10.9
519	0.38	4.2
520	0.50	5.0
522	0.41	15.0
524	0.46	4.7
526	0.30 to 0.55	10.3 to 19.0
527	—	—
528	0.44	4.6

TABLE 12  
POST TEST NOZZLE VISUAL EVALUATION  
ABLATIVE NOZZLE CHARACTERIZATION  
Liquid Propellant Test Series

<u>Nozzle</u>	<u>Evaluation</u>
352	Bore very rough, uneven erosion, spalling, insert undercut
377	Bore rough, uneven erosion and undercuts
380	Bore rough, uneven erosion, spalling, coating remaining on entrance and exit sections
381	Bore smooth, uneven erosion
382	Bore smooth, uneven erosion, coating remaining on exit cone
390	Bore smooth, even erosion, laminations
391	Bore rough, even erosion, cylindrical cracks
392	Bore rough, uneven erosion, cylindrical cracks
395	Bore rough, uneven erosion, spalling
396	Bore smooth, uneven erosion
408	Bore rough, uneven erosion, spalling, some cylindrical cracks
409	Bore rough, even erosion, spalling, laminations
412	Bore smooth, even erosion
415	Bore smooth, even erosion
420	Bore smooth, even erosion
424	Bore smooth, uneven erosion
425	Bore smooth, even erosion, cylindrical cracks
426	Bore rough, even erosion, cylindrical cracks
427	Bore rough, even erosion, cylindrical cracks
436	Bore rough, even erosion, slight cylindrical cracks

TABLE 12 (Continued)  
 POST TEST NOZZLE VISUAL EVALUATION  
 ABLATIVE NOZZLE CHARACTERIZATION  
 Liquid Propellant Test Series

<u>Nozzle</u>	<u>Evaluation</u>
438	Bore rough, even erosion, slight cylindrical cracks
445	Bore rough, even erosion, slight spalling, cylindrical cracks
447	Bore rough, even erosion, spalling, cylindrical cracks
450	Bore rough, even erosion, spalling, cylindrical cracks
453	Bore rough, even erosion
461	Bore rough, even erosion, spalling
462	Bore rough, even erosion, spalling
465	Bore smooth, even erosion, laminations
466	Bore smooth, even erosion
472	Bore rough, uneven erosion, laminations
473	Bore smooth, even erosion
475	Bore rough, uneven erosion, spalling, coating remaining on entrance and part of exit section
476	Bore smooth, even erosion, slight spalling
477	Bore smooth, even erosion
478	Bore rough, even erosion, spalling
479	Bore rough, even erosion, slight spalling
481	Bore smooth, even erosion, slight spalling
484	Bore smooth, slight erosion, partially undercut at entrance section
485	Bore rough, uneven erosion, spalling, coating remaining on entrance and exit section
486	Bore rough, uneven erosion, spalling, coating remaining on entrance section

TABLE 12 (Continued)  
POST TEST NOZZLE EROSION EVALUATION  
ABLATIVE NOZZLE CHARACTERIZATION

Liquid Propellant Test Series

<u>Nozzle</u>	<u>Evaluation</u>
487	Bore rough, even erosion, spalling, coating remaining on entrance and exit section
488	Bore rough, uneven erosion, spalling, coating remaining on entrance and exit section
492	Bore smooth, even erosion
493	Bore smooth, even erosion, one cylindrical crack
494	Bore rough, even erosion, spalling, insert eroded
495	Bore rough, even erosion, spalling
496	Bore rough, even erosion, spalling
497	Bore smooth, even erosion, cylindrical cracks
498	Bore smooth, even erosion
499	Bore smooth, even erosion, laminations
500	Bore smooth, even erosion
501	Bore rough, even erosion, cylindrical cracks
502	Bore rough, even erosion, cylindrical cracks
503	Bore rough, even erosion, slight cylindrical cracks
504	Bore rough, even erosion, spalling
505	Bore rough, even erosion, slight spalling, cylindrical cracks
507	Bore rough, even erosion, deep cylindrical cracks
509	Bore rough, even erosion, laminations
514	Bore rough, even erosion, spalling, coating remaining on entrance and exit section
515	Bore rough, uneven erosion, spalling, coating remaining on entrance and exit section
516	Bore smooth, even erosion

TABLE 12 (Continued)  
 POST TEST NOZZLE VISUAL EVALUATION  
 ABLATIVE NOZZLE CHARACTERIZATION  
 Liquid Propellant Test Series

<u>Nozzle</u>	<u>Evaluation</u>
517	Bore rough, even erosion, spalling
518	Bore smooth, even erosion
519	Bore rough, even erosion, one cylindrical crack
520	Bore smooth, even erosion
522	Bore smooth, even erosion, cylindrical cracks
524	Bore smooth, even erosion, one cylindrical crack
526	Bore rough and filled, even erosion, material flow
527	Nozzle section blown out
528	Bore rough, even erosion, some spalling, inlet section partially separated from holder



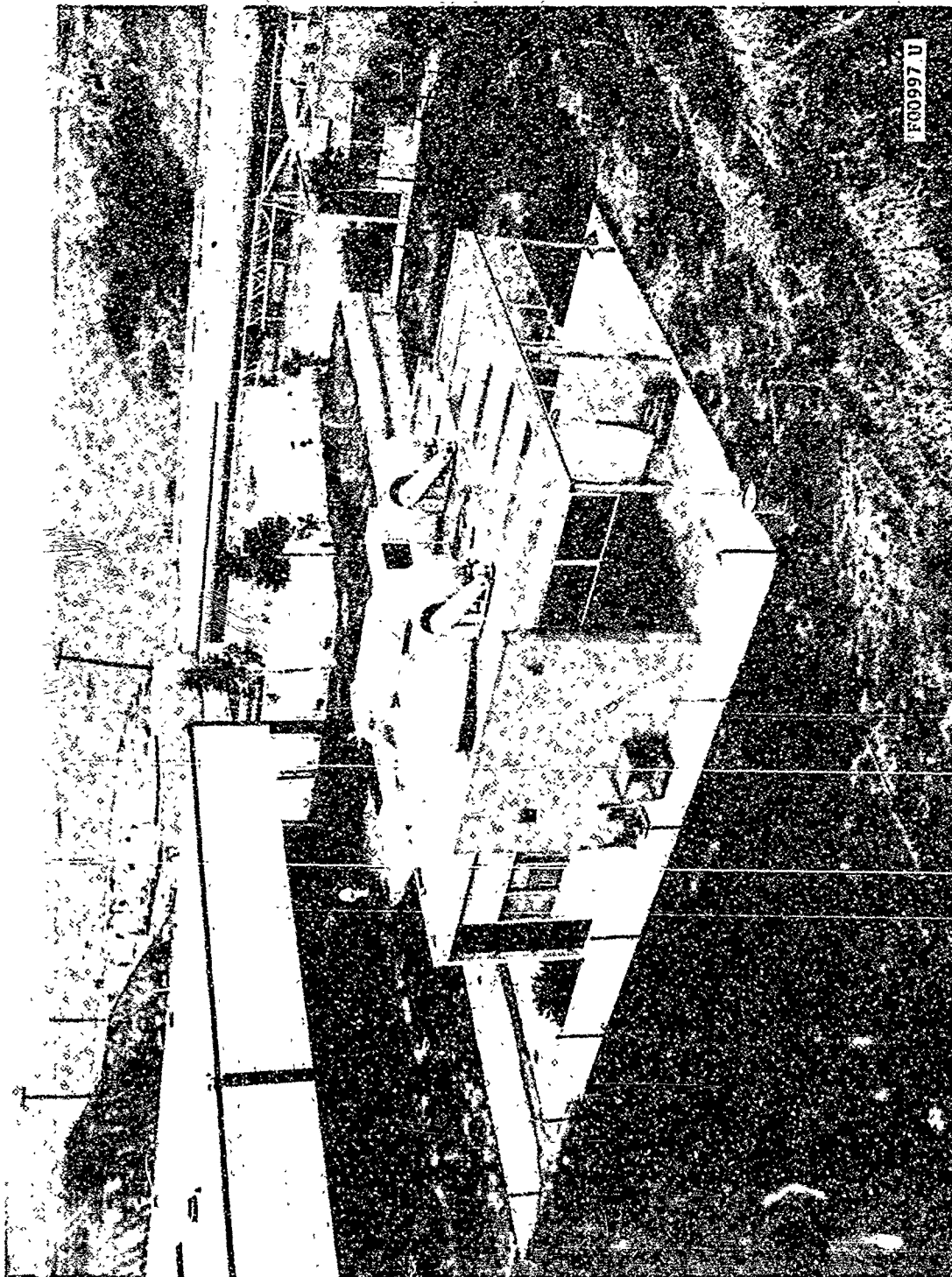


FIGURE 1. AEROTHERMOCHEMICAL LABORATORY TEST CELLS 6 AND 7

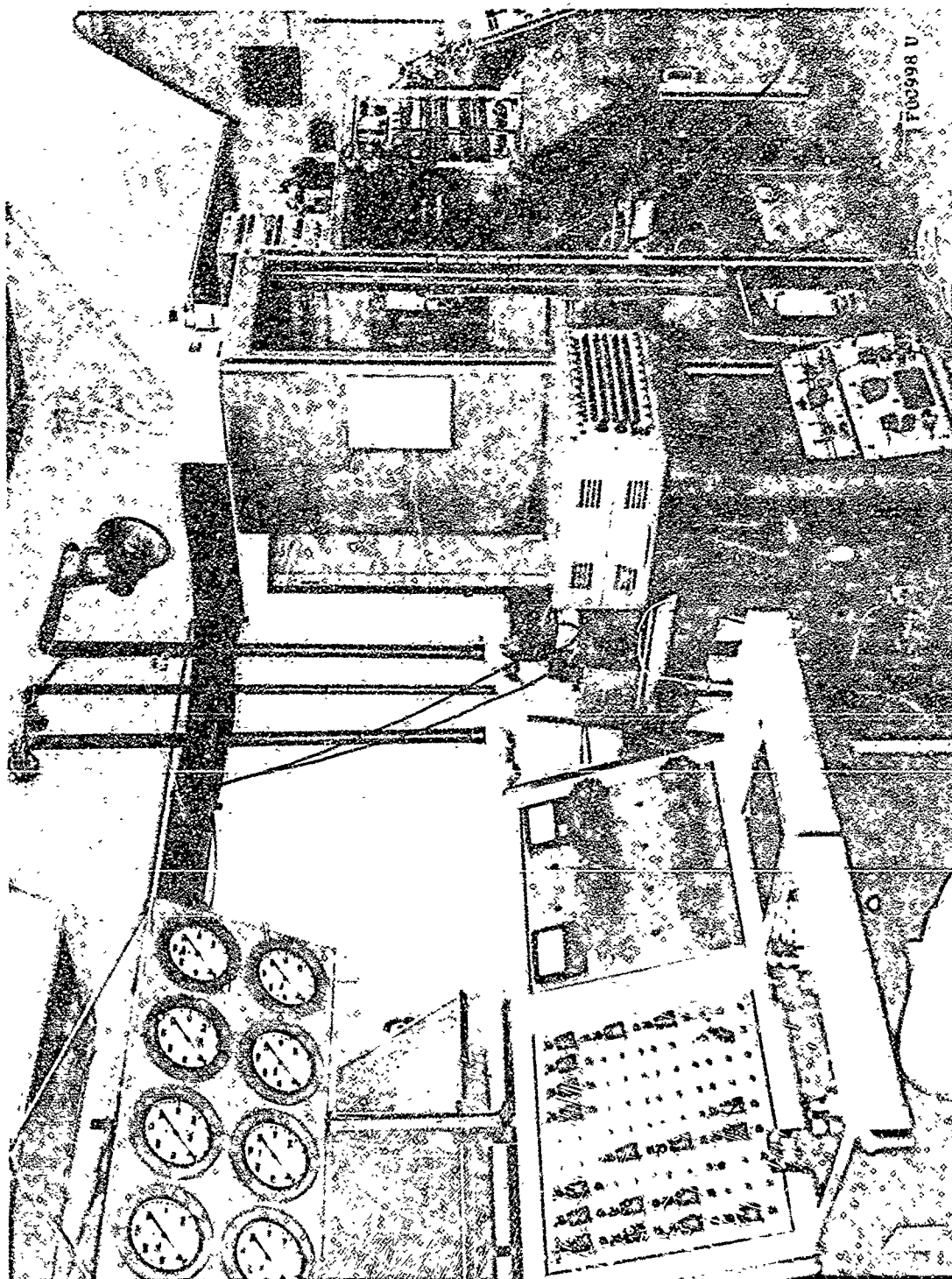


FIGURE 2. ATC TEST CELL 6 CONTROL ROOM

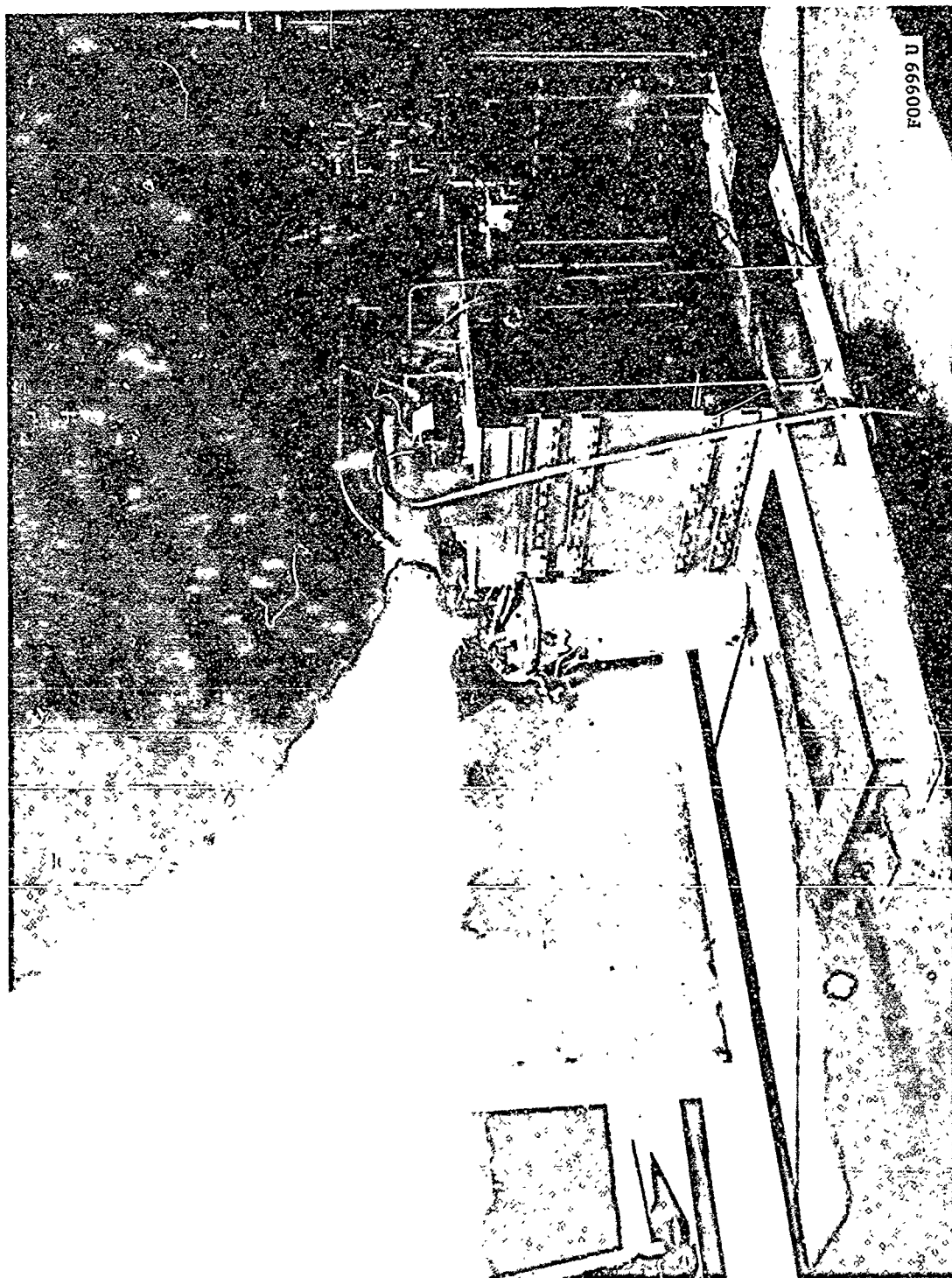
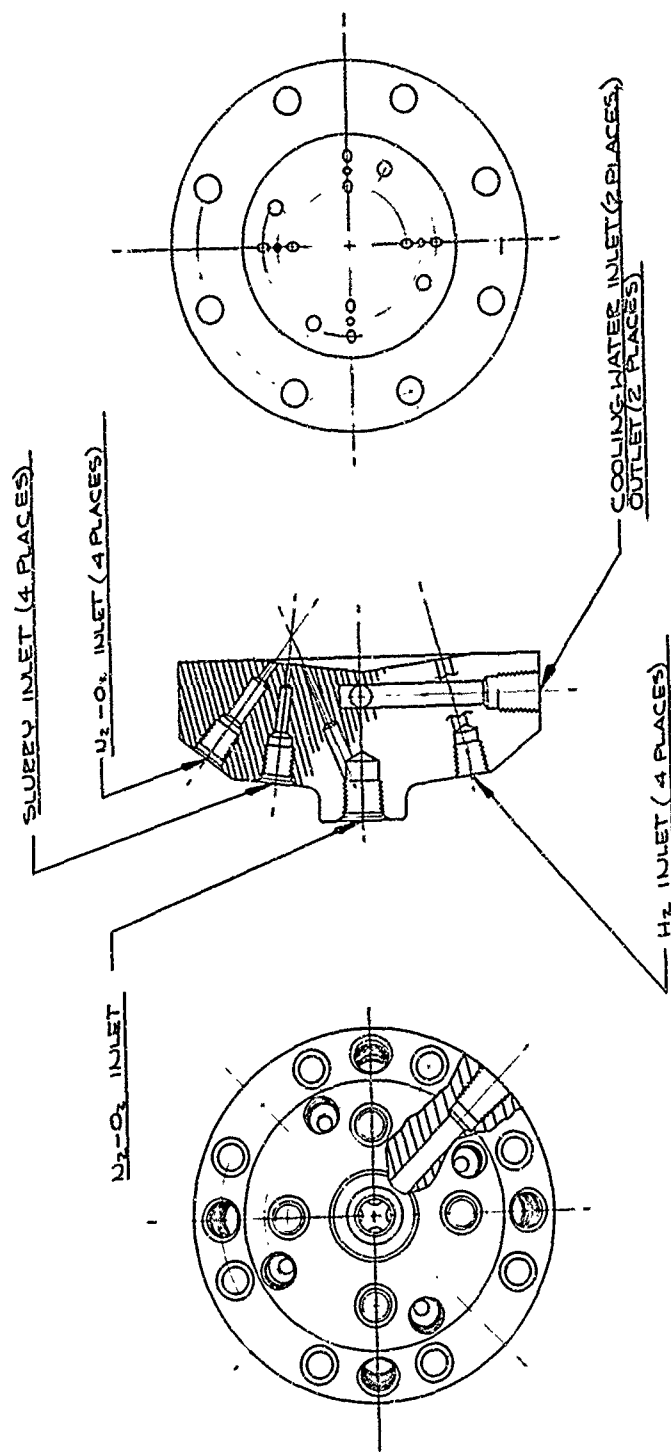


FIGURE 3. ATC TEST CELL 6 SIMULATOR FIRING



F01000 U

FIGURE 4. SOLID PROPELLANT SIMULATOR ROCKET MOTOR  
INJECTOR - WRIGHT FIELD NOZZLE TEST (COPPER)

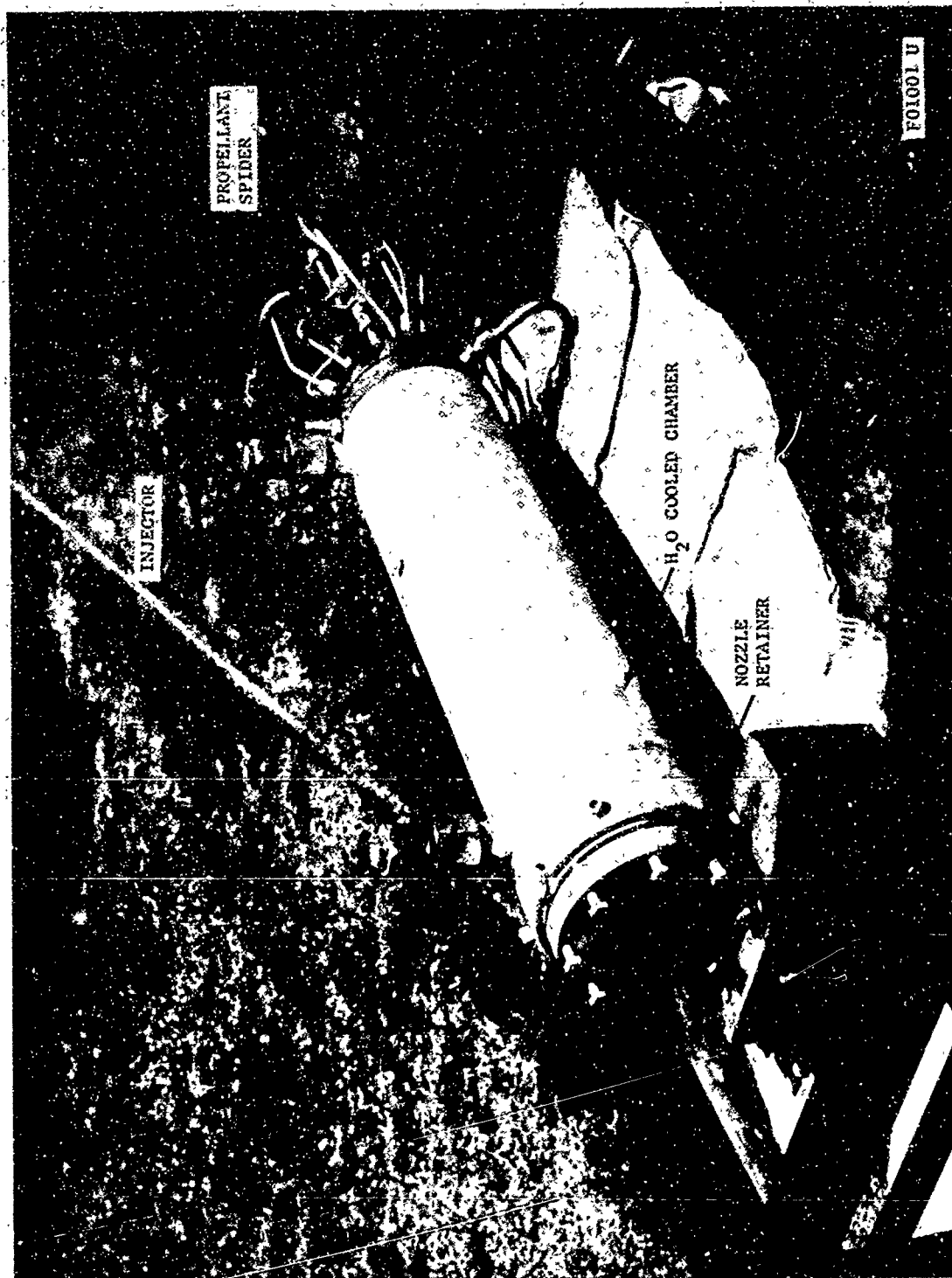
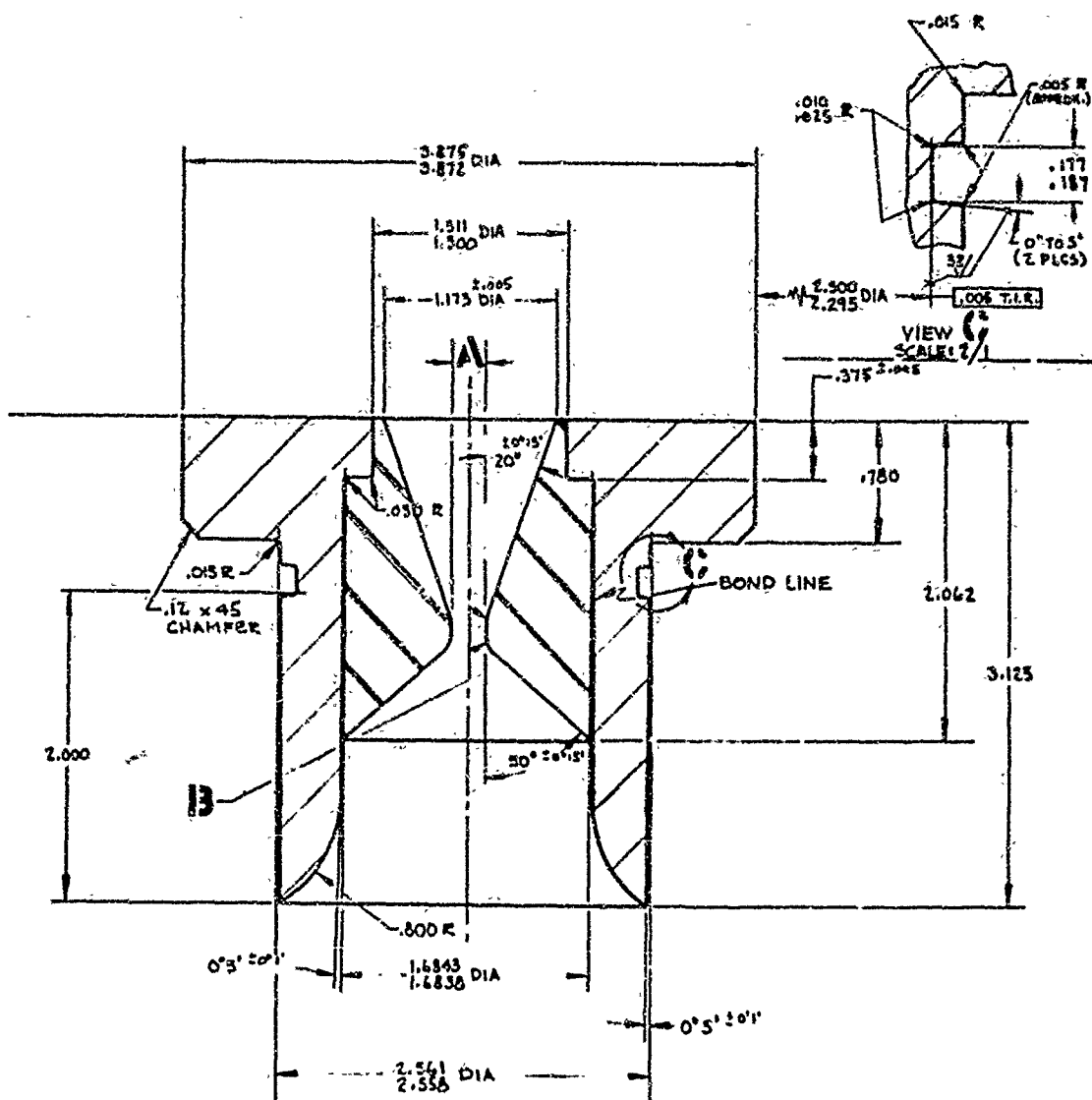


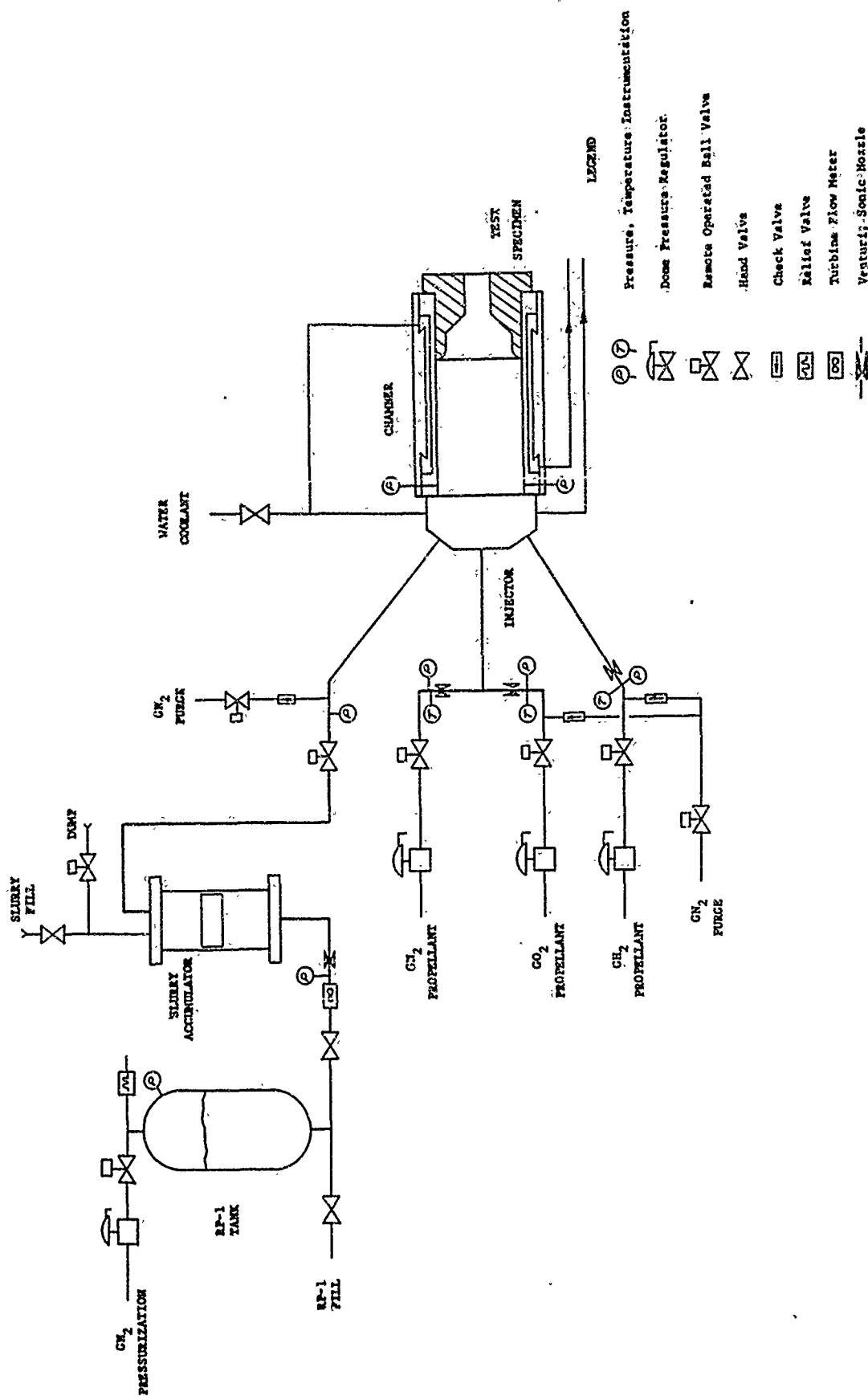
FIGURE 5. SOLID PROPELLANT SIMULATOR ROCKET MOTOR HARDWARE



NOTE: A SHRINK FACTOR OF .001 IN/IN HAS BEEN ADDED TO THE PART DIMENSIONS TO PRODUCE THE DIMENSIONS SHOWN

F01002 U

FIGURE 6. TYPICAL TEST NOZZLE SPECIMEN SCHEMATIC



FOI003 U

FIGURE 7. SOLID PROPELLANT SIMULATED ROCKET MOTOR TEST CELL SCHEM

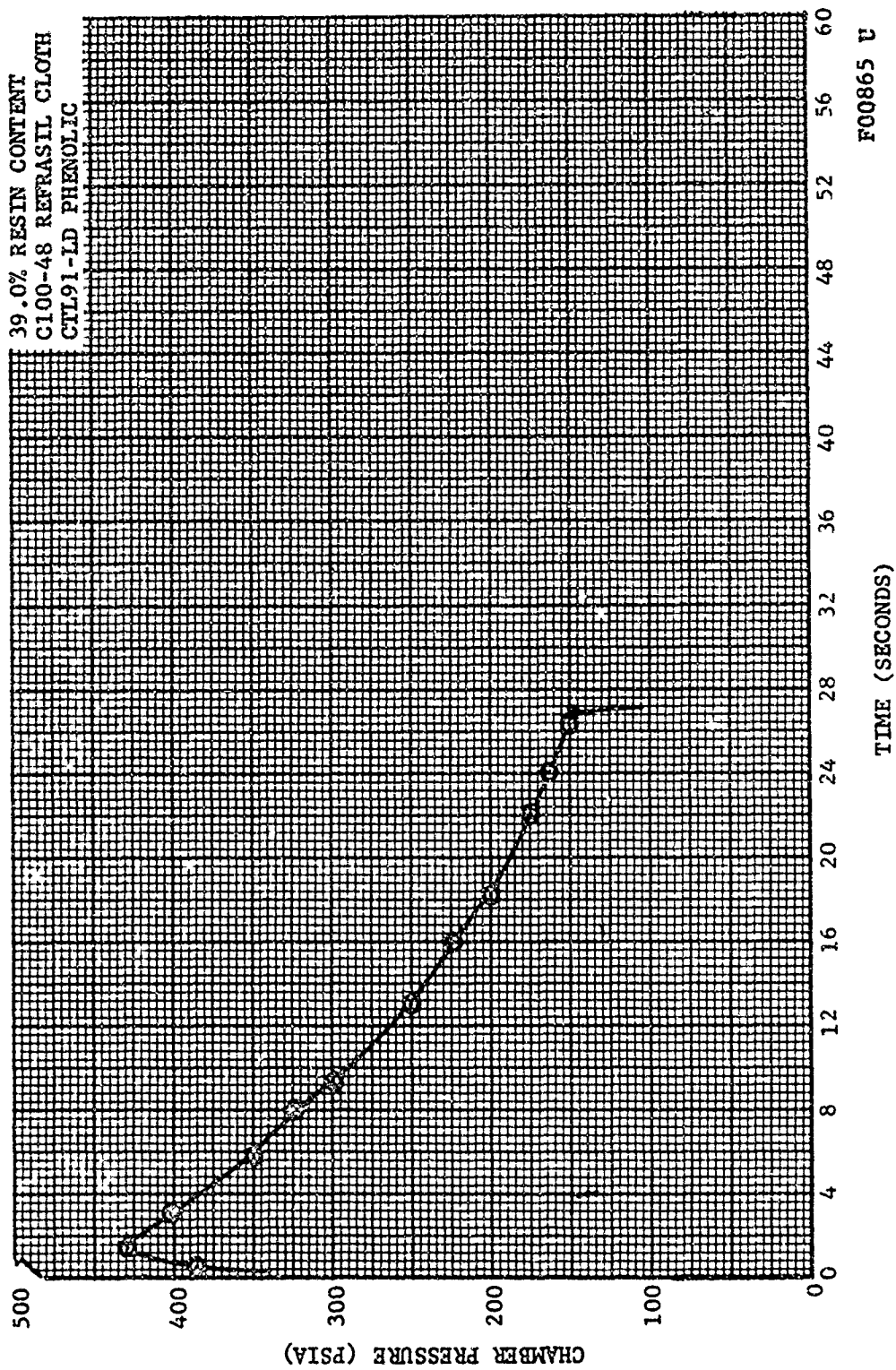


FIGURE 8. CHAMBER PRESSURE VERSUS TIME - MANC-1 NOZZLE



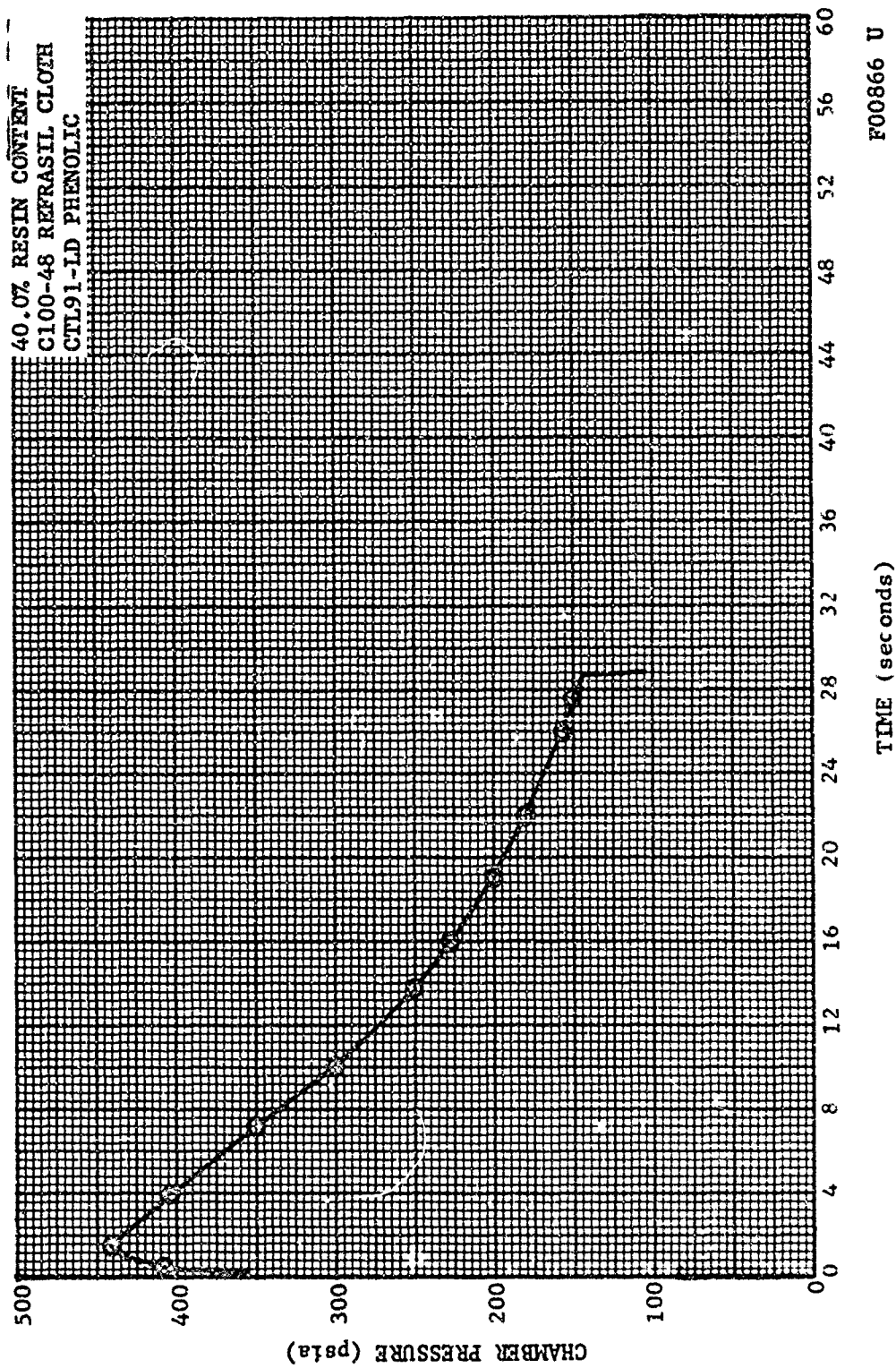


FIGURE 9. CHAMBER PRESSURE VERSUS TIME - MANC-2 NOZZLE

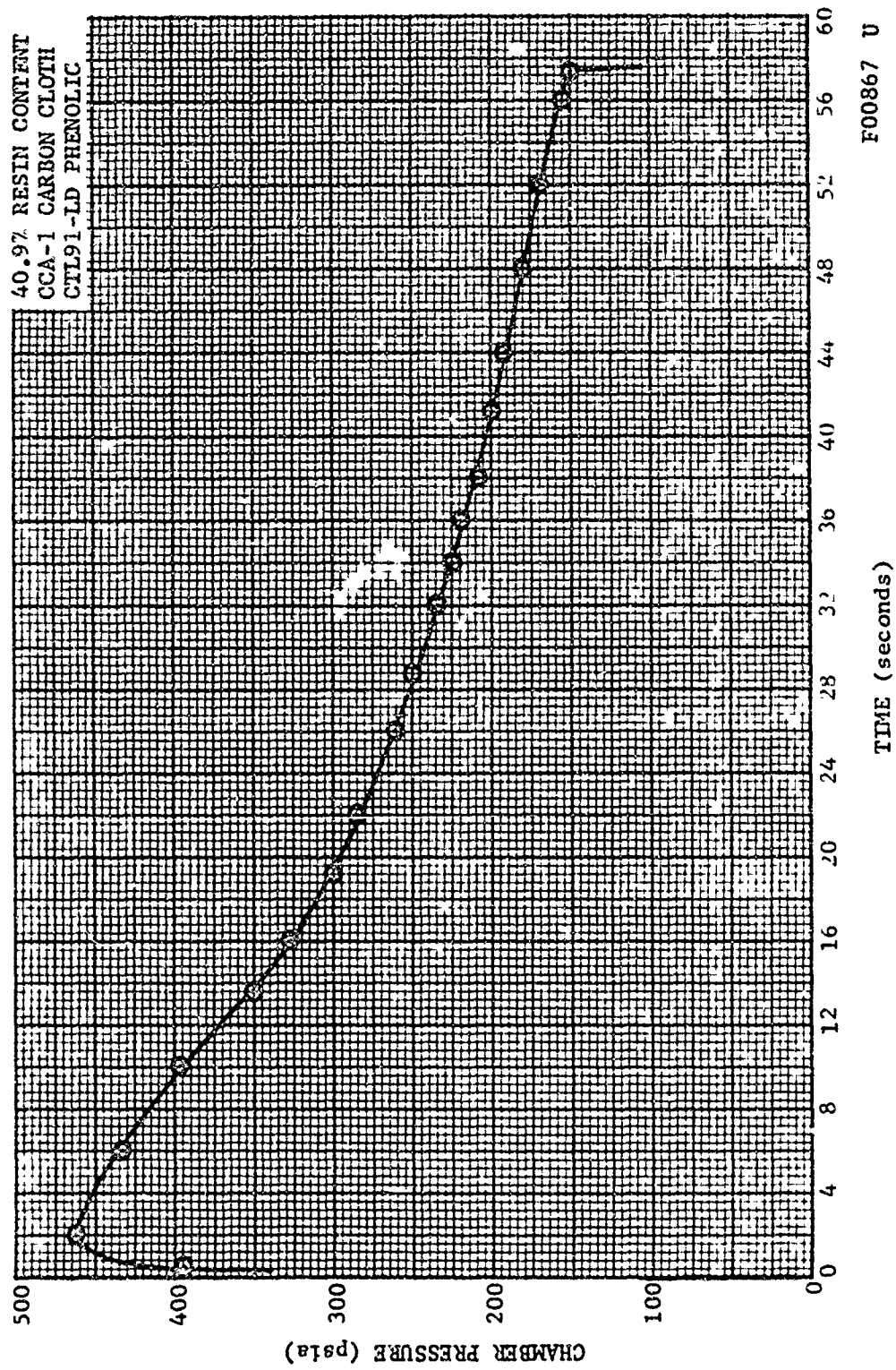


FIGURE 10. CHAMBER PRESSURE VERSUS TIME - MANC-3 NOZZLE

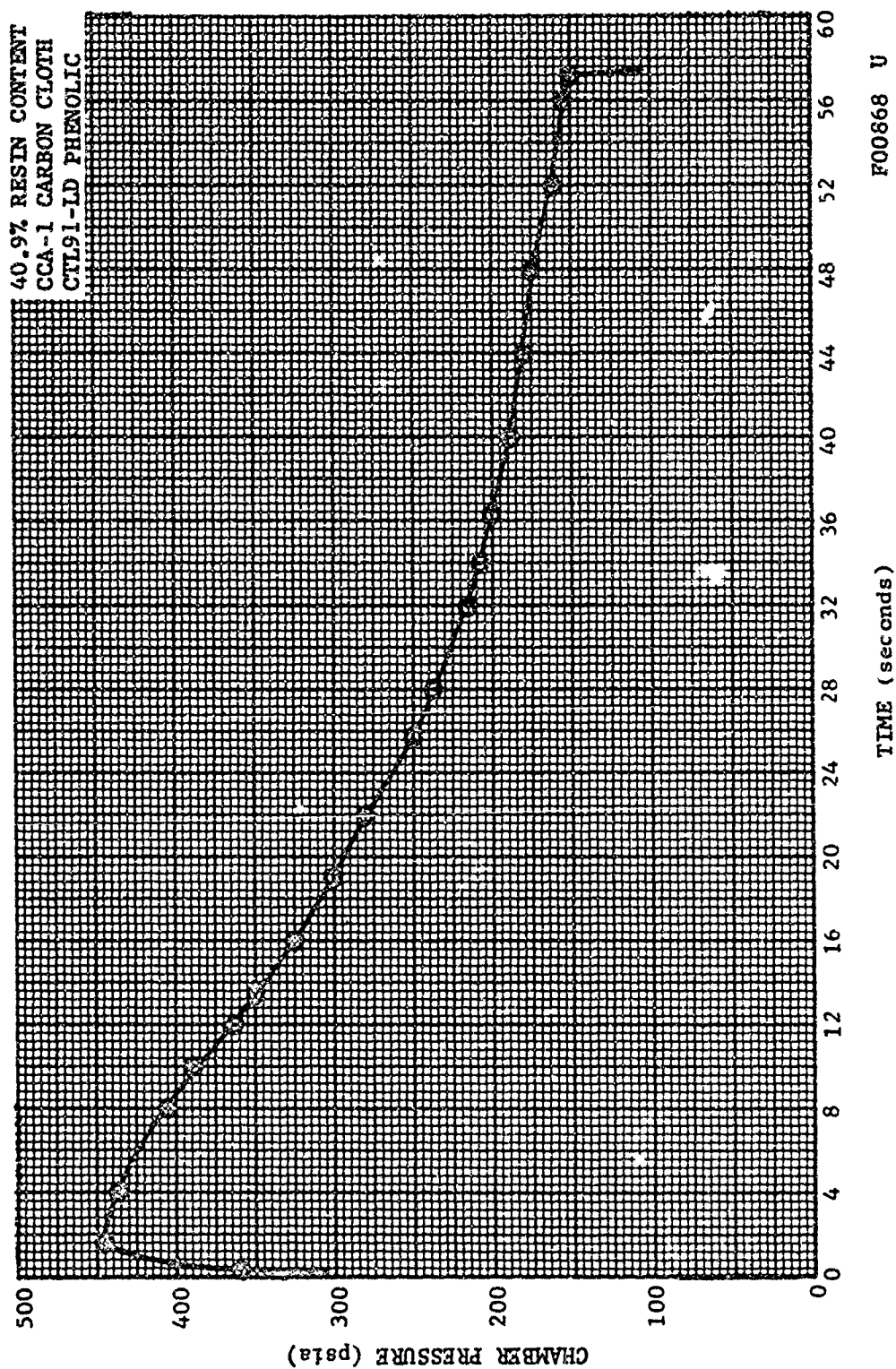


FIGURE 11. CHAMBER PRESSURE VERSUS TIME - MANC-4 NOZZLE

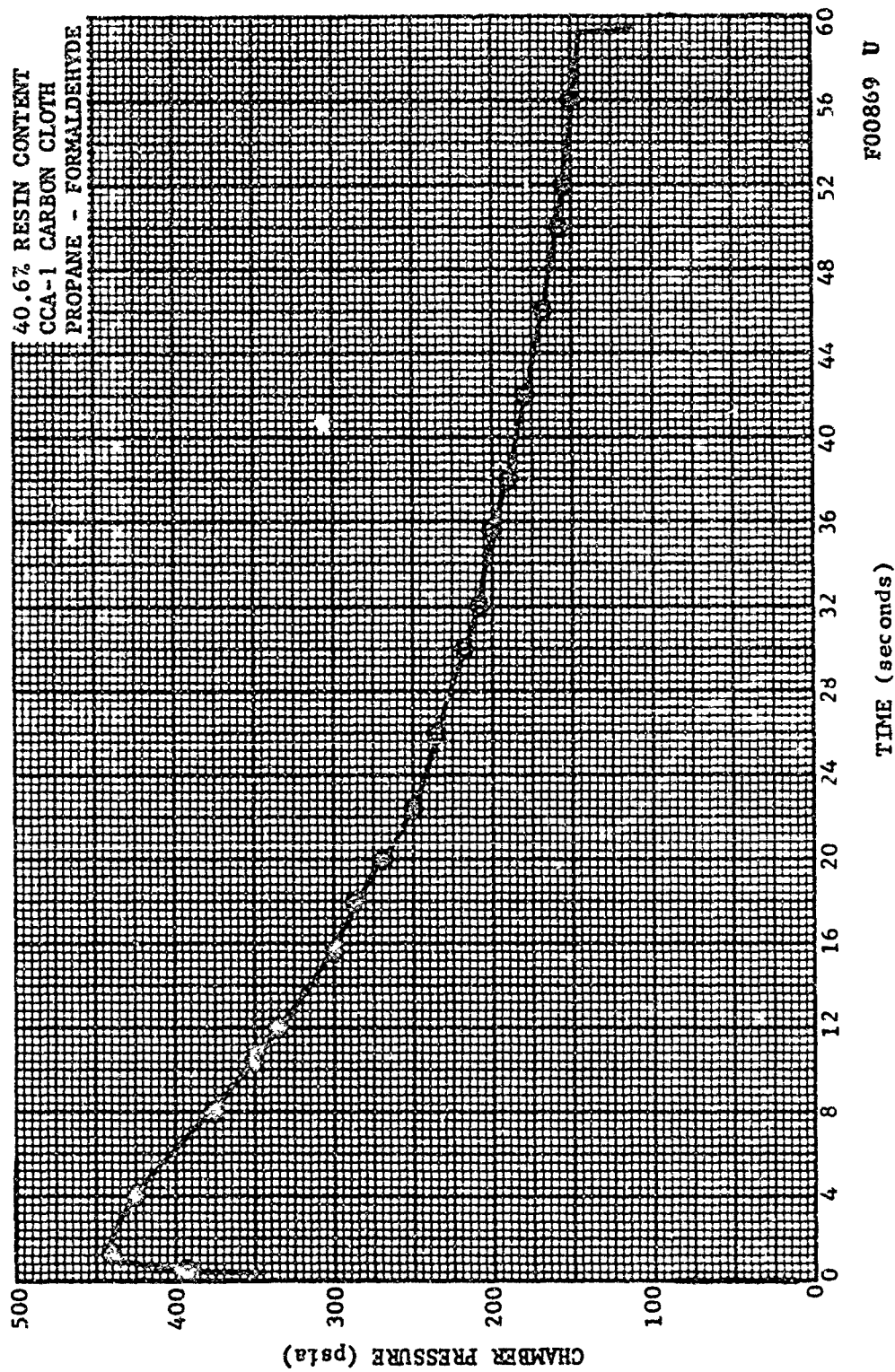


FIGURE 12. CHAMBER PRESSURE VERSUS TIME - ASD 394 NOZZLE

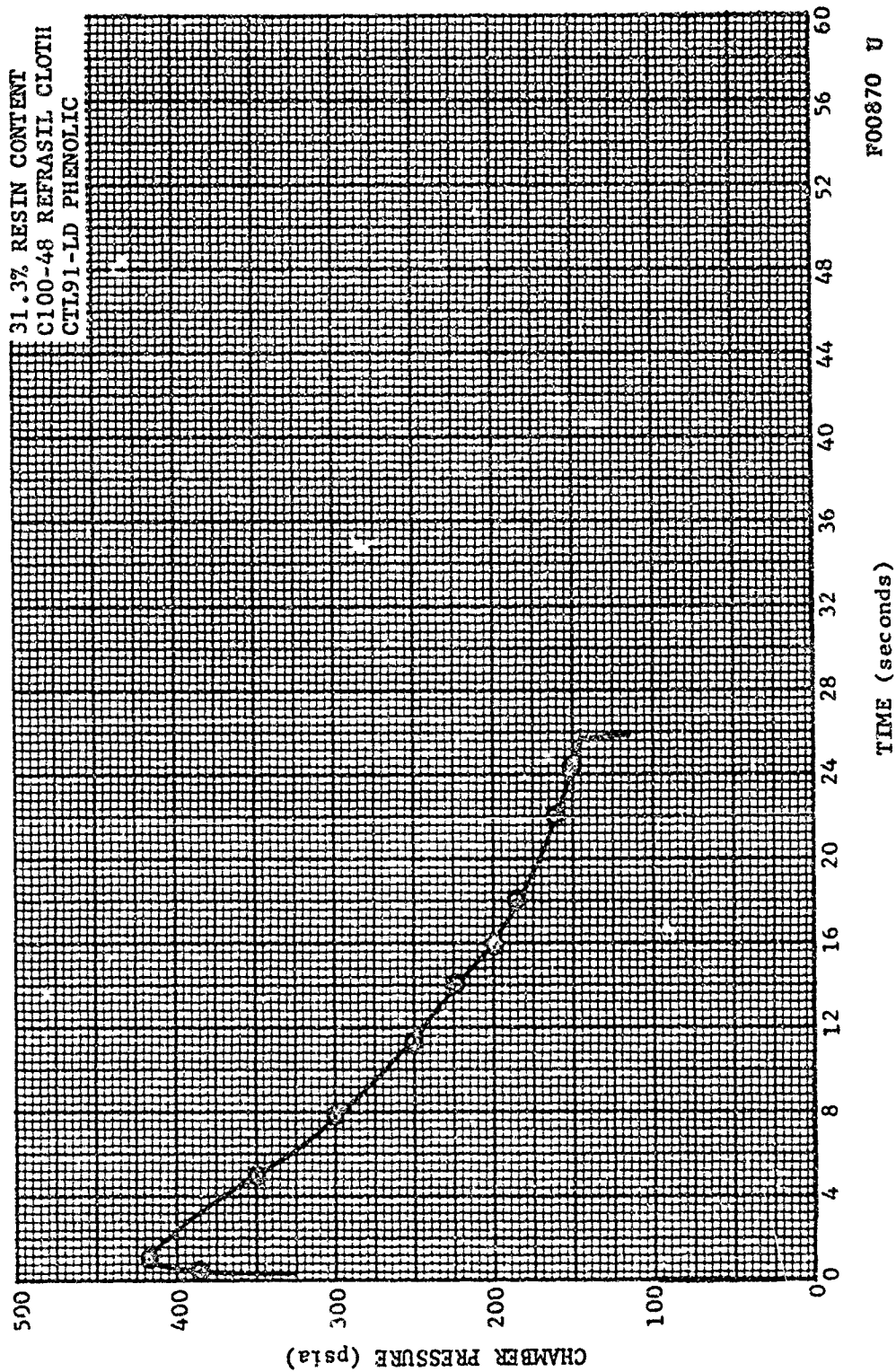


FIGURE 13. CHAMBER PRESSURE VERSUS TIME - ASD 397 NOZZLE



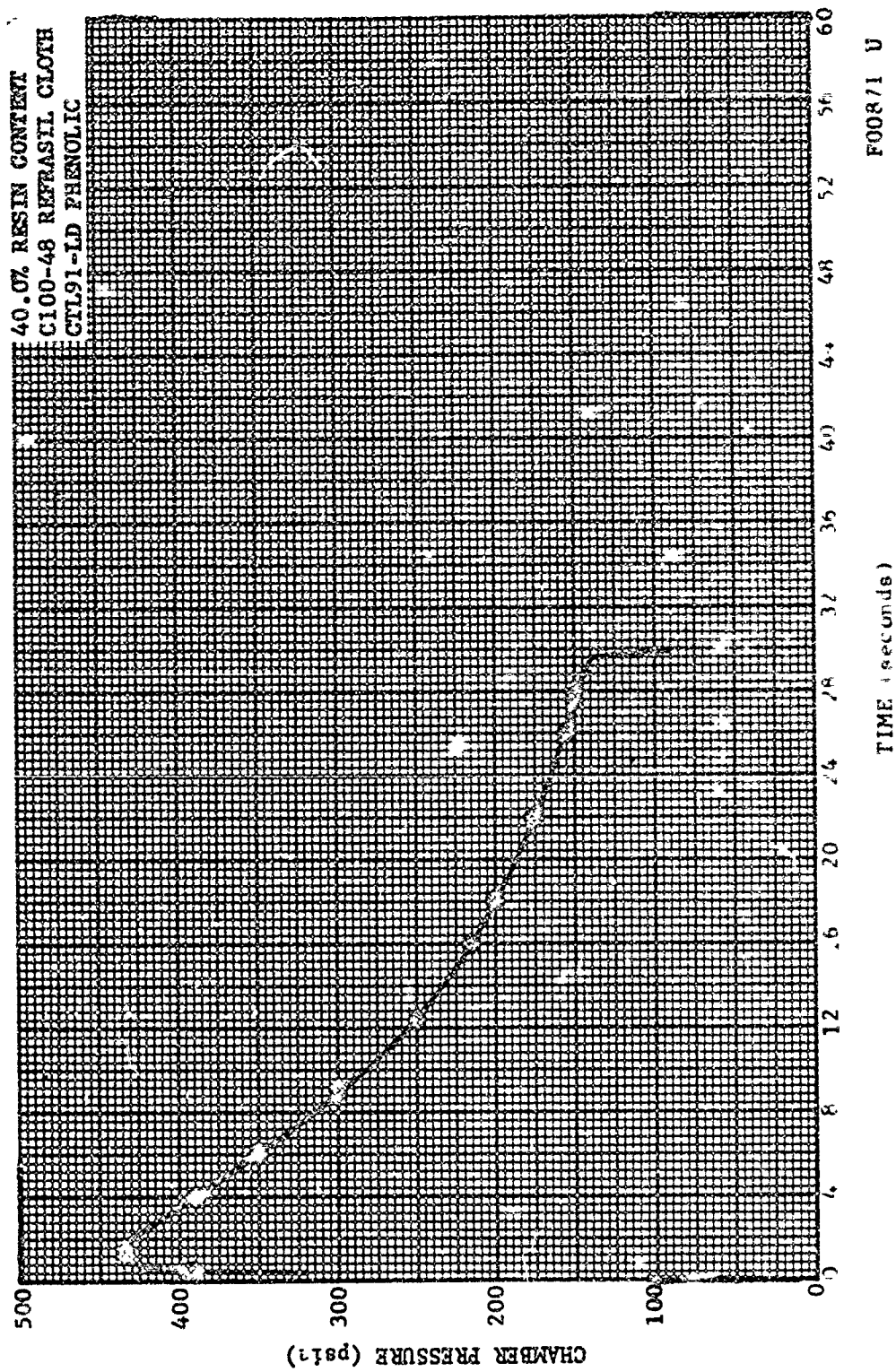


FIGURE 14 CHAMBER PRESSURE VERSUS TIME ASD 398 NOZZLE

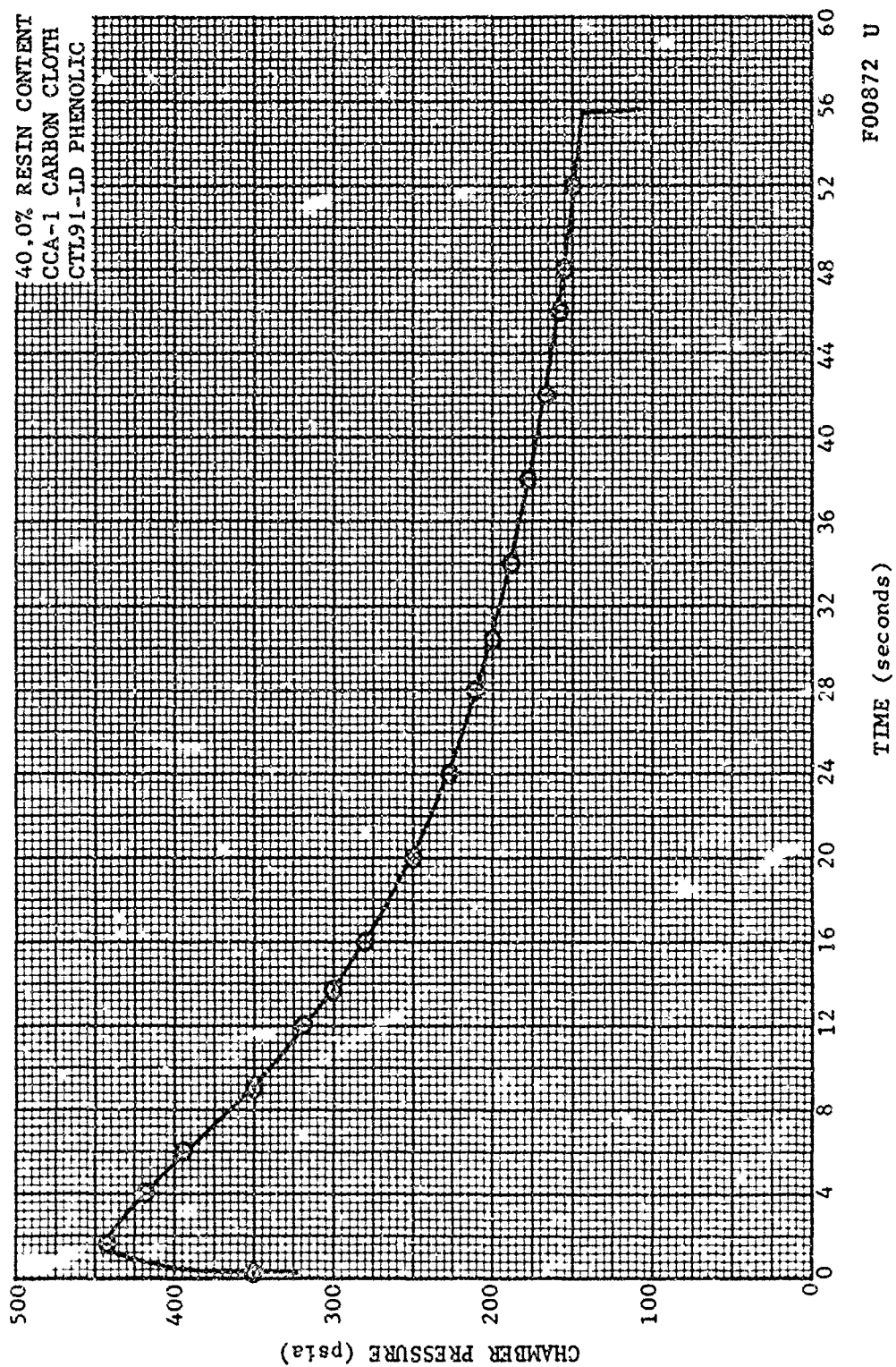


FIGURE 15. CHAMBER PRESSURE VERSUS TIME - ASD 400 NOZZLE

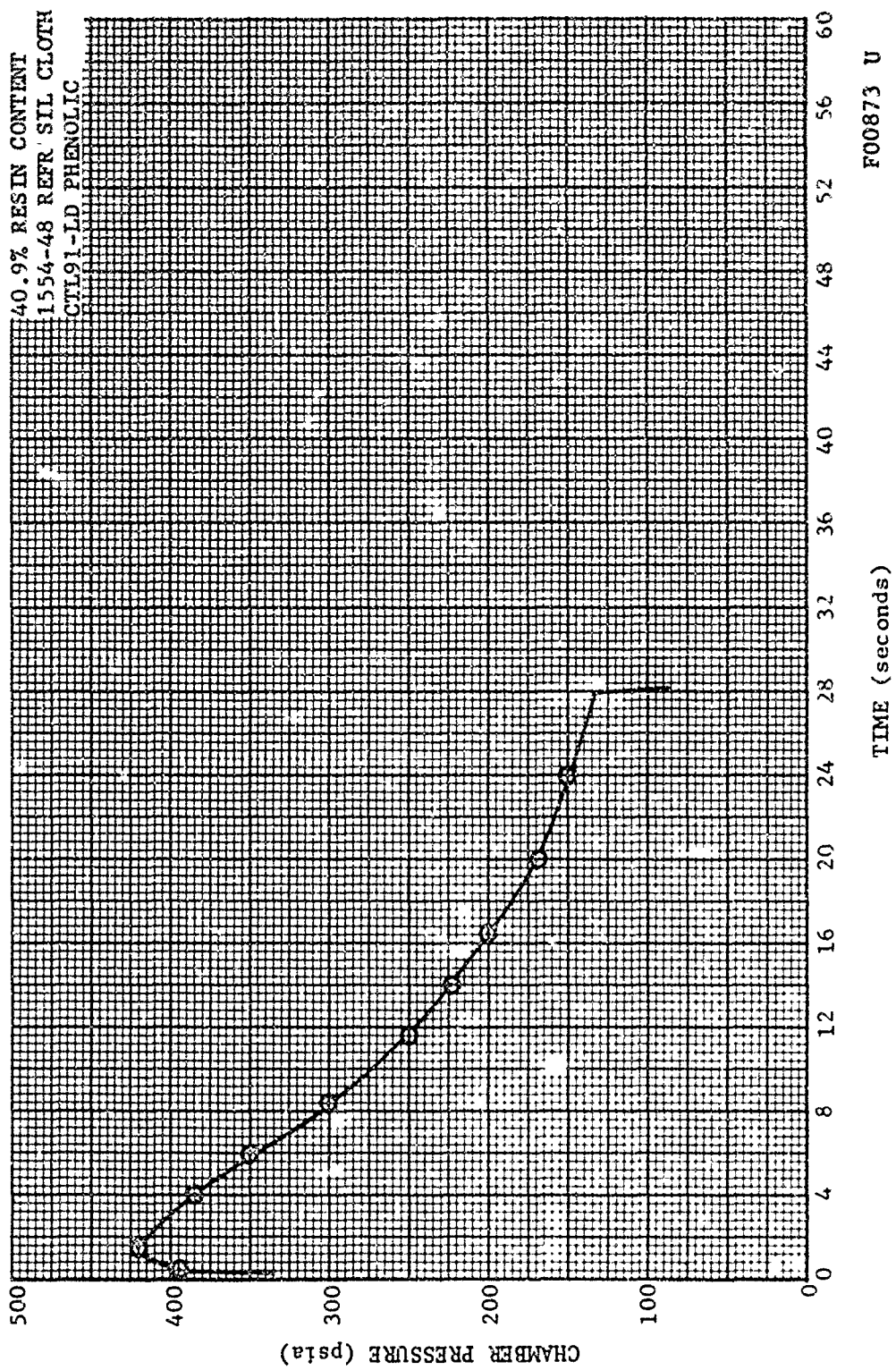


FIGURE 16. CHAMBER PRESSURE VERSUS TIME - ASD 414 NO. ZLE



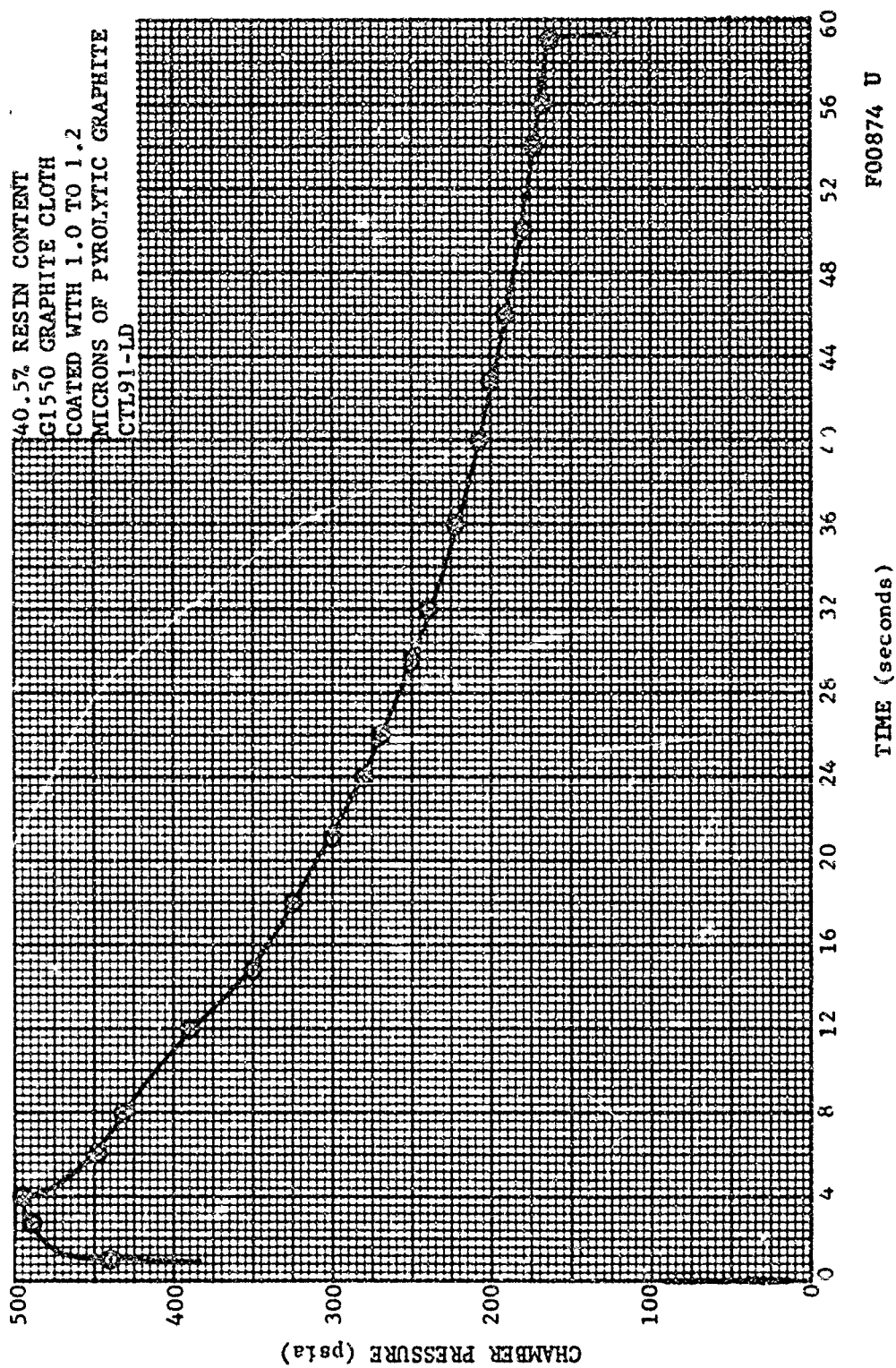


FIGURE 17. CHAMBER PRESSURE VERSUS TIME - ASD 416 NOZZLE

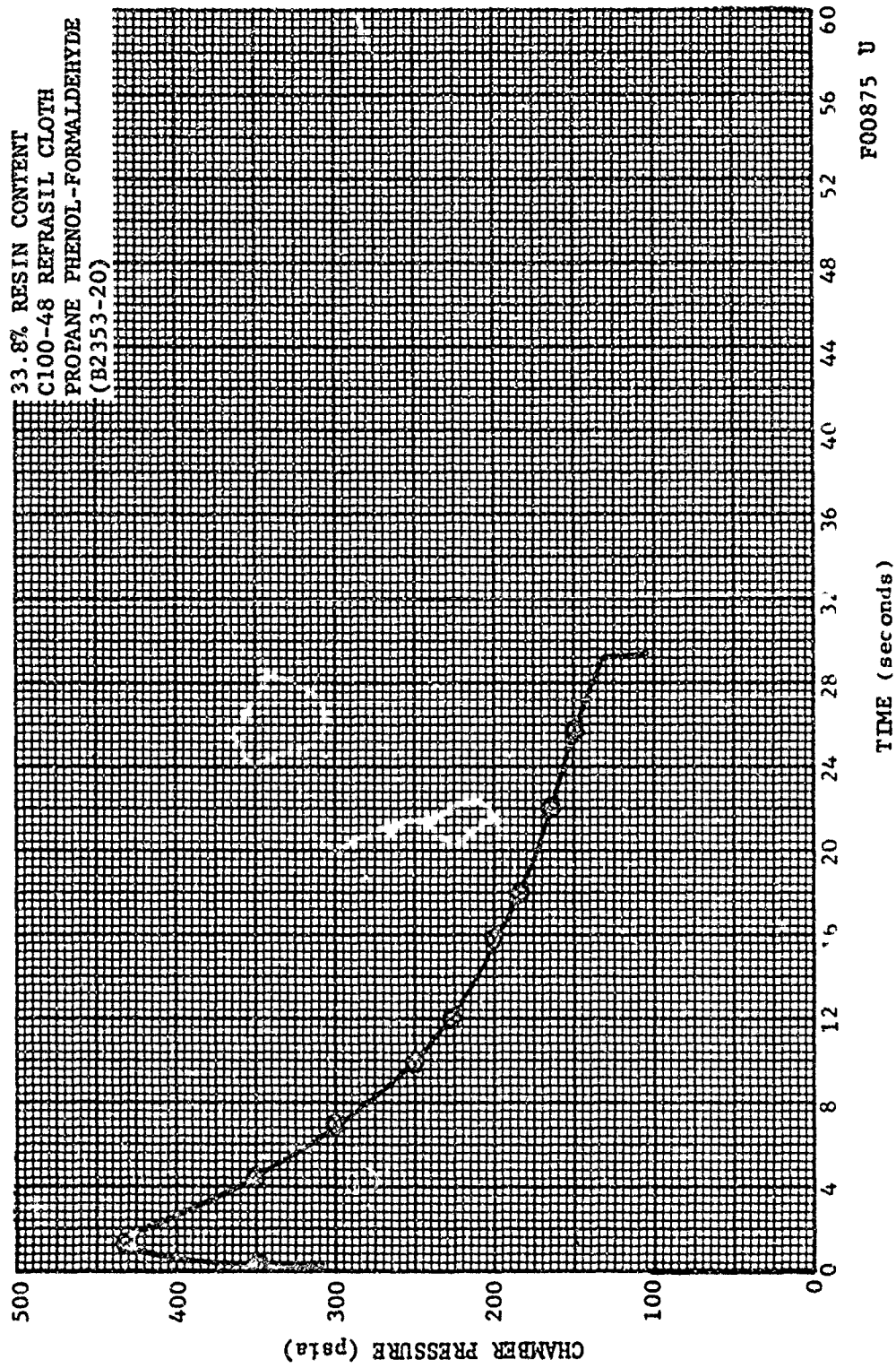


FIGURE 18 CHAMBER PRESSURE VERSUS TIME - ASD 418 NOZZLE

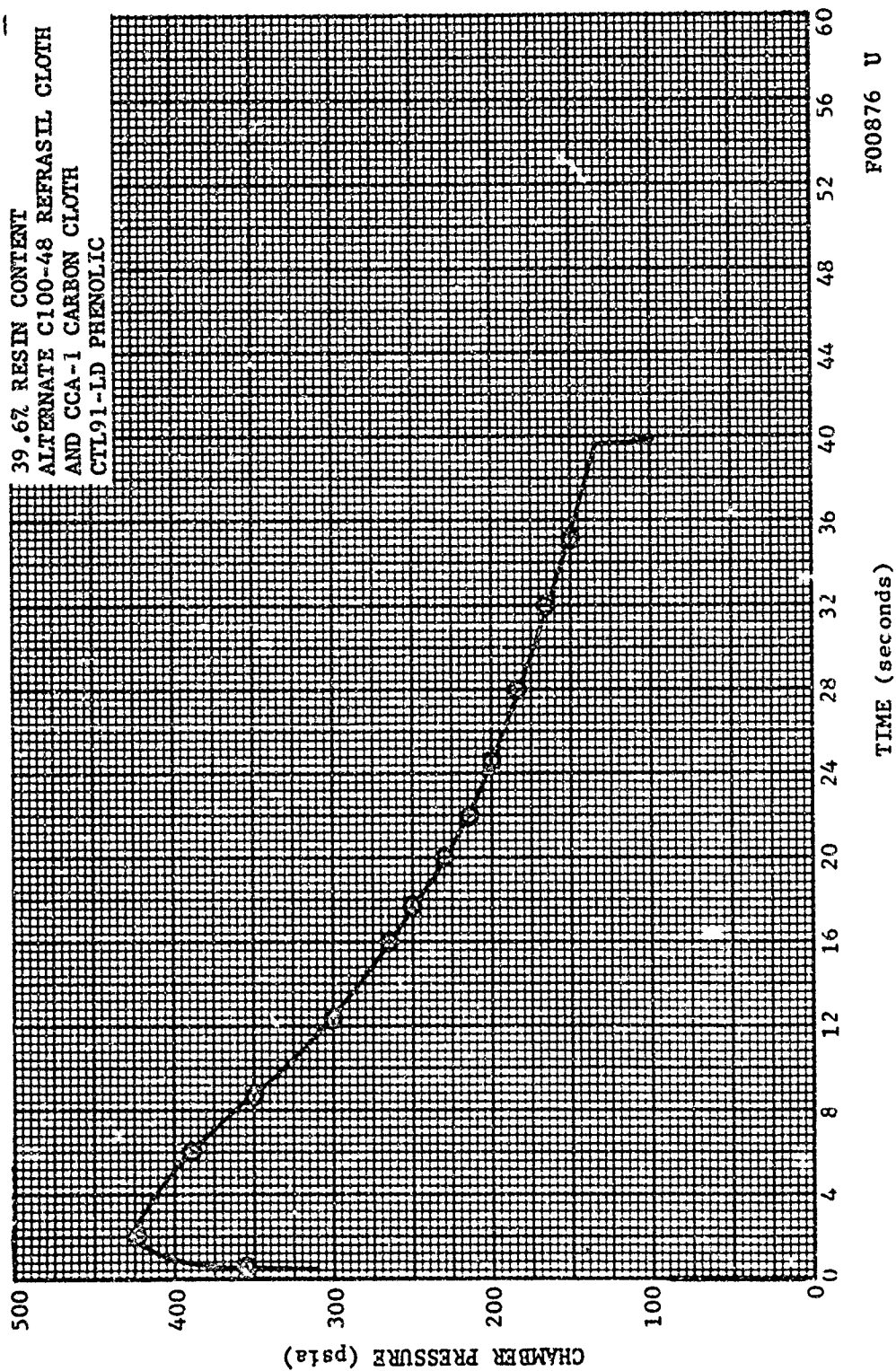


FIGURE 19. CHAMBER PRESSURE VERSUS TIME - ASD 419 NOZZLE

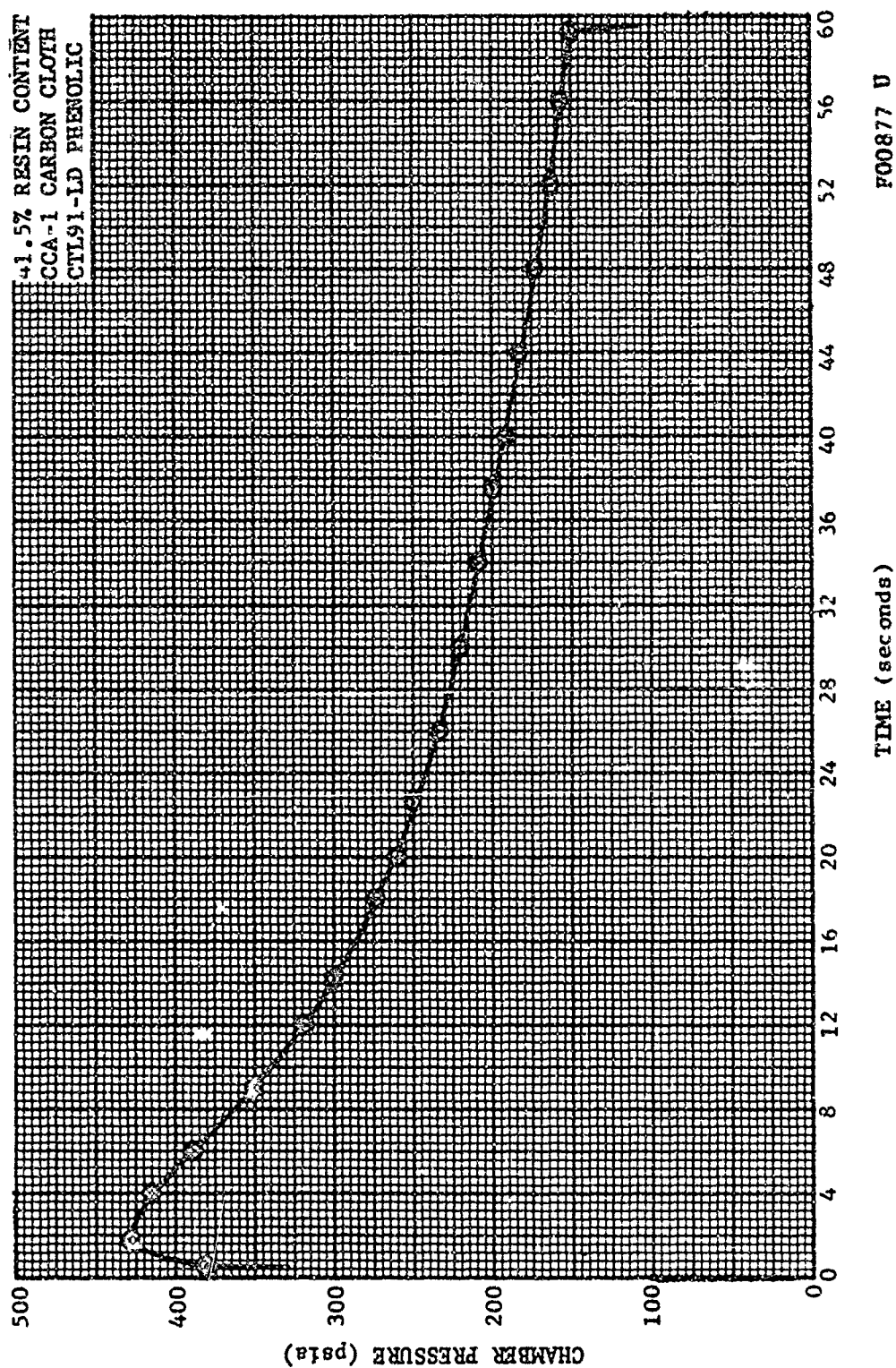


FIGURE 20. CHAMBER PRESSURE VERSUS TIME - ASD 421 NOZZLE

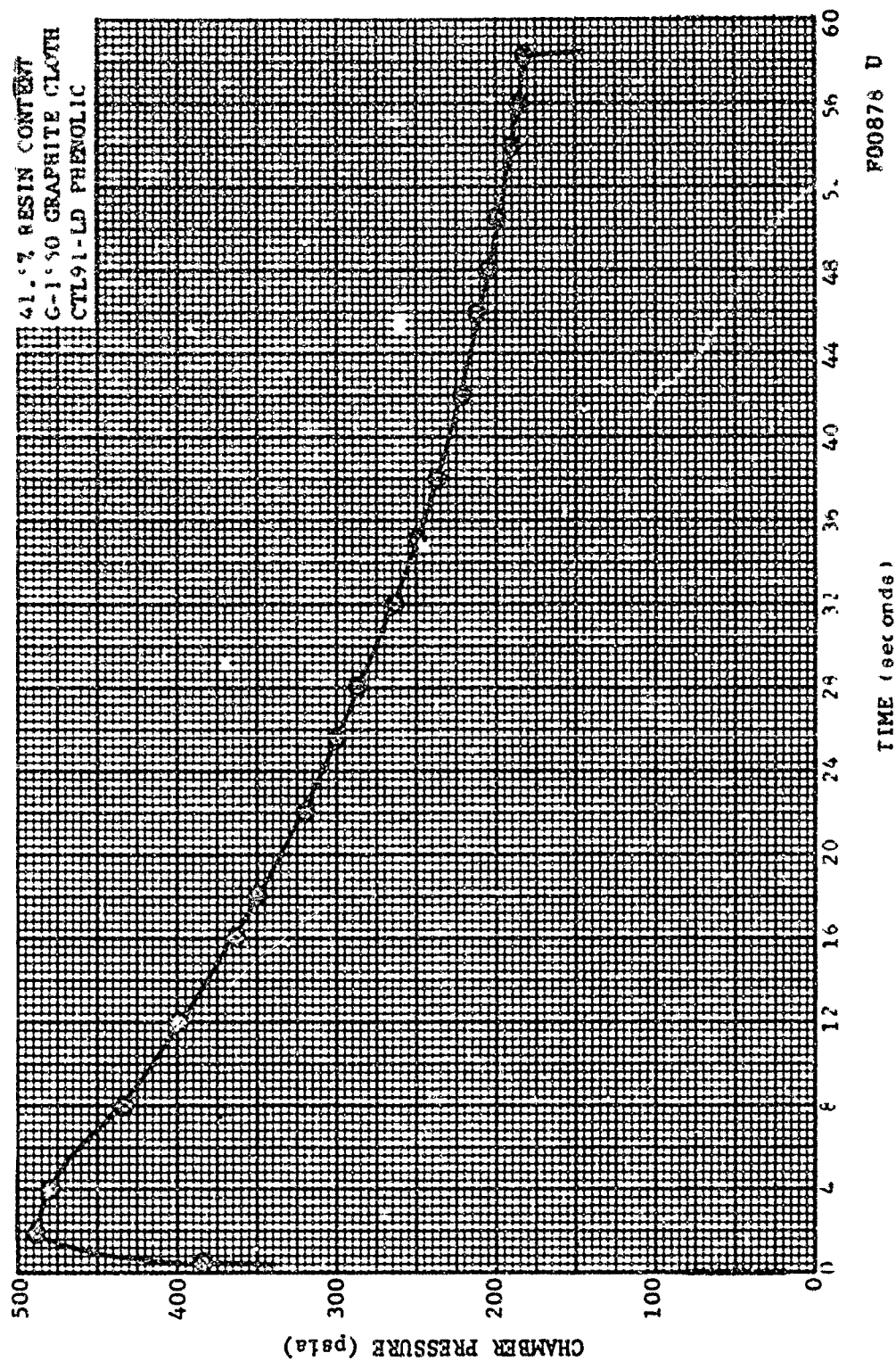


FIGURE 21 CHAMBER PRESSURE VERSUS TIME AND 428 NOZZLE

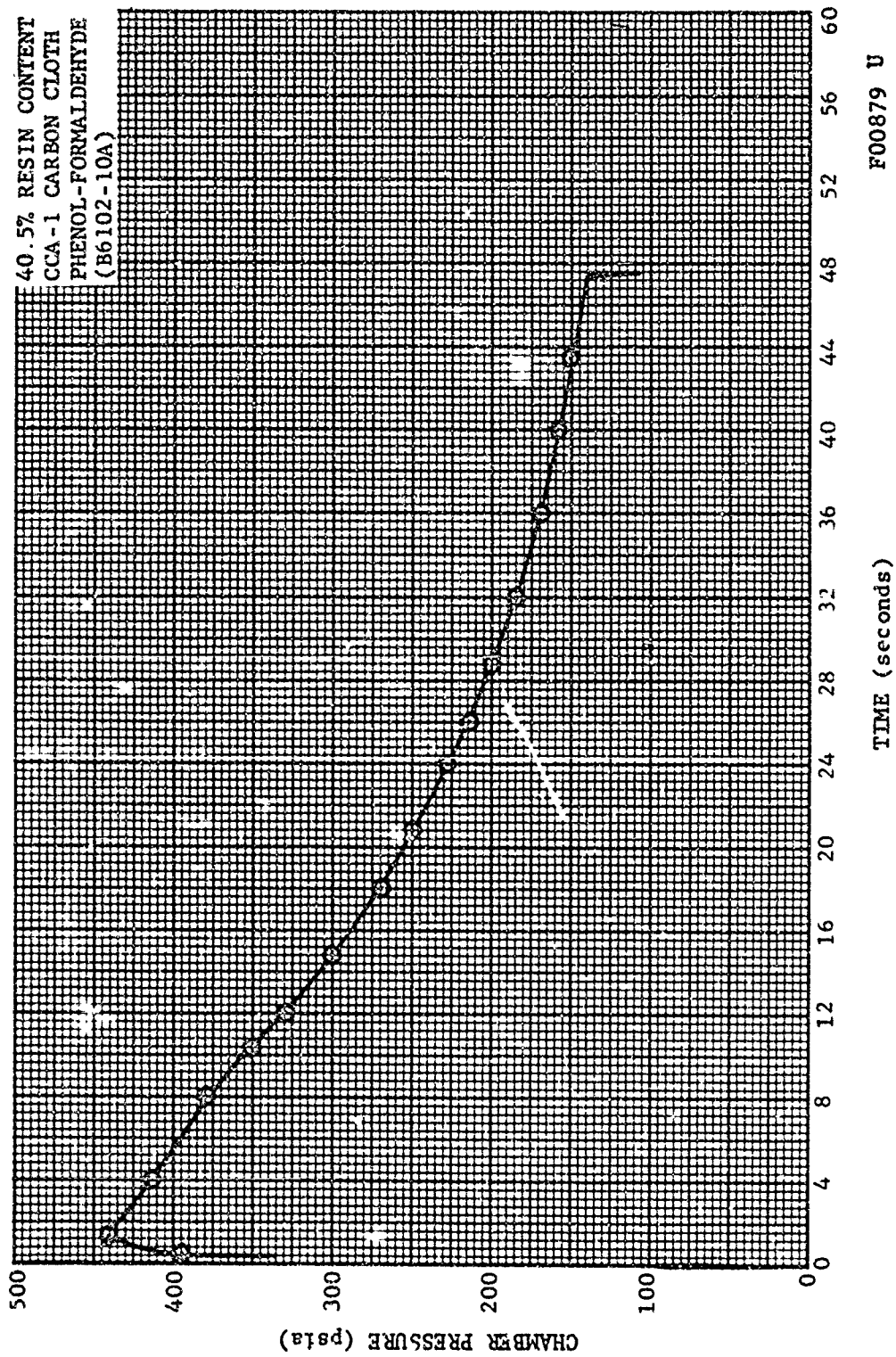


FIGURE 22. CHAMBER PRESSURE VERSUS TIME - ASD 430 NOZZLE



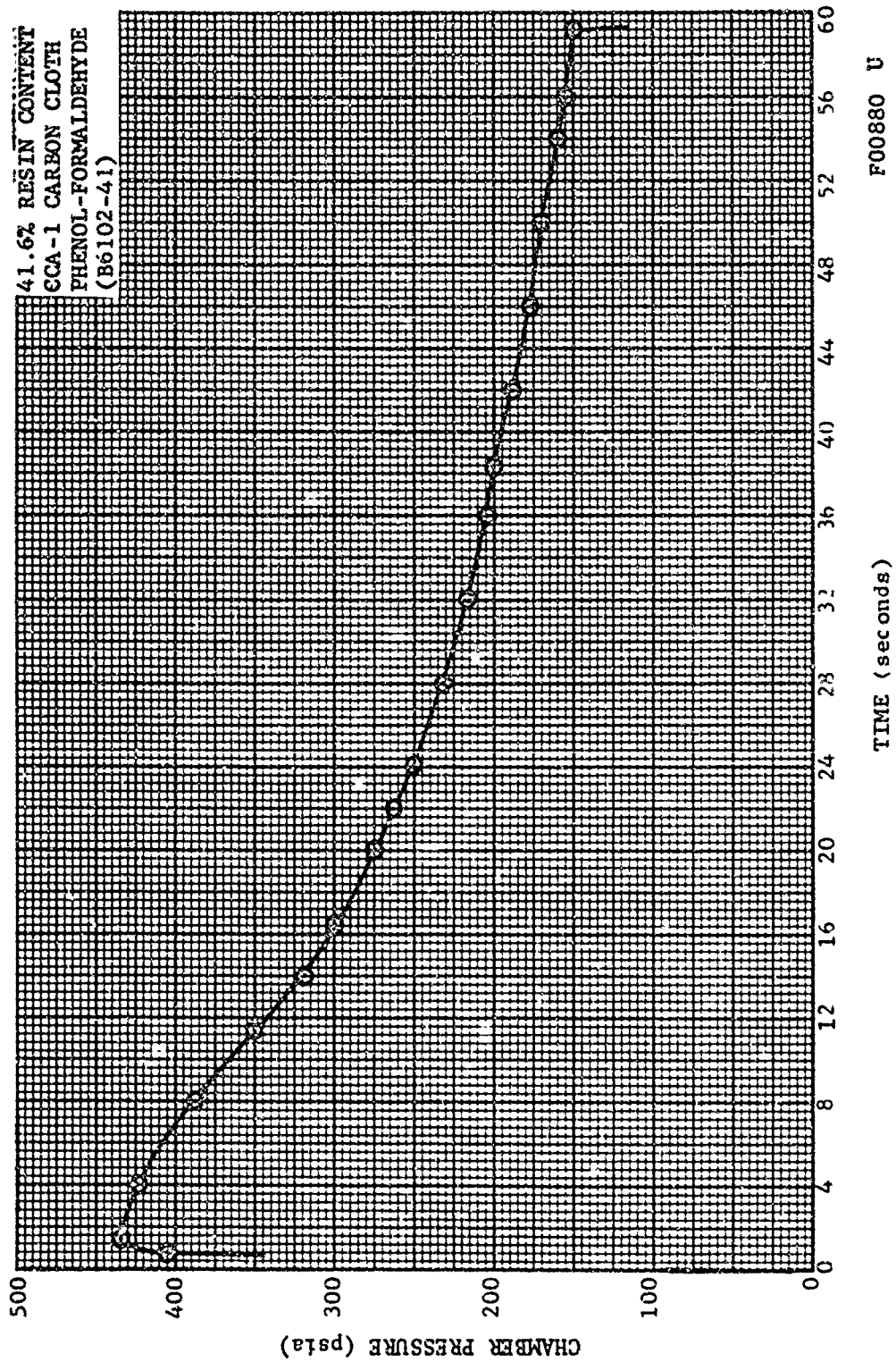


FIGURE 23. CHAMBER PRESSURE VERSUS TIME - ASD 431 NOZZLE

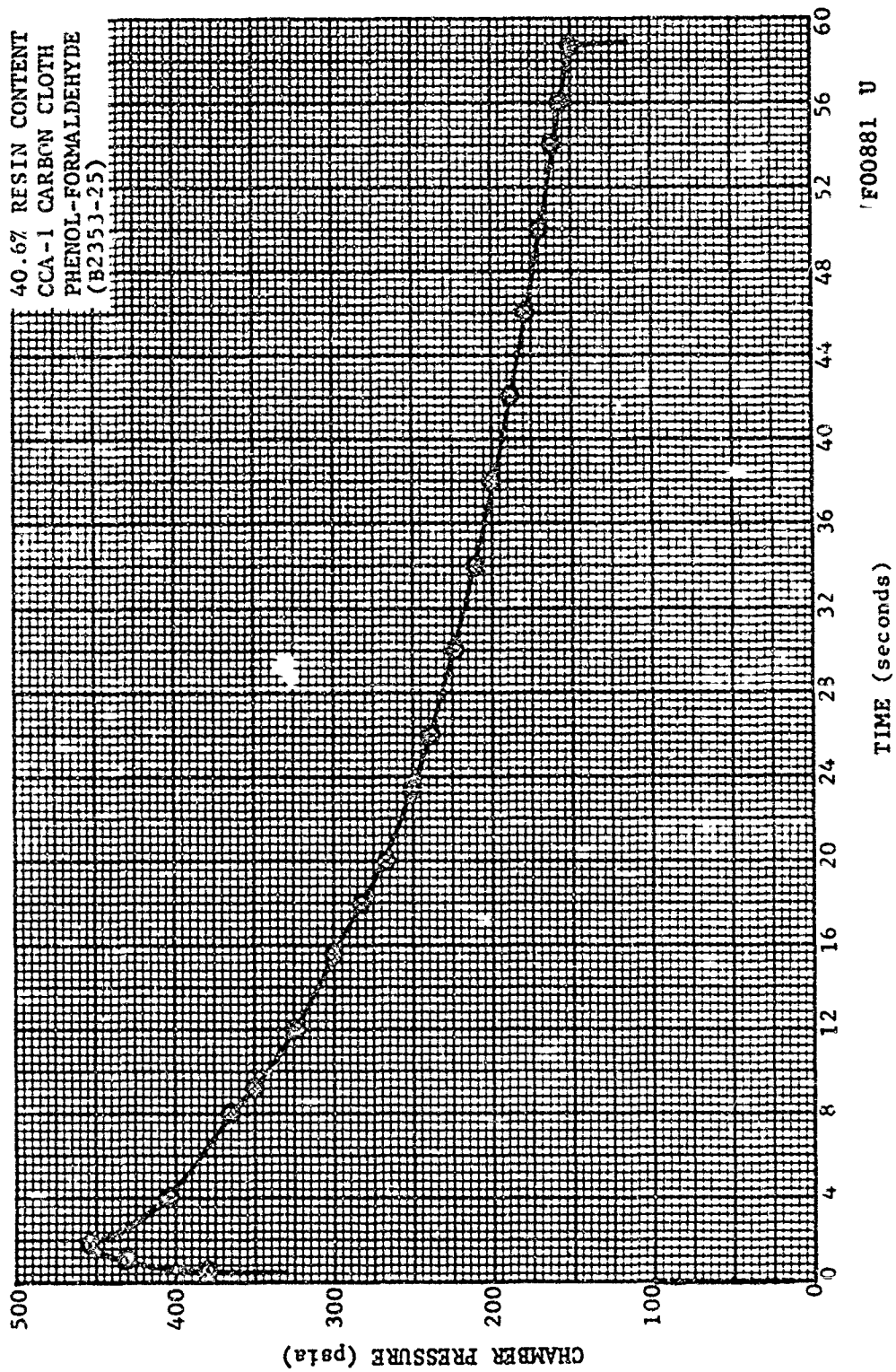


FIGURE 24. CHAMBER PRESSURE VERSUS TIME - ASD 432 NOZZLE



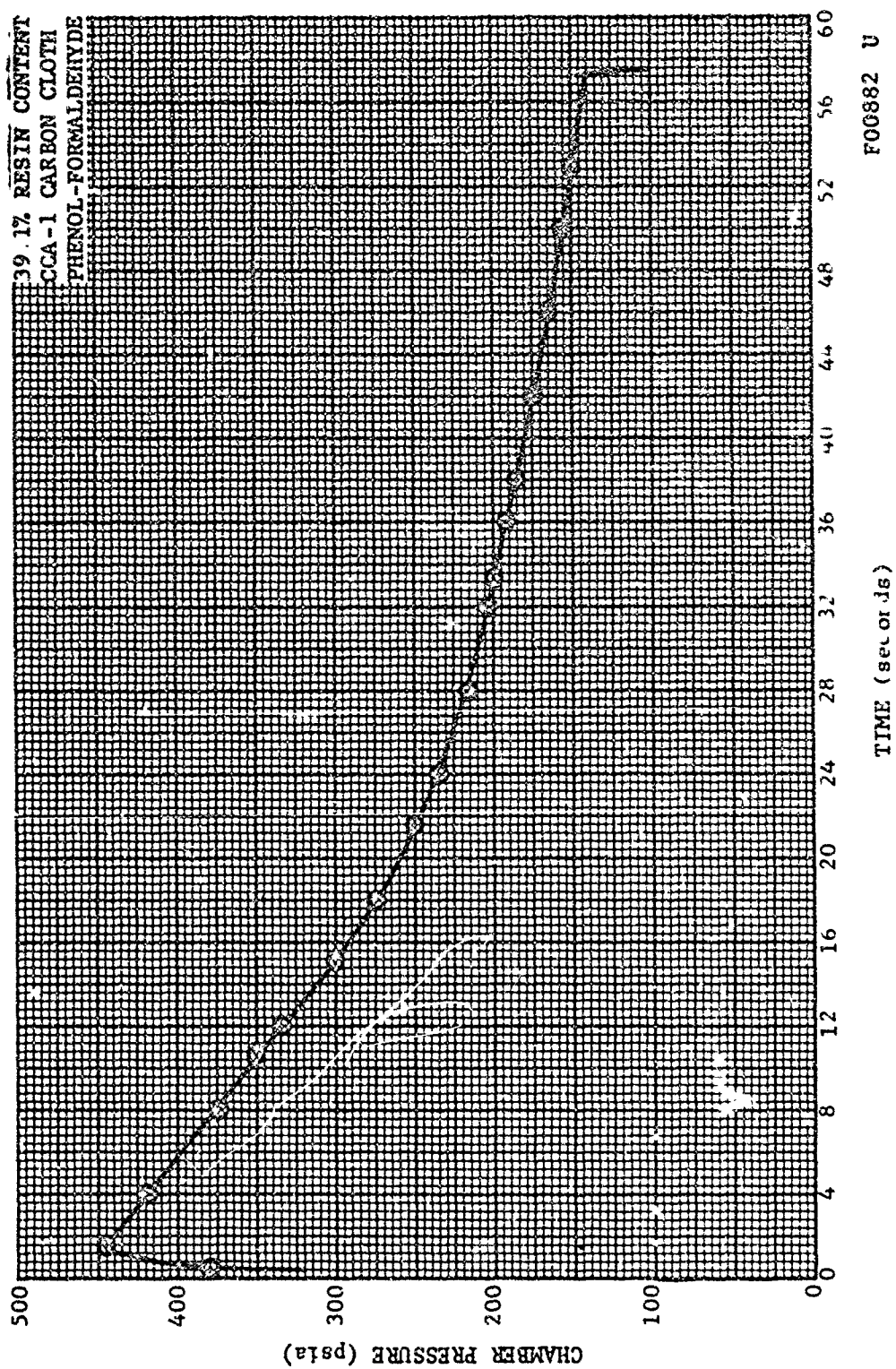


FIGURE 25. CHAMBER PRESSURE VERSUS TIME - ASD 433 NOZZLE

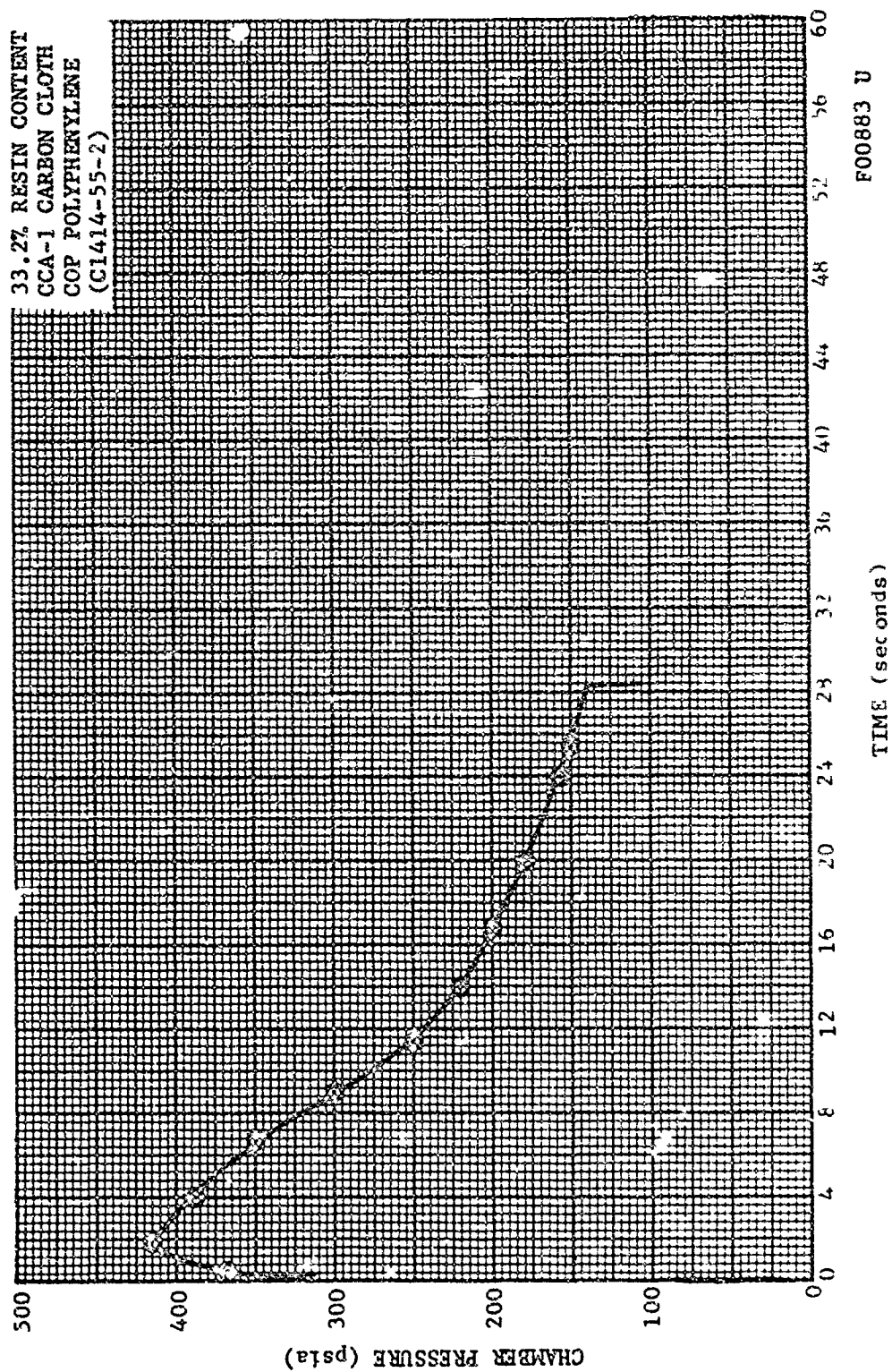


FIGURE 26. CHAMBER PRESSURE VERSUS TIME - ASD 434 NOZZLE

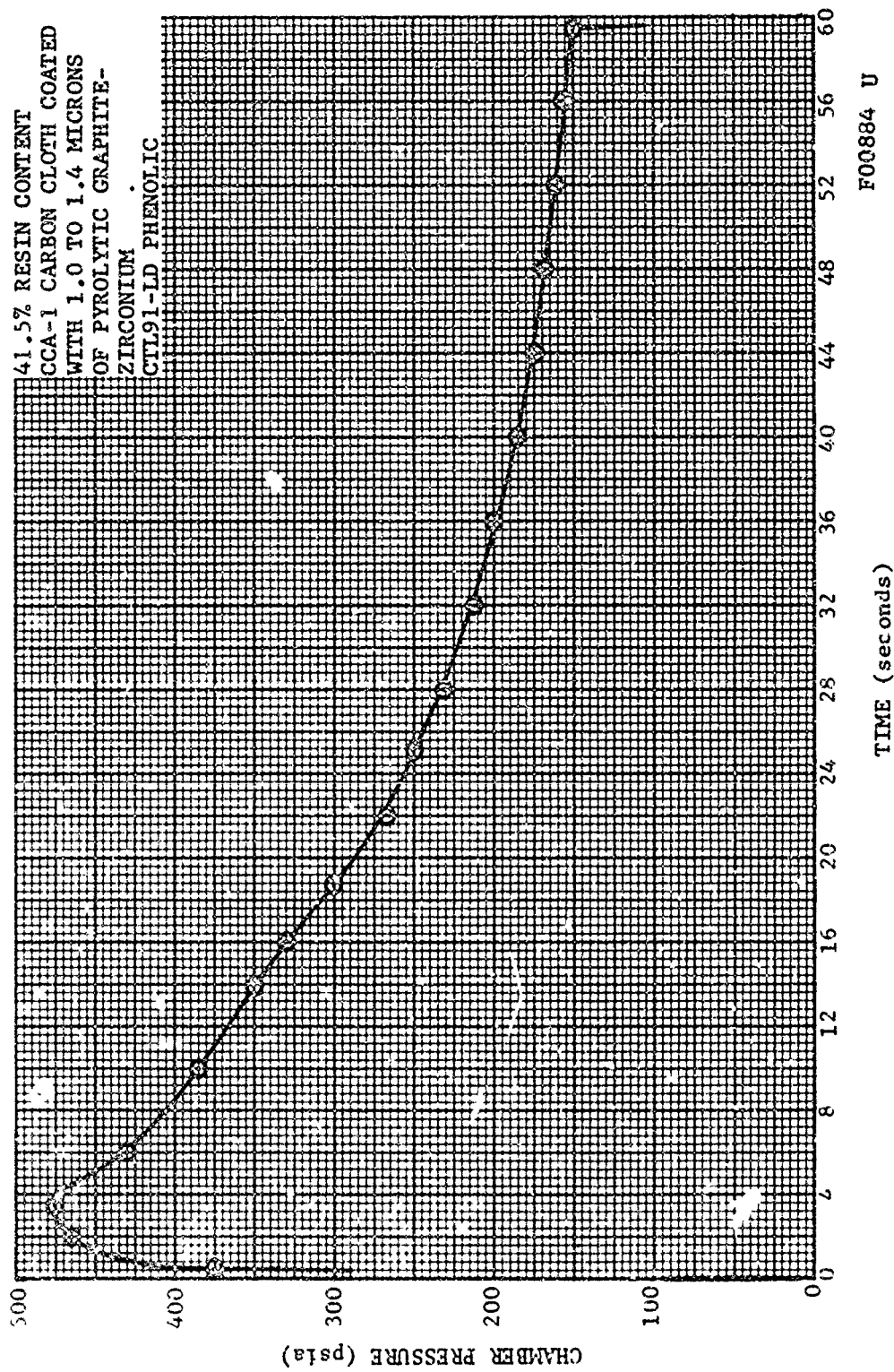


FIGURE 27. CHAMBER PRESSURE VERSUS TIME - ASD 435 NOZZLE

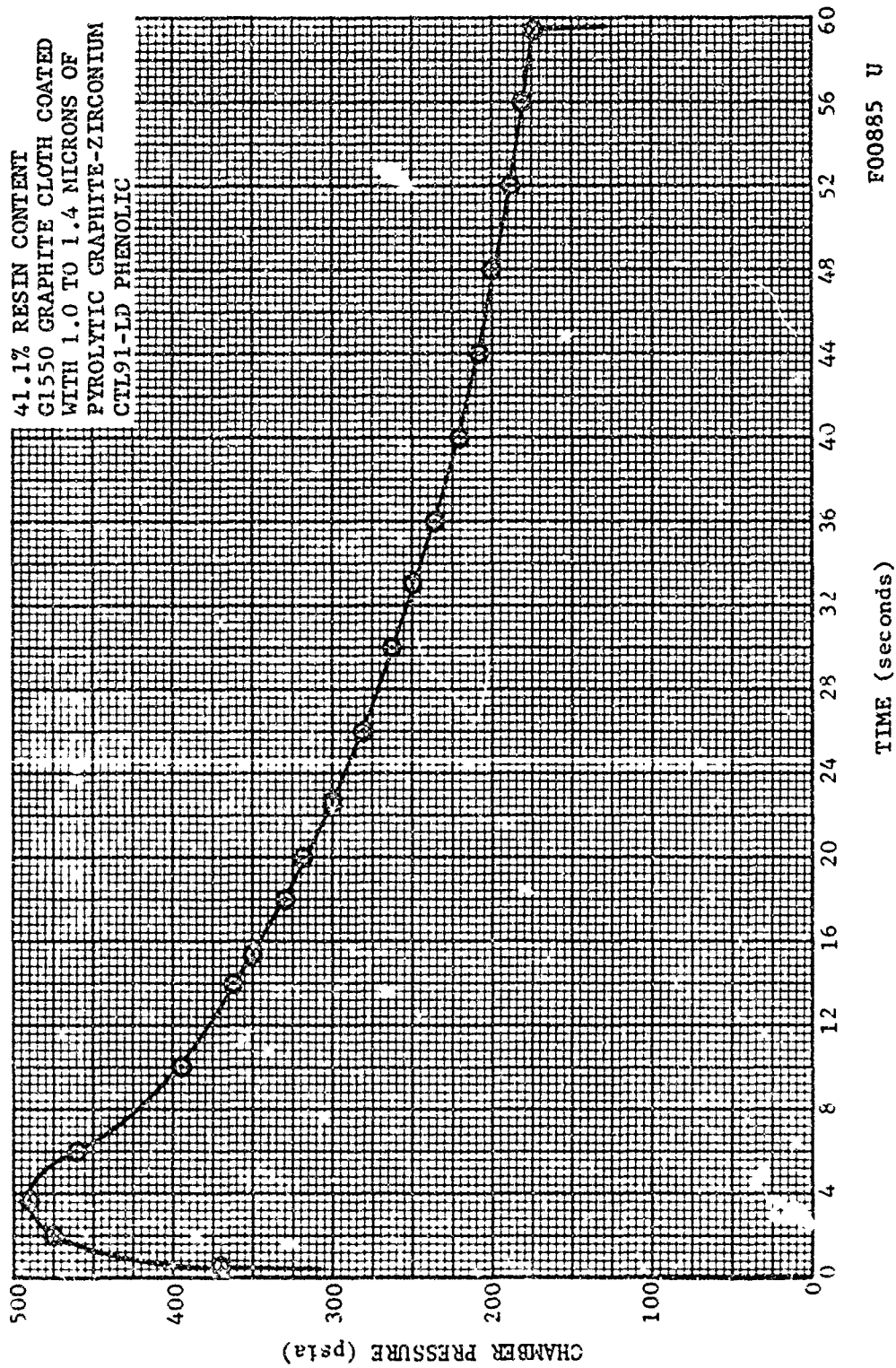


FIGURE 28. CHAMBER PRESSURE VERSUS TIME - ASD 437 NOZZLE

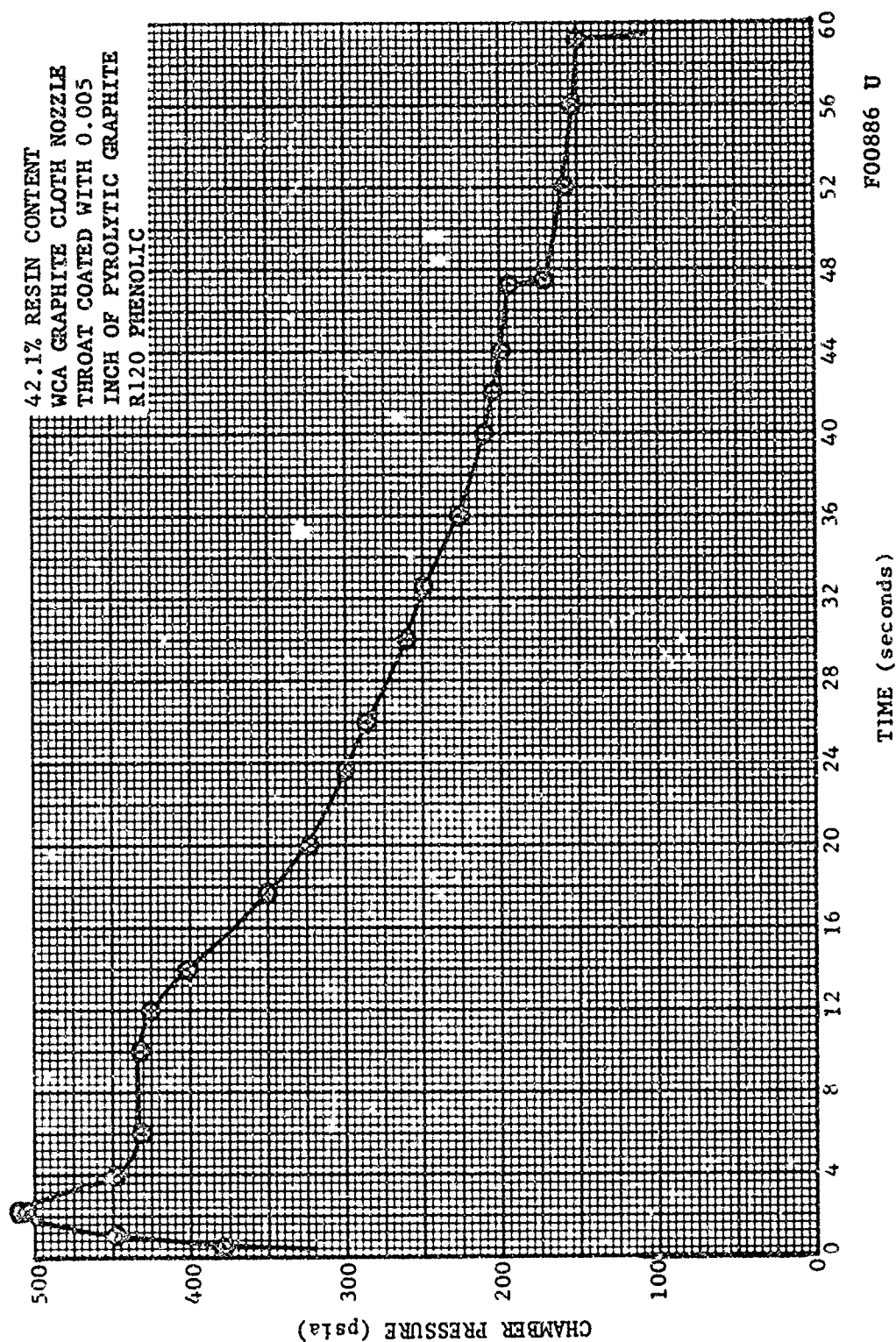


FIGURE 29. CHAMBER PRESSURE VERSUS TIME - ASD 439 NOZZLE



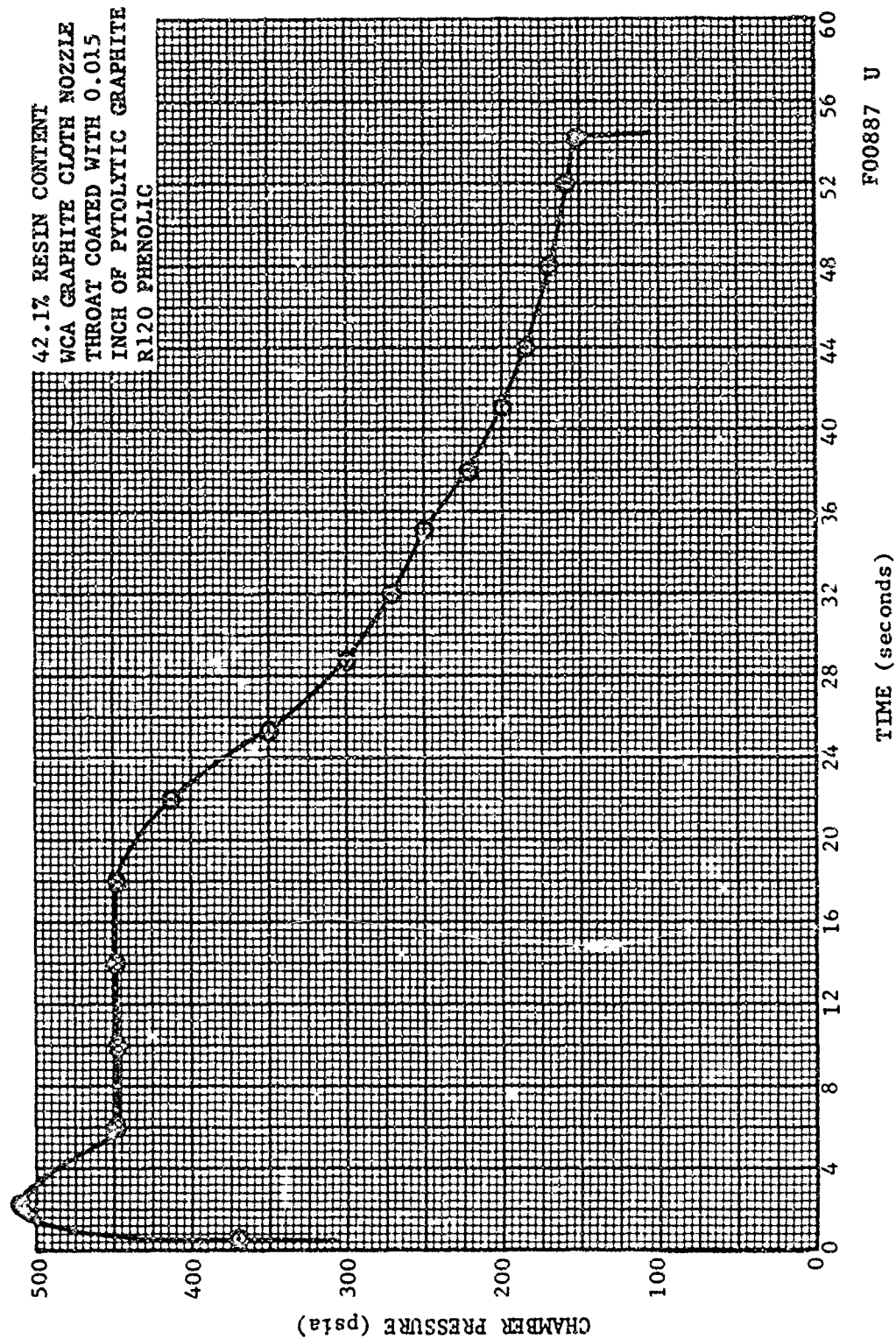


FIGURE 30. CHAMBER PRESSURE VERSUS TIME - ASD 440 NOZZLE

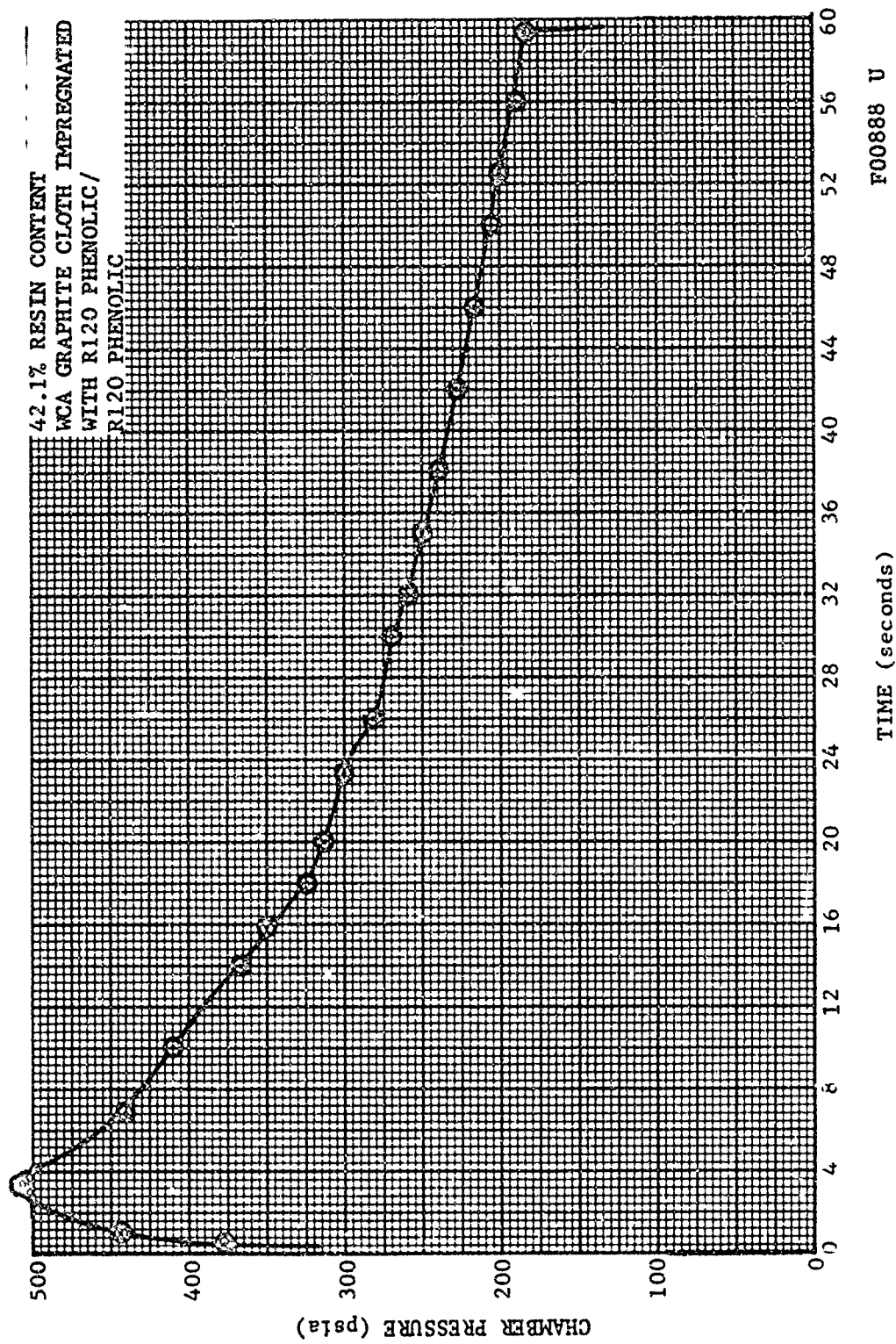


FIGURE 31. CHAMBER PRESSURE VERSUS TIME - ASD 441 NOZZLE

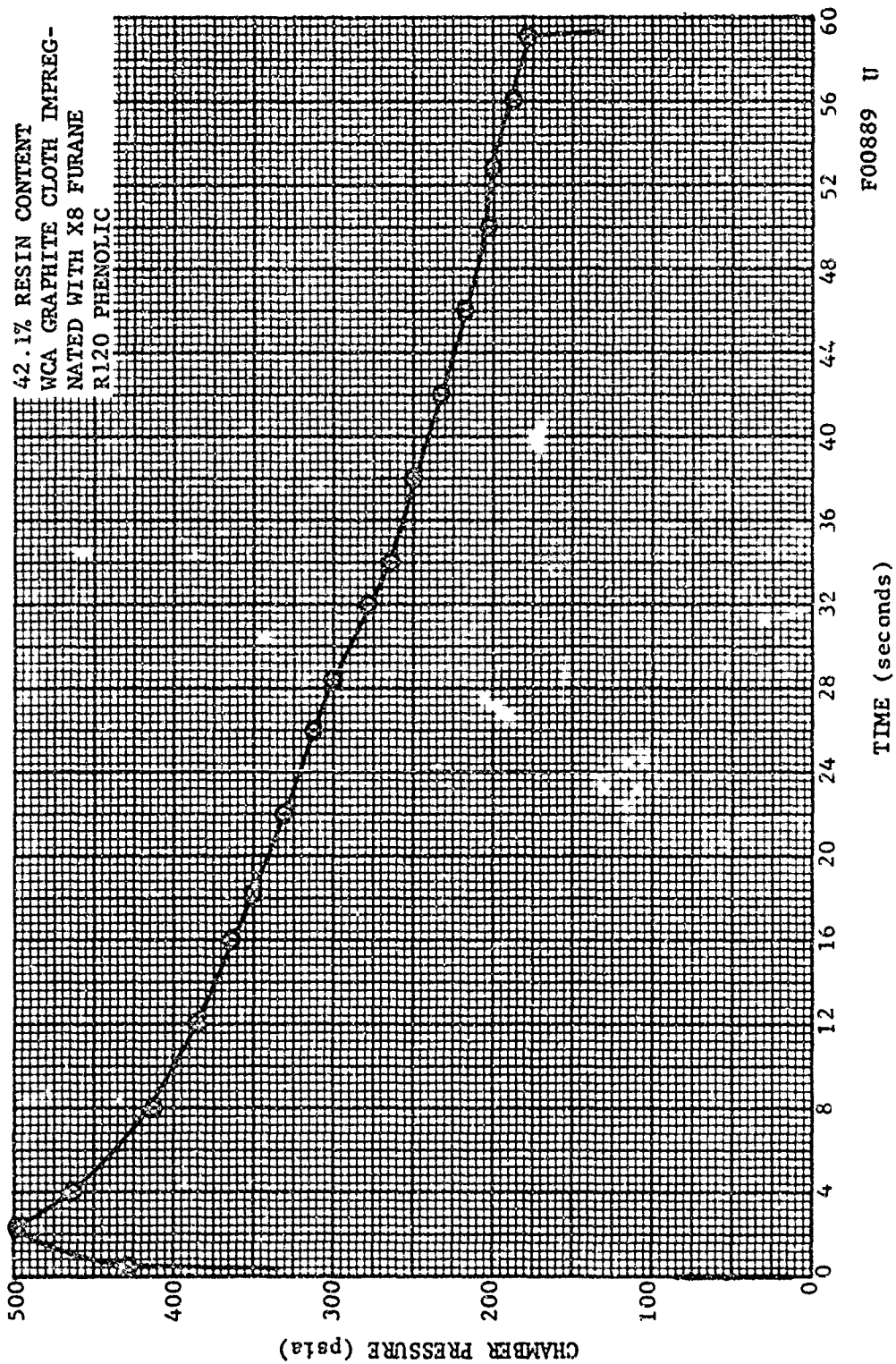


FIGURE 32. CHAMBER PRESSURE VERSUS TIME - ASD 442 NOZZLE



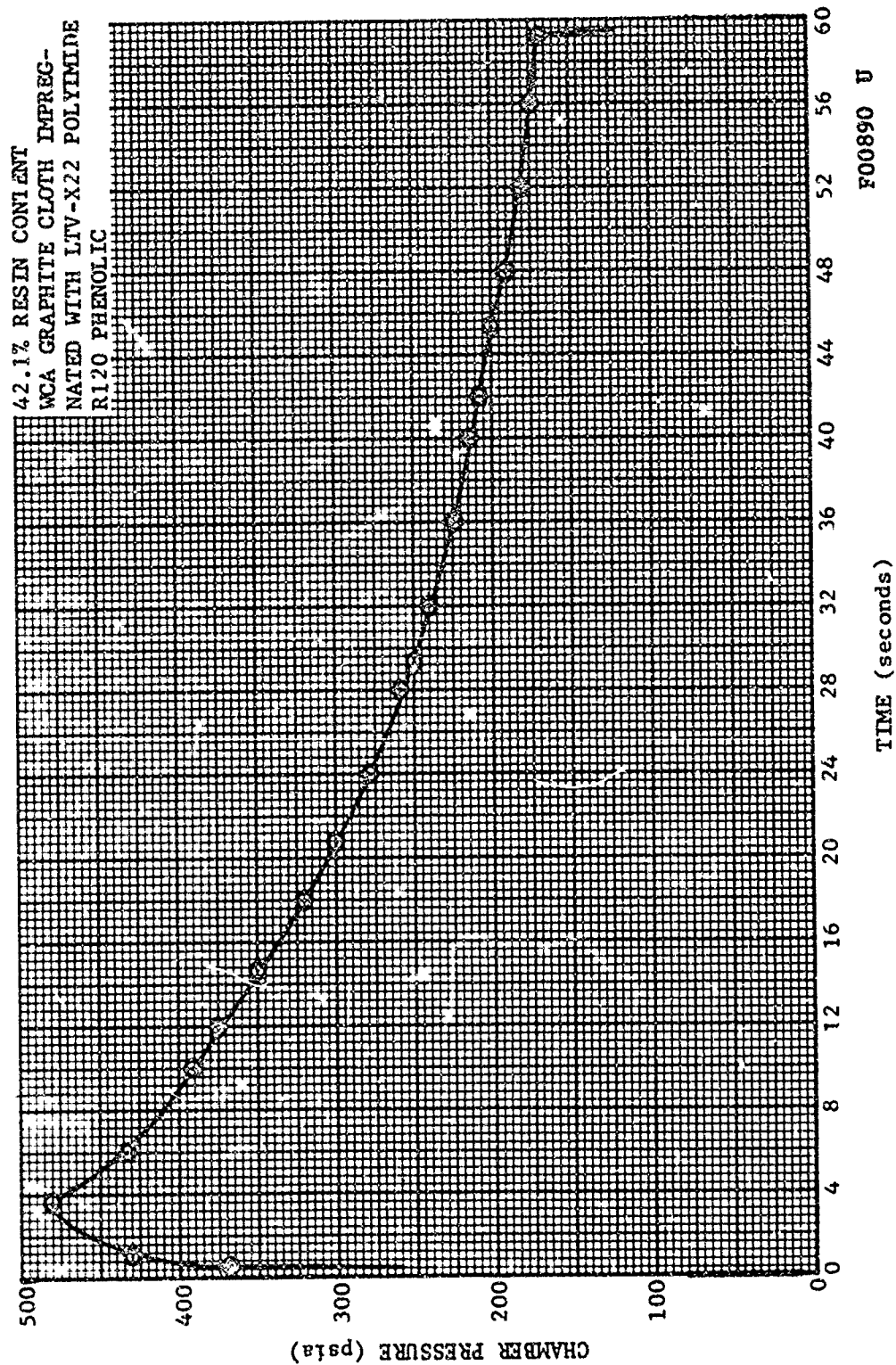


FIGURE 33. CHAMBER PRESSURE VERSUS TIME - ASD 443 NOZZLE

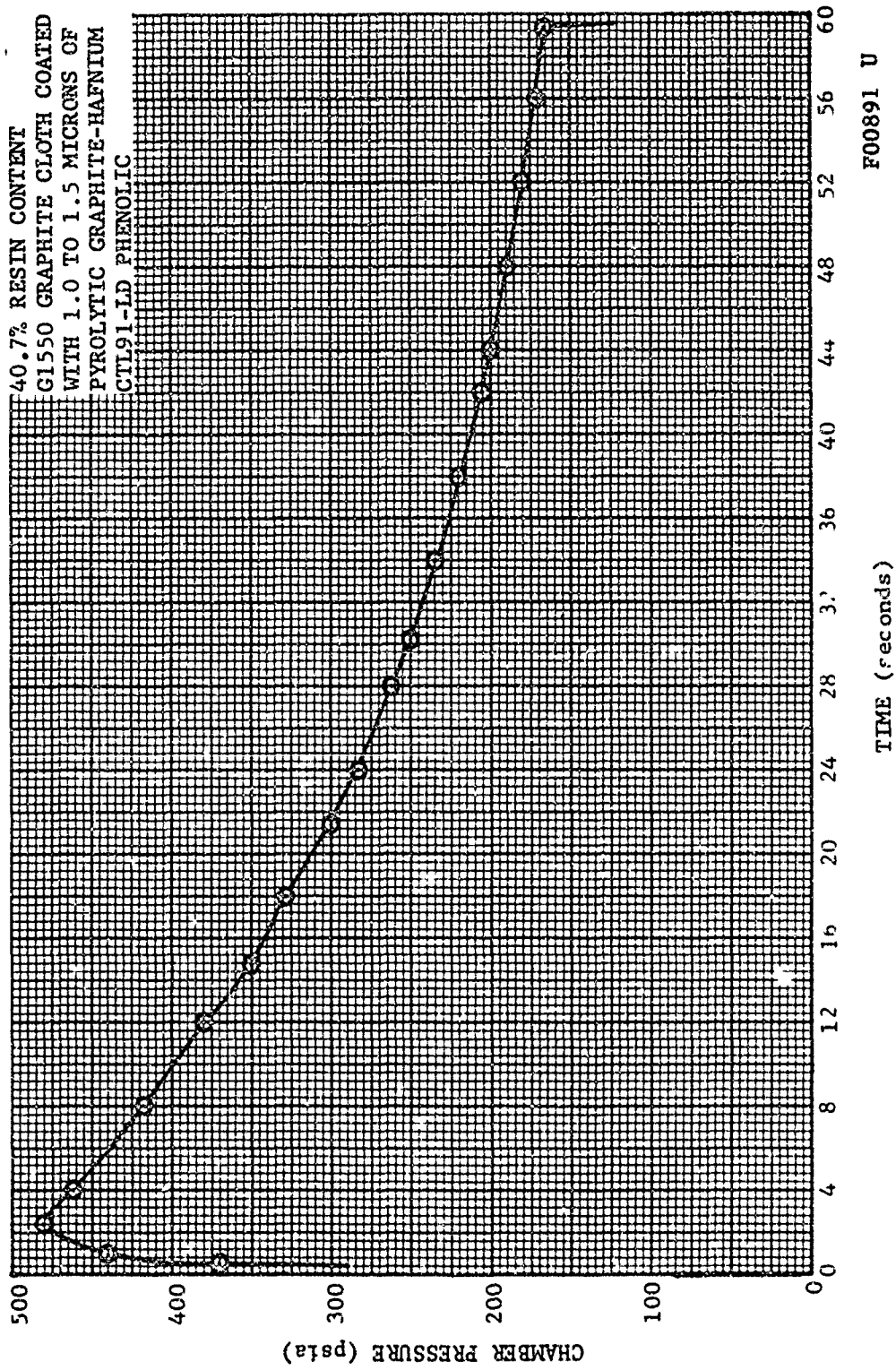


FIGURE 34. CHAMBER PRESSURE VERSUS TIME - ASD 444 NOZZLE

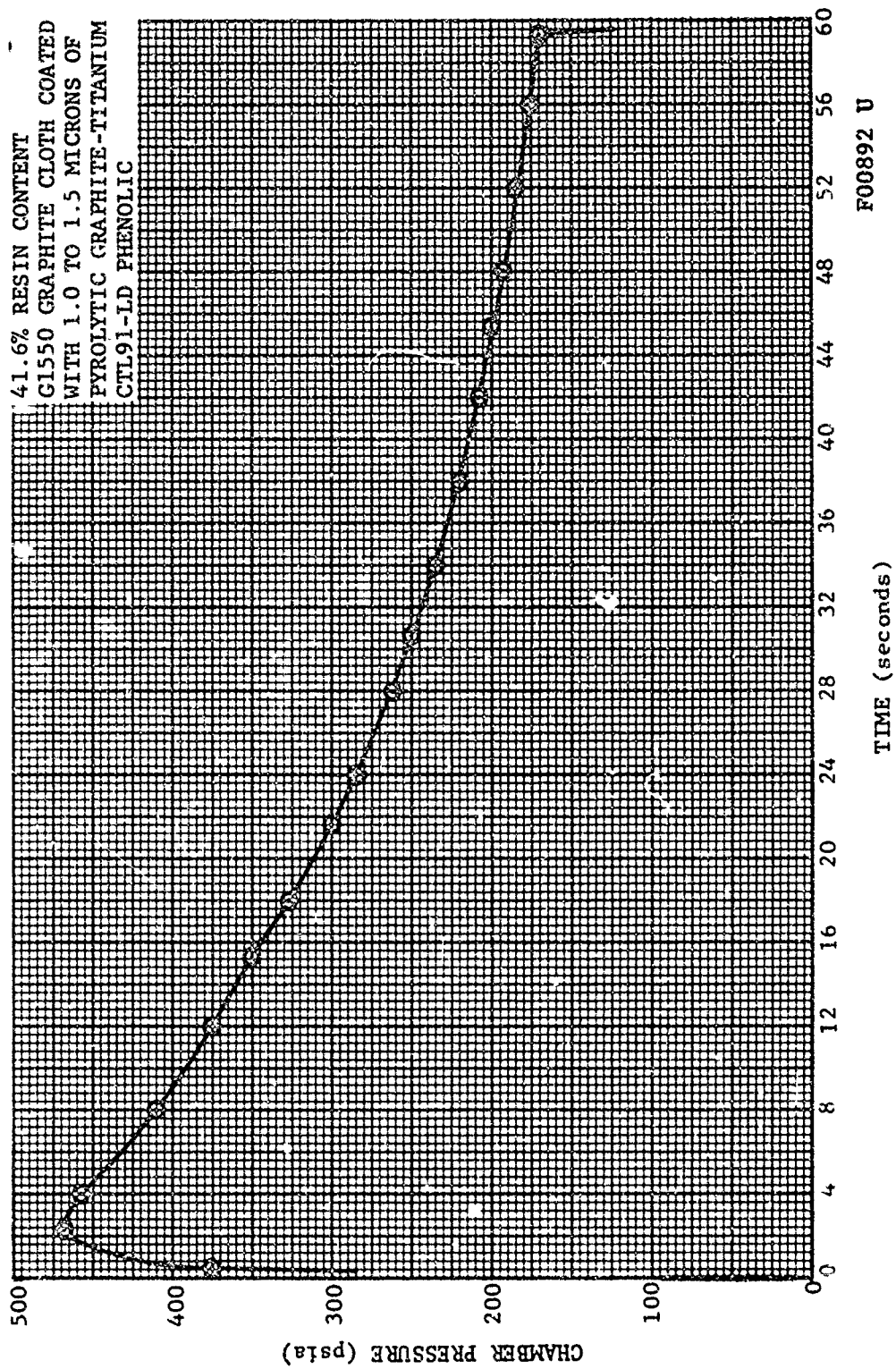


FIGURE 35. CHAMBER PRESSURE VERSUS TIME - ASD 446 NOZZLE

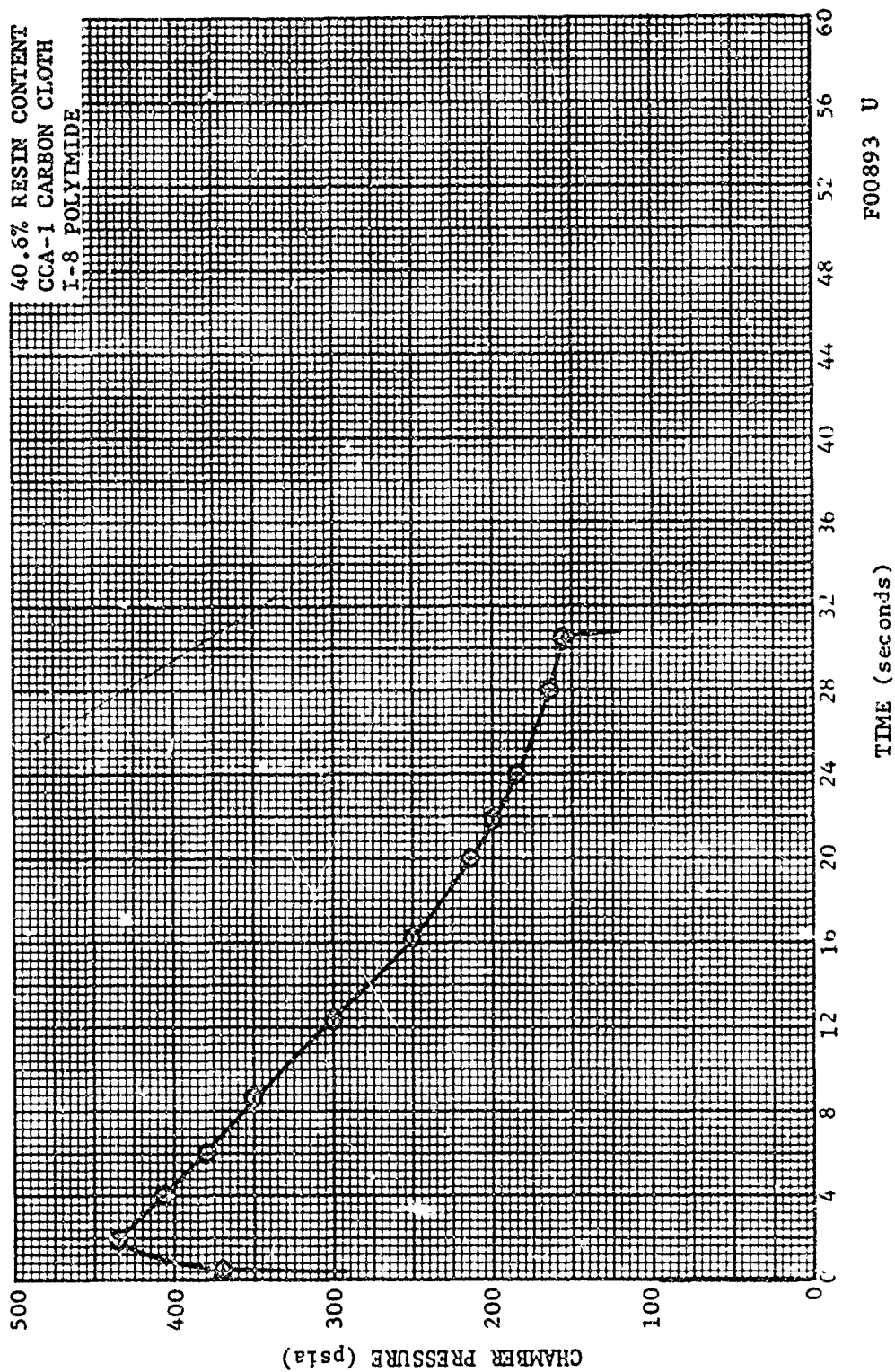


FIGURE 36. CHAMBER PRESSURE VERSUS TIME - ASD 448 NOZZLE

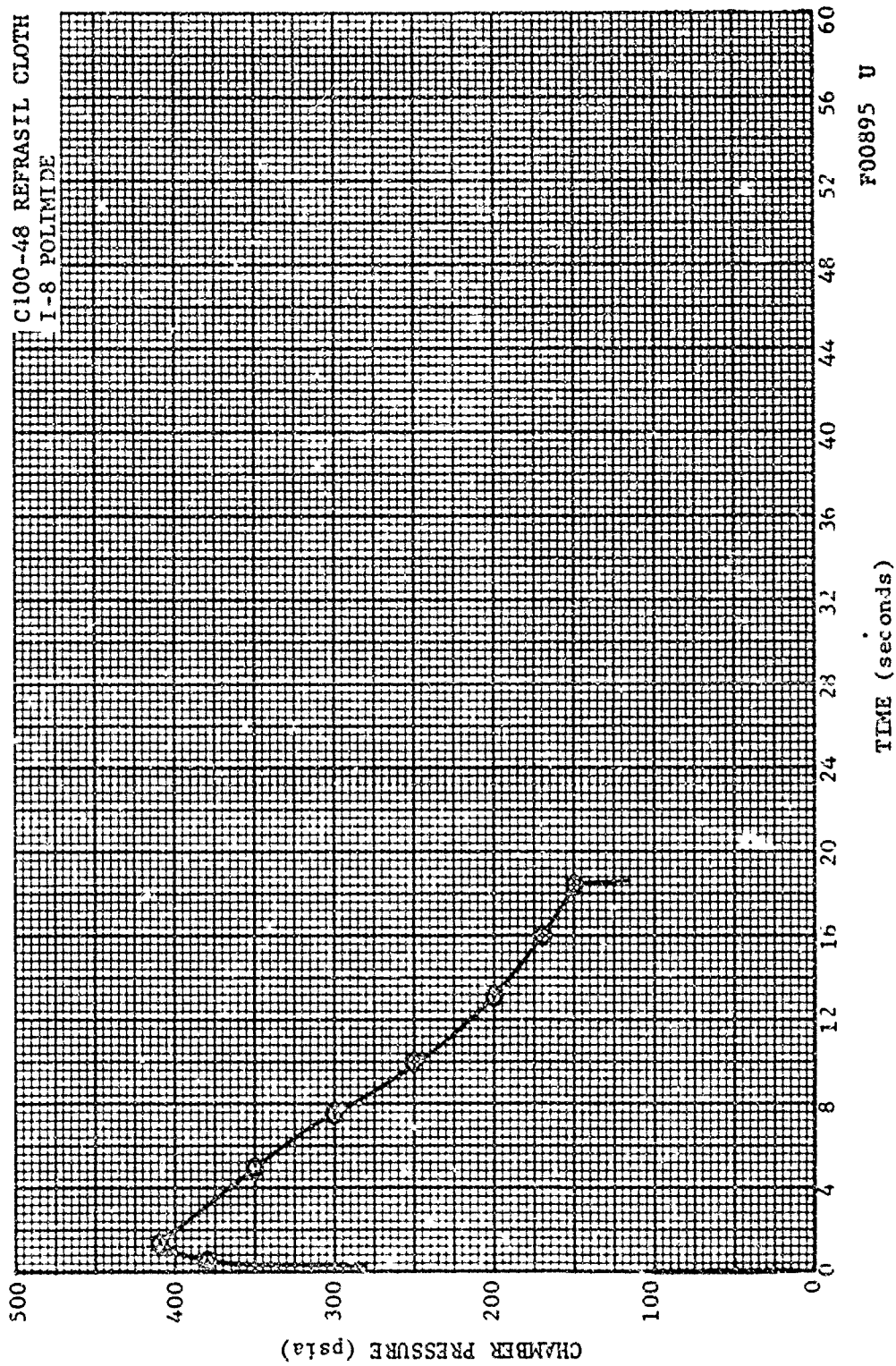


FIGURE 37. CHAMBER PRESSURE VERSUS TIME - ASD 452 NOZZLE



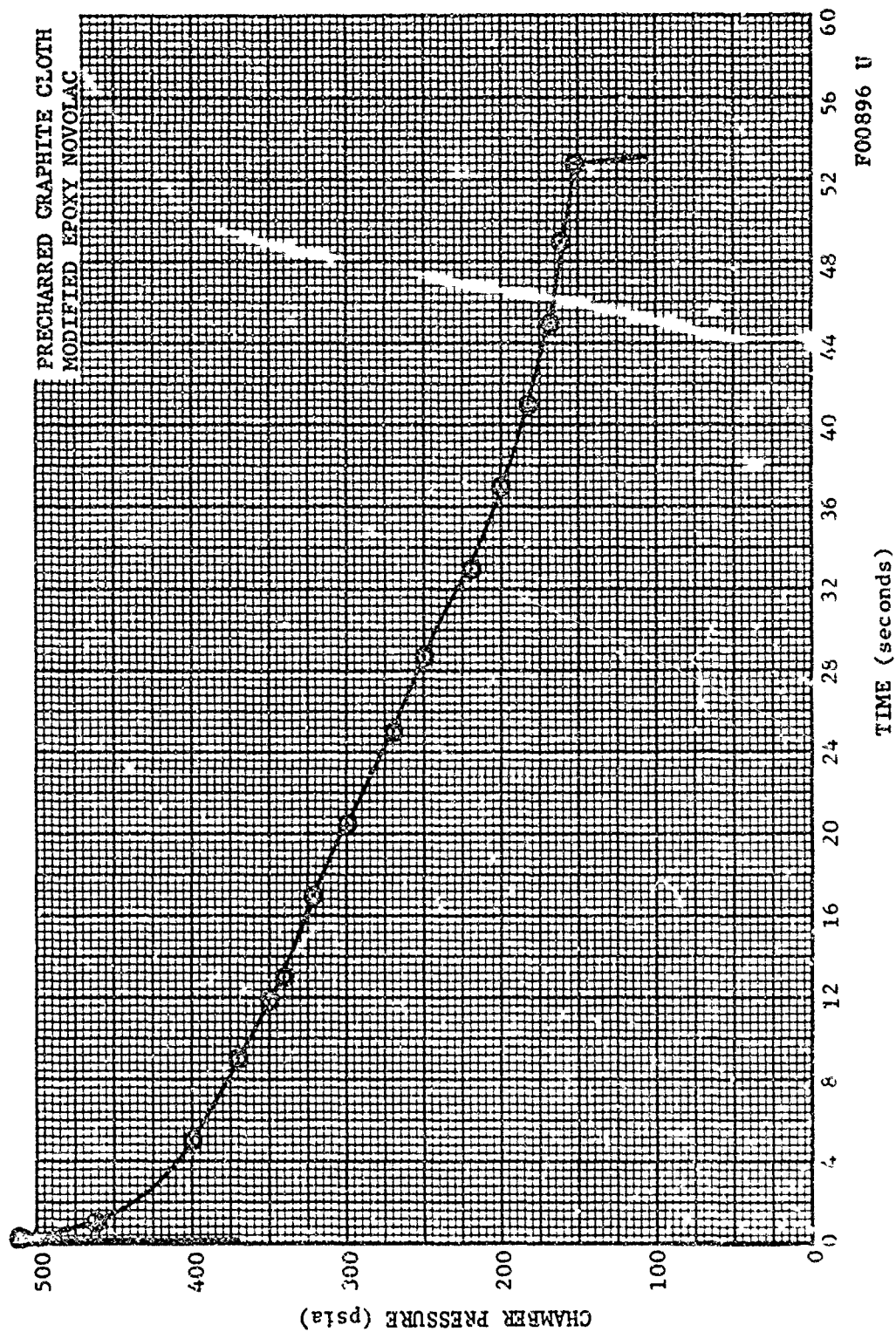


FIGURE 38. CHAMBER PRESSURE VERSUS TIME - ASD 356 NOZZLE

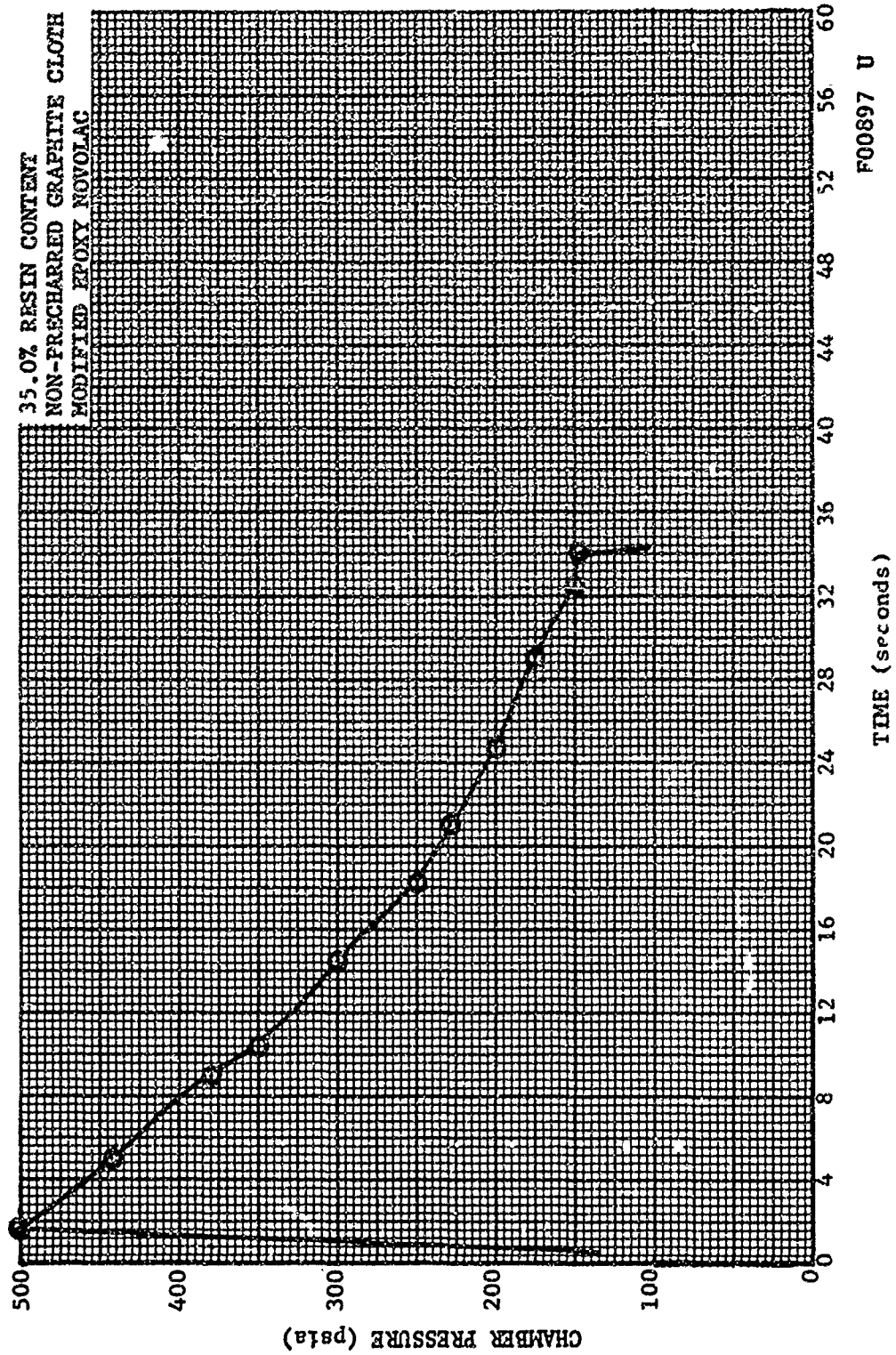


FIGURE 39. CHAMBER PRESSURE VERSUS TIME - ASD 358 NOZZLE

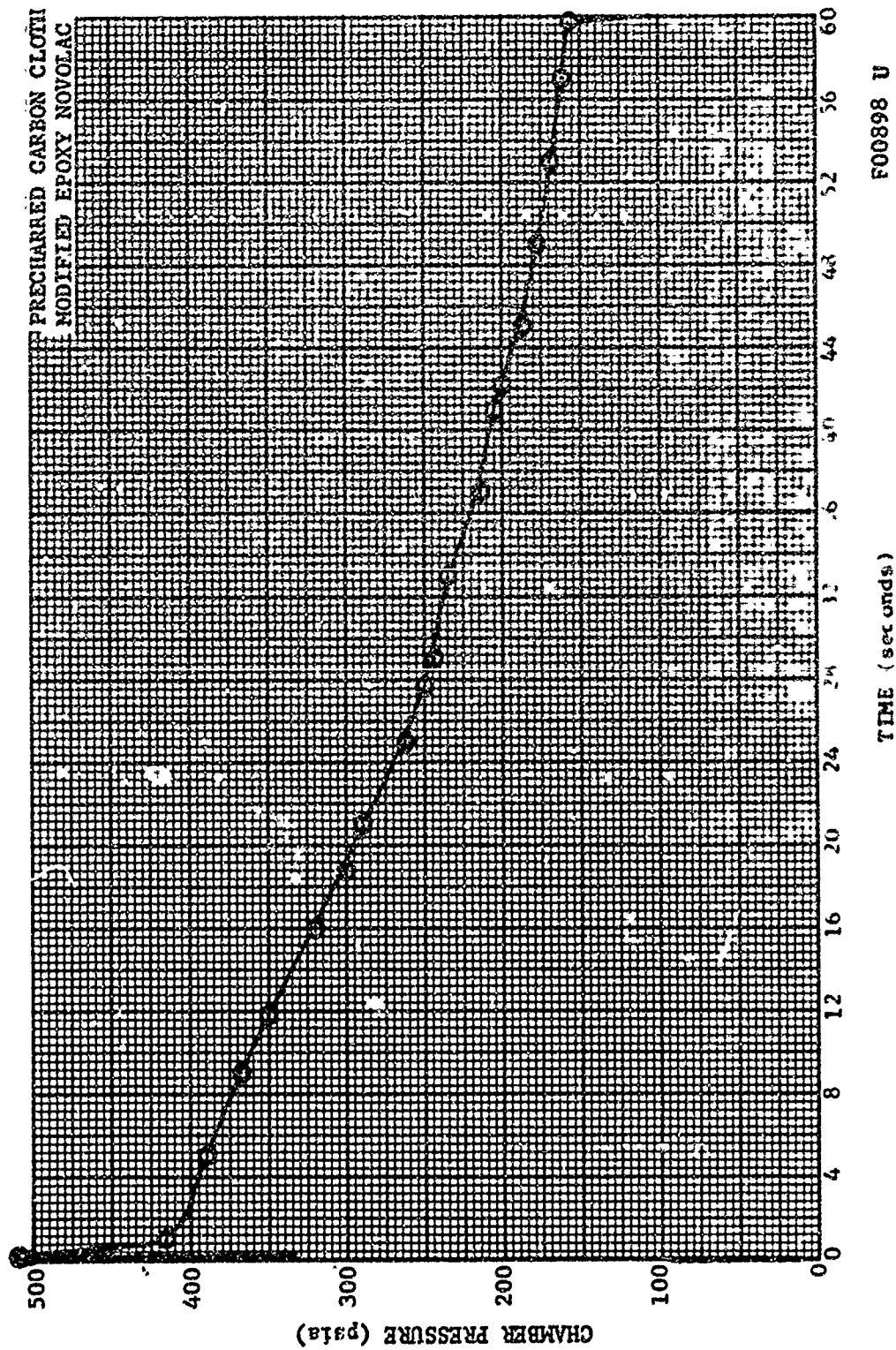
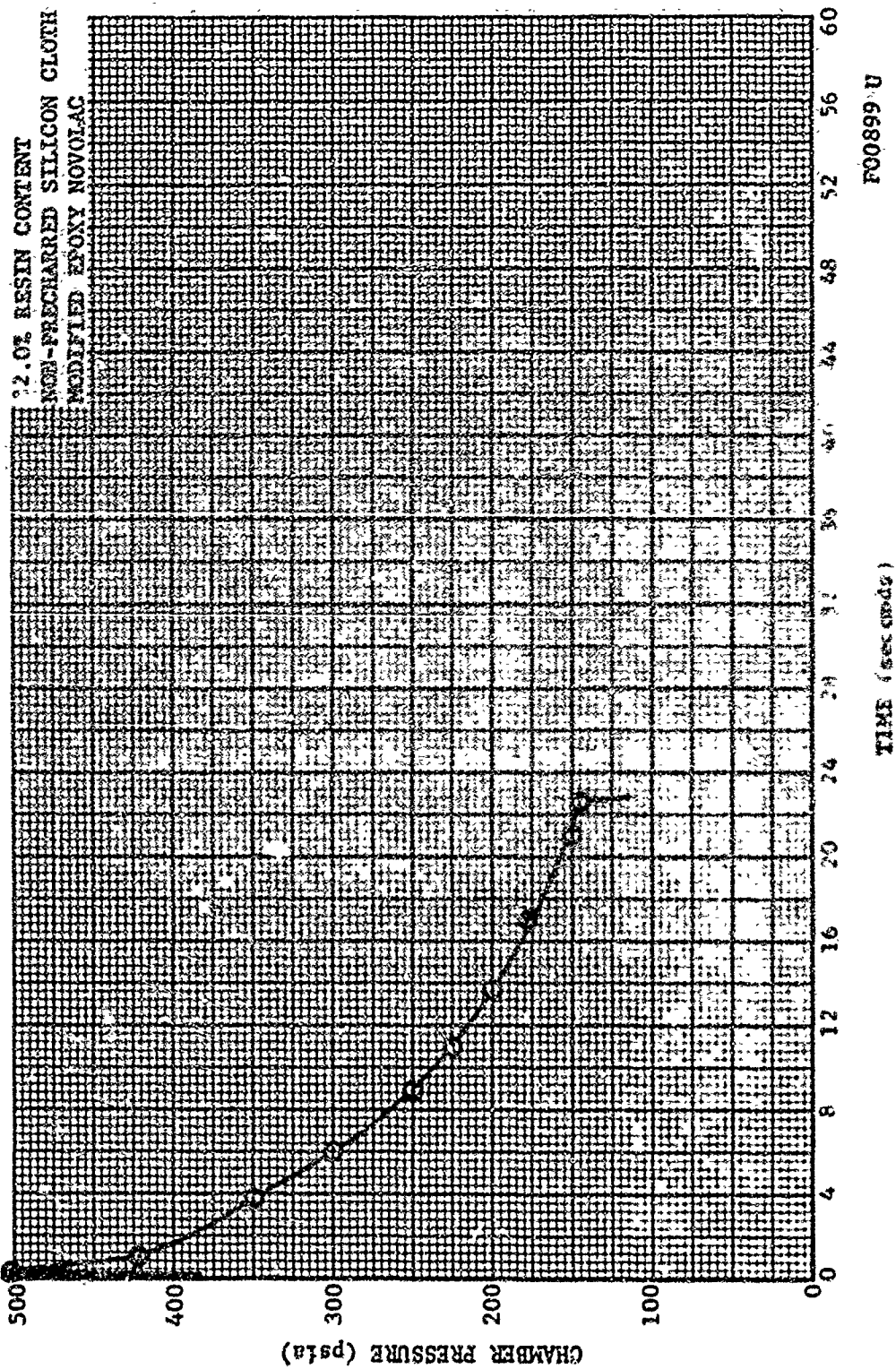


FIGURE 40 CHAMBER PRESSURE VERSUS TIME - ASD 160 NOZZLE





FO0899 U

FIGURE 41 CHAMBER PRESSURE VERSUS TIME - ASD 306 NOZZLE

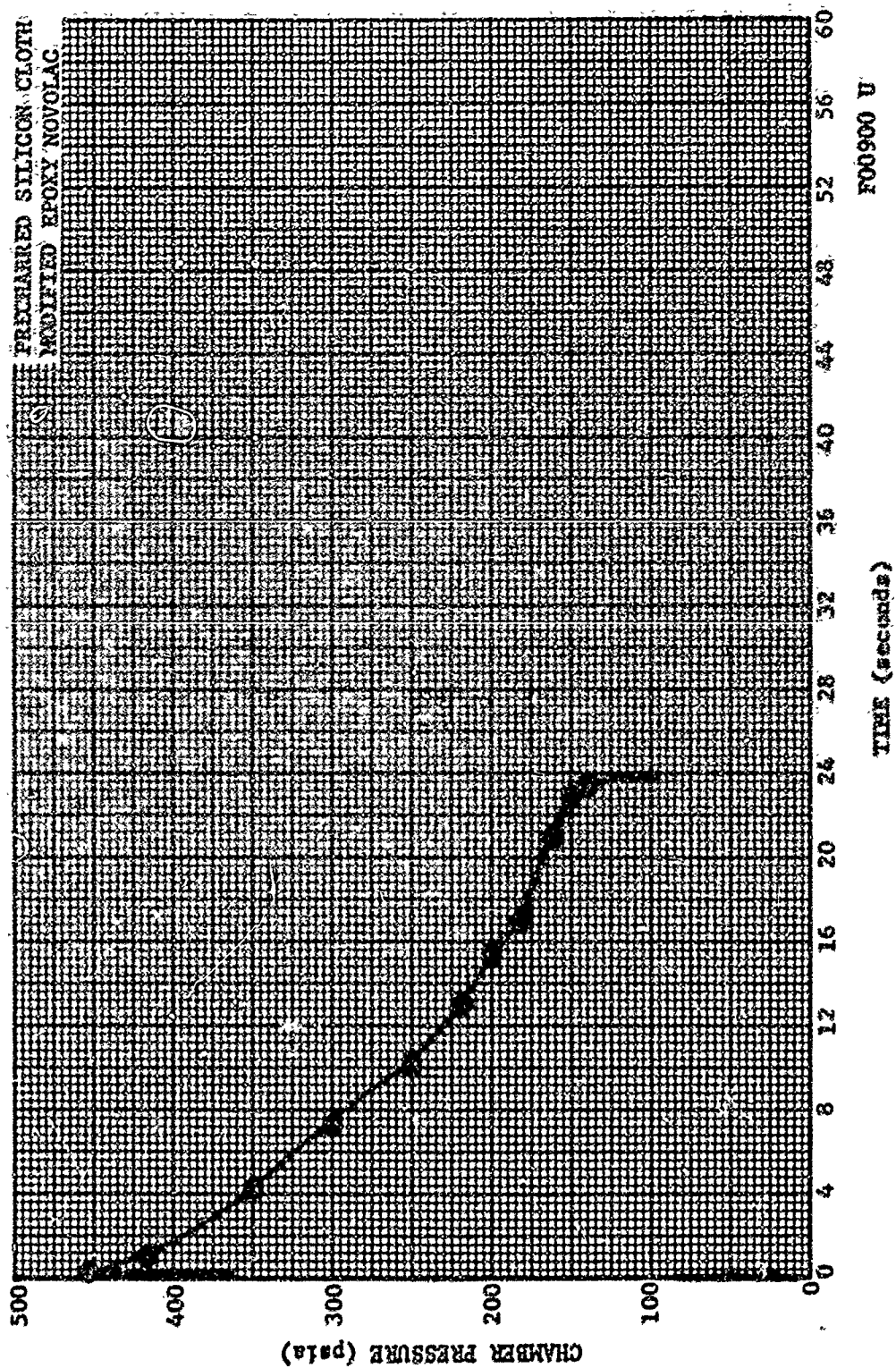


FIGURE 42. CHAMBER PRESSURE VERSUS TIME - ASD 368 NOZZLE.

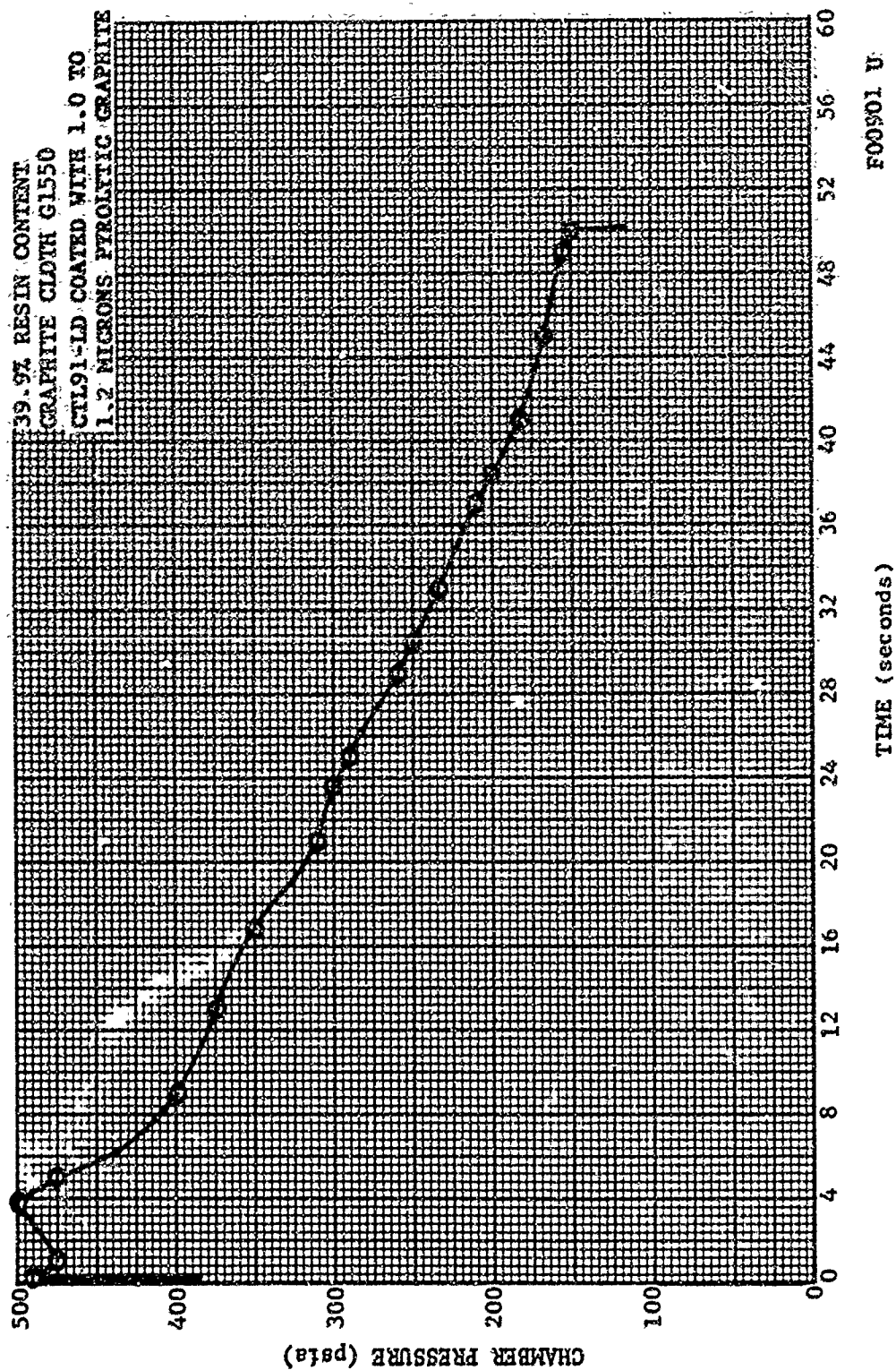


FIGURE 43. CHAMBER PRESSURE VERSUS TIME - ASD 4.17 NOZZLE

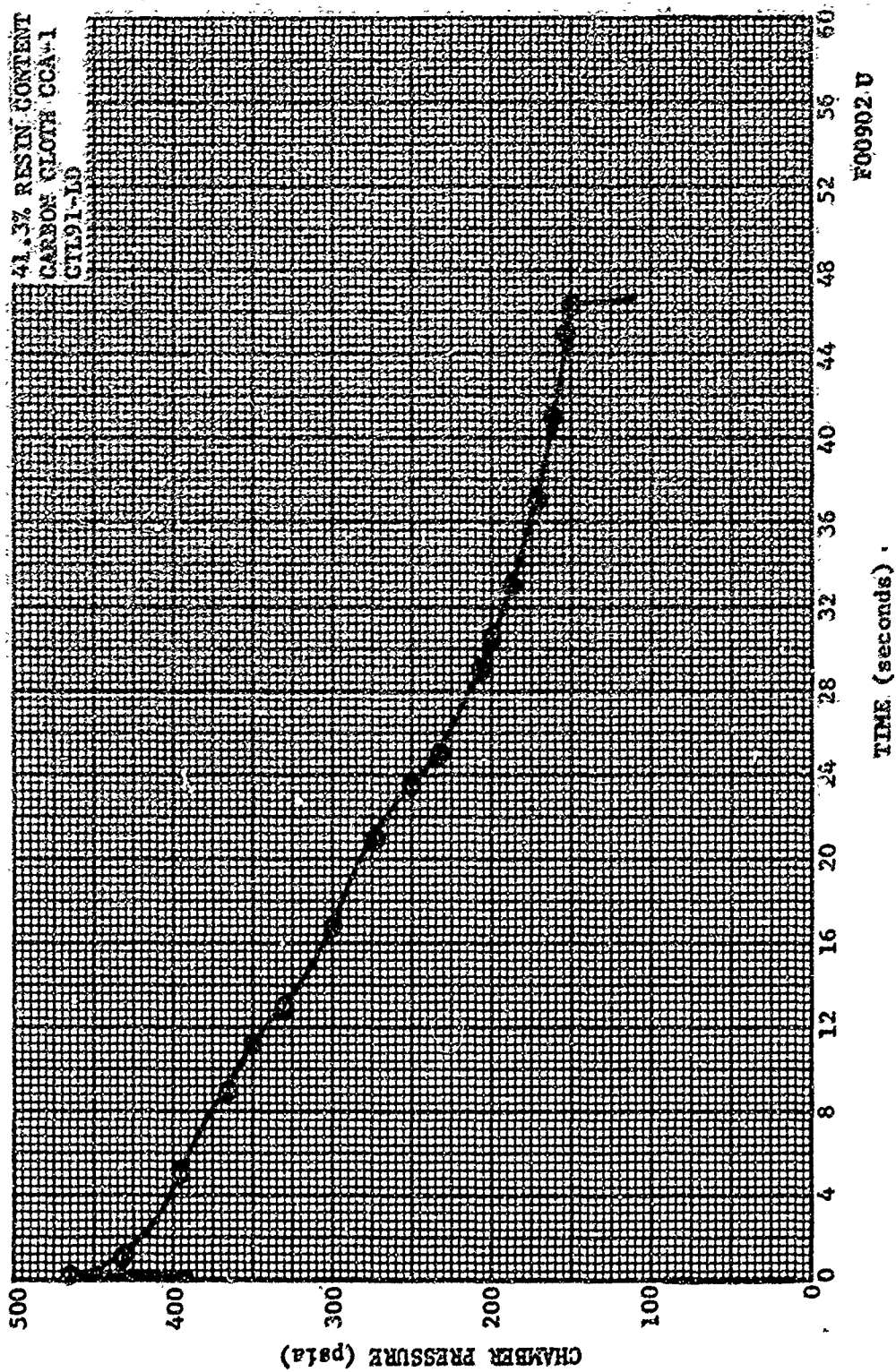


FIGURE 44. CHAMBER PRESSURE VERSUS TIME - ASD 422 NOZZLE

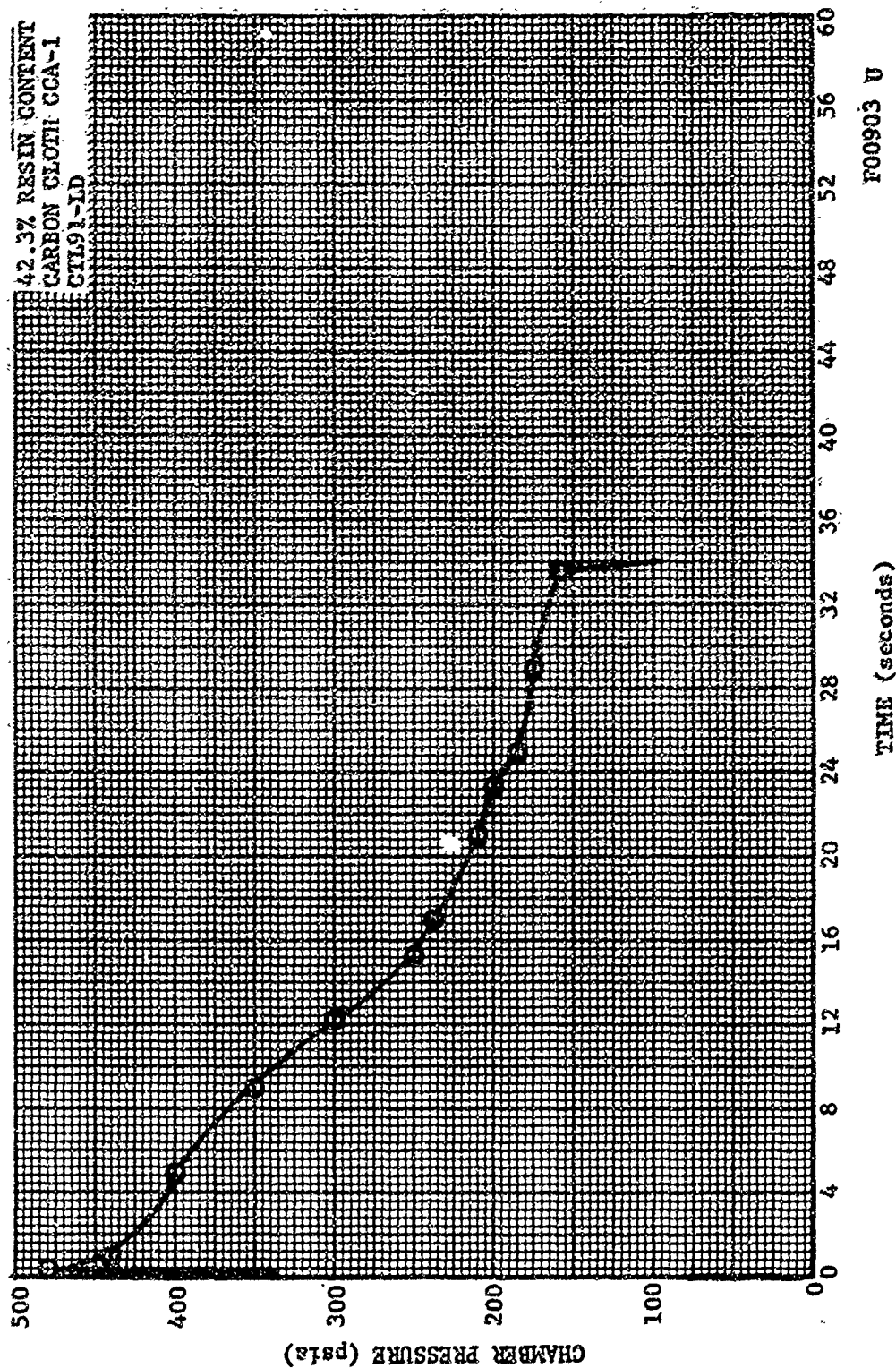


FIGURE 45. CHAMBER PRESSURE VERSUS TIME - ASD 423 NOZZLE



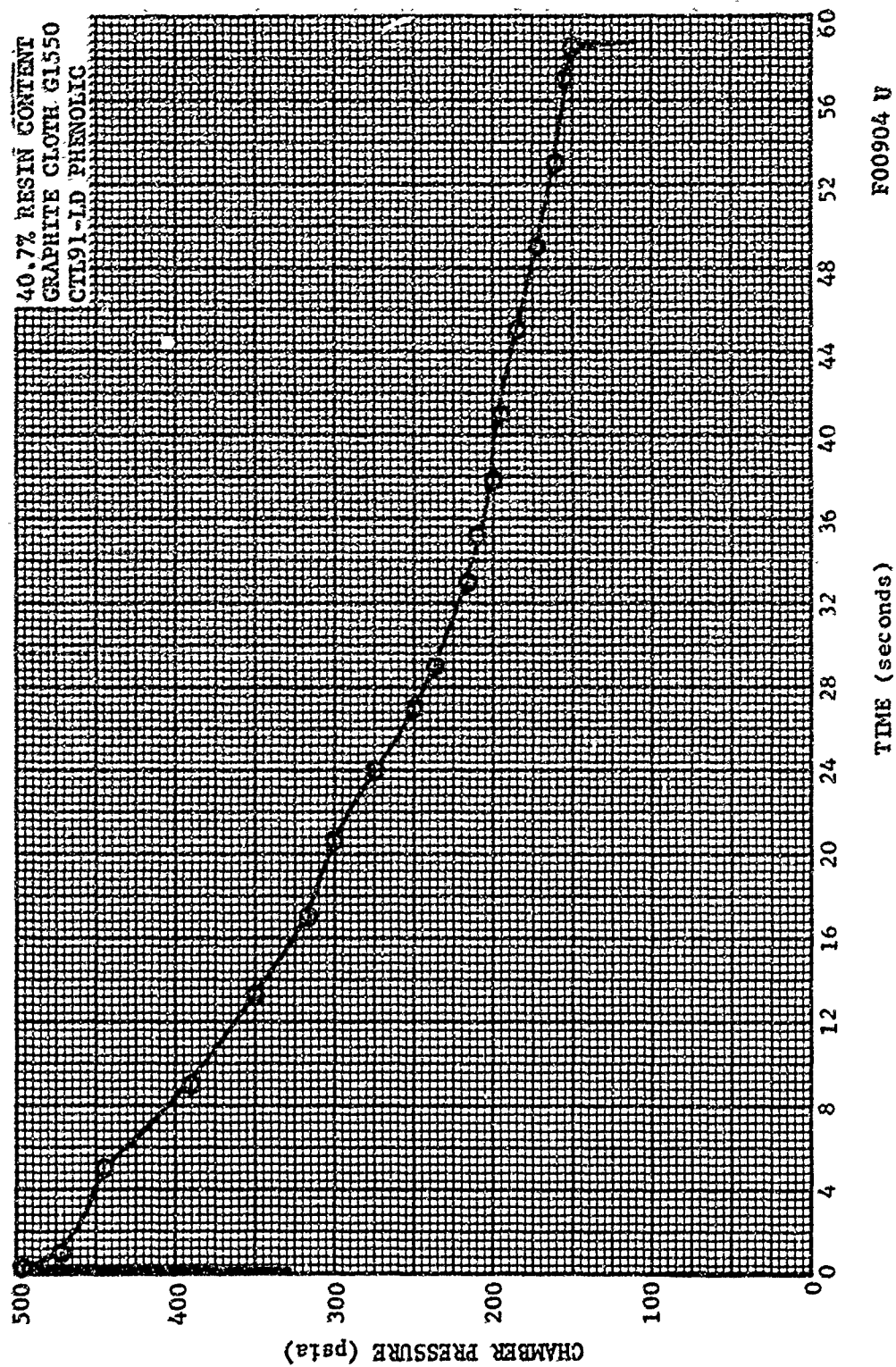


FIGURE 46. CHAMBER PRESSURE VERSUS TIME - ASD 429 NOZZLE

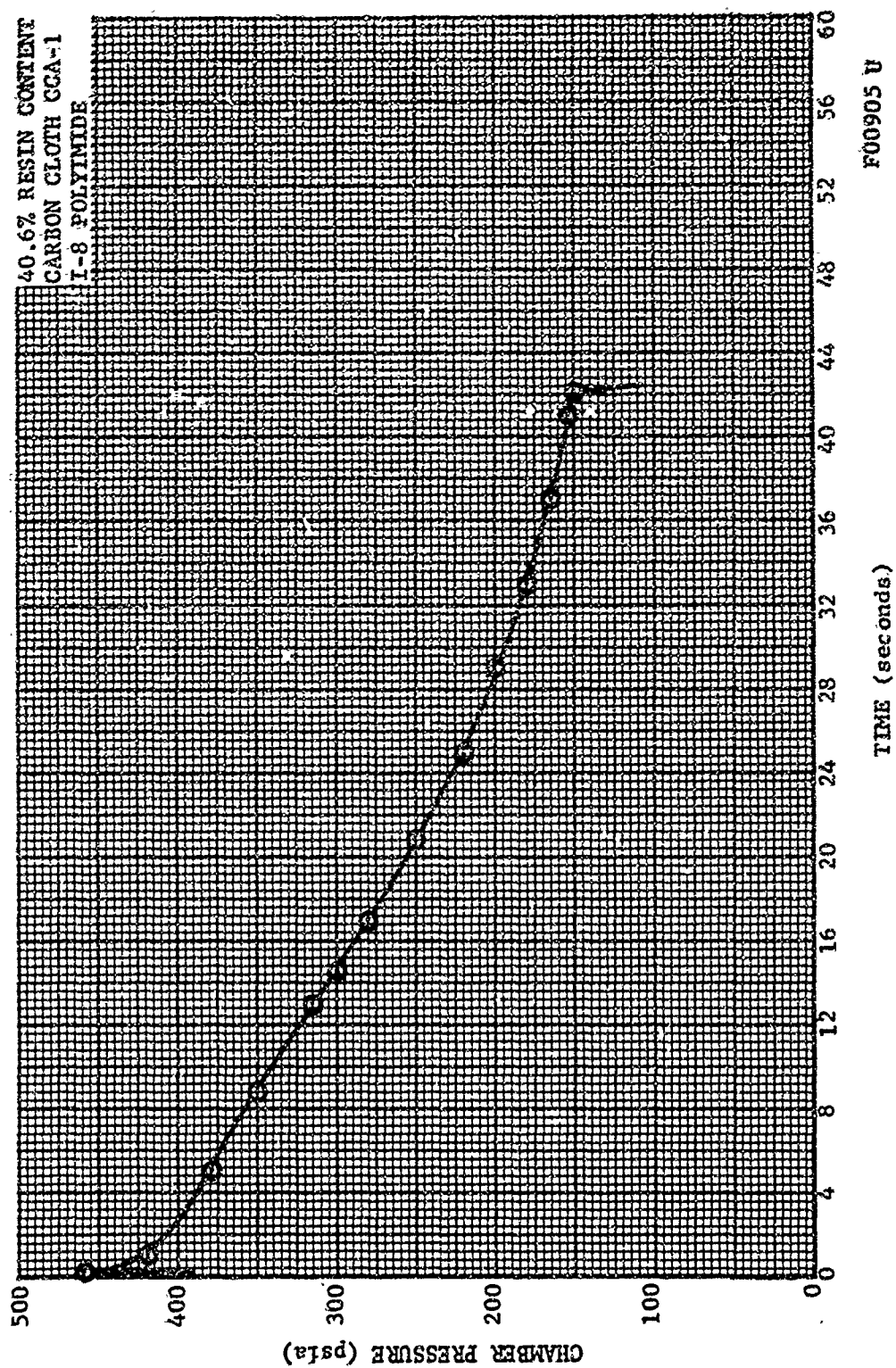


FIGURE 47. CHAMBER PRESSURE VERSUS TIME - ASD 449 NOZZLE

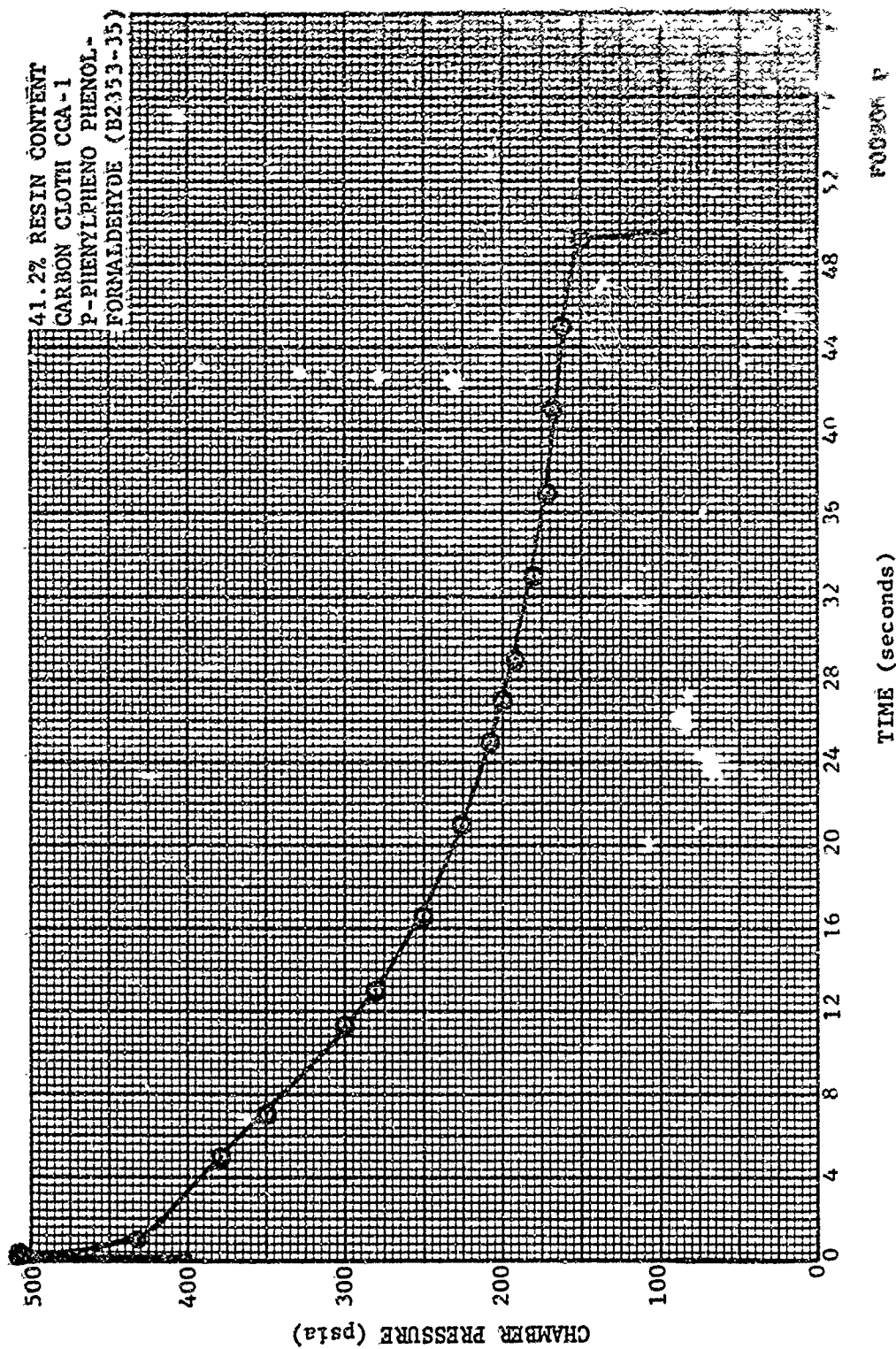


FIGURE 48. CHAMBER PRESSURE VERSUS TIME - ASD 455 NOZZLE



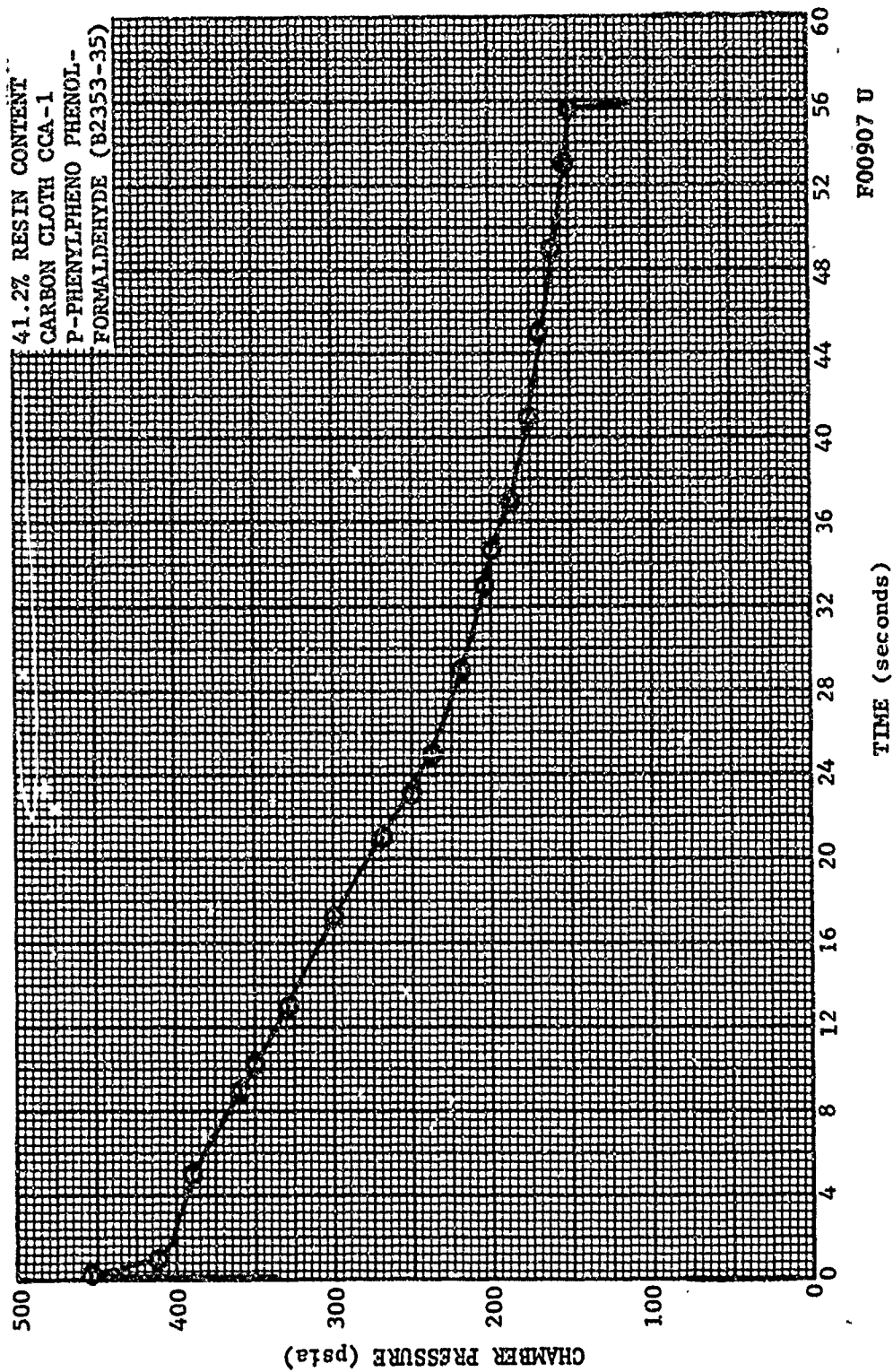


FIGURE 49. CHAMBER PRESSURE VERSUS TIME - ASD 456 NOZZLE

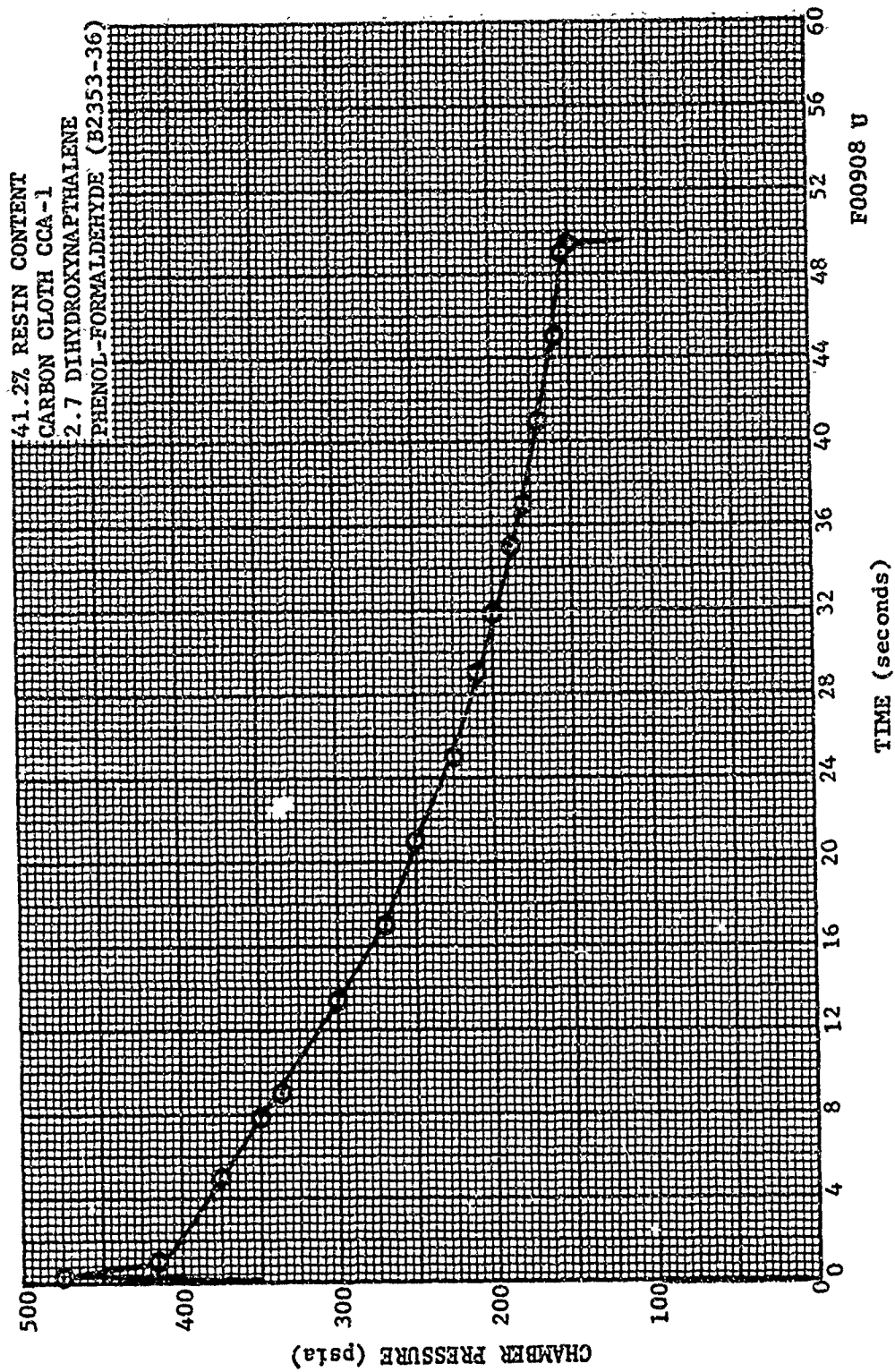


FIGURE 50. CHAMBER PRESSURE VERSUS TIME - ASD 457 NOZZLE

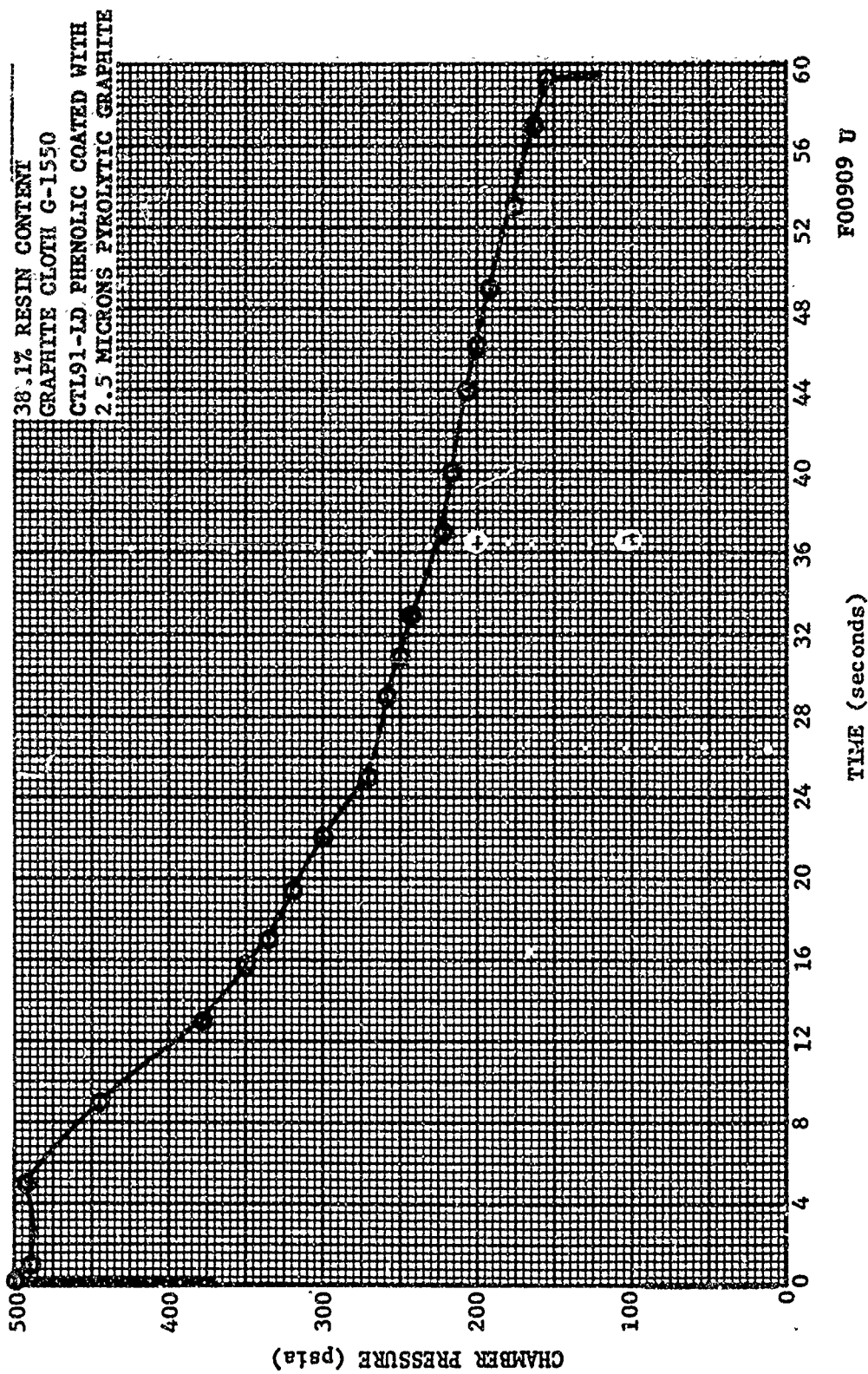


FIGURE 51. CHAMBER PRESSURE VERSUS TIME - ASD 459 NOZZLE

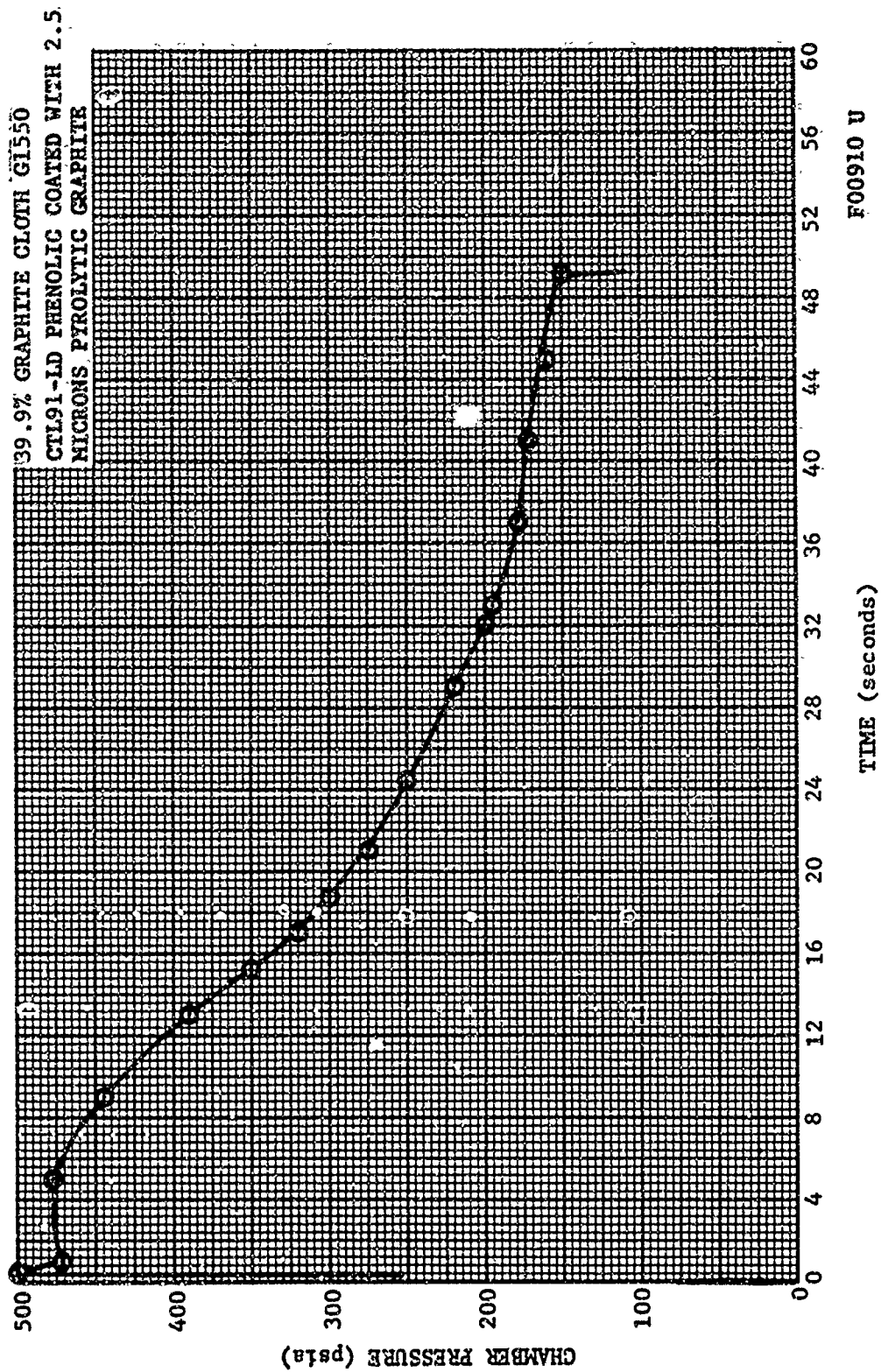


FIGURE 52. CHAMBER PRESSURE VERSUS TIME - ASD 460 NOZZLE

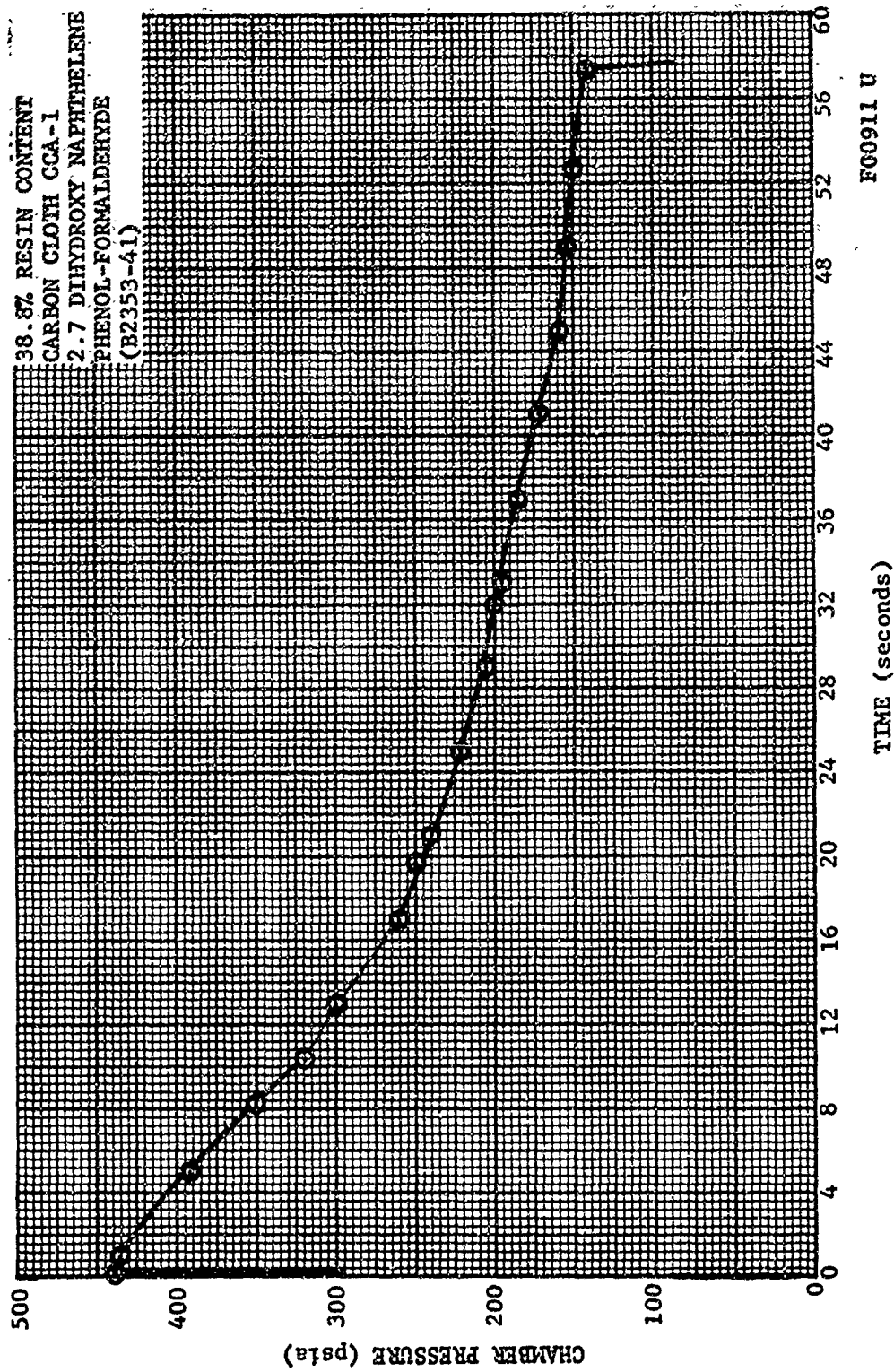


FIGURE 53. CHAMBER PRESSURE VERSUS TIME - ASD 463 NOZZLE



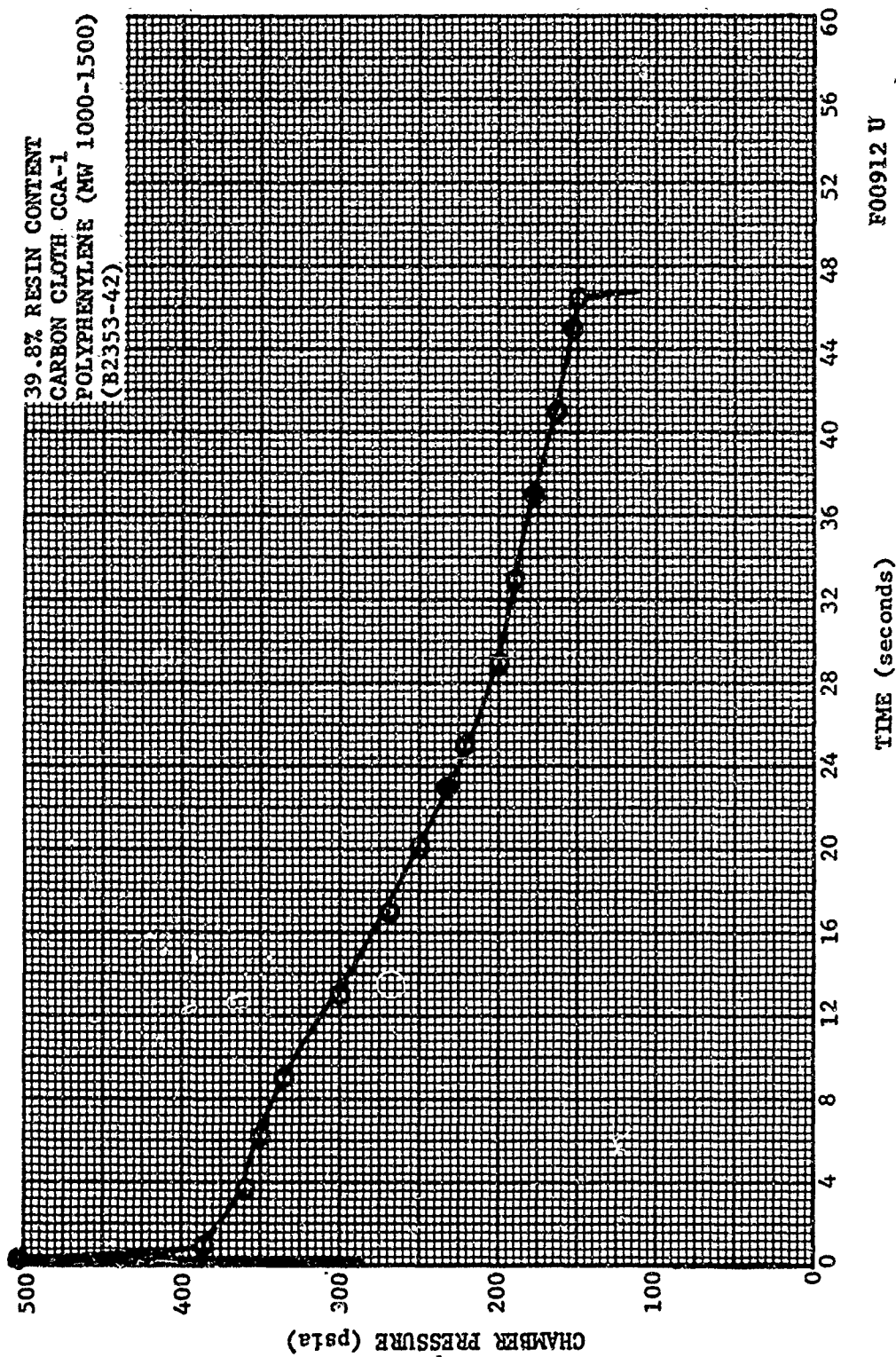


FIGURE 54. CHAMBER PRESSURE VERSUS TIME - ASD 467 NOZZLE

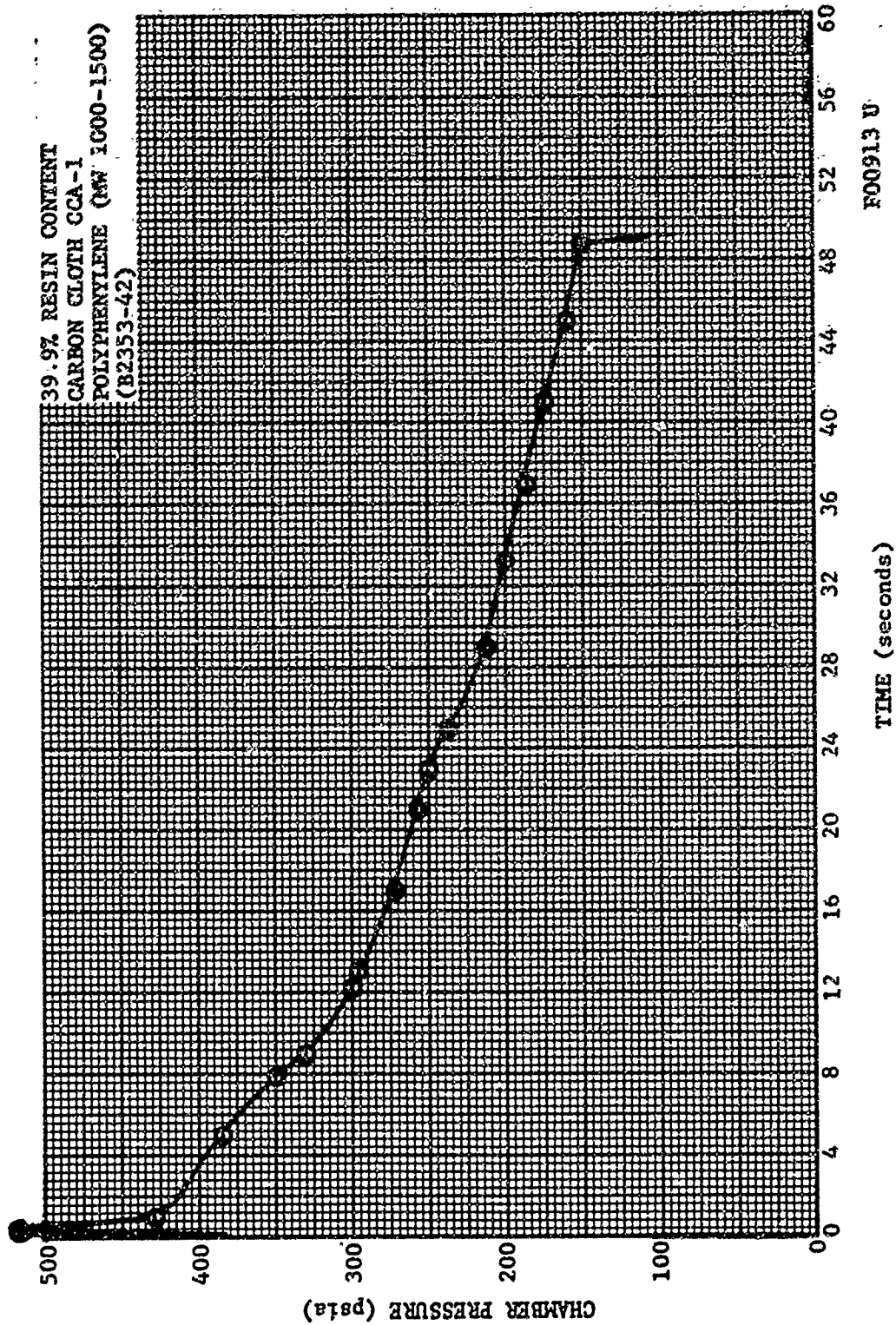
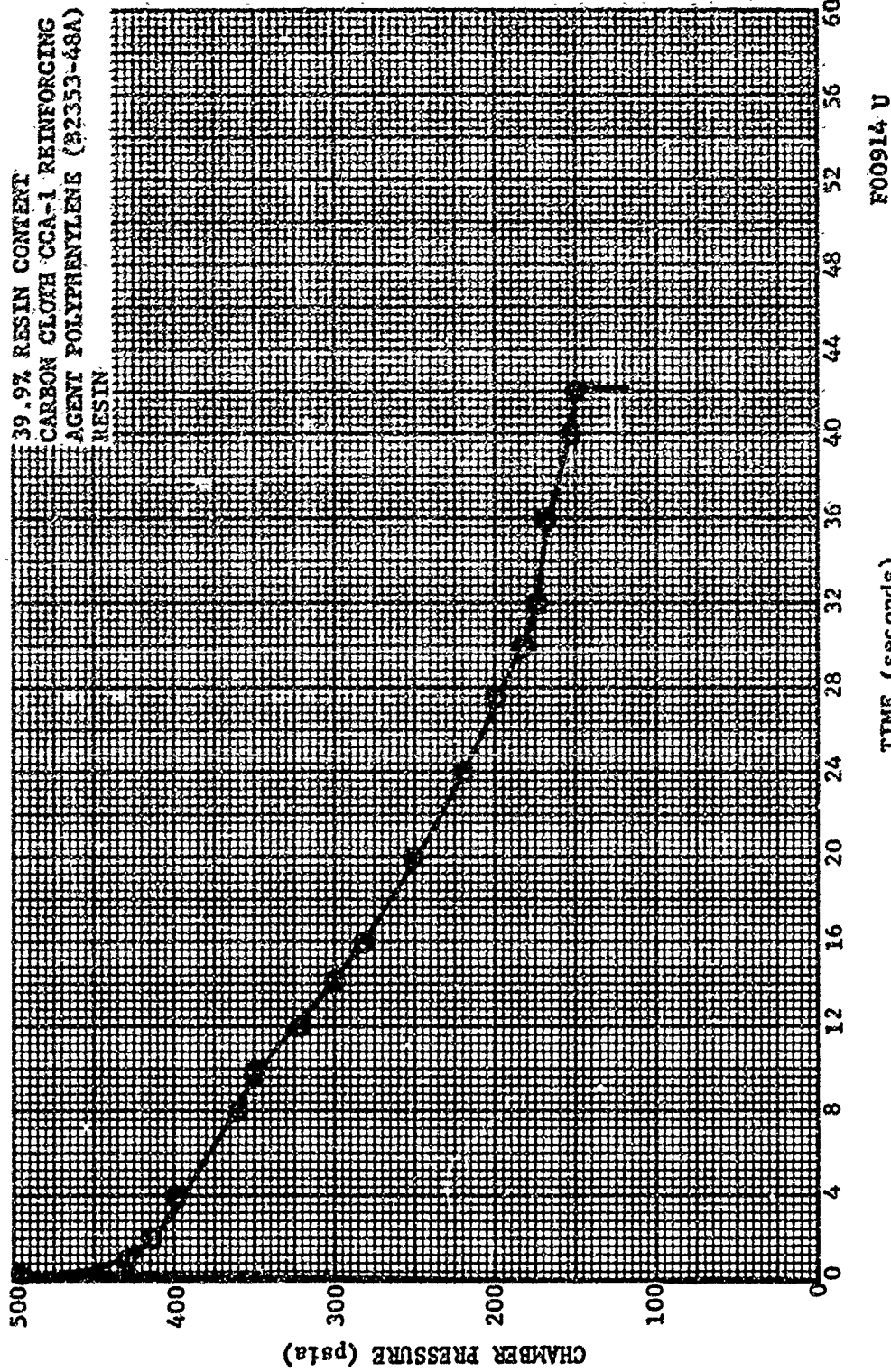


FIGURE 55. CHAMBER PRESSURE VERSUS TIME - ASD 468 NOZZLE

39.9% RESIN CONTENT  
 CARBON CLOTH CCA-1 REINFORCING  
 AGENT POLYPHENYLENE (B2353-48A)  
 RESIN



F00914 U

FIGURE 56. CHAMBER PRESSURE VERSUS TIME - ASD 471 NOZZLE



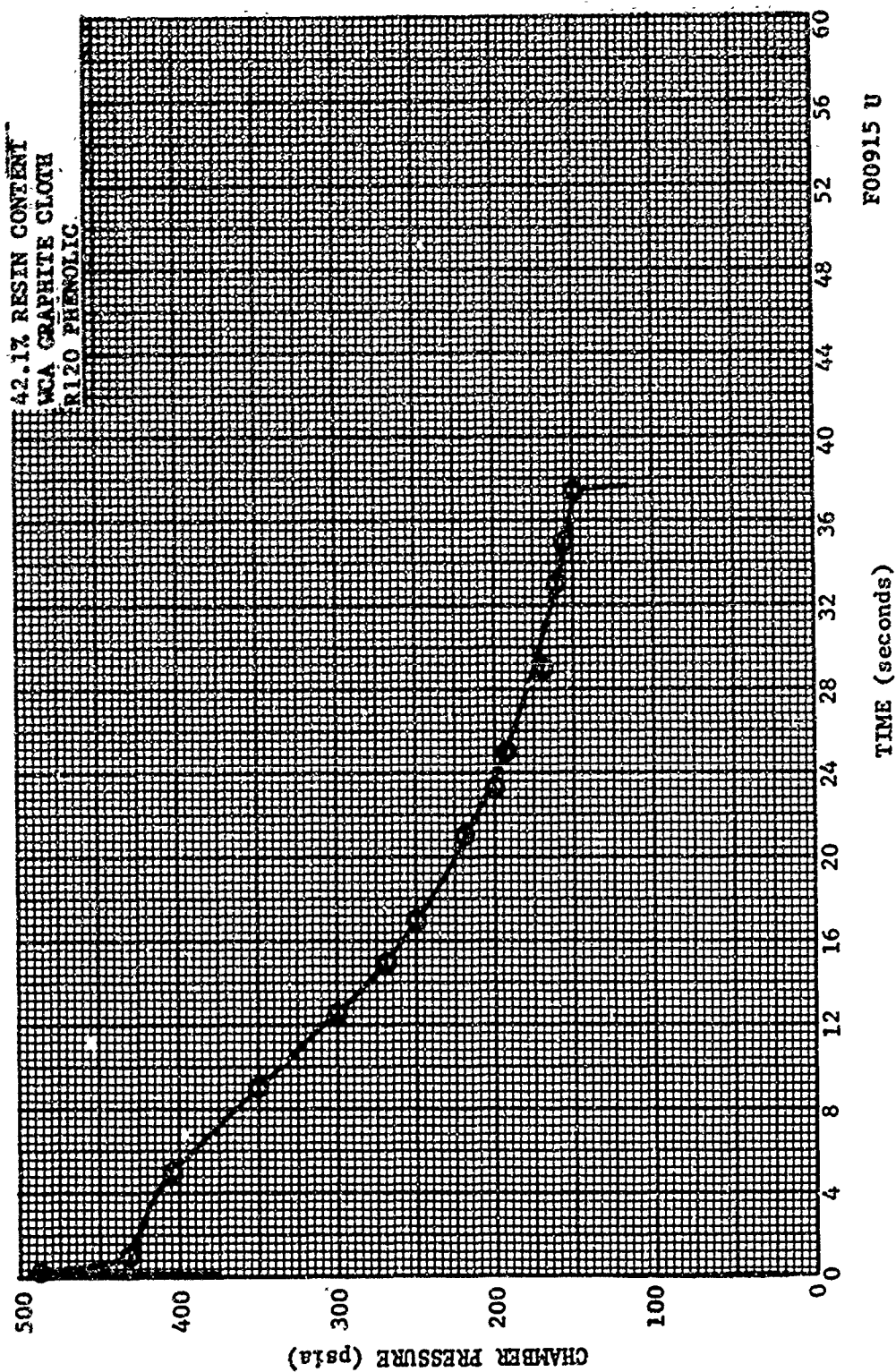


FIGURE 57. CHAMBER PRESSURE VERSUS TIME - ASD 480 NOZZLE

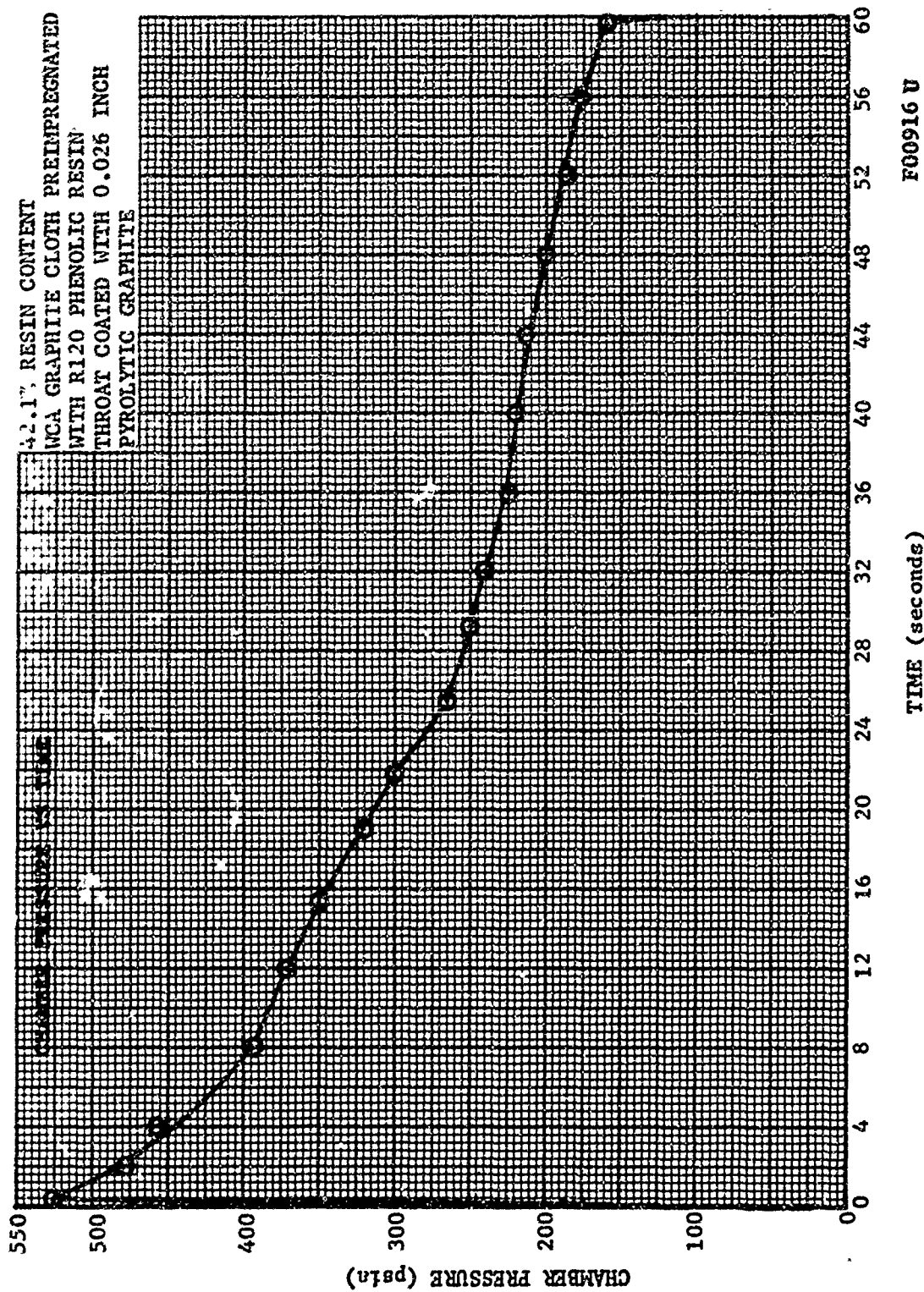


FIGURE 58. CHAMBER PRESSURE VERSUS TIME - ASD 482 NOZZLE

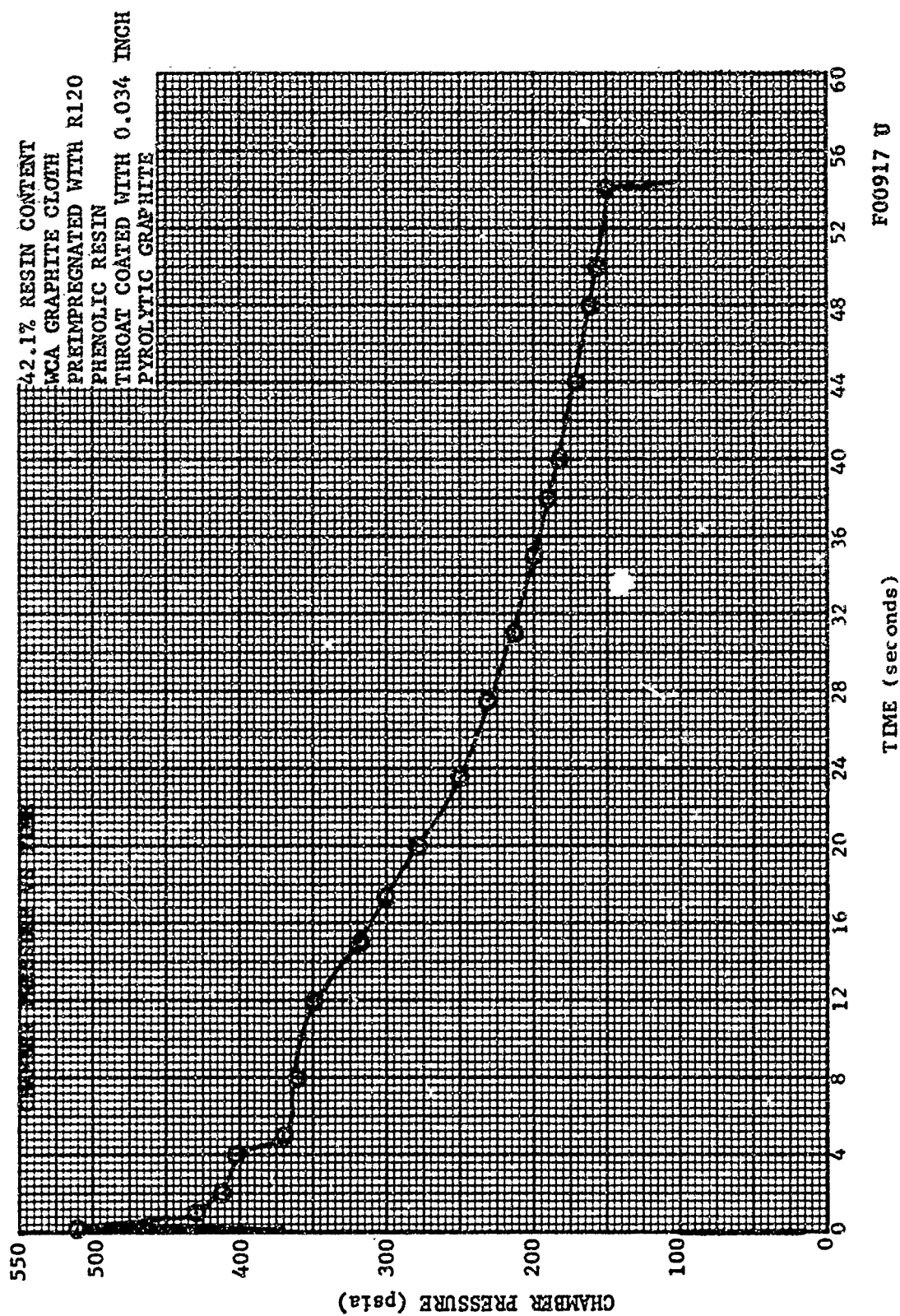


FIGURE 59 CHAMBER PRESSURE VERSUS TIME - ASD 483 NOZZLE

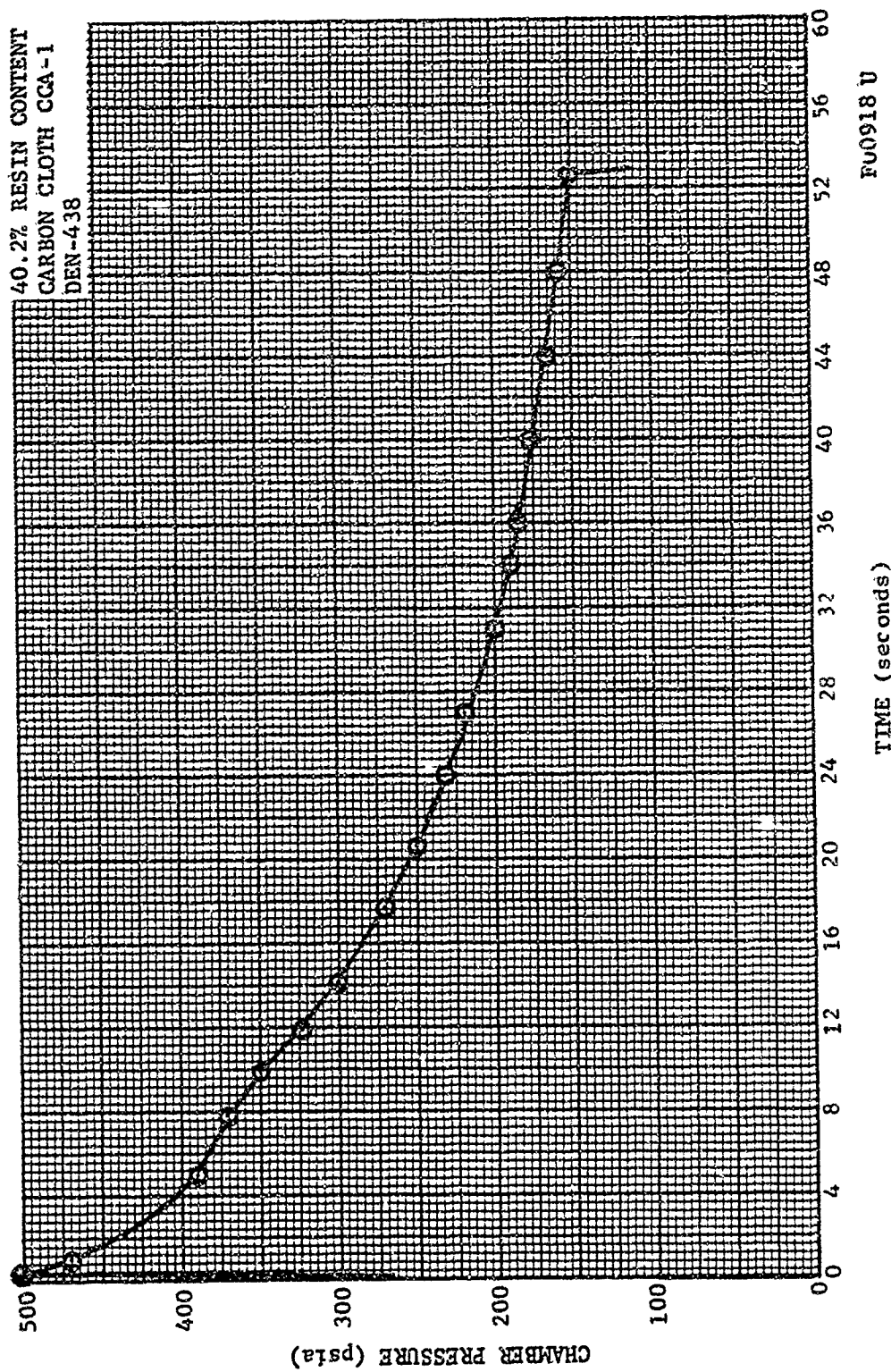


FIGURE 60. CHAMBER PRESSURE VERSUS TIME - ASD 489 NOZZLE

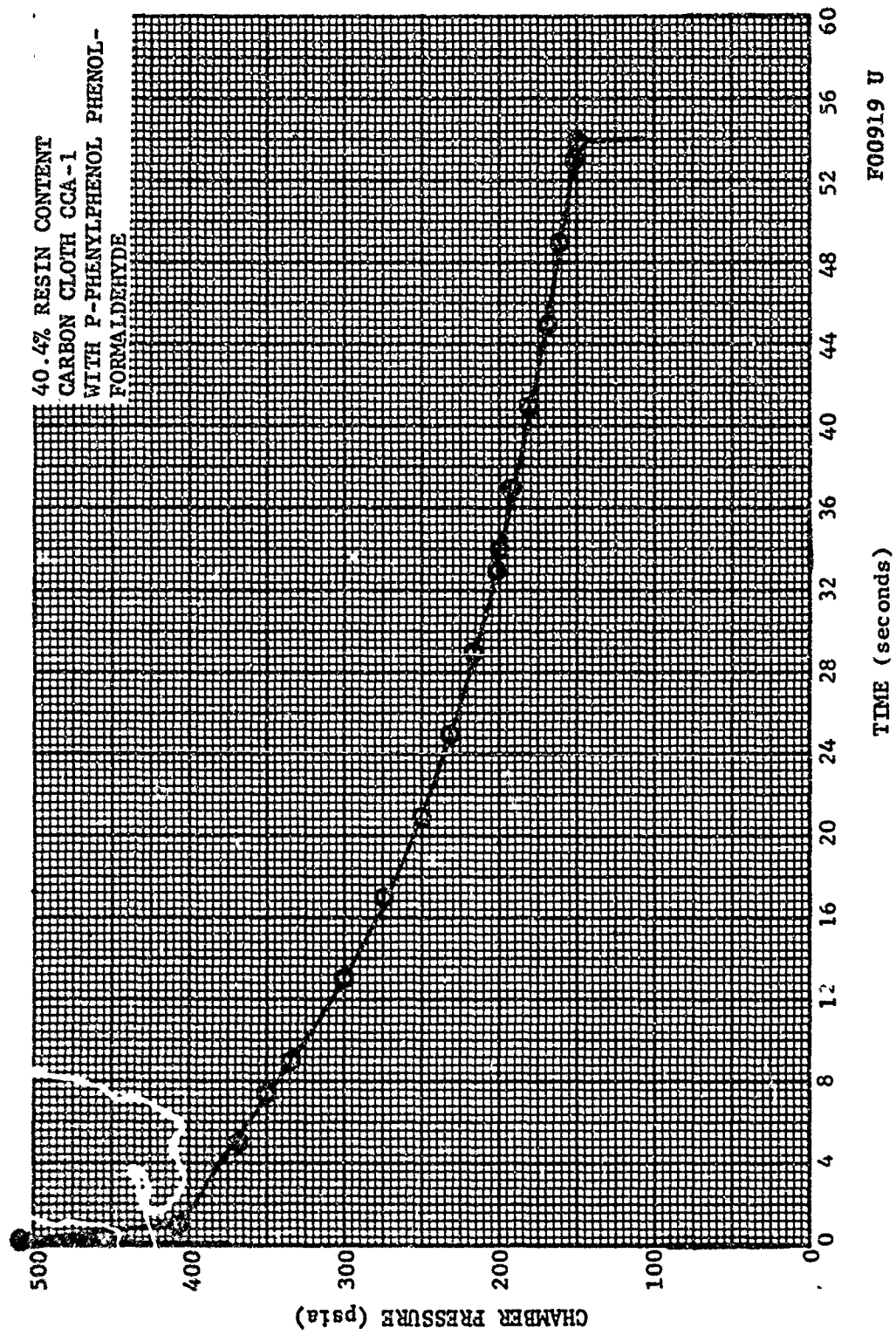


FIGURE 61. CHAMBER PRESSURE VERSUS TIME - ASD 490 NOZZLE



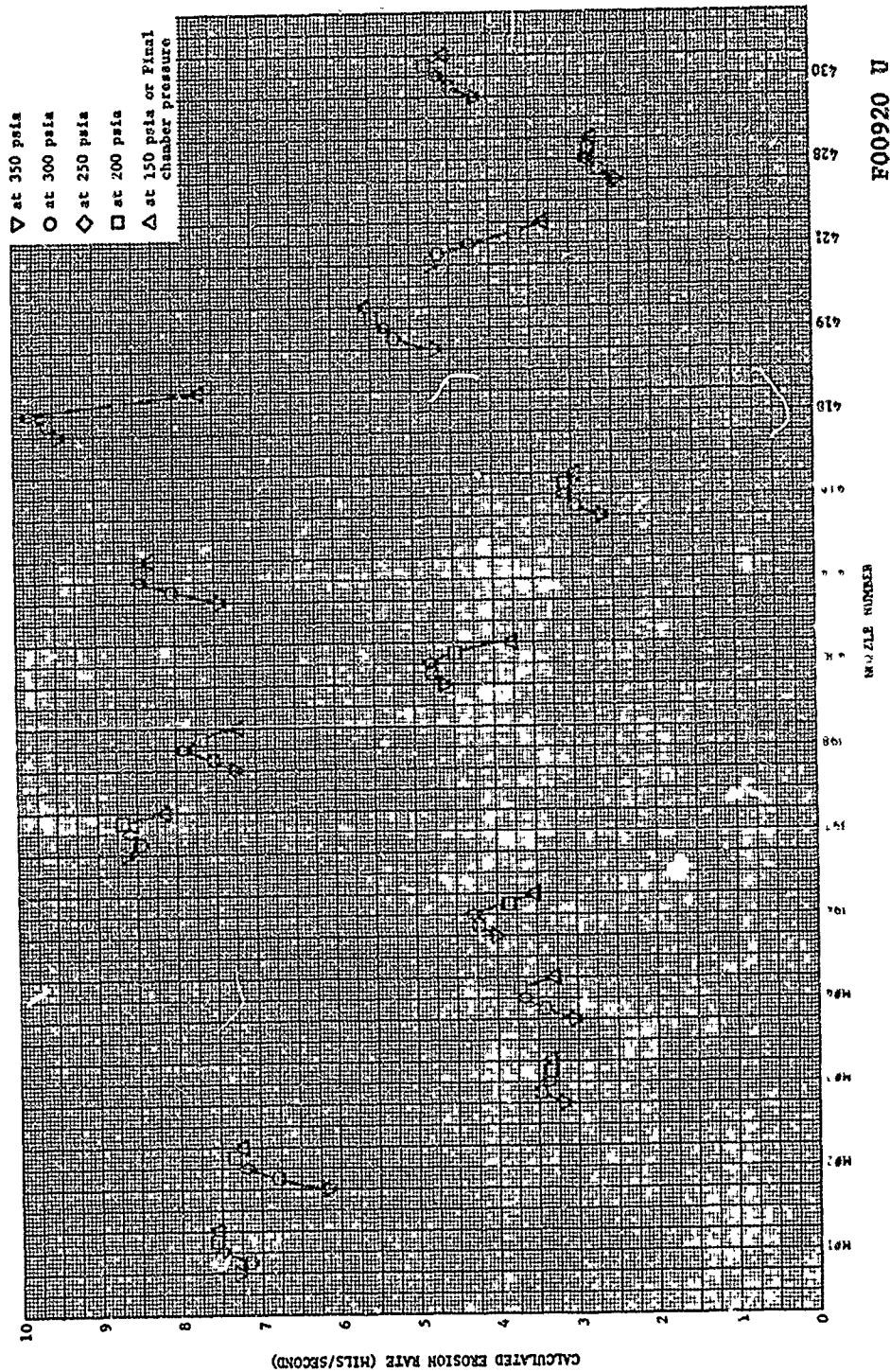
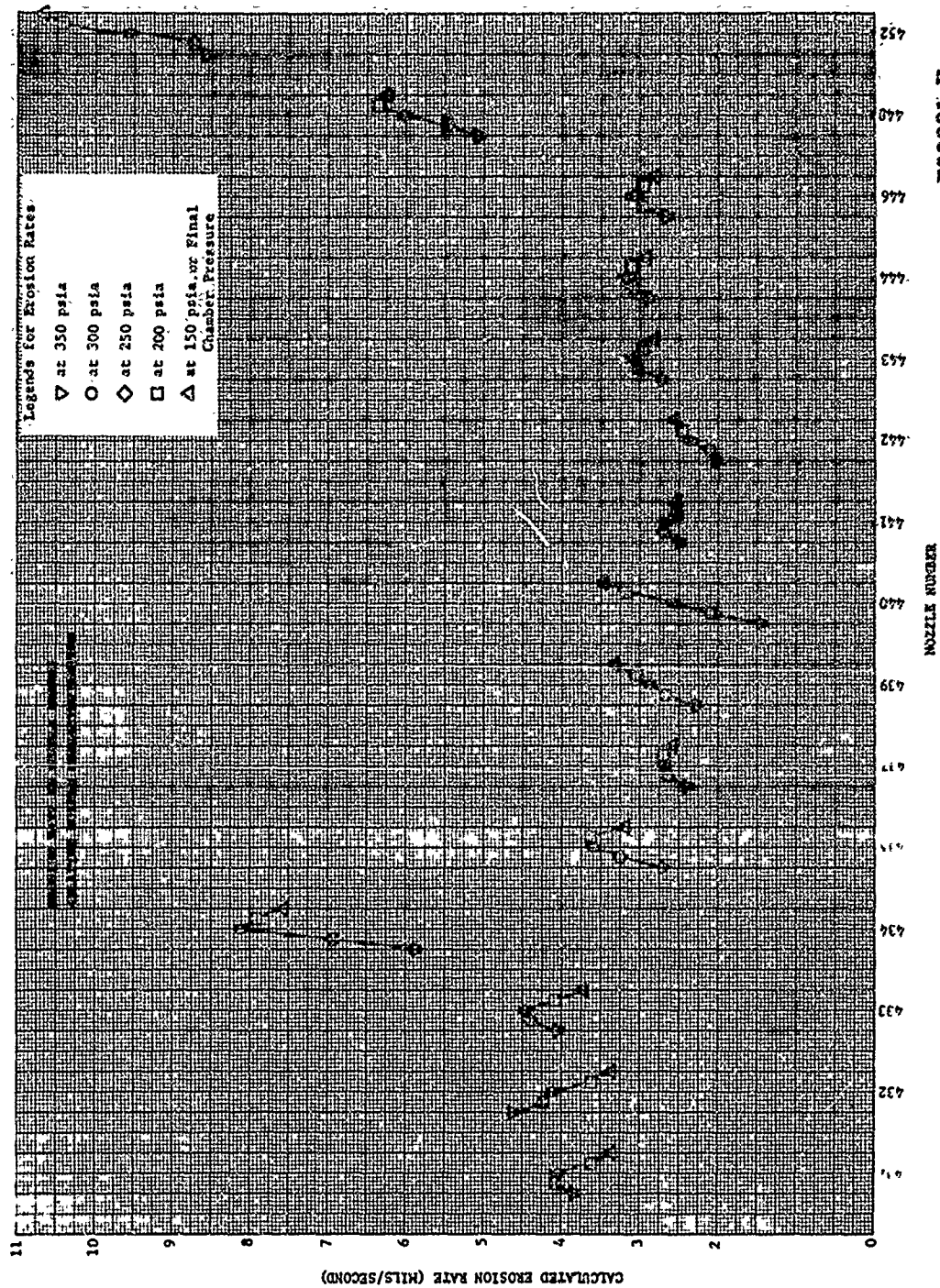


FIGURE 62A. EROSION RATE VERSUS NOZZLE NUMBER ABLATIVE NOZZLE  
CHARACTERIZATION - TEST SERIES 2



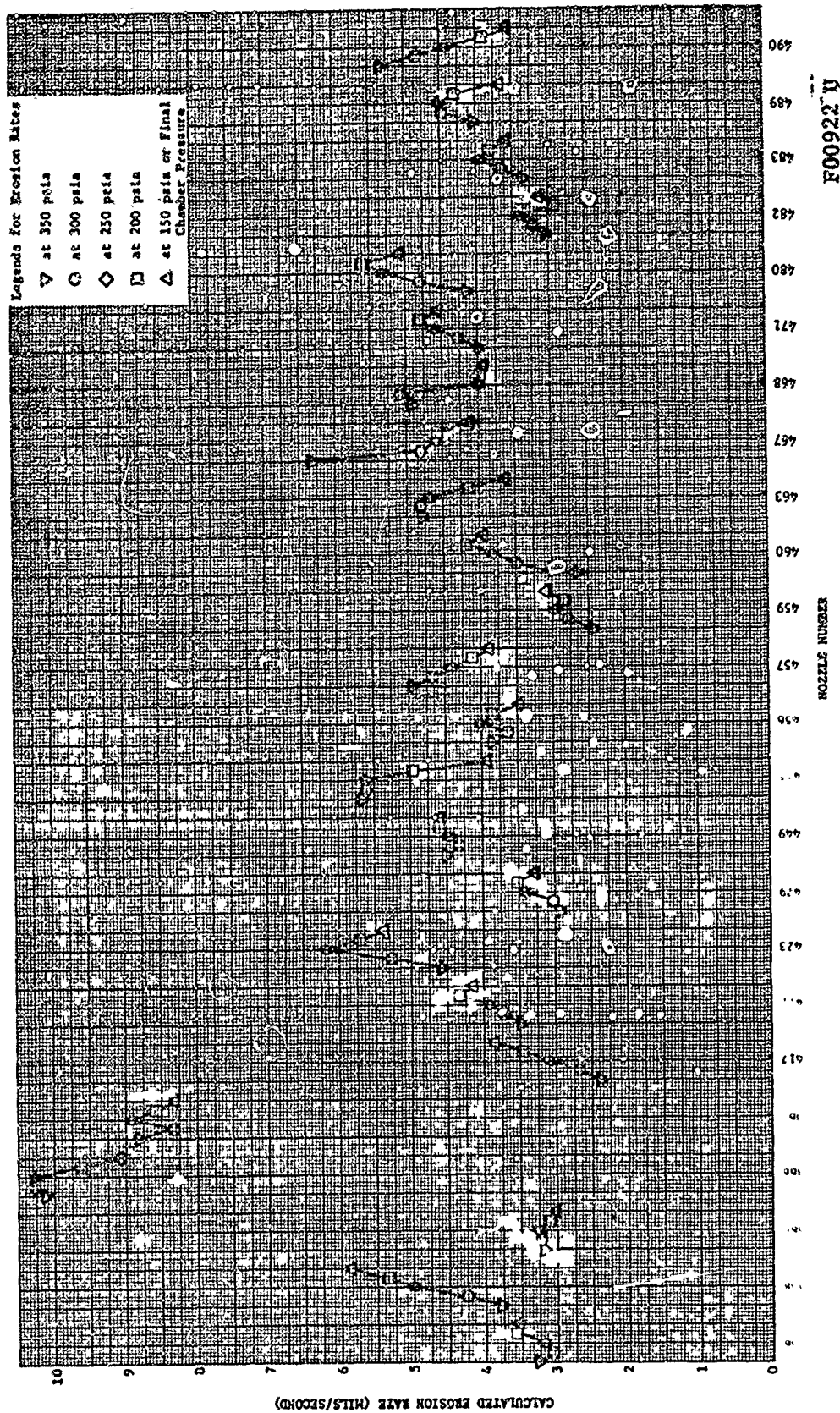
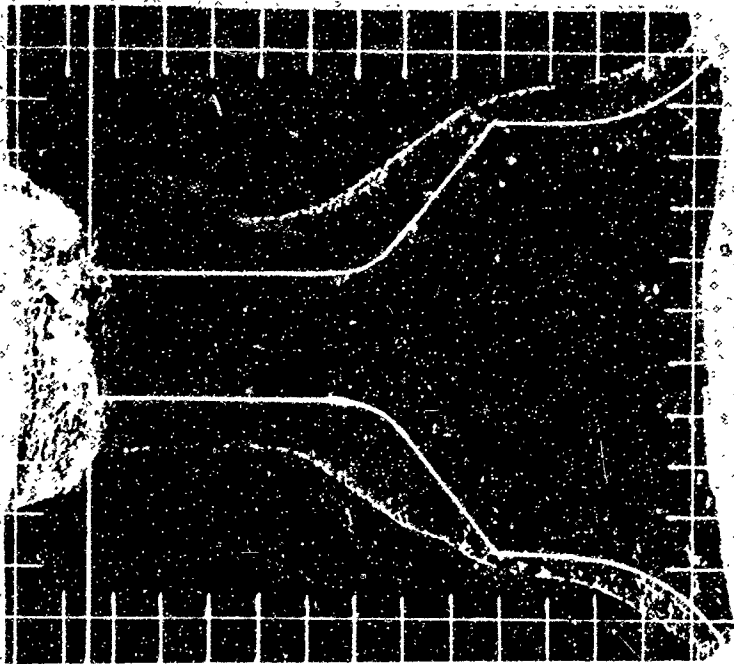


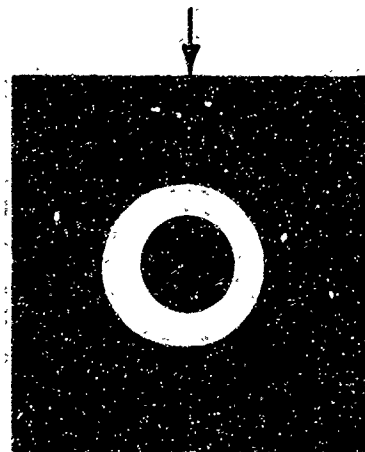
FIGURE 62B. EROSION RATE VERSUS NOZZLE NUMBER ABLATIVE NOZZLE CHARACTERIZATION - TEST SERIES 2



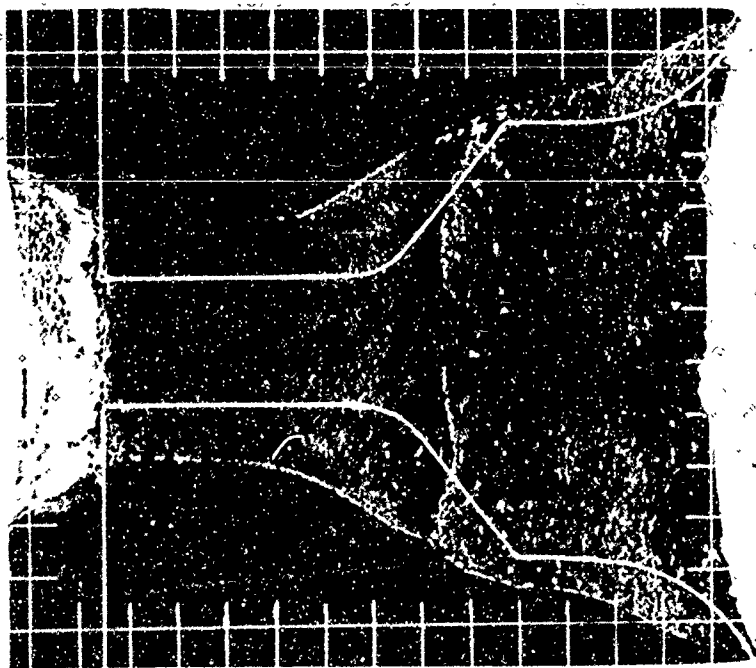
NOZZLE NO. MANC-1



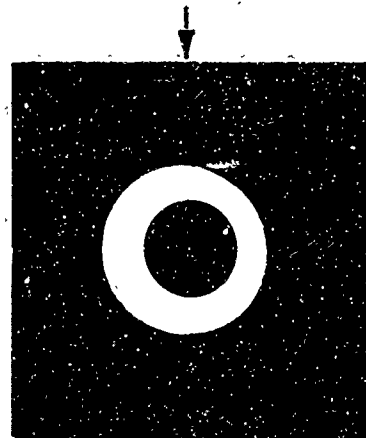
12 O'CLOCK



NOZZLE NO. MANC-2



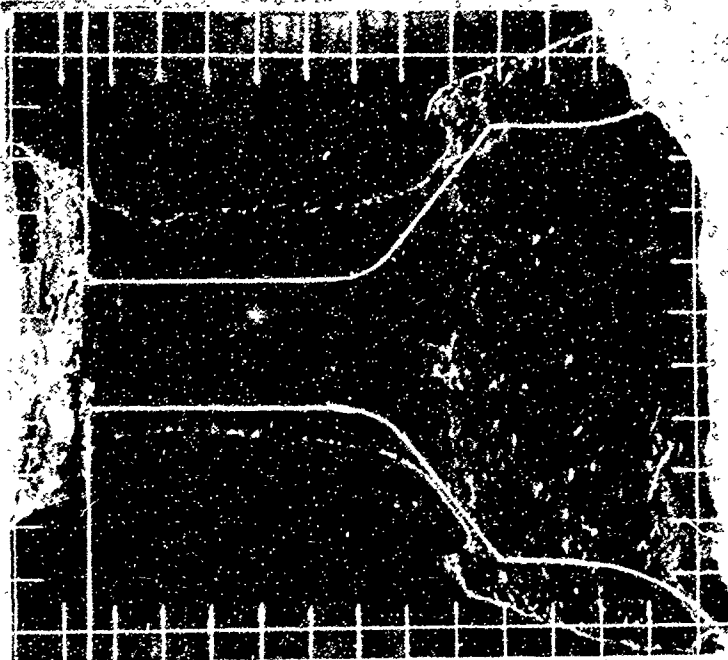
12 O'CLOCK



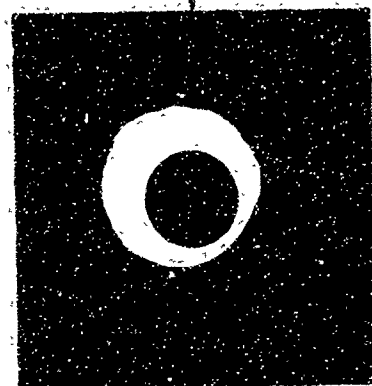
R13889 U

FIGURE 63. PROFILE AND AXIAL NOZZLE PHOTOGRAPHS

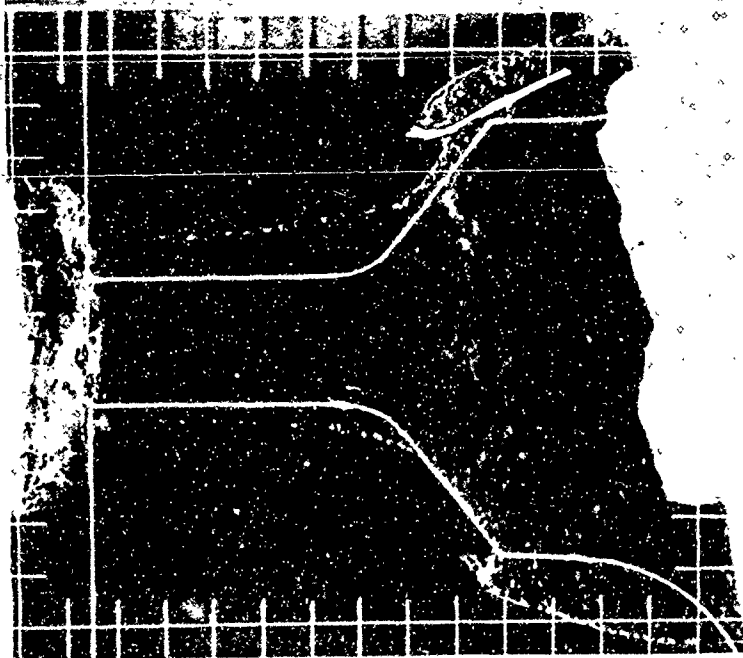
NOZZLE NO. MANC-3



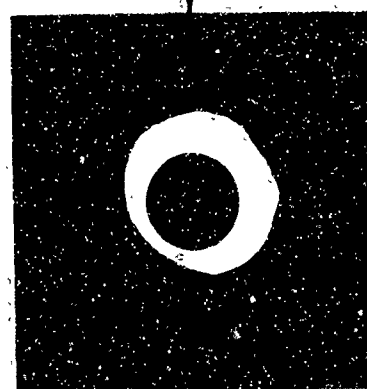
12 O'CLOCK



NOZZLE NO. MANC-4



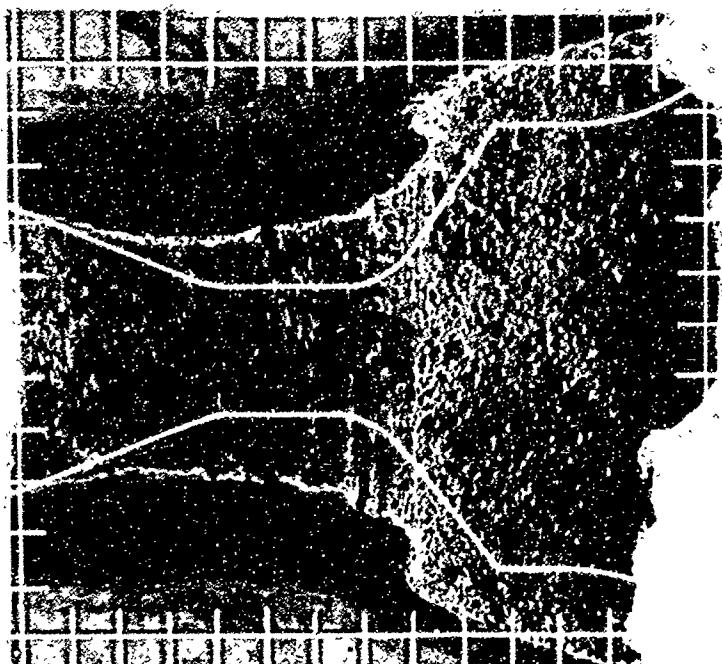
12 O'CLOCK



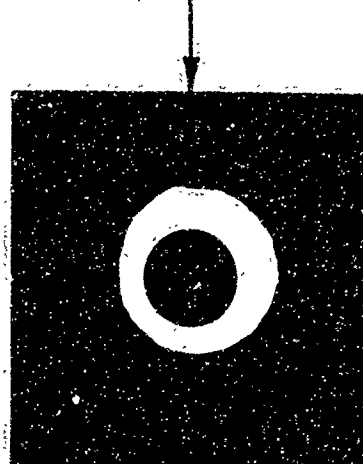
RY3888 U

FIGURE 64. PROFILE AND AXIAL NOZZLE PHOTOGRAPHS

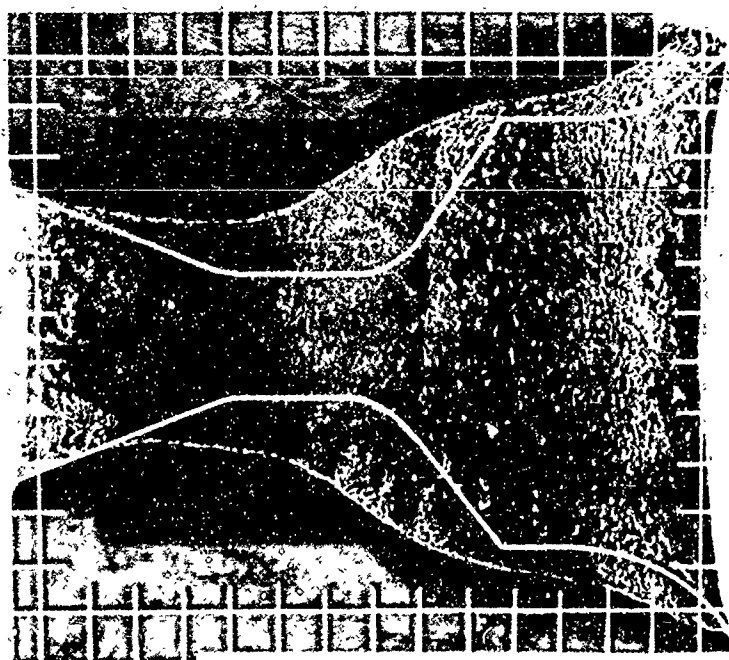
NOZZLE NO. ASD-94



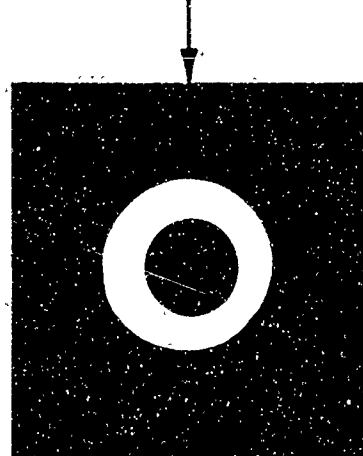
12 O'CLOCK



NOZZLE NO. ASD-397



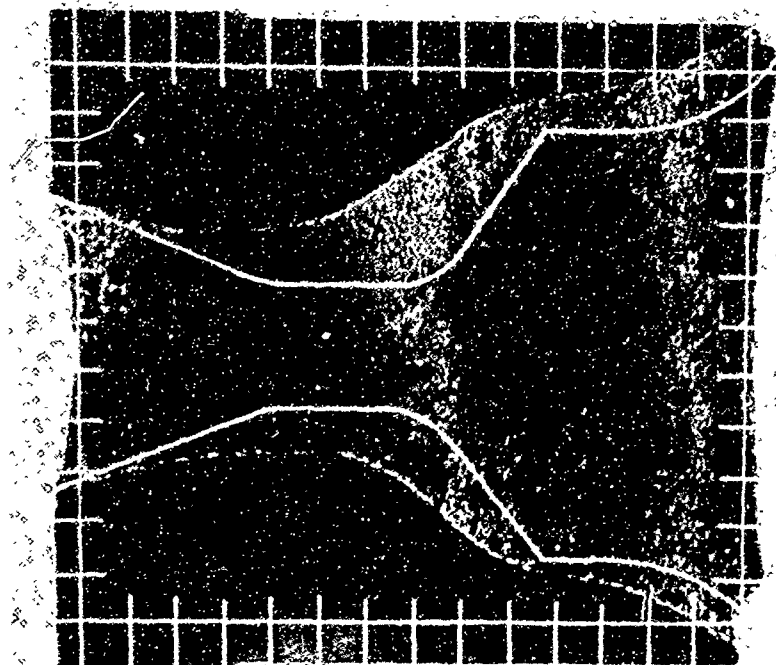
12 O'CLOCK



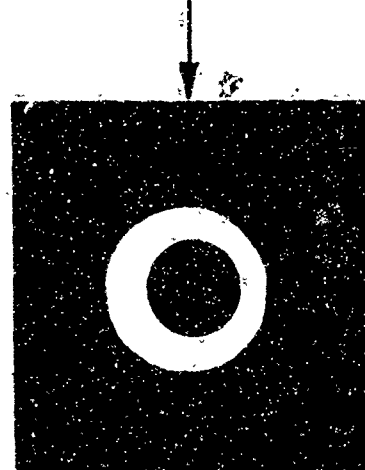
R13887 U

FIGURE 65. PROFILE AND AXIAL NOZZLE PHOTOGRAPHS

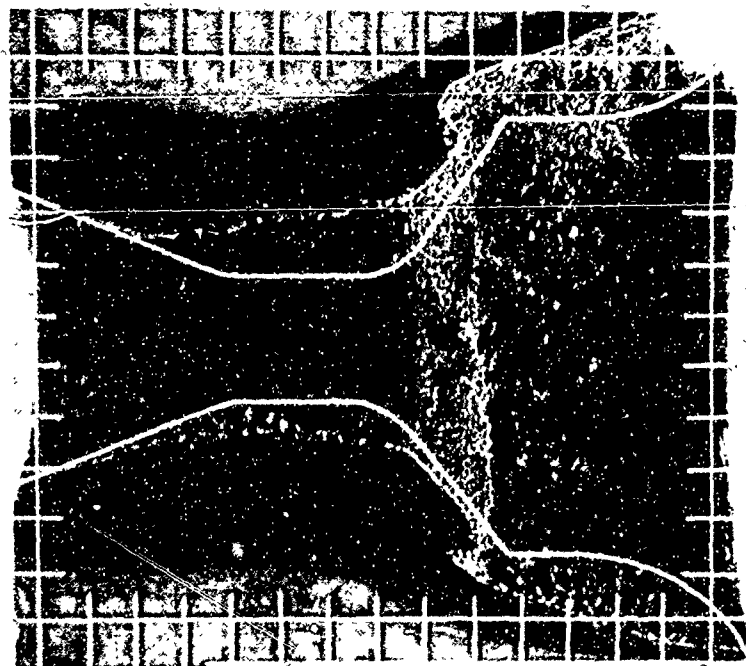
NOZZLE NO. ASD-398



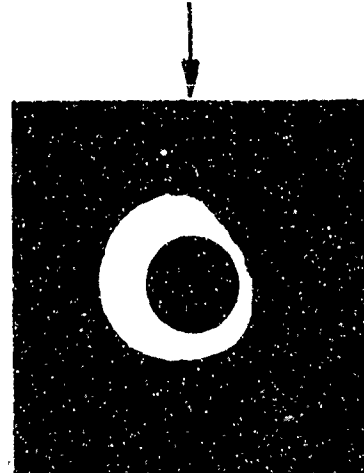
12 O'CLOCK



NOZZLE NO. ASD-400



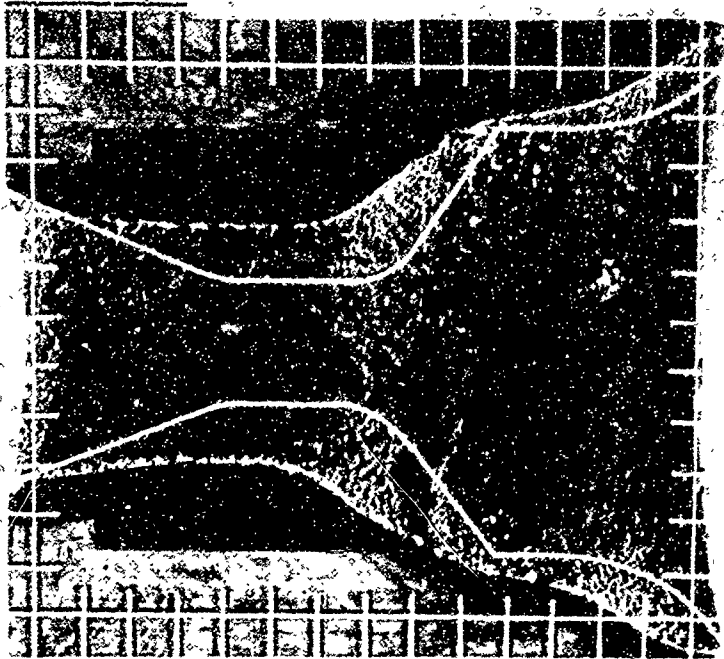
12 O'CLOCK



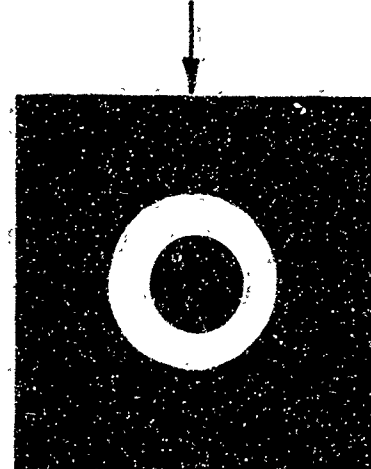
R13886U

FIGURE 66. PROFILE AND AXIAL NOZZLE PHOTOGRAPHS

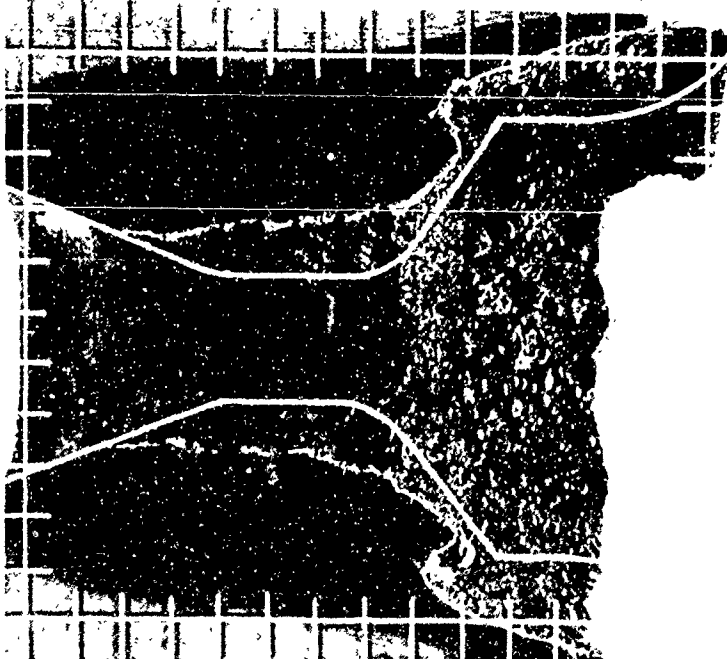
NOZZLE NO. ASD-414



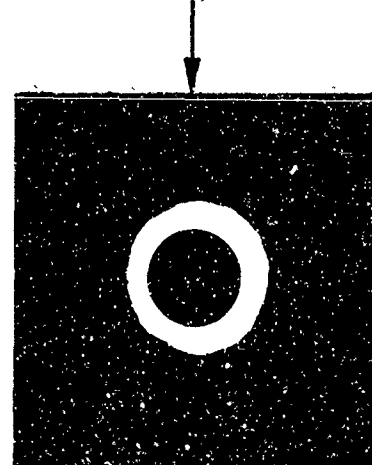
12 O'CLOCK



NOZZLE NO. ASD-416



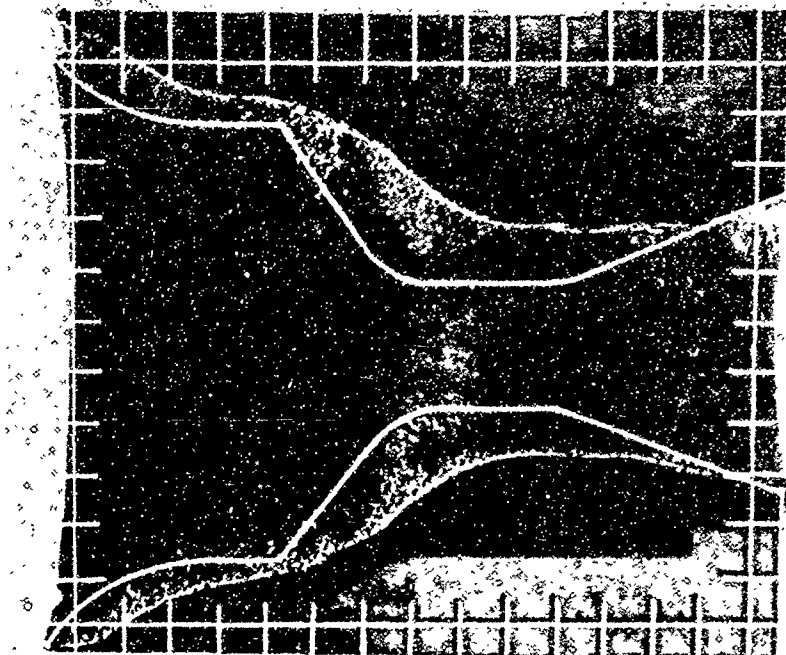
12 O'CLOCK



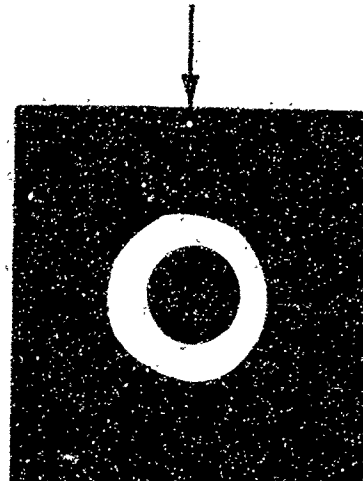
R13885U

FIGURE 67. PROFILE AND AXIAL NOZZLE PHOTOGRAPHS

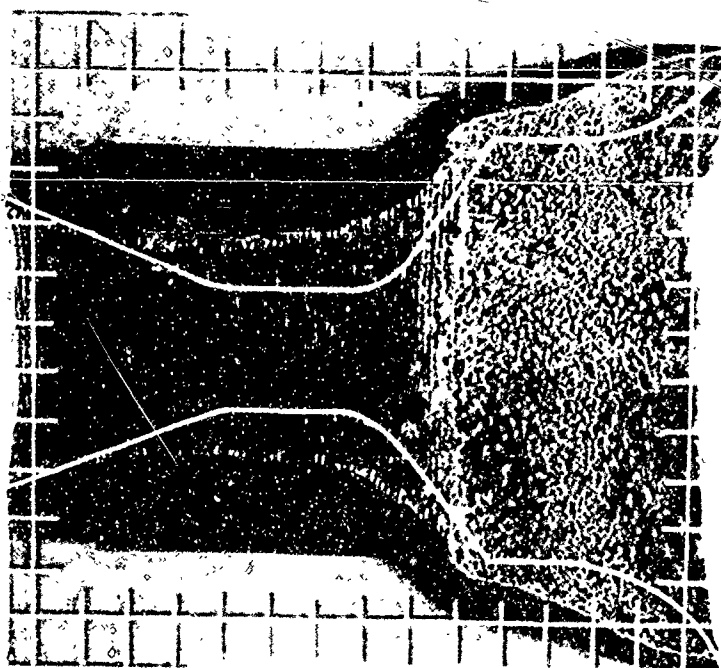
NOZZLE NO. ASD-418



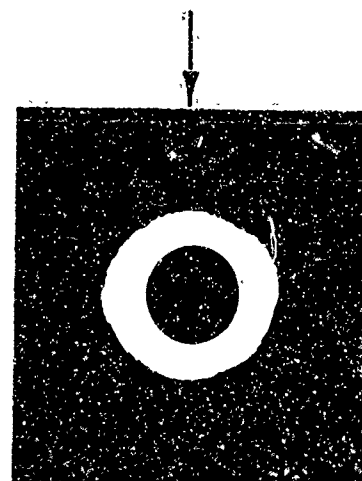
12 O'CLOCK



NOZZLE NO. ASD-419



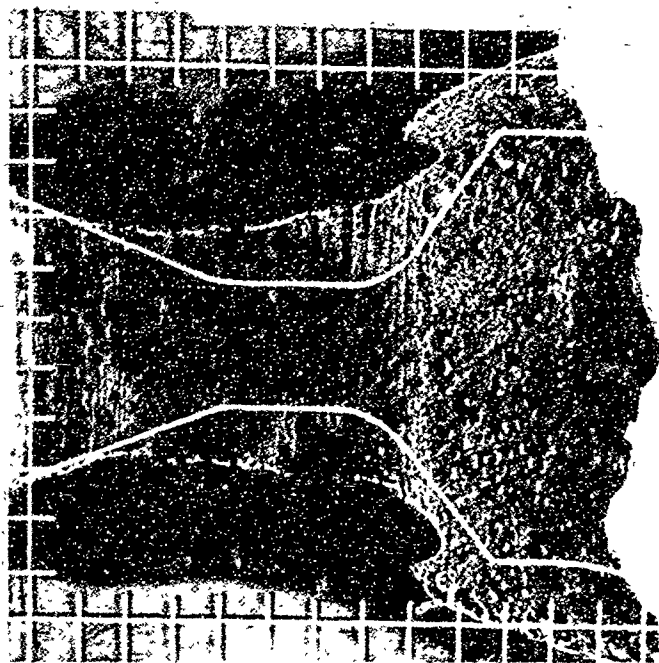
12 O'CLOCK



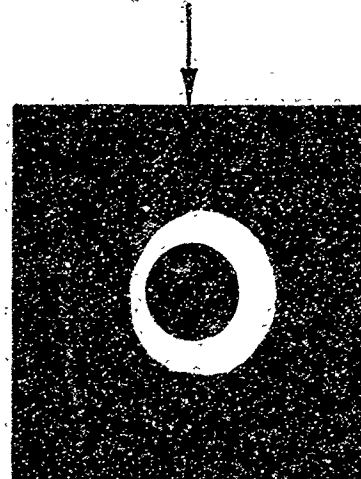
R13884U

FIGURE 68. PROFILE AND AXIAL NOZZLE PHOTOGRAPHS

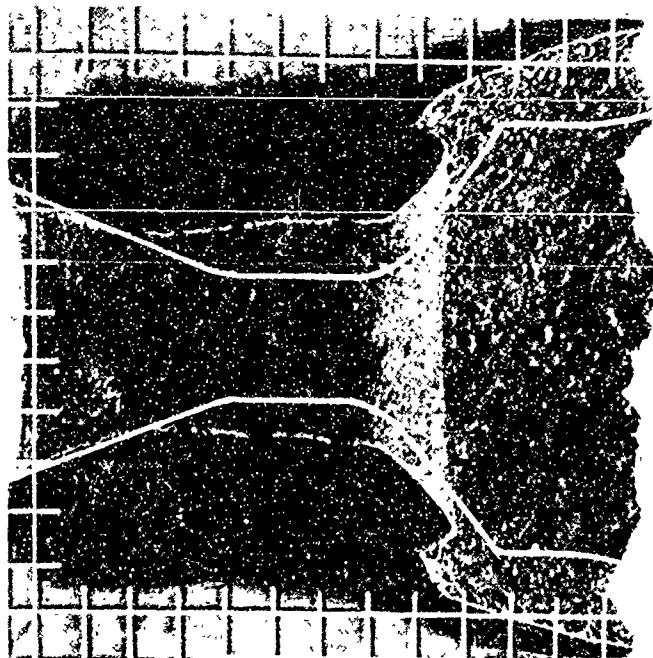
NOZZLE NO. ASD-421



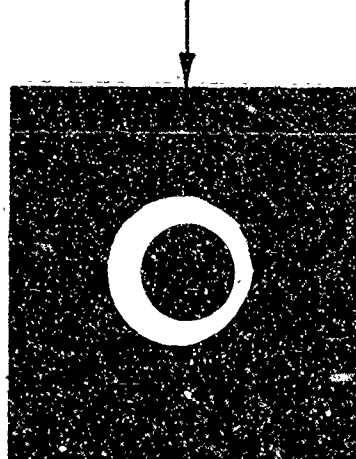
12 O'CLOCK



NOZZLE NO. ASD-428



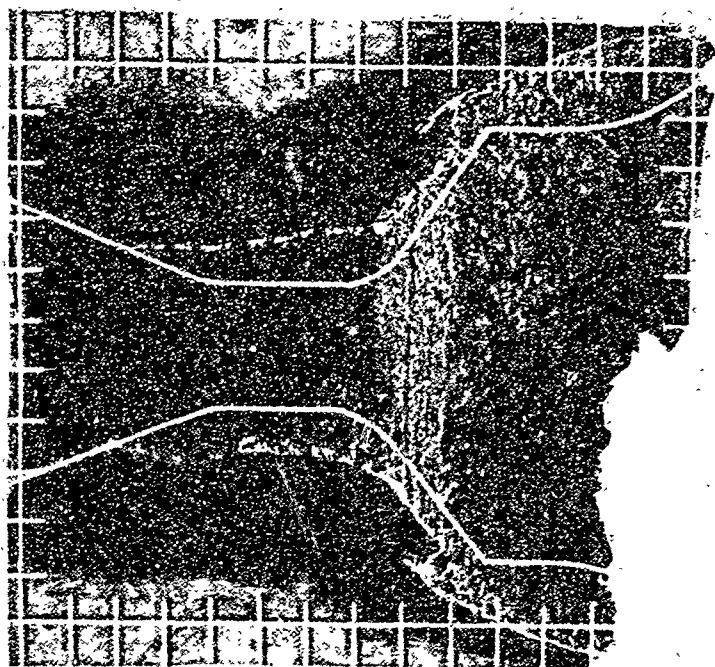
12 O'CLOCK



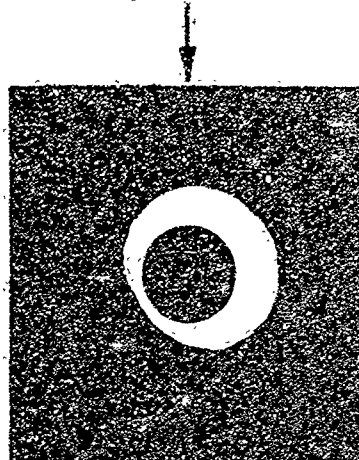
R13883U

FIGURE 69. PROFILE AND AXIAL NOZZLE PHOTOGRAPHS

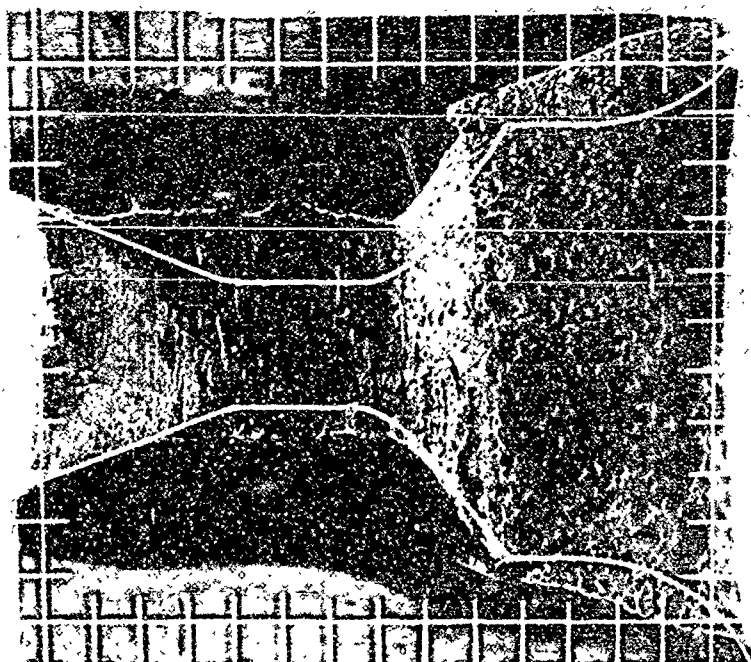
NOZZLE NO. ASD-430



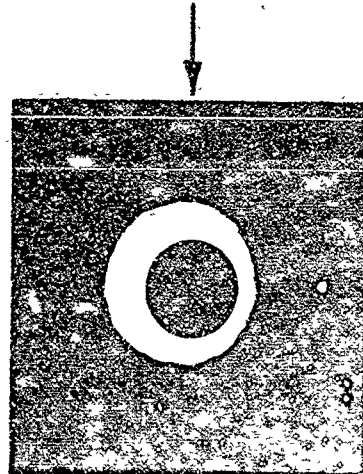
12 O'CLOCK



NOZZLE NO. ASD-431



12 O'CLOCK

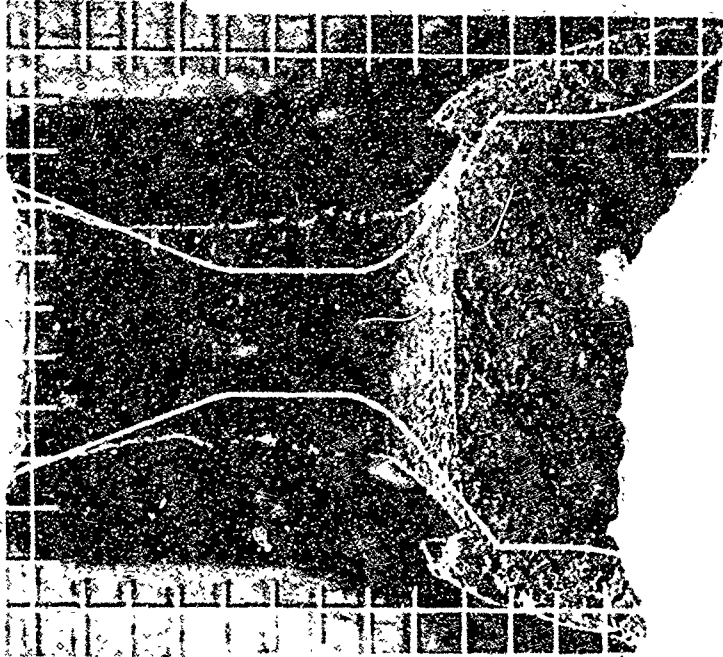


R13862U

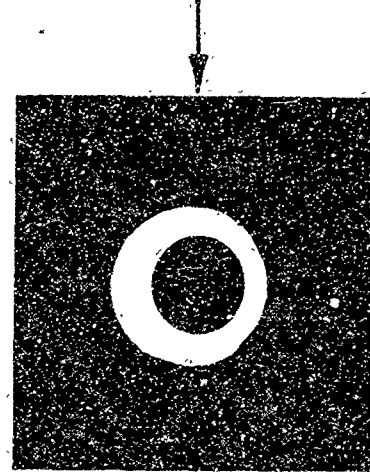
FIGURE 70. PROFILE AND AXIAL NOZZLE PHOTOGRAPHS



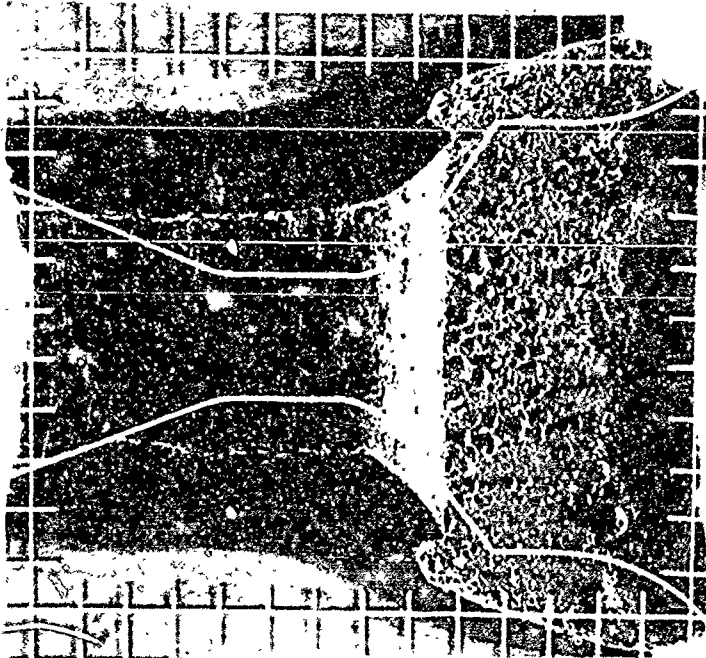
NOZZLE NO. ASD-432



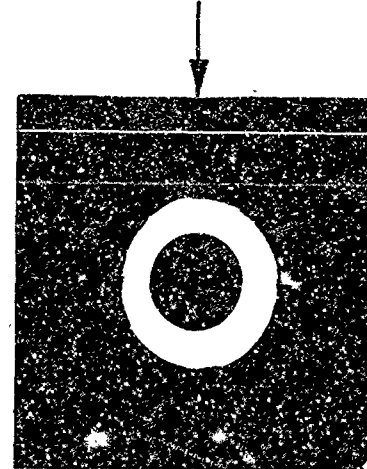
12 O'CLOCK



NOZZLE NO. ASD-433



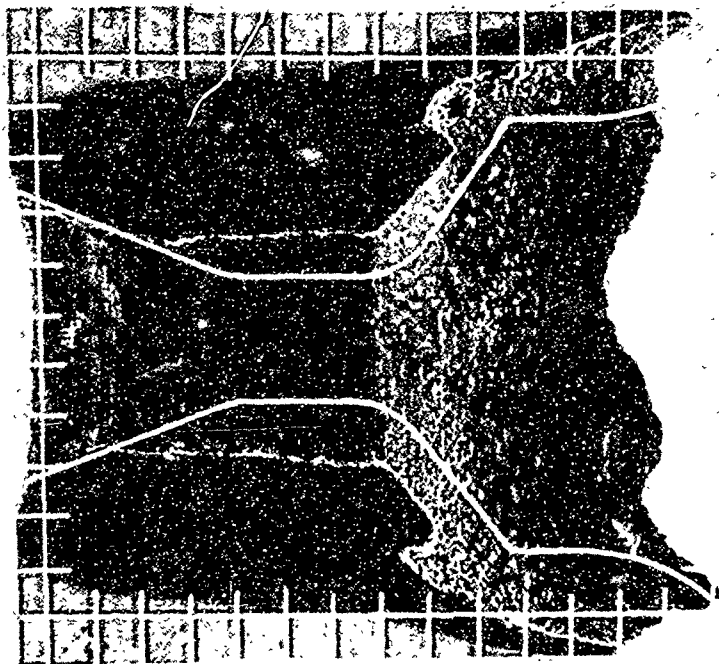
12 O'CLOCK



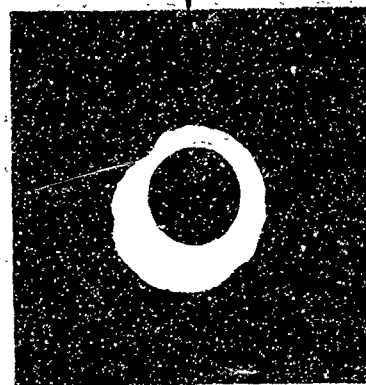
R13881U

FIGURE 71. PROFILE AND AXIAL NOZZLE PHOTOGRAPHS

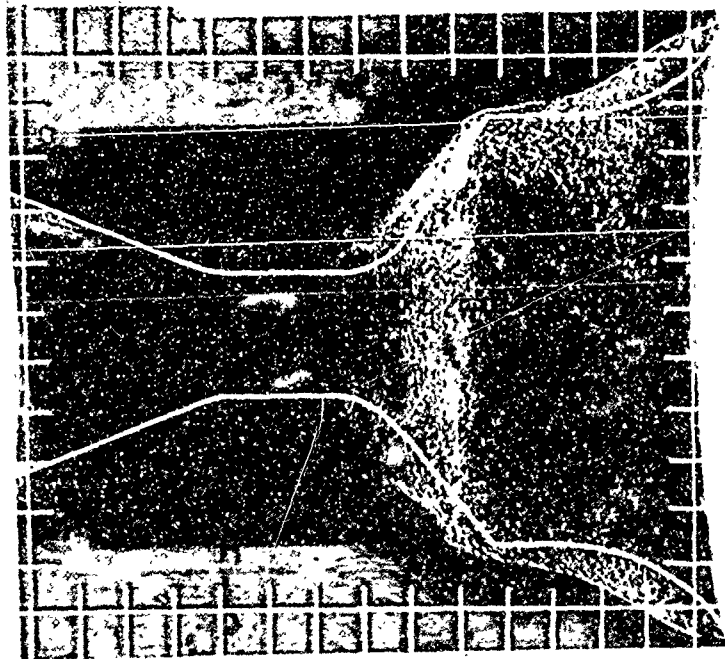
NOZZLE NO. ASD-434



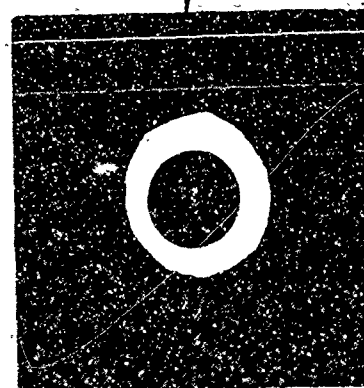
12 O'CLOCK



NOZZLE NO. ASD-435



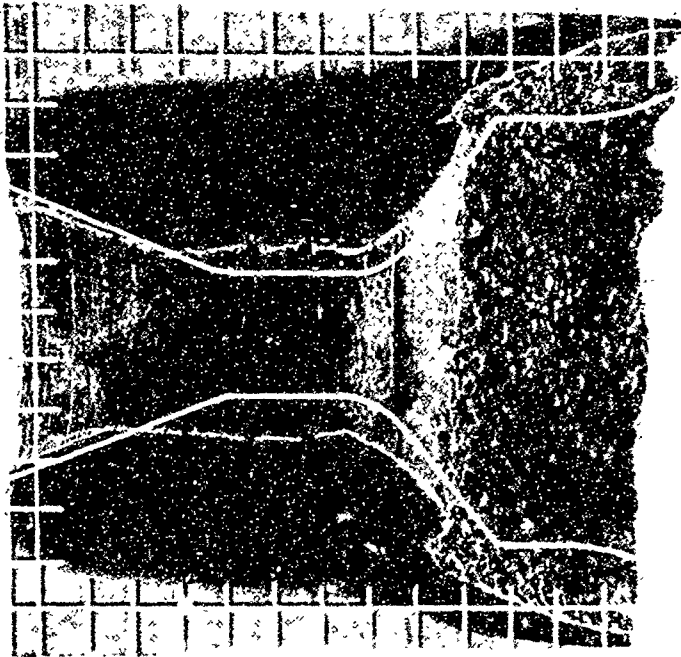
12 O'CLOCK



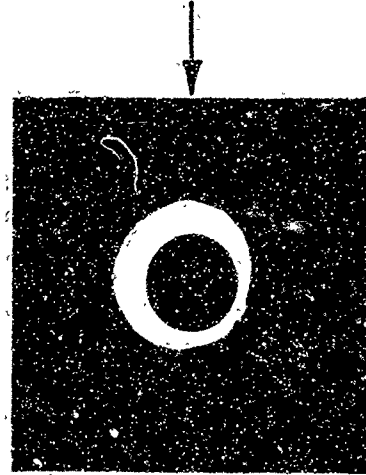
R13880U

FIGURE 72. PROFILE AND AXIAL NOZZLE PHOTOGRAPHS

NOZZLE NO. ASD-437



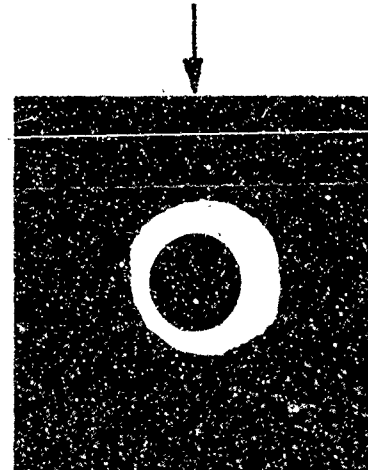
12 O'CLOCK



NOZZLE NO. ASD-439



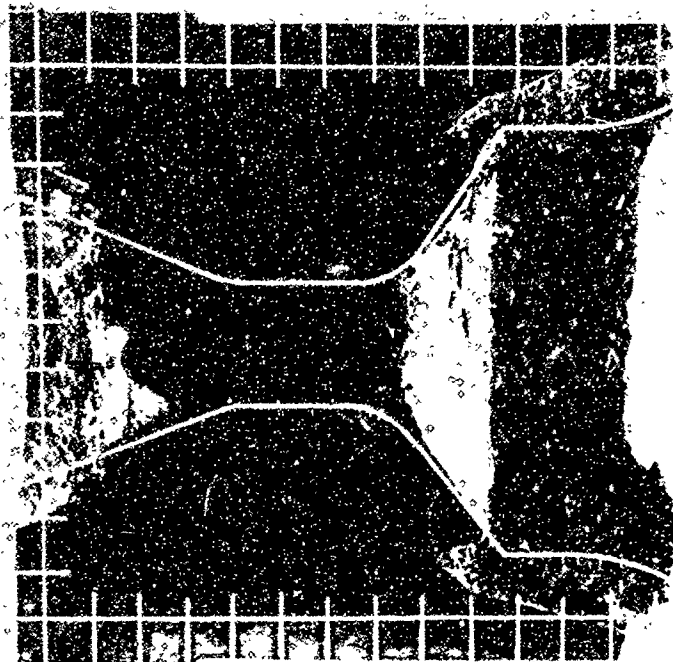
12 O'CLOCK



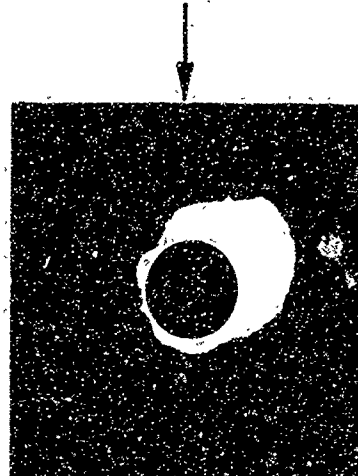
R13879U

FIGURE 73. PROFILE AND AXIAL NOZZLE PHOTOGRAPHS

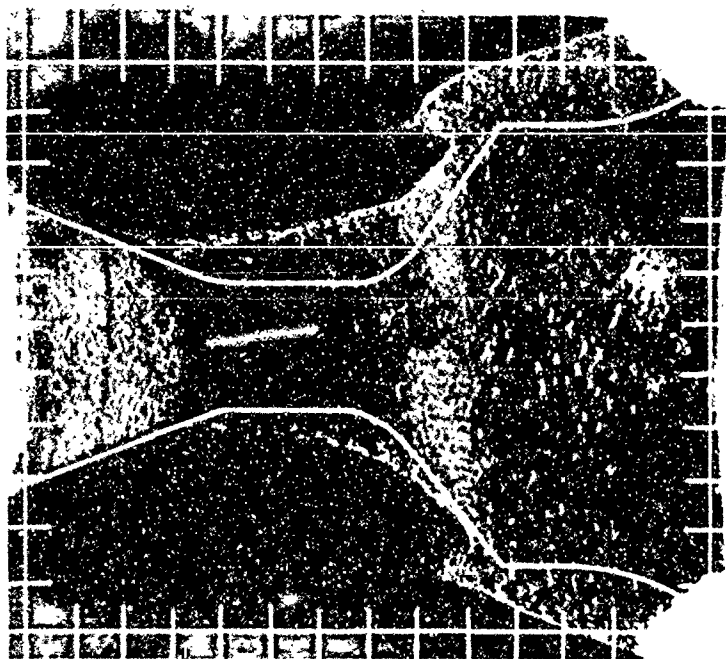
NOZZLE NO. ASD-440



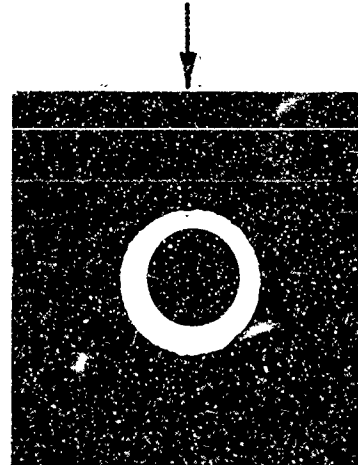
12 O'CLOCK



NOZZLE NO. ASD-441



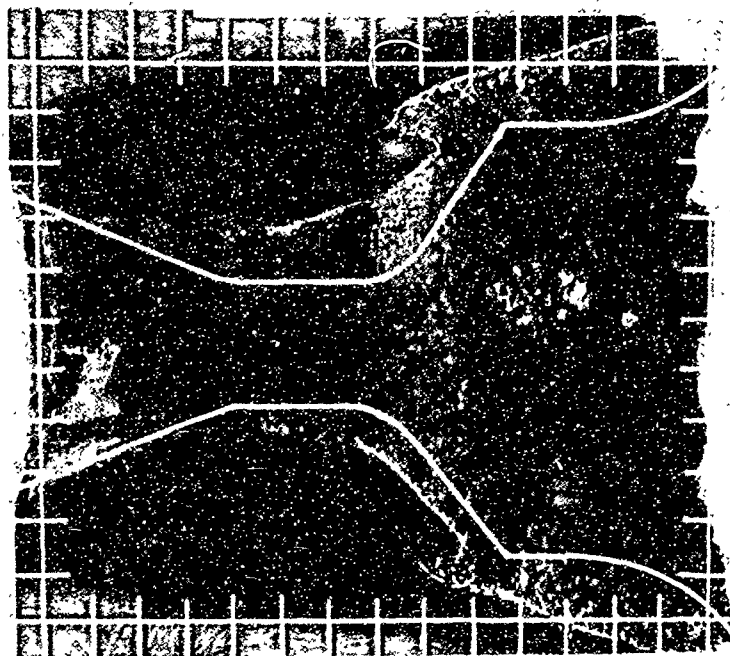
12 O'CLOCK



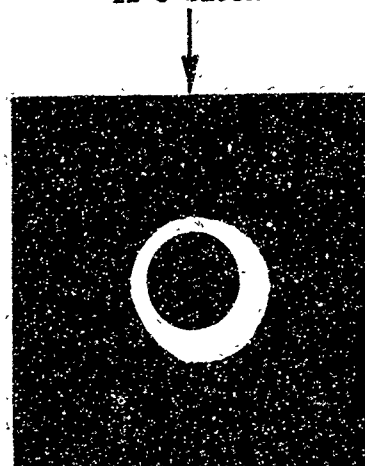
R13878U

FIGURE 74. PROFILE AND AXIAL NOZZLE PHOTOGRAPHS

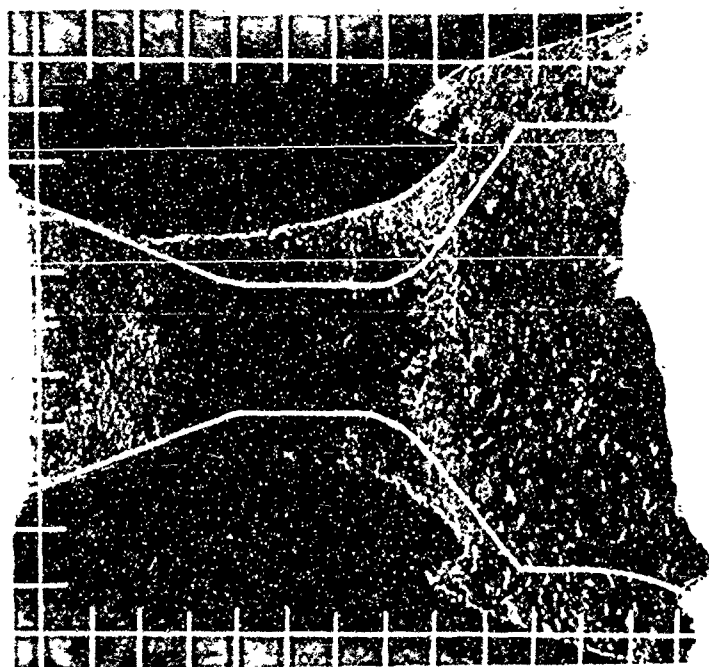
NOZZLE NO. ASD-442



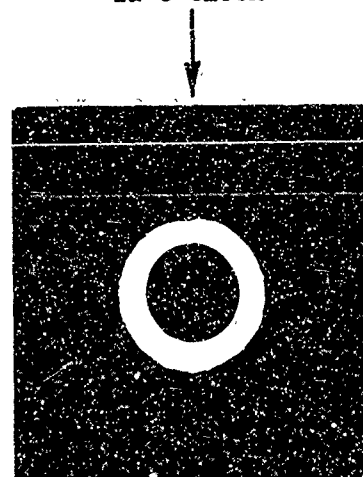
12 O'CLOCK



NOZZLE NO. ASD-443



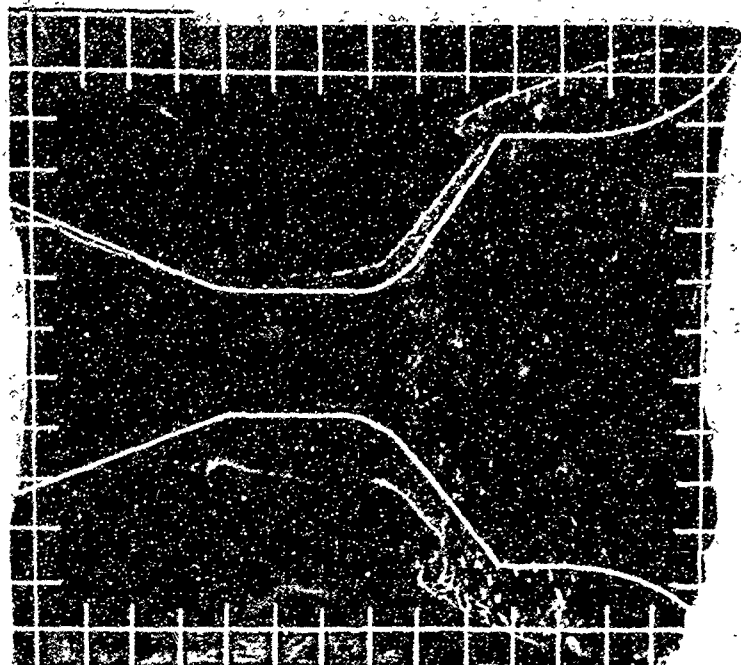
12 O'CLOCK



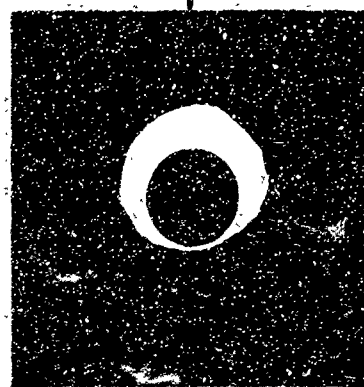
R13877U

FIGURE 75. PROFILE AND AXIAL NOZZLE PHOTOGRAPHS

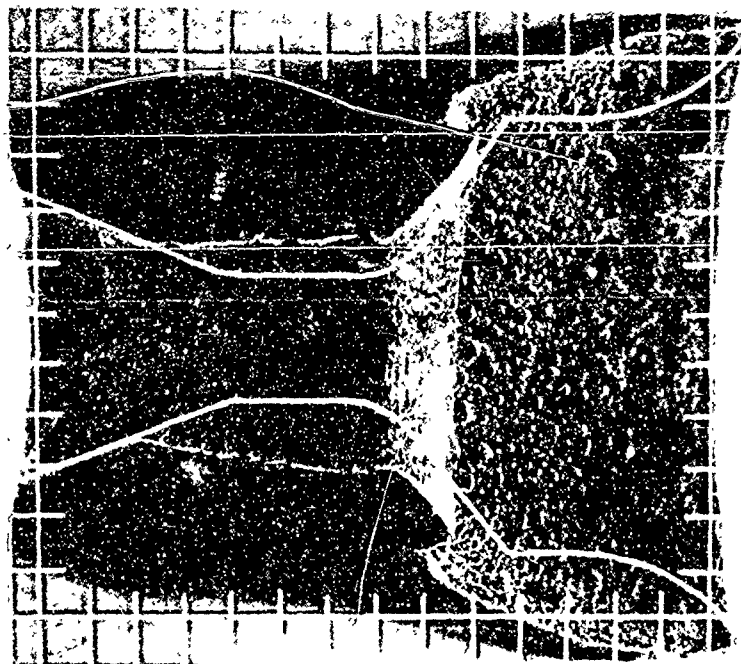
NOZZLE NO. ASD-444



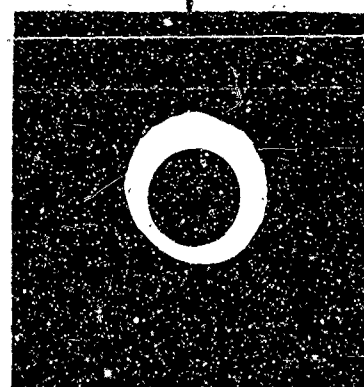
12 O'CLOCK



NOZZLE NO. ASD-446



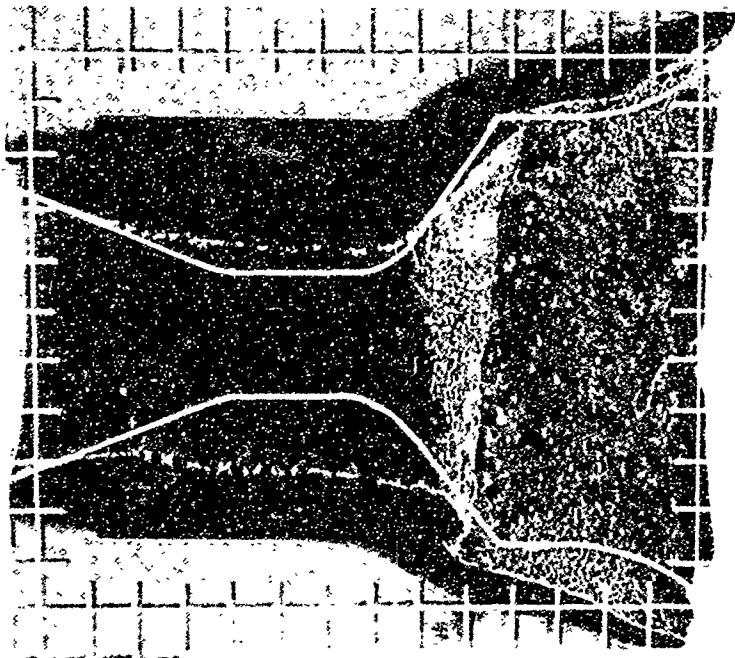
12 O'CLOCK



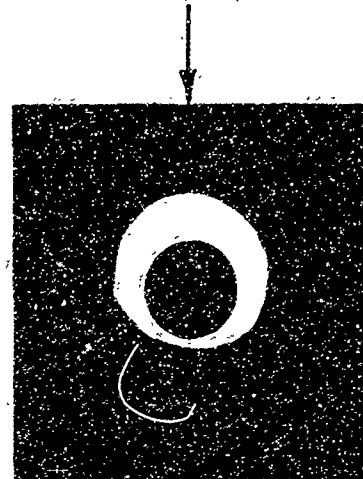
R13876U

FIGURE 76. PROFILE AND AXIAL NOZZLE PHOTOGRAPHS

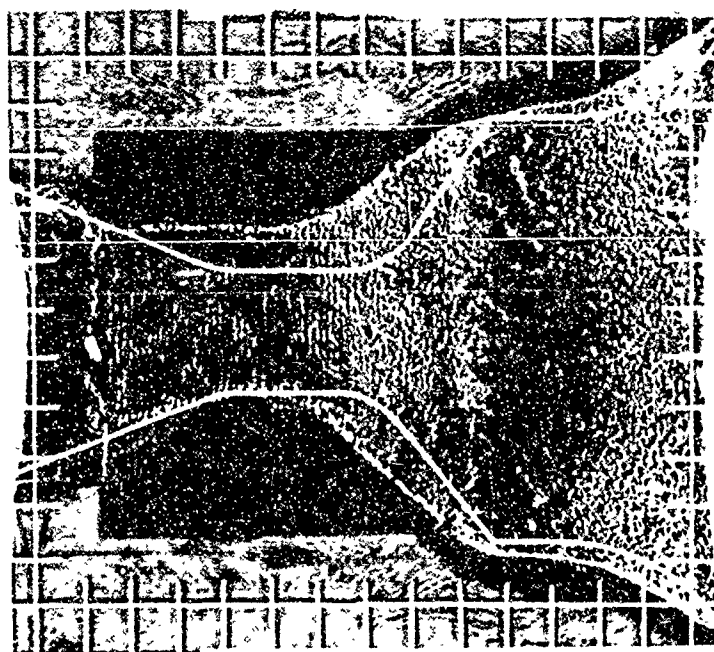
NOZZLE NO. ASD-448



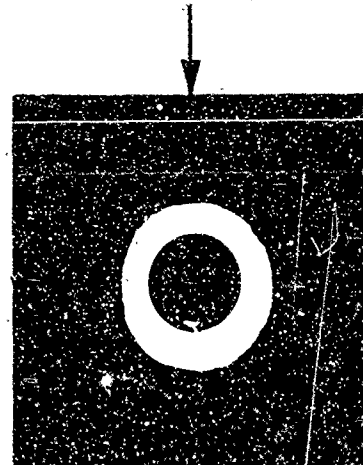
12 O'CLOCK



NOZZLE NO. ASD-452



12 O'CLOCK

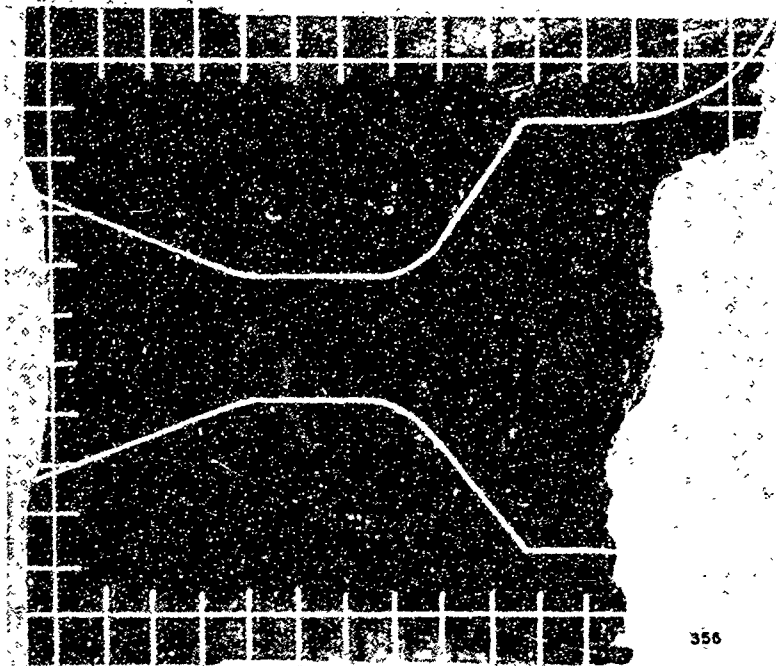


R13875U

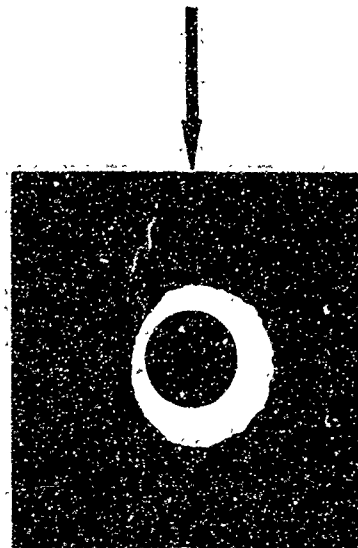
FIGURE 77. PROFILE AND AXIAL NOZZLE PHOTOGRAPHS



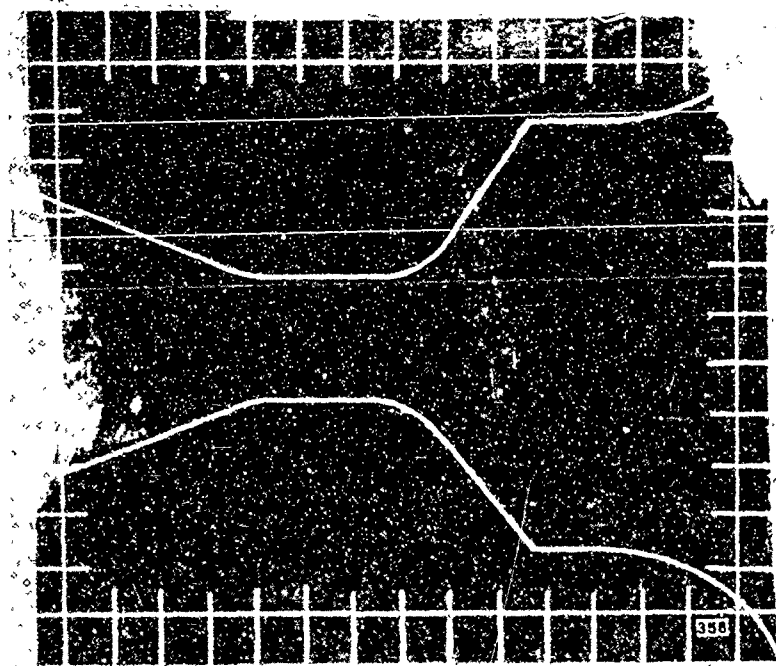
NOZZLE NO. ASD-356



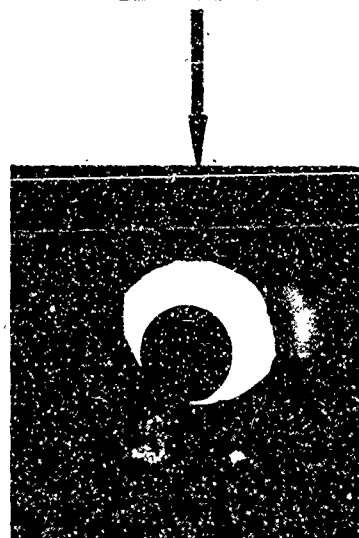
12 O'CLOCK



NOZZLE NO. ASD-358



12 O'CLOCK



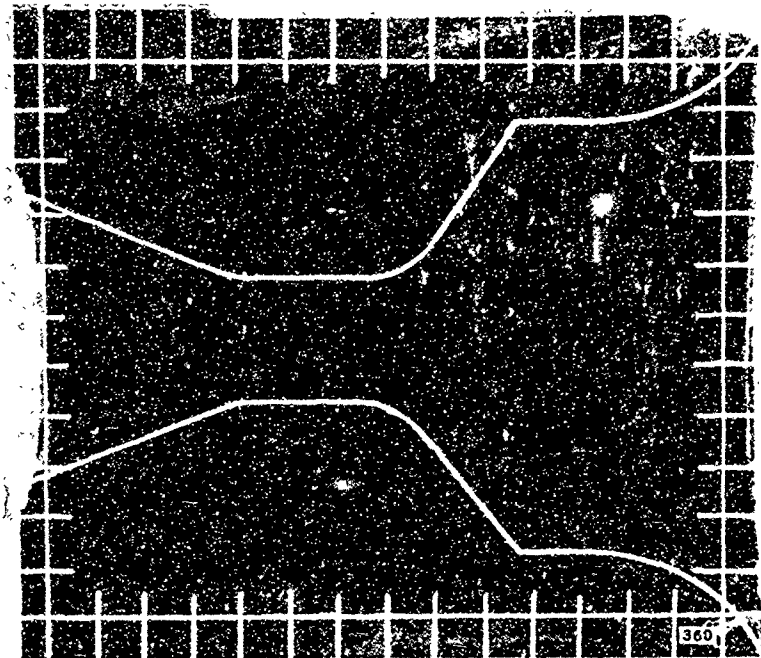
F00923 U

GRID SCALE — | —  
.20 INCH

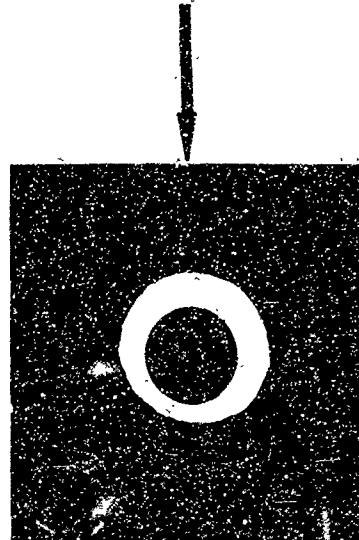
FIGURE 78. PROFILE AND AXIAL NOZZLE PHOTOGRAPHS



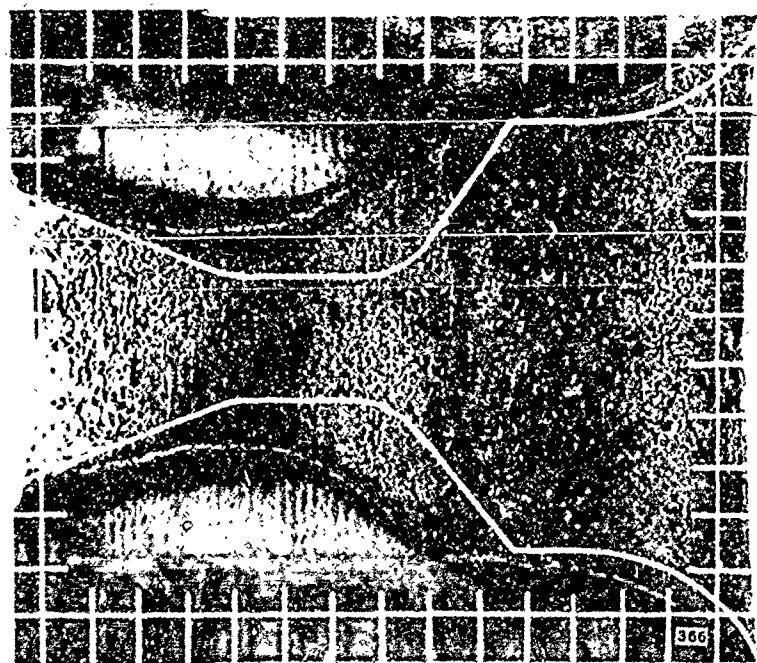
NOZZLE NO. ASD-360



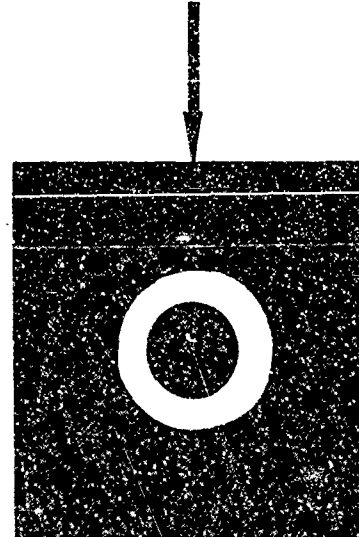
12 O'CLOCK



NOZZLE NO. ASD-366



12 O'CLOCK

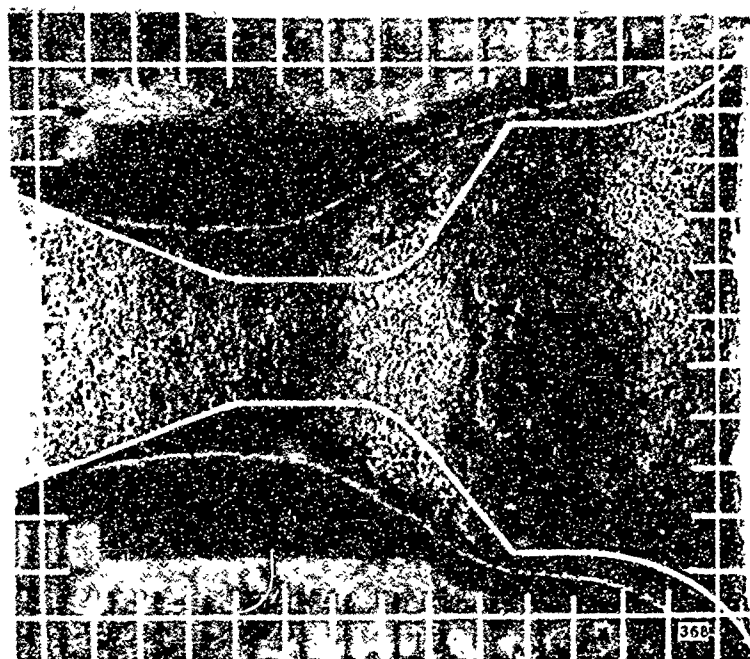


F00924 U

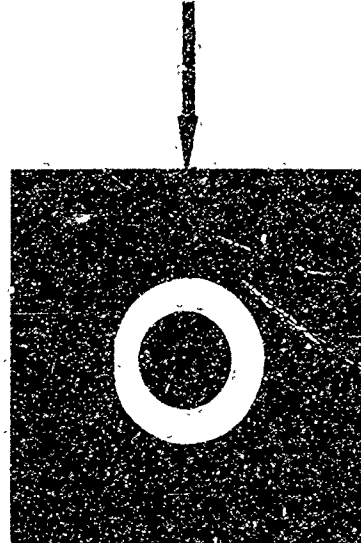
GRID SCALE  
.20 INCH

FIGURE 79. PROFILE AND AXIAL NOZZLE PHOTOGRAPHS

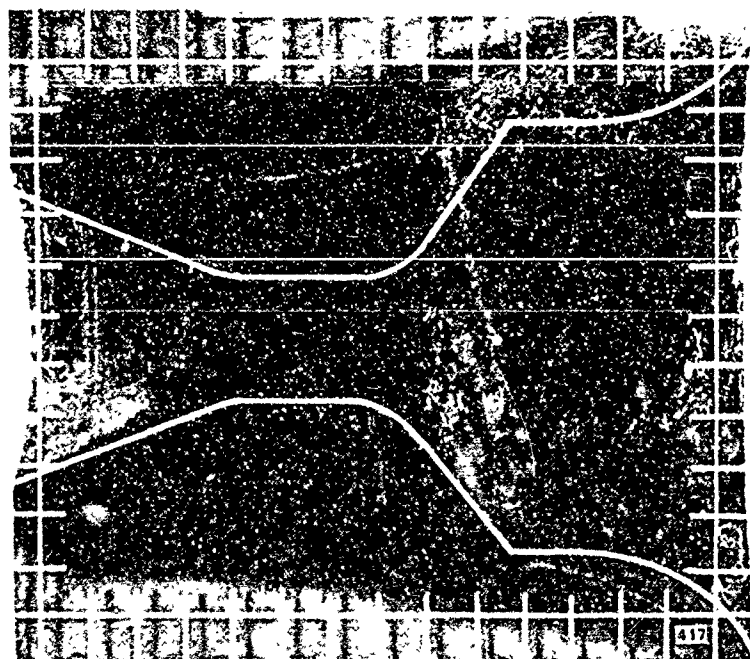
NOZZLE NO. ASD-368



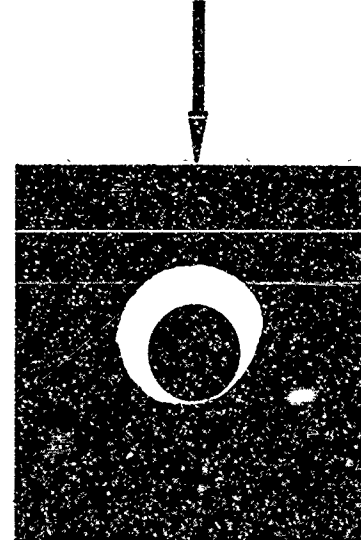
12 O'CLOCK



NOZZLE NO. ASD-417



12 O'CLOCK



F00925 U

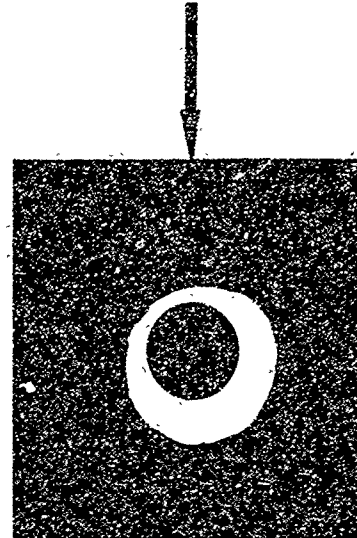
GRID SCALE — | —  
.20 INCH

FIGURE 80. PROFILE AND AXIAL NOZZLE PHOTOGRAPHS

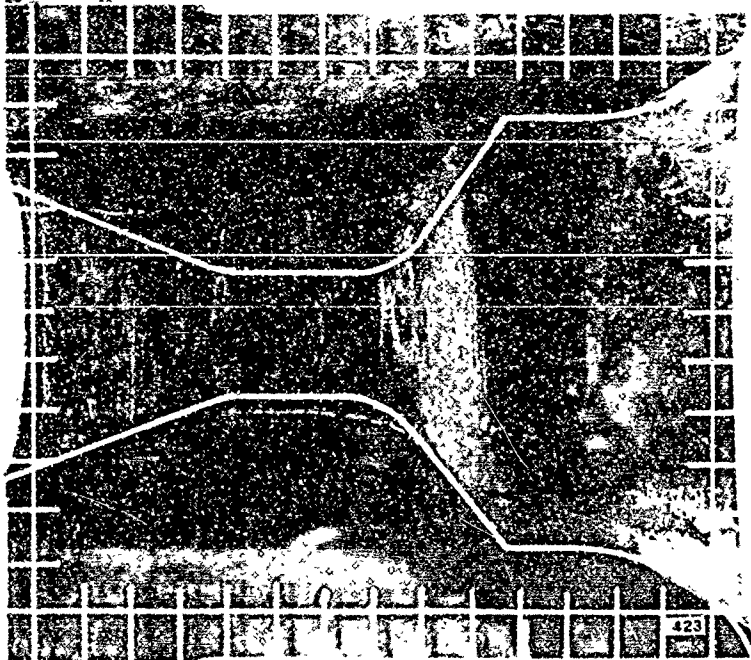
NOZZLE NO. ASD-422



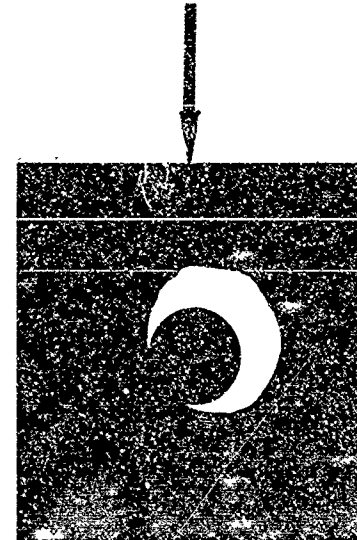
12 O'CLOCK



NOZZLE NO. ASD-423



12 O'CLOCK

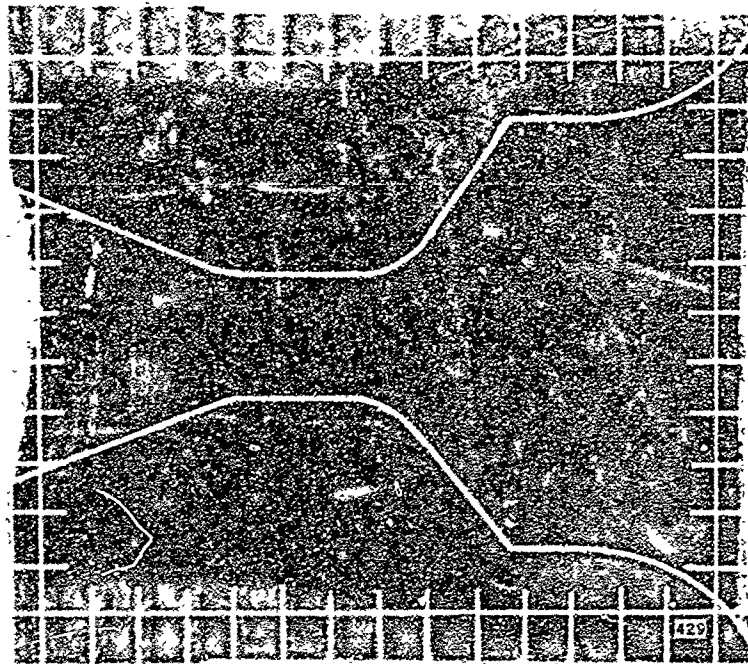


F00926 U

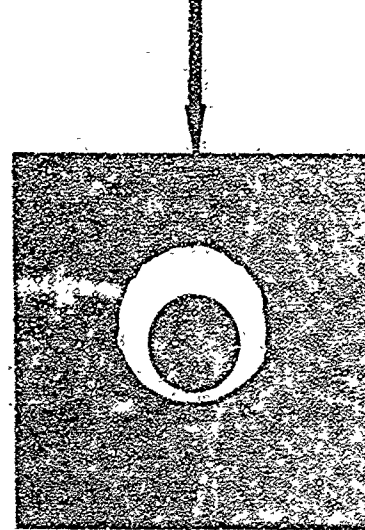
GRID SCALE — | | —  
.20 INCH

FIGURE 81. PROFILE AND AXIAL NOZZLE PHOTOGRAPHS

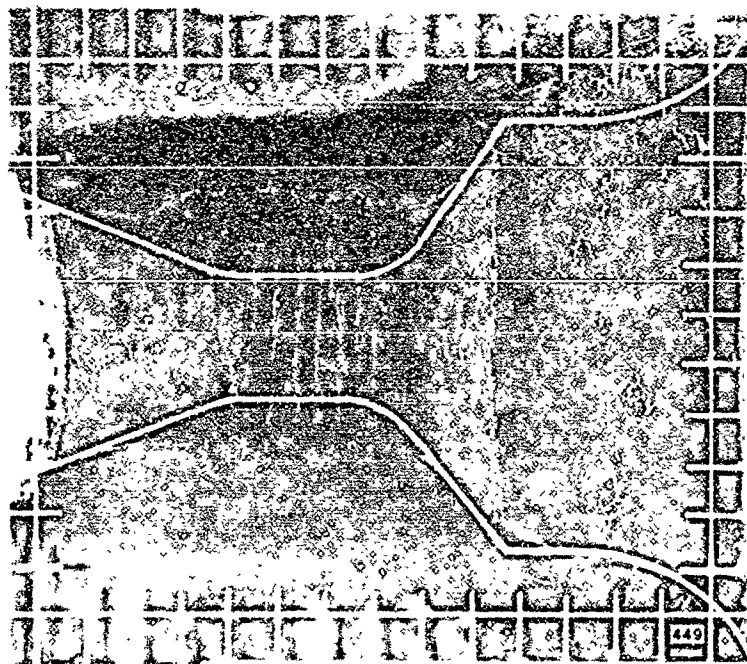
NOZZLE NO. ASD-429



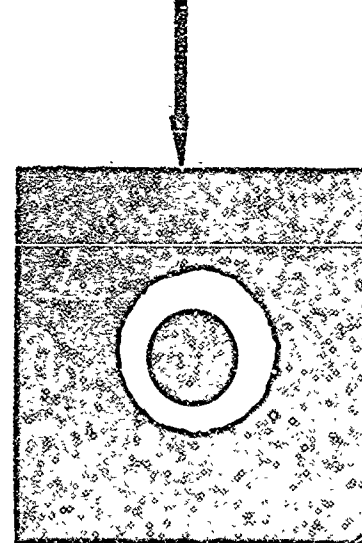
12 O'CLOCK



NOZZLE NO. ASD-449



12 O'CLOCK

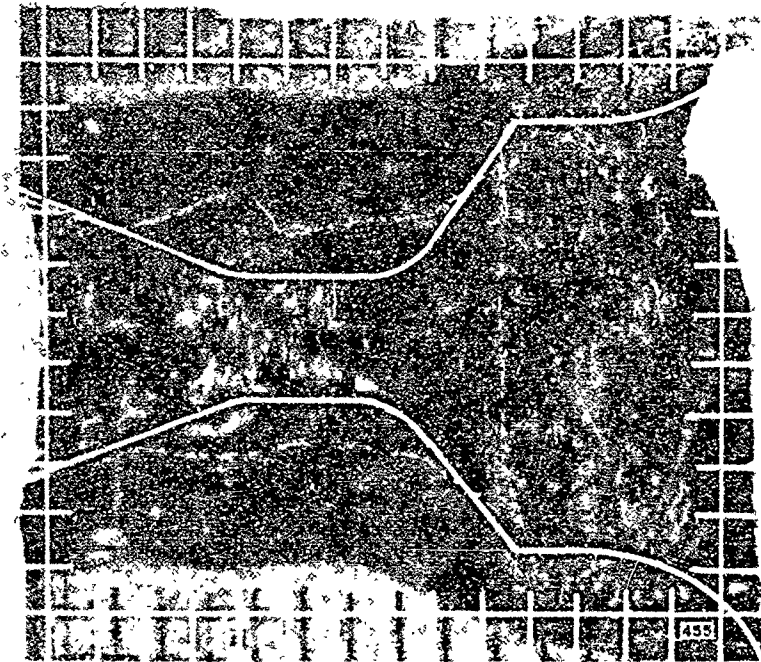


F00927 U

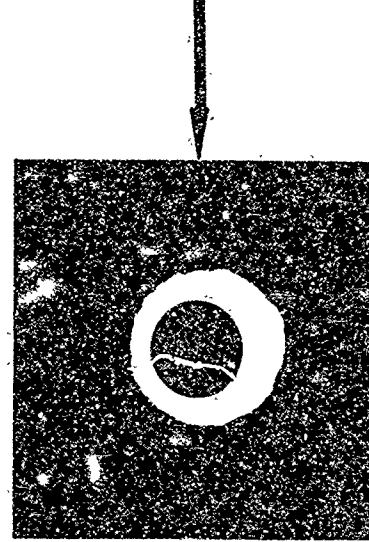
GRID SCALE — | —  
.20 INCH

FIGURE 82. PROFILE AND AXIAL NOZZLE PHOTOGRAPHS

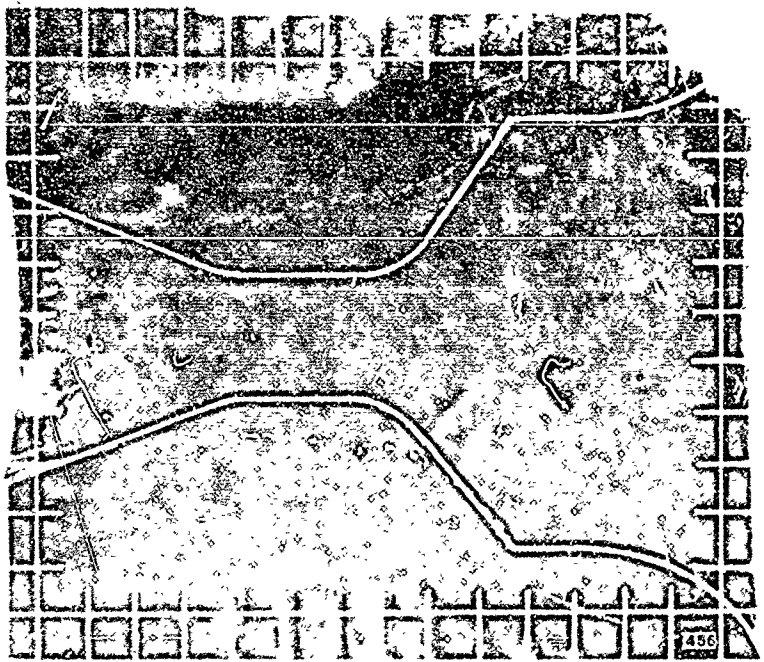
NOZZLE NO. ASD-455



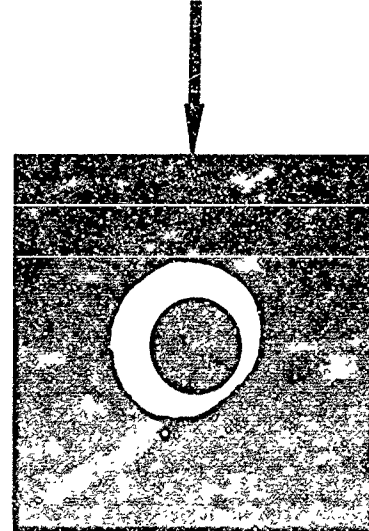
12 O'CLOCK



NOZZLE NO. ASD-456



12 O'CLOCK



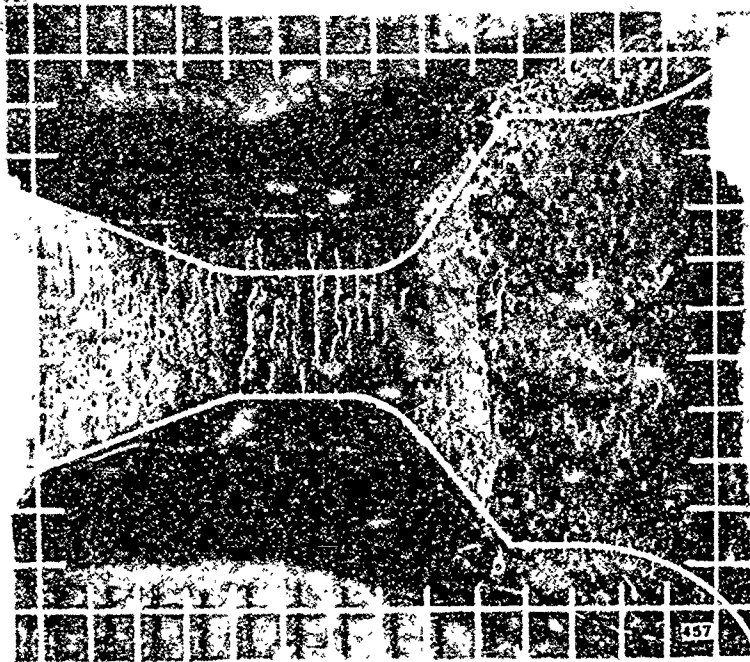
F00928 U

GRID SCALE →  
.20 INCH

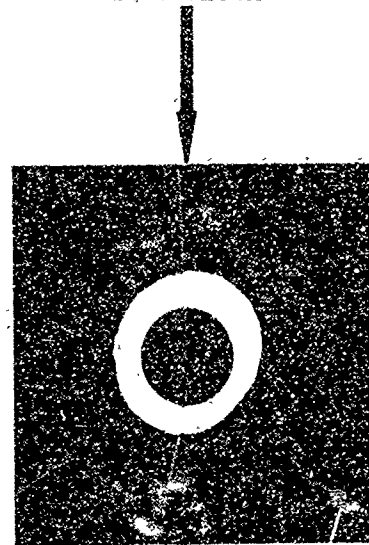
FIGURE 83. PROFILE AND AXIAL NOZZLE PHOTOGRAPHS



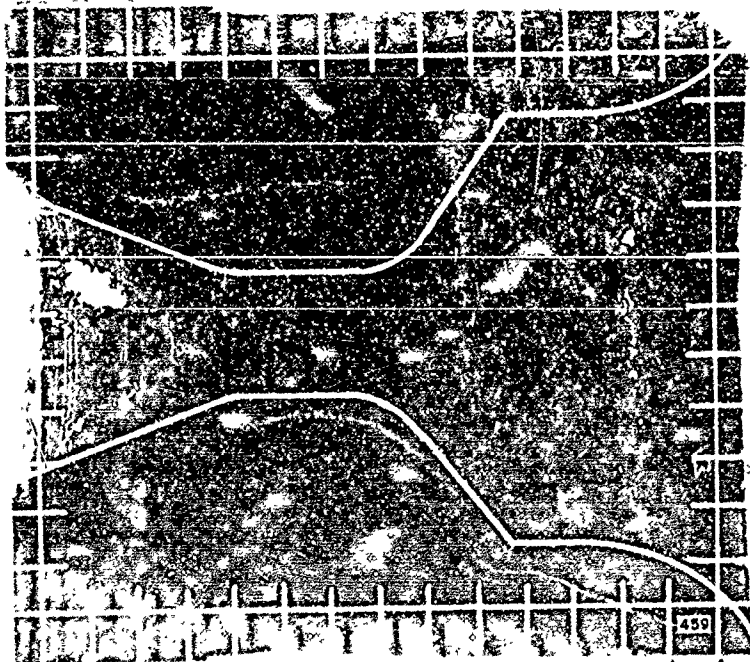
NOZZLE NO. ASD-457



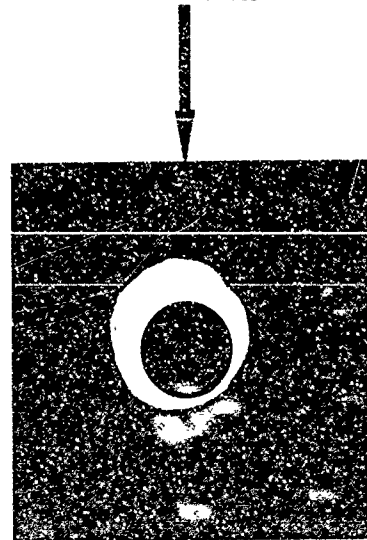
12 O'CLOCK



NOZZLE NO. ASD-459



12 O'CLOCK

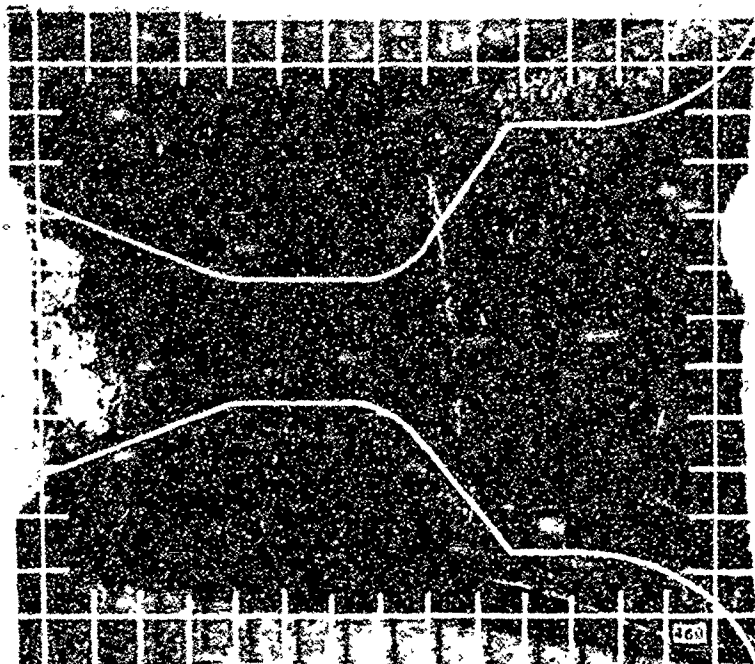


F00929 U

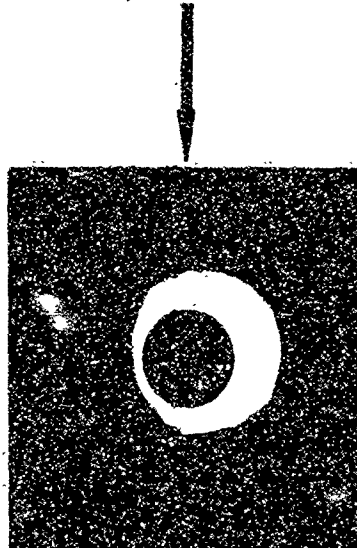
GRID SCALE --| |  
.20 INCH

FIGURE 84. PROFILE AND AXIAL NOZZLE PHOTOGRAPHS

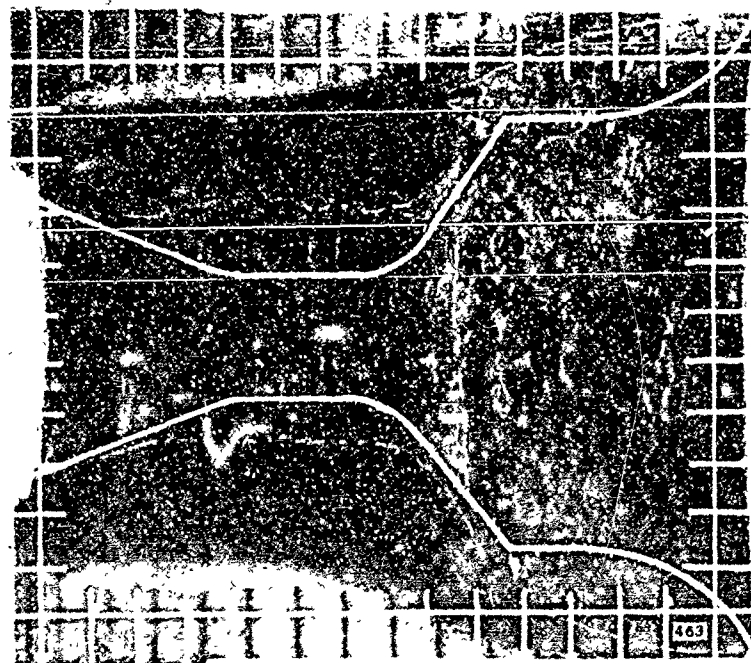
NOZZLE NO. ASD-460



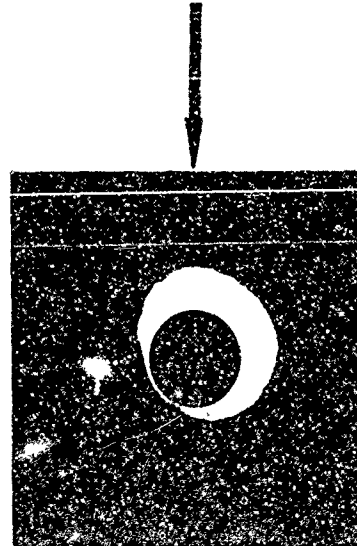
12 O'CLOCK



NOZZLE NO. ASD-463



12 O'CLOCK

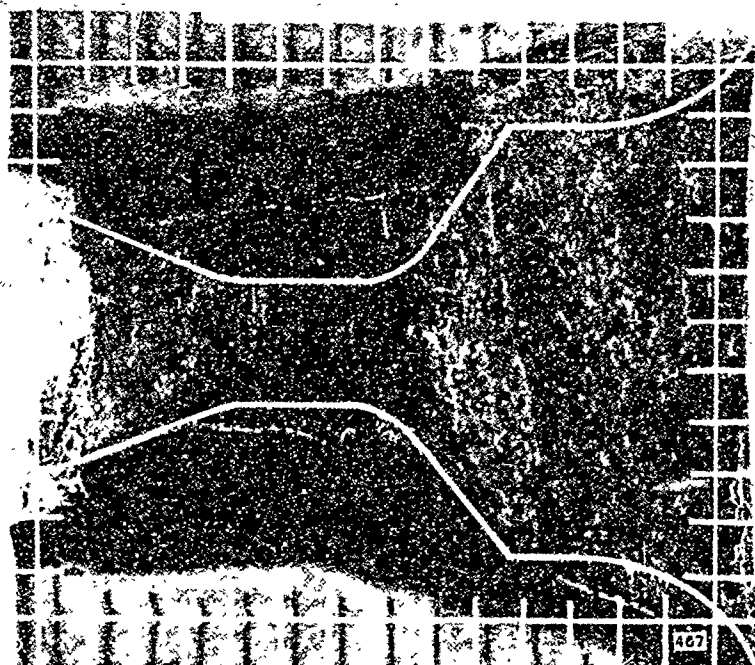


GRID SCALE → |←  
.20 INCH

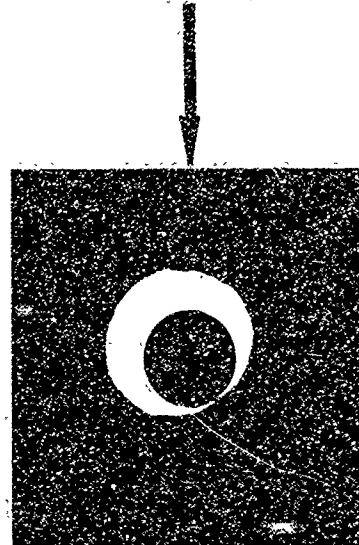
F00930 U

FIGURE 85. PROFILE AND AXIAL NOZZLE PHOTOGRAPHS

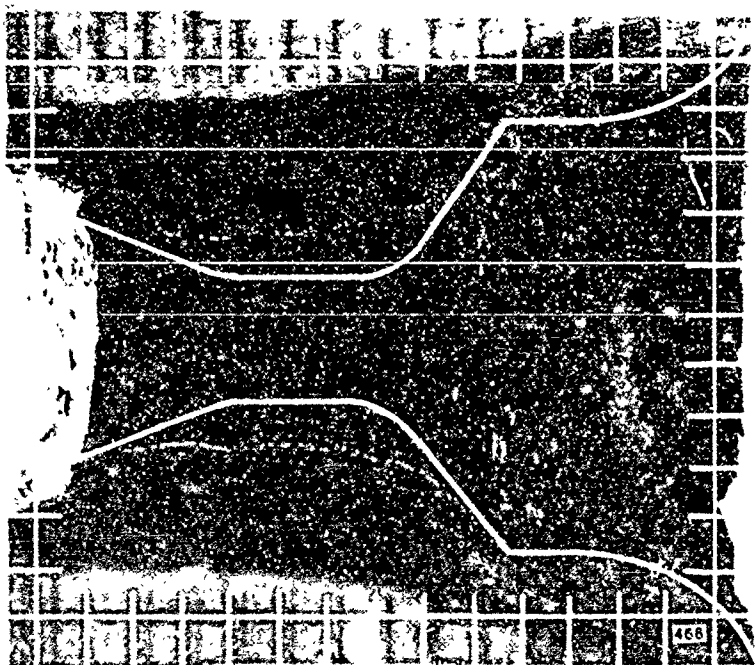
NOZZLE NO. ASD-467



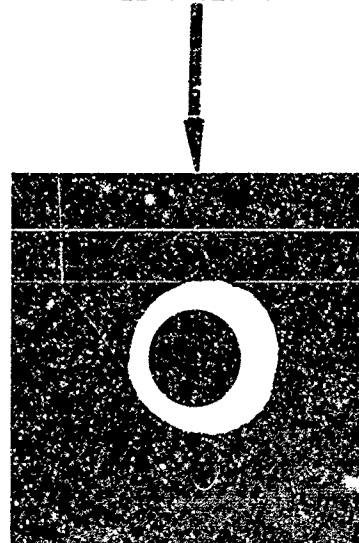
12 O'CLOCK



NOZZLE NO. ASD-468



12 O'CLOCK



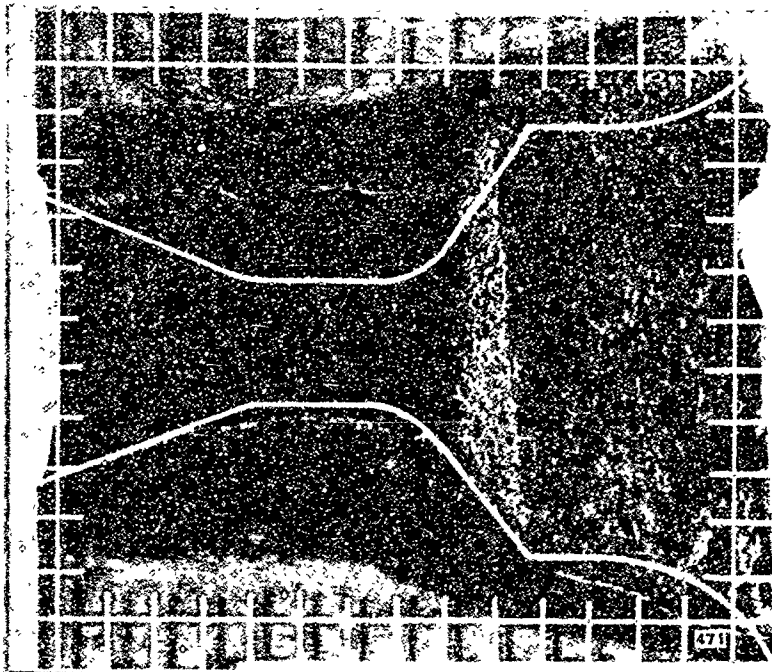
F00931 U

GRID SCALE → | | ←  
.20 INCH

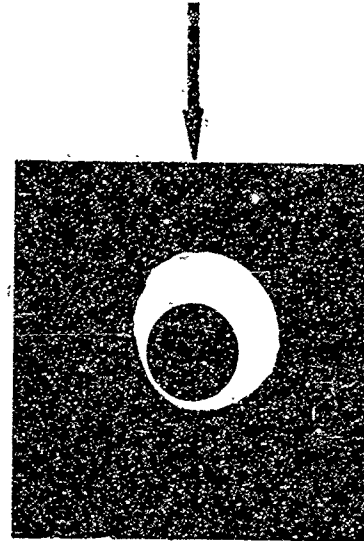
FIGURE 86. PROFILE AND AXIAL NOZZLE PHOTOGRAPHS



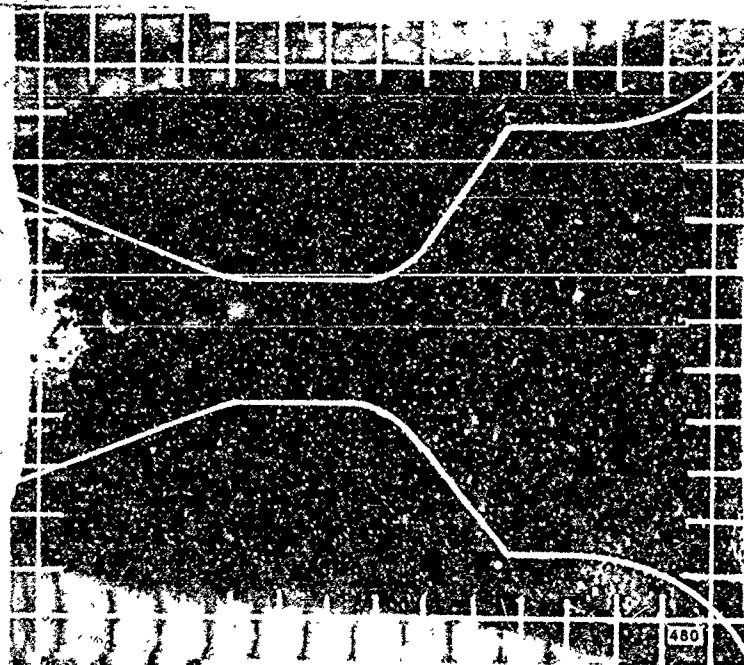
NOZZLE NO. ASD-471



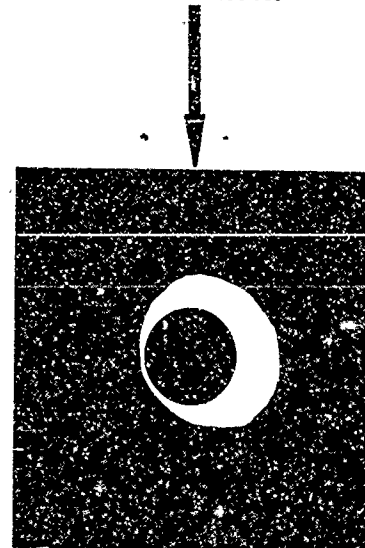
12 O'CLOCK



NOZZLE NO. ASD-480



12 O'CLOCK

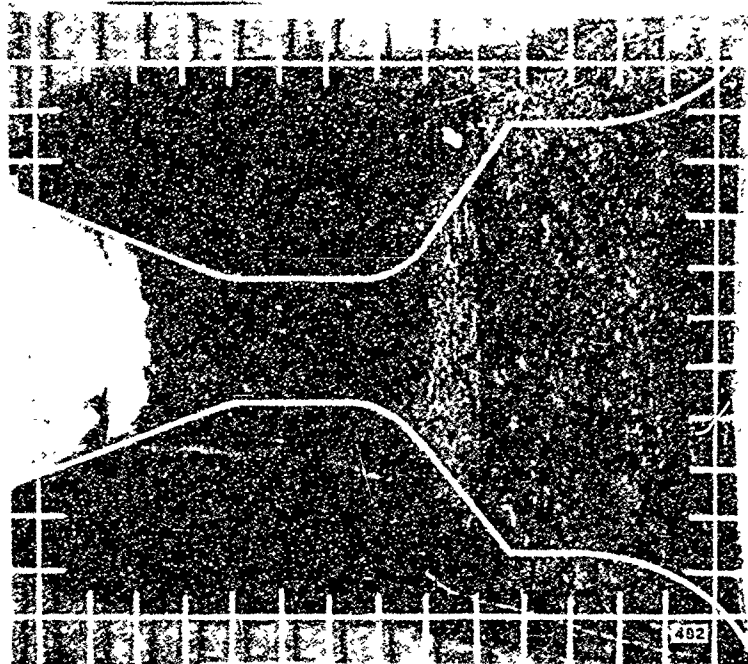


F00932 U

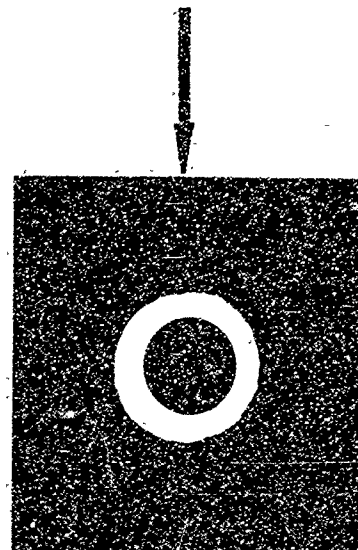
GRID SCALE → | ←  
.20 INCH

FIGURE 87. PROFILE AND AXIAL NOZZLE PHOTOGRAPHS

NOZZLE NO. ASD-482



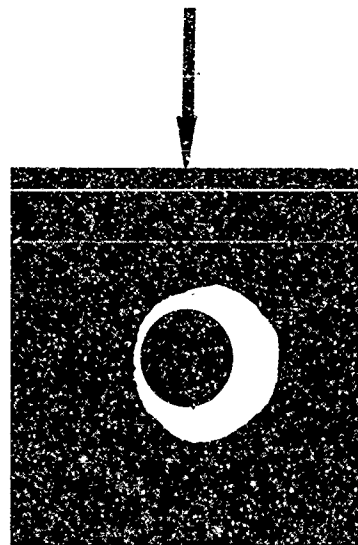
12 O'CLOCK



NOZZLE NO. ASD-483



12 O'CLOCK

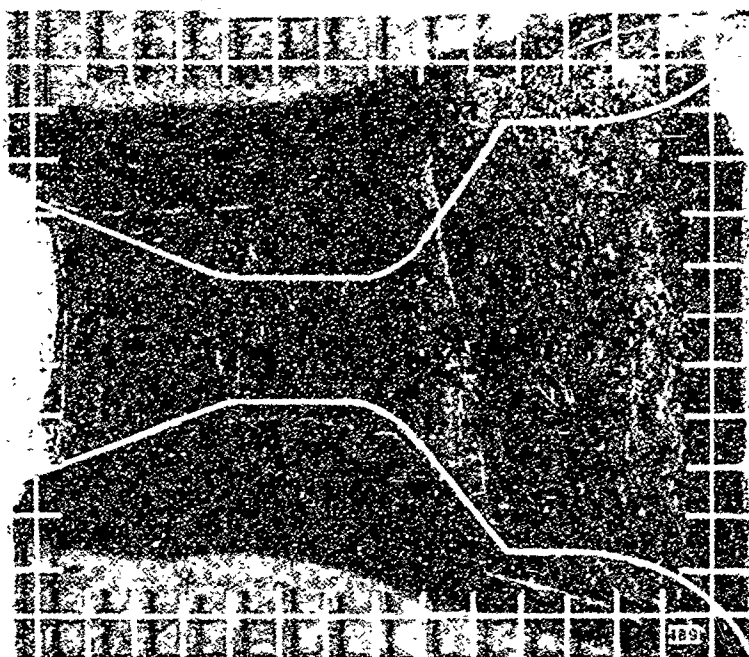


GRID SCALE → | ←  
.20 INCH

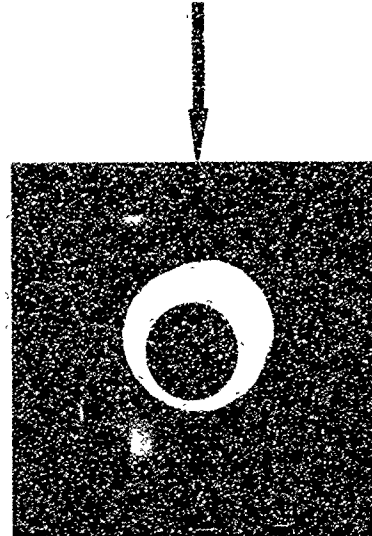
F00933 U

FIGURE 88. PROFILE AND AXIAL NOZZLE PHOTOGRAPHS

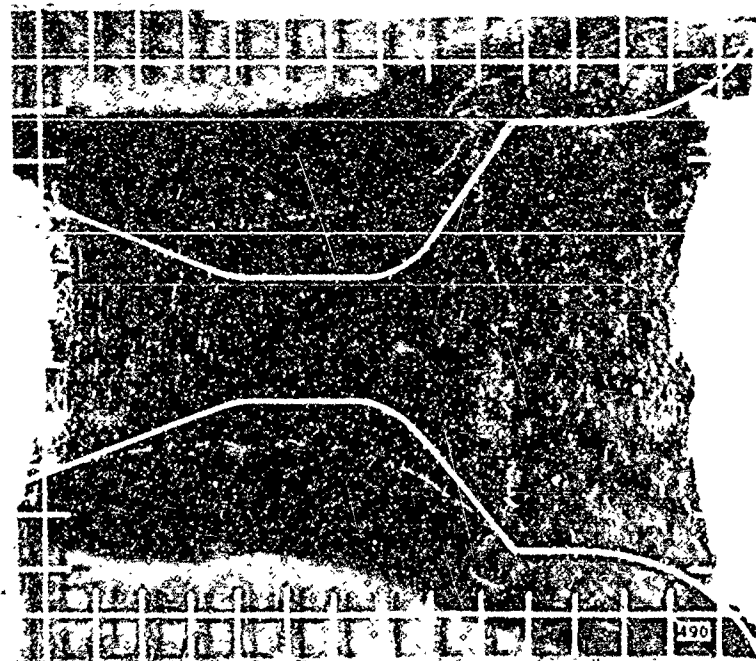
NOZZLE NO. ASD-489



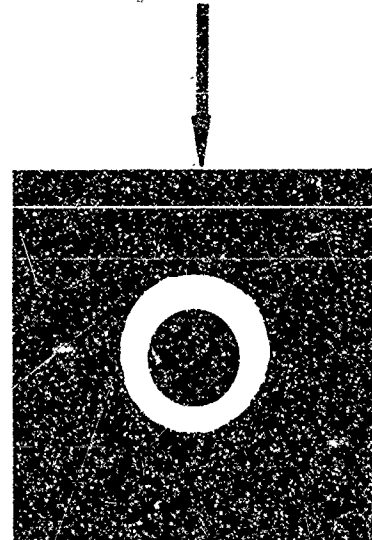
12 O'CLOCK



NOZZLE NO. ASD-490



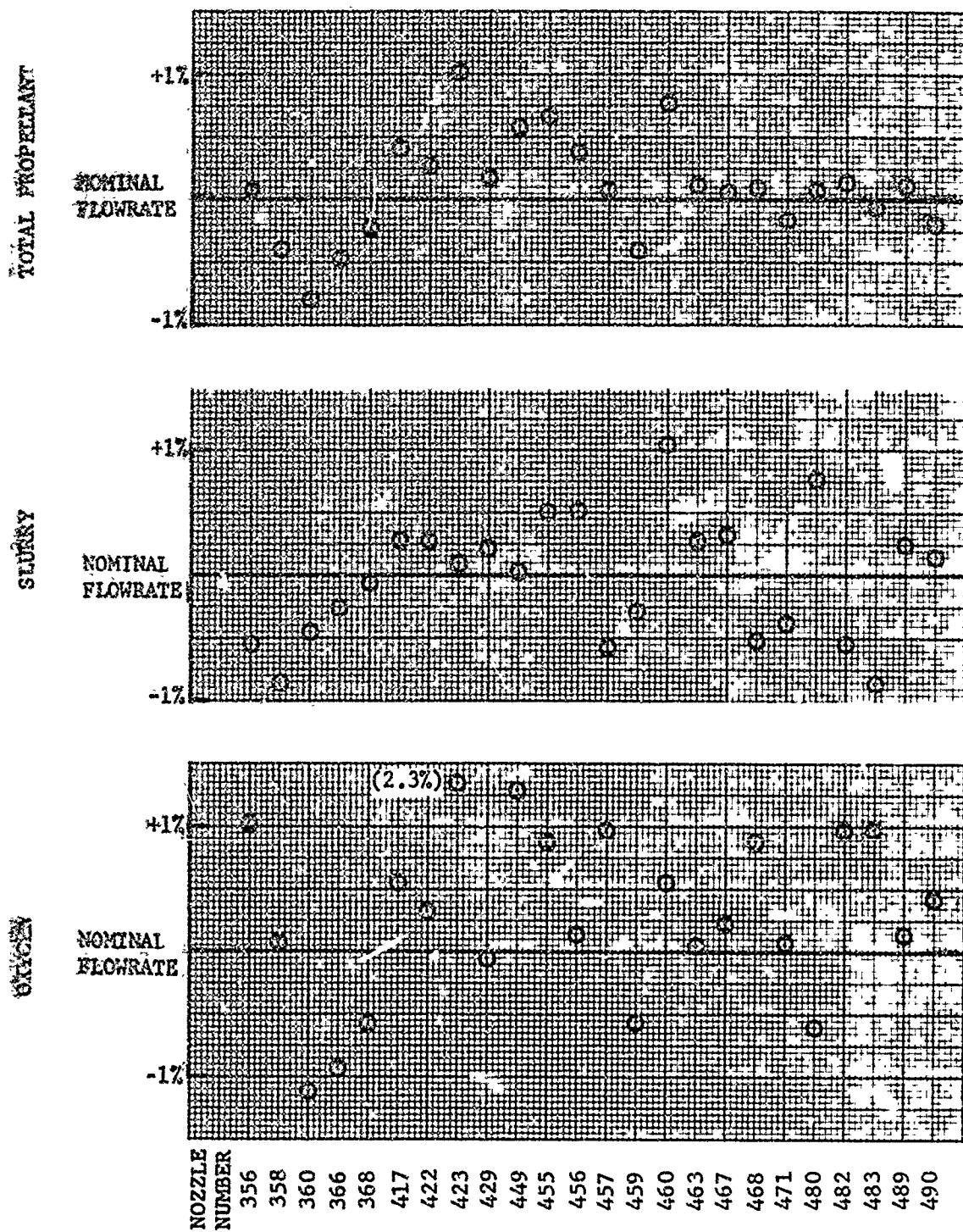
12 O'CLOCK



F00934 U

GRID SCALE → | ←  
.20 INCH

FIGURE 89. PROFILE AND AXIAL NOZZLE PHOTOGRAPHS



F00935 U

FIGURE 90. TEST-TO-TEST PROPELLANT FLOWRATE VARIATION FROM NOMINAL CONDITION

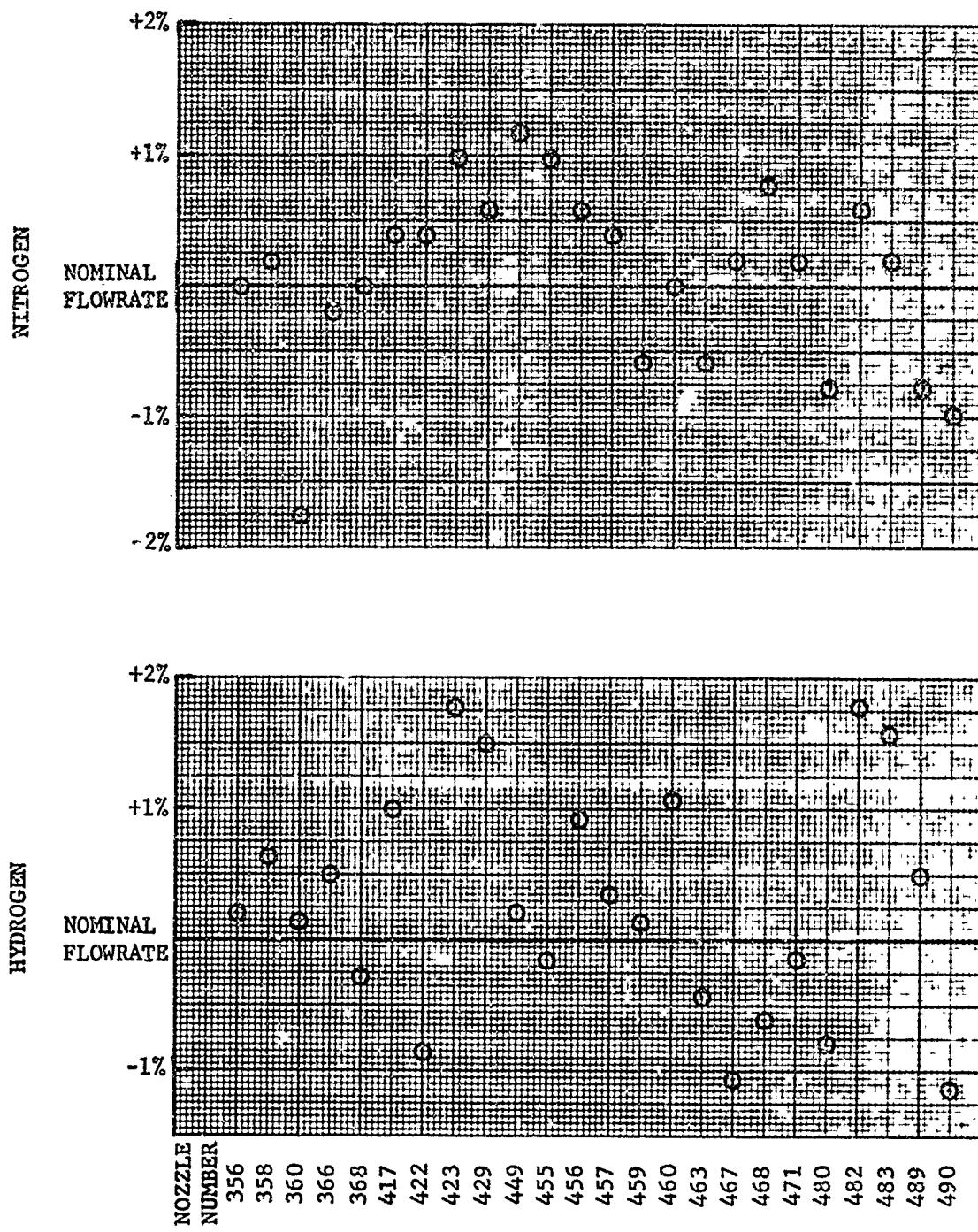


FIGURE 91. TEST-TO-TEST PROPELLANT FLOWRATE VARIATION FROM NOMINAL CONDITION



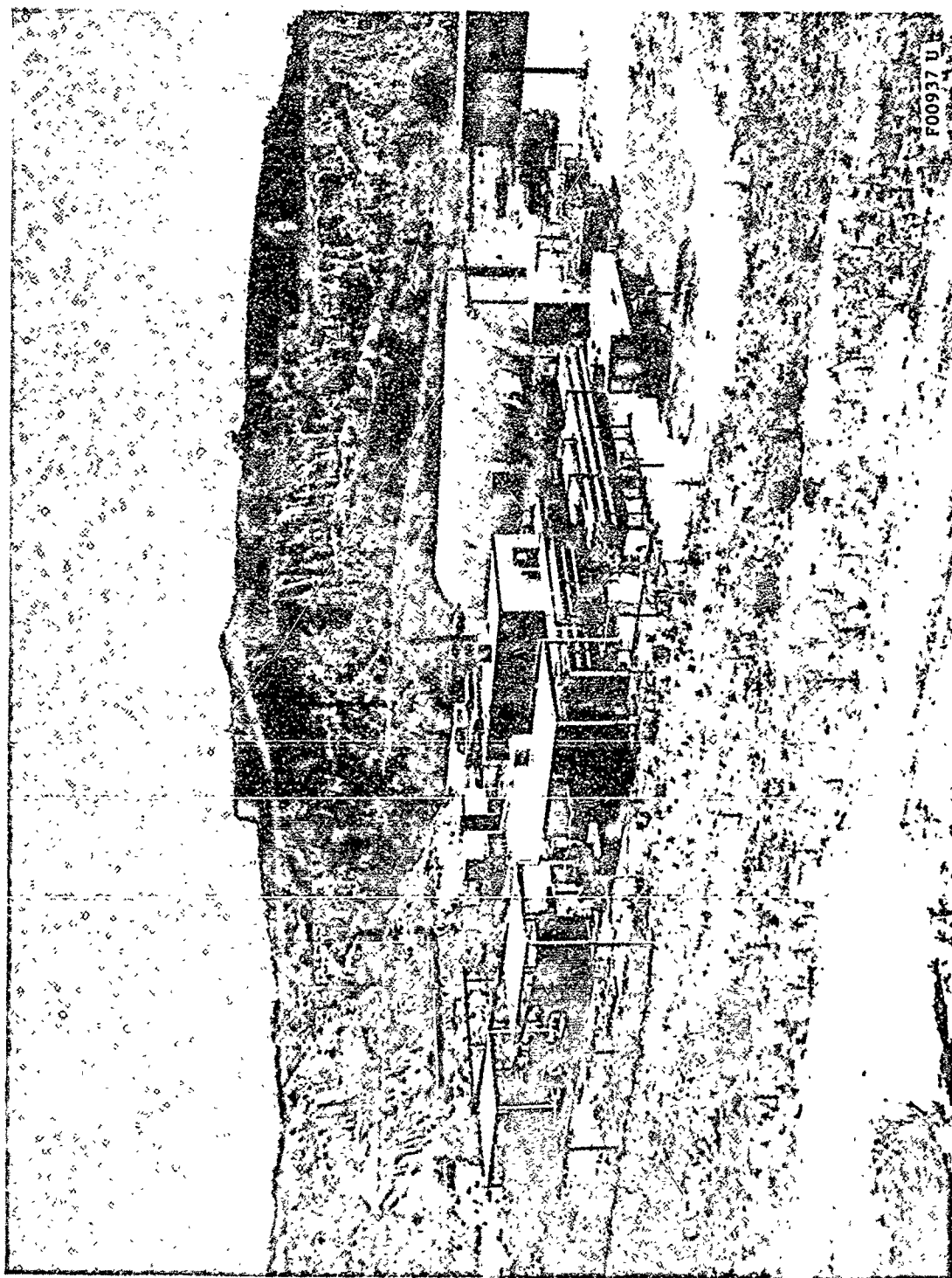


FIGURE 92. AERONUTRONIC EL TORO TEST SITE

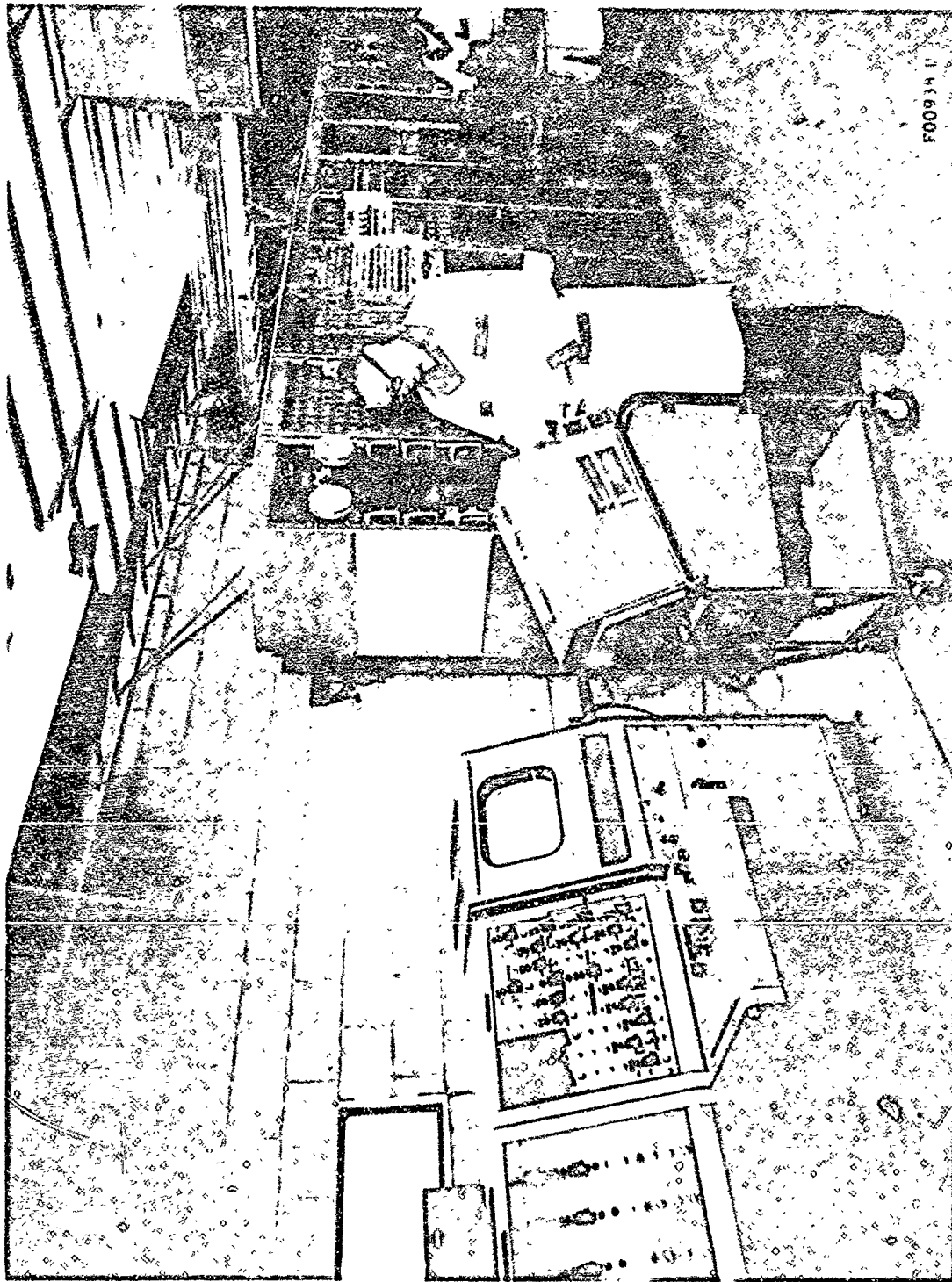
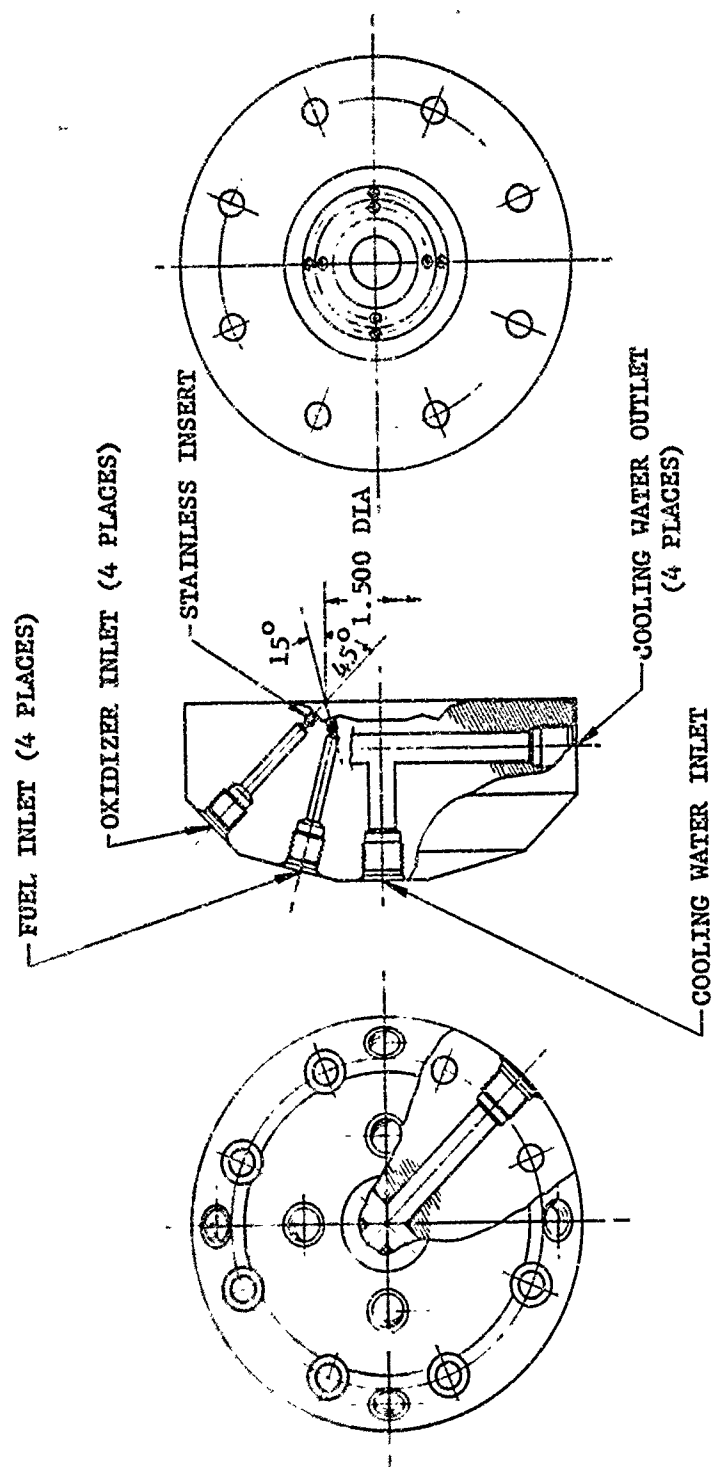


FIGURE 93 CONTROL COMPLEX AT EL TORO

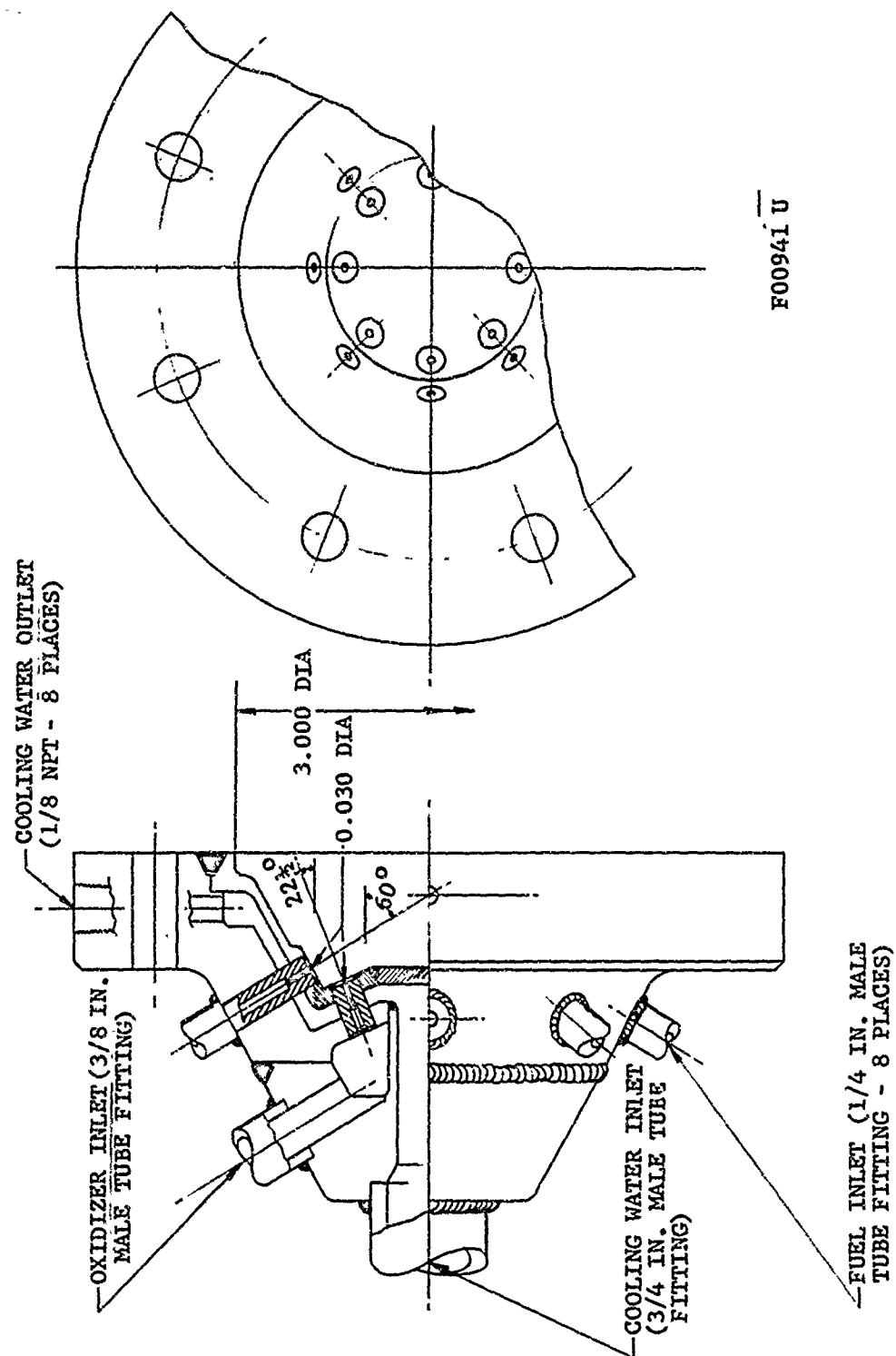






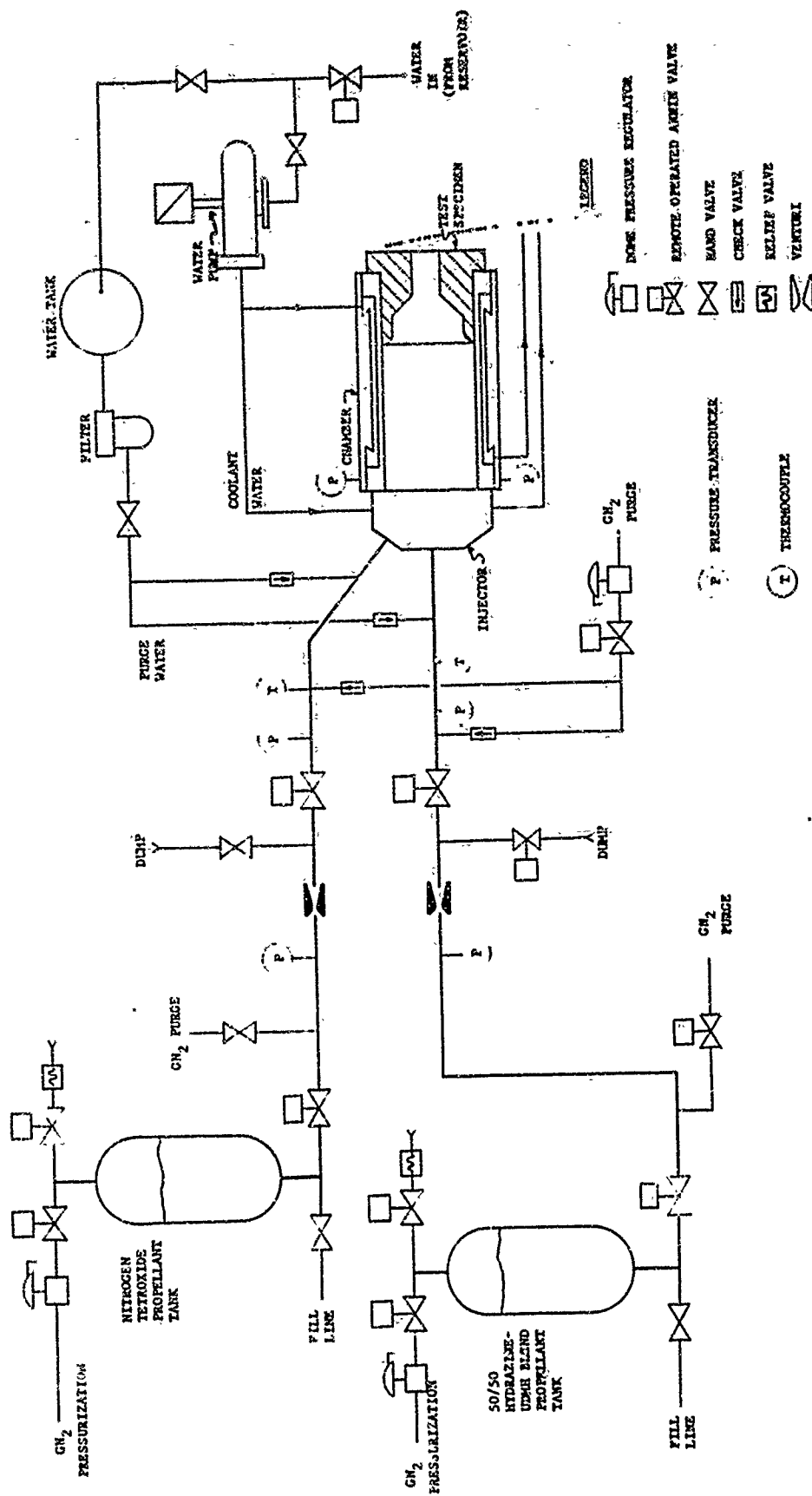
F00940 U

FIGURE 95.  $N_2O_4$  - AEROZINE INJECTOR - WRIGHT FIELD NOZZLE TEST (COPPER)



F00941 U

FIGURE 96.  $N_2O_4$  - AEROZINE INJECTOR - WRIGHT FIELD NOZZLE TEST (STAINLESS)



FO0942 U

FIGURE 97. EL TORO CELL B SCHEMATIC - WRIGHT FIELD ABLATIVE NOZZLE TEST SERIES

DATA FROM AERONUTRONIC PUBLICATION C-2327  
1ST QUARTERLY REPORT - APPLICATION OF  
MATERIALS TO ADVANCED ROCKET NOZZLES  
AND HOT GAS CONTROL SYSTEMS

OCT. 15, 1963

H. M. BLAES et. al.

AF 33(657)-11217

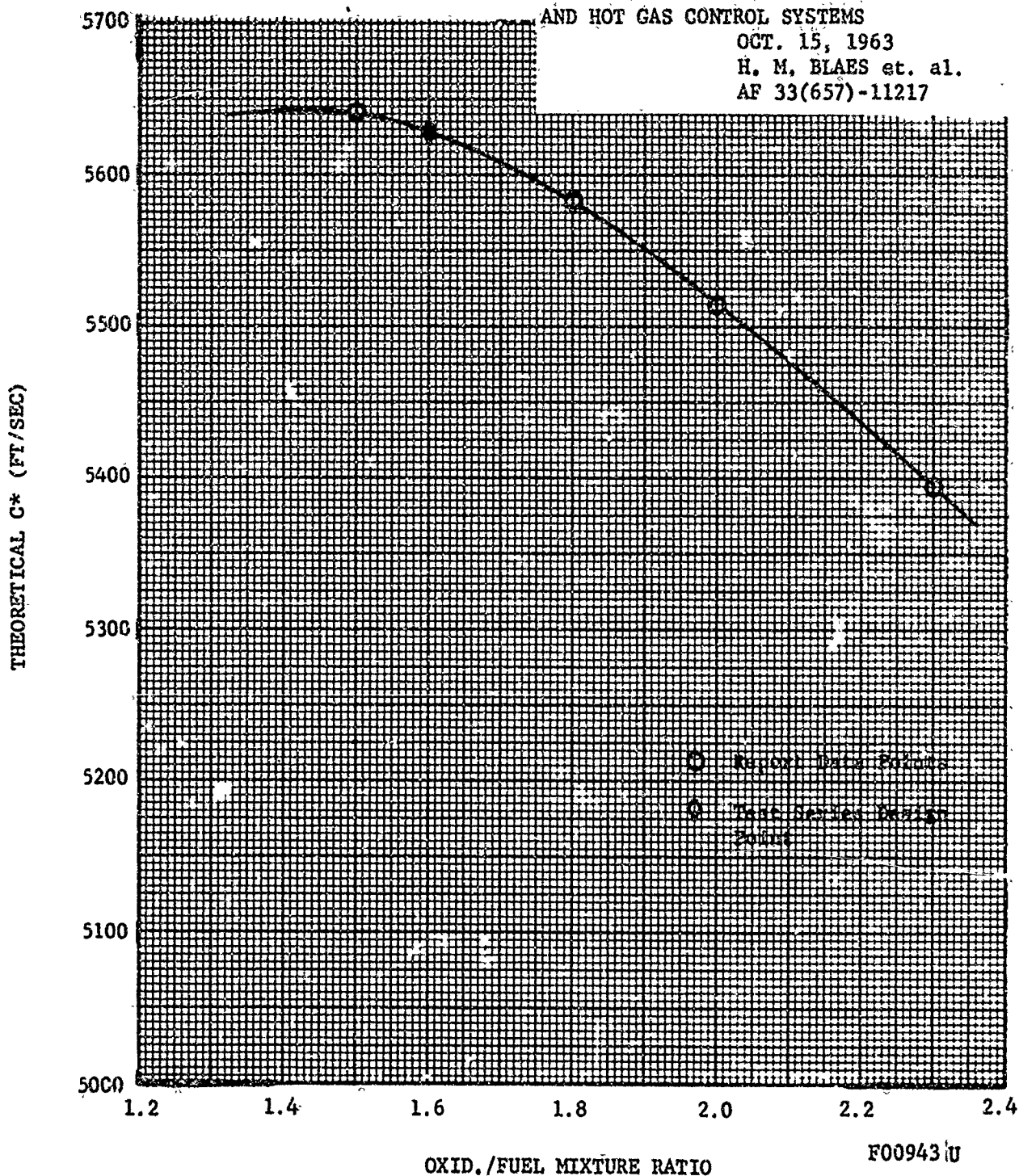
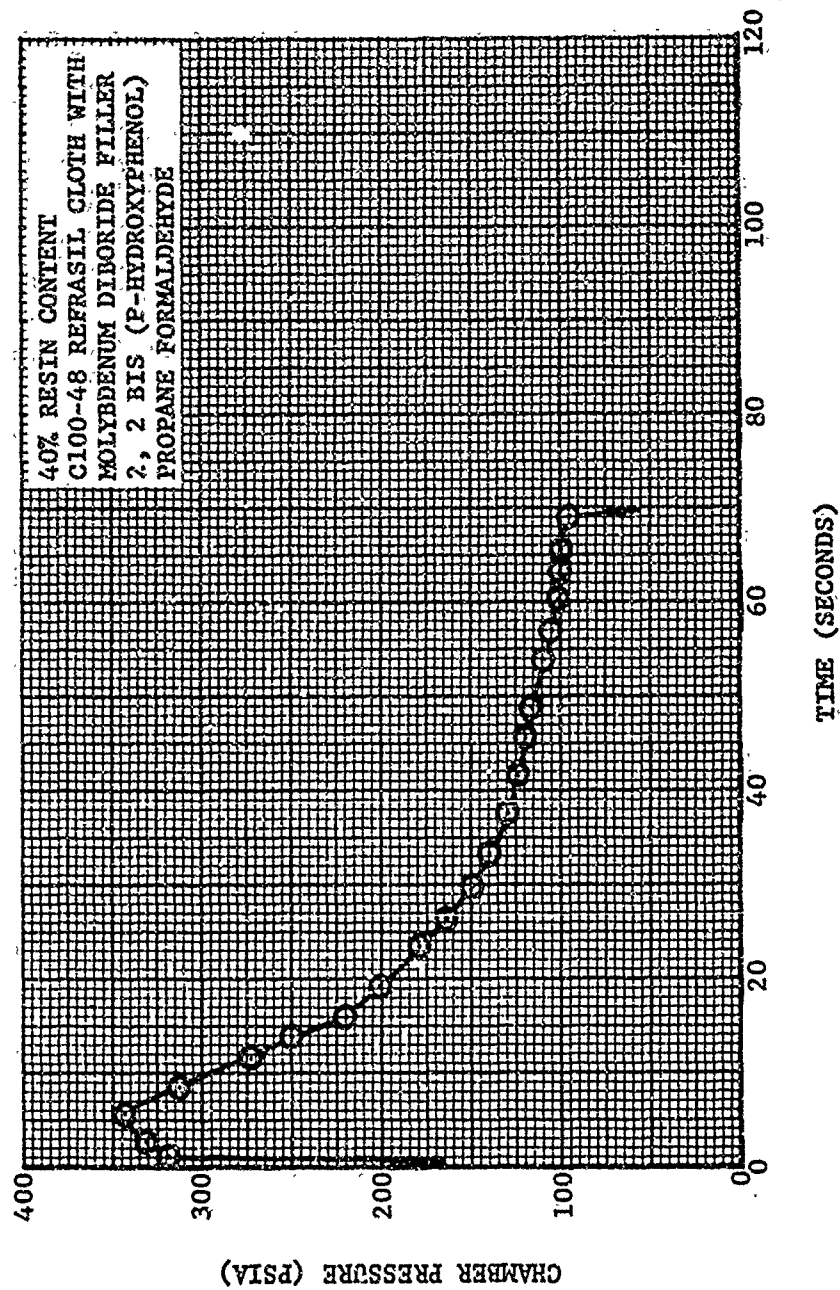
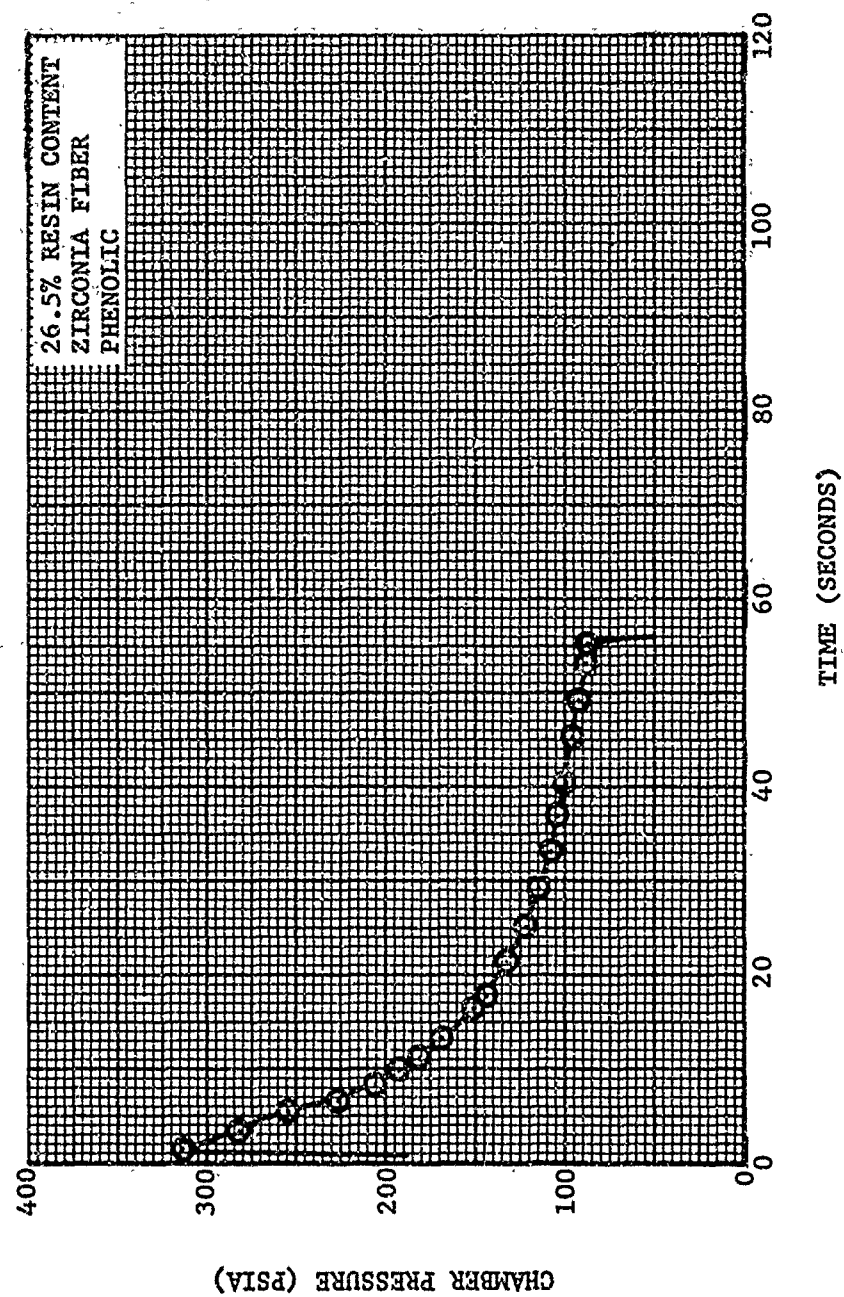


FIGURE 98. THEORETICAL C\* VERSUS MIXTURE RATIO  $N_2O_4/50\% N_2H_4-50\% UDMH$  PROPELLANT AT 300 PSIA CHAMBER PRESSURE



R14194 U

FIGURE 99. CHAMBER PRESSURE VERSUS TIME - ASD 352 NOZZLE



R14193 U

FIGURE 100. CHAMBER PRESSURE VERSUS TIME - ASD 377 NOZZLE

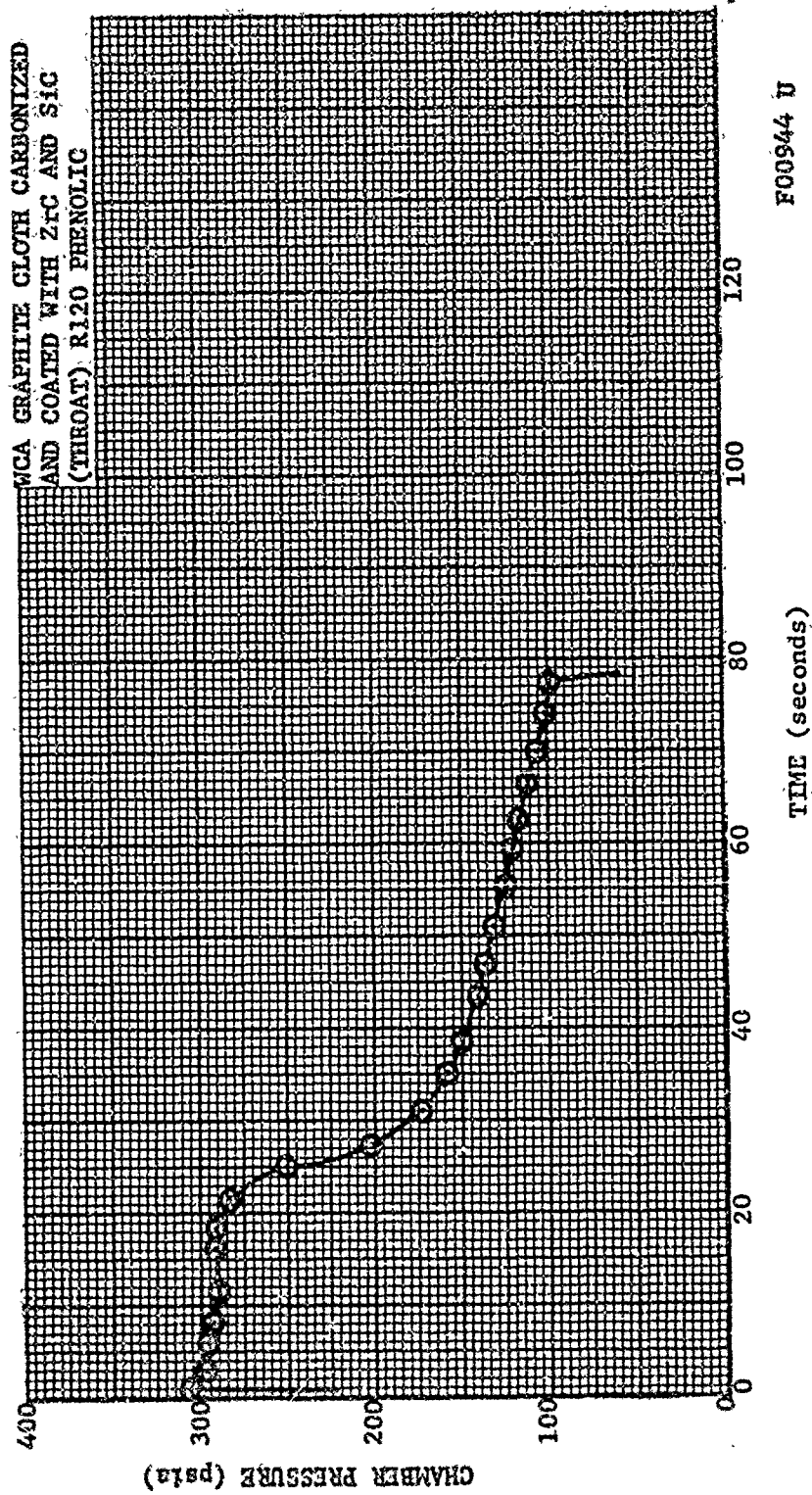
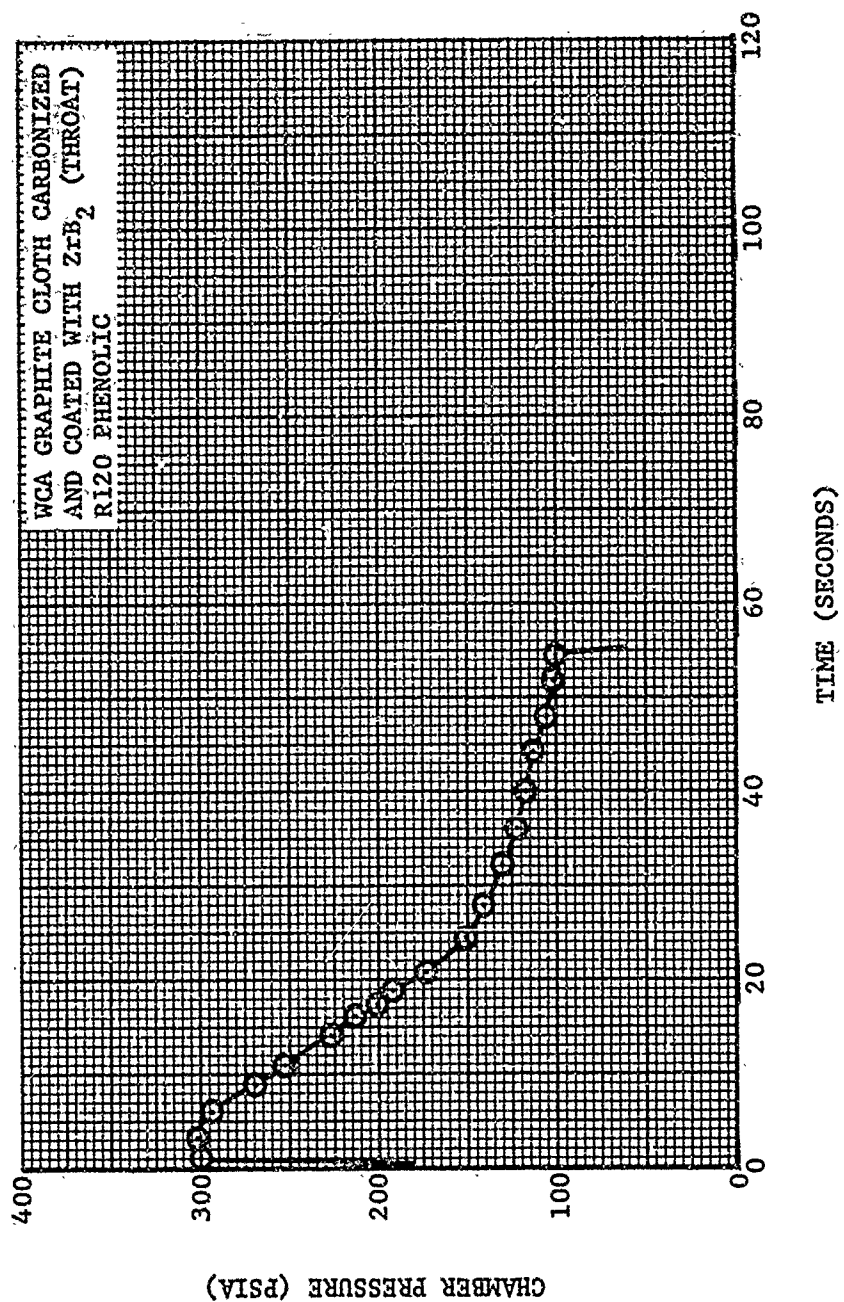


FIGURE 101. CHAMBER PRESSURE VERSUS TIME - ASD 380 NOZZLE





R14192 U

FIGURE 102. CHAMBER PRESSURE VERSUS TIME - ASD 381 NOZZLE



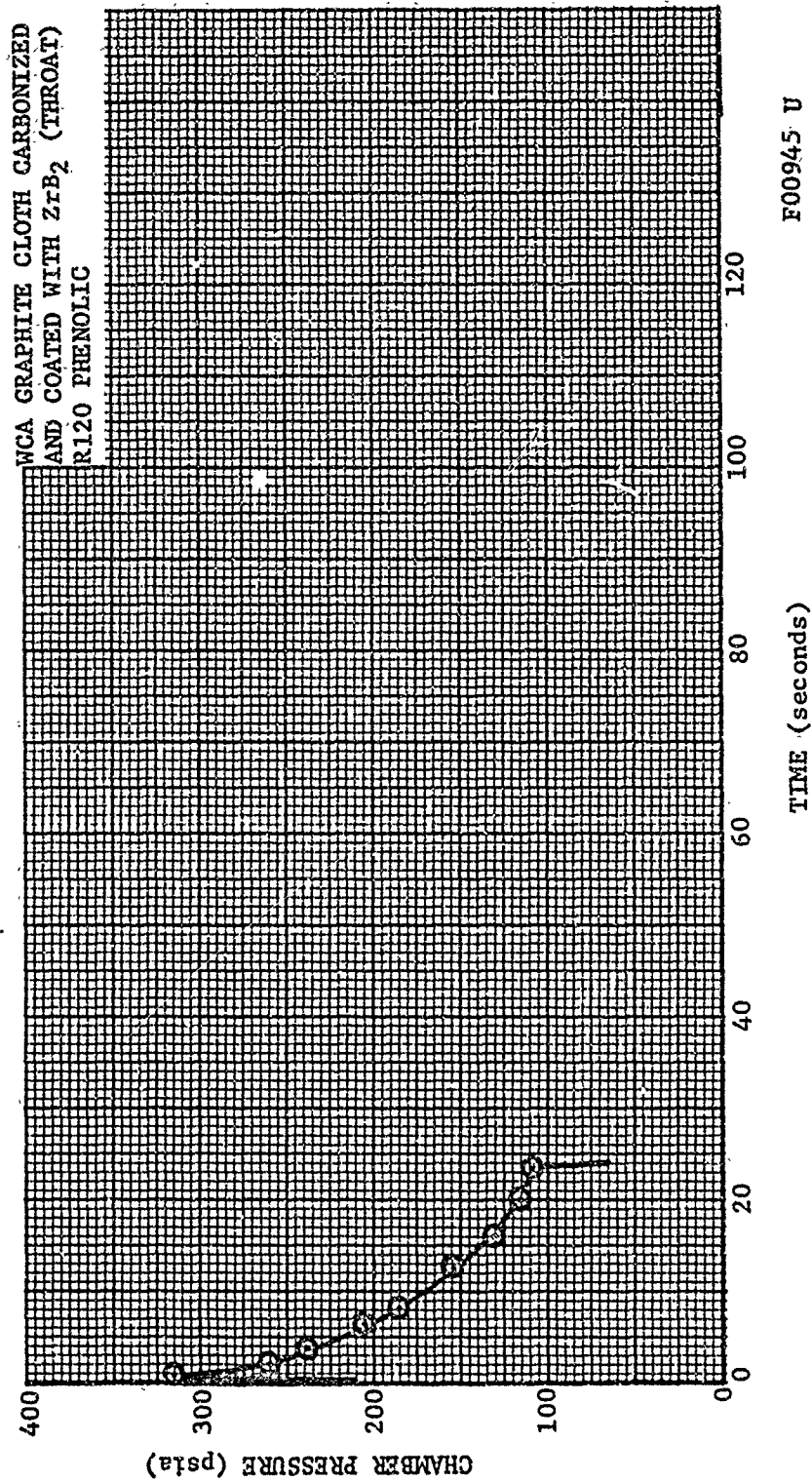
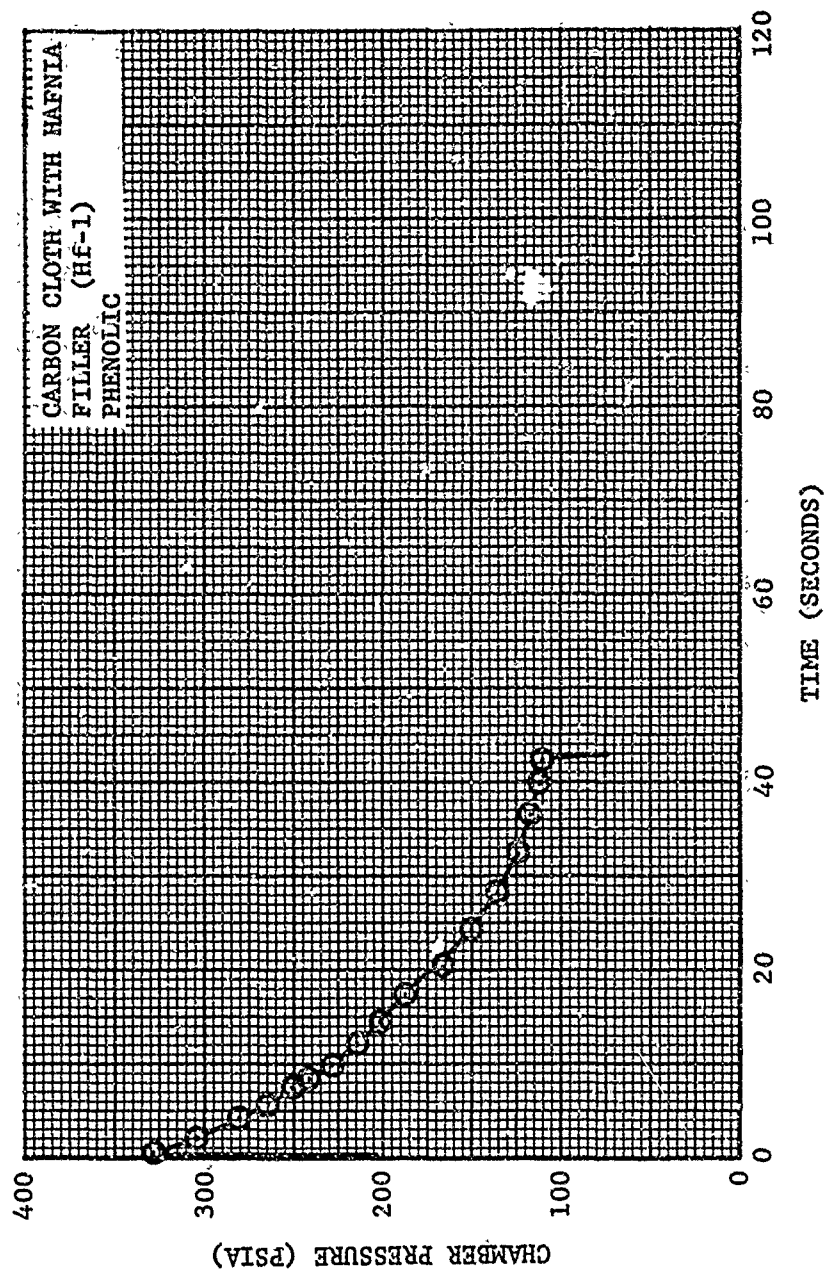


FIGURE 103. CHAMBER PRESSURE VERSUS TIME - ASD 382 NOZZLE



R14197 U

FIGURE 104. CHAMBER PRESSURE VERSUS TIME - ASD 390 NOZZLE

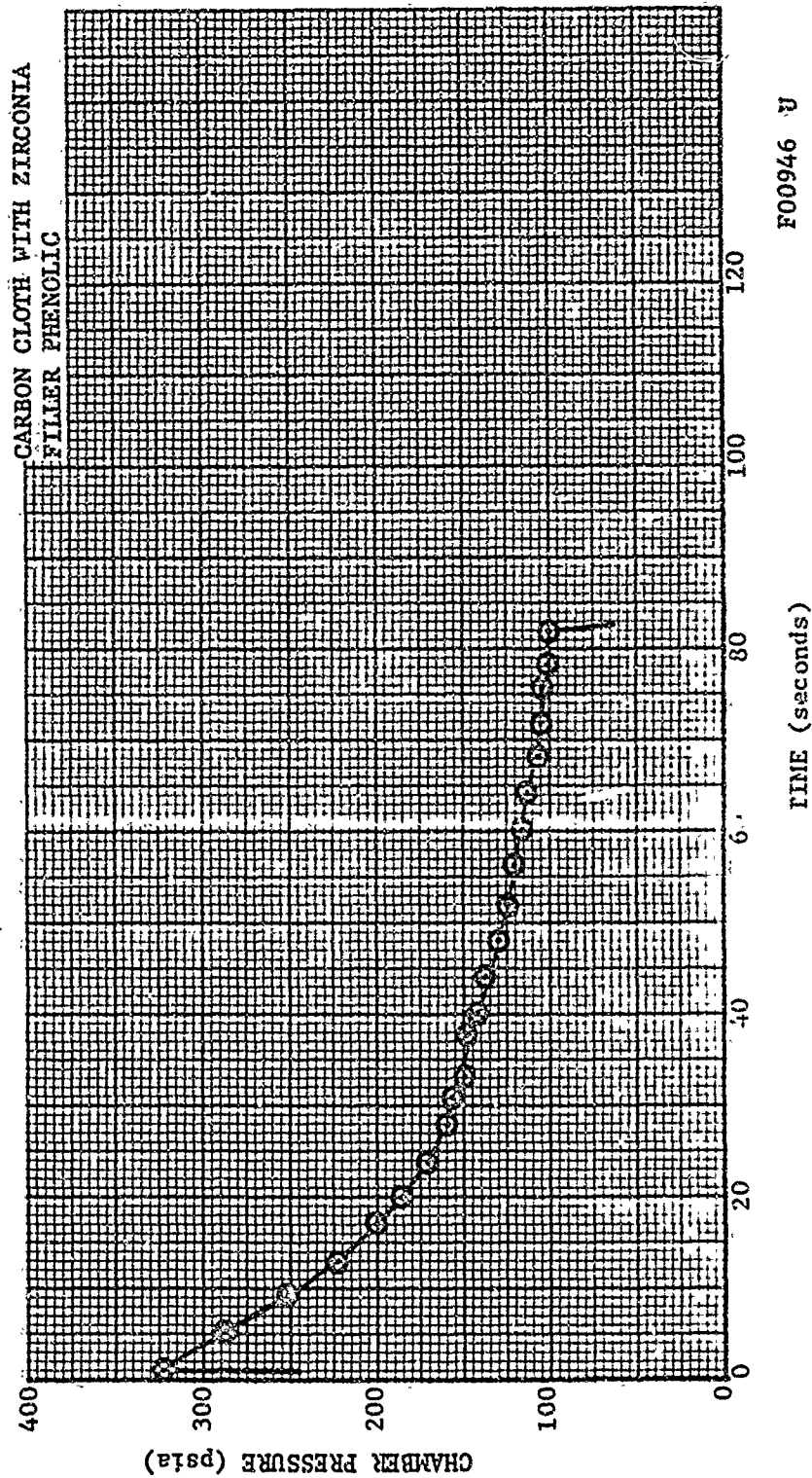


FIGURE 105. CHAMBER PRESSURE VERSUS TIME - ASD 391 NOZZLE

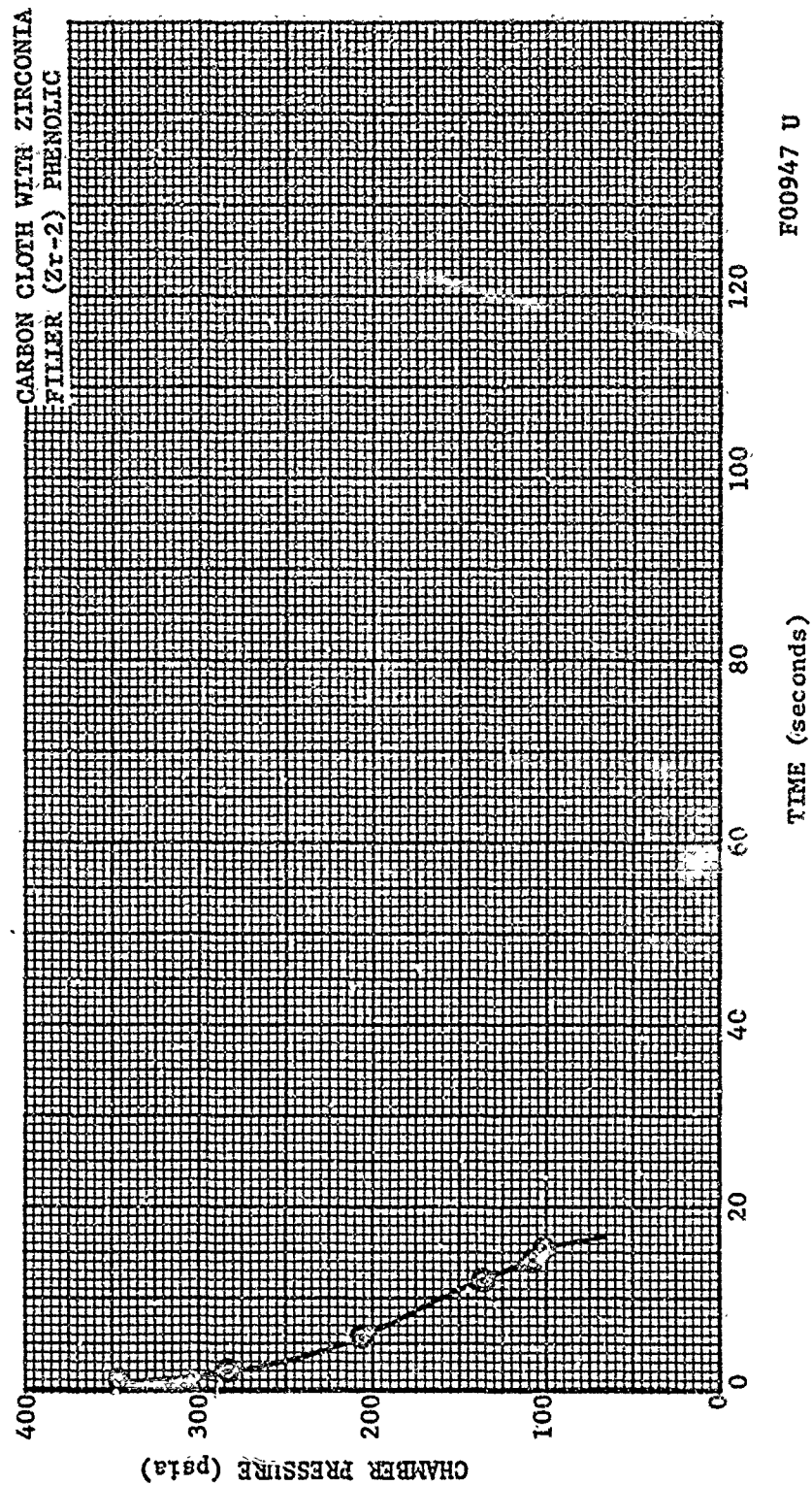


FIGURE 106. CHAMBER PRESSURE VERSUS TIME - ASF 392 NOZZLE

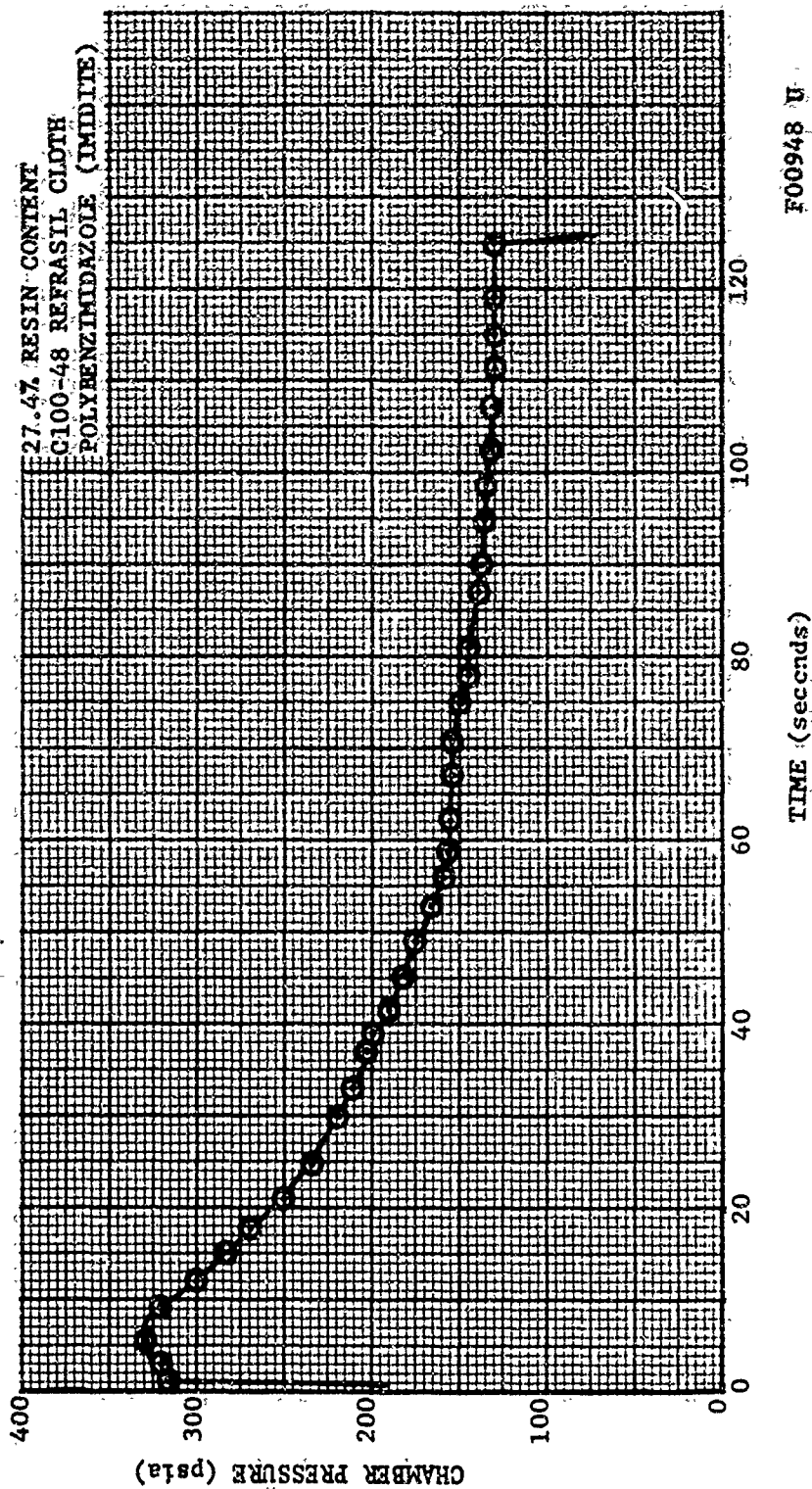


FIGURE 107. CHAMBER PRESSURE VERSUS TIME - ASD 395 NOZZLE

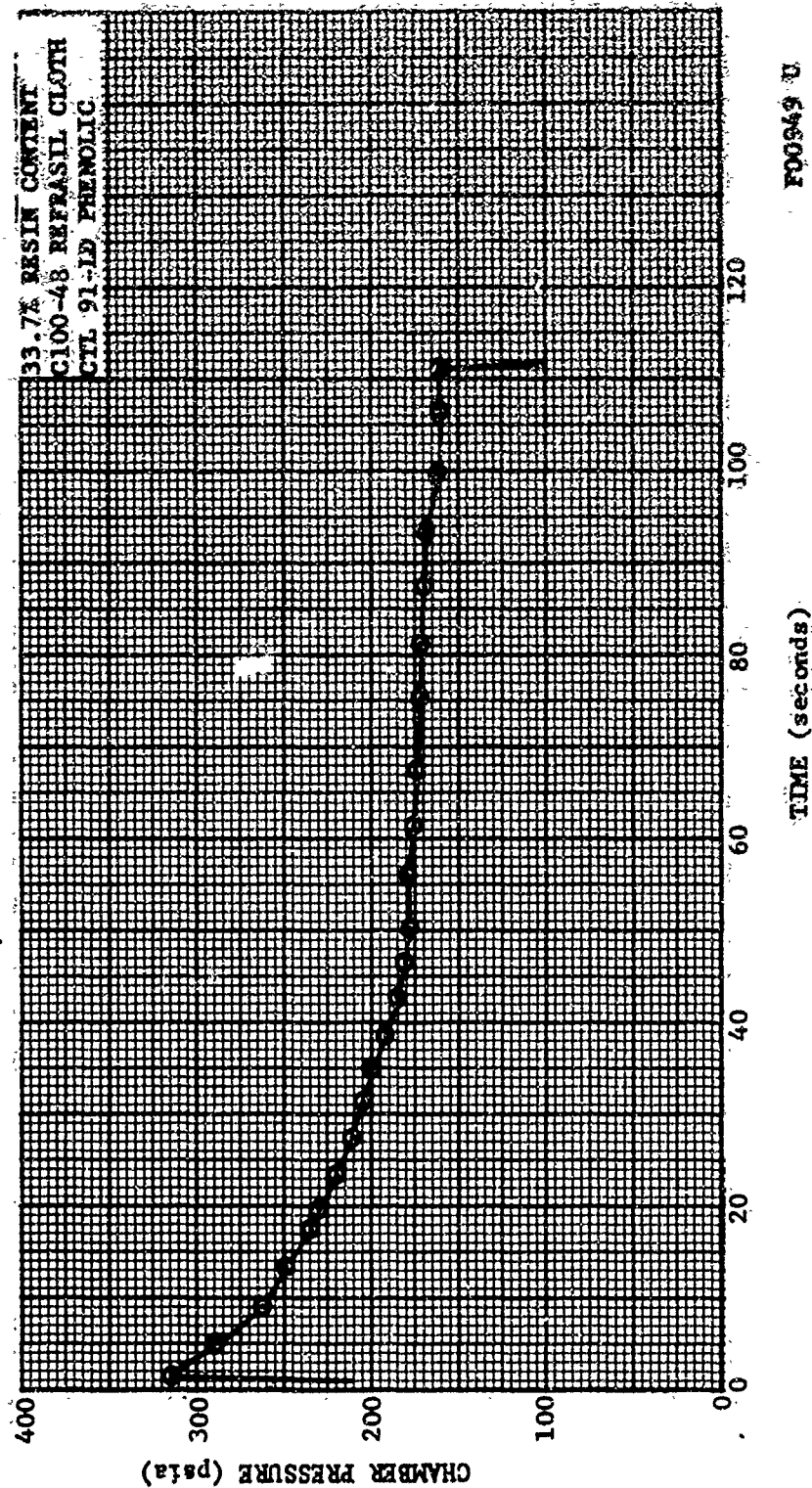
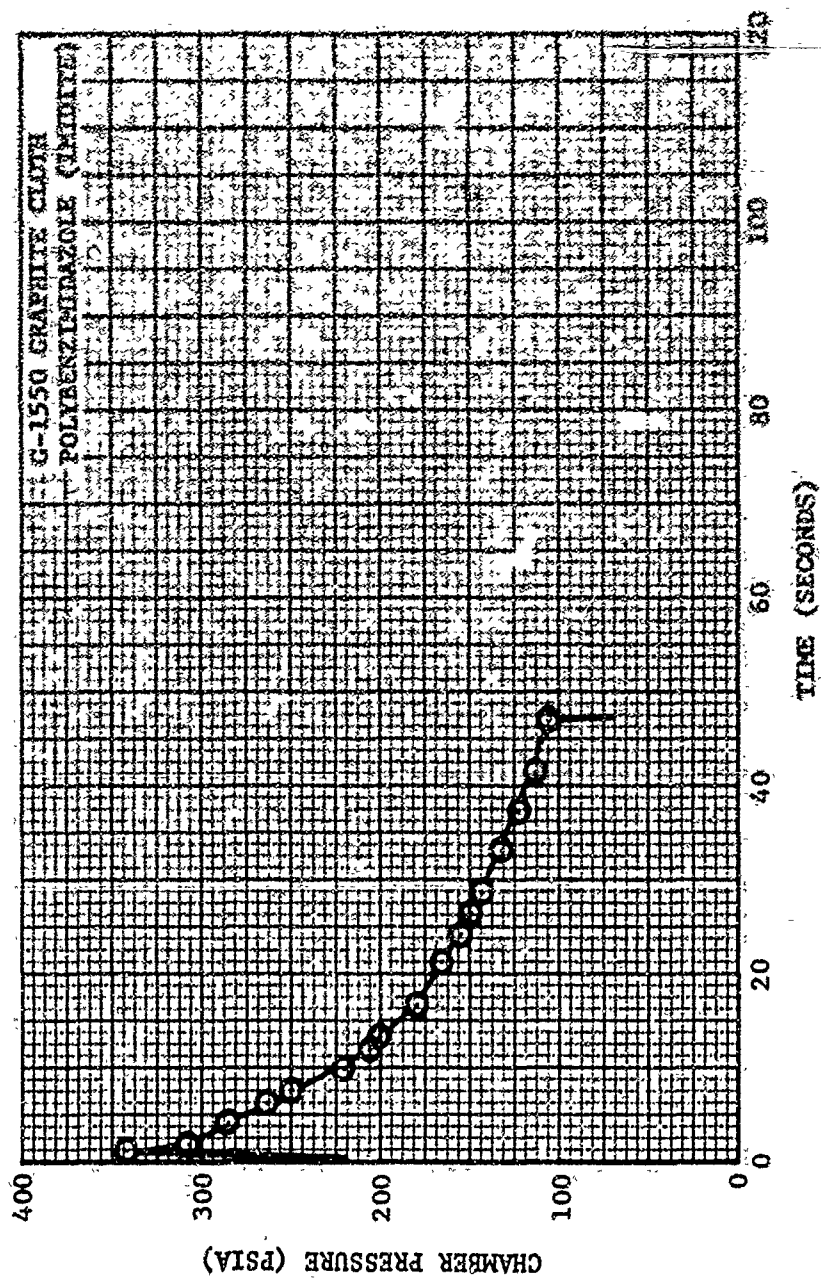


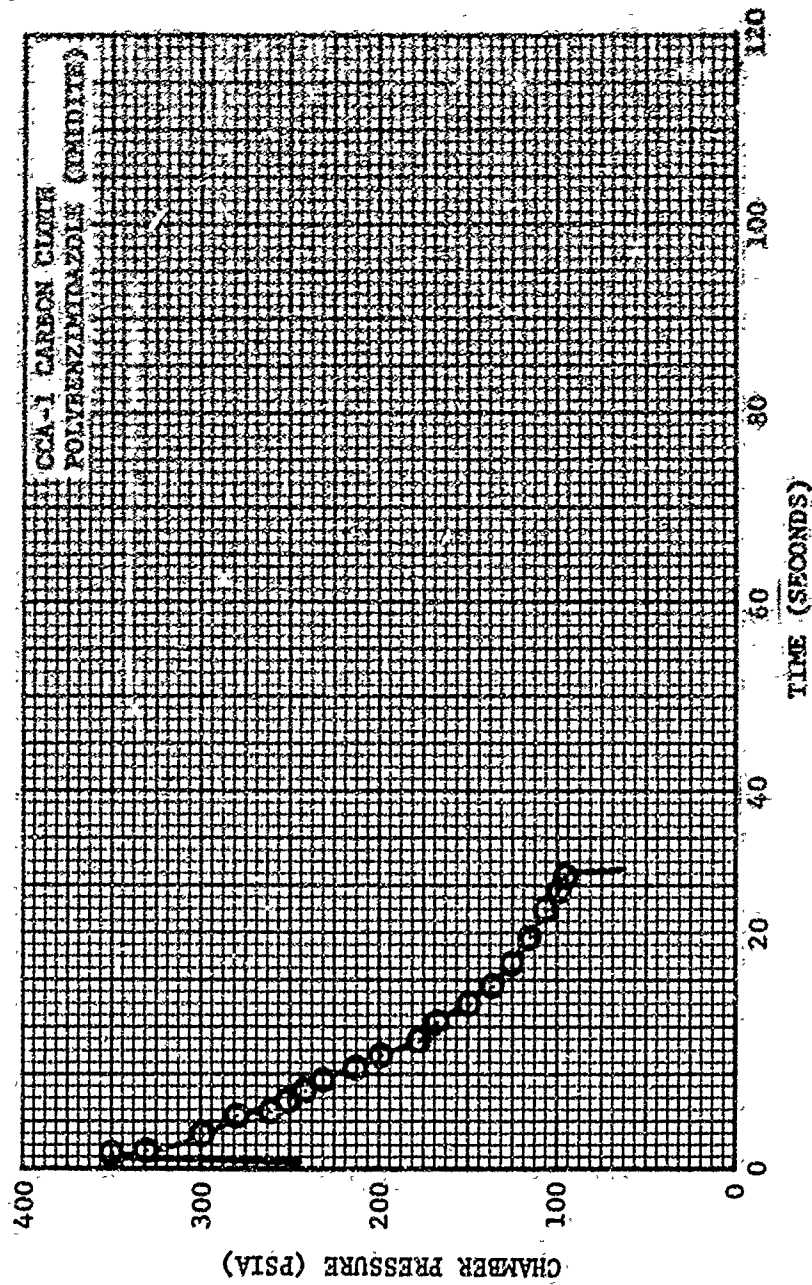
FIGURE 108. CHAMBER PRESSURE VERSUS TIME - ASD 396 NOZZLE





W14128 D

FIGURE 109. CHAMBER PRESSURE VERSUS TIME - ASD 409 NOZZLE



814195 U

FIGURE 110. CHAMBER PRESSURE VERSUS TIME - ASD 409 NOZZLE



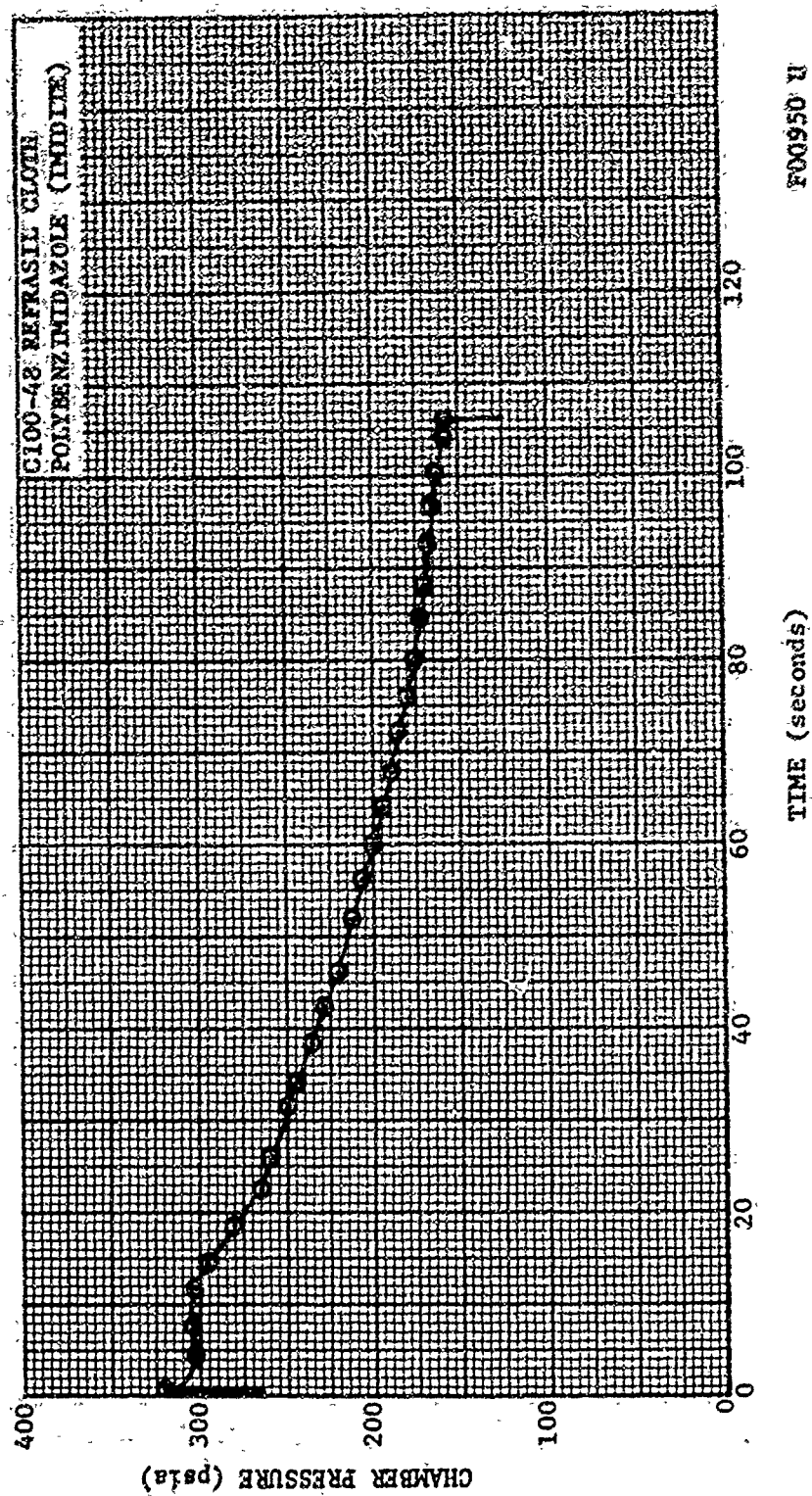


FIGURE 111: CHAMBER PRESSURE VERSUS TIME - ASD 412 NOZZLE

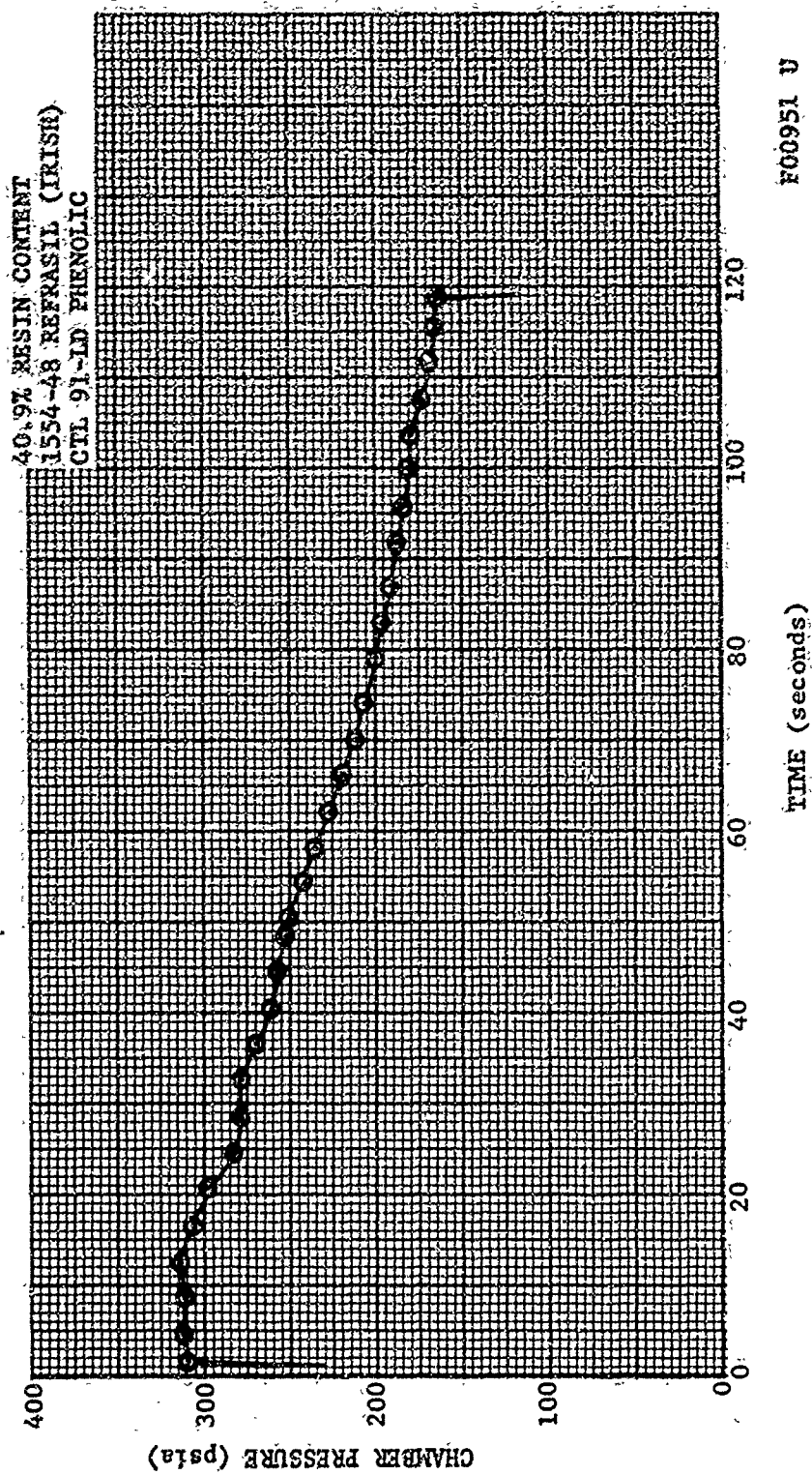


FIGURE 112. CHAMBER PRESSURE VERSUS TIME - ASD 415. NOZZLE

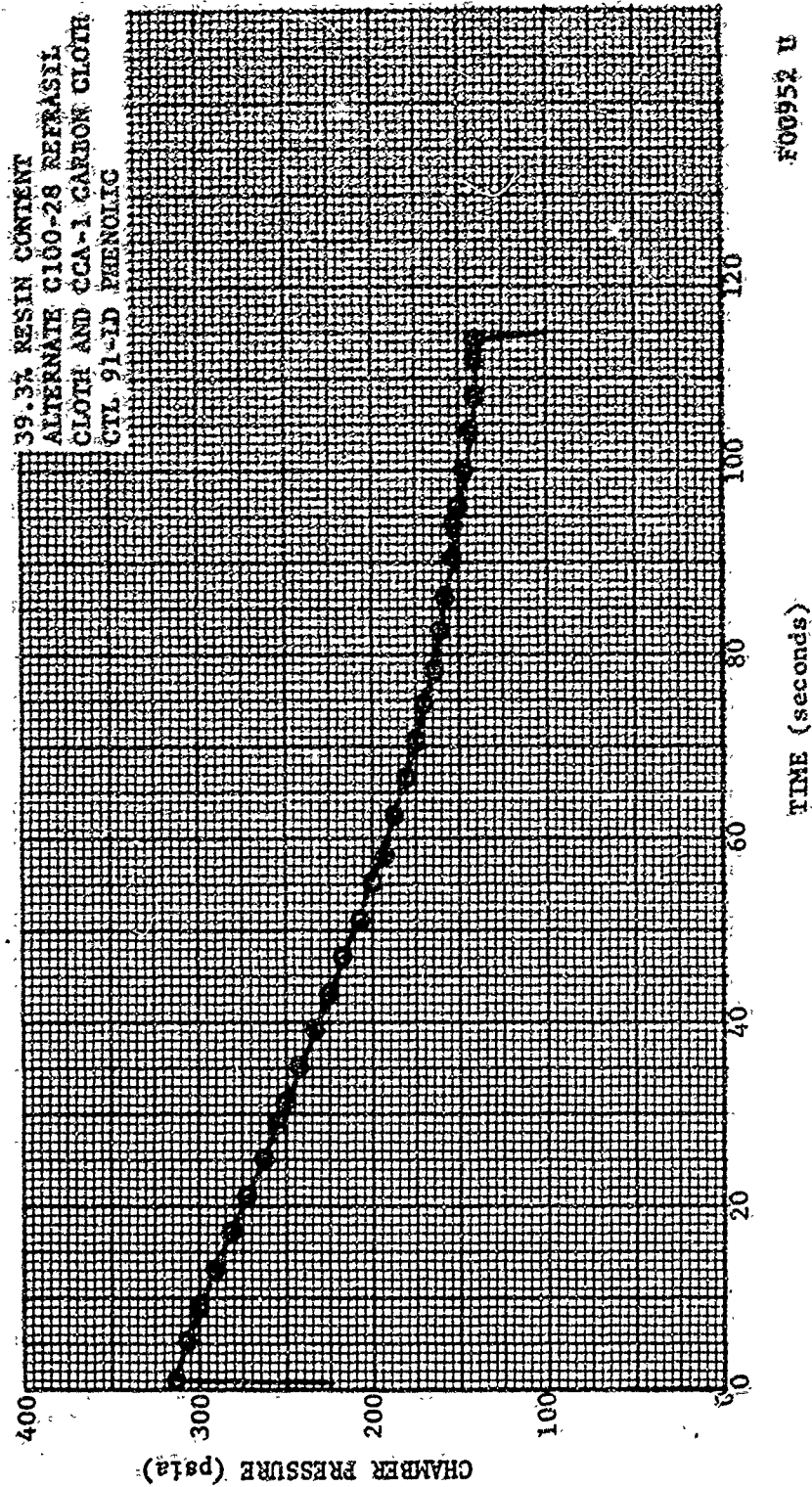


FIGURE 113. CHAMBER PRESSURE VERSUS TIME - ASD 420 NOZZLE

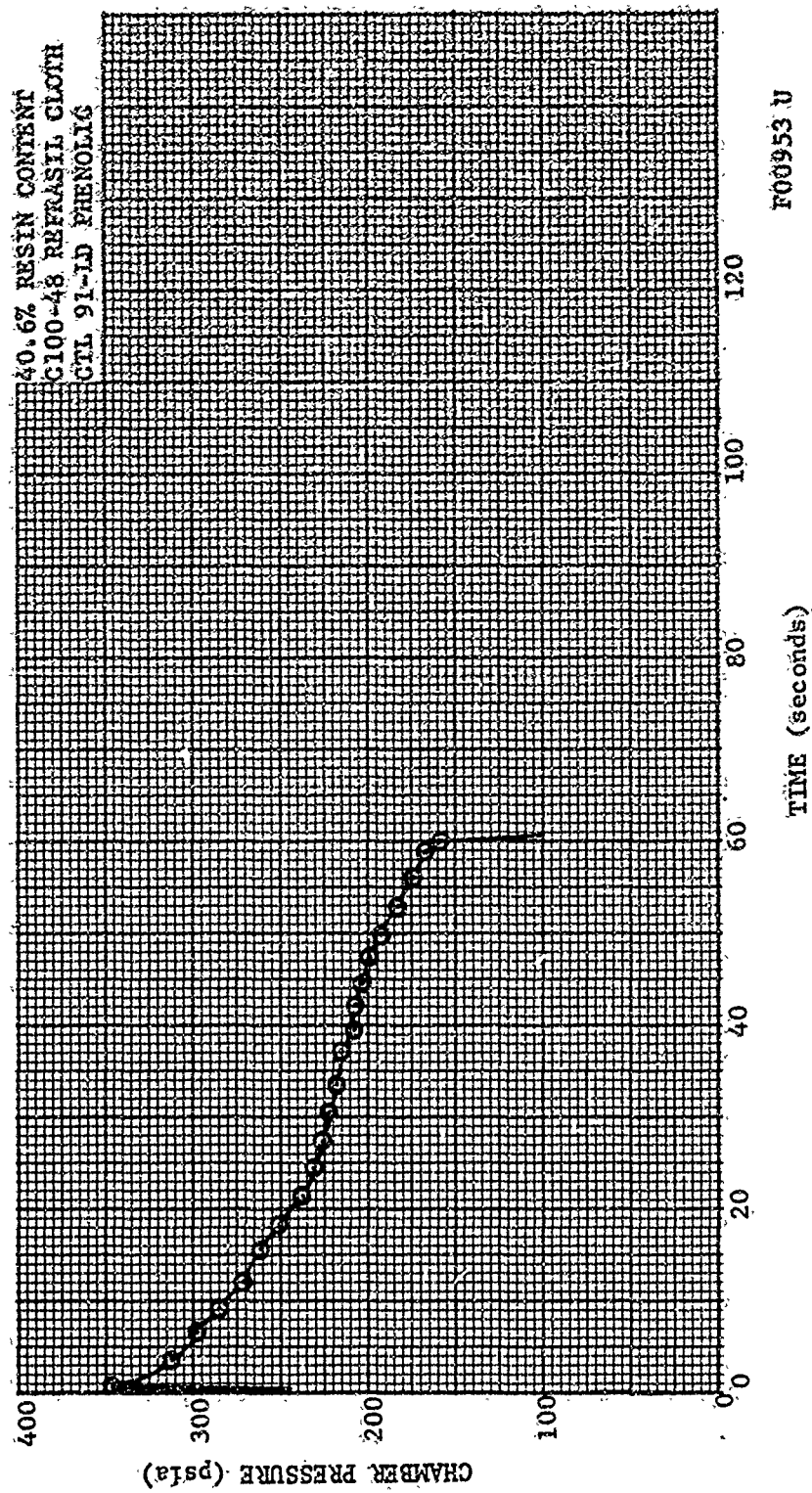
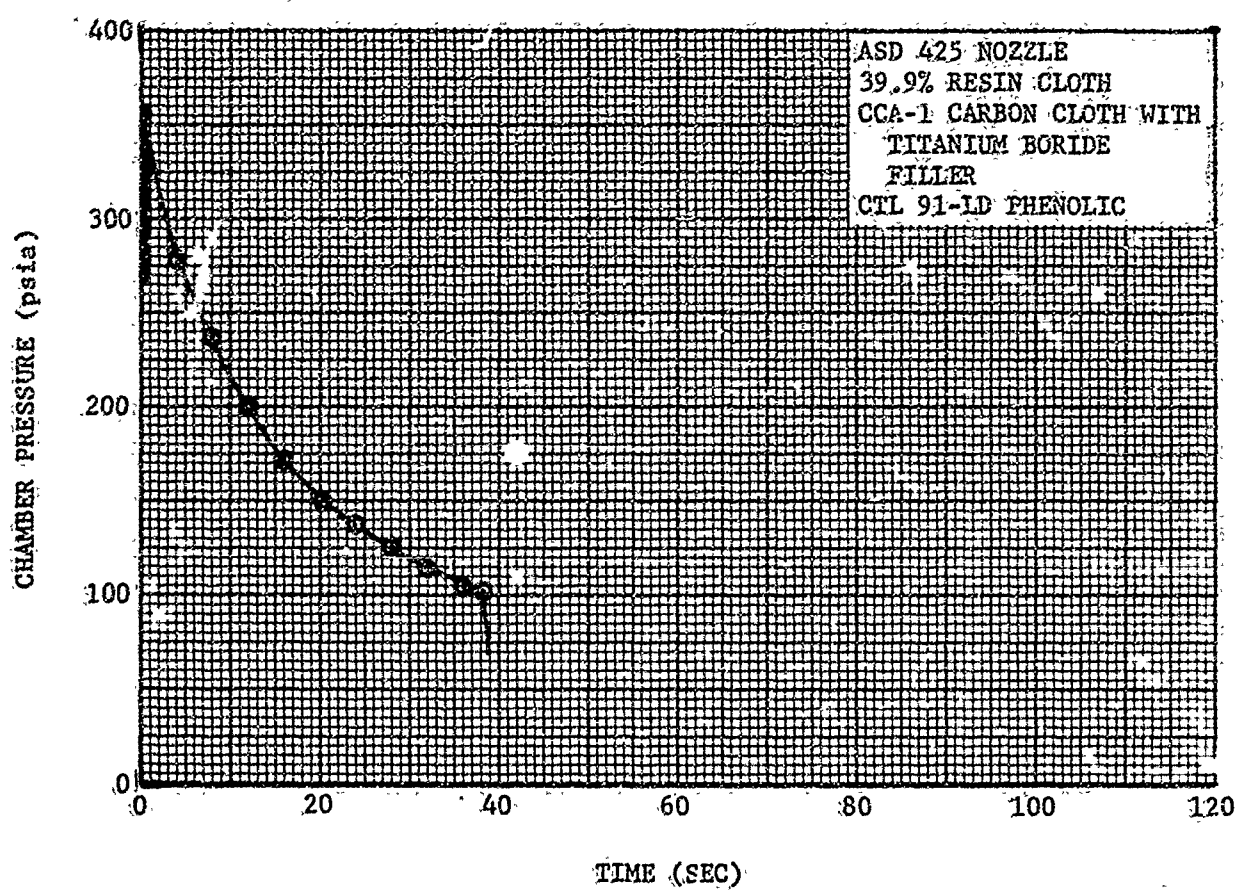
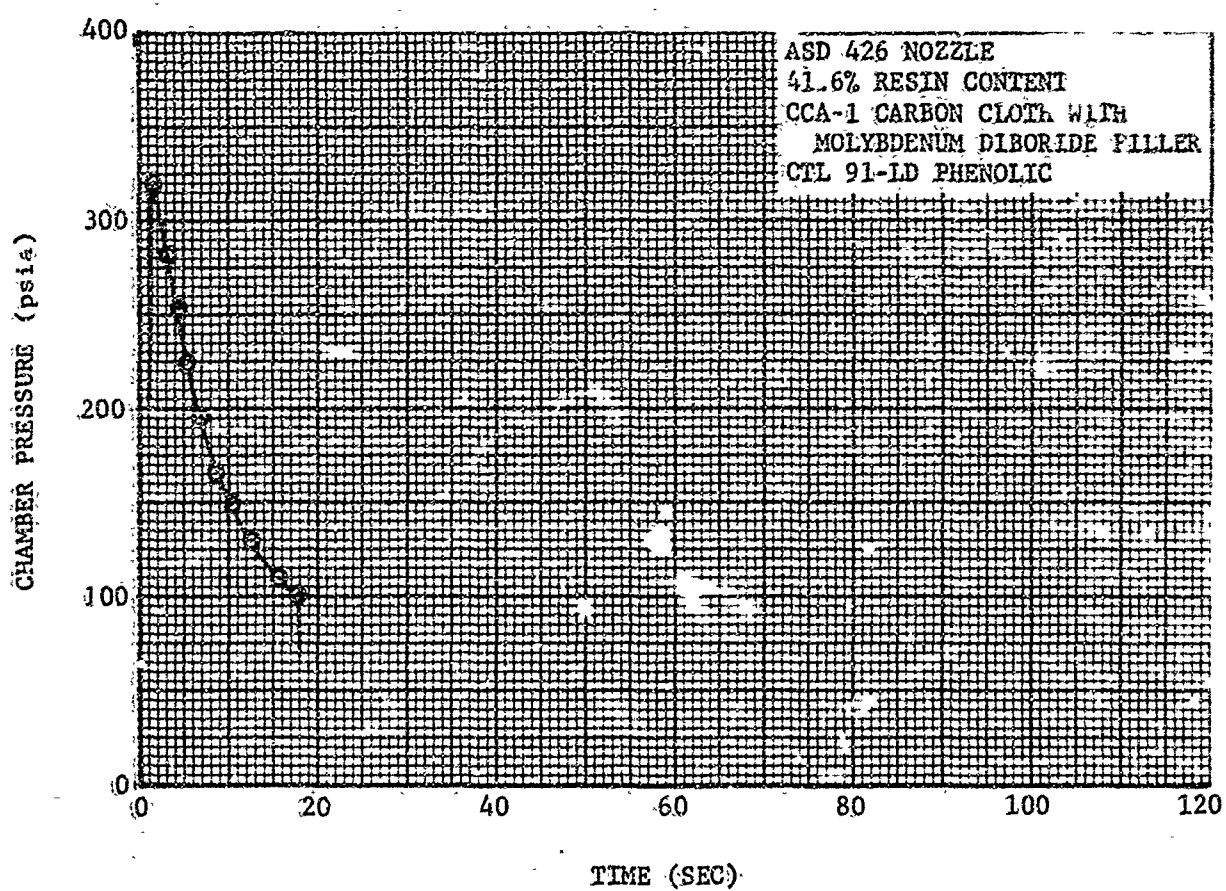


FIGURE 114. CHAMBER PRESSURE VERSUS TIME - ASD 424 NOZZLE



R14184 U

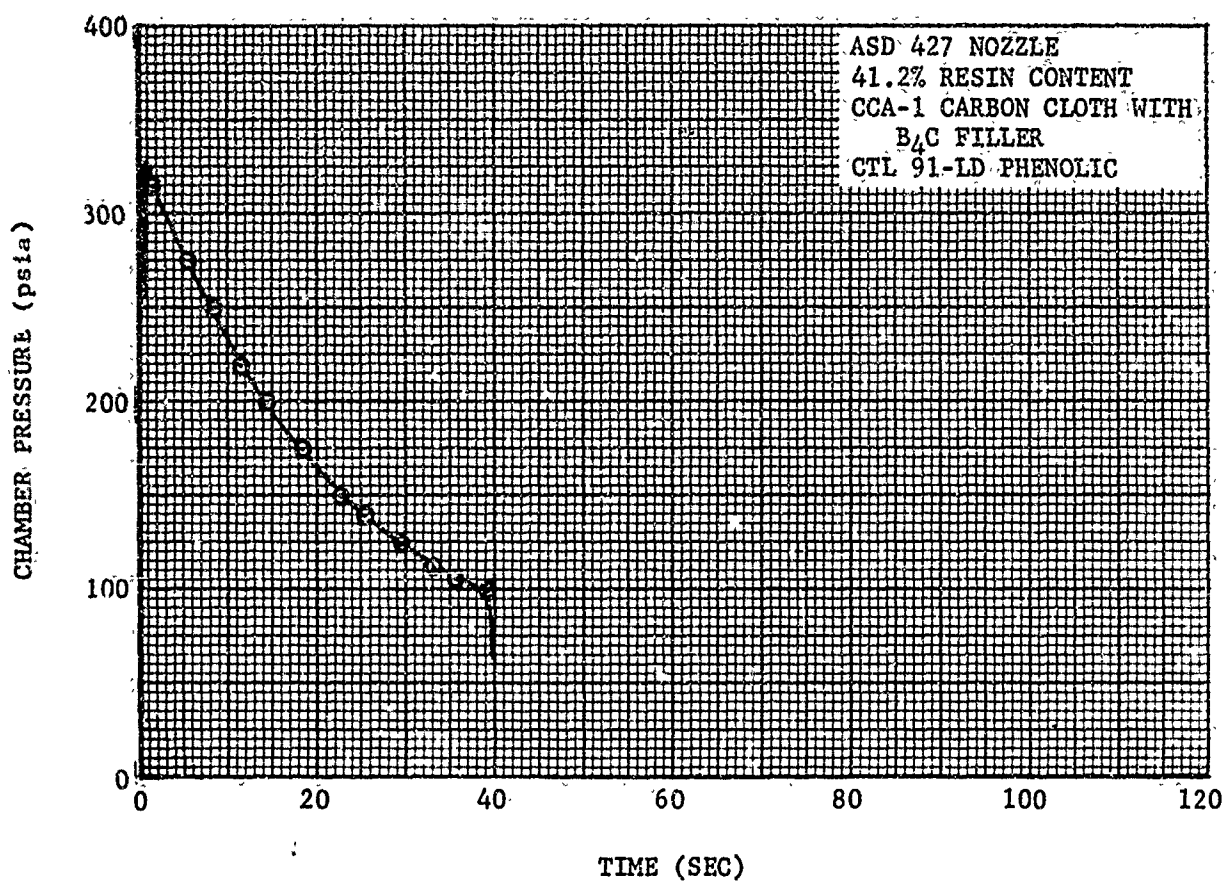
FIGURE 115. CHAMBER PRESSURE VERSUS TIME - ASD 425 NOZZLE



R14183 U

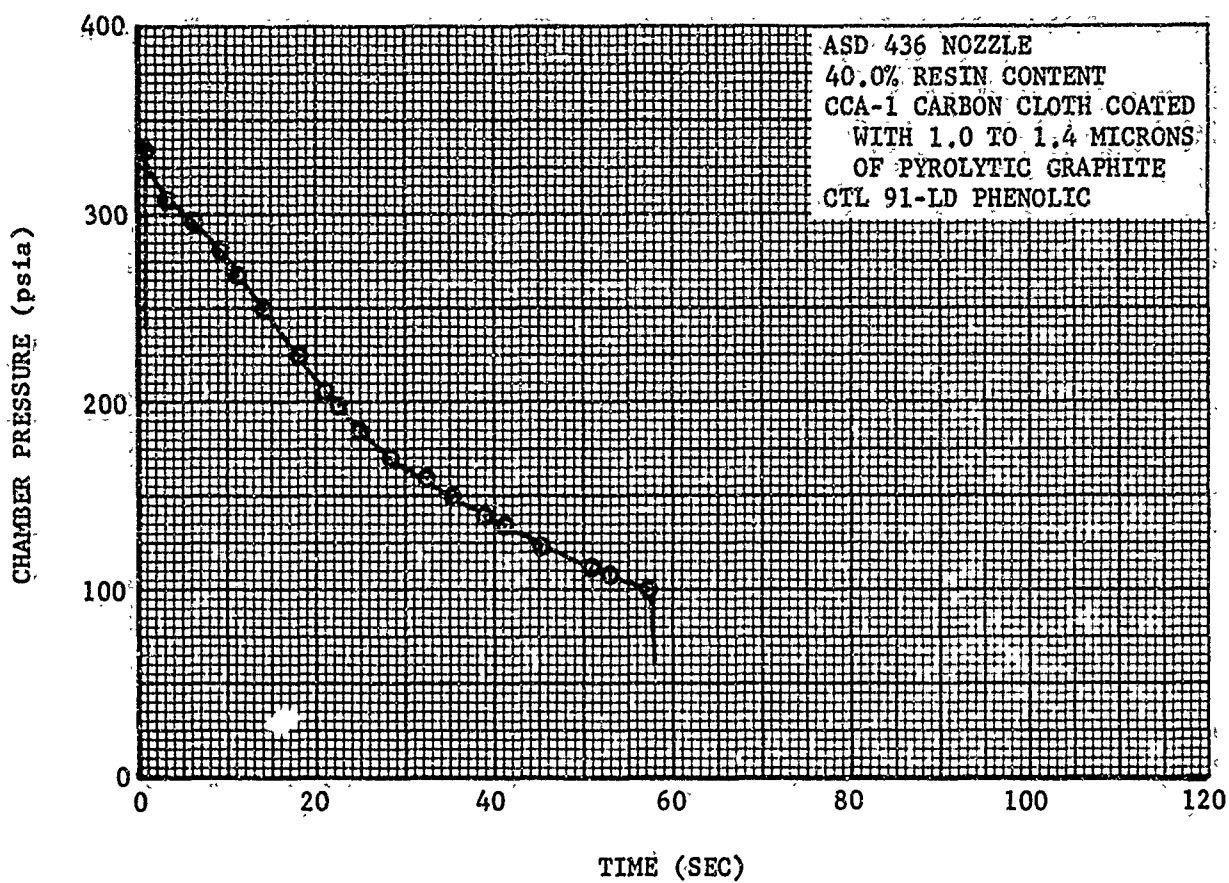
FIGURE 116. CHAMBER PRESSURE VERSUS TIME - ASD 426 NOZZLE





R14169 U

FIGURE 117. CHAMBER PRESSURE VERSUS TIME - ASD 427 NOZZLE



R14170 U

FIGURE 118. CHAMBER PRESSURE VERSUS TIME - ASD 436 NOZZLE



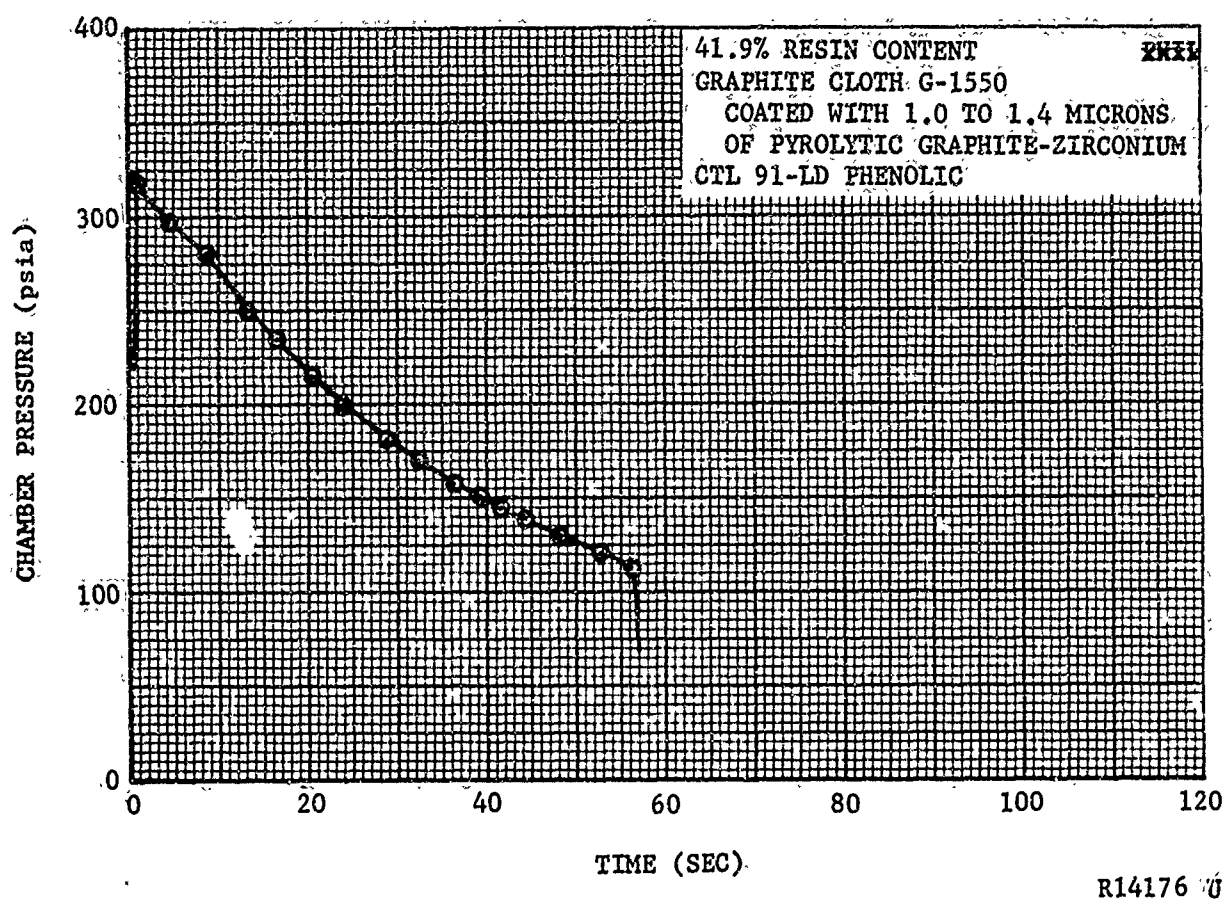
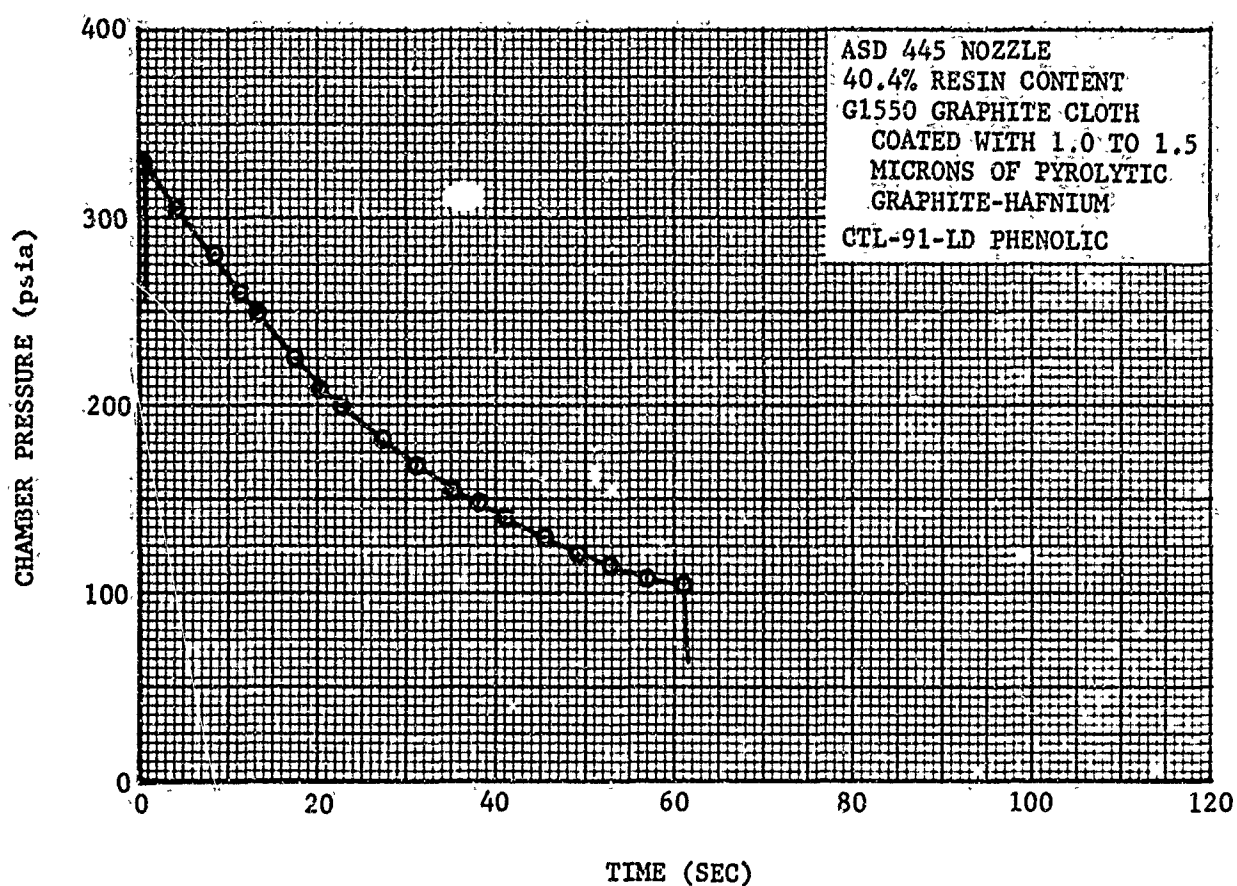
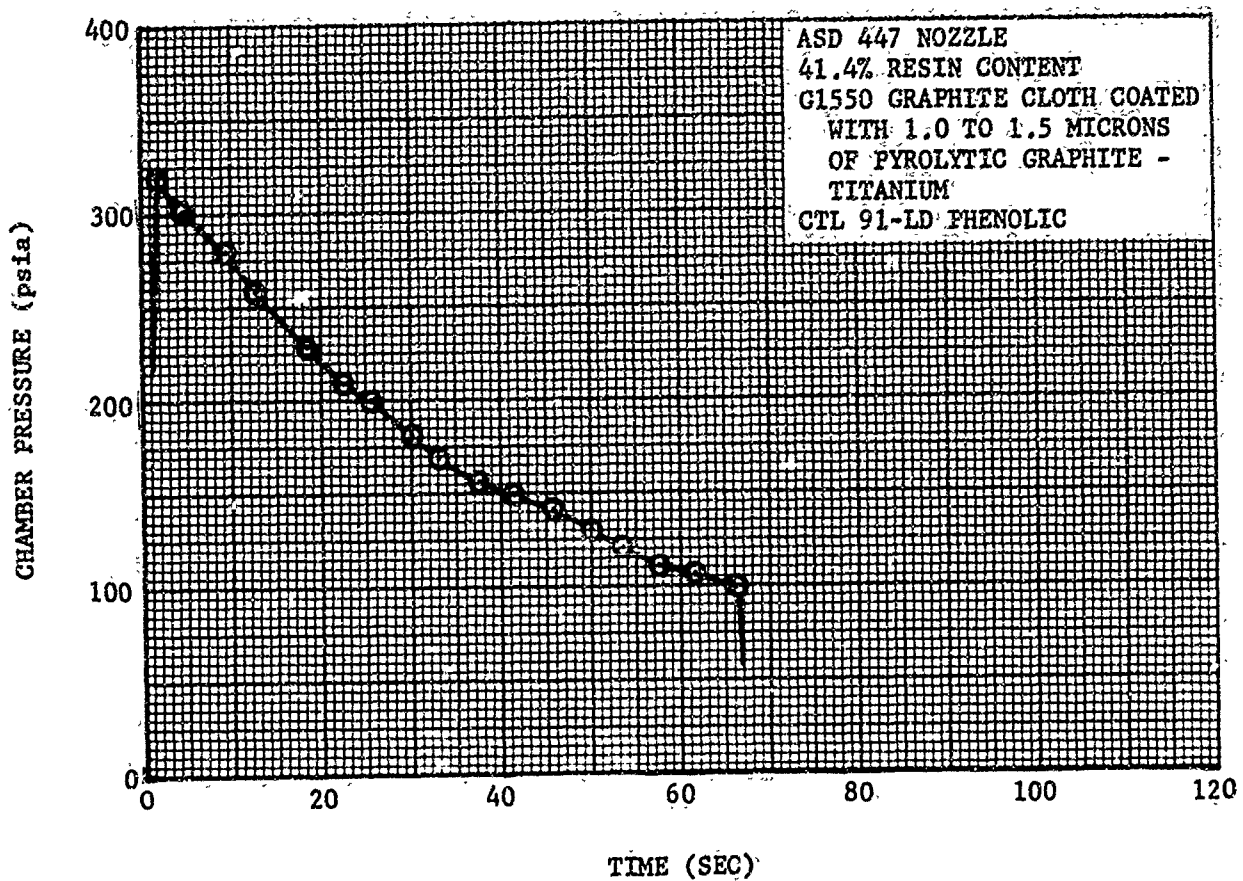


FIGURE 119. CHAMBER PRESSURE VERSUS TIME - ASD 438 NOZZLE



R14177 U

FIGURE 120. CHAMBER PRESSURE VERSUS TIME - ASD 445 NOZZLE



R14173 U

FIGURE 121. CHAMBER PRESSURE VERSUS TIME - ASD 447 NOZZLE

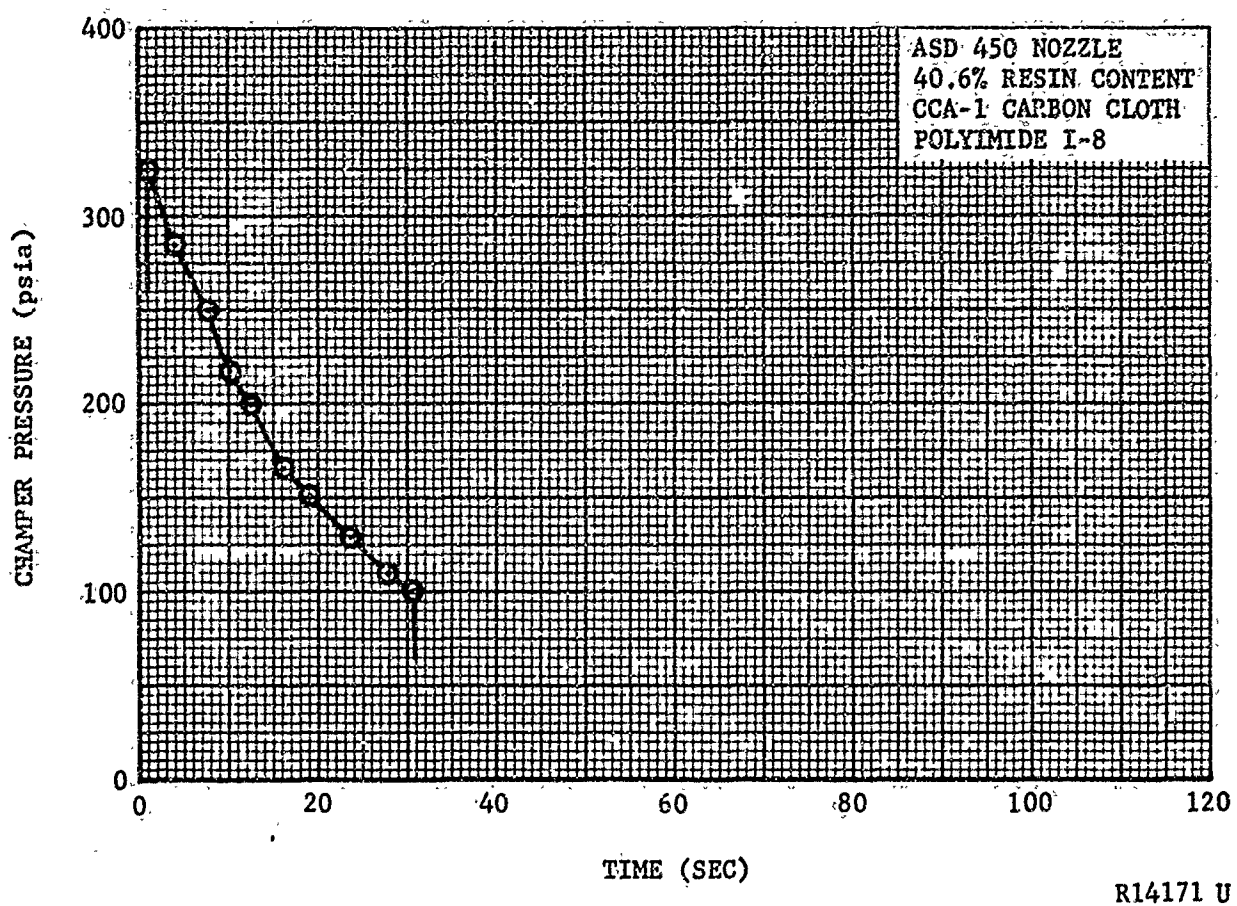
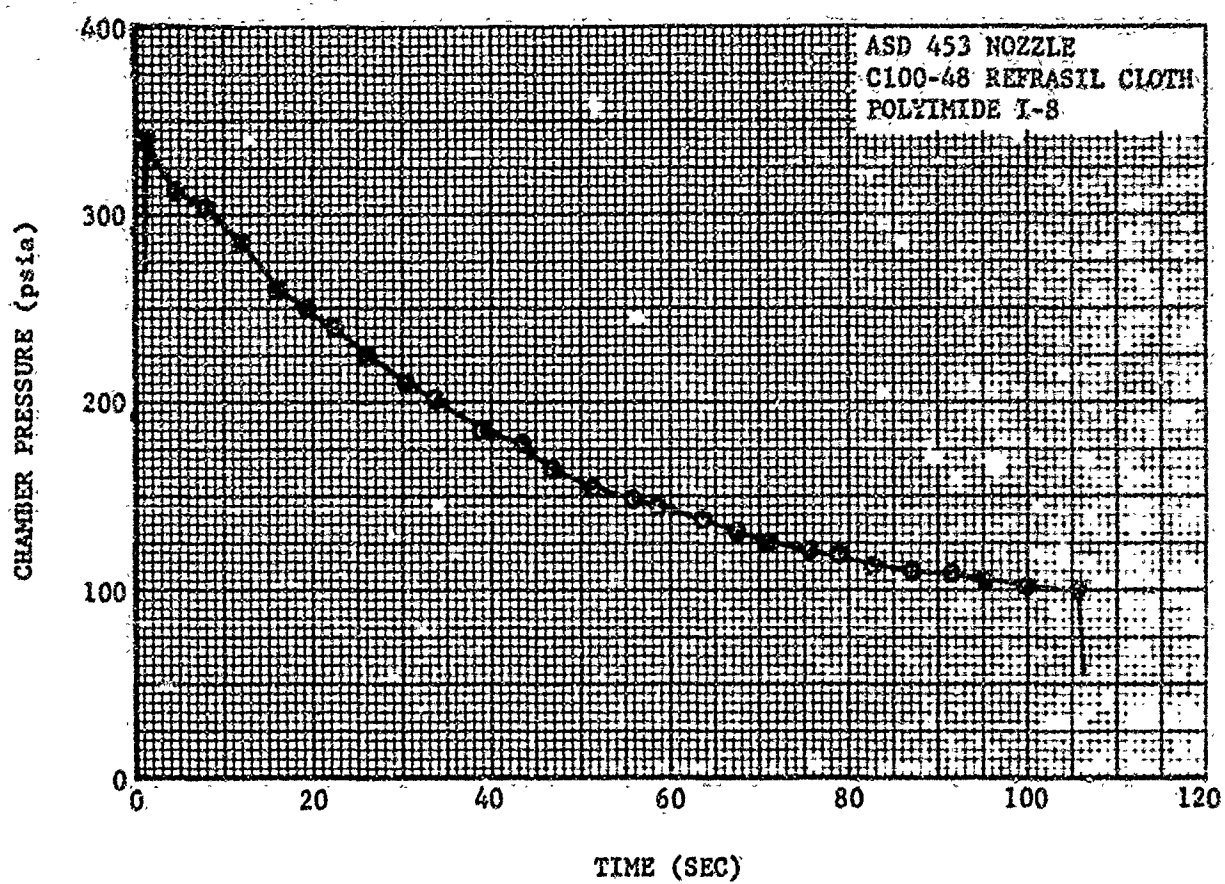
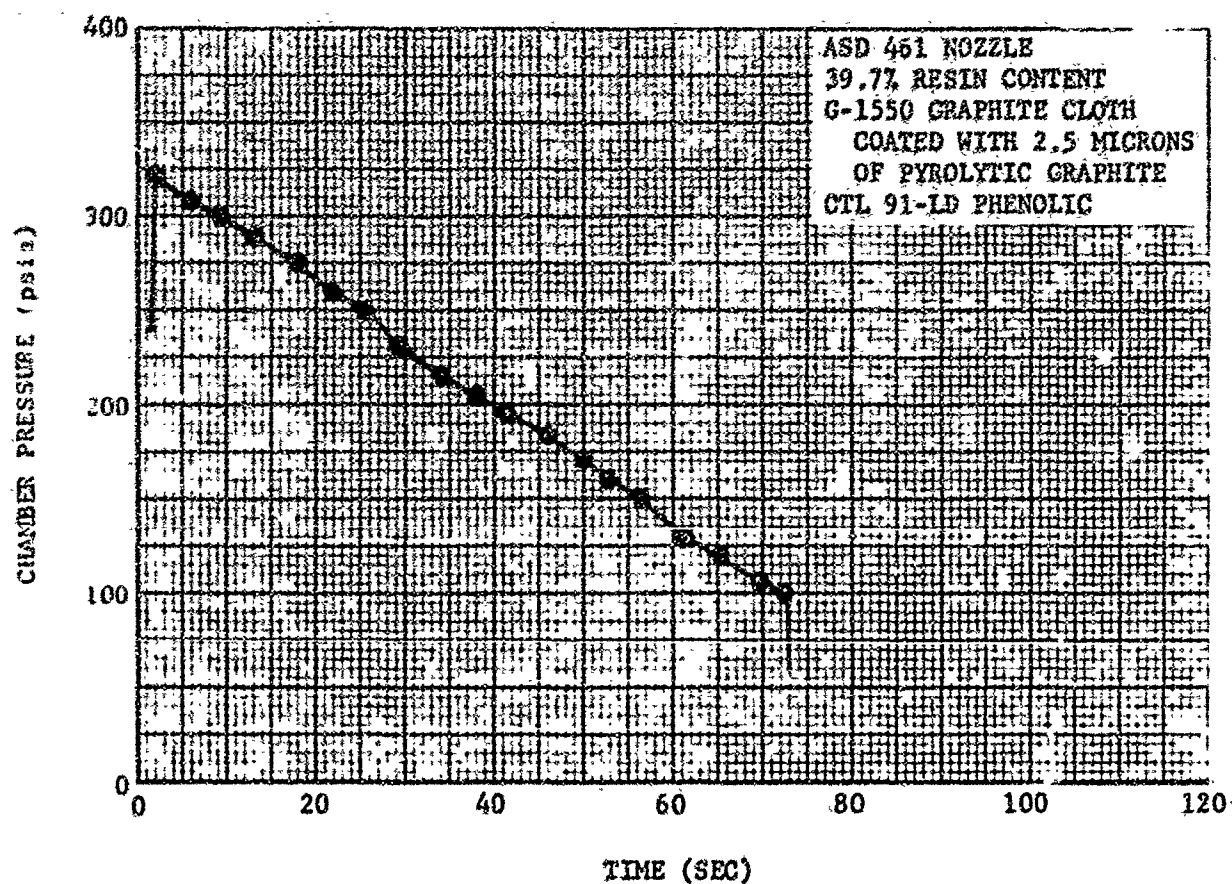


FIGURE 122. CHAMBER PRESSURE VERSUS TIME - ASD 450 NOZZLE



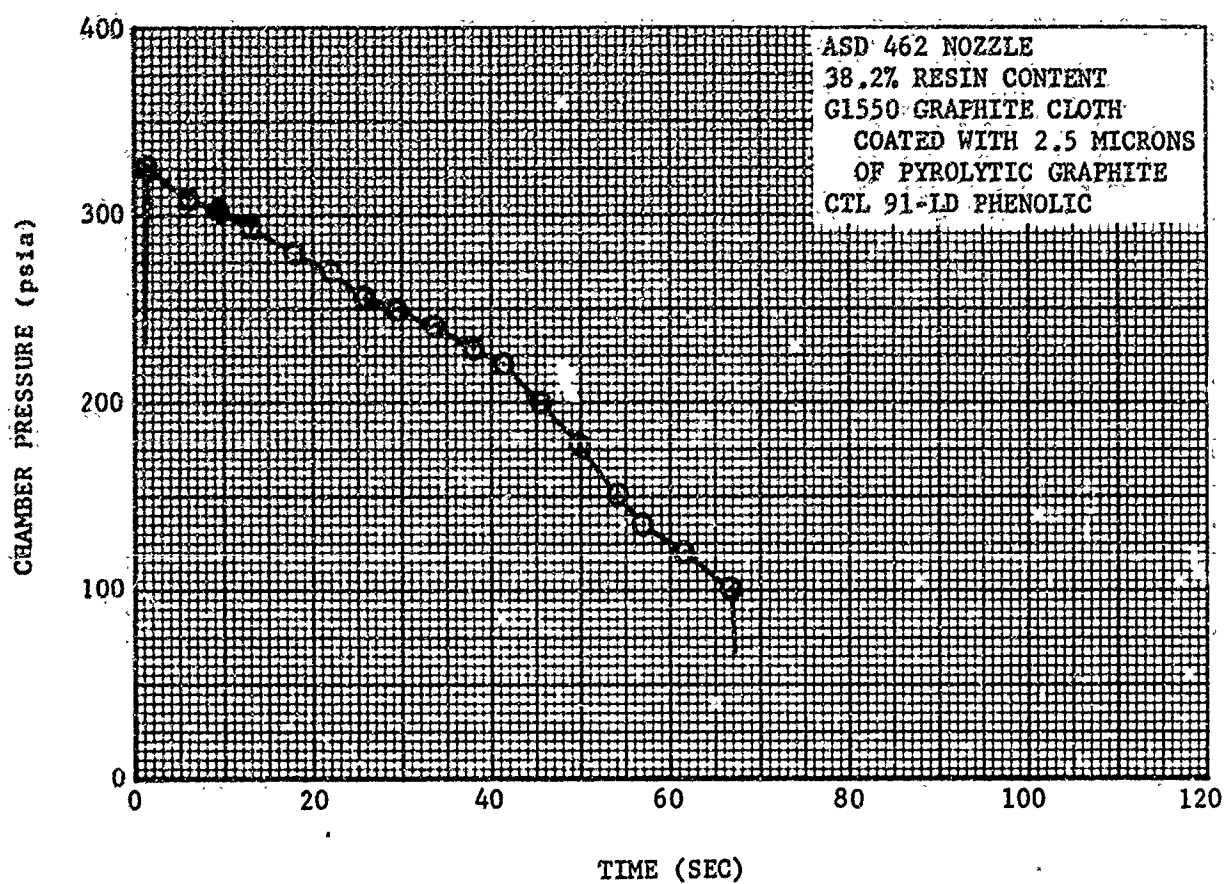
R14172 U

FIGURE 123. CHAMBER PRESSURE VERSUS TIME - ASD 453 NOZZLE



R14167 U

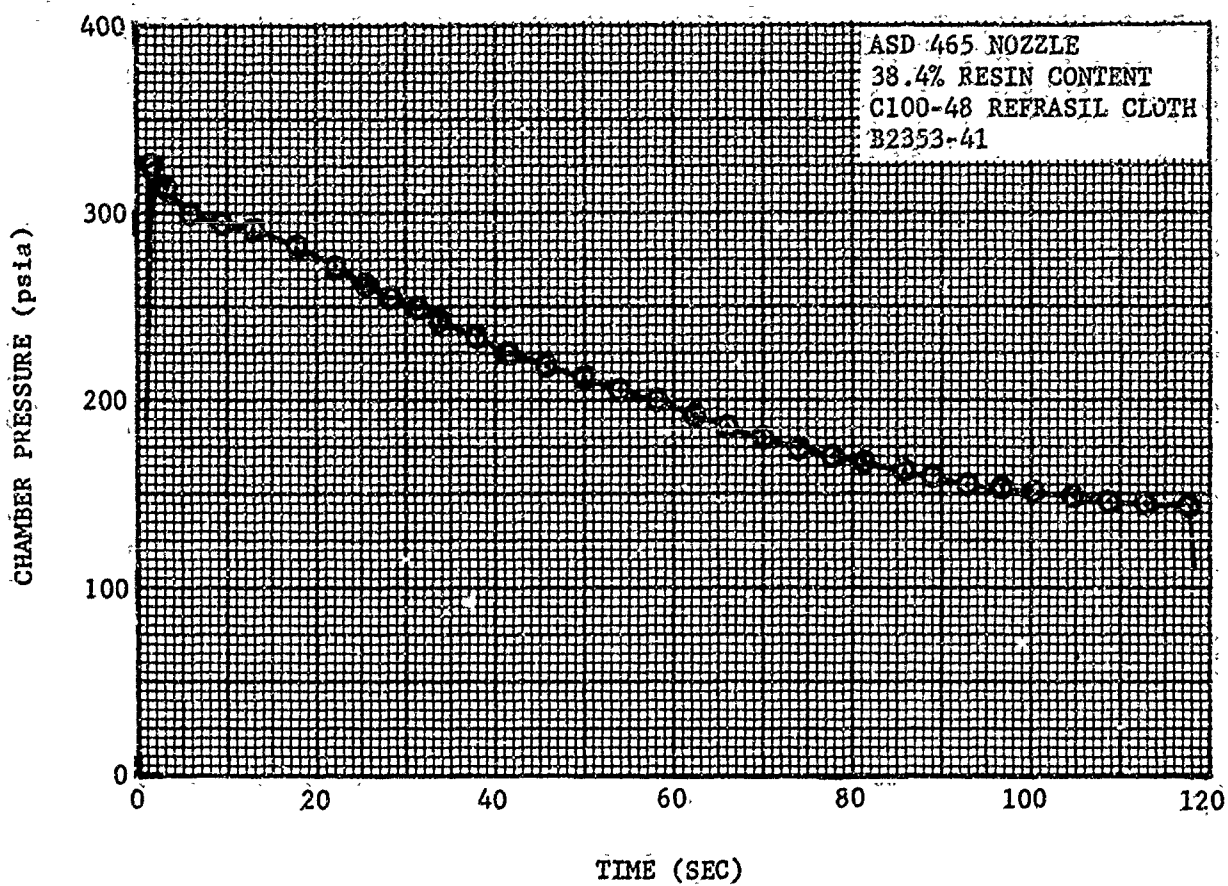
FIGURE 124. CHAMBER PRESSURE VERSUS TIME - ASD 461 NOZZLE



R14178 U

FIGURE 125. CHAMBER PRESSURE VERSUS TIME - ASD 462 NOZZLE

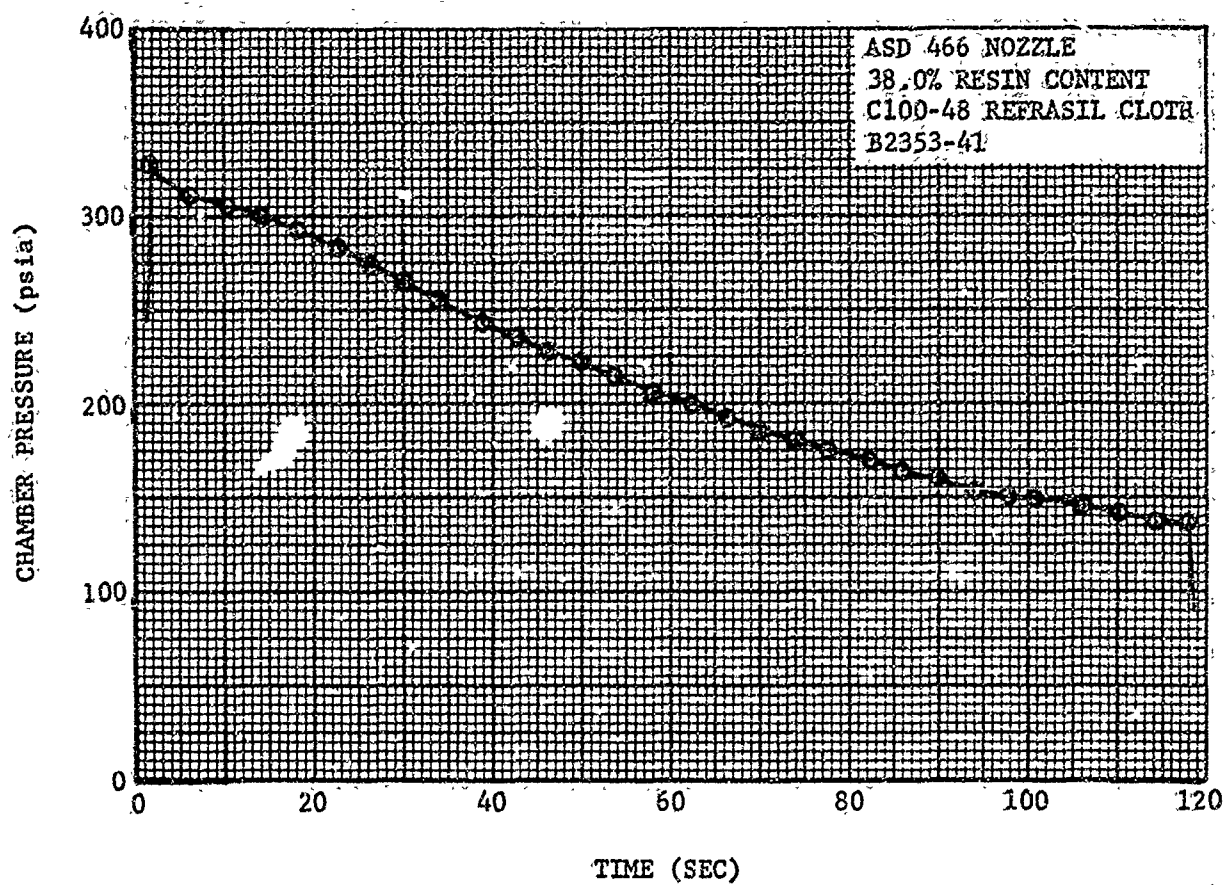




R14168 U

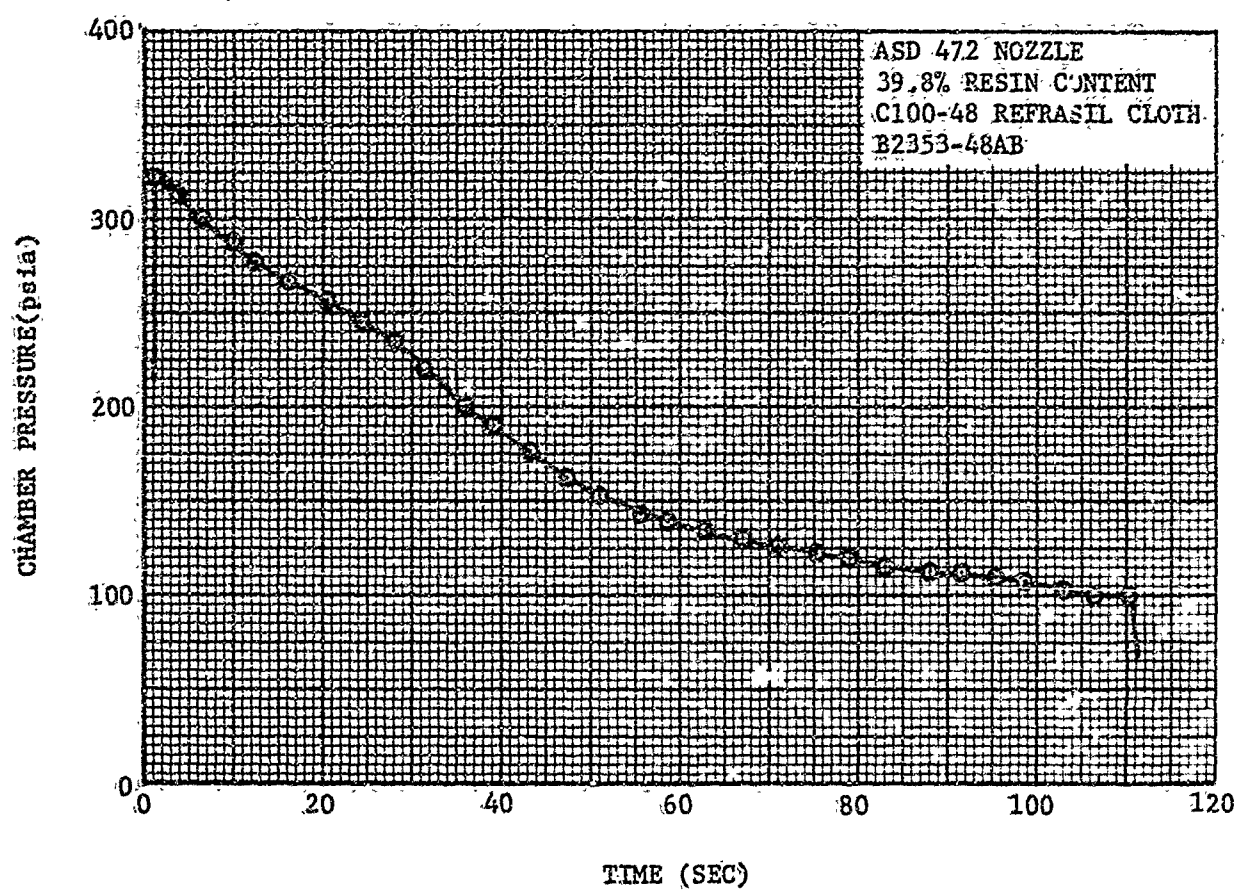
FIGURE 126. CHAMBER PRESSURE VERSUS TIME - ASD 465 NOZZLE





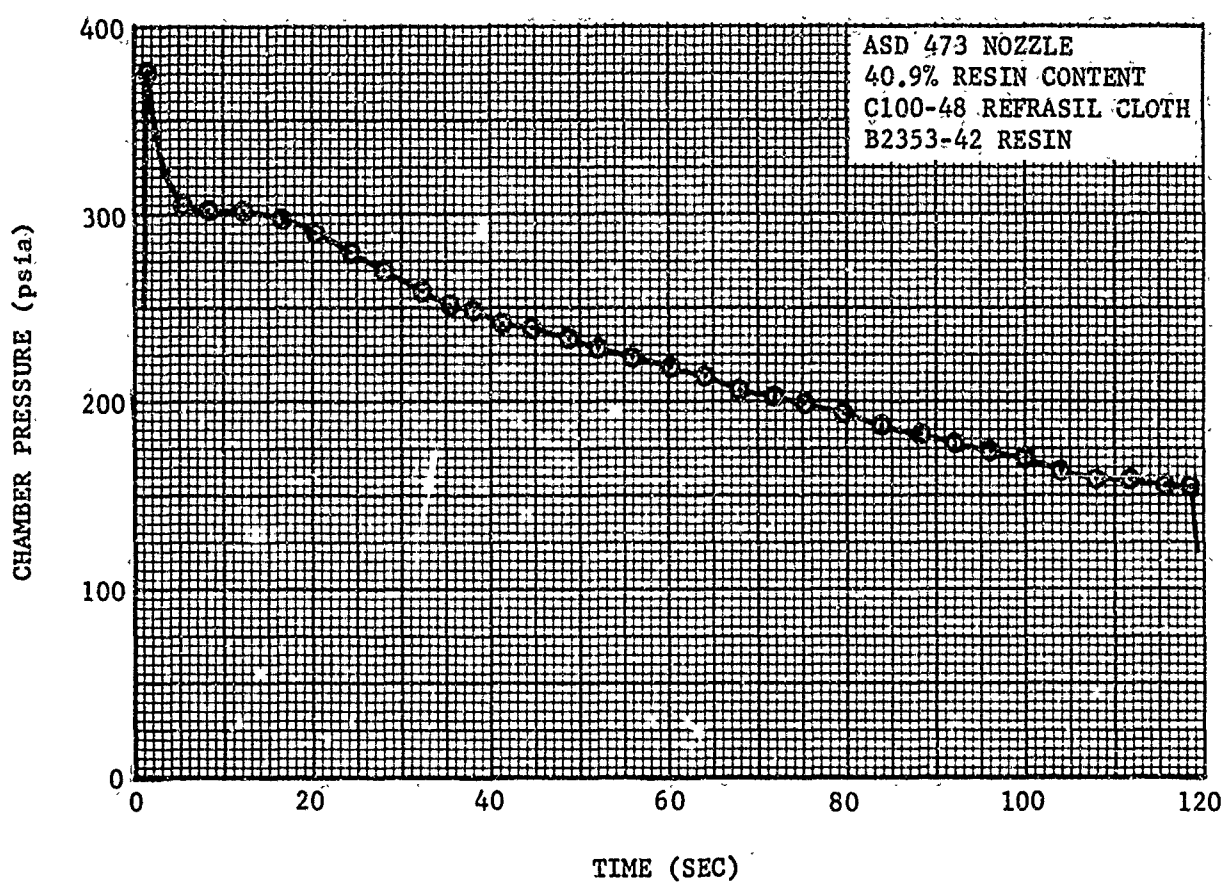
R14179 U

FIGURE 127. CHAMBER PRESSURE VERSUS TIME - ASD 466 NOZZLE



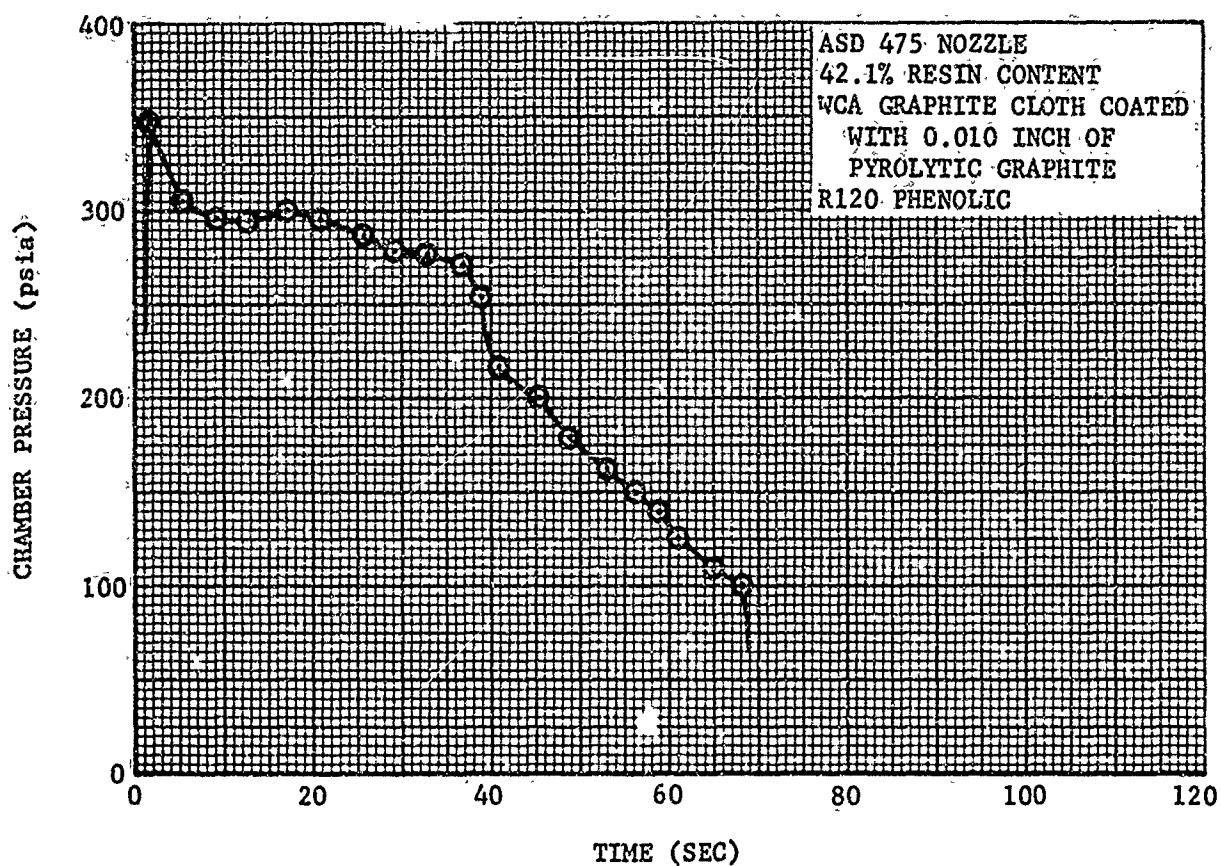
R14180 U

FIGURE 128. CHAMBER PRESSURE VERSUS TIME - ASD 472 NOZZLE



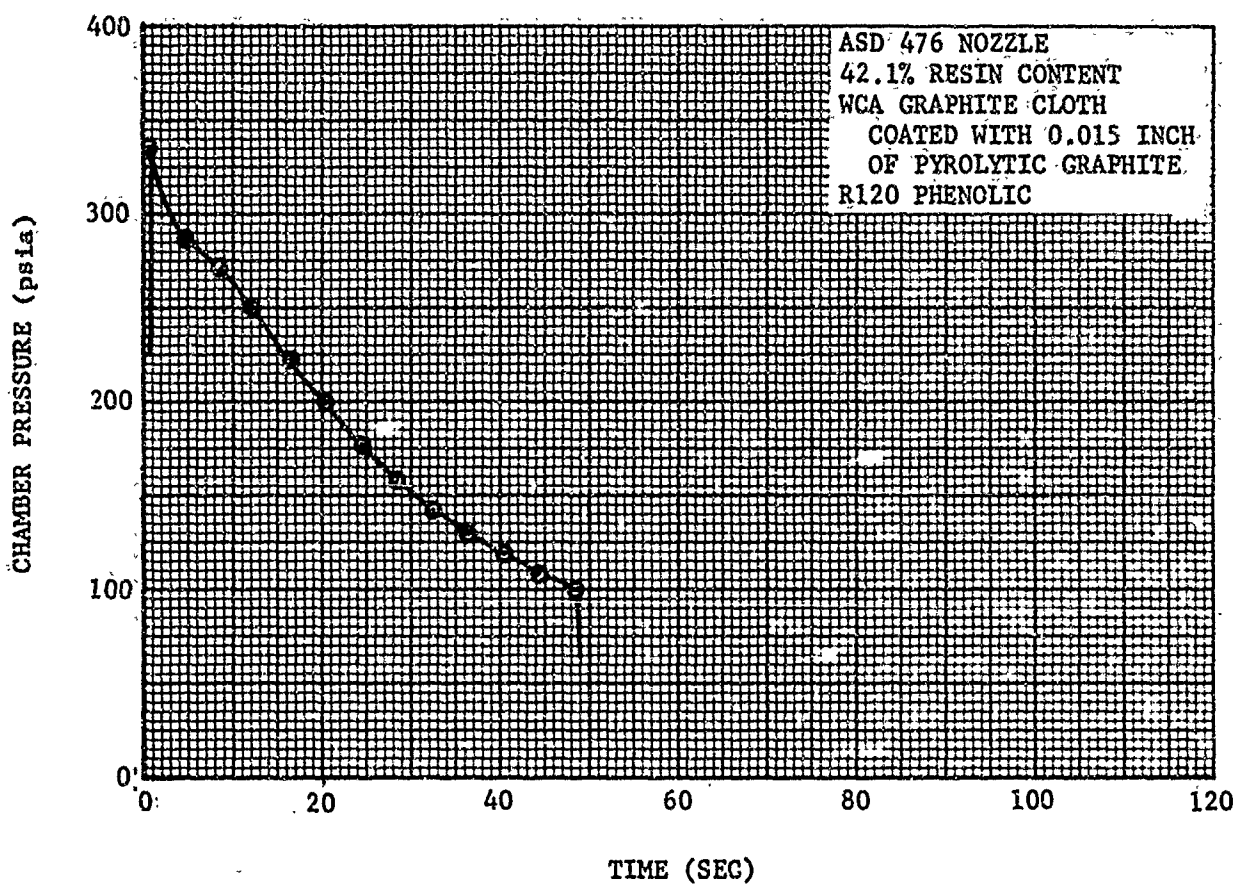
R14166 U

FIGURE 129. CHAMBER PRESSURE VERSUS TIME - ASD 473 NOZZLE



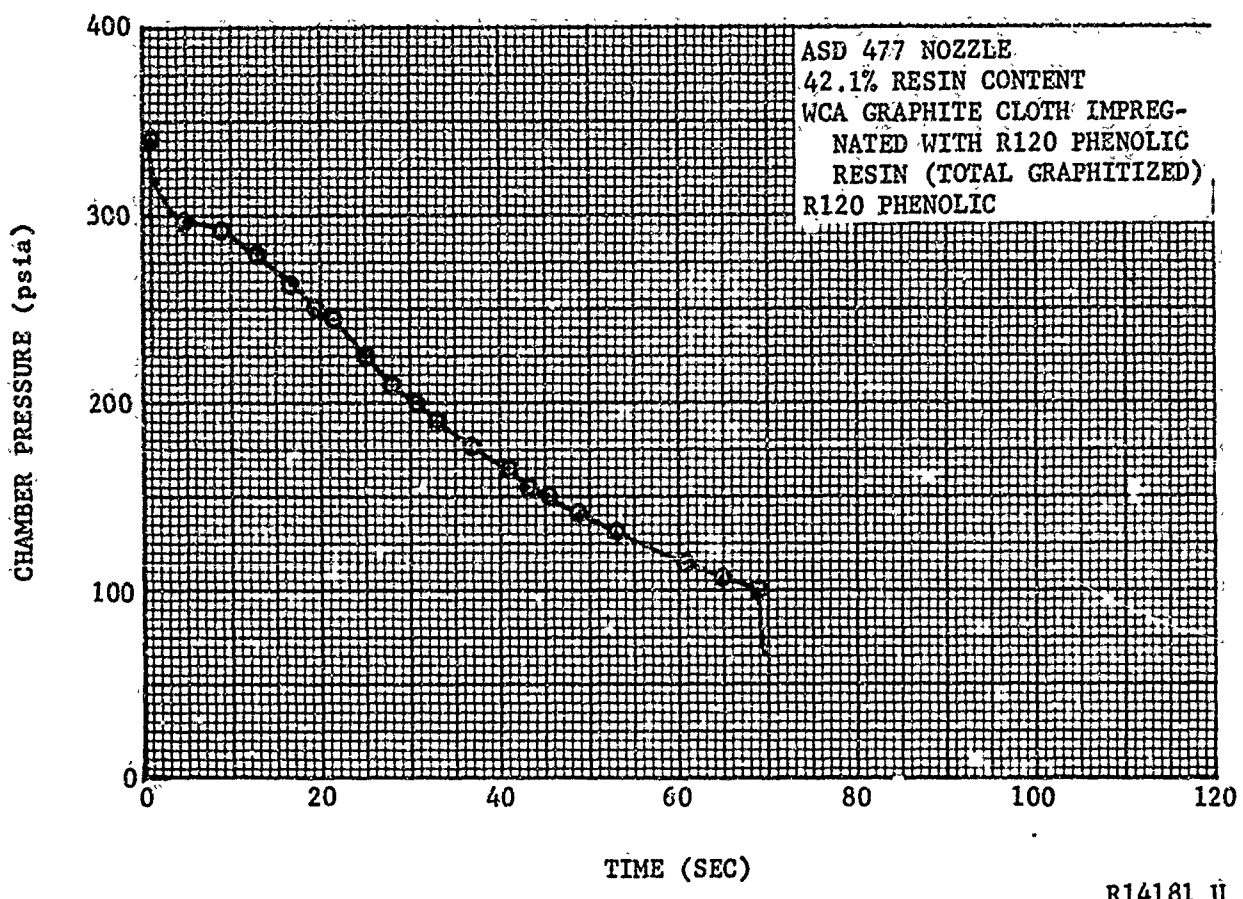
R14185 U

FIGURE 130. CHAMBER PRESSURE VERSUS TIME - ASD 475 NOZZLE



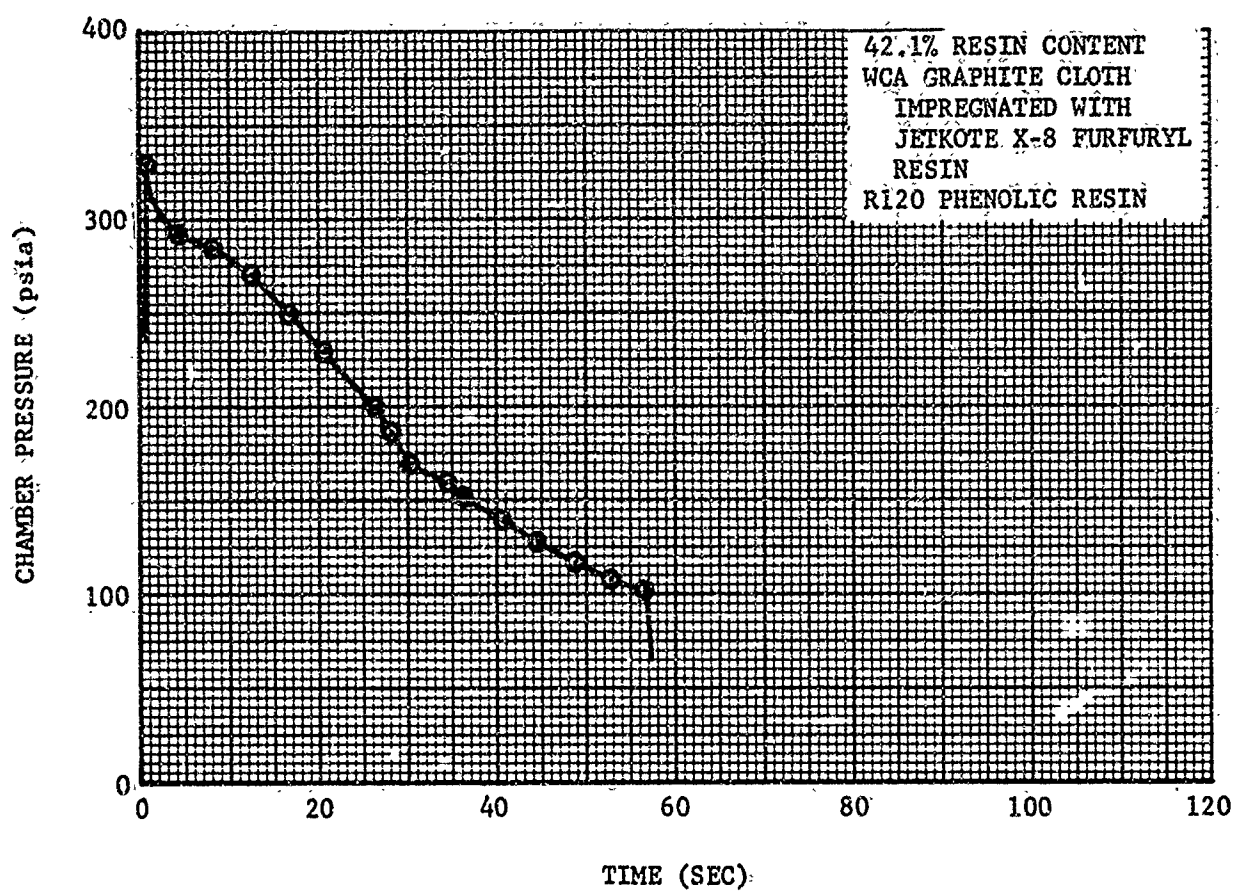
R14182 U

FIGURE 131. CHAMBER PRESSURE VERSUS TIME - ASD 476 NOZZLE



R14181 U

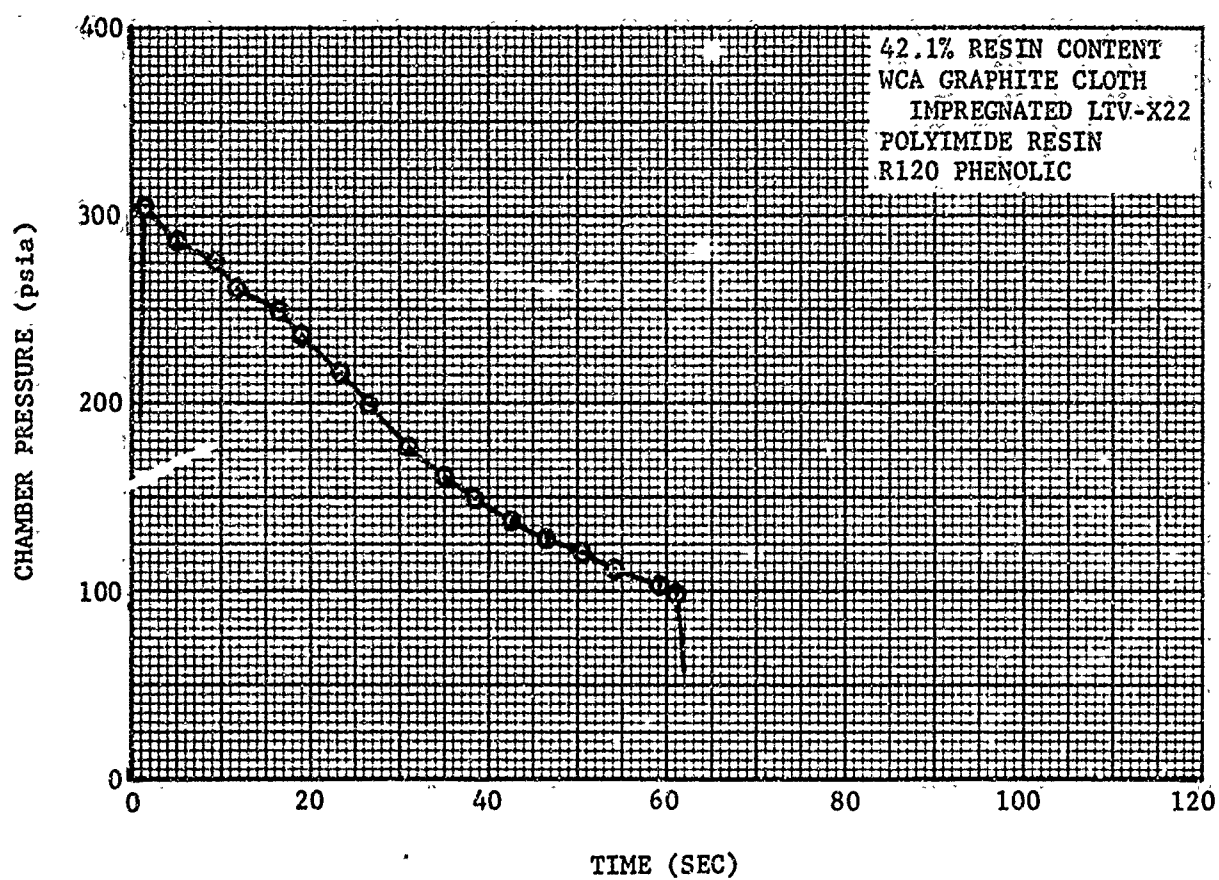
FIGURE 132. CHAMBER PRESSURE VERSUS TIME - ASD 477 NOZZLE



R14175 U

FIGURE 133. CHAMBER PRESSURE VERSUS TIME - ASD 478 NOZZLE





R14174 U

FIGURE 134. CHAMBER PRESSURE VERSUS TIME - ASD 479 NOZZLE



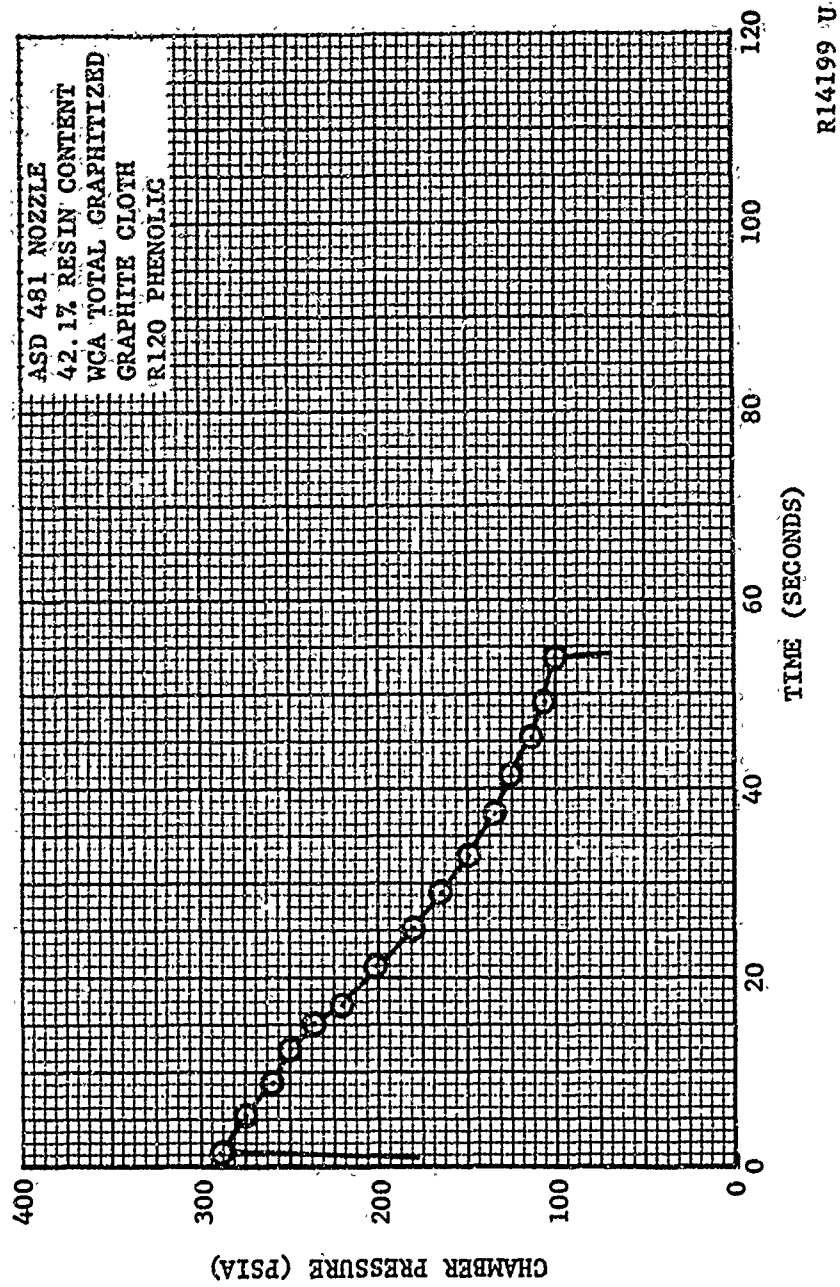


FIGURE 135. CHAMBER PRESSURE VERSUS TIME - ASD 481 NOZZLE

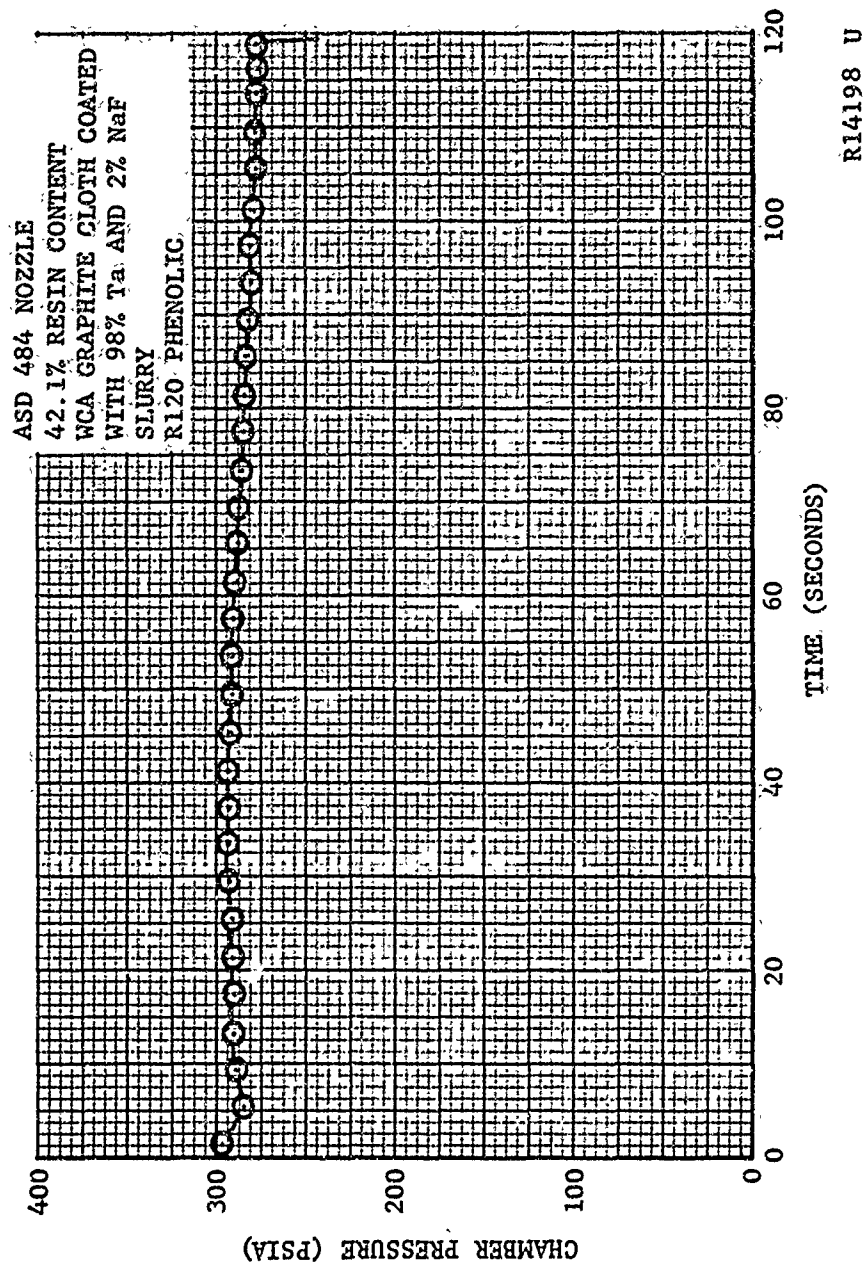
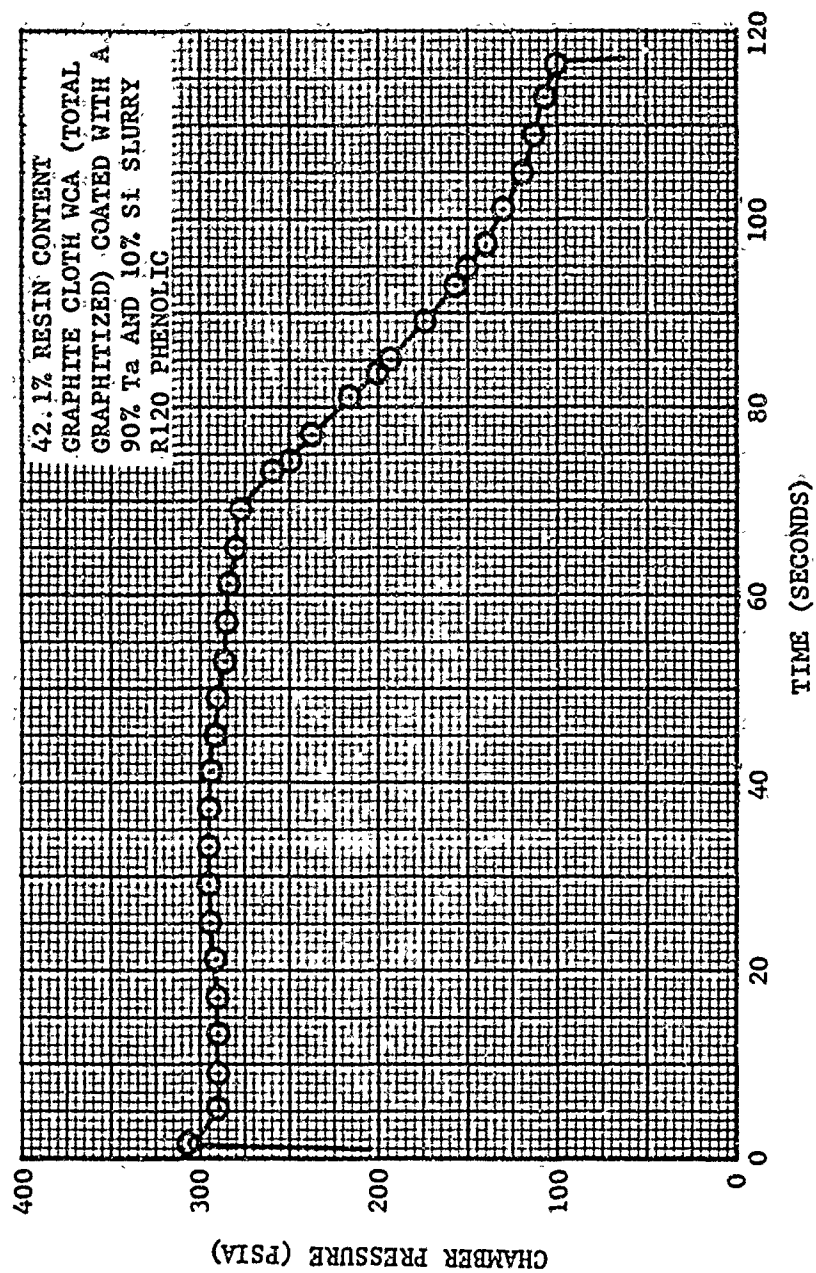
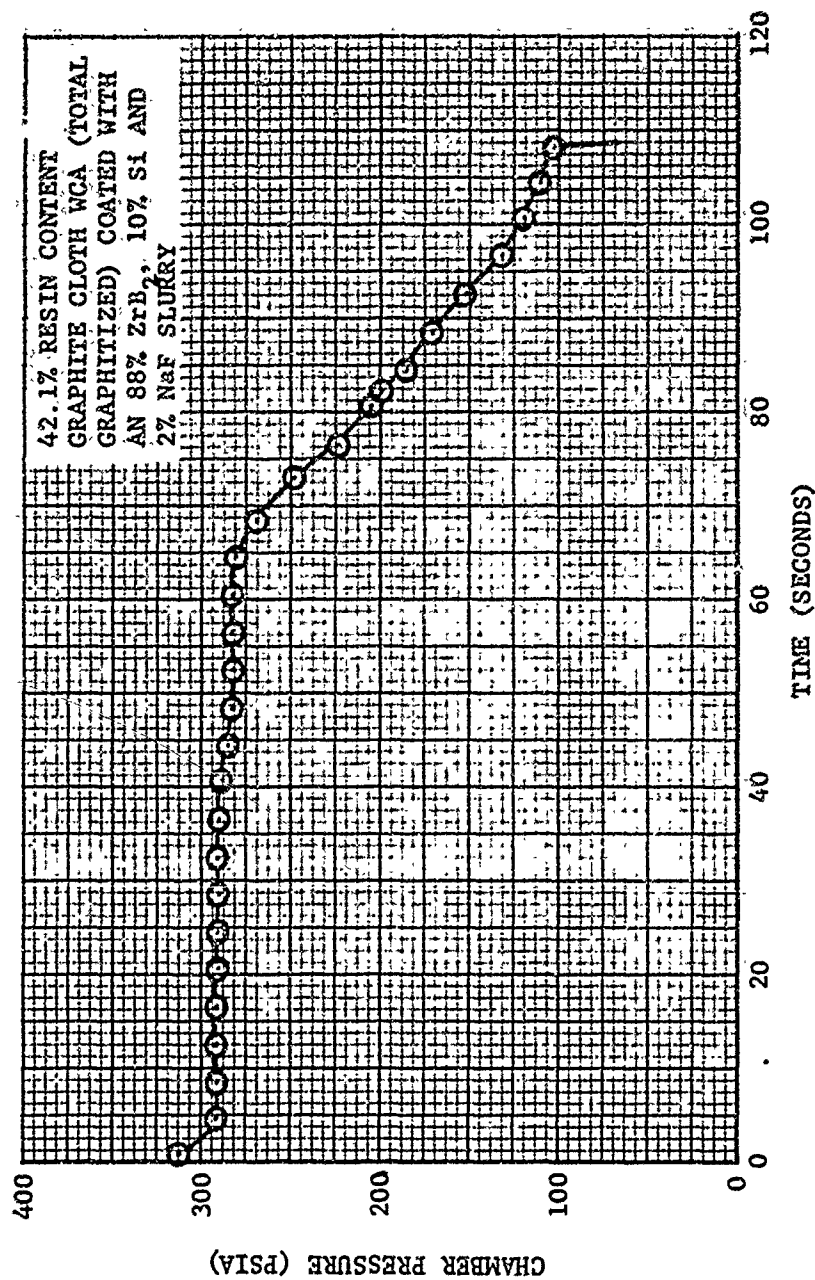


FIGURE 136. CHAMBER PRESSURE VERSUS TIME - ASD 484 NOZZLE



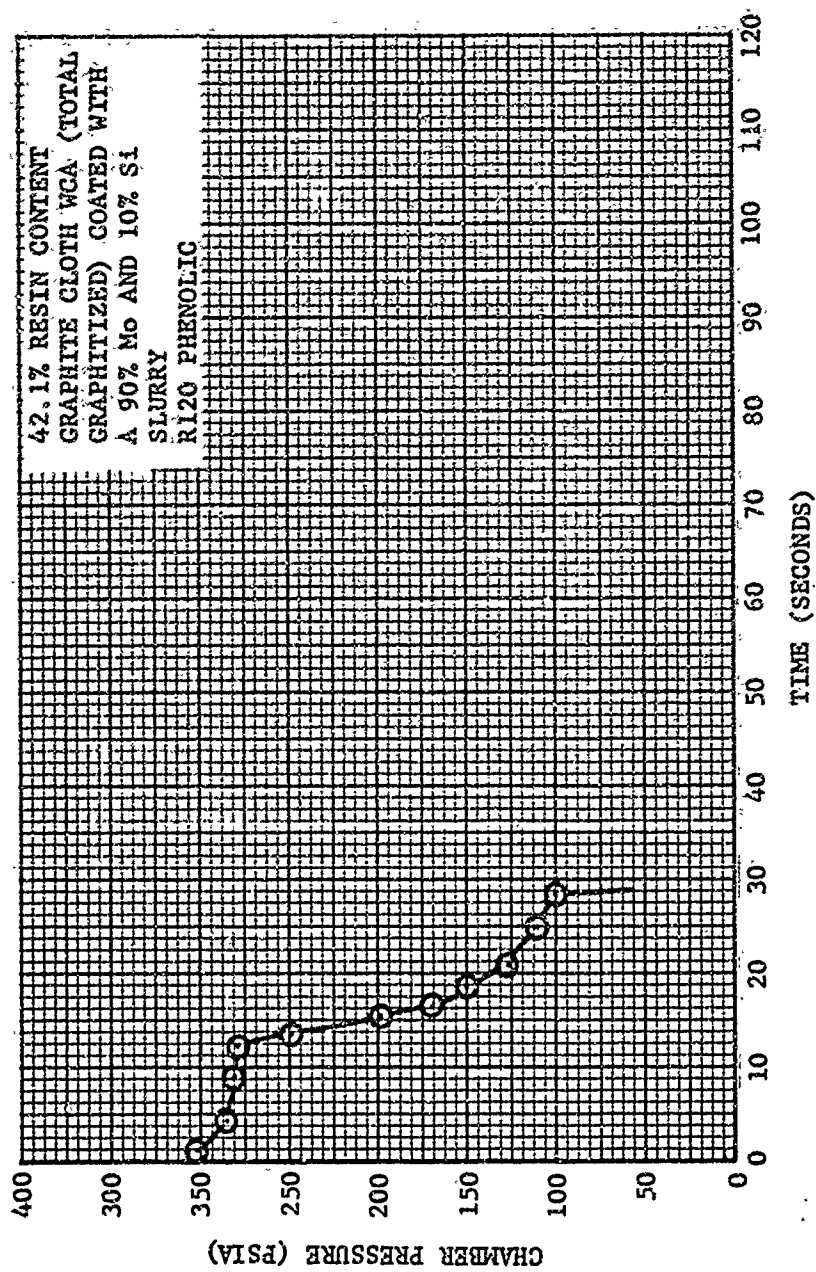
R14202 U

FIGURE 137. CHAMBER PRESSURE VERSUS TIME - ASD 485 NOZZLE



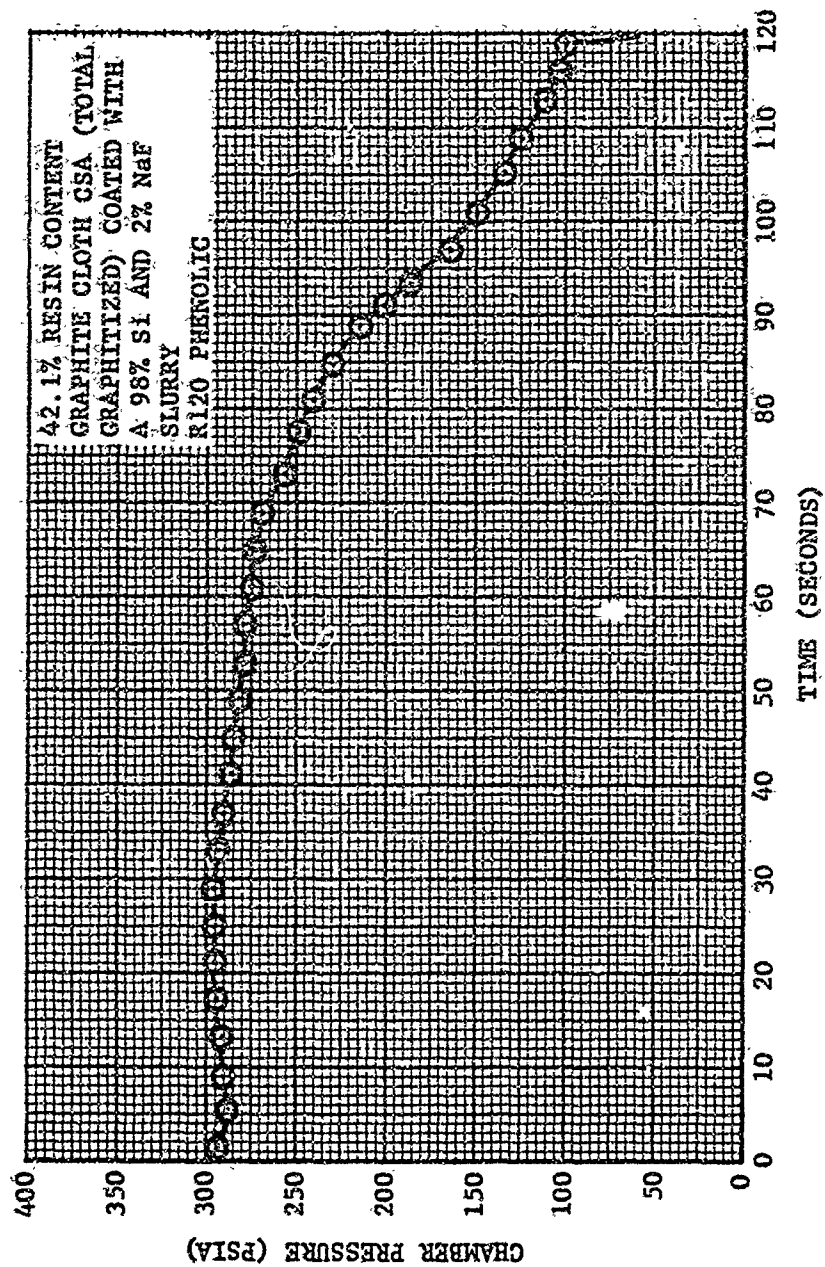
R14207 U

FIGURE 138. CHAMBER PRESSURE VERSUS TIME - ASD 486 NOZZLE



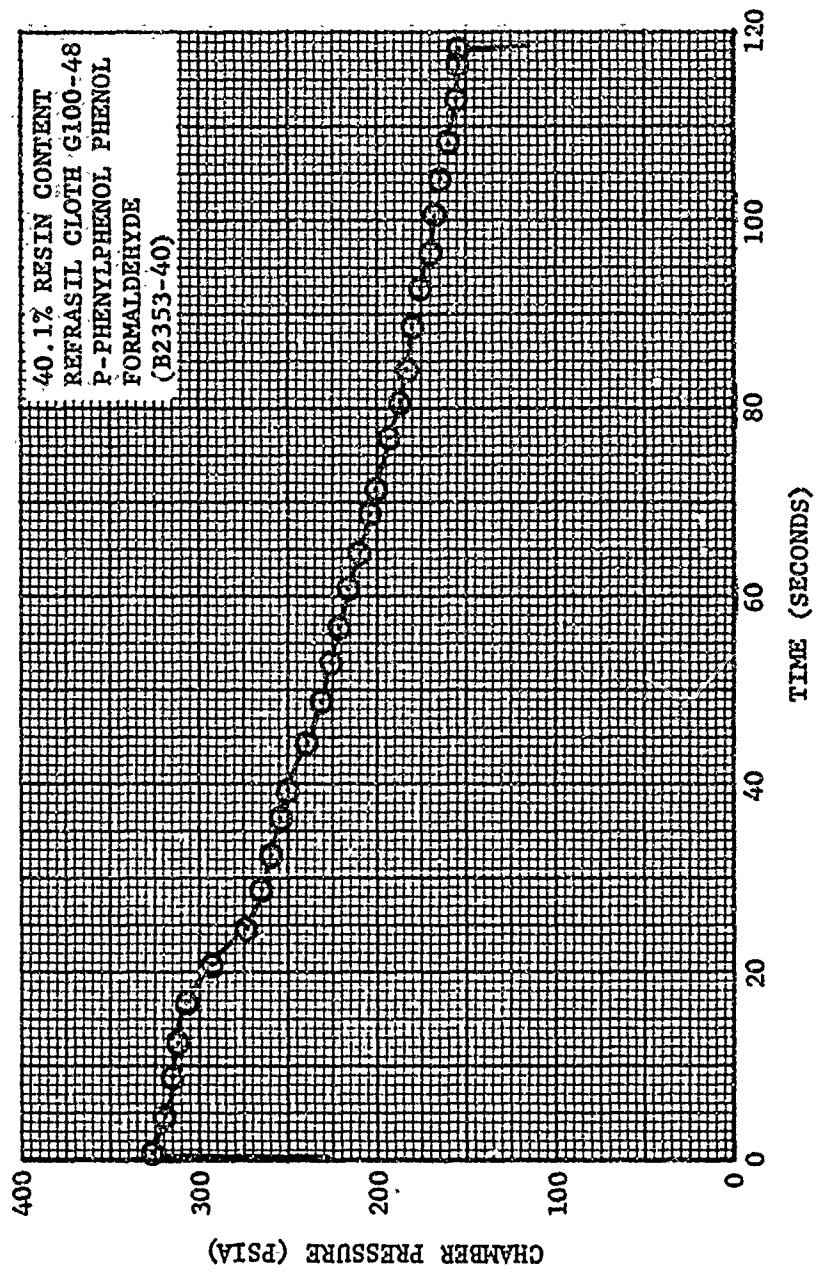
R14205 U

FIGURE 139. CHAMBER PRESSURE VERSUS TIME - ASD 487 NOZZLE



R14204 U

FIGURE 140. CHAMBER PRESSURE VERSUS TIME - ASD 488 NOZZLE



R14203 U

FIGURE 141. CHAMBER PRESSURE VERSUS TIME - ASD 492 NOZZLE



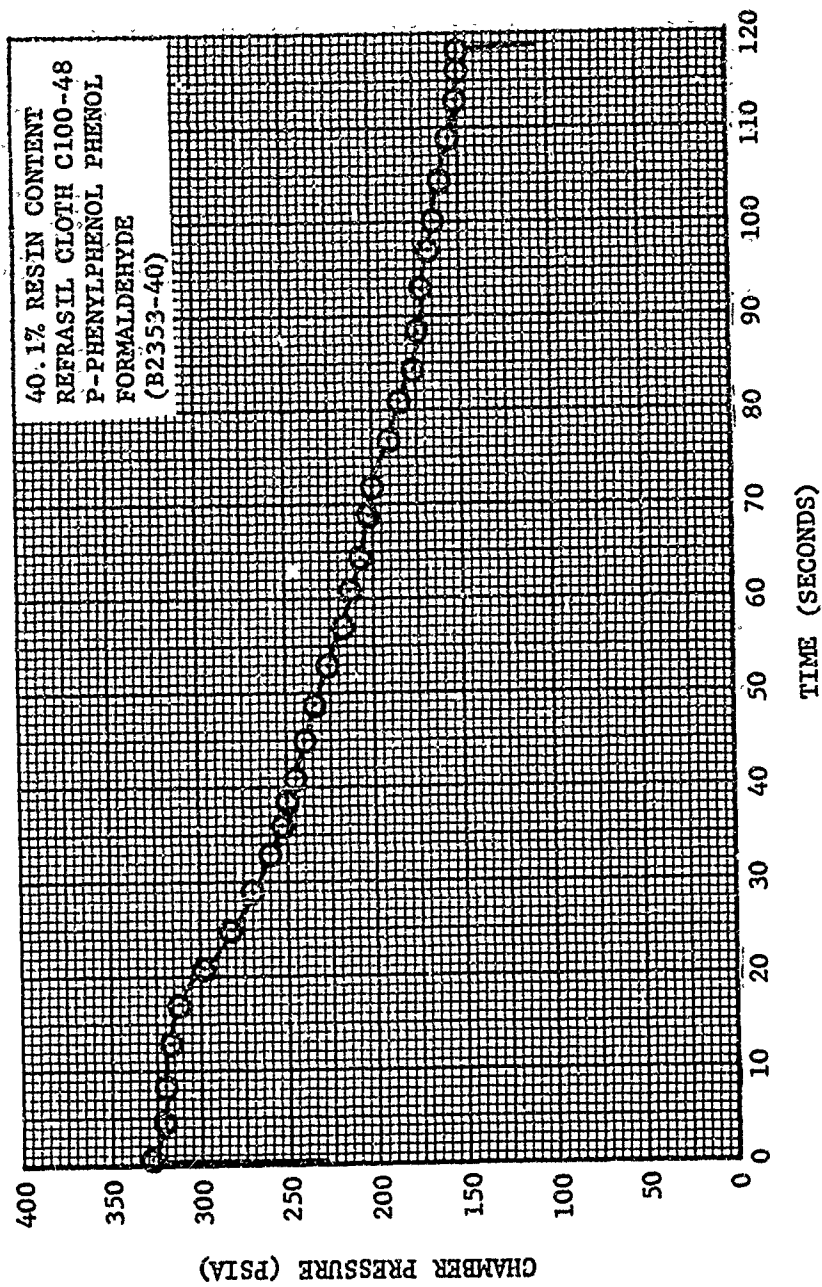
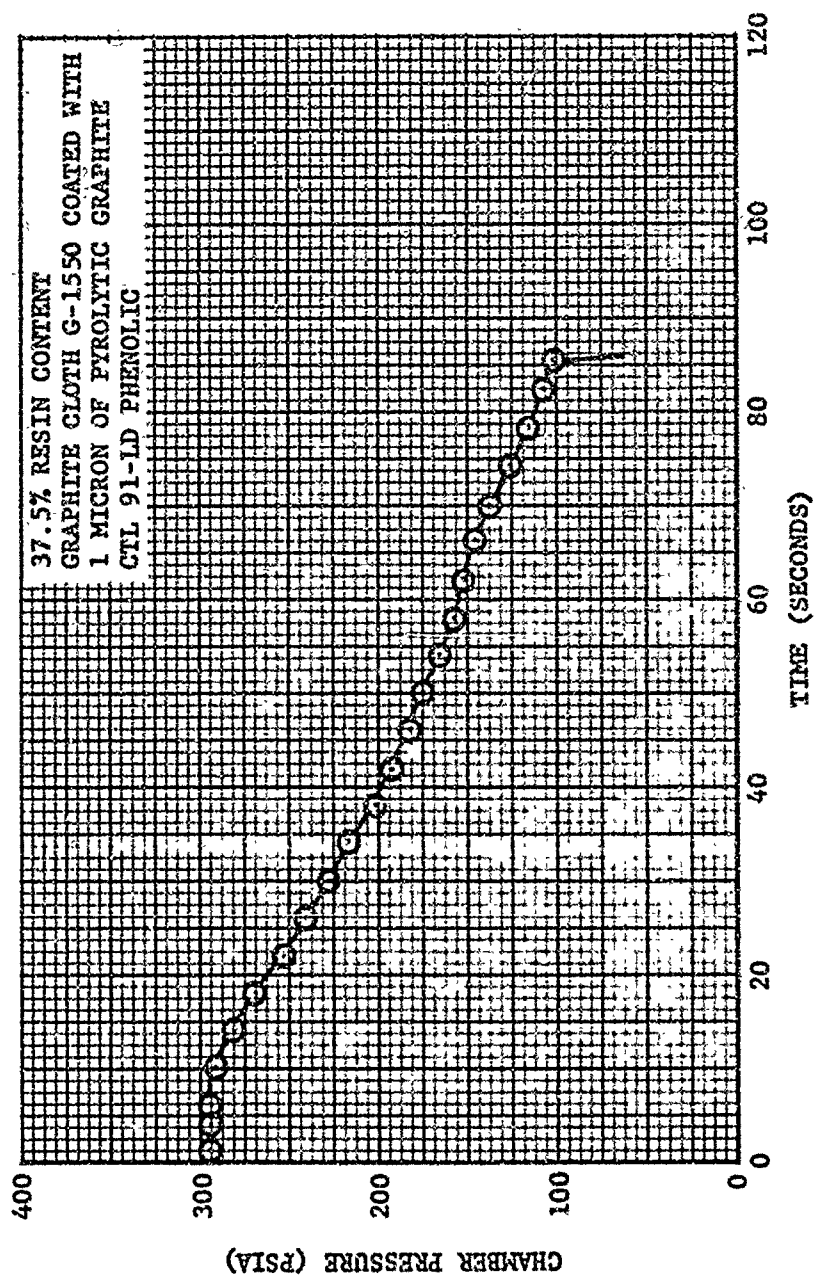


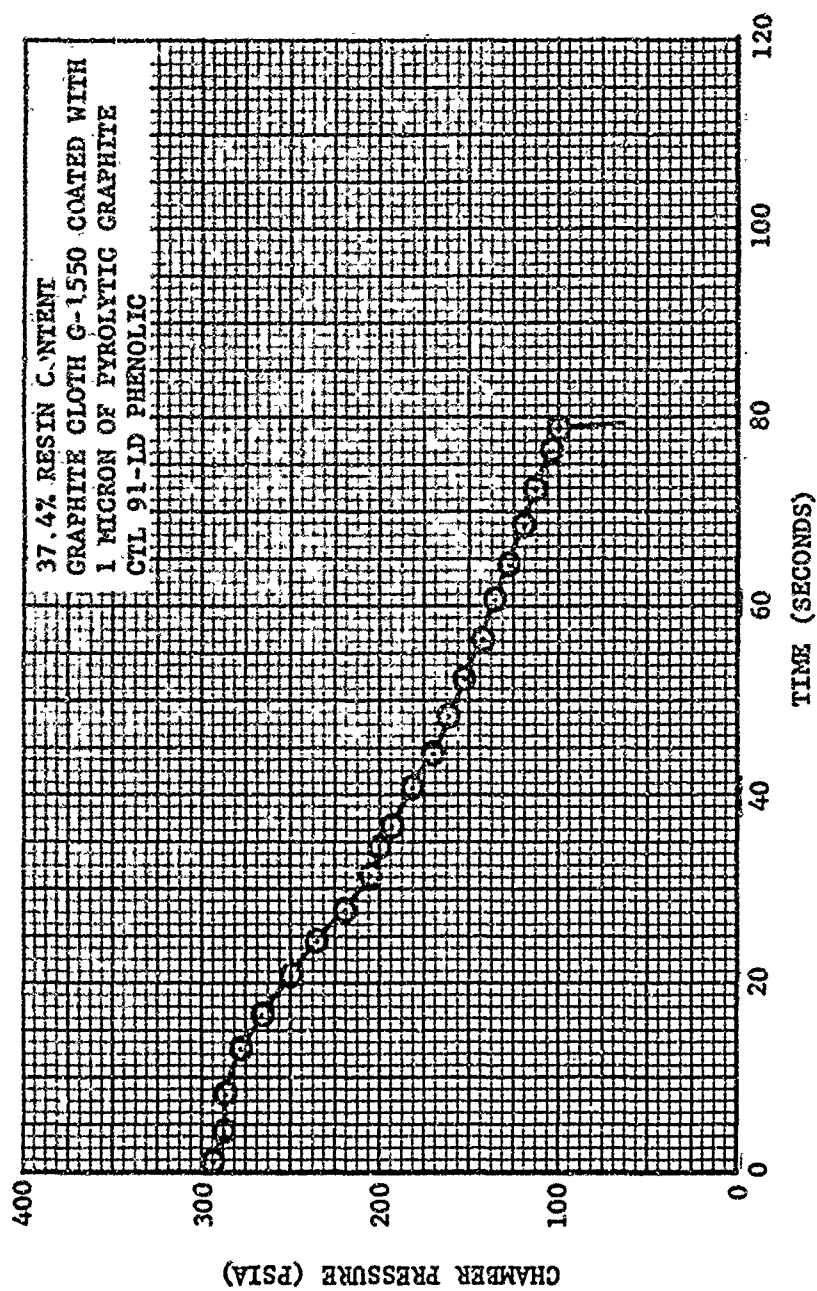
FIGURE 142. CHAMBER PRESSURE VERSUS TIME - ASD 493 NOZZLE





R14201 U

FIGURE 143. CHAMBER PRESSURE VERSUS TIME - ASD 494 NOZZLE



R14200 U

FIGURE 144. CHAMBER PRESSURE VERSUS TIME - ASD 495 NOZZLE

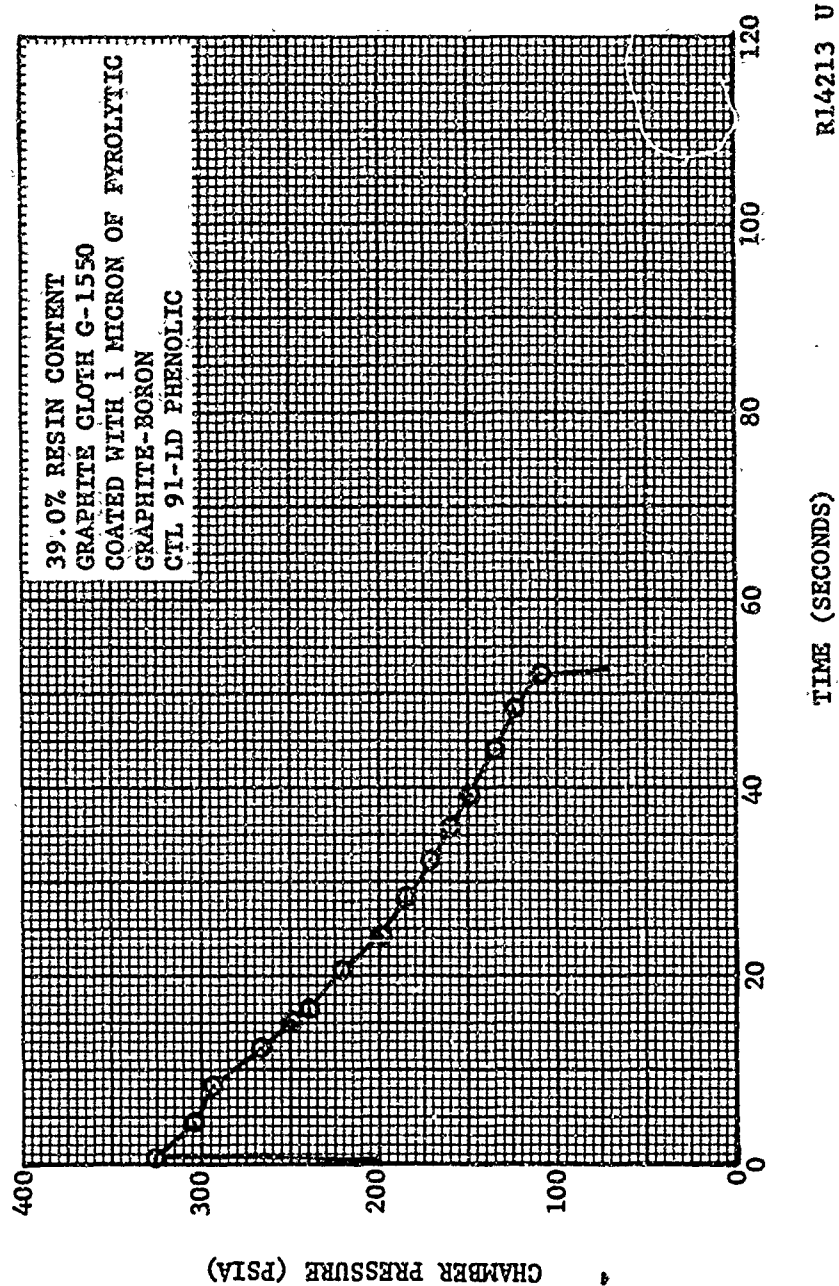


FIGURE 145. CHAMBER PRESSURE VERSUS TIME - ASD 496 NOZZLE

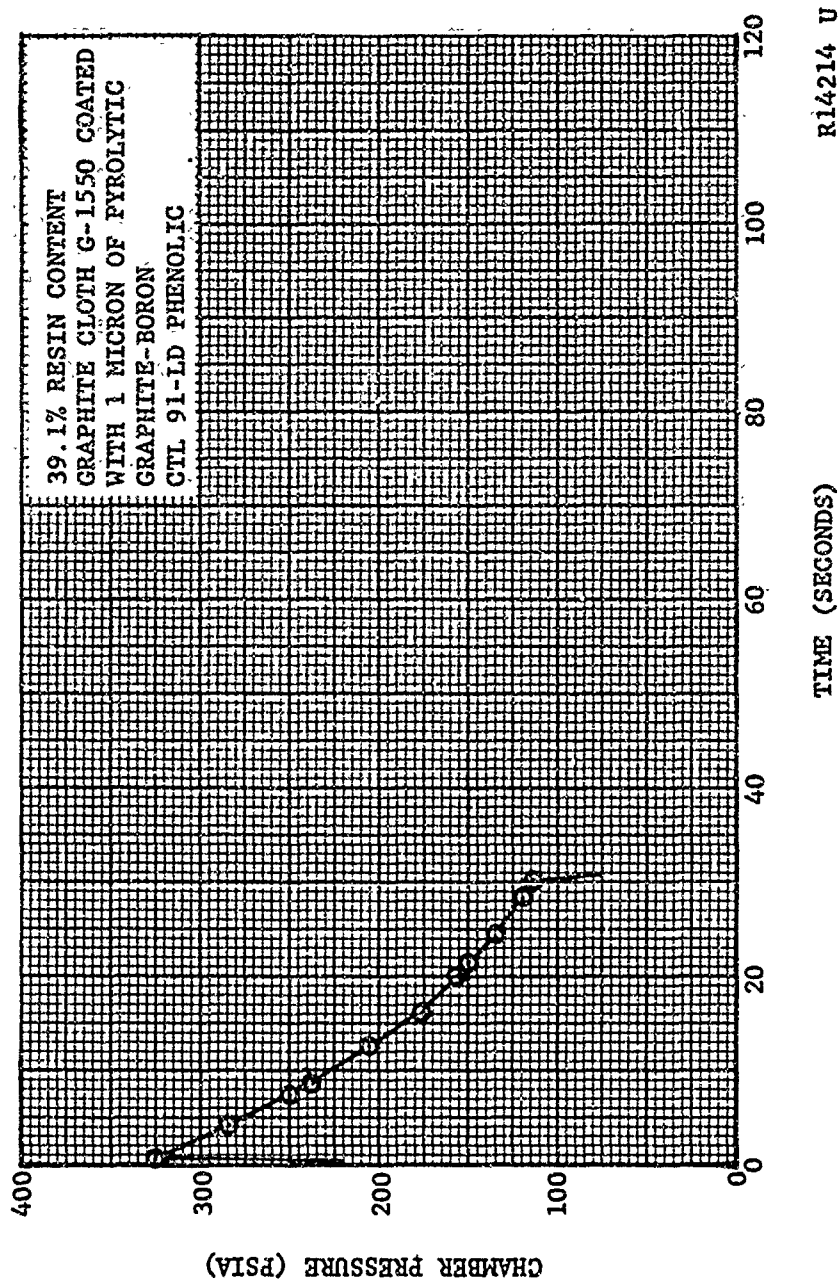
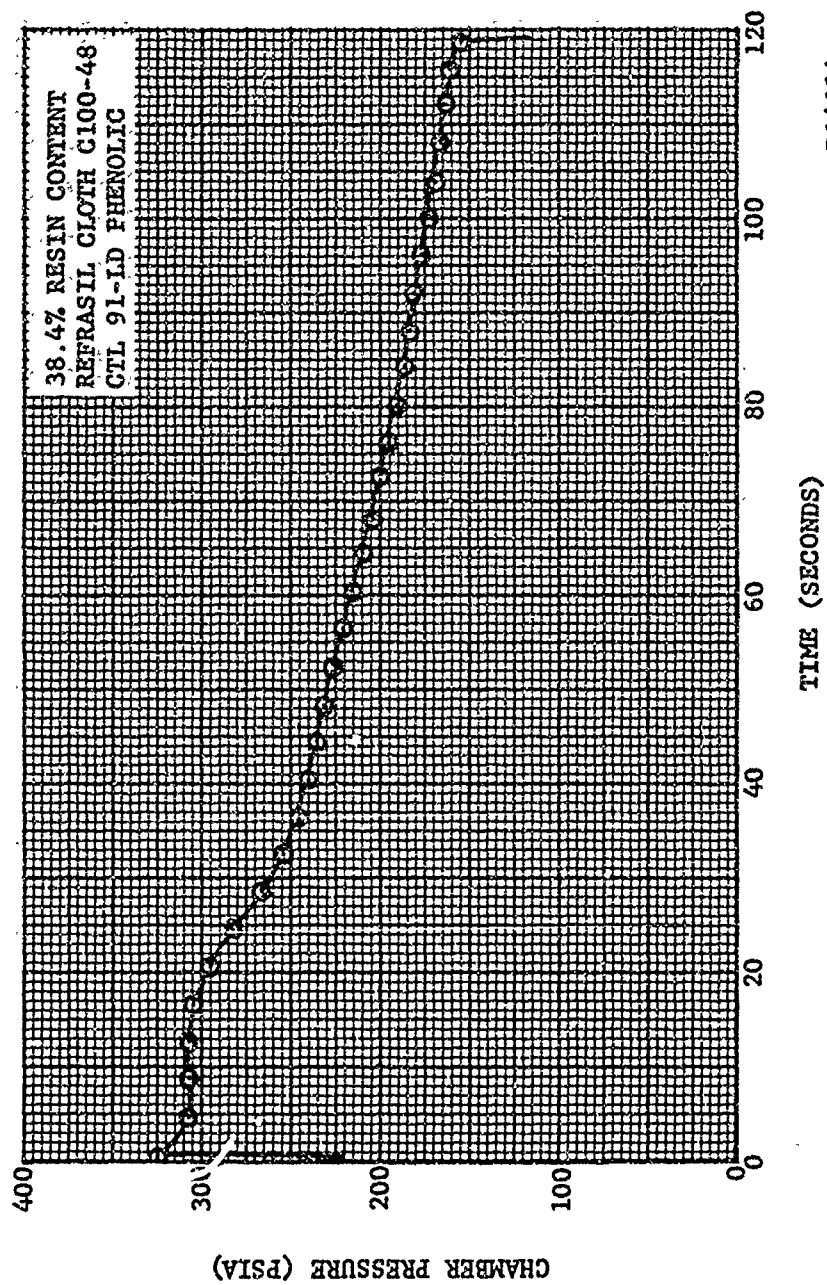


FIGURE 146. CHAMBER PRESSURE VERSUS TIME - ASD 497 NOZZLE



R14214 U

FIGURE 147. CHAMBER PRESSURE VERSUS TIME - ASD 498 NOZZLE

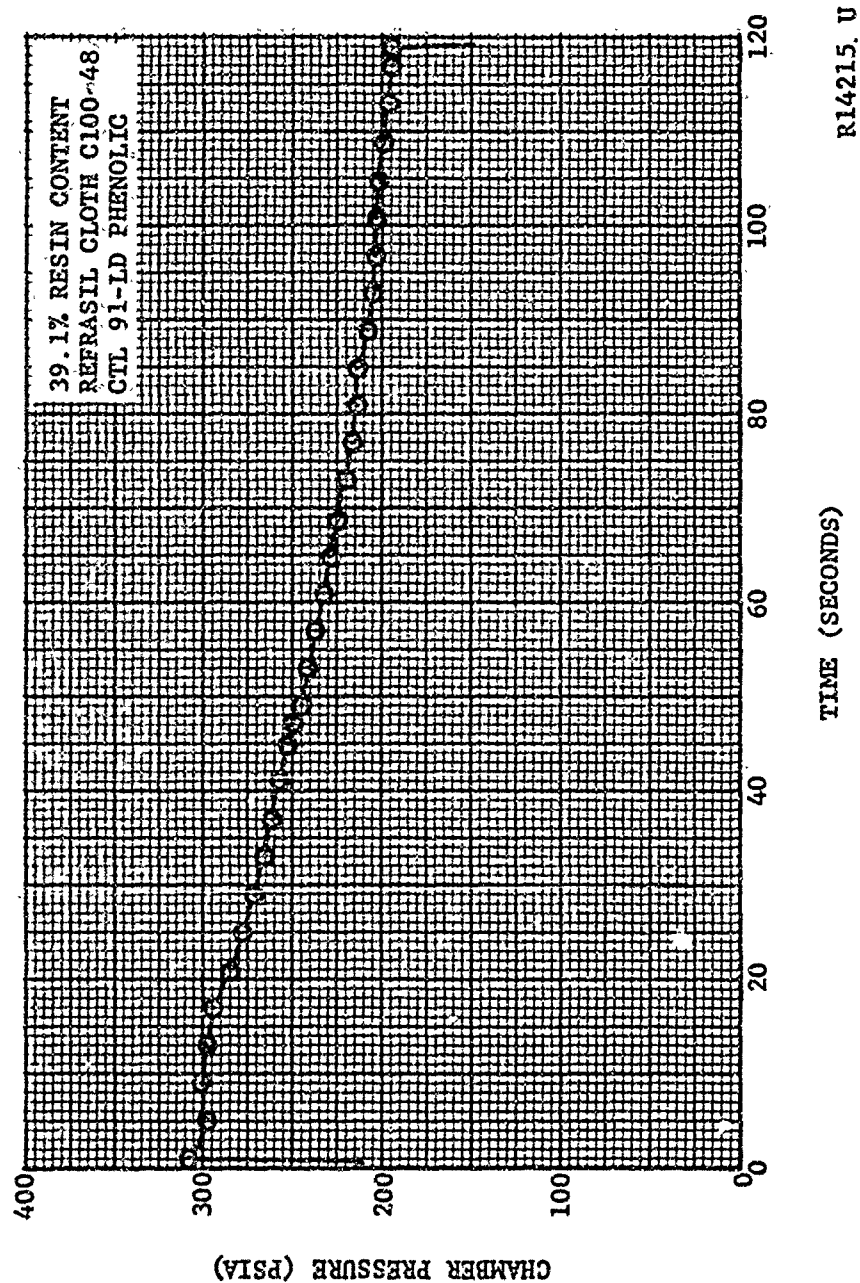


FIGURE 148. CHAMBER PRESSURE VERSUS TIME - ASD.499 NOZZLE

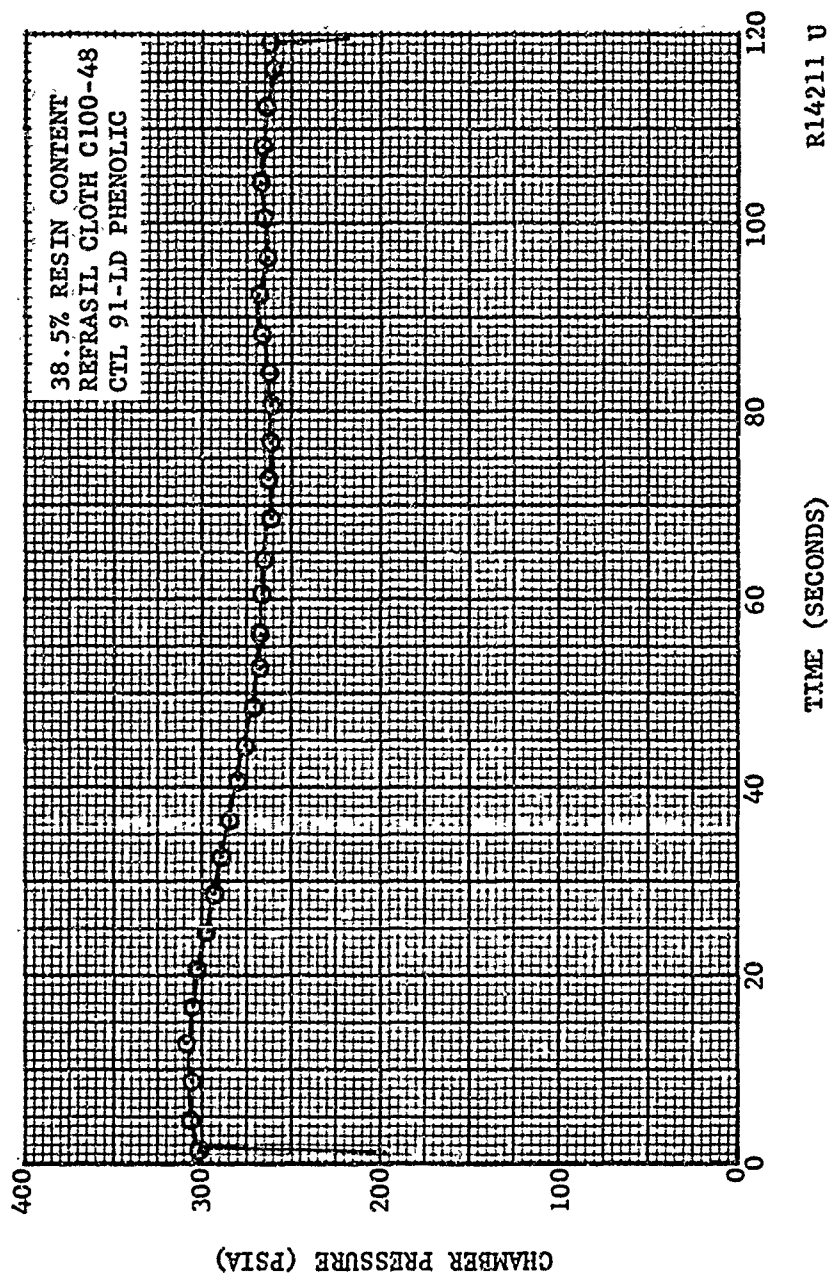


FIGURE 149. CHAMBER PRESSURE VERSUS TIME - ASD 500 NOZZLE



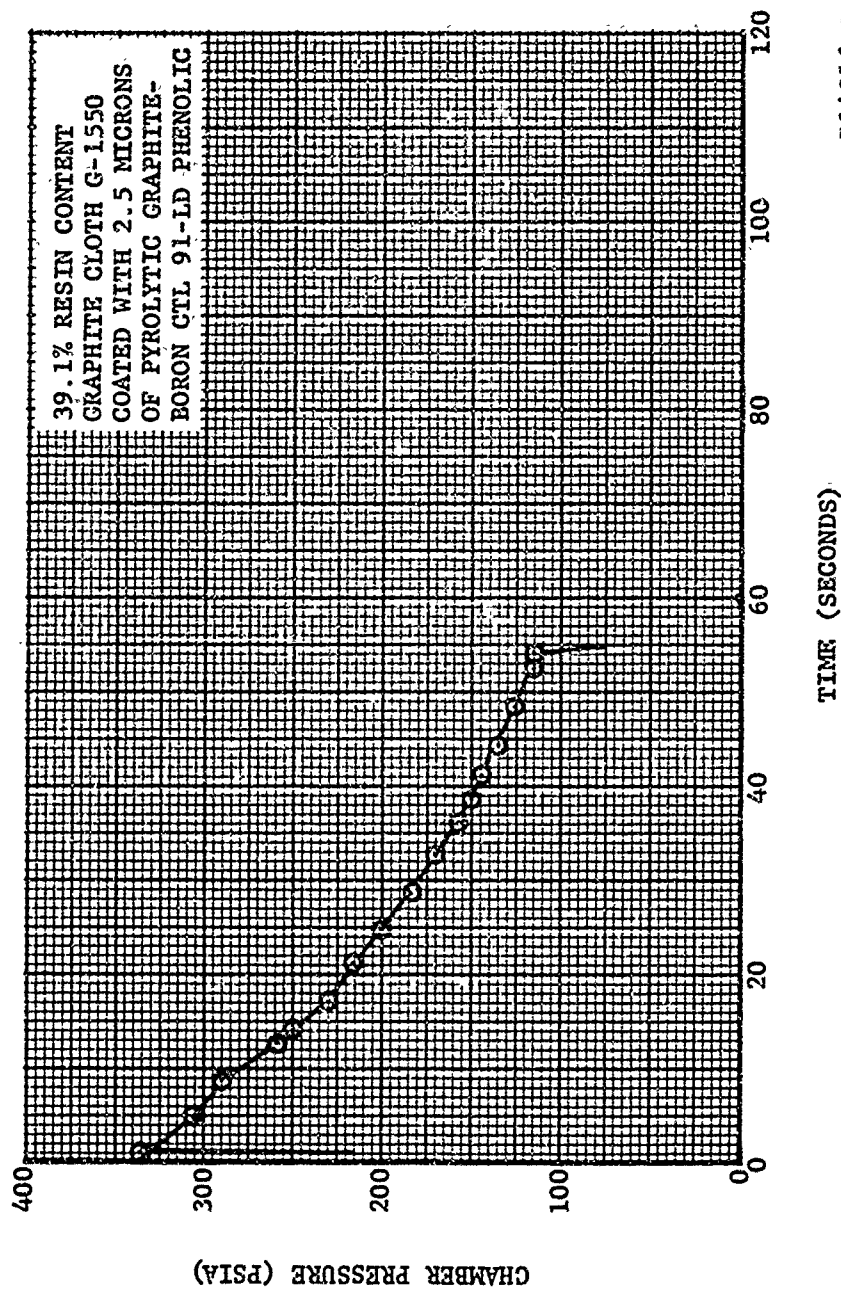


FIGURE 150. CHAMBER PRESSURE VERSUS TIME - ASD 501 NOZZLE



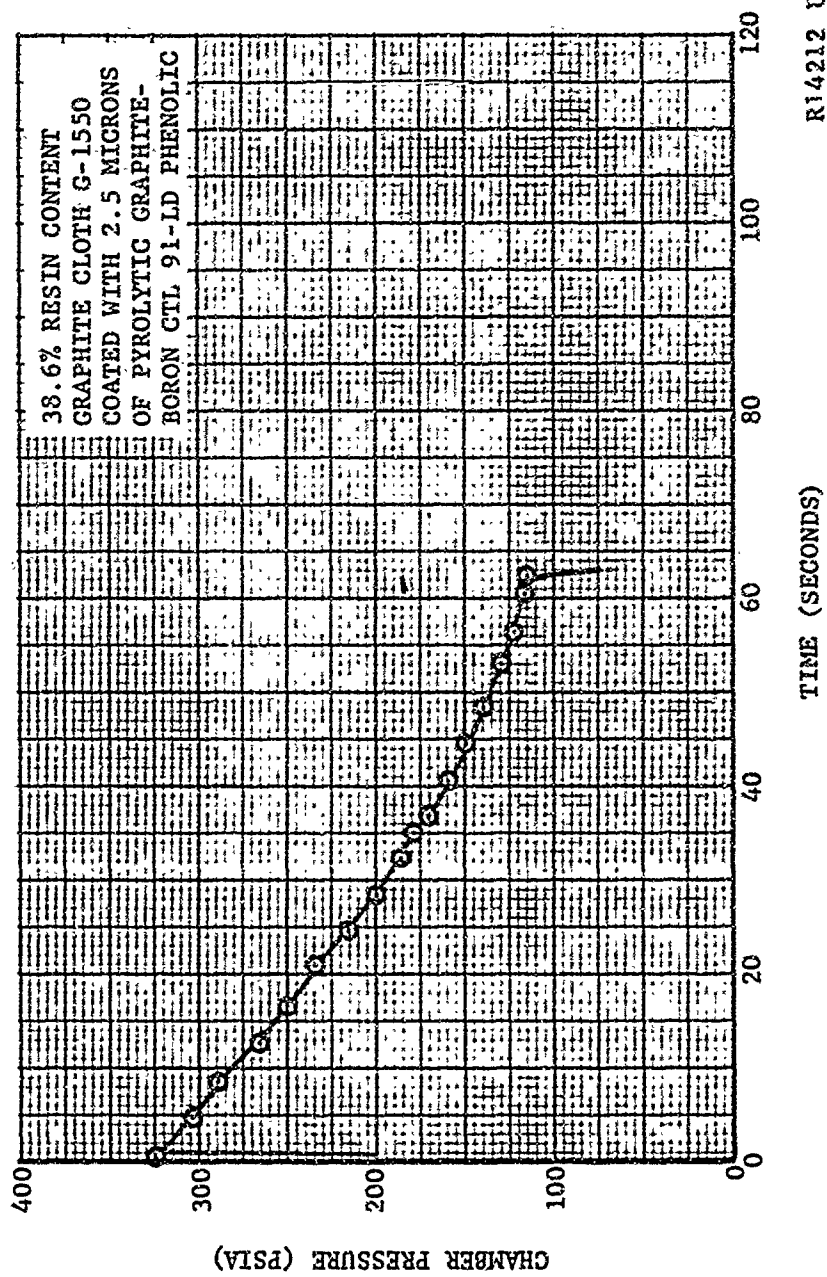
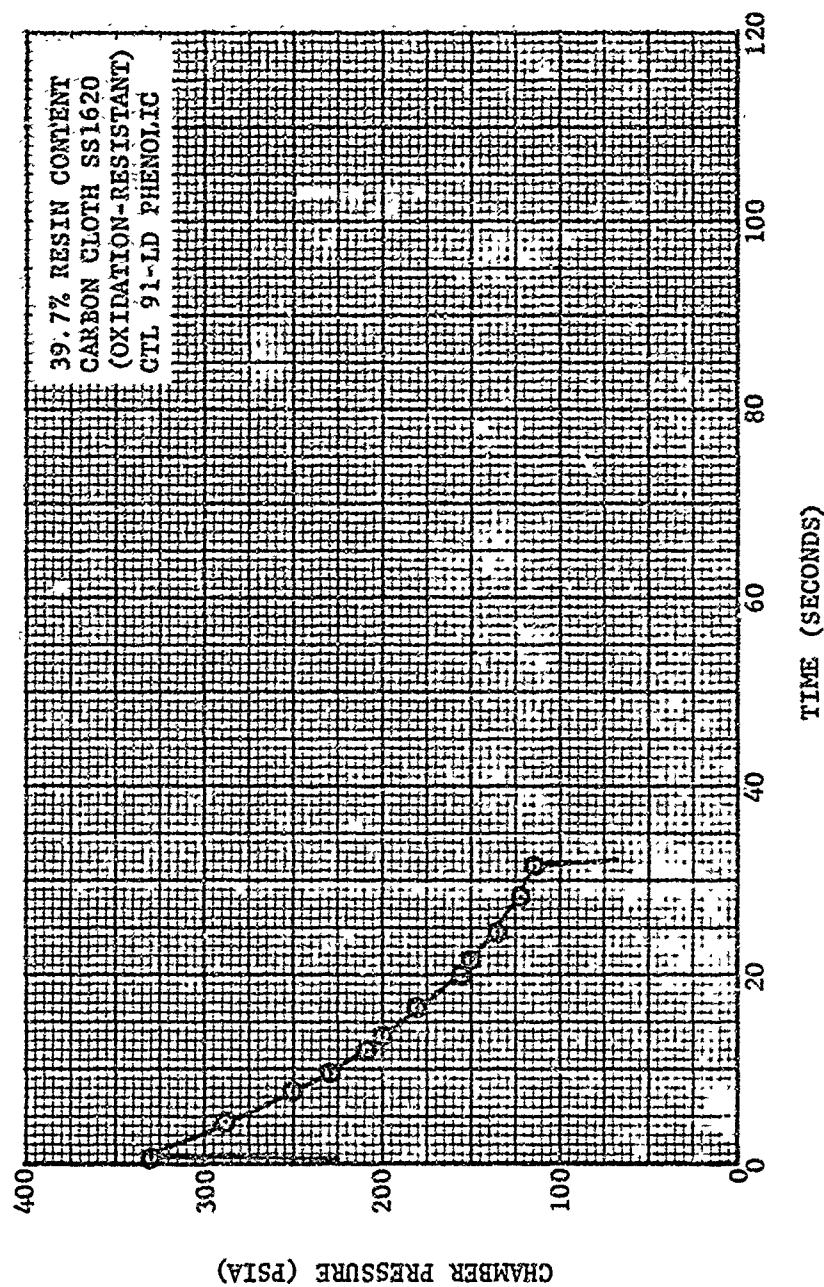
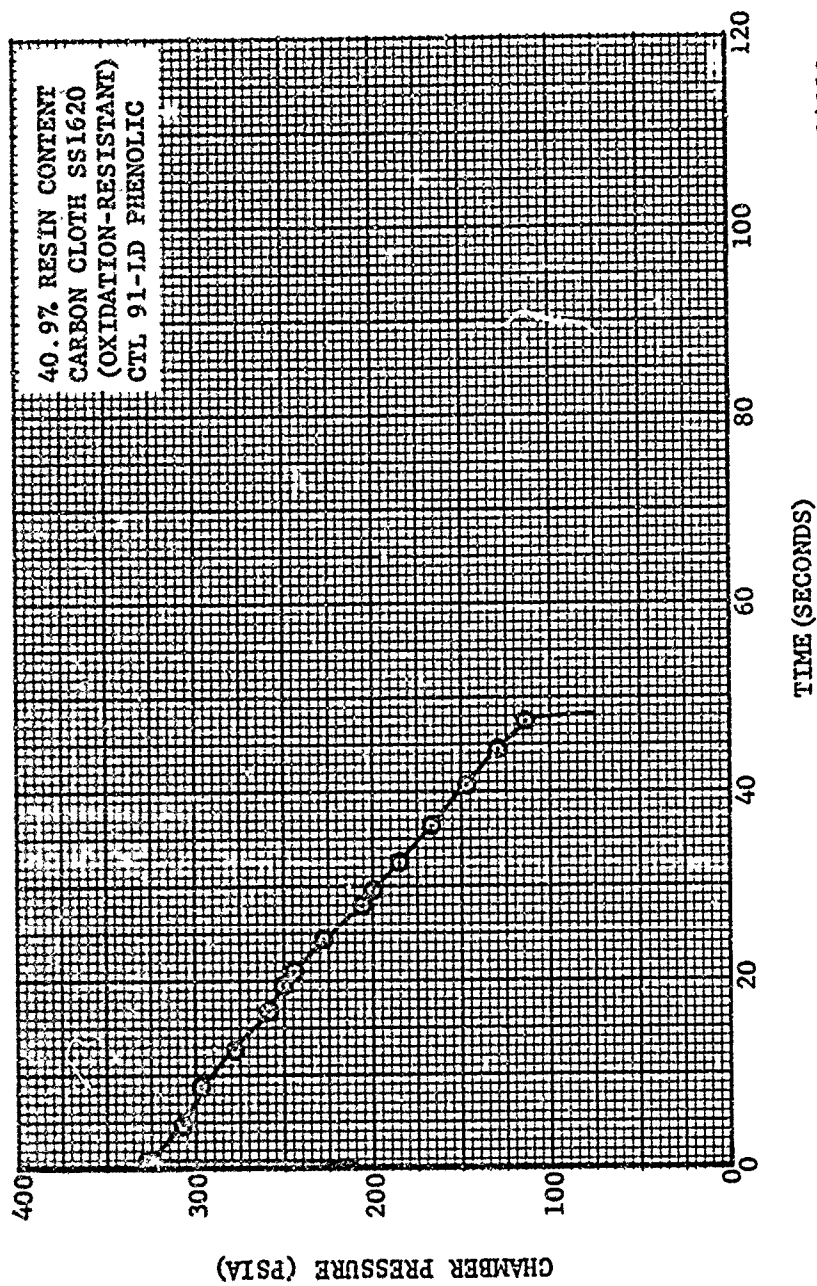


FIGURE 151. CHAMBER PRESSURE VERSUS TIME - ASD 502 NOZZLE



R14218

FIGURE 152. CHAMBER PRESSURE VERSUS TIME - ASD 503 NOZZLE



R14219 U

FIGURE 153. CHAMBER PRESSURE VERSUS TIME - ASD 504 NOZZLE

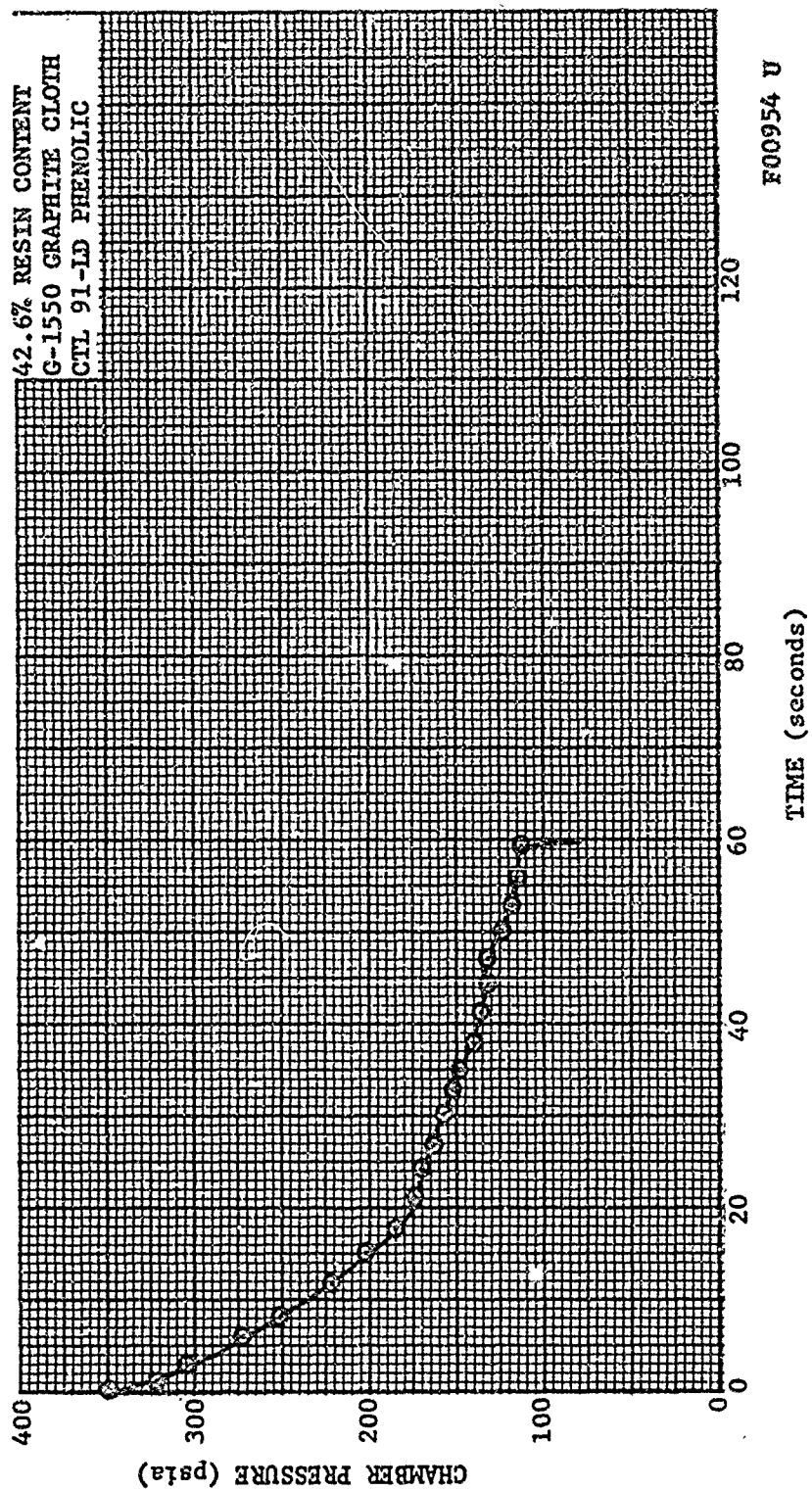


FIGURE 154. CHAMBER PRESSURE VERSUS TIME - ASD 505 NOZZLE

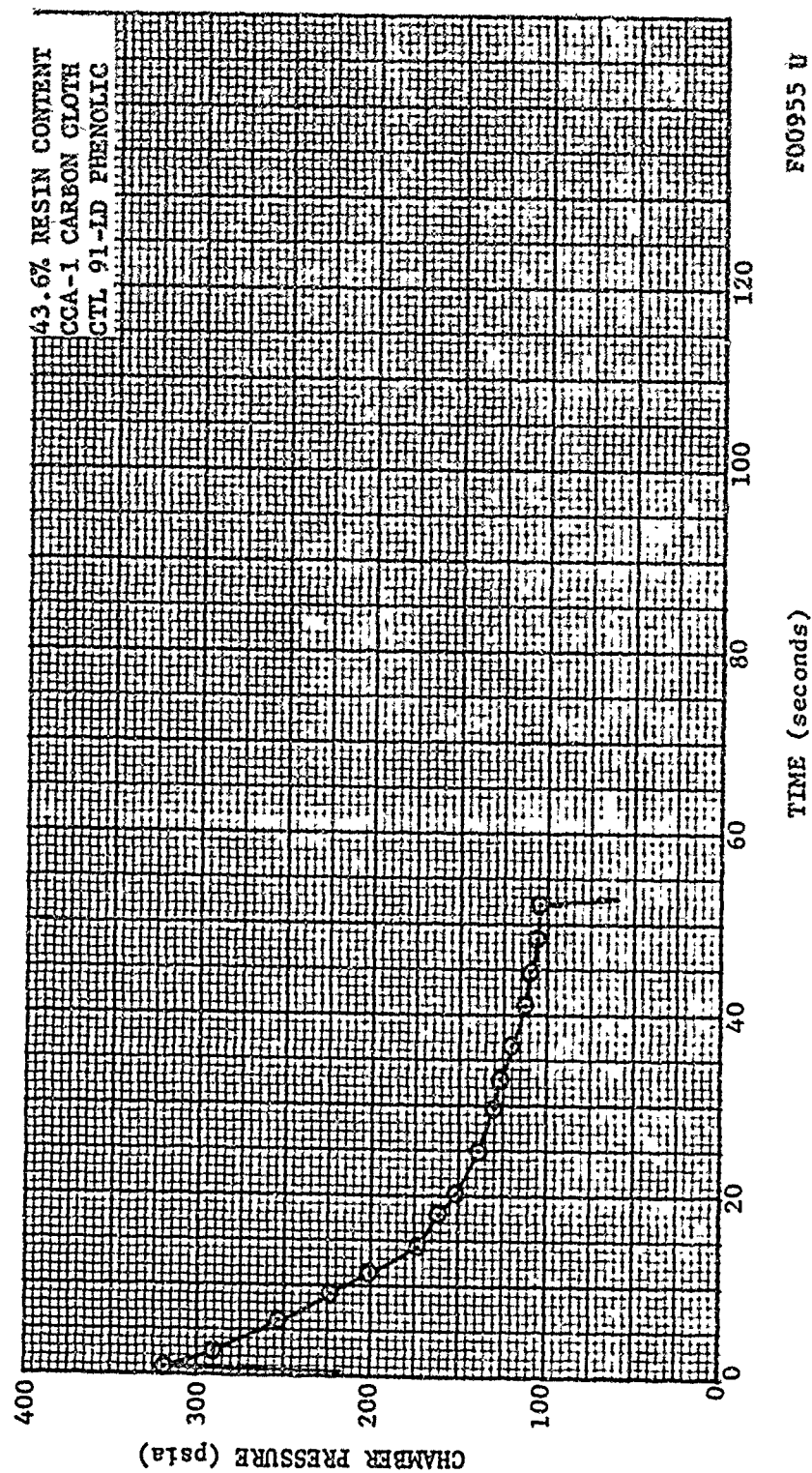


FIGURE 155. CHAMBER PRESSURE VERSUS TIME - ASD 507 NOZZLE

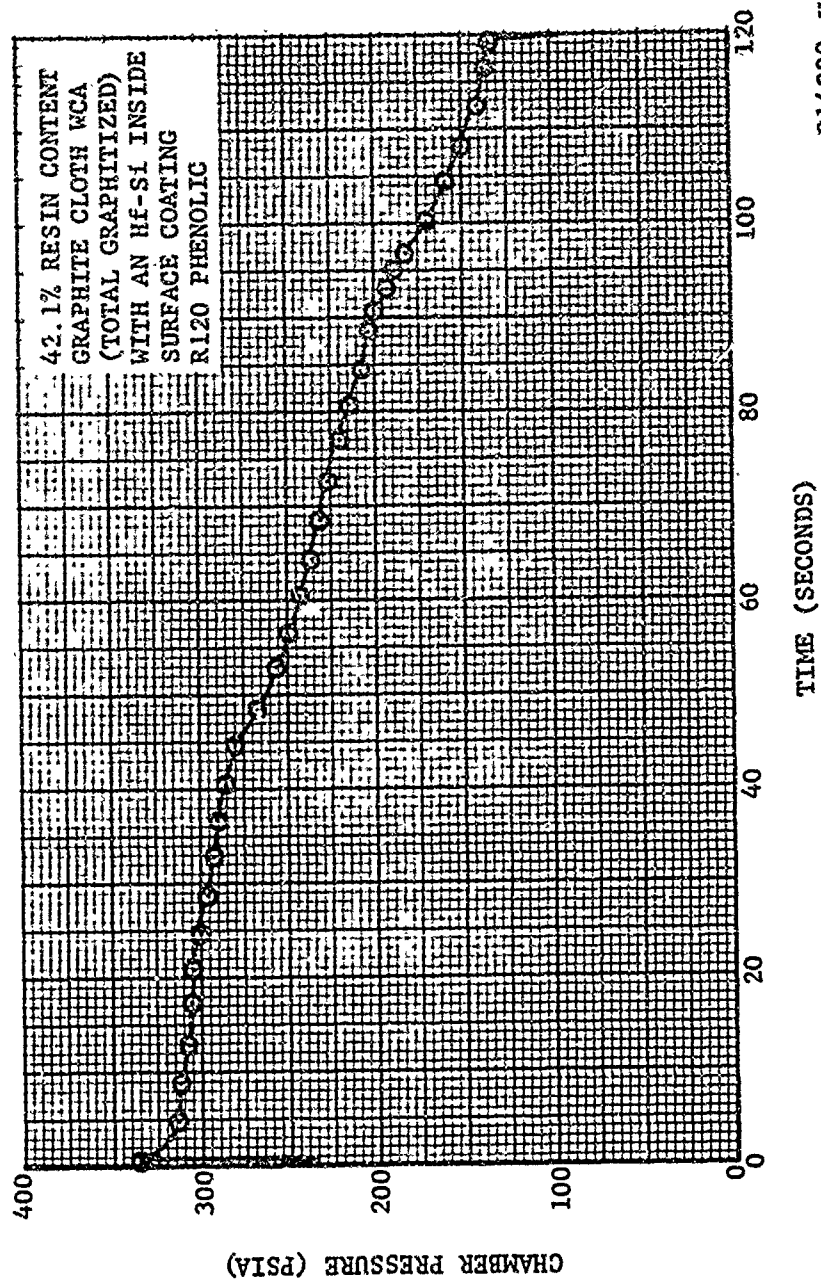


FIGURE 156. CHAMBER PRESSURE VERSUS TIME - ASD 509 NOZZLE



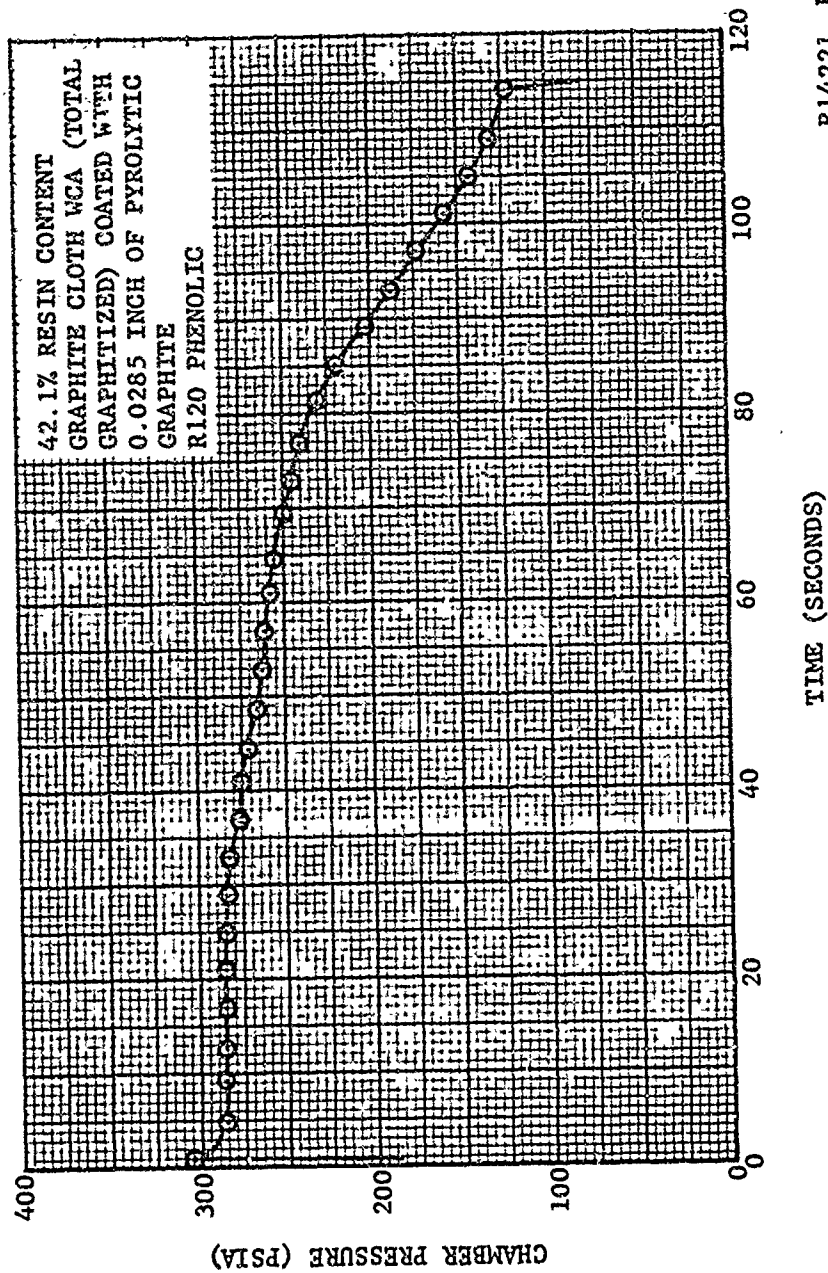


FIGURE 157. CHAMBER PRESSURE VERSUS TIME - ASD 514 NOZZLE

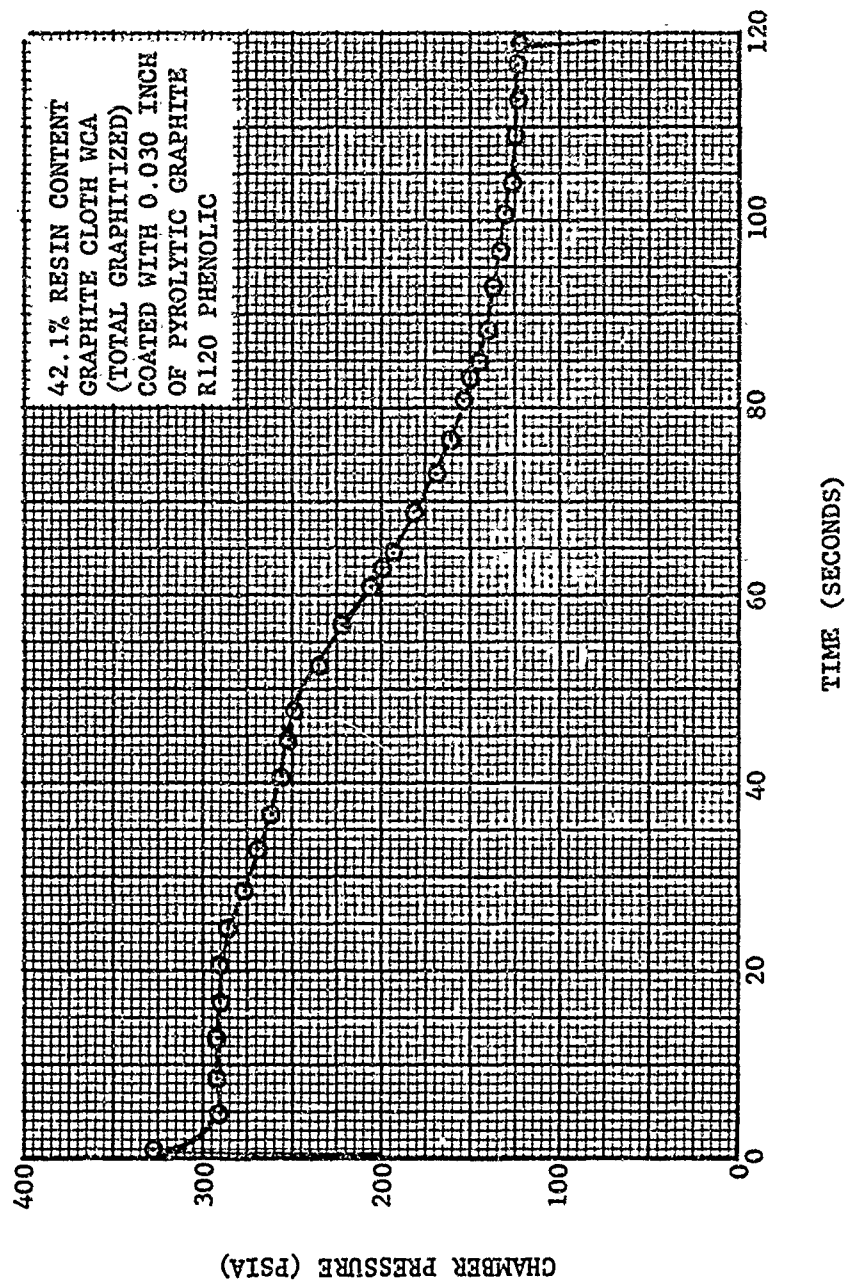
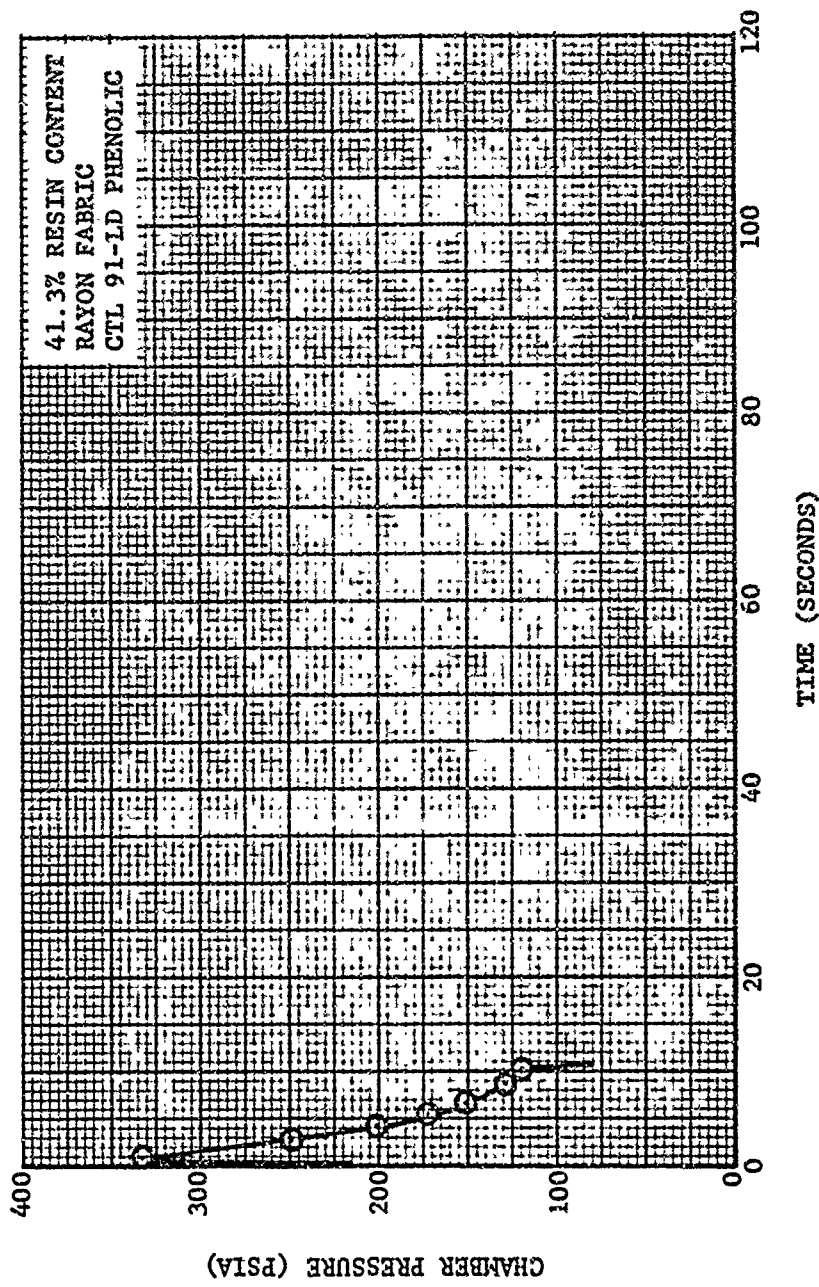


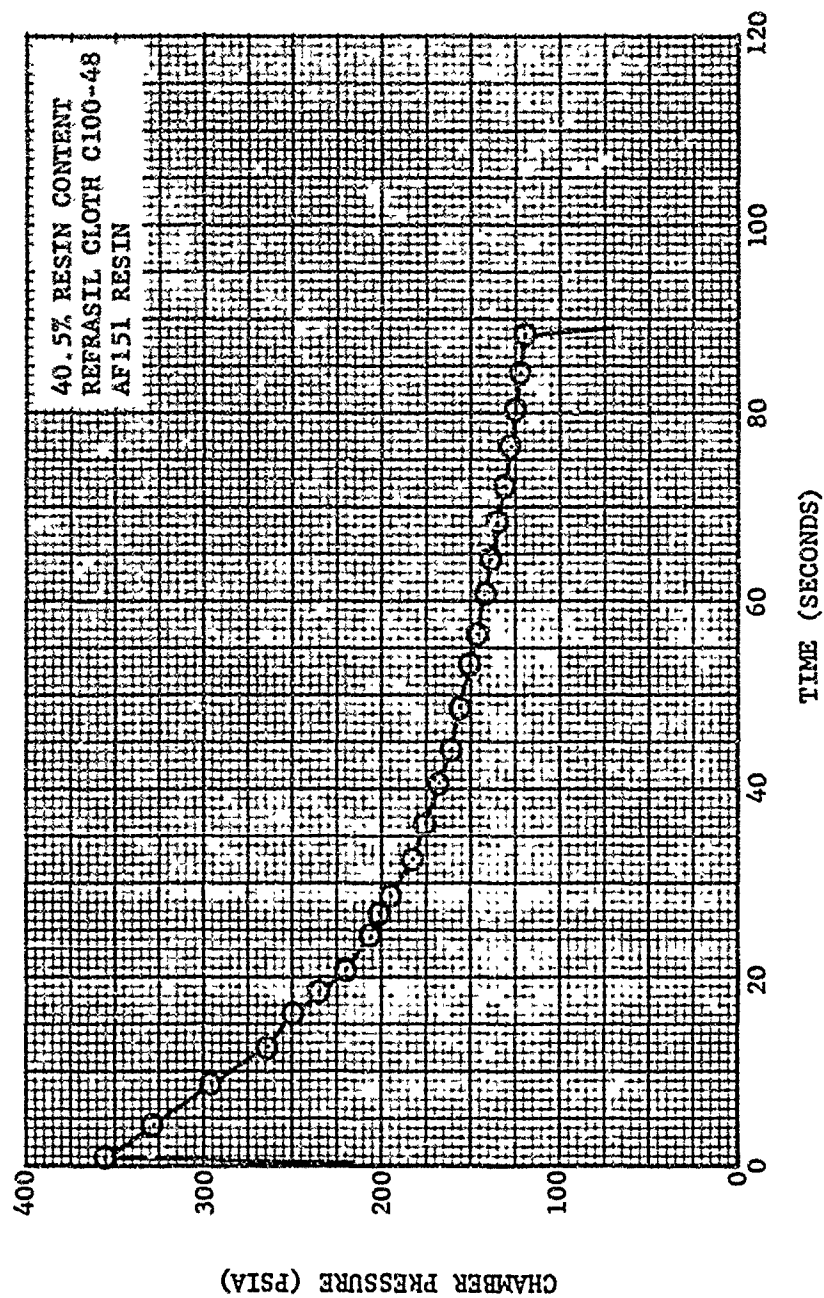
FIGURE 158. CHAMBER PRESSURE VERSUS TIME - ASD 515 NOZZLE





RI4227 U

FIGURE 159. CHAMBER PRESSURE VERSUS TIME - ASD 516 NOZZLE



R14224

FIGURE 160. CHAMBER PRESSURE VERSUS TIME - ASD 517 NOZZLE

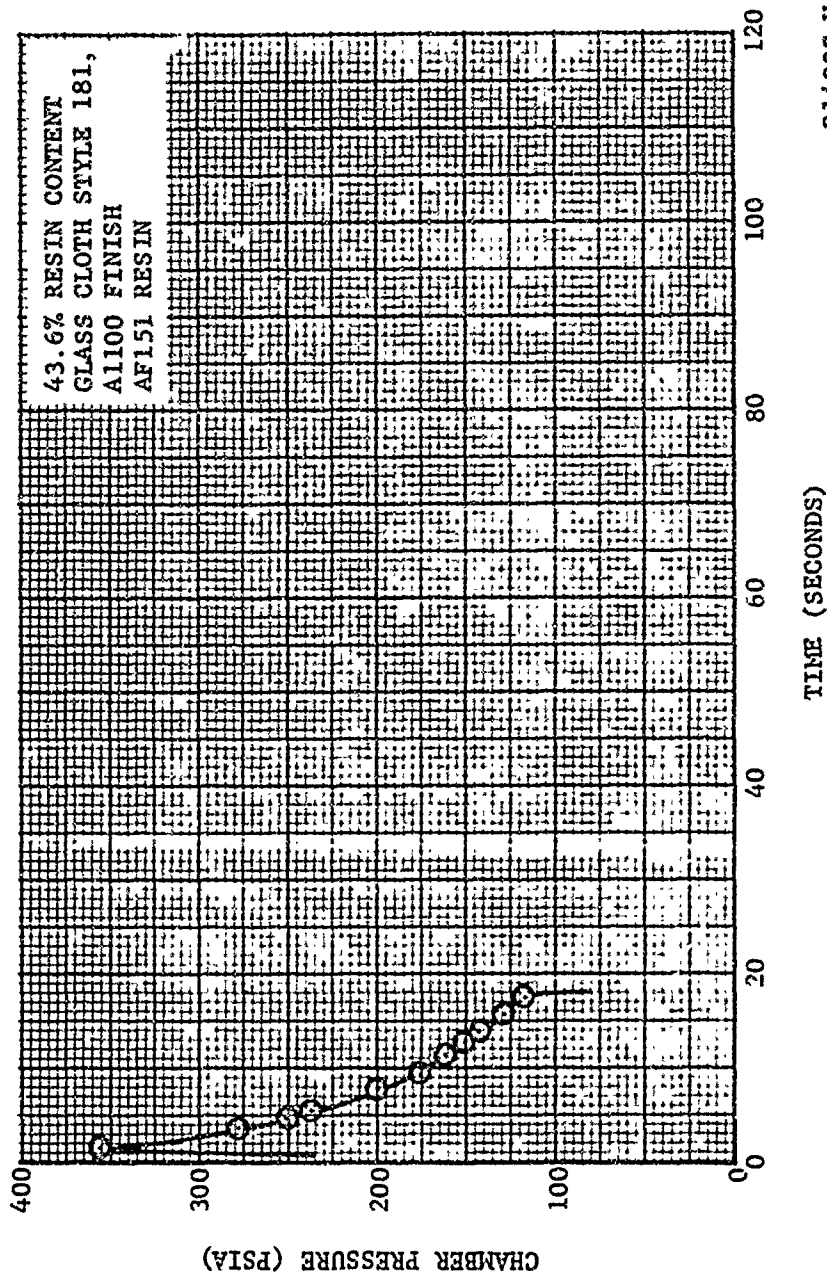


FIGURE 101. CHAMBER PRESSURE VERSUS TIME - ASD 518 NOZZLE

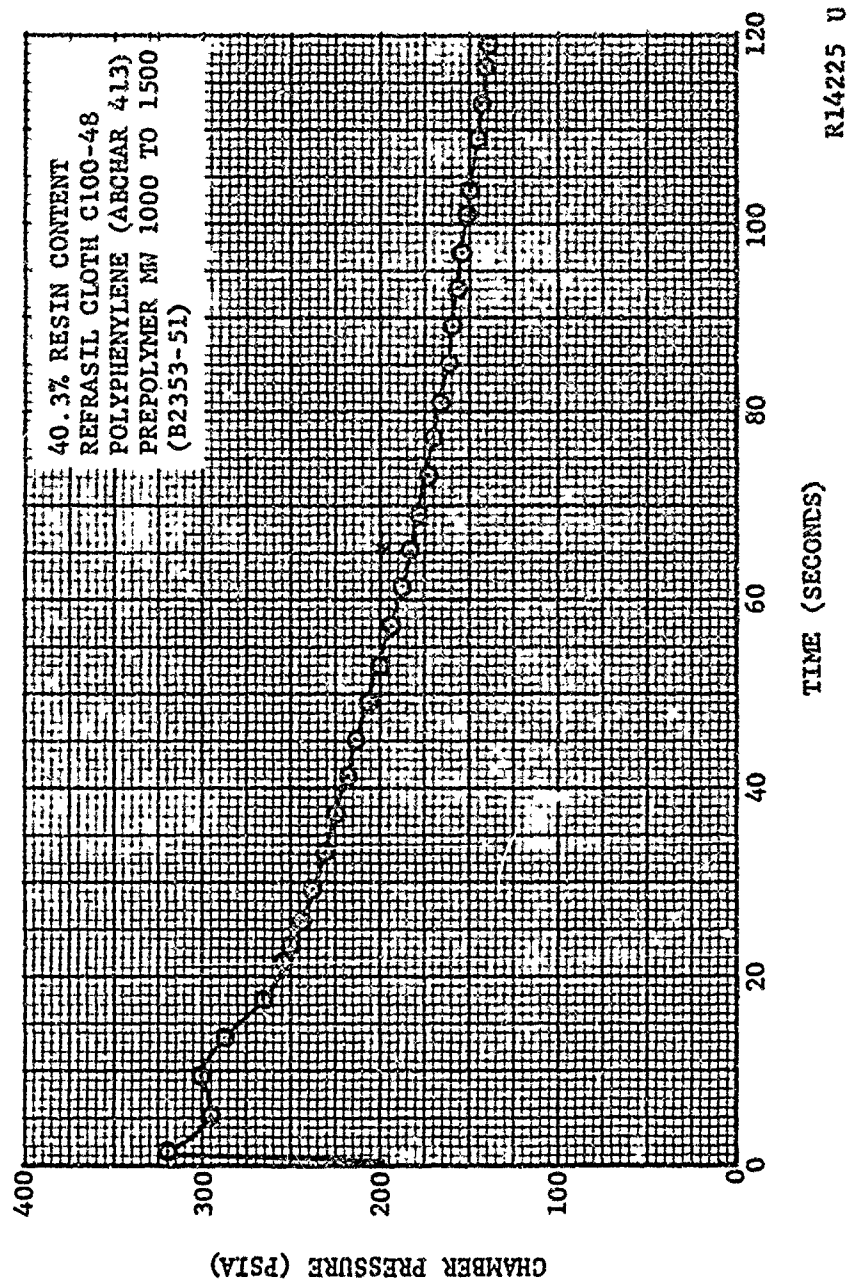
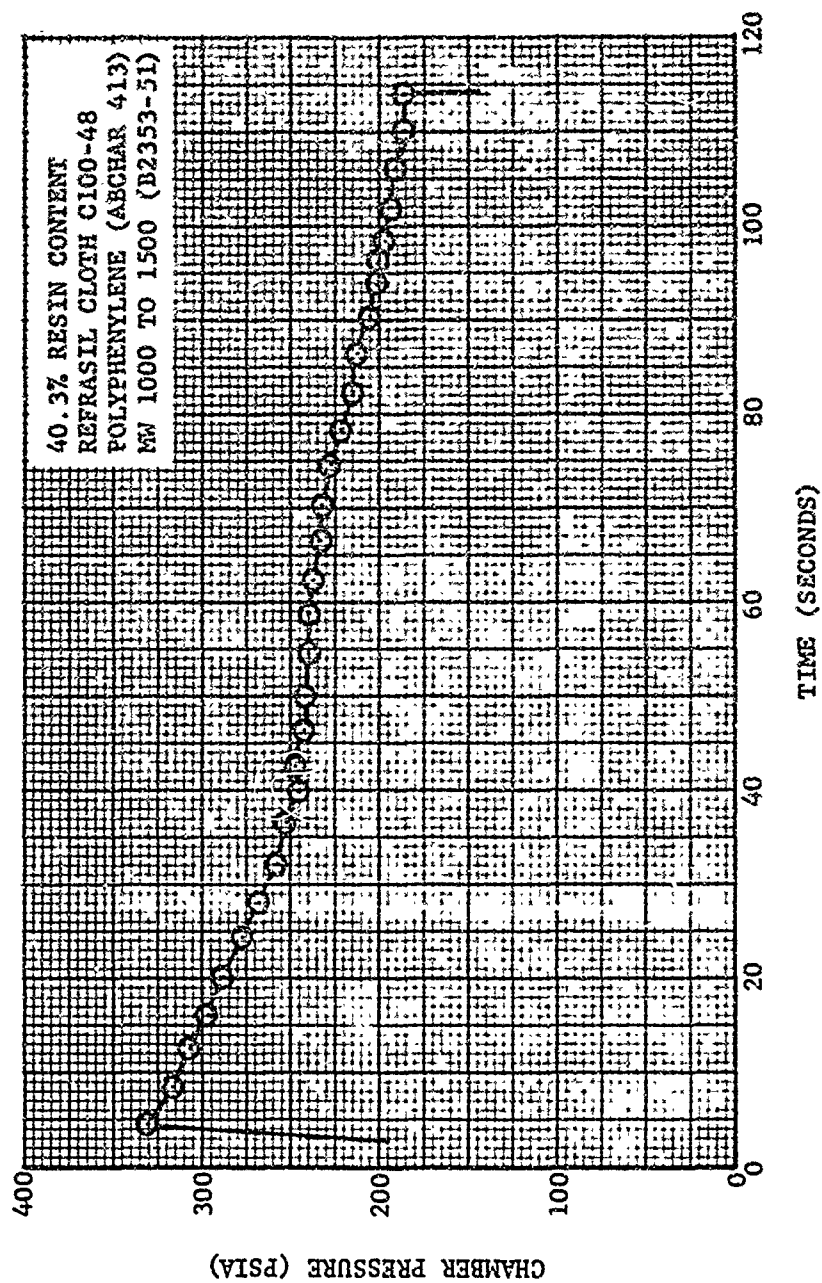


FIGURE 162. CHAMBER PRESSURE VERSUS TIME - ASD 519 NOZZLE



RI4222 U

FIGURE 163. CHAMBER PRESSURE VERSUS TIME - ASD 520 NOZZLE

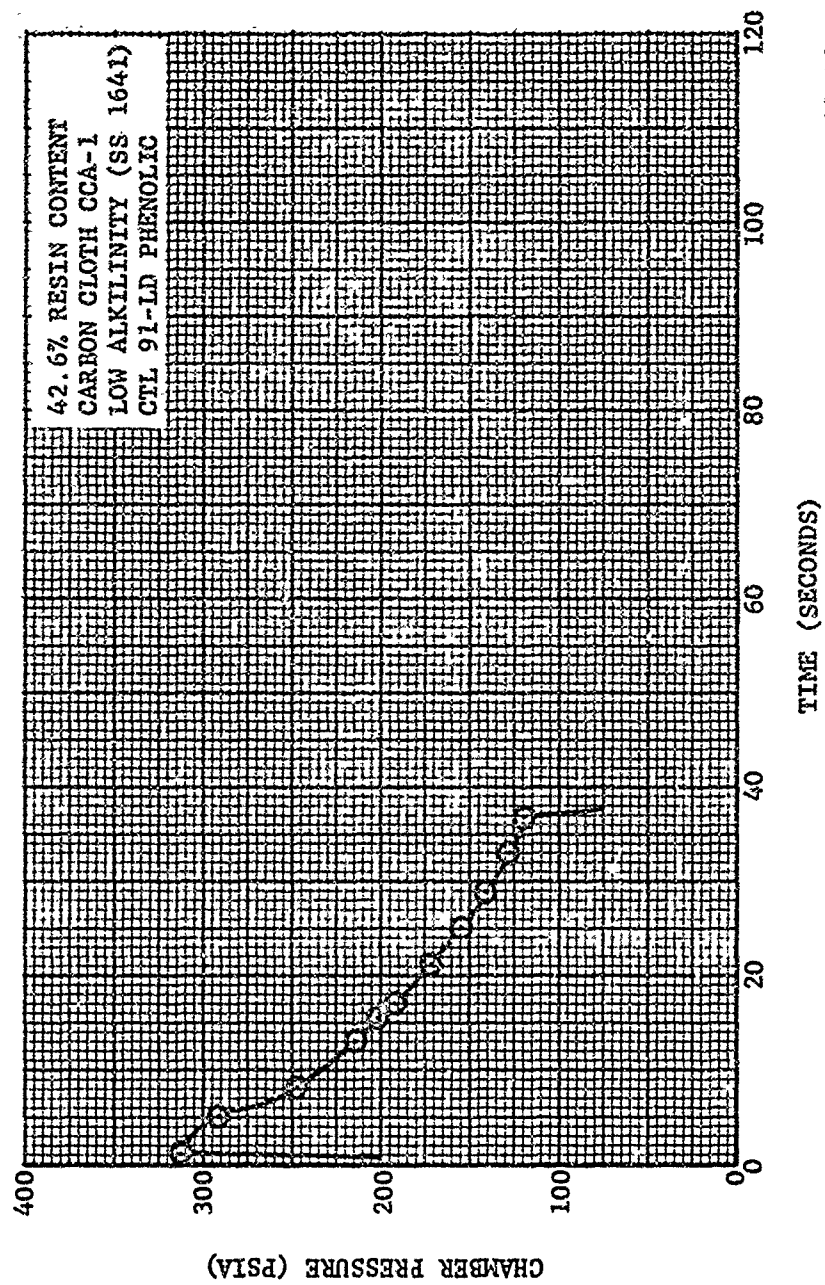
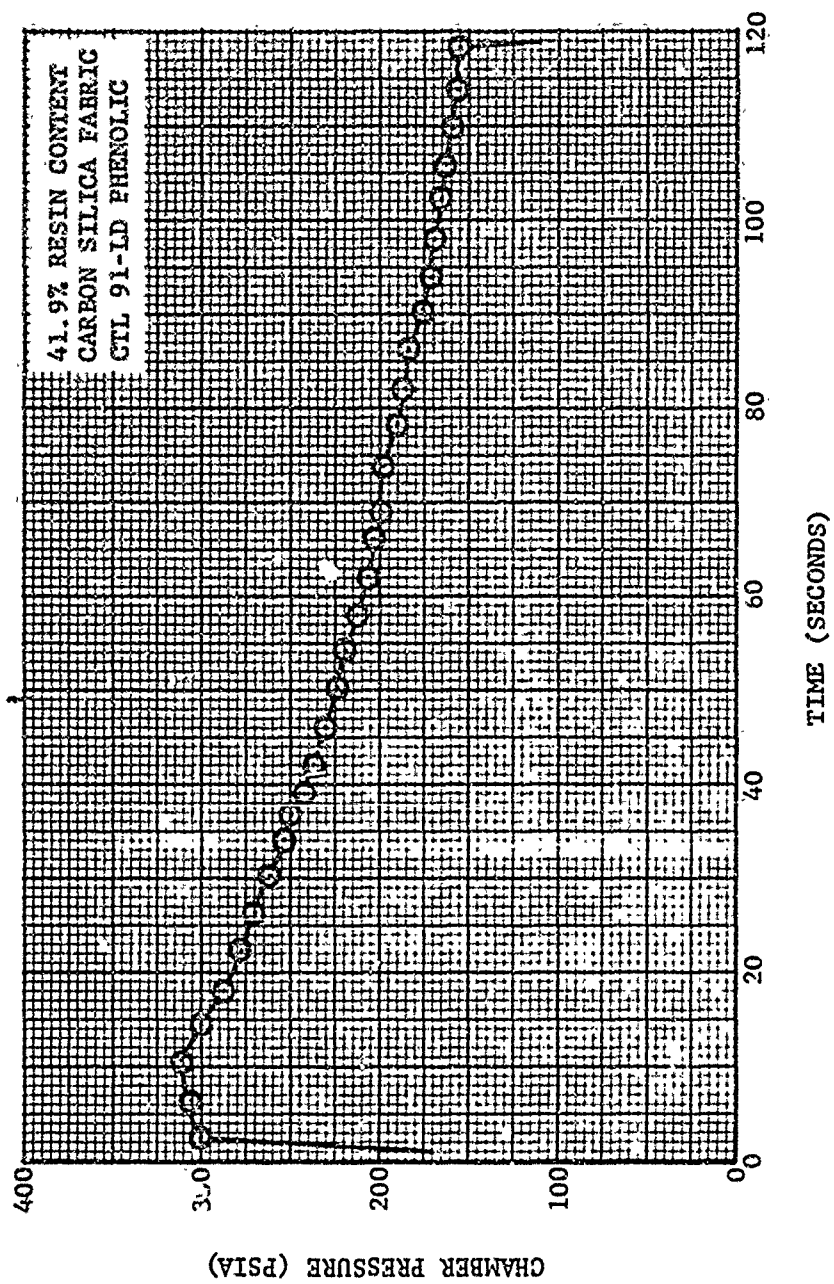


FIGURE 164. CHAMBER PRESSURE VERSUS TIME - ASD 522 NOZZLE



R14231 U

FIGURE 165. CHAMBER PRESSURE VERSUS TIME - ASD 524 NOZZLE



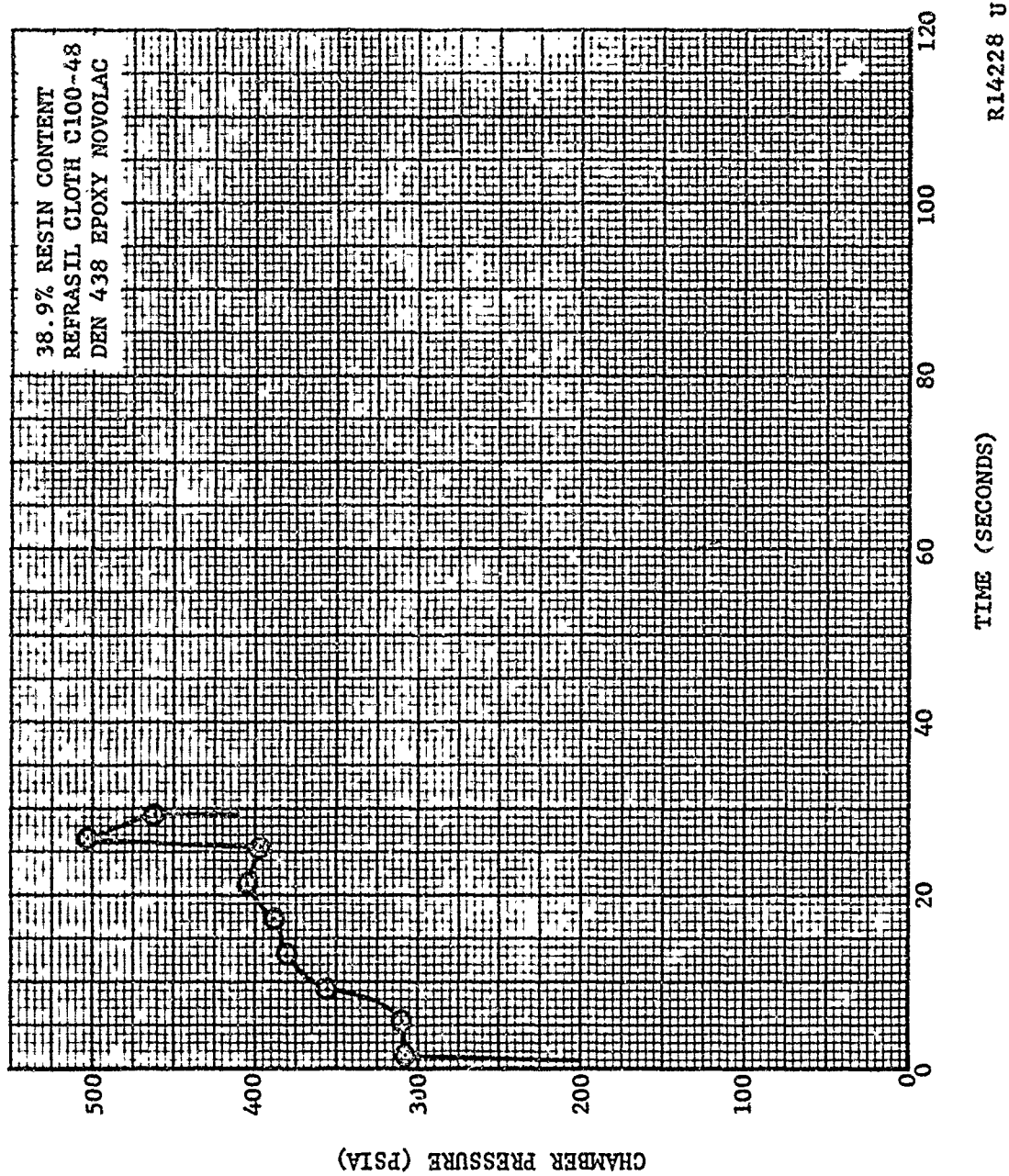


FIGURE 166. CHAMBER PRESSURE VERSUS TIME - ASD 526 NOZZLE



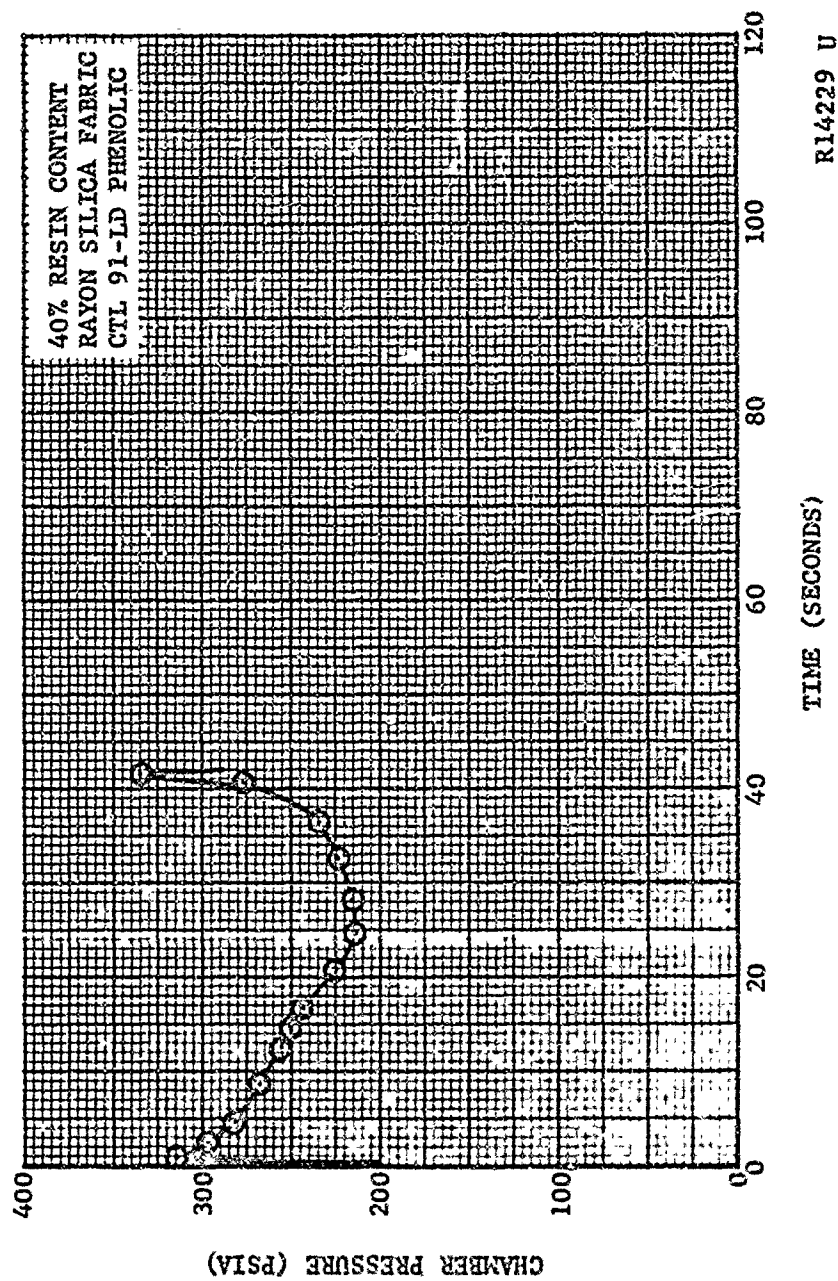
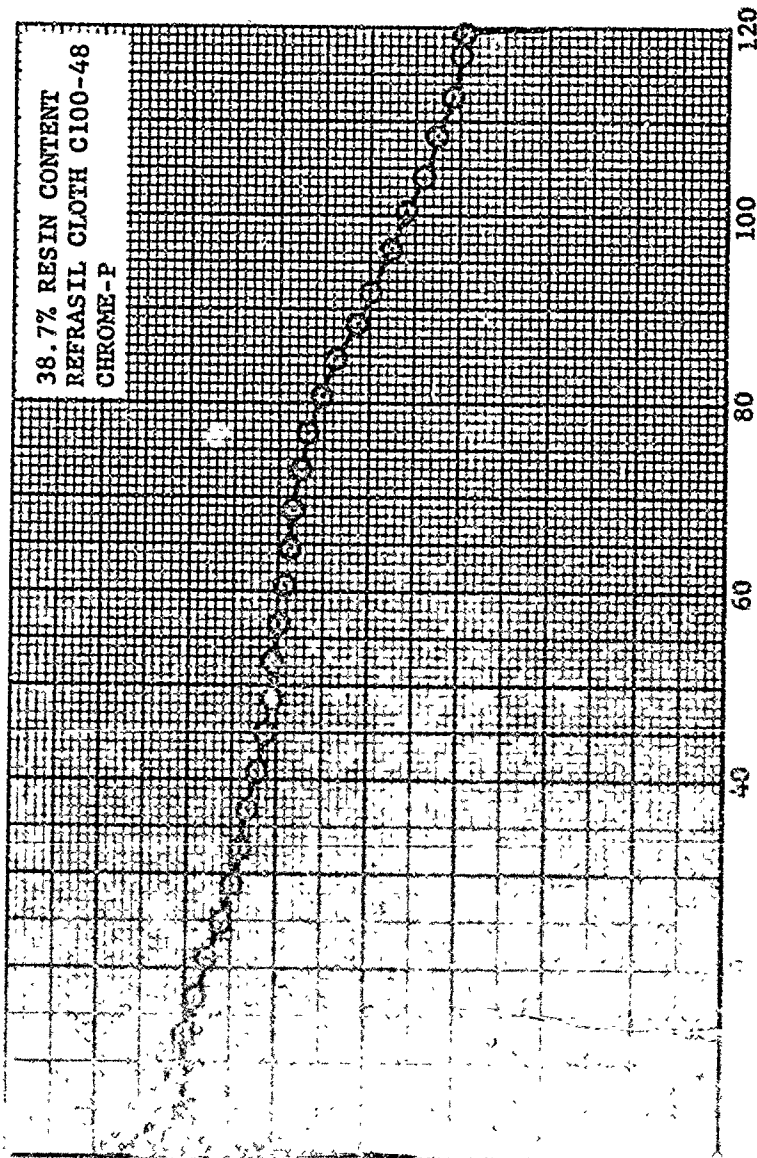


FIGURE 167. CHAMBER PRESSURE VERSUS TIME - ASD 527 NOZZLE

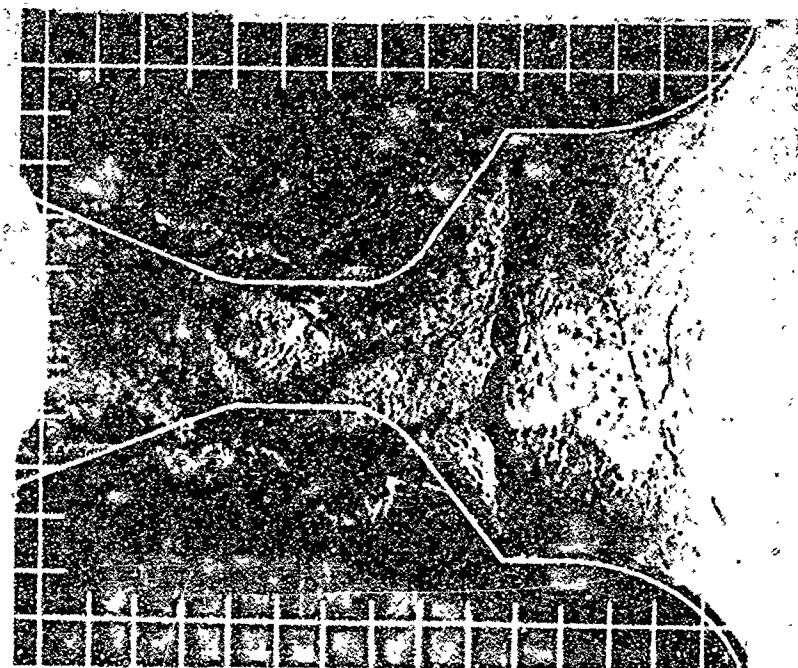


TIME (SECONDS)

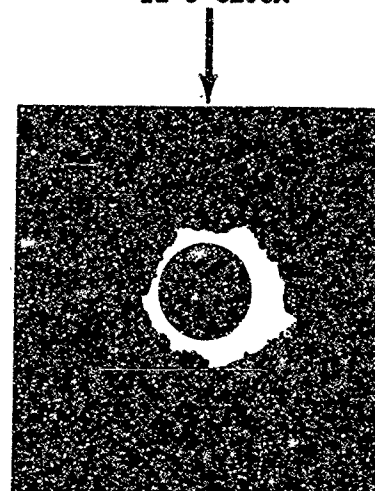
R14230 U

FIGURE 105. CHAMBER PRESSURE VERSUS TIME - ASD 528 NOZZLE

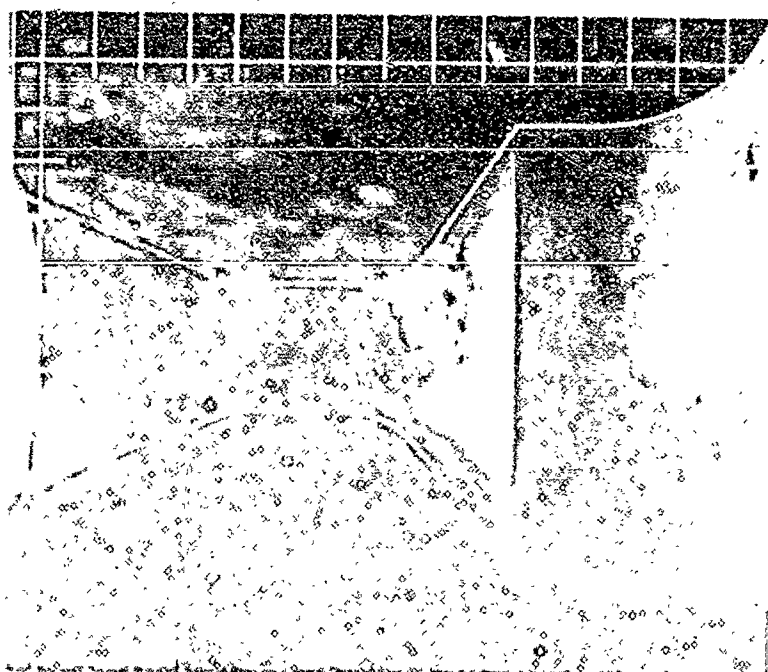
NOZZLE NO. ASD-352



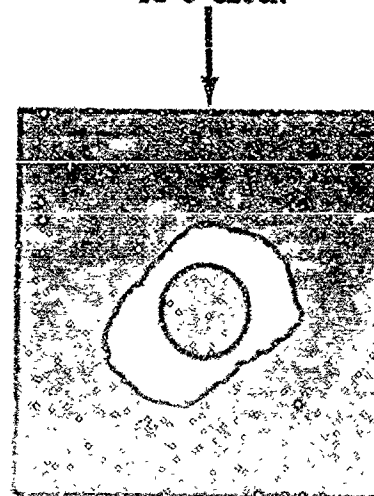
12 O'CLOCK



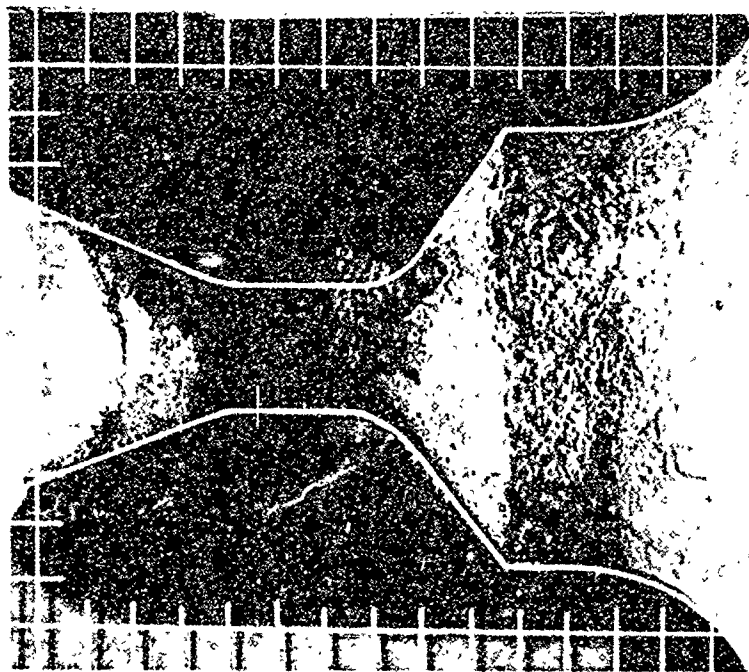
NOZZLE NO. ASD-377



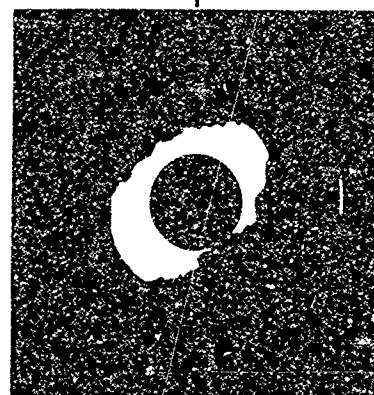
12 O'CLOCK



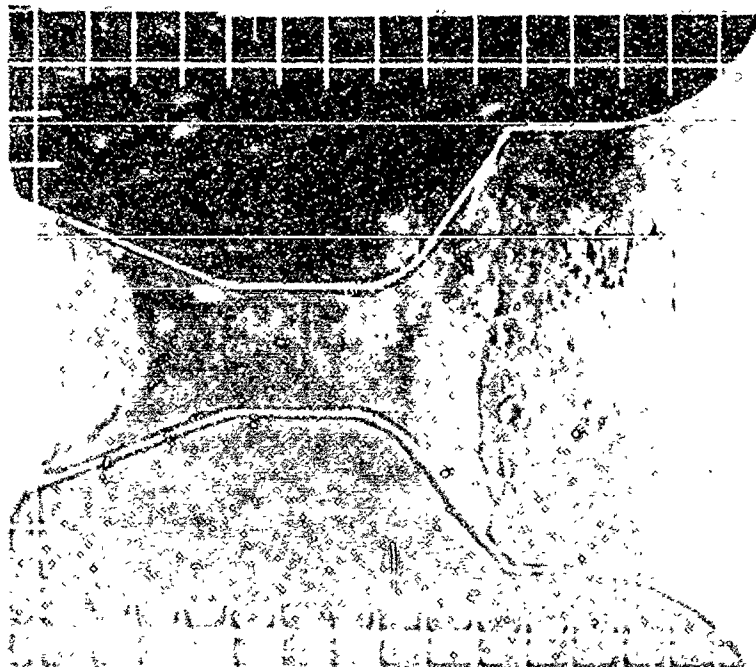
NOZZLE NO. ASD-380



12 O'CLOCK



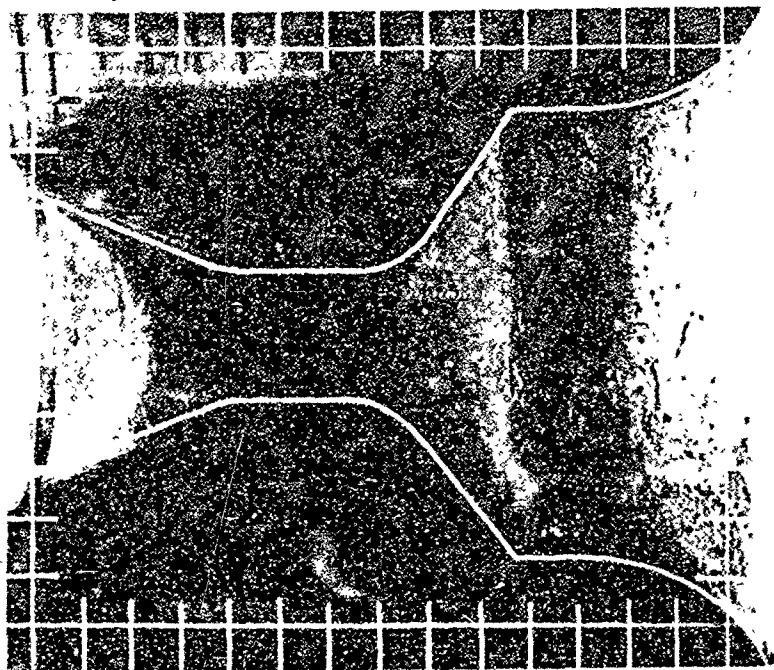
NOZZLE NO. ASD-381



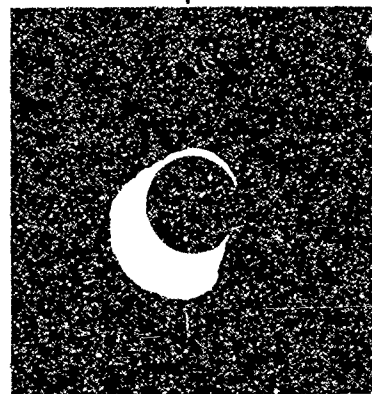
12 O'CLOCK



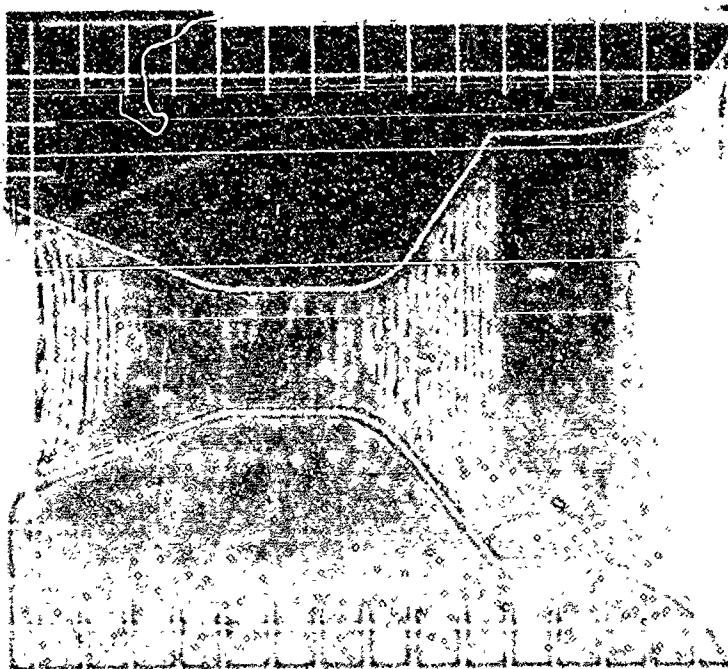
NOZZLE NO. ASD-382



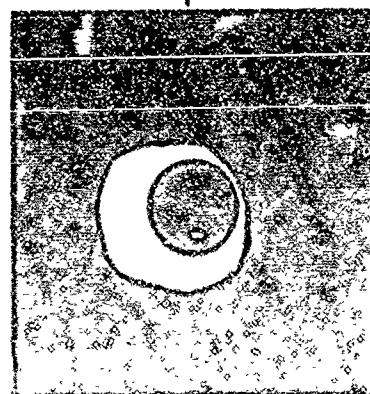
12 O'CLOCK



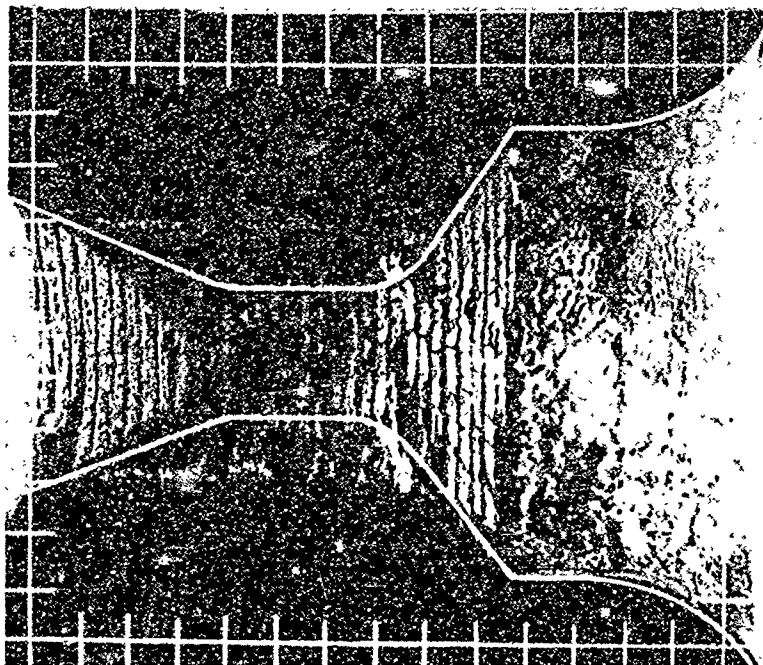
NOZZLE NO. ASD-390



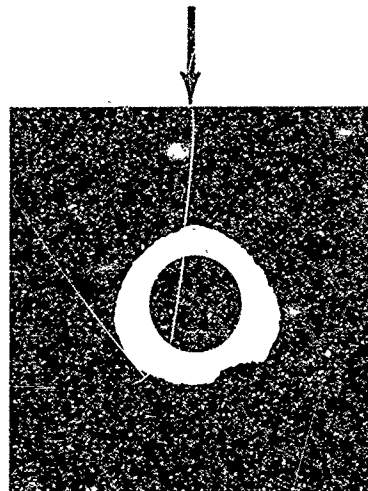
12 O'CLOCK



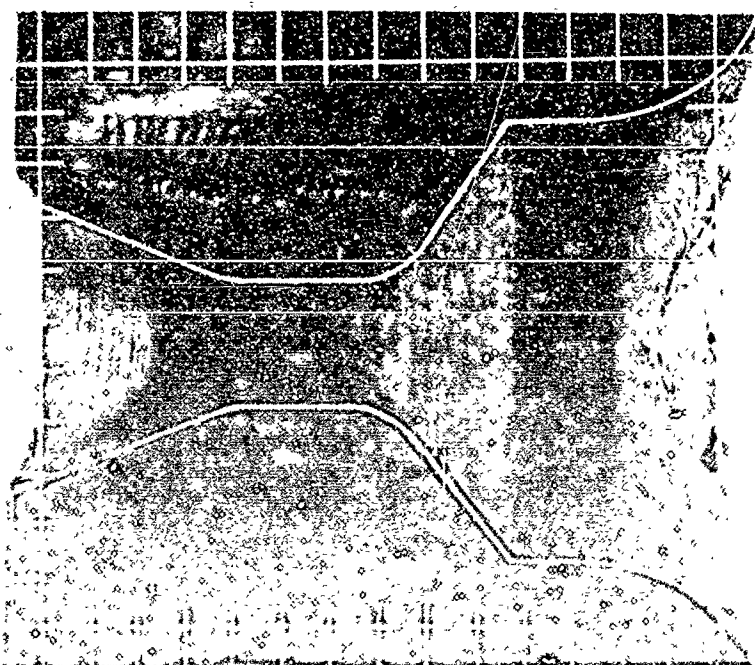
NOZZLE NO. ASD-391



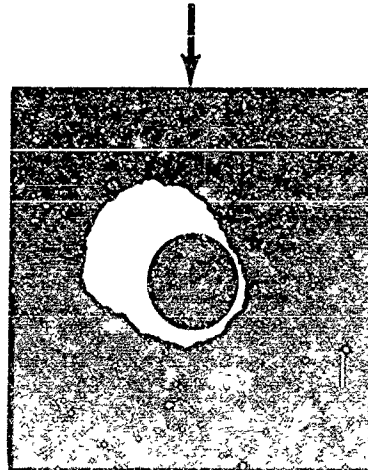
12 O'CLOCK



NOZZLE NO. ASD-392



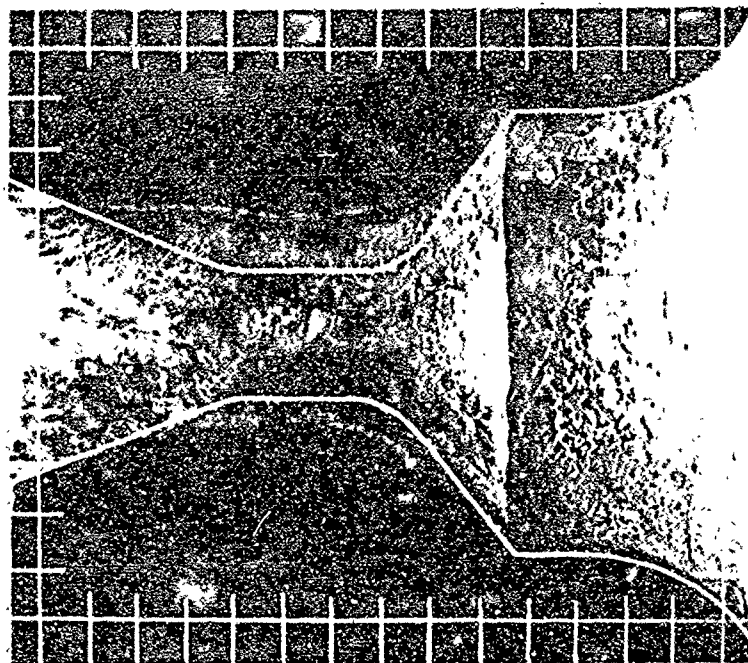
12 O'CLOCK



R13894U



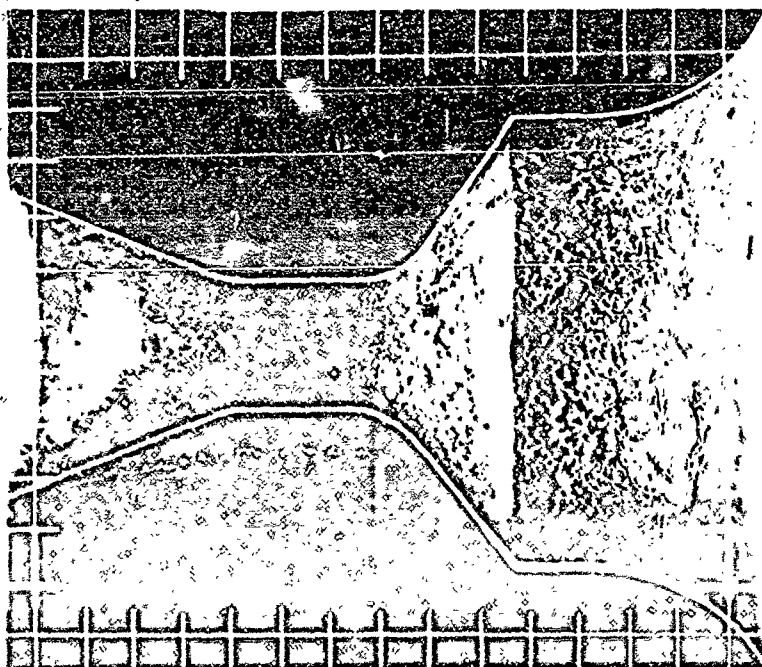
NOZZLE NO. ASD-395



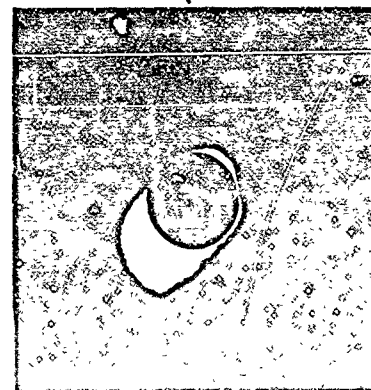
12 O'CLOCK



NOZZLE NO. ASD-396



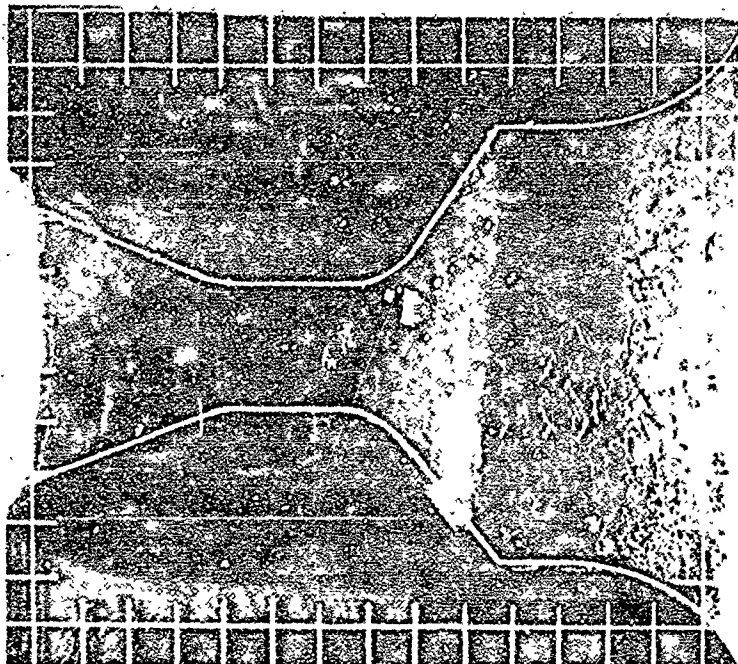
12 O'CLOCK



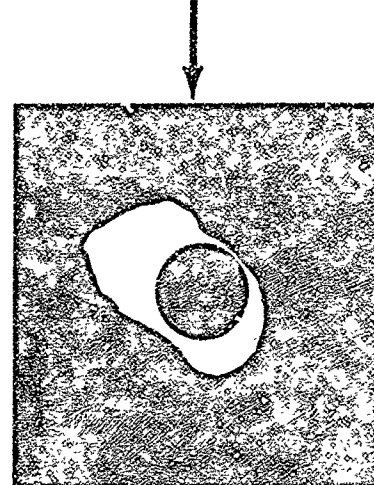
R13895U

FIGURE 173. PROFILE AND AXIAL NOZZLE PHOTOGRAPHS

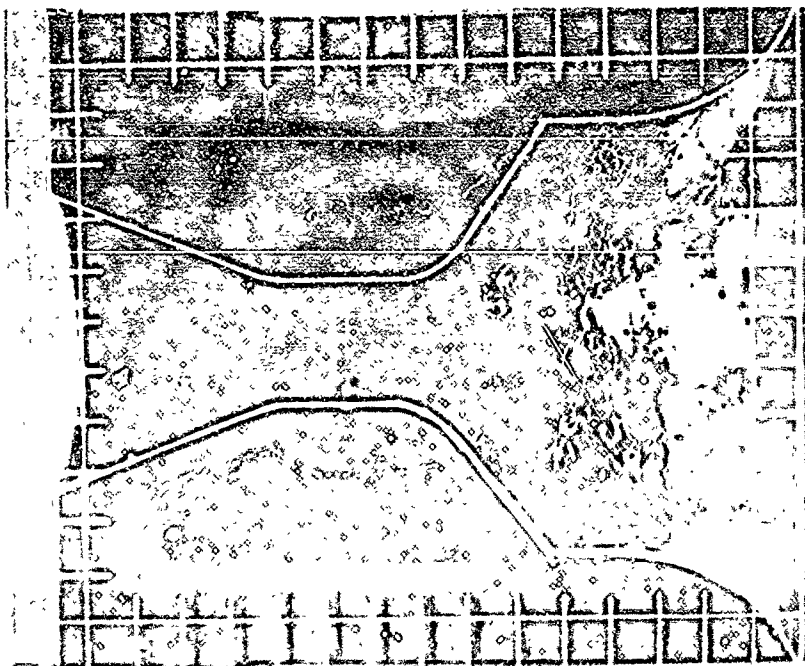
NOZZLE NO. ASD-408



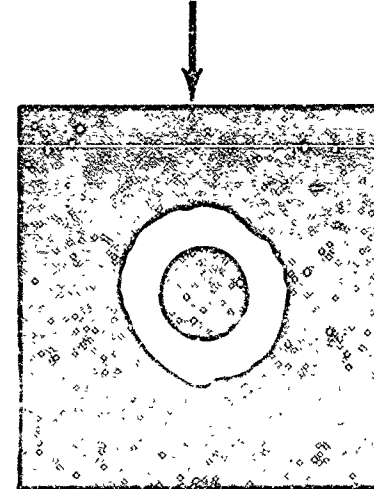
12 O'CLOCK



NOZZLE NO. ASD-409



12 O'CLOCK

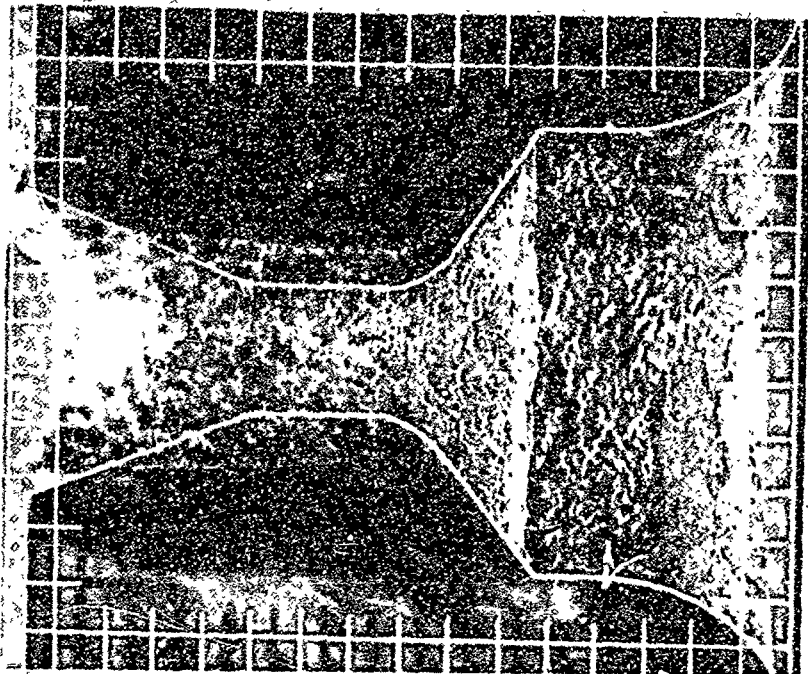


R13896U

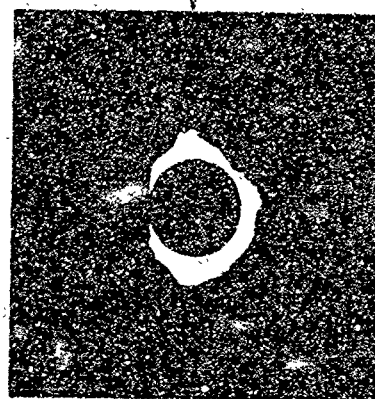
FIGURE 174. PROFILE AND AXIAL NOZZLE PHOTOGRAPHS



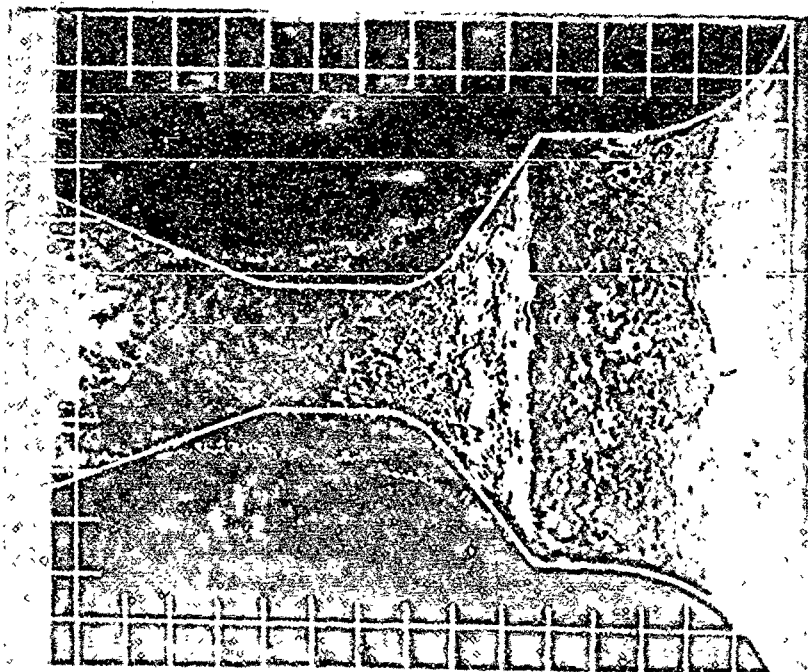
NOZZLE NO. ASD-412



12 O'CLOCK



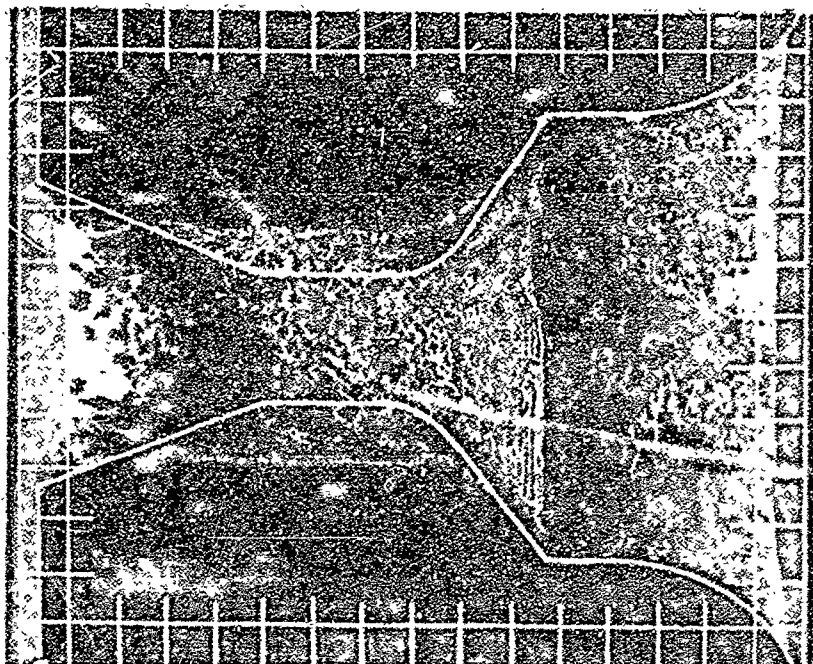
NOZZLE NO. ASD-415



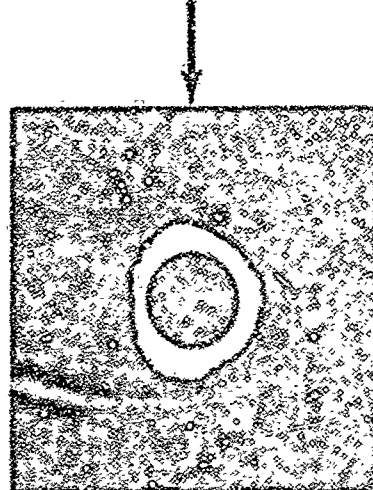
12 O'CLOCK



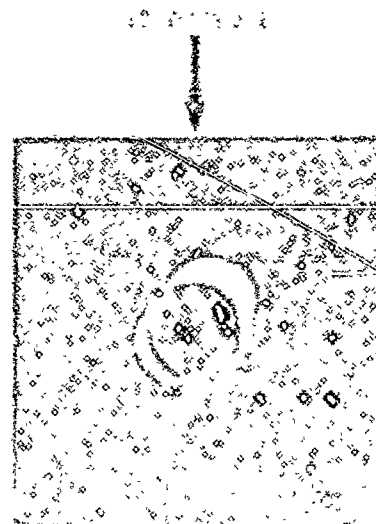
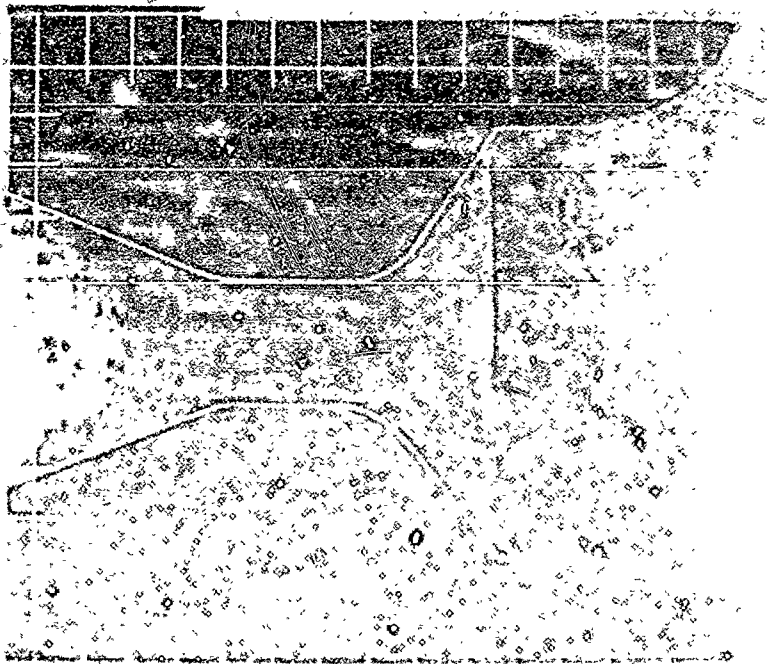
NOZZLE NO. ASD-420



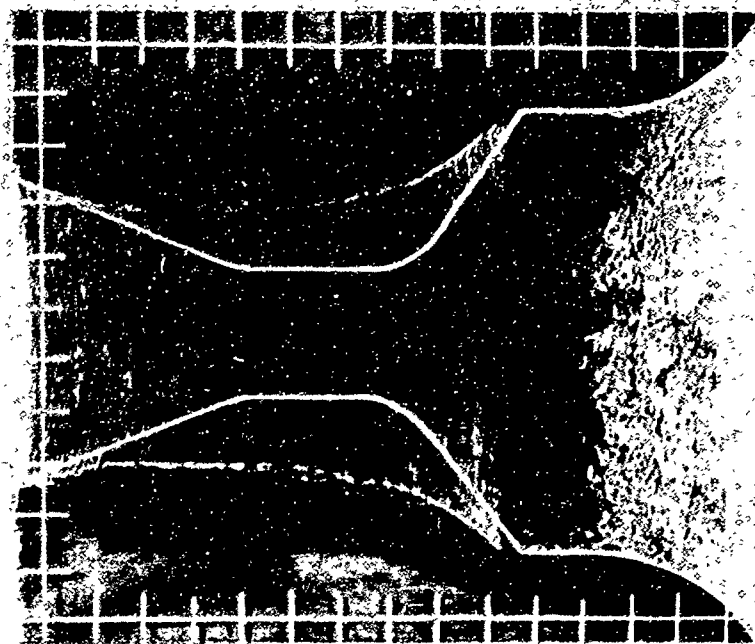
12 O'CLOCK



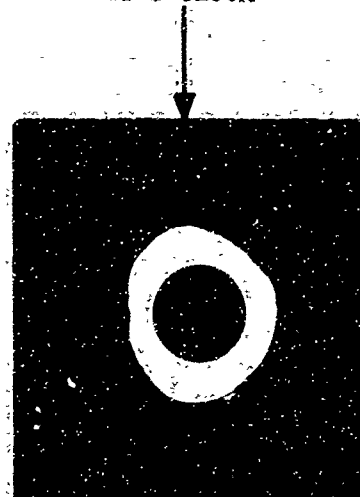
NOZZLE NO. ASD-424



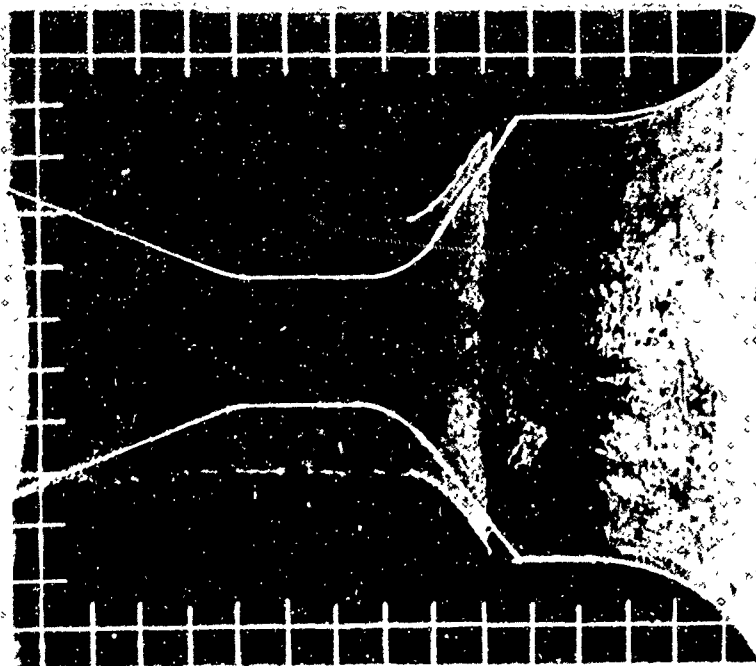
NOZZLE NO. ASD-425



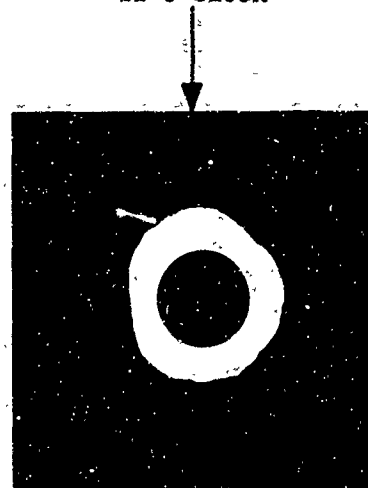
12 O'CLOCK



NOZZLE NO. ASD-426



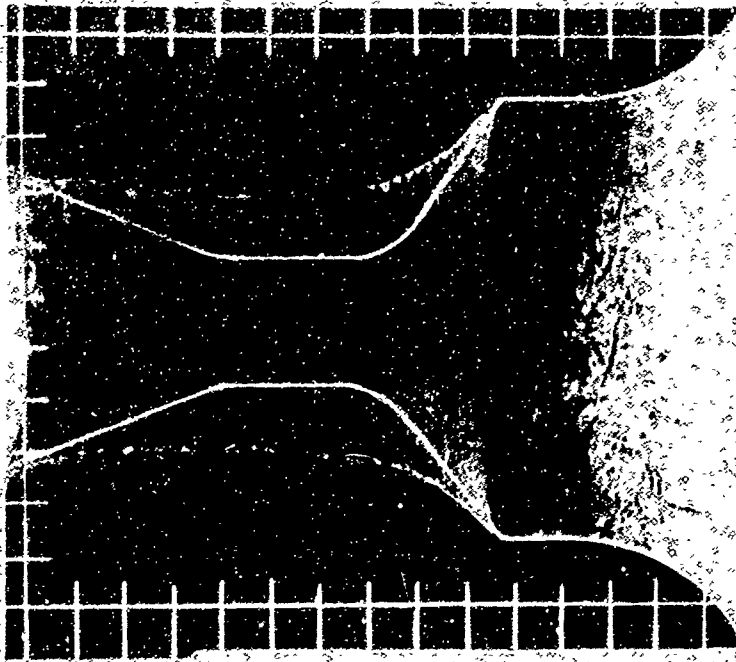
12 O'CLOCK



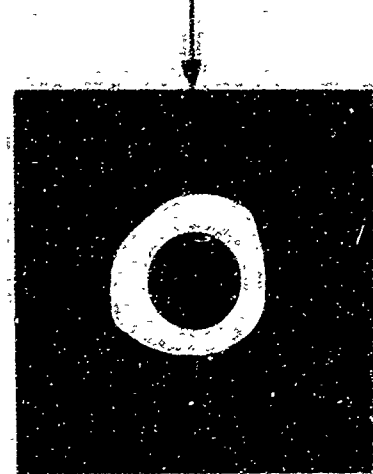
F00956 U

FIGURE 177. PROFILE AND AXIAL NOZZLE PHOTOGRAPHS

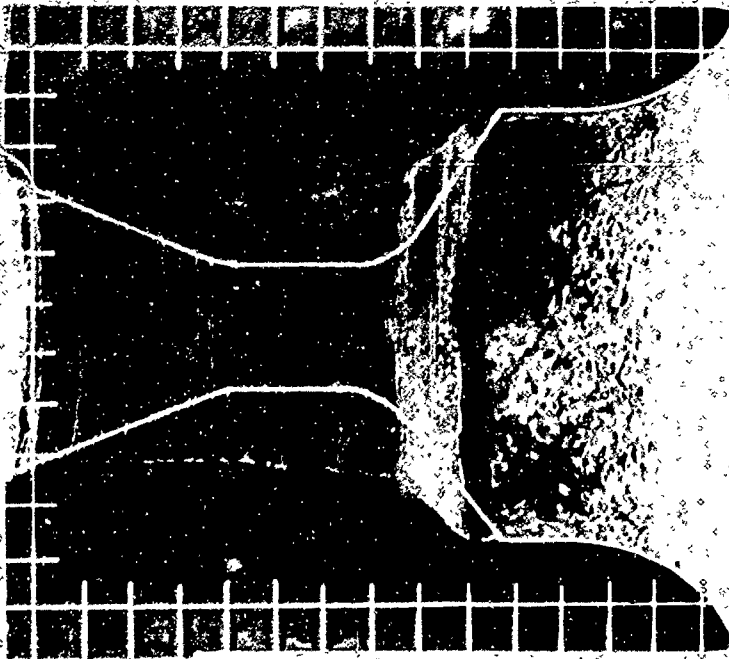
NOZZLE NO. ASD-427



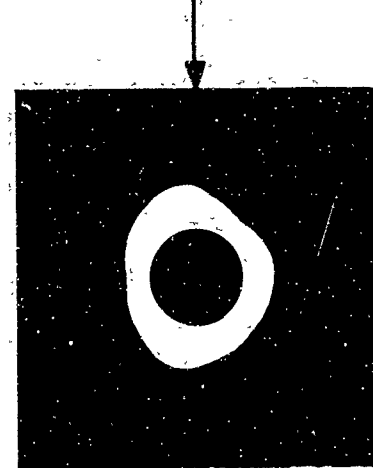
12 O'CLOCK



NOZZLE NO. ASD-436



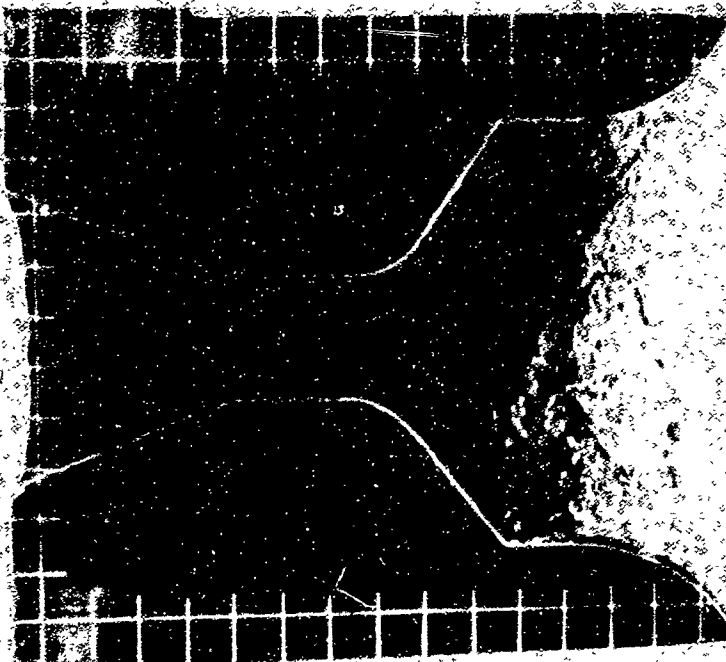
12 O'CLOCK



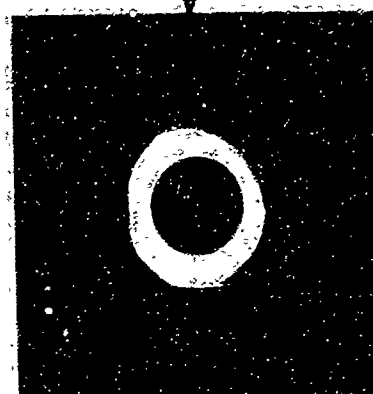
F00957 U

FIGURE 178. PROFILE AND AXIAL NOZZLE PHOTOGRAPHS

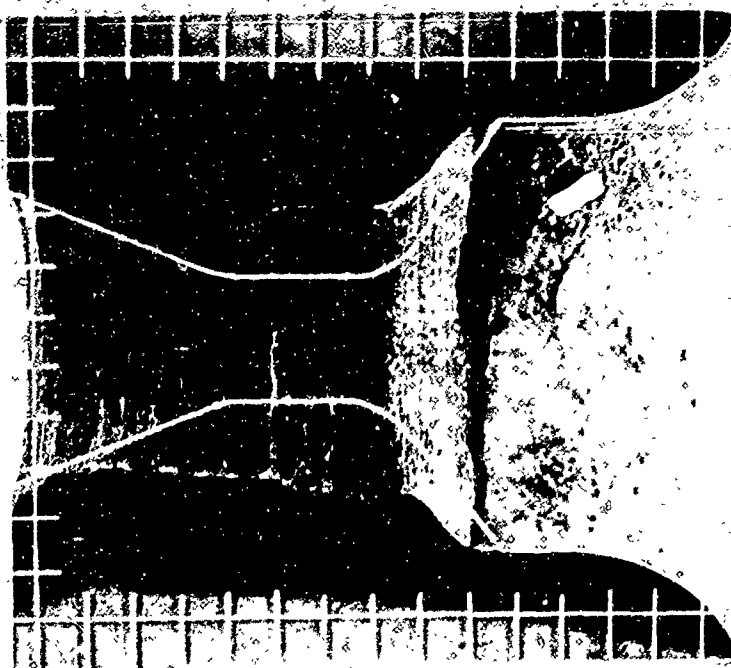
NOZZLE NO. ASD-438



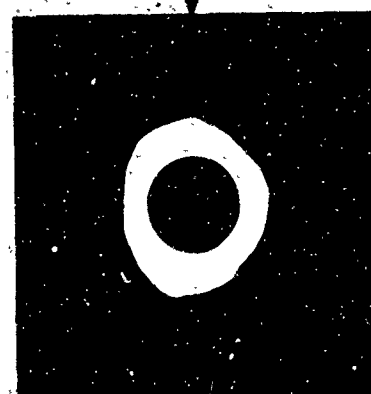
12 O'CLOCK



NOZZLE NO. ASD-445



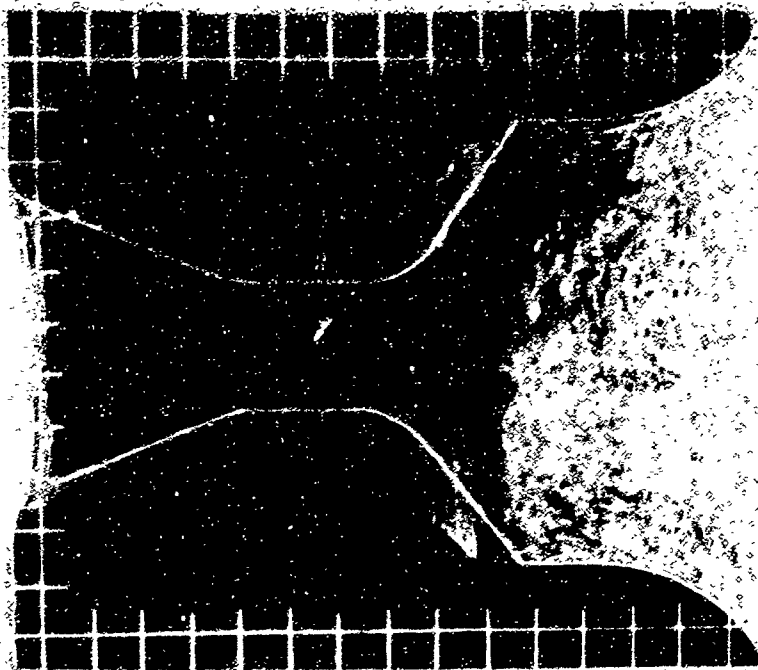
12 O'CLOCK



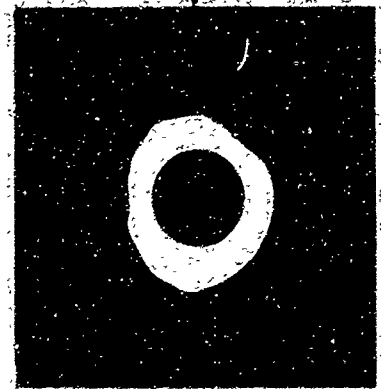
F00958 U

FIGURE 179. PROFILE AND AXIAL NOZZLE PHOTOGRAPHS

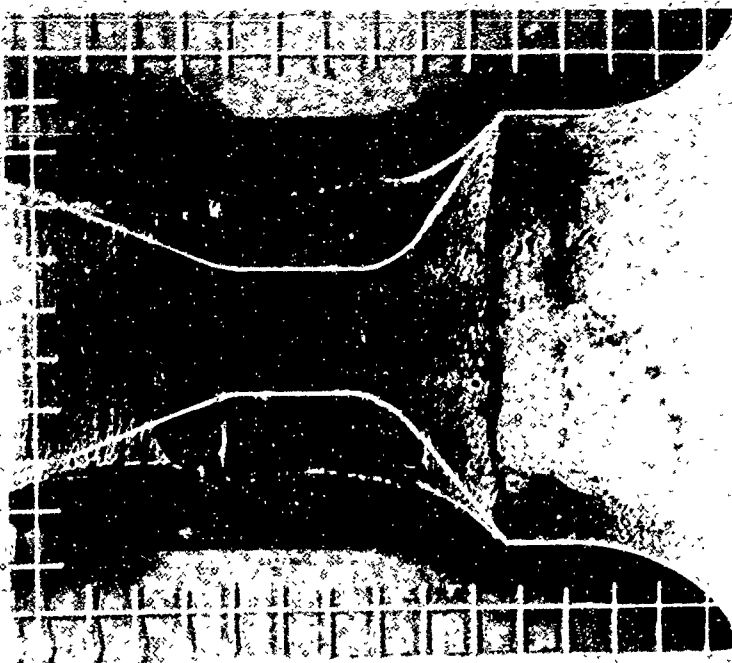
NOZZLE NO. ASD-447



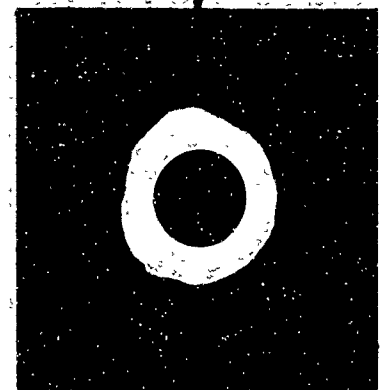
12 O'CLOCK



NOZZLE NO. ASD 450



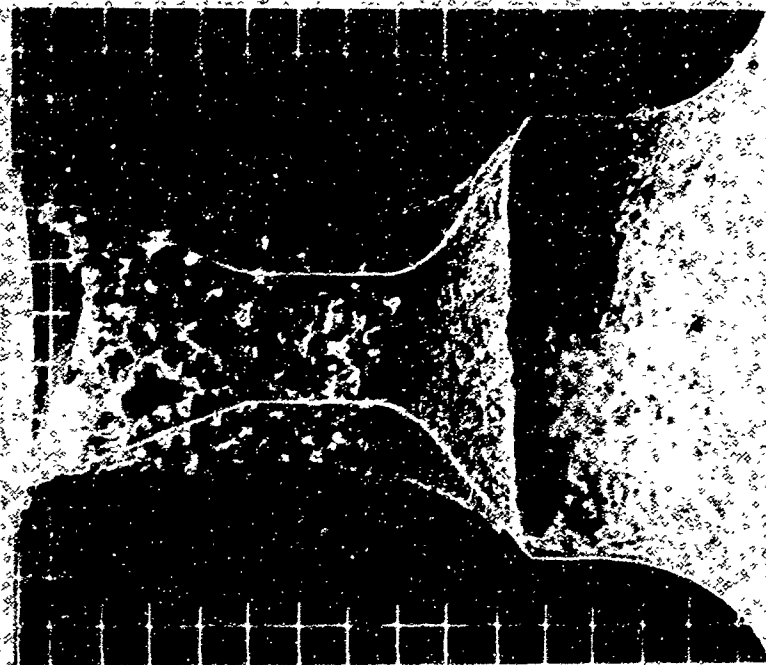
12 O'CLOCK



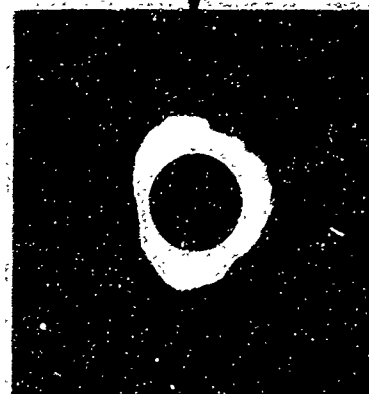
F00959 U

FIGURE 180. PROFILE AND AXIAL NOZZLE PHOTOGRAPHS

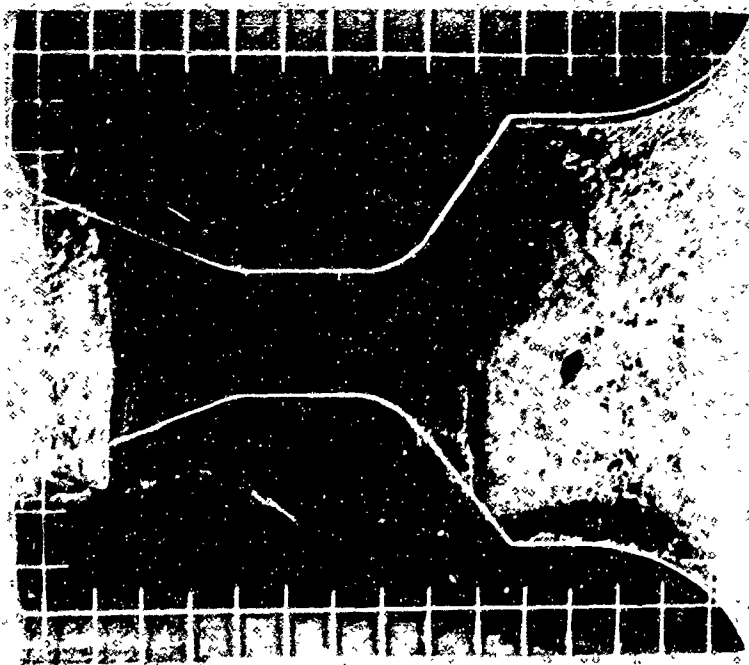
NOZZLE NO. ASD-453



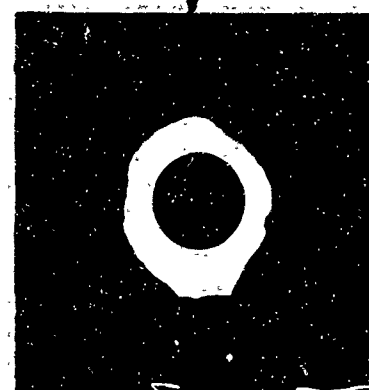
12 O'CLOCK



NOZZLE NO. ASD-461



12 O'CLOCK

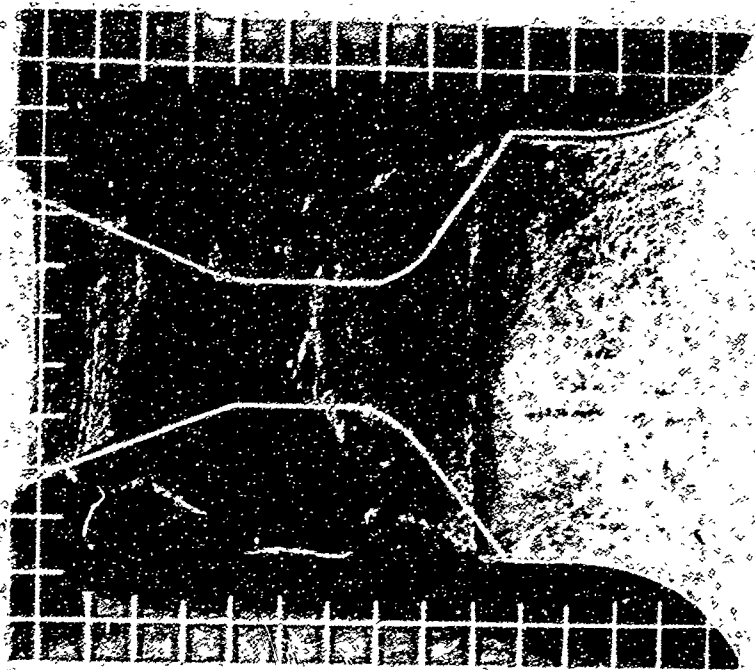


F00960 U

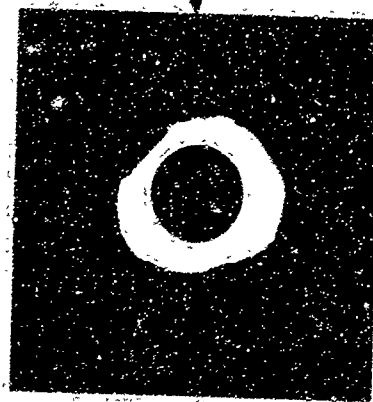
FIGURE 181. PROFILE AND AXIAL NOZZLE PHOTOGRAPHS



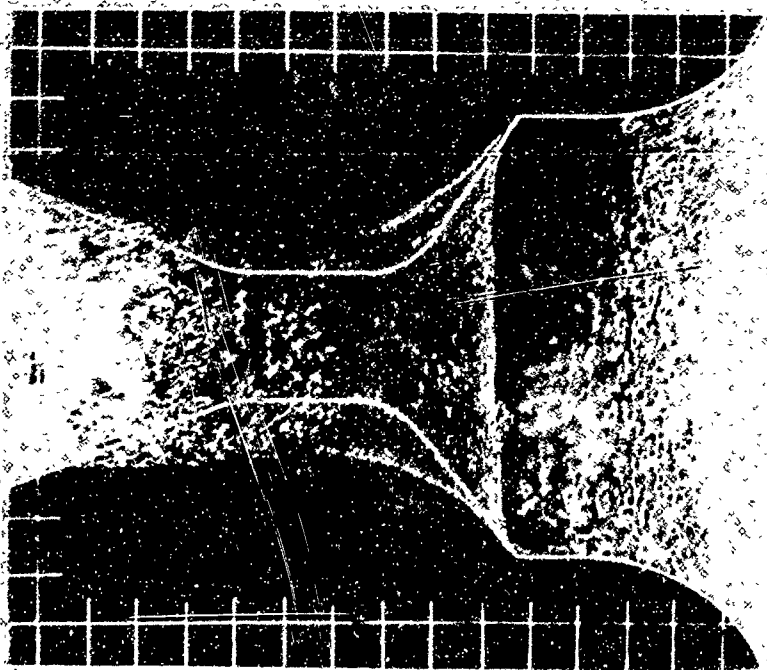
NOZZLE NO. ASD-462



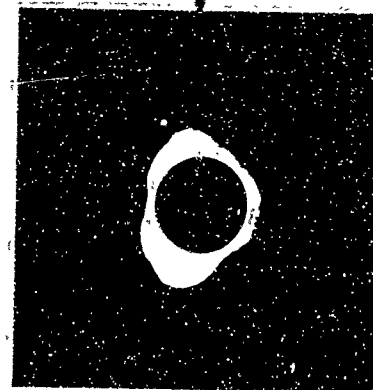
12 O'CLOCK



NOZZLE NO. ASD-465



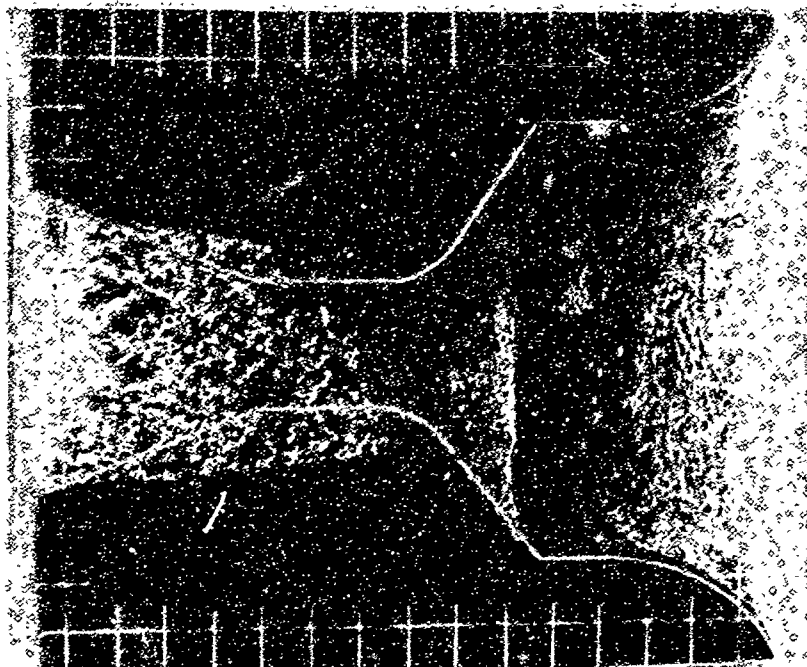
12 O'CLOCK



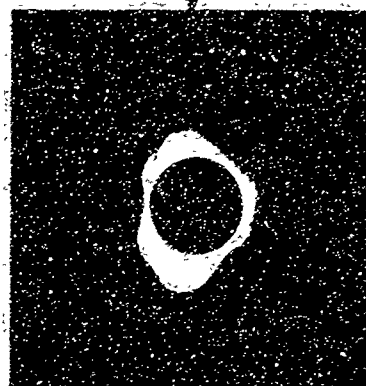
F00961 U

FIGURE 182. PROFILE AND AXIAL NOZZLE PHOTOGRAPHS

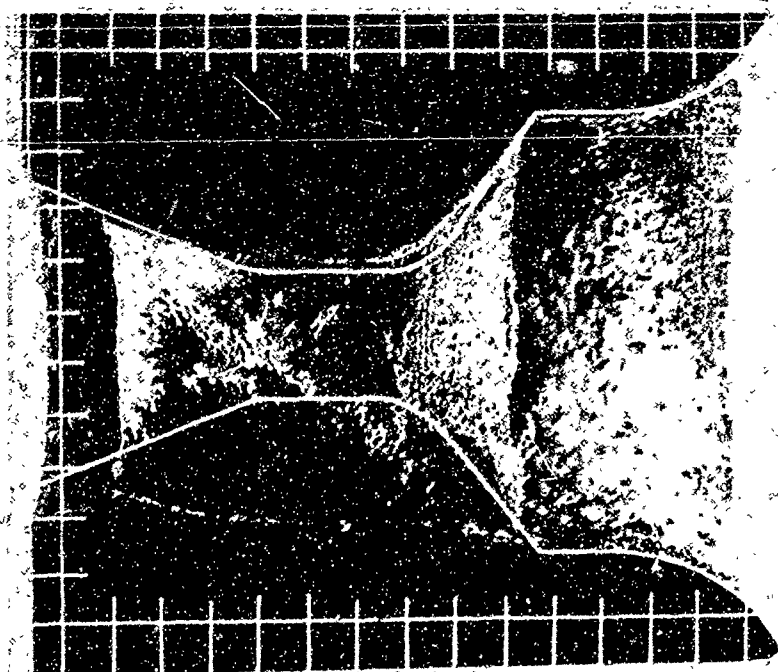
NOZZLE NO. ASD-466



12 O'CLOCK



NOZZLE NO. ASD-472



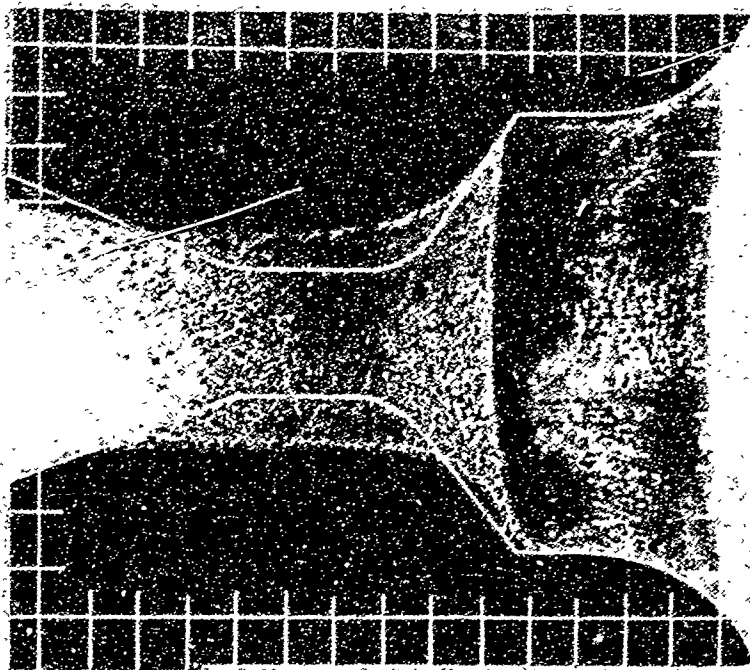
12 O'CLOCK



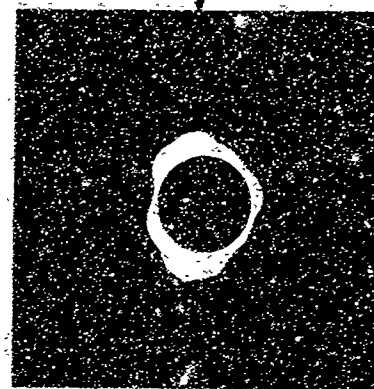
F00962 U

FIGURE 183. PROFILE AND AXIAL NOZZLE PHOTOGRAPHS

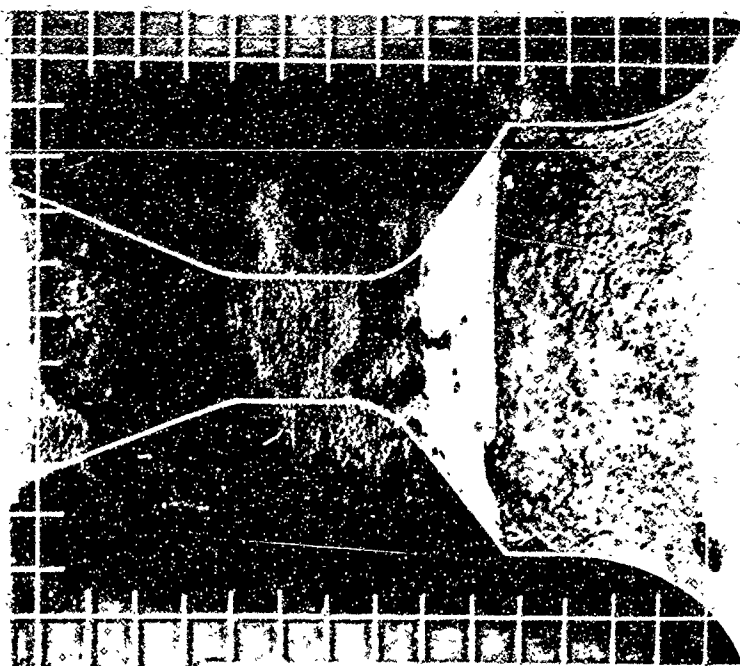
NOZZLE NO. ASD-473



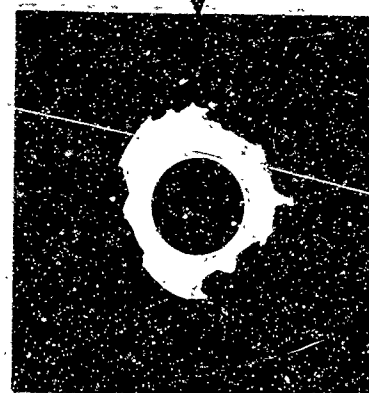
12 O'CLOCK



NOZZLE NO. ASD-475



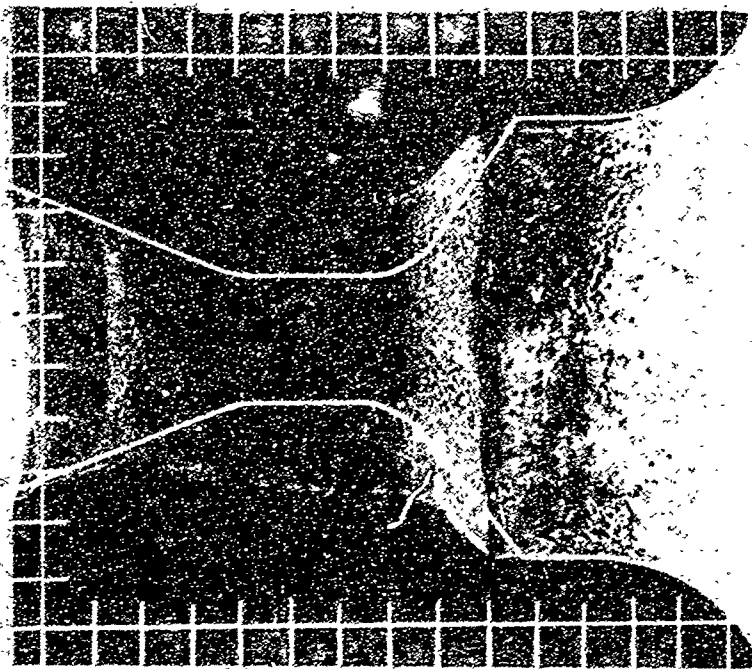
12 O'CLOCK



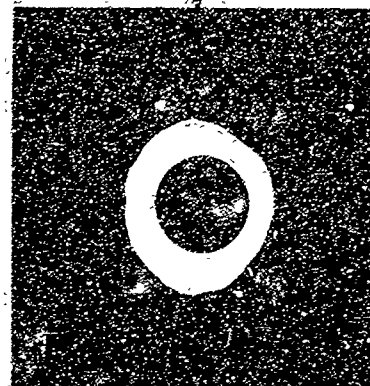
F00963 U

FIGURE 184. PROFILE AND AXIAL NOZZLE PHOTOGRAPHS

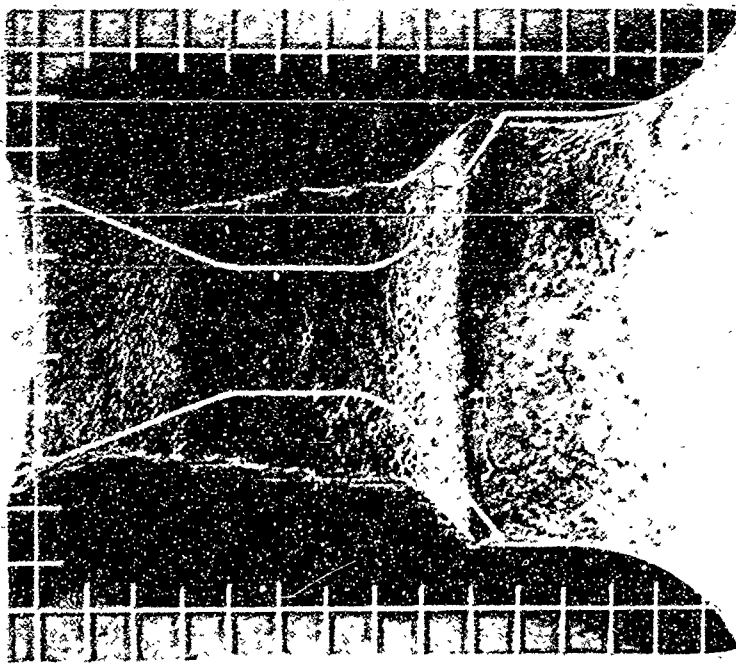
NOZZLE NO. ASD-476



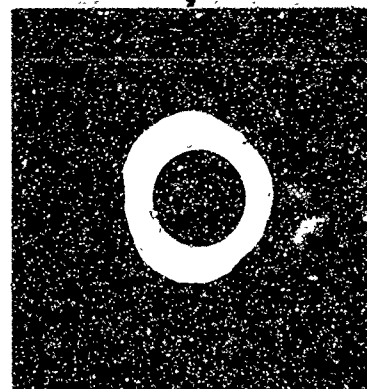
12 O'CLOCK



NOZZLE NO. ASD-477



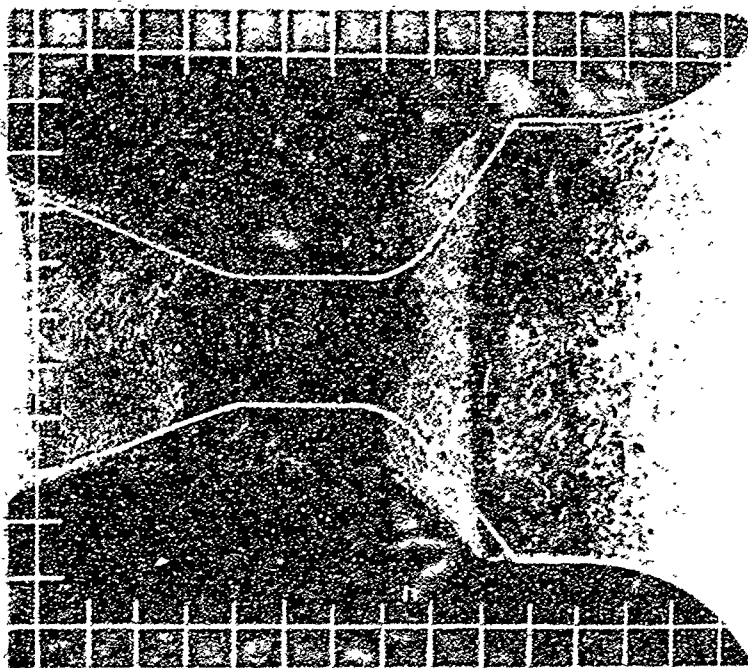
12 O'CLOCK



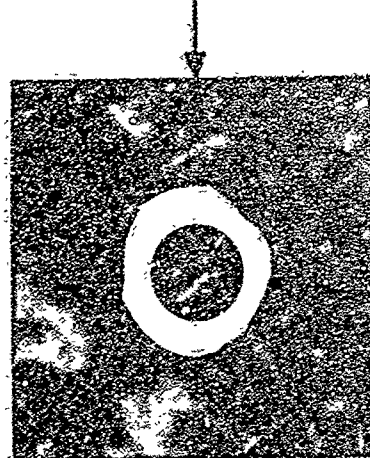
F00964 U

FIGURE 185. PROFILE AND AXIAL NOZZLE PHOTOGRAPHS

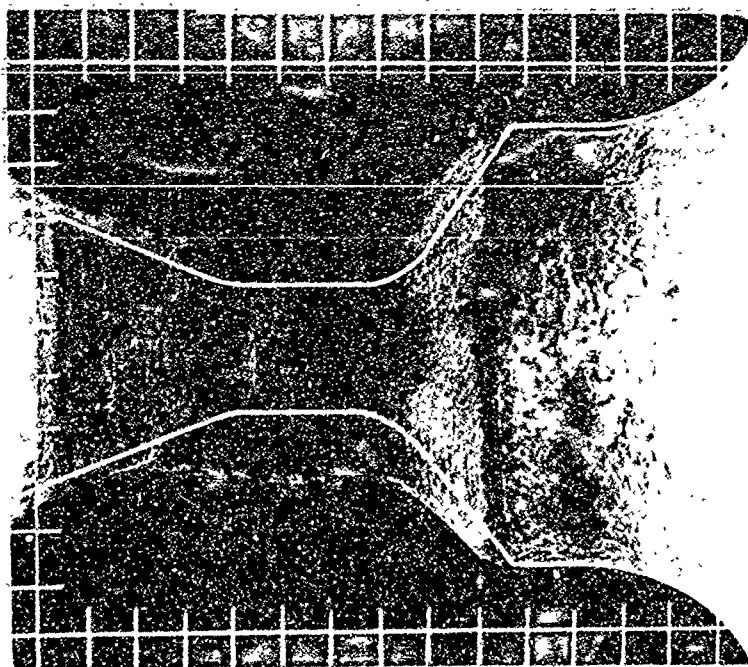
NOZZLE NO. ASD-478



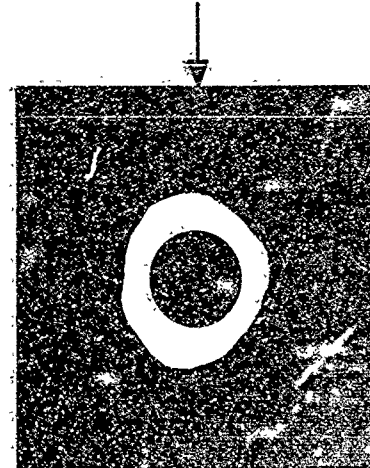
12 O'CLOCK



NOZZLE NO. ASD-479



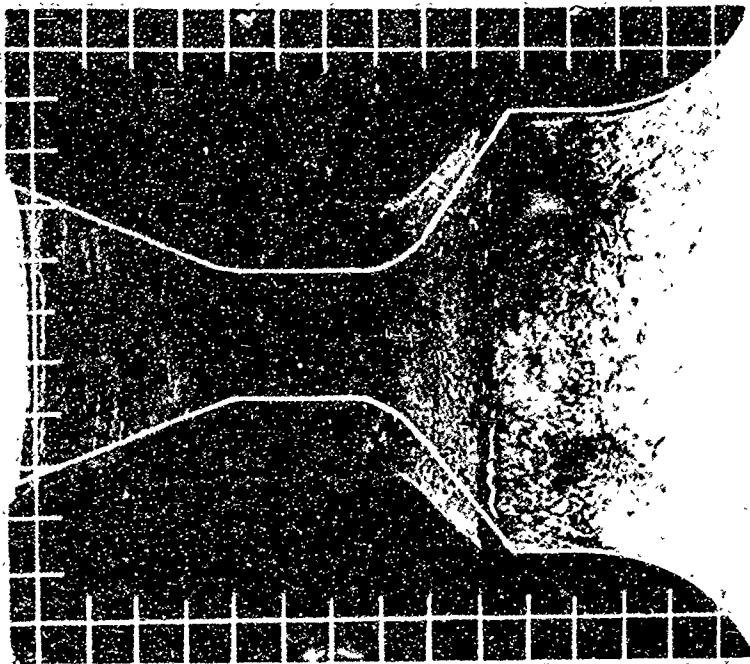
12 O'CLOCK



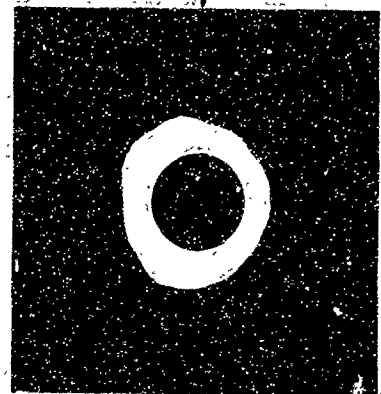
F00965 U

FIGURE 186. PROFILE AND AXIAL NOZZLE PHOTOGRAPHS

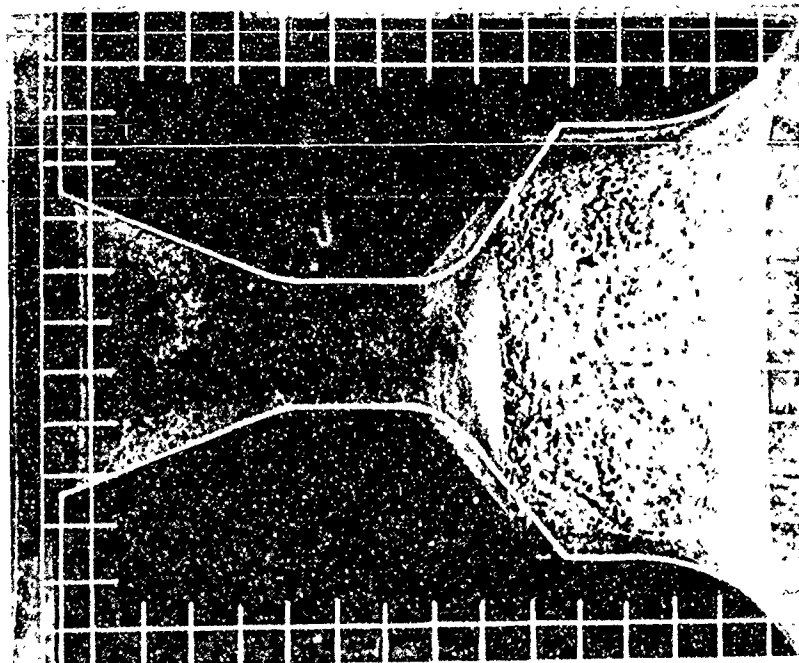
NOZZLE NO. ASD-481



12 O'CLOCK



NOZZLE NO. ASD-484



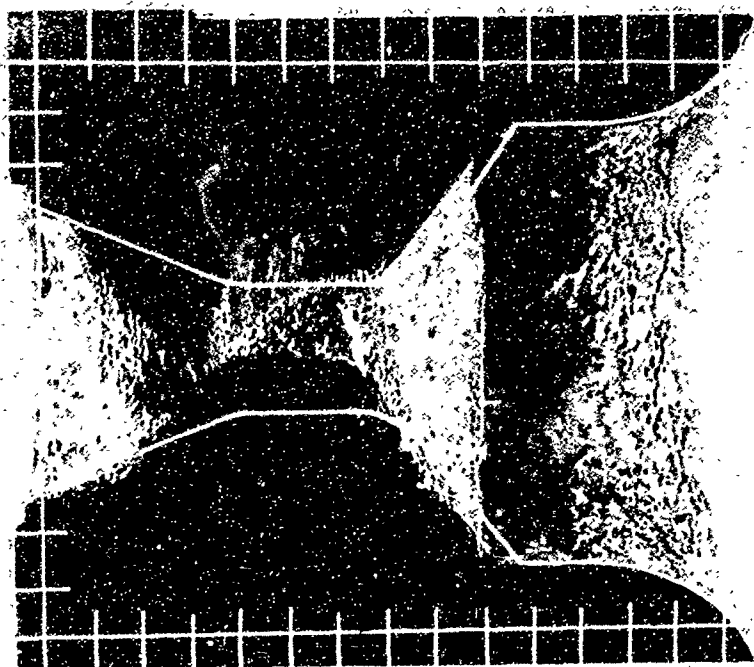
12 O'CLOCK



F00966 U

FIGURE 187. PROFILE AND AXIAL NOZZLE PHOTOGRAPHS

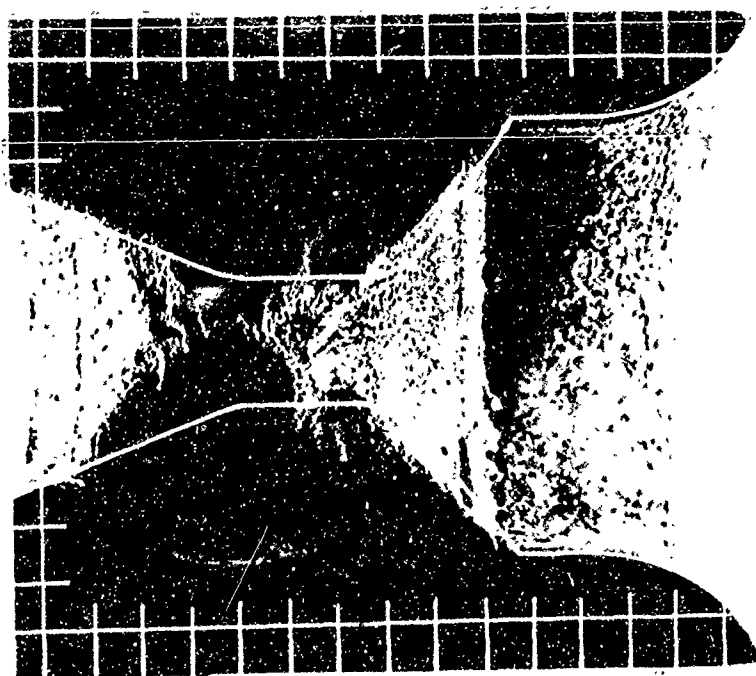
NOZZLE NO. ASD-485



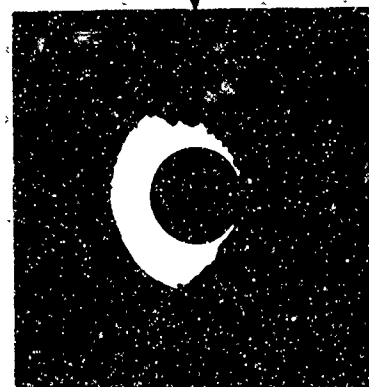
12 O'CLOCK



NOZZLE NO. ASD-486



12 O'CLOCK

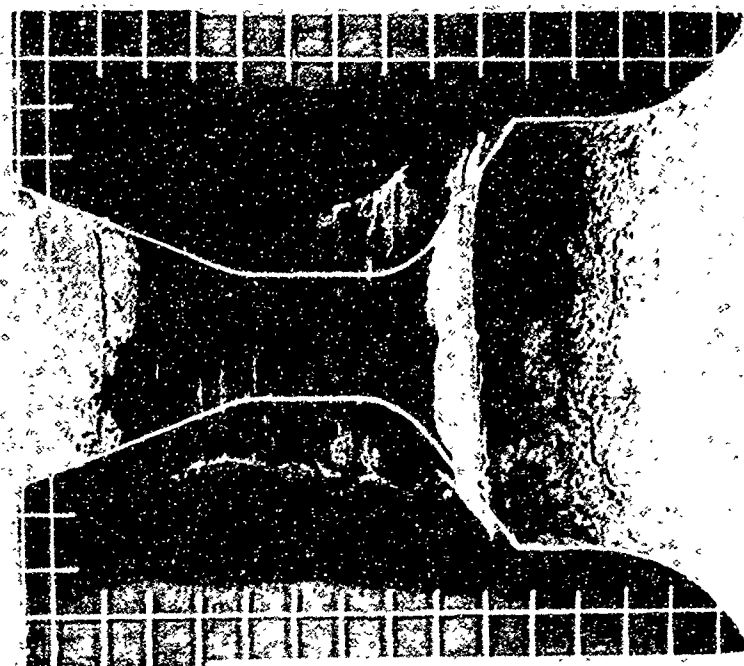


F00967 U

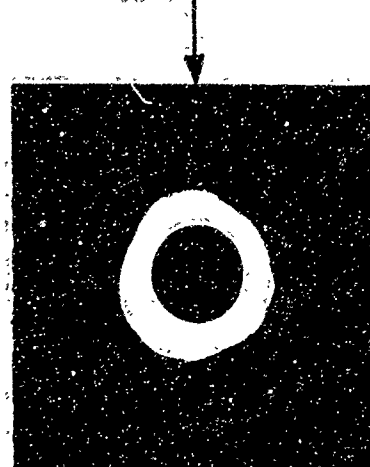
FIGURE 188. PROFILE AND AXIAL NOZZLE PHOTOGRAPHS



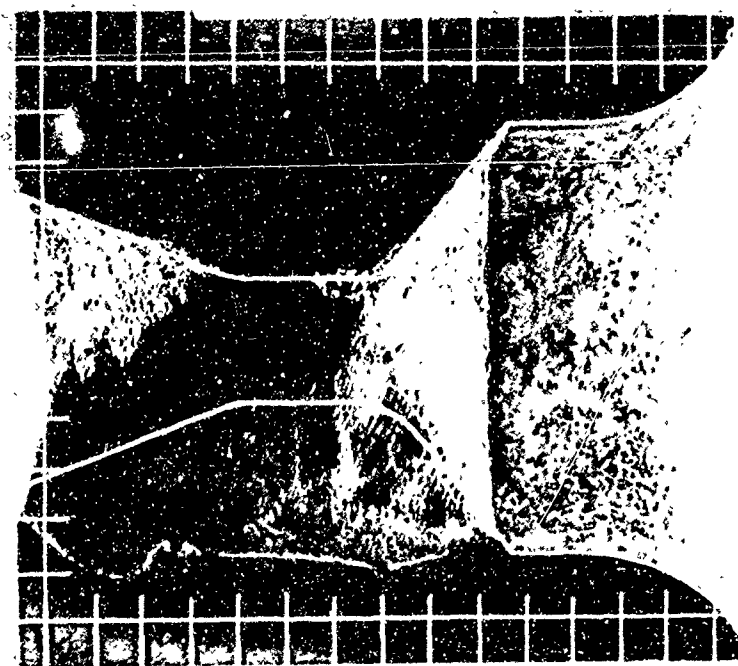
NOZZLE NO. ASD-487



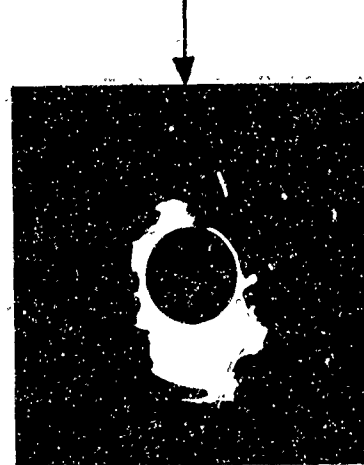
12 O'CLOCK



NOZZLE NO. ASD-488



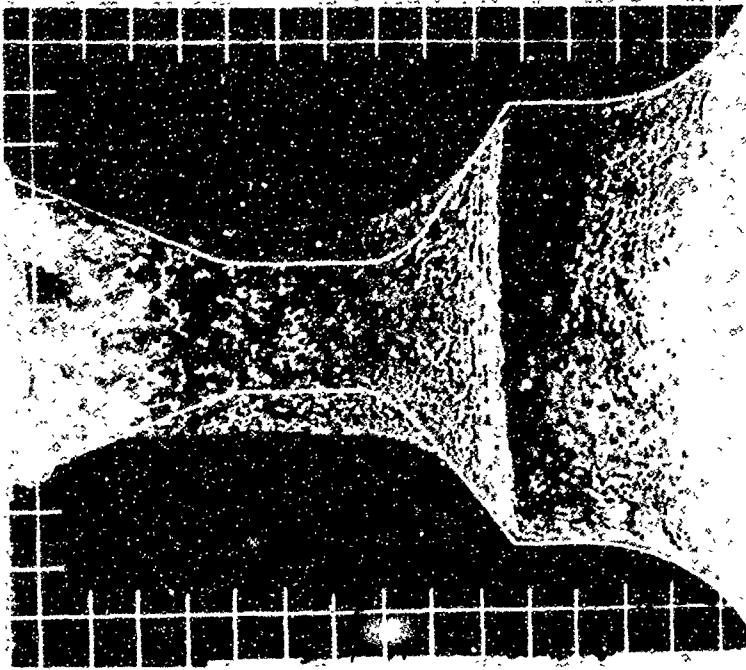
12 O'CLOCK



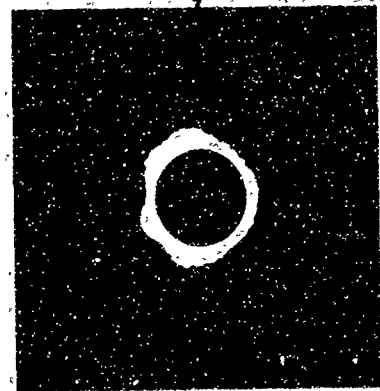
F00968 U

FIGURE 189. PROFILE AND AXIAL NOZZLE PHOTOGRAPHS

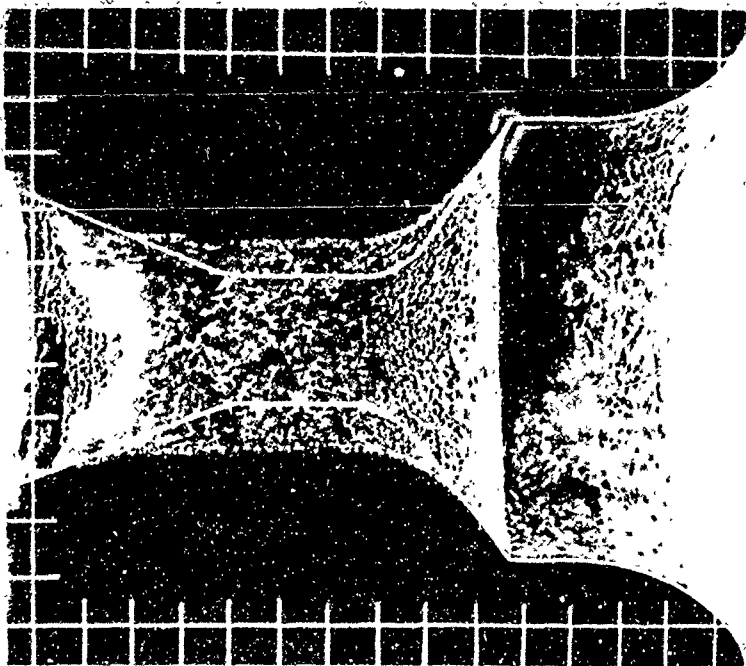
NOZZLE NO. ASD-492



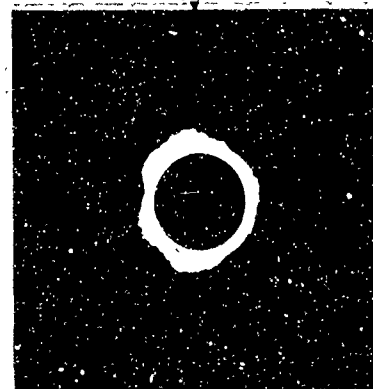
12 O'CLOCK



NOZZLE NO. ASD-493



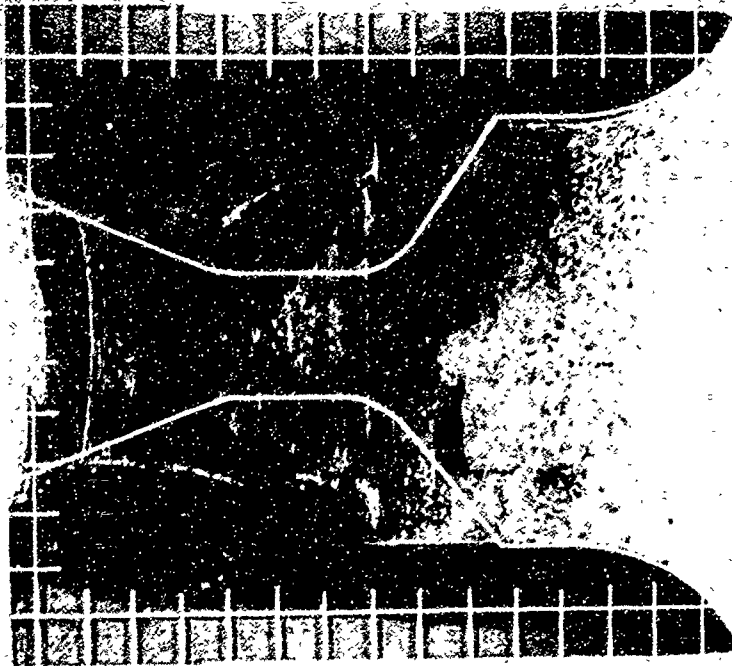
12 O'CLOCK



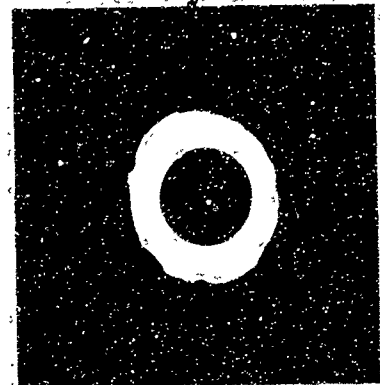
F00969 U

FIGURE 190. PROFILE AND AXIAL NOZZLE PHOTOGRAPHS

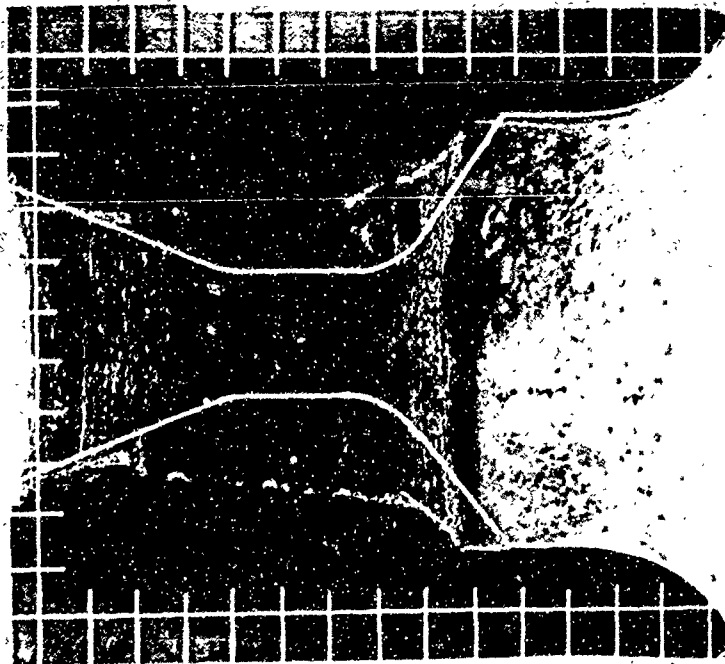
NOZZLE NO. ASD-494



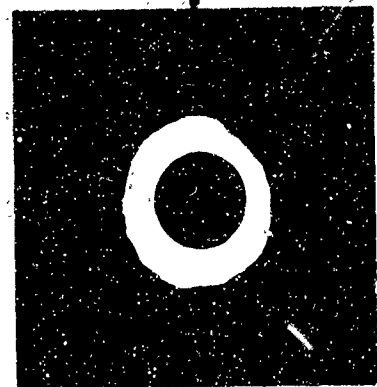
12 O'CLOCK



NOZZLE NO. ASD-495



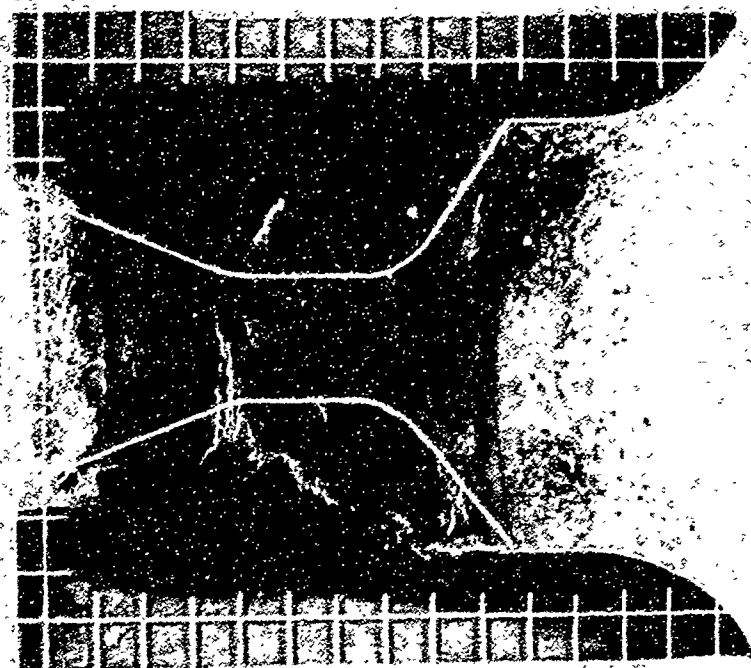
12 O'CLOCK



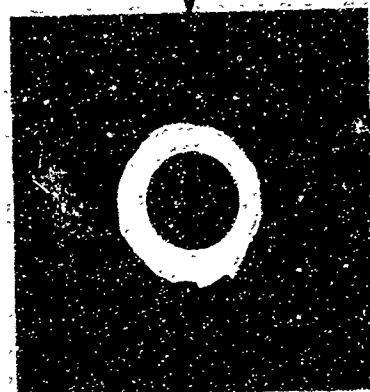
F00970 U

FIGURE 191. PROFILE AND AXIAL NOZZLE PHOTOGRAPHS

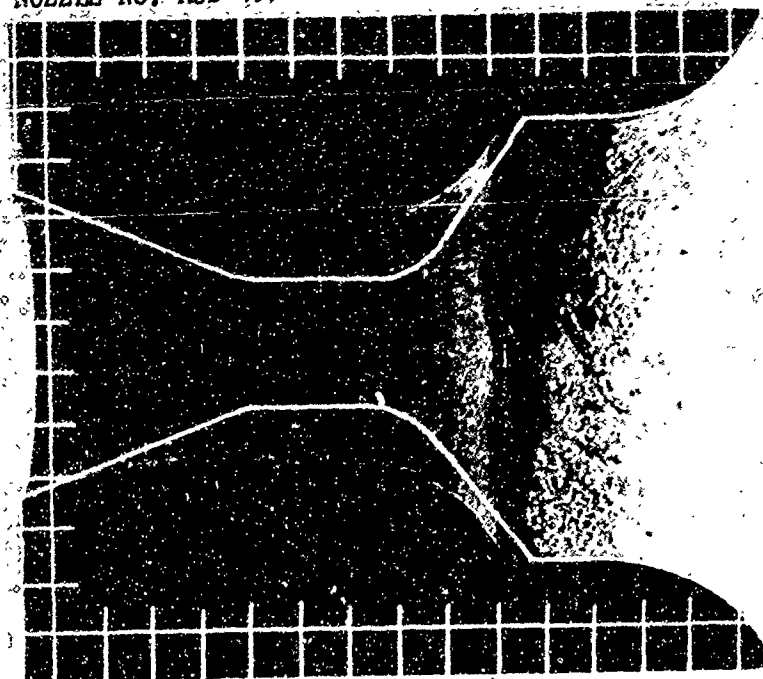
NOZZLE NO. ASD-496



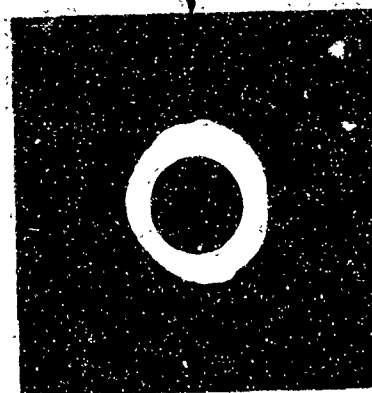
12 O'CLOCK



NOZZLE NO. ASD-497



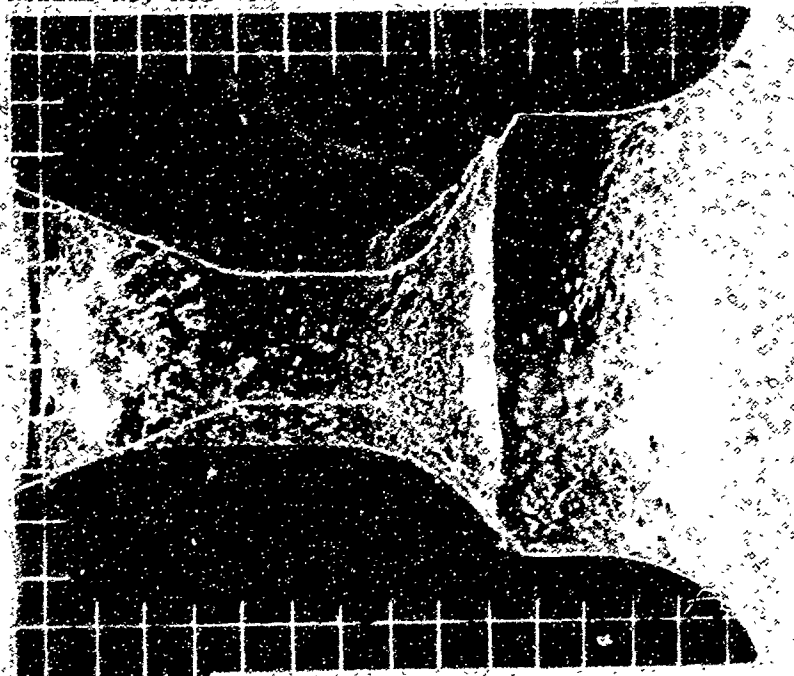
12 O'CLOCK



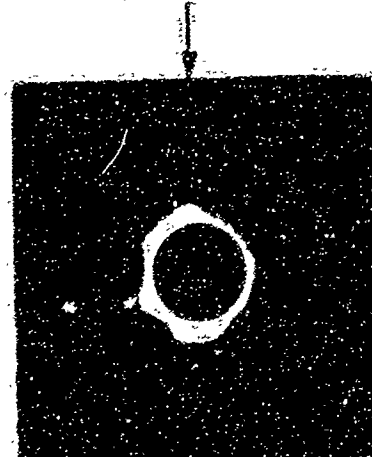
F00971 U

FIGURE 192. PROFILE AND AXIAL NOZZLE PHOTOGRAPHS

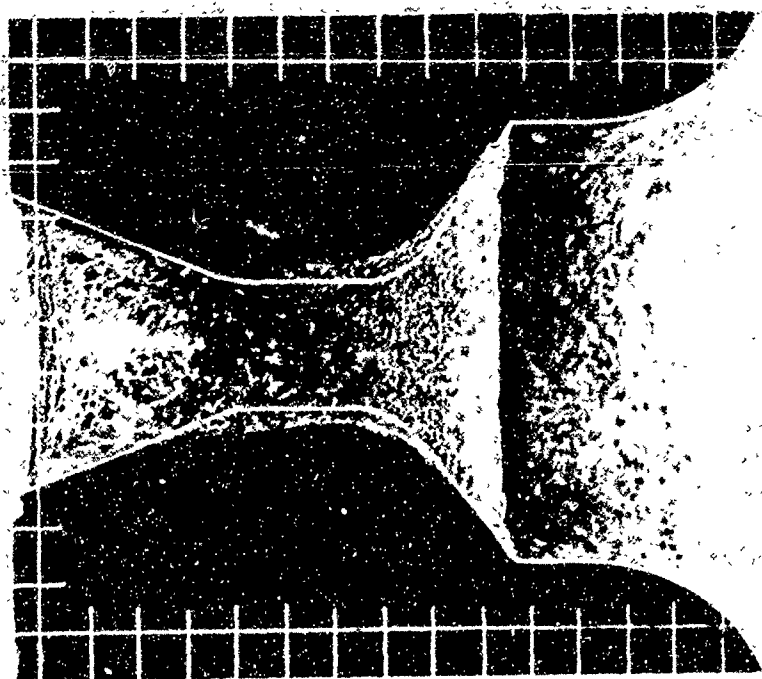
NOZZLE NO. ASD-498



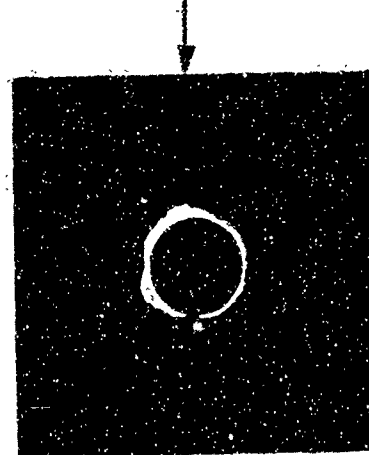
12 O'CLOCK



NOZZLE NO. ASD-499



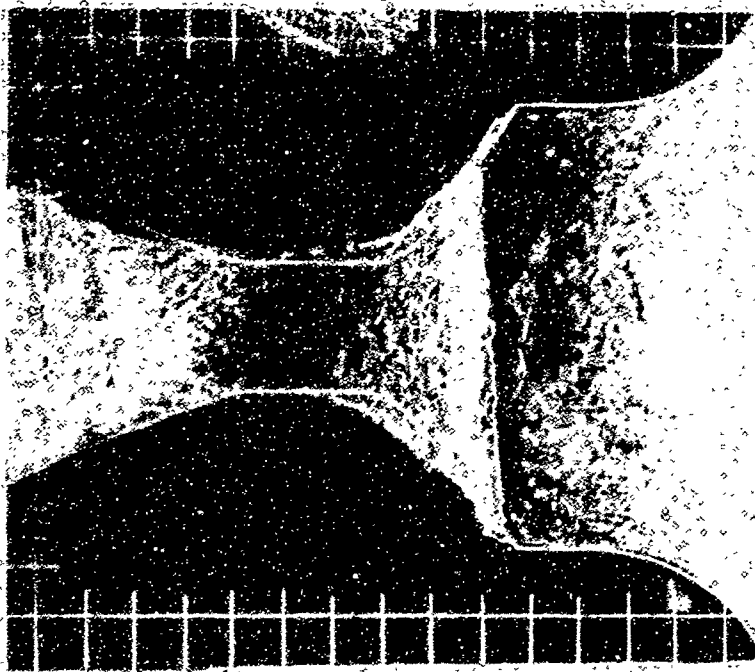
12 O'CLOCK



F00972 U

FIGURE 193. PROFILE AND AXIAL NOZZLE PHOTOGRAPHS

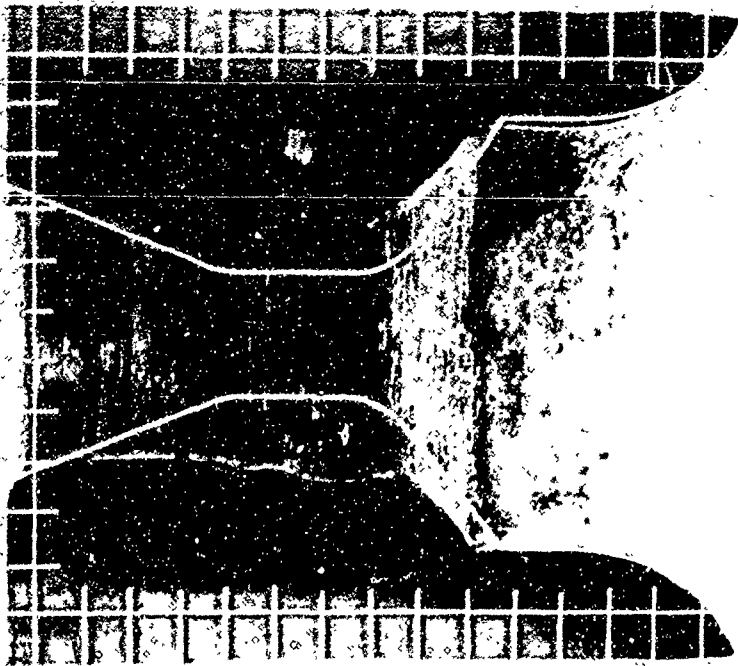
NOZZLE NO. ASD-500



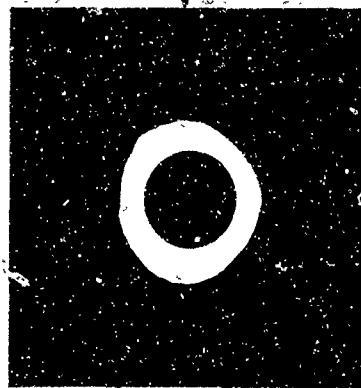
12 O'CLOCK



NOZZLE NO. ASD-501



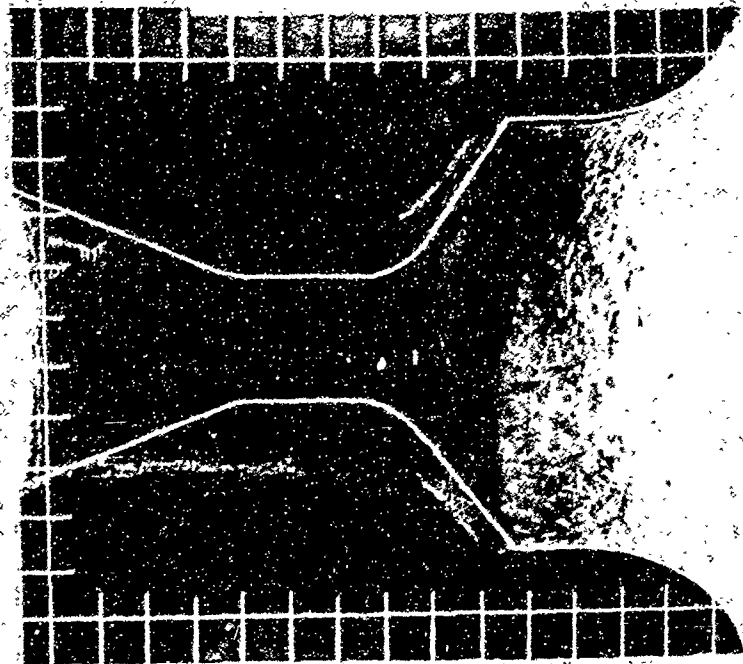
12 O'CLOCK



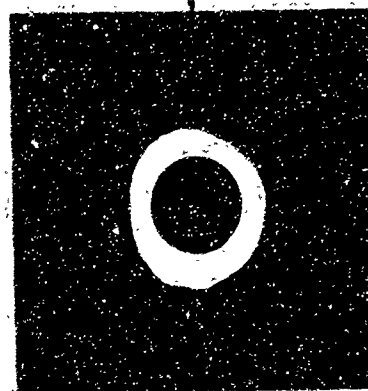
F00973 U

FIGURE 194. PROFILE AND AXIAL NOZZLE PHOTOGRAPHS

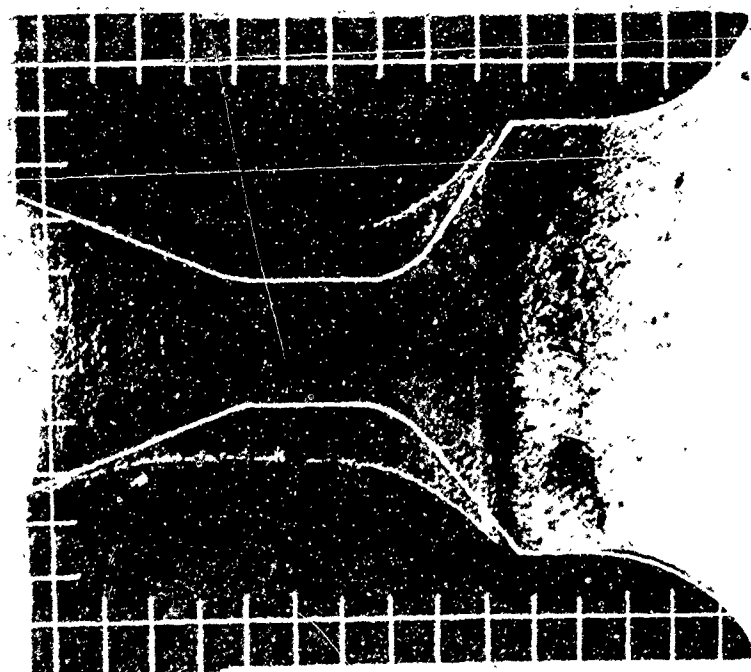
NOZZLE NO. ASD-502



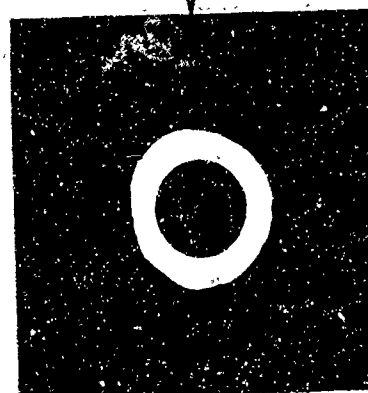
12 O'CLOCK



NOZZLE NO. ASD-503



12 O'CLOCK

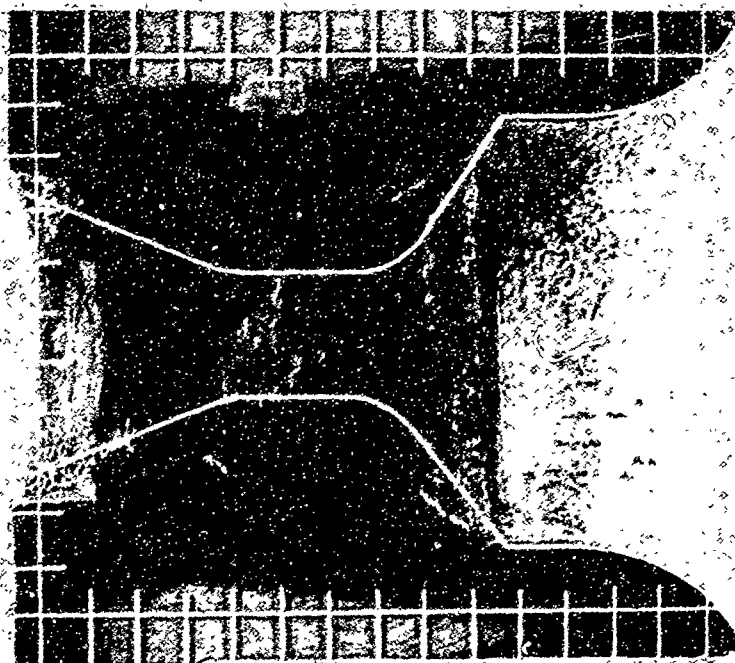


F00974 U

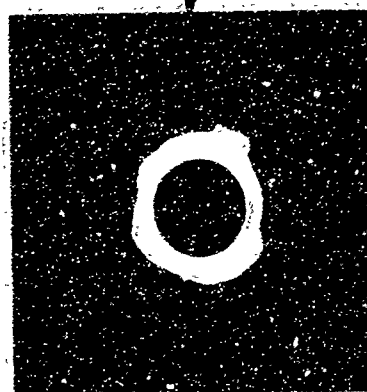
FIGURE 195. PROFILE AND AXIAL NOZZLE PHOTOGRAPHS



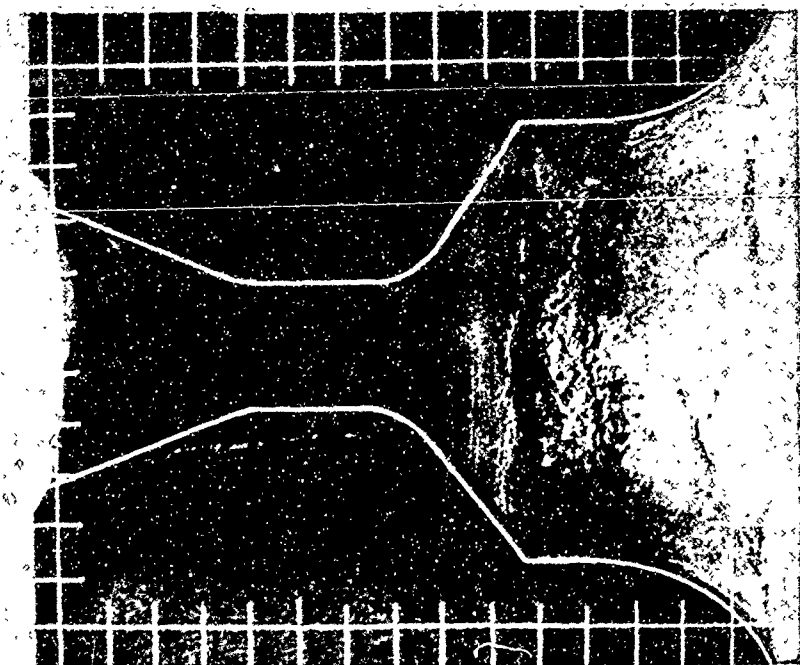
NOZZLE NO. ASD-504



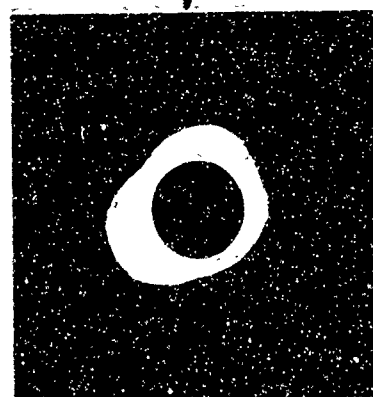
12 O'CLOCK



NOZZLE NO. ASD-505



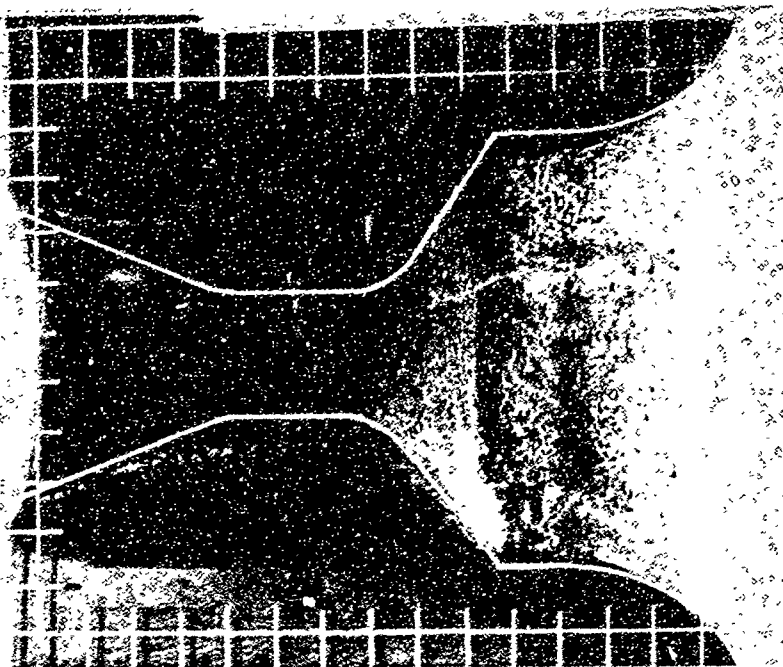
12 O'CLOCK



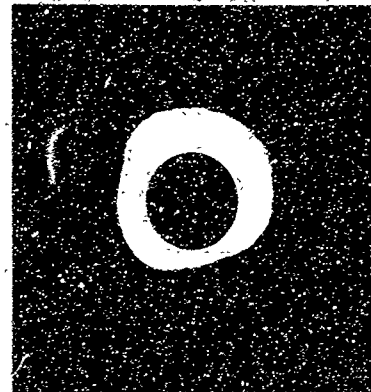
F00975 U

FIGURE 196. PROFILE AND AXIAL NOZZLE PHOTOGRAPHS

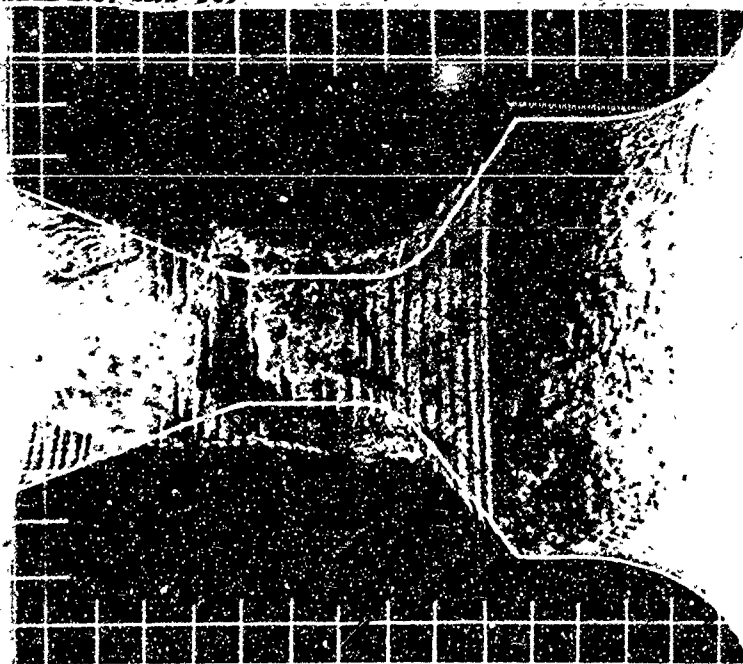
NOZZLE NO. ASD-507



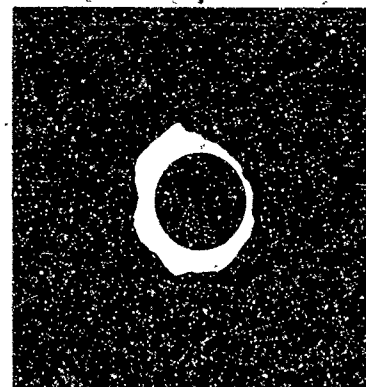
12 O'CLOCK



NOZZLE NO. ASD-509



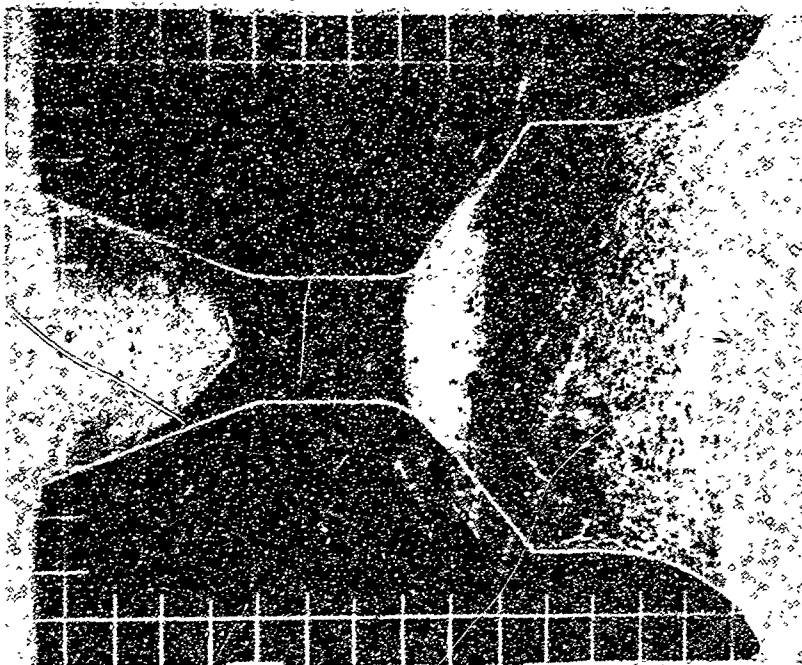
12 O'CLOCK



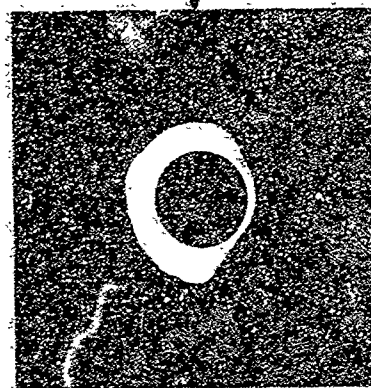
R13890U

FIGURE 197. PROFILE AND AXIAL NOZZLE PHOTOGRAPHS

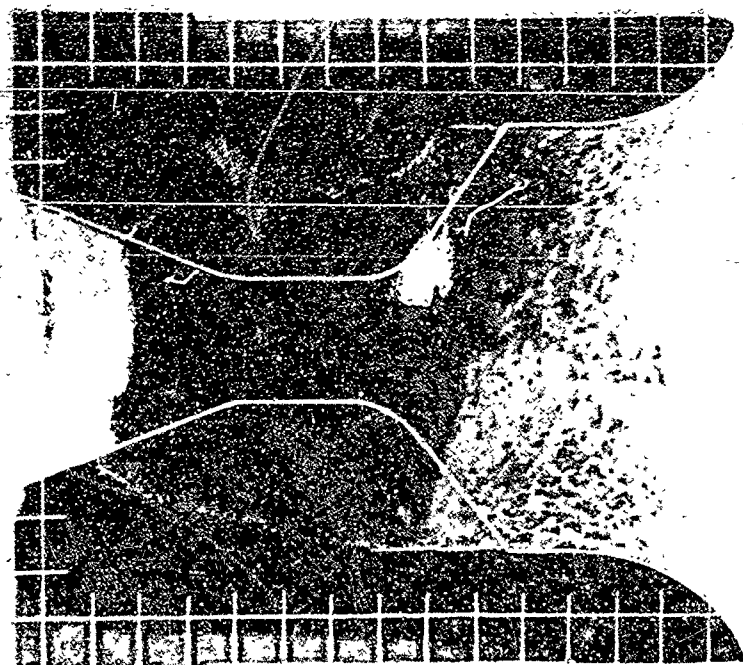
NOZZLE NO. ASD-514



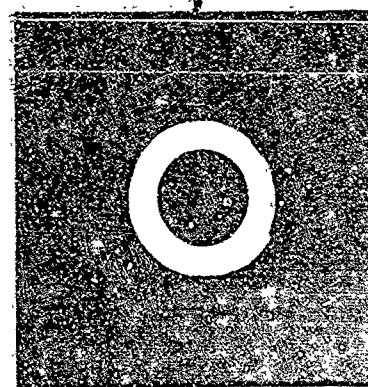
12 O'CLOCK



NOZZLE NO. ASD-515



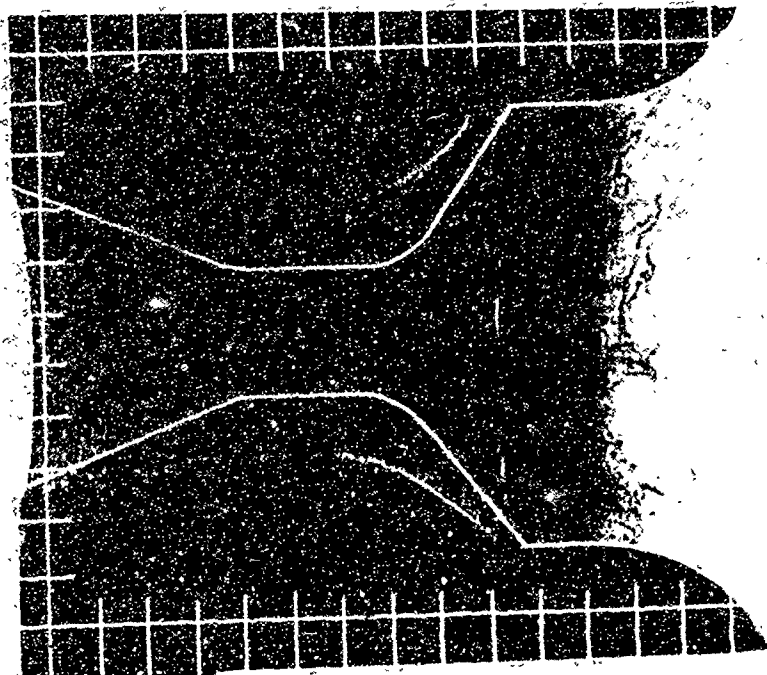
12 O'CLOCK



F00976 U

FIGURE 198. PROFILE AND AXIAL NOZZLE PHOTOGRAPHS

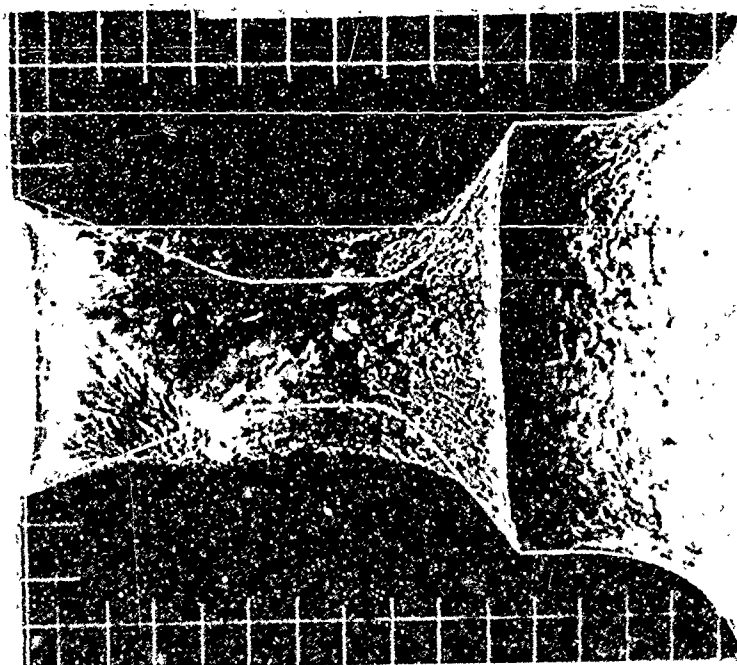
NOZZLE NO. ASD-516



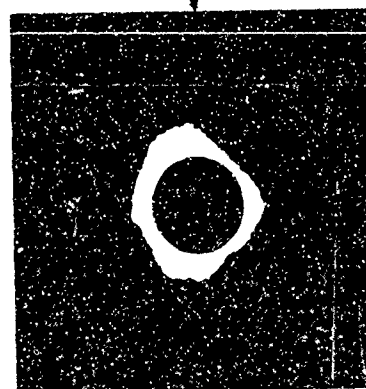
12 O'CLOCK



NOZZLE NO. ASD-517



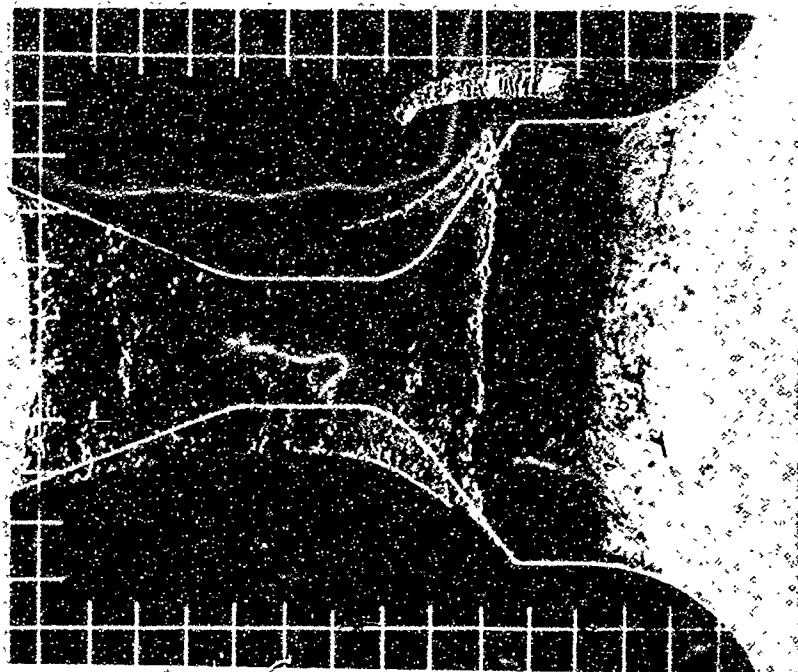
12 O'CLOCK



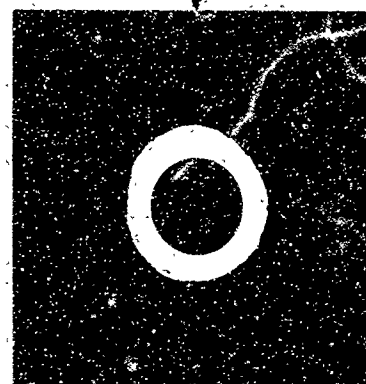
F00977 U

FIGURE 199. PROFILE AND AXIAL NOZZLE PHOTOGRAPHS

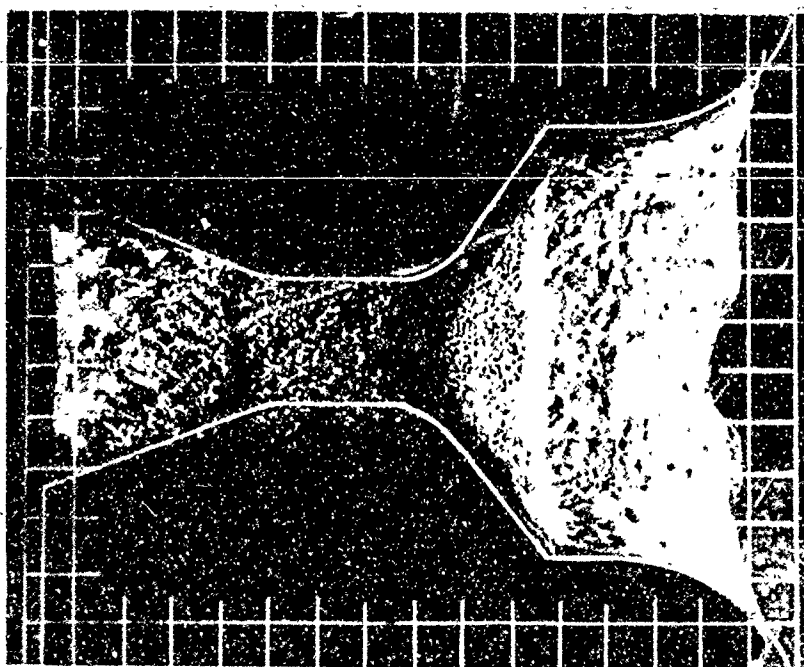
NOZZLE NO. ASD-518



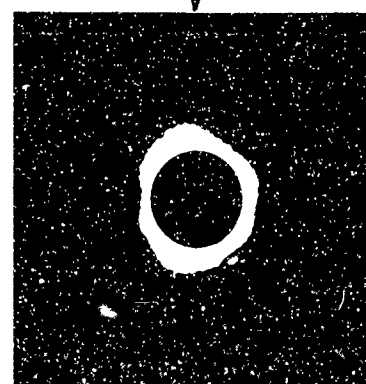
12 O'CLOCK



NOZZLE NO. ASD-519



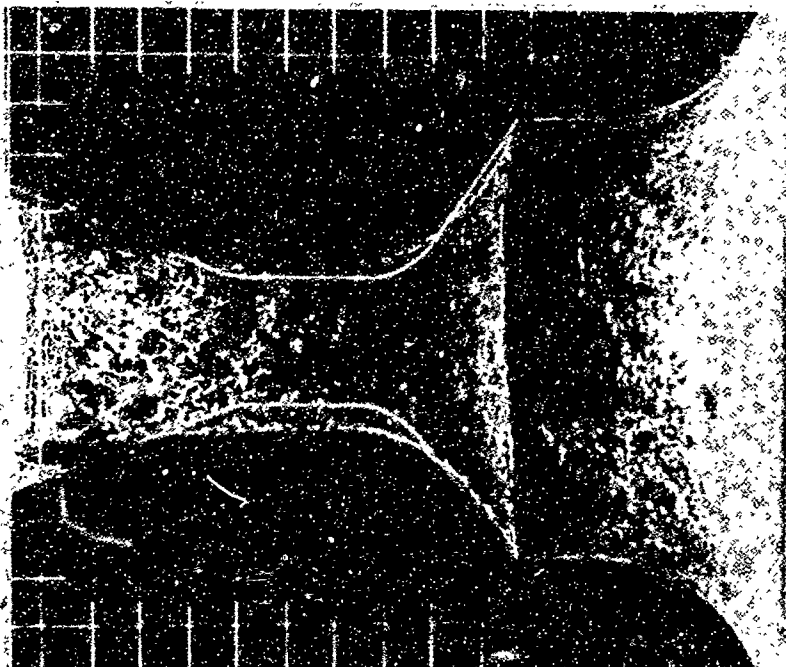
12 O'CLOCK



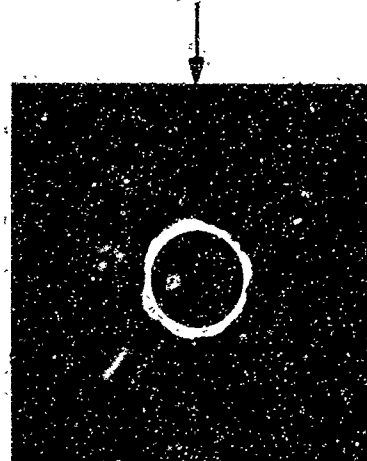
F00978 U

FIGURE 200. PROFILE AND AXIAL NOZZLE PHOTOGRAPHS

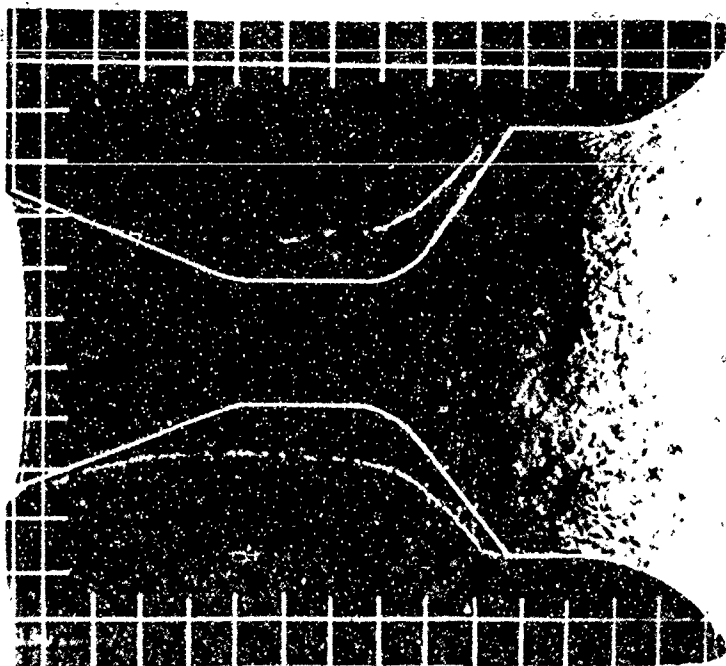
NOZZLE NO. ASD-520



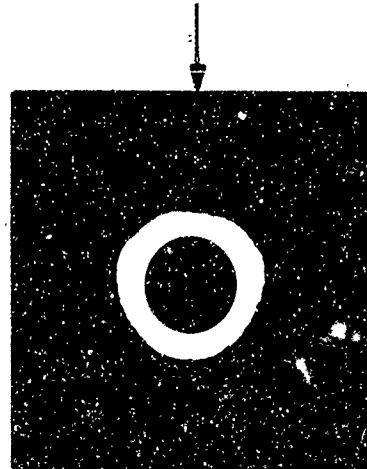
12 O'CLOCK



NOZZLE NO. ASD-522



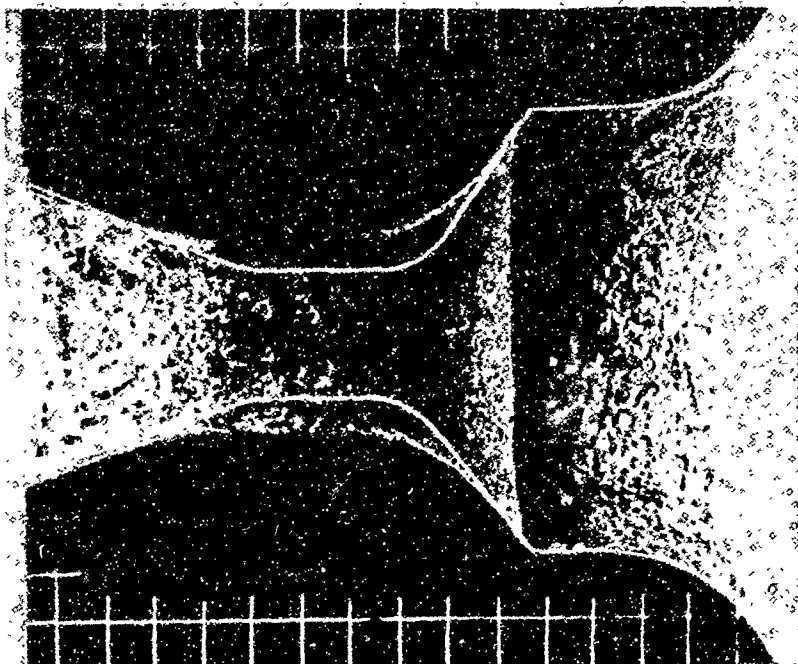
12 O'CLOCK



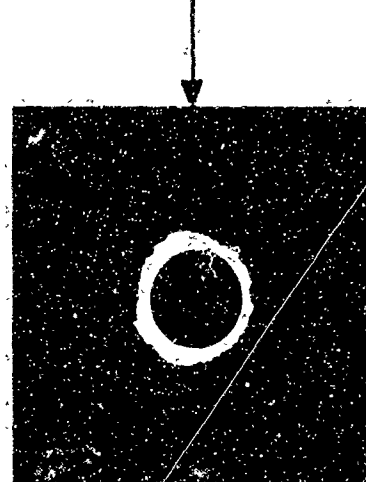
F00979 U

FIGURE 201. PROFILE AND AXIAL NOZZLE PHOTOGRAPHS

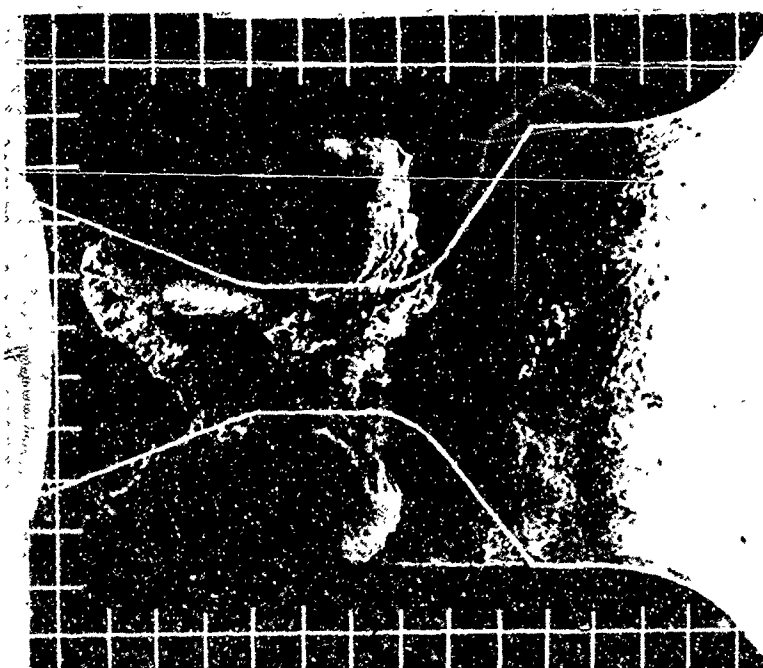
NOZZLE NO. ASD-524



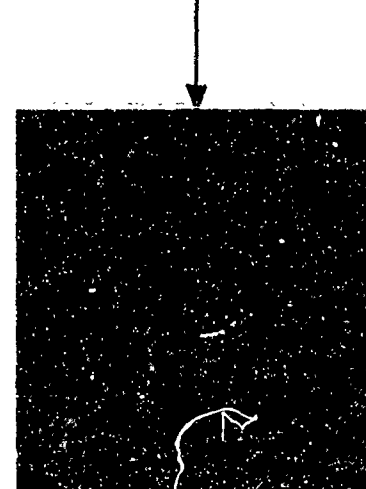
12 O'CLOCK



NOZZLE NO. ASD-526



12 O'CLOCK

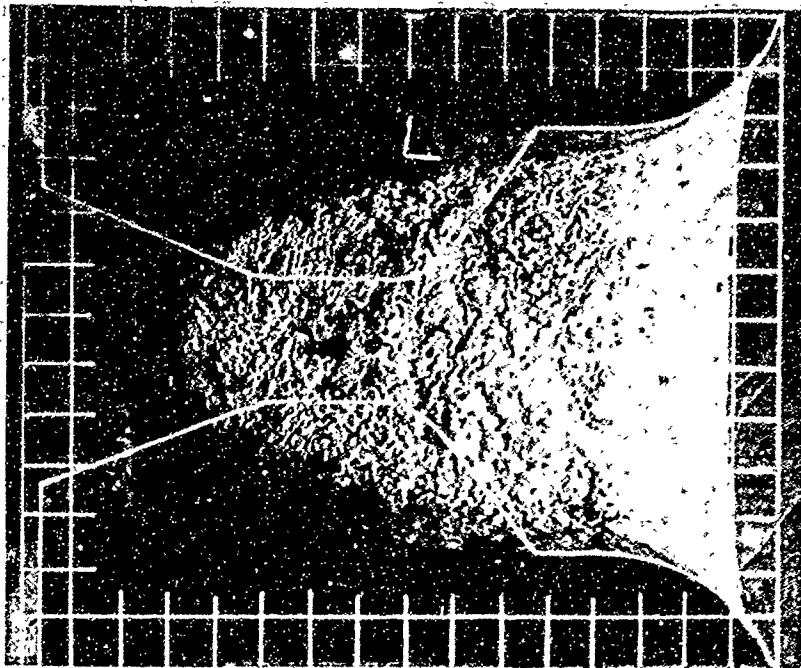


F00930 U

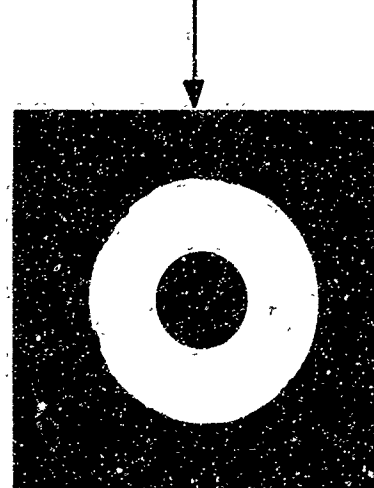
FIGURE 202. PROFILE AND AXIAL NOZZLE PHOTOGRAPHS



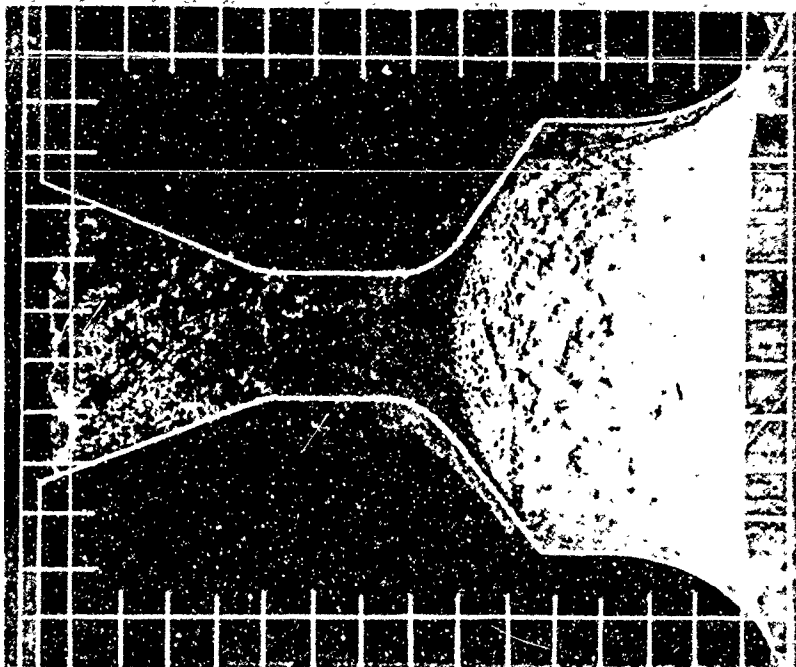
NOZZLE NO. ASD-527



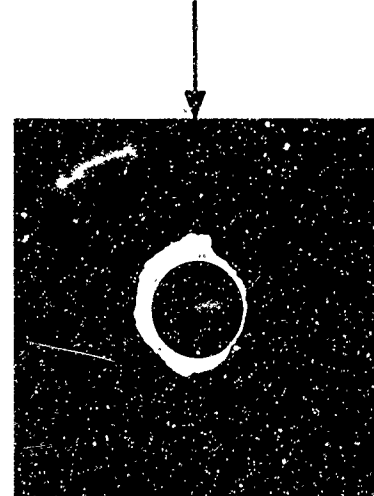
12 O'CLOCK



NOZZLE NO. ASD-528



12 O'CLOCK



F00981 U

FIGURE 203. PROFILE AND AXIAL NOZZLE PHOTOGRAPHS

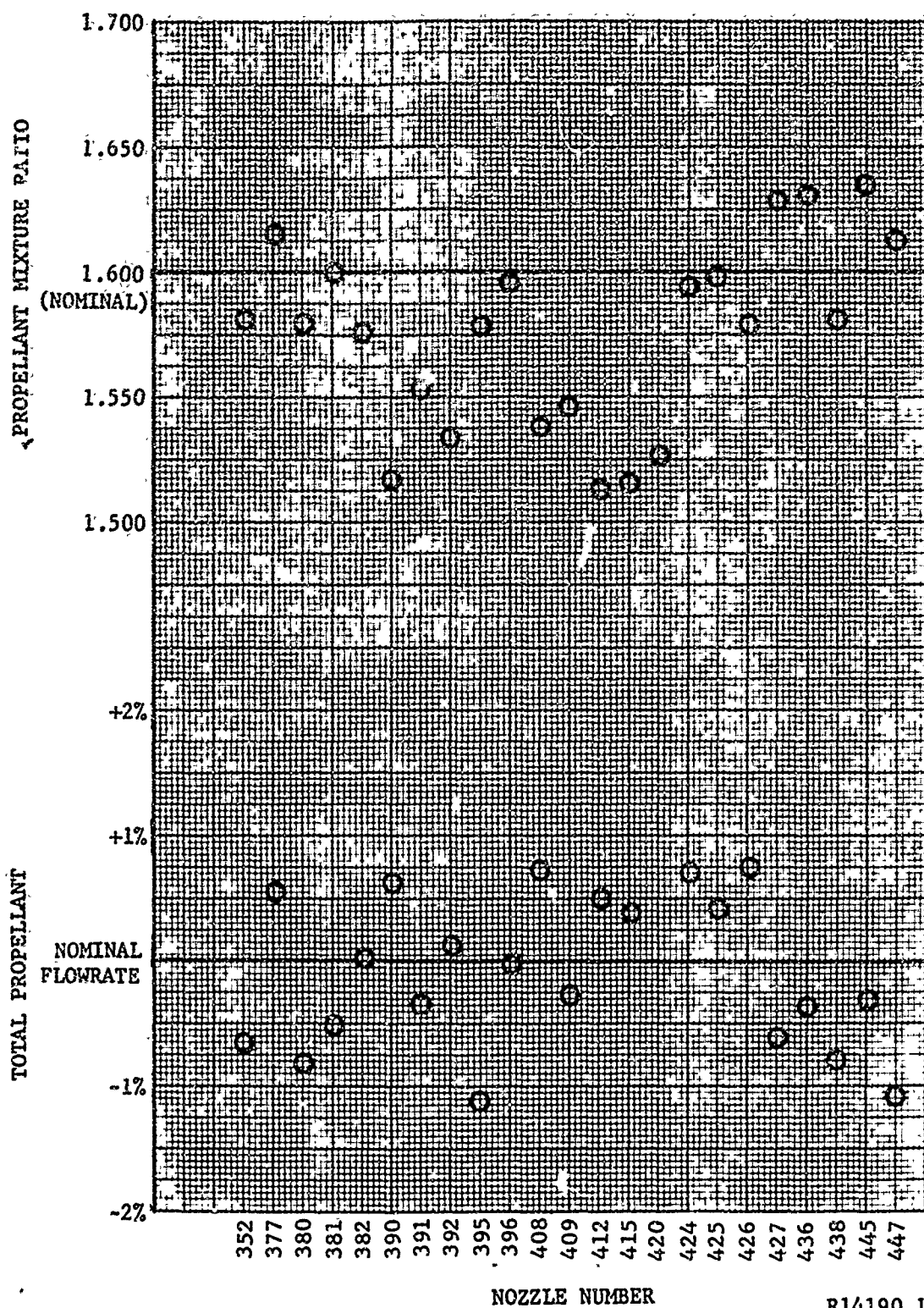


FIGURE 204A. TEST-TO-TEST PROPELLANT MIXTURE RATIO AND TOTAL PROPELLANT FLOWRATE VARIATION

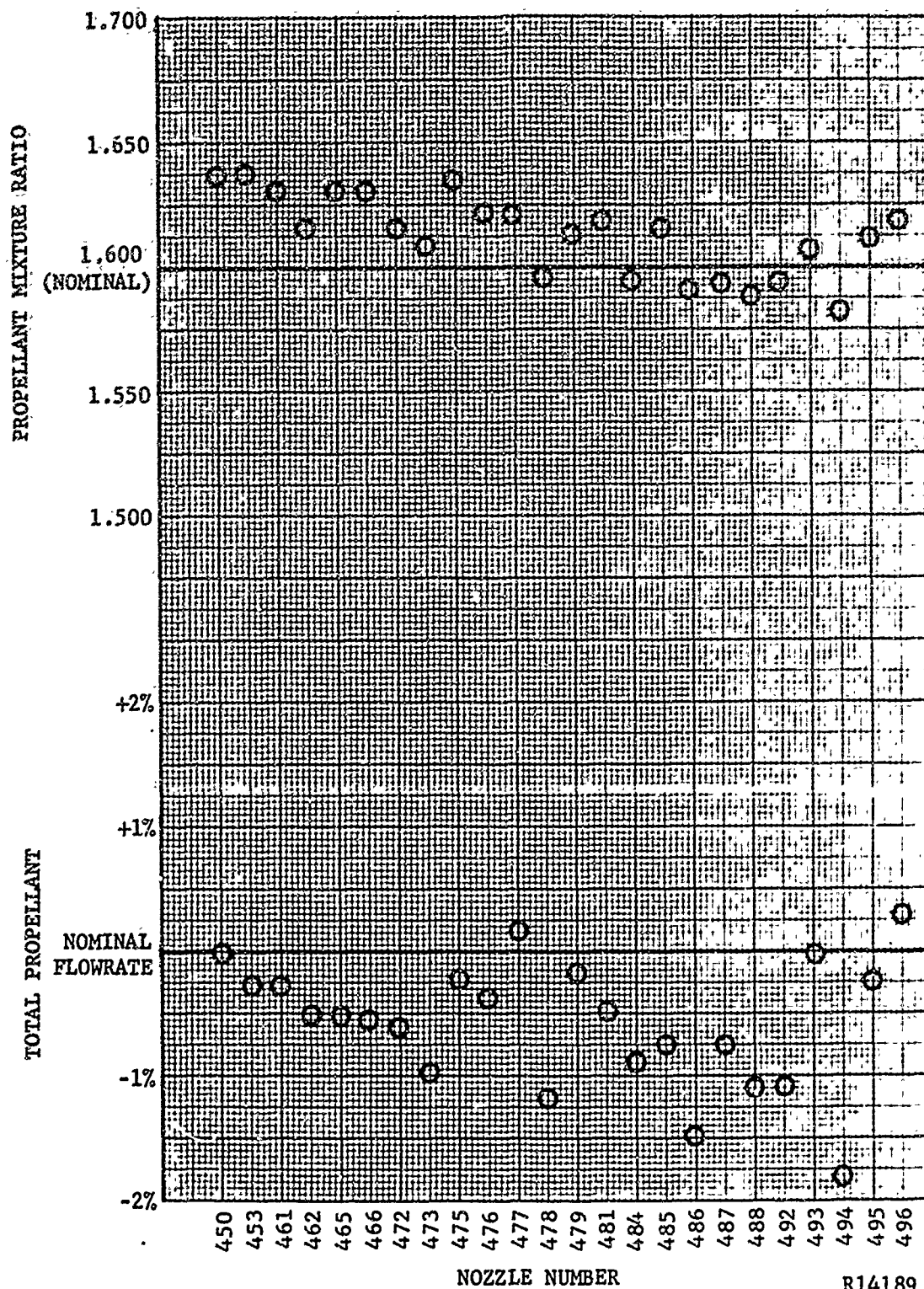
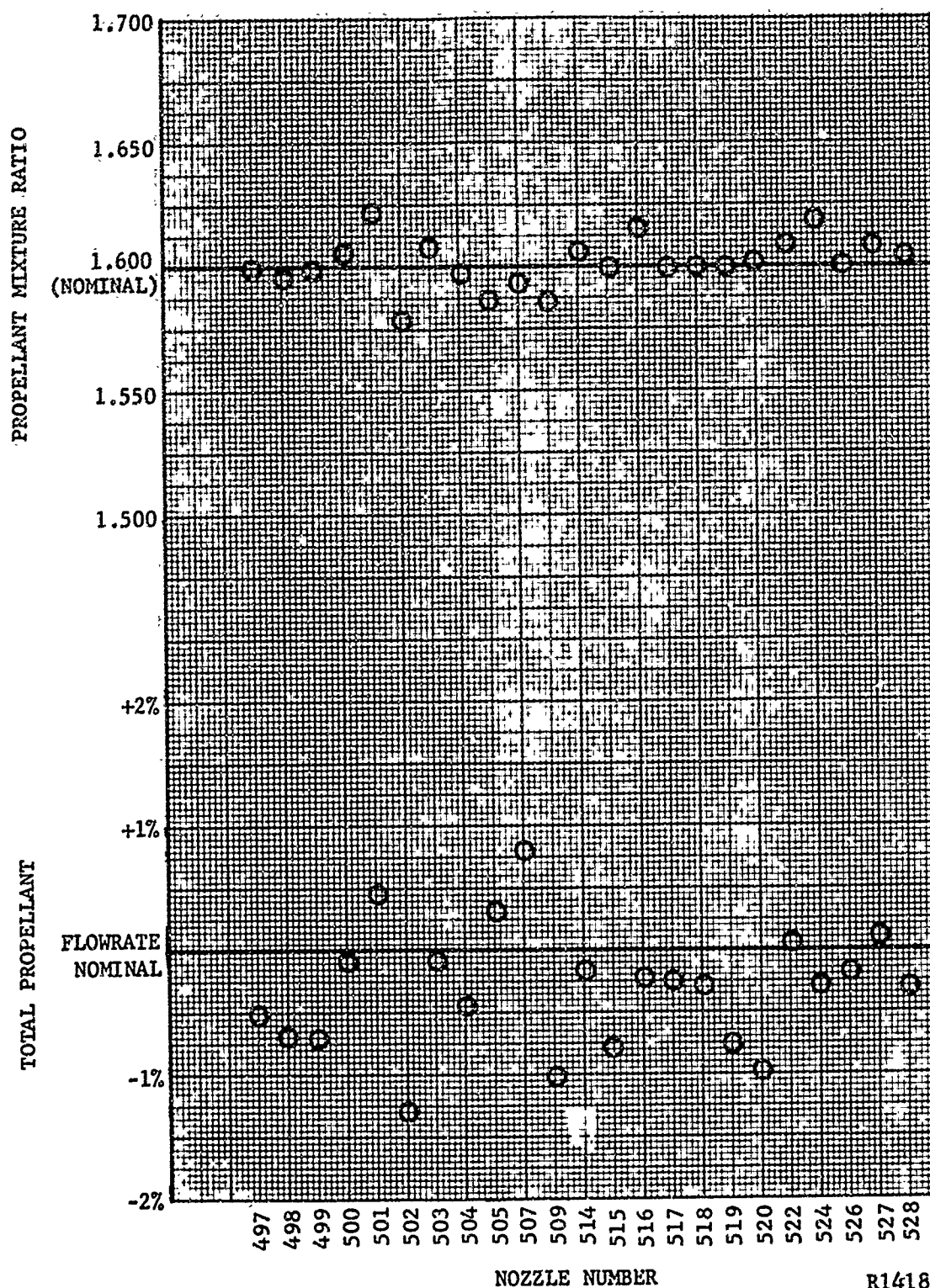


FIGURE 204B. TEST-TO-TEST PROPELLANT MIXTURE RATIO AND TOTAL PROPELLANT FLOWRATE VARIATION



FIXTURE 204C. TEST-TO-TEST PROPELLANT MIXTURE RATIO AND TOTAL PROPELLANT FLOWRATE VARIATION

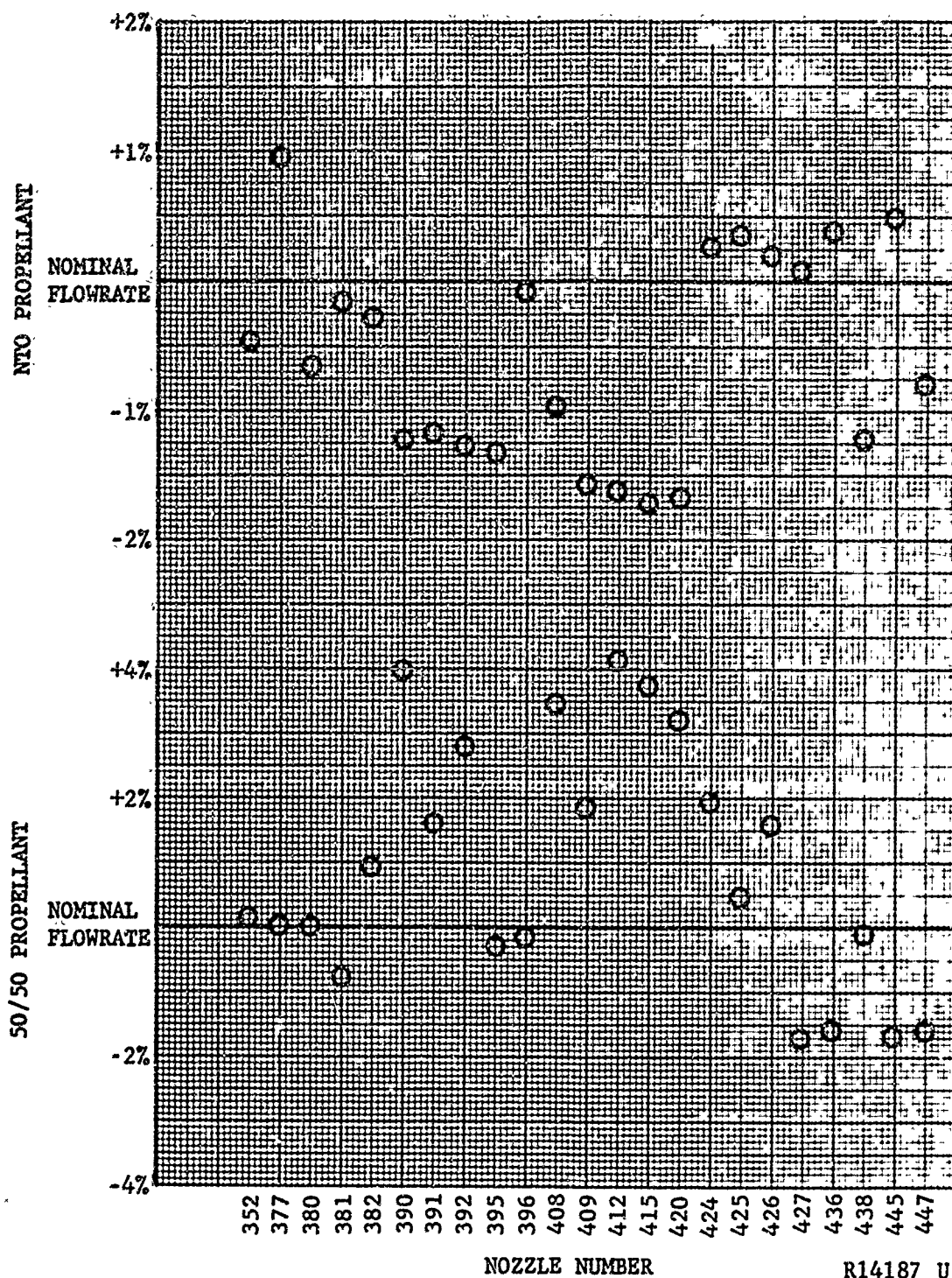
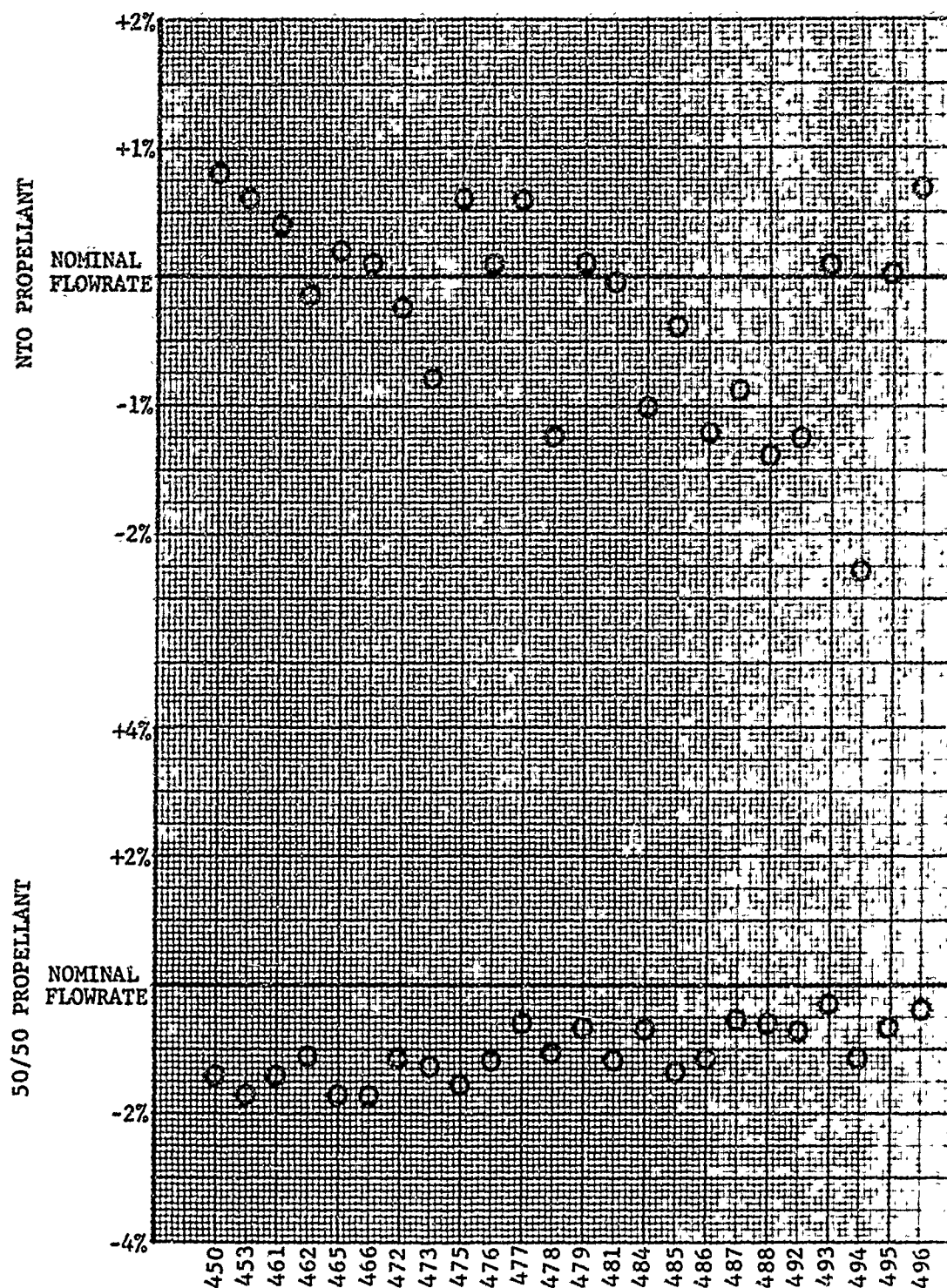


FIGURE 205A TEST-TO-TEST PROPELLANT FLOWRATE VARIATION FROM NOMINAL CONDITION

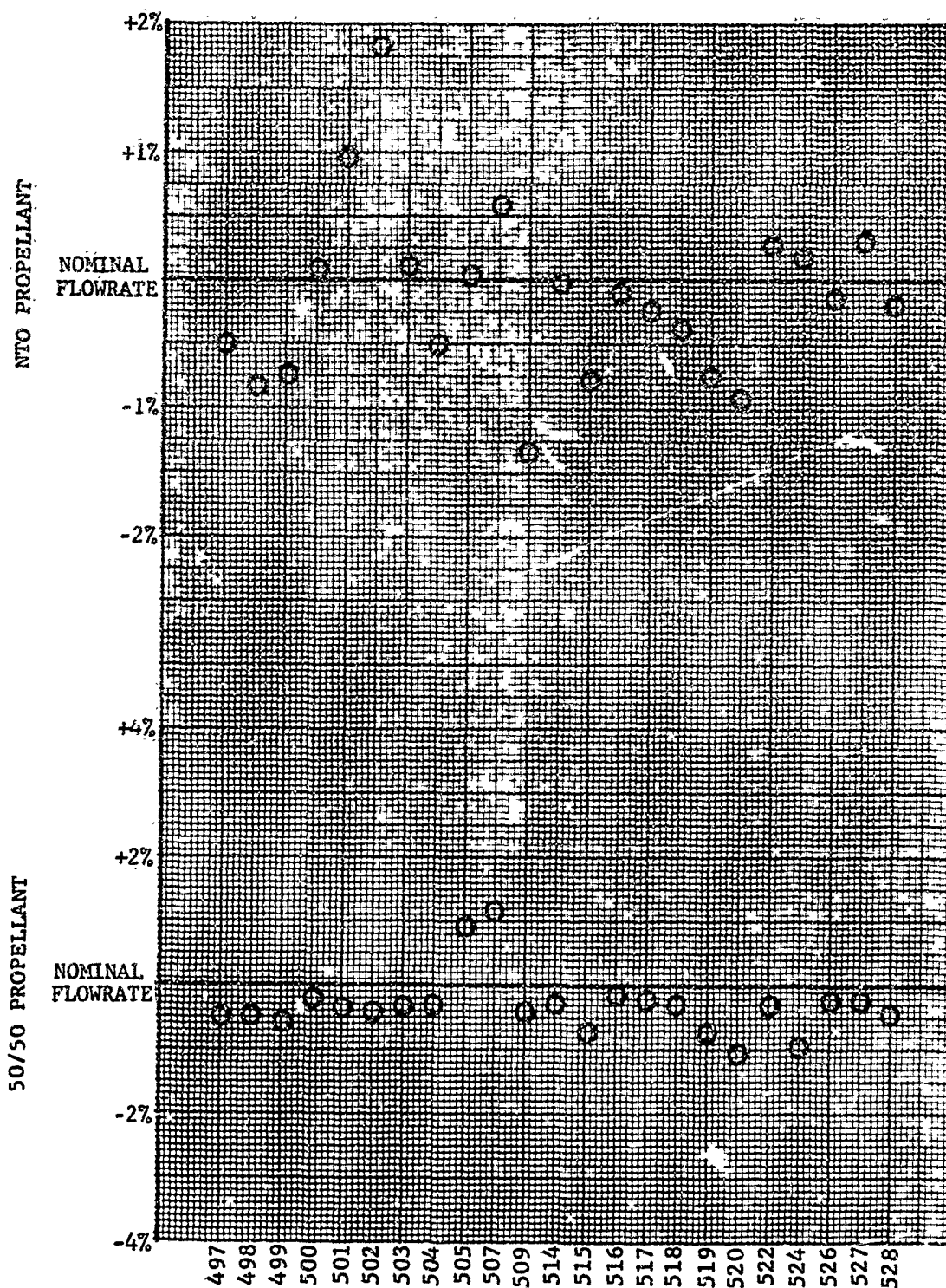




NOZZLE NUMBER

R14186 U

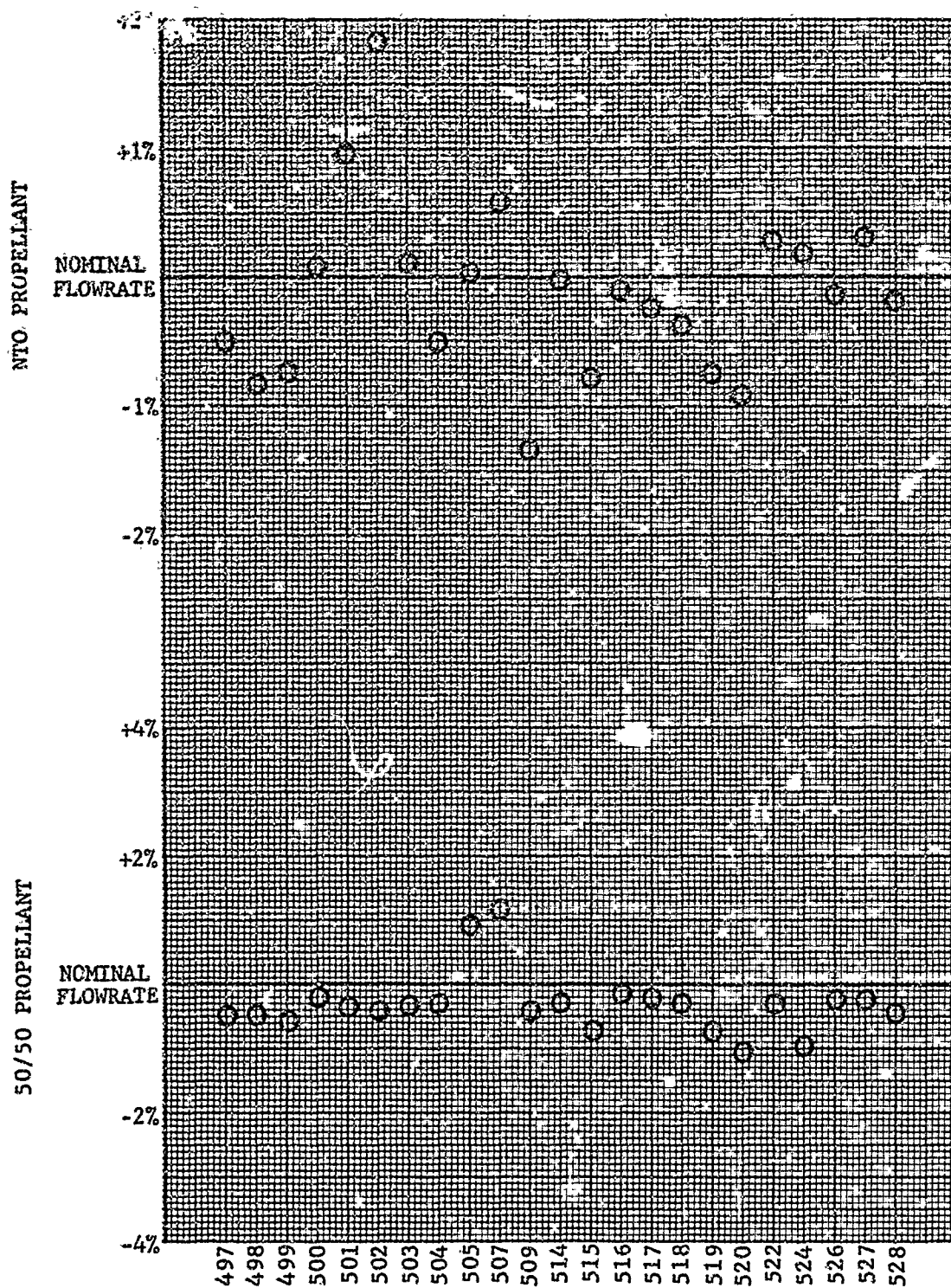
FIGURE 205B. TEST-TO-TEST PROPELLANT FLOWRATE VARIATION FROM NOMINAL CONDITION



R14191 U

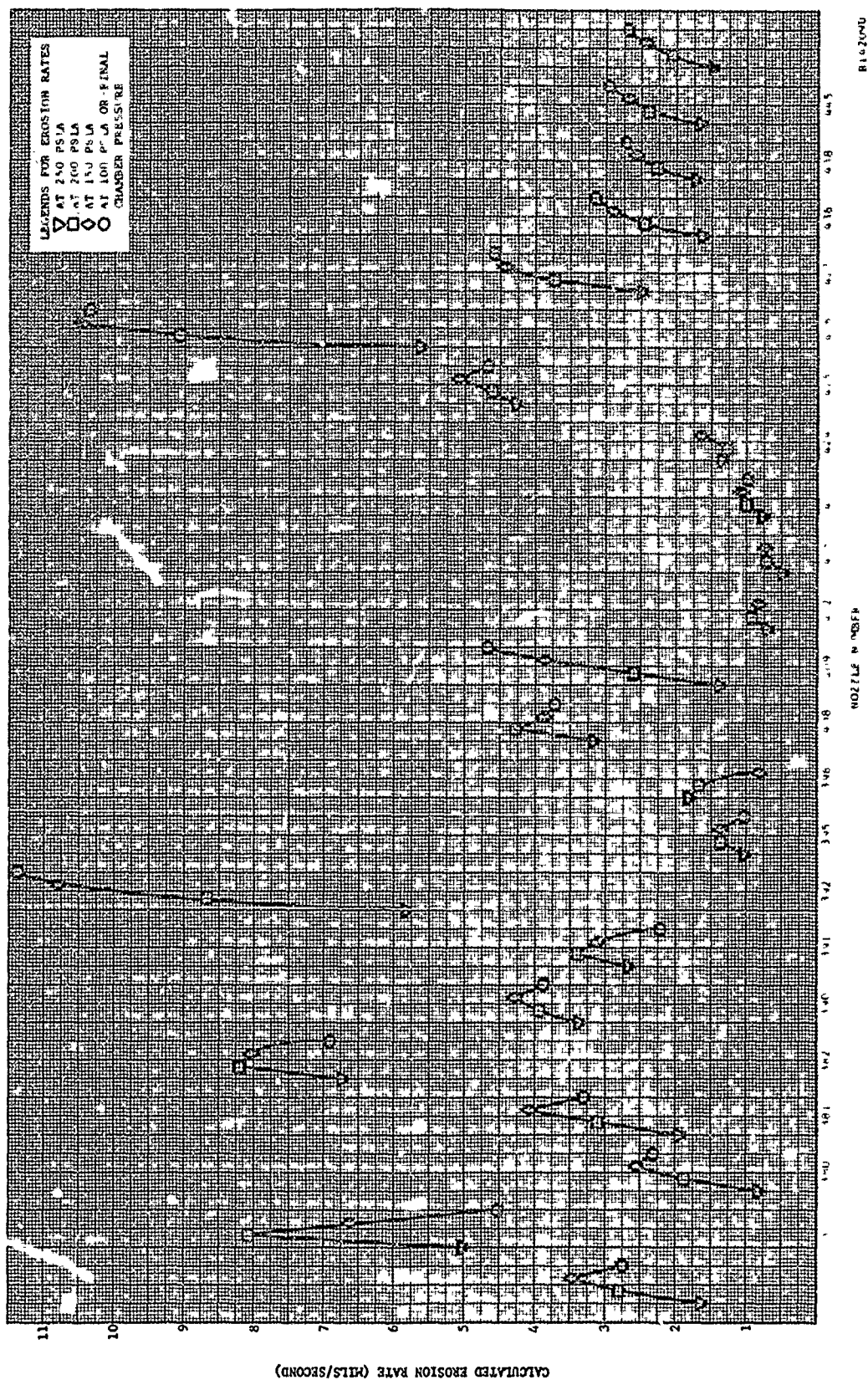
FIGURE 205C. TEST-TO-TEST PROPELLANT FLOWRATE VARIATION FROM NOMINAL CONDITION NOZZLE NUMBER





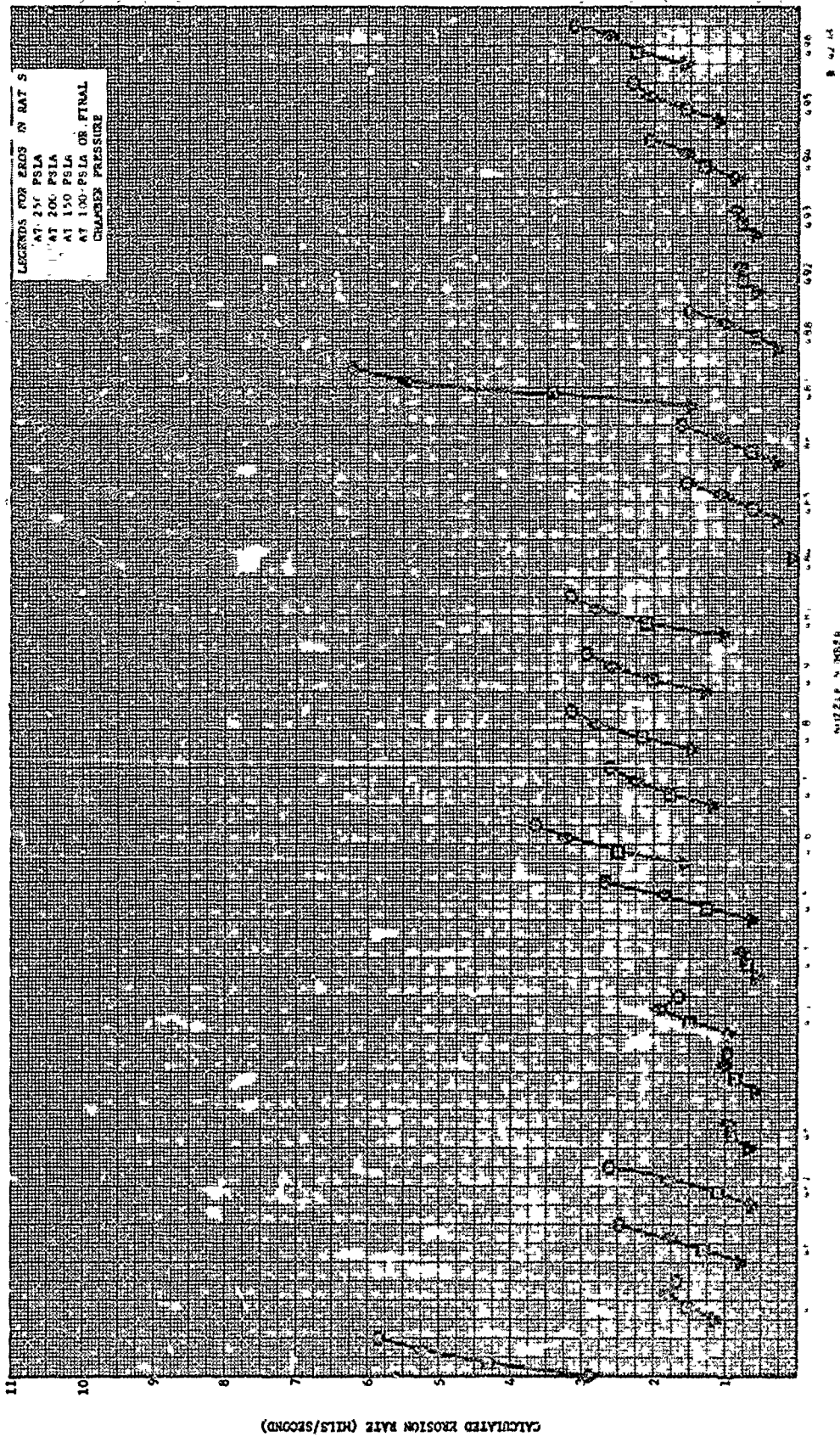
R14191 U

FIGURE 205C. TEST-TO-TEST PROPELLANT FLOWRATE VARIATION FROM NOMINAL CONDITION NOZZLE NUMBER



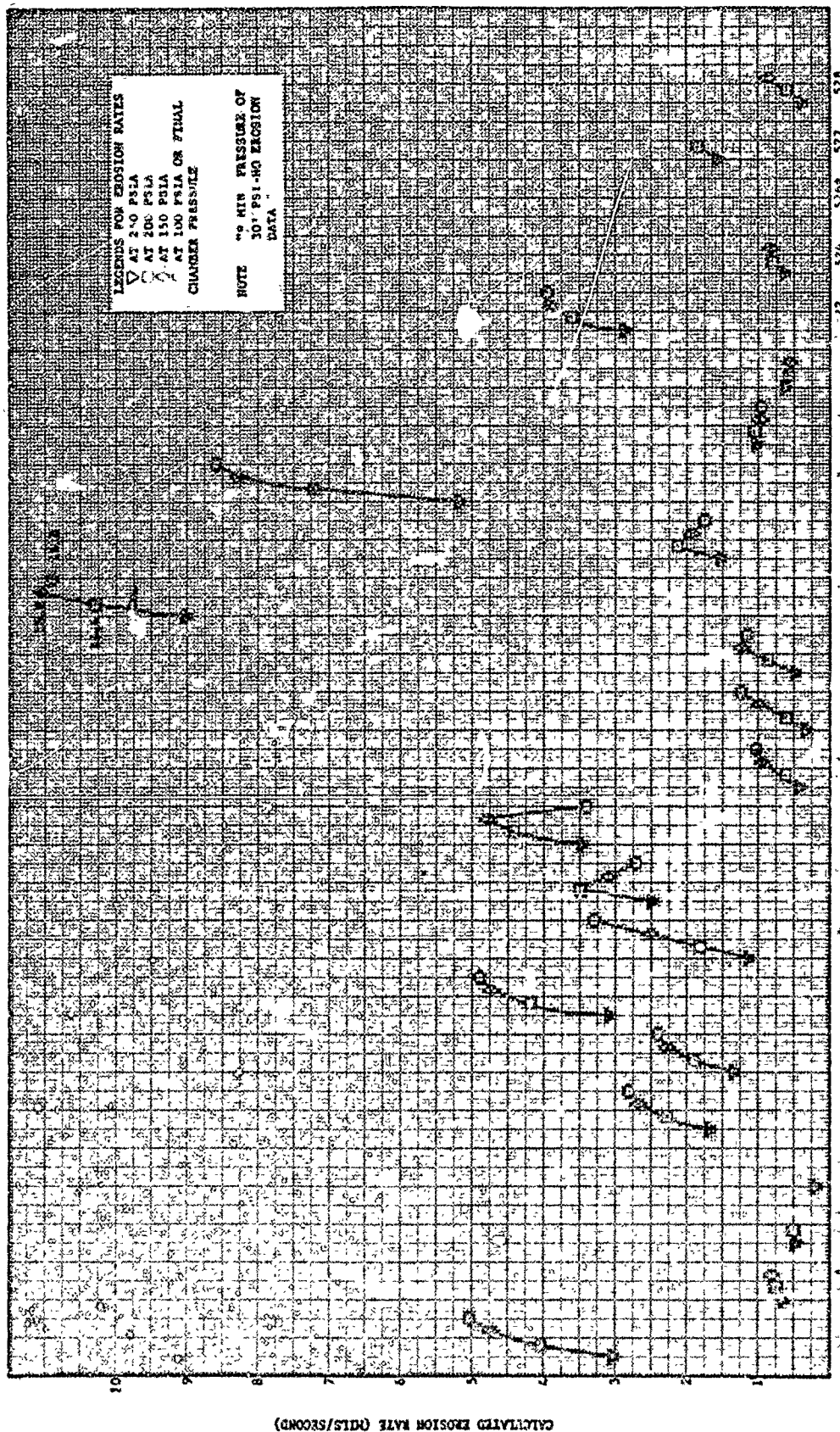
8103000

FIGURE 20-A EROSION RATE VERSUS NOZZLE NUMBER ABLATIVE NOZZLE CHARACTERIZATION



EROSION RATE VERSUS NOZZLE NUMBER ABLATIVE NOZZLE CHARACTERIZATION





RI - 4

520 521 522 523 524 525 526 527 528

EROSION RATE VERSUS DISTANCE IN CHAMBER AREA (INCHES) CHARACTERIZATION

Unclassified

Security Classification

DOCUMENT CONTROL DATA - R&D		
(Security classification of title, body of abstract and indexing annotation must be entered when the overall report is classified)		
1. ORIGINATING ACTIVITY (Corporate author)		2a. REPORT SECURITY CLASSIFICATION
Philco Corporation Aeronutronic Division Newport Beach, California		Unclassified
		2b. GROUP
		N/A
3. REPORT TITLE		
Research on Ablative Plastic Characterization in Simulated Motor Exhaust		
4. DESCRIPTIVE NOTES (Type of report and inclusive dates)		
Summary Report 15 June 1964 to 30 June 1965		
5. AUTHOR(S) (Last name, first name, initial)		
Mayo, G. S. Ostrow, S. L. Marcus, R. E.		
6. REPORT DATE	7a. TOTAL NO. OF PAGES	7b. NO. OF REFS
July 1965	277	0
8a. CONTRACT OR GRANT NO.	8b. ORIGINATOR'S REPORT NUMBER(S)	
AF 33(615)-1632	AFML-TR-65-245, Part I	
b. PROJECT NO.	9b. OTHER REPORT NO(S) (Any other numbers that may be assigned this report)	
7340	U-3356	
c. Task No.		
734001		
d.		
10. AVAILABILITY/LIMITATION NOTICES Each transmittal of this document outside the agencies of the U. S. Government must have prior approval of the Plastics and Composites Branch, MANC, Nonmetallic Materials Division, Air Force Materials Laboratory, Wright-Patterson AFB, Ohio 45433		
11. SUPPLEMENTARY NOTES		12. SPONSORING MILITARY ACTIVITY
		Air Force Materials Laboratory (MANC) Wright-Patterson AFB, Ohio
13. ABSTRACT New chemical compositions and physical constructions of ablative materials were exposed in a small scale, high temperature Aeronutronic solid propellant rocket motor simulator and a liquid propellant (nitrogen tetroxide - 50 percent hydrazine and 50 percent unsymmetrical dimethylhydrazine) combustion gas environment to determine the potential usefulness of these materials for hyperenvironmental conditions associated with current and future solid and liquid propellant motors. Material erosion and thermal insulation characteristics of the research nozzles were evaluated by comparisons of chamber pressure versus time data, erosion and resin degradation rates, and visual photographic data. Research nozzle specimens were exposed in two (2) groups to the exhaust environment of a simulated solid propellant having a flame temperature of 5800°F and being highly aluminized. Test Series 1 contained thirty (30) nozzle specimens and Test Series 2 contained twenty-four (24) specimens. Test results and preliminary specimen evaluation indicated that the Aeronutronic solid propellant simulator exhaust environment provided the specified exhaust environment with the required repeatable test screening characteristics to enable valid material evaluations. A total of seventy (70) nozzles were exposed to the exhaust environment of the liquid rocket motor (NTO/50-50). In the initial phase the motor injector was modified to provide optimum erosion geometry characteristics prior to research nozzle testing. Test results indicated that the specified nominal test conditions were met and enabled valid material evaluation. Several new ablative plastic composites were found to have ablative performance characteristics superior to the state-of-the-art carb n-phenolic and silica-phenolic composites.		

DD FORM 1 JAN 64 1473

Unclassified

Security Classification

Unclassified

Security Classification

14. KEY WORDS	LINK A		LINK B		LINK C	
	ROLE	WT	ROLE	WT	ROLE	WT
Plastics Ablation Nozzle Materials Solid Propellant Liquid Propellant						

### INSTRUCTIONS

**1. ORIGINATING ACTIVITY:** Enter the name and address of the contractor, subcontractor, grantee, Department of Defense activity or other organization (corporate author) issuing the report.

**2a. REPORT SECURITY CLASSIFICATION:** Enter the overall security classification of the report. Indicate whether "Restricted Data" is included. Marking is to be in accordance with appropriate security regulations.

**2b. GROUP:** Automatic downgrading is specified in DoD Directive 5200.10 and Armed Forces Industrial Manual. Enter the group number. Also, when applicable, show that optional markings have been used for Group 3 and Group 4 as authorized.

**3. REPORT TITLE:** Enter the complete report title in all capital letters. Titles in all cases should be unclassified. If a meaningful title cannot be selected without classification, show title classification in all capitals in parenthesis immediately following the title.

**4. DESCRIPTIVE NOTES:** If appropriate, enter the type of report, e.g., interim, progress, summary, annual, or final. Give the inclusive dates when a specific reporting period is covered.

**5. AUTHOR(S):** Enter the name(s) of author(s) as shown on or in the report. Enter last name, first name, middle initial. If military, show rank and branch of service. The name of the principal author is an absolute minimum requirement.

**6. REPORT DATE:** Enter the date of the report as day, month, year; or month, year. If more than one date appears on the report, use date of publication.

**7a. TOTAL NUMBER OF PAGES:** The total page count should follow normal pagination procedures, i.e., enter the number of pages containing information.

**7b. NUMBER OF REFERENCES:** Enter the total number of references cited in the report.

**8a. CONTRACT OR GRANT NUMBER:** If appropriate, enter the applicable number of the contract or grant under which the report was written.

**8b, 8c, & 8d. PROJECT NUMBER:** Enter the appropriate military department identification, such as project number, subproject number, system numbers, task number, etc.

**9a. ORIGINATOR'S REPORT NUMBER(S):** Enter the official report number by which the document will be identified and controlled by the originating activity. This number must be unique to this report.

**9b. OTHER REPORT NUMBER(S):** If the report has been assigned any other report numbers (either by the originator or by the sponsor), also enter this number(s).

**10. AVAILABILITY/LIMITATION NOTICES:** Enter any limitations on further dissemination of the report, other than those

imposed by security classification, using standard statements such as:

- (1) "Qualified requesters may obtain copies of this report from DDC."
- (2) "Foreign announcement and dissemination of this report by DDC is not authorized."
- (3) "U. S. Government agencies may obtain copies of this report directly from DDC. Other qualified DDC users shall request through \_\_\_\_\_."
- (4) "U. S. military agencies may obtain copies of this report directly from DDC. Other qualified users shall request through \_\_\_\_\_."
- (5) "All distribution of this report is controlled. Qualified DDC users shall request through \_\_\_\_\_."

If the report has been furnished to the Office of Technical Services, Department of Commerce, for sale to the public, indicate this fact and enter the price, if known.

**11. SUPPLEMENTARY NOTES:** Use for additional explanatory notes.

**12. SPONSORING MILITARY ACTIVITY:** Enter the name of the departmental project office or laboratory sponsoring (paying for) the research and development. Include address.

**13. ABSTRACT:** Enter an abstract giving a brief and factual summary of the document indicative of the report, even though it may also appear elsewhere in the body of the technical report. If additional space is required, a continuation sheet shall be attached.

It is highly desirable that the abstract of classified reports be unclassified. Each paragraph of the abstract shall end with an indication of the military security classification of the information in the paragraph, represented as (TS), (S), (C), or (U).

There is no limitation on the length of the abstract. However, the suggested length is from 150 to 225 words.

**14. KEY WORDS:** Key words are technically meaningful terms or short phrases that characterize a report and may be used as index entries for cataloging the report. Key words must be selected so that no security classification is required. Identifiers, such as equipment model designation, trade name, military project code name, geographic location, may be used as key words but will be followed by an indication of technical context. The assignment of links, rules, and weights is optional.

Unclassified

Security Classification